https://ntrs.nasa.gov/search.jsp?R=19850012651 2020-03-20T18:45:09+00:00Z

NASA-CP-2349 19850012651

NASA Conference Publication 2349

Future of Ultraviolet Astronomy Based on Six Years of IUE Research

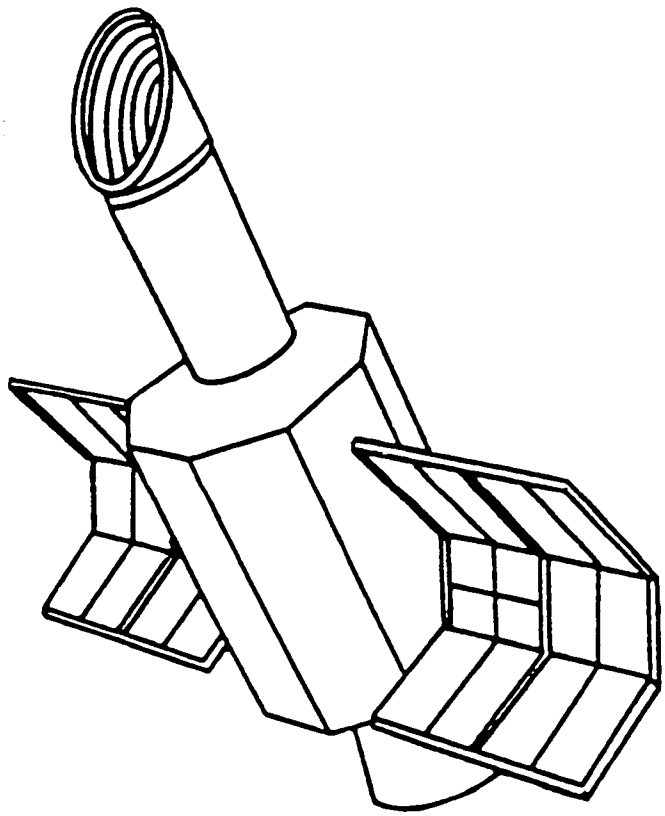

Proceedings of a symposium held at
NASA Goddard Space Flight Center
Greenbelt, Maryland
April 3-5, 1984

NASA

NASA Conference Publication 2349

Future of Ultraviolet Astronomy Based on Six Years of IUE Research

Edited by
Jaylee M. Mead
Robert D. Chapman
and Yoji Kondo
Goddard Space Flight Center

Proceedings of a symposium held at
NASA Goddard Space Flight Center
Greenbelt, Maryland
April 3–5, 1984

National Aeronautics
and Space Administration

**Scientific and Technical
Information Branch**

1984

PREFACE

This is the third in a series of biennial NASA International Ultraviolet Explorer (IUE) Symposia. The first two conferences took place in the spring of 1980 and 1982.

The current symposium commemorates the successful completion of the first six years of the IUE Guest Observer Program and inaugurates the seventh year. Launched into a quasi-geosynchronous orbit on 26 January 1978, the IUE satellite observatory has been used as an important tool for astronomical research by over a thousand astronomers from all over the world. The objects studied with the IUE encompass practically all astronomical sources, ranging from nearby solar system objects, such as comets and planets, to extragalactic objects, including quasars. The content of this conference proceedings demonstrates the breadth of the research being conducted with the IUE.

We wish to acknowledge the contributions made by a cadre of scientists, engineers, and technicians, who have made the IUE a resounding success. This includes, in particular, the enthusiastic guest observers, many of whom were present at this symposium.

Proceedings Editors: Jaylee M. Mead, Robert D. Chapman, Yoji Kondo

Scientific Organizing Committee:

T. R. Ayres
R. D. Chapman (Co-Chm.)
A. P. Cowley
R. Giacconi
Y. Kondo (Chm.)
B. Margon
R. M. Nelson
J. B. Oke
J. C. Raymond
B. D. Savage
G. A. Wegner
E. J. Weiler

Local Organizing Committee:

S. R. Heap
J. N. Heckathorn
A. V. Holm
J. K. Kalinowski
J. M. Mead (Chm.)

IUE SYMPOSIUM PARTICIPANTS

Ahmad, I. D.
Aizenman, M. L.
Ake, T.
Altner, B.
Arpingny, C.
Ayres, T.
Baliunas, S.
Barker, P. K.
Baumert, N. H.
Bell, R. A.
Bennett, J.
Bianchi, L.
Blair, W. P.
Boggess, A.
Bohlin, R.
Böhm, K.-H.
Böhm-Vitense, E.
Bond, H.
Bonnell, J.
Bowers, C.
Boyce P.
Bregman, J. N.
Bromage, G. E.
Brosius, J.
Brown, D.
Brugel, E.
Bruhweiler, F.
Bruner, G.
Brunk, W. E.
Bruzual, G.
Butterworth, P. S.
Caldwell, J.
Cardelli, J. A.
Carpenter, K.
Carruthers, G. R.
Chapman, R. D.
Che, T. B.
Clayton, G.
Córdova, F.
Cowley, A.
De La Pena, M.
Doazan, V.
Dossin, F.
Dubin, M.
Dufour, R. J.
Dupree, A.
Durrance, S. T.
Egret, D.
Evans, N. R.
Feibelman, W. A.
Feldman, P.
Ferguson, H. C.
Finley, D. S.
Fitzpatrick, E. L.
Garmany, K.
Giampapa, M. S.
Gilra, D. P.
Grady, C. A.
Grewing, M.
Guinan, E. F.
Gull, T.
Hackney, K. R. H.
Hackney, R. L.
Hallam, K.
Heap, S. R.
Hecht, J.
Heck, A.
Heckathorn, H.
Heckathorn, J.
Henry, R. B. C.
Hettrick, M.
Holberg, J.
Holm, A.
Hulbert, S. J.
Hutchings, J. B.
Imhoff, C. L.
Johnson, H.
Kalinowski, K.
Kenyon, S.
Kimble, R.
Kinney, A. L.
Kondo. Y.
Lamb, S.
Lamontagne, R.
Landsman, W.
Linsky, J.
Little-Marenin, I.
Locke, M.
Long. K. S.
Maran, S.
Massa, D.
McCluskey, G. E.
Mead, J.
Michalitsianos, A. G.
Moos, W.
Morrison, N. D.
Mushotzky, R.
Nava, D.
Netzer, H.
Ockert, M.
Oliversen, N.
Oliversen, R.
Opal, C.
Parsons, S.
Peery, B.
Peters, G.
Plavec, M. J.
Polidan, R. S.
Proffitt, C.
Rahe, J.
Raymond, J. C.
Roman, N. G.
Savage, B.
Schaefer, B.
Schiffer, F. H.
Scott, E.
Shipman, H. L.
Shore, S.
Simon, T.
Sion, E.
Skinner, T.
Stalio, R.
Starrfield, S.
Stecher, T.
Steiman-Cameron, T.
Stencel, R.
Swank, J.
Szkody, P.
Thomas, F. G.
Thomas, R.
Timothy, J. G.
Viotti, R.
Vitello, P.
Wade, R.
Wagener, R.
Walborn, N.
Walter, S.
Wamsteker, W.
Warren, W.
Weaver, H. A.
Weistrop, D.
Wende, C.
Wilson, L. A.
Woods, T.

TABLE OF CONTENTS

Page

NEBULAE AND CLUSTERS

INTERSTELLAR MEDIUM

WHITE DWARFS

VARIABLE STARS

Page

INVITED PAPERS

IUE ABSORPTION LINE STUDIES OF HIGHLY IONIZED INTERSTELLAR GAS

Blair D. Savage
Washburn Observatory, The University of Wisconsin-Madison

Abstract

IUE high dispersion echelle spectra of galactic and extragalactic sources have generally revealed the presence of absorption by interstellar Si IV and C IV. Occasionally N V has been detected. The observational results relating to these species will be reviewed for H II regions, supernova remnants, galactic disk gas, galactic halo gas, and extragalactic gas. For the various regions, the likely origin of the ionization is considered.

INTRODUCTION

Lyman Spitzer in his classic theoretical paper, "On a Possible Interstellar Galactic Corona" (Spitzer 1956), first suggested the possible existence of a hot (10^6K) phase of the interstellar medium heated by stellar ejecta. This hot medium was required to provide the pressure support to stabilize the clouds found at large distances from the galactic plane. Spitzer also pointed out the importance of orbiting ultraviolet telescopes for directly recording the absorption lines of the highly ionized gas expected to exist in the hot medium.

The first ultraviolet detection of the highly ionized interstellar medium came shortly after the launch of the Copernicus satellite in 1972 (Rogerson et al. 1972). Detailed studies by Jenkins (1978 a and b) established the pervasiveness of this new low density high temperature component of the interstellar gas. Unfortunately the Copernicus satellite O VI survey of Jenkins was limited to stars brighter than V = 6.9. In addition, only a few bright stars were scanned to search for C IV absorption because of the low sensitivity of Copernicus at 1550 A.

With its ability to obtain spectra of hot stars as faint as V = 14, the IUE has provided an important complement to the Copernicus studies of the highly ionized species in the interstellar medium.

Table 1 lists basic information about the various highly ionized interstellar species accessible to the IUE. For completeness, information is also given for other species accessible to the Copernicus Satellite in the 912 to 1200 A region. The table lists wavelengths, f values, the energy required to produce and destroy the ion, the solar elemental abundance ratio with respect to hydrogen, and the temperature for which the ionic abundance is a maximum according to the "coronal ionization" calculations of Shull and van Steenberg (1982) and Baliunas and Butler (1980). In these calculations, electron collisional ionization is balanced by electronic and dielectronic recombination using the most up to date cross-sections. The Baliunas and

Butler calculation for Si IV also includes the effects of charge exchange. The column labeled "sensitivity" lists $f[n(x)/n(H)]_{\odot}[n(ion)/n(x)]T_{max}$. This product is a rough measure of the detectability of a particular line assuming equilibrium collisional ionization, solar abundances, and equal amounts of gas at all temperatures between 0.5×10^5 and 3×10^5 K. The product suggests the most sensitive species are C IV and O VI followed by Si IV, N V, S VI, and S IV. The sensitivity of C IV and O VI are comparable while Si IV and N V are about 5 to 10 times less sensitive. Care should be used when intercomparing species associated with different elements to infer interstellar temperatures. The solar abundance ratios may not apply in the region being studied. For example, in the Orion Nebula the nitrogen abundance given by Dufour, Shields and Talbot (1982) is 3 x smaller than the value listed in Table 1. IUE has the sensitivity to probe such distant interstellar regions that galactocentric abundance gradients may even become important. Finally, if the gaseous regions being studied contain dust, the enhanced depletion of one element with respect to another may also be important.

IONIZATION MECHANISMS

The comment column of Table 1 gives a number of possible ionization mechanisms for each of the ions listed. The large range of possibilities listed demonstrates the problem associated with understanding the origin of the highly ionized gas in the interstellar medium.

Photoionization by Hot Young Stars

Those species requiring less than 54 eV for their production may be created by direct photoionization by normal Population I hot stars. 54 eV is important since hot stars with normal helium abundances have large He II discontinuities at 228 A. For example, for the log g = 4.5 and solar abundance hot star model atmosphere calculations of Hummer and Mihalas (1970), the ratio of the number of emitted He^+ ionizing photons to H ionizing photons is 1.2×10^{-6}, 1.9×10^{-5}, and 1.2×10^{-4} at T_{eff} = 40,000, 50,000, and 60,000 K, respectively. O3 stars are believed to have $T_{eff} \simeq 50{,}000$ K (Kudritzki 1980). Thus, stars O3 or cooler might produce detectable amounts of Si IV, S IV, and C IV but would not be capable of producing much N V, S VI, or O VI. Detailed photoionization calculations of the expected column densities of Si IV and C IV in normal H II regions surrounding Population I stars are found in Black *et al.* (1980) and Cowie, Taylor, and York (1981). Both calculations make use of the model atmospheres of Kurucz (1979). The column densities scale with $n_e^{1/2}$. For n_e = 1, observable amounts ($\sim 10^{13}$ cm^{-2}) of Si IV and C IV are predicted for stars with T_{eff} 30,000 and 35,000 K, respectively. The ratio N(C IV)/N(Si IV) increases from about 0.04 to 0.9 as T_{eff} increases from 35,000 to 50,000 K. The results obtained in such calculations will depend on the quality of the model atmosphere calculations in the region of the rapid fall off in the Planck function. Properly allowing for such effects as atmospheric extension and winds might have a large effect on the computed emergent spectrum. Another problem concerns the basic atomic parameters. For example, the Si^{2+} photoionization cross-sections of Reilman and Manson (1979) are 4 to 5 times smaller than those usually adopted. The origin of this discrepancy

is unknown. Also, the expected C IV to Si IV ratio must be modified if C and Si are depleted because of the survival of dust in H II regions. In the diffuse interstellar medium, the gas phase carbon abundance is 1/3 solar (Hobbs et al., 1982) while the gas phase Si abundance is 1/10 solar (Phillips, Gondhalekar and Pettini 1982). The detection of the 9.7 μm silicate feature from dust in many H II regions including Orion (for a review see Savage and Mathis 1978), suggests that the depletion of Si may be large. As a consequence of these concerns, the observed C IV to Si IV column density ratio may not provide very many clues about the nature of the ionization process.

Photoionization by Hot Evolved Stars

Hot white dwarfs and the central stars of planetary nebulae can have surface temperatures greatly exceeding 50,000 K. In a recent paper, Dupree and Raymond (1983) considered the photoionizing effects of hot white dwarfs on the creation of highly ionized species in the interstellar medium. Helium rich white dwarfs can produce Si IV and C IV while hydrogen rich white dwarfs which do not have a strong 54 eV He^+ discontinuity also produce N V and O VI. Aside from producing their own surrounding H II regions which have been detected, these stars may also be important in explaining the distributed C IV found in the milky way plane and halo.

Photoionization by Stellar X-Ray Sources

McCray, Wright and Hatchett (1977) pointed out that X-ray photoionization can create zones of highly ionized elements in the interstellar gas around an X-ray source. The expected high ionization column densities depend on the source spectrum and luminosity and on the density distribution of the surrounding ambient gas.

Photoionization by the Extragalactic Background

Extragalactic EUV and XUV radiation can affect the ionization of gas at large distances from the galactic plane. Above E = 1 keV the background radiation can be measured directly (Schwartz 1979). At lower energies the background must be estimated by counting up the likely emission from quasars and active galaxies. Such estimates have been made by Sherman (1980).

Hartquist, Pettini and Tallant (1984) and Chevalier and Fransson (1984) have calculated the ionization of interstellar gas by the extragalactic background. They find that this source of ionization could play a very important role in the galactic halo.

Collisional Ionization in the Hot Interstellar Medium

The evidence for a hot phase to the interstellar medium is the soft X-ray background (McCammon et al. 1983) and the O VI measurements of the Copernicus satellite (Jenkins 1978 a and b). The volume occupied by this phase could range from less than 10% to more than 80 or 90% (McCammon 1981). All of the species listed in Table 1 can be produced by electron collisional ionization in a medium with $0.5\times10^5<T<5\times10^5$ K. The soft X-rays imply gas with higher temperatures. Possibly the O VI lines and other high ionization lines are

produced in the interface region between the X-ray emitting gas and cooler clouds, i.e., at evaporating cloud boundaries (McKee and Cowie 1977). If this is the case, the relative abundances of the highly ionized species will depend on the run of density and temperature through the interface. Furthermore since this boundary layer can be thin, time dependent effects may be important. For evaporative interfaces the ion ratios may be estimated from the time dependent ionization calculations of Weaver et al. (1977). Adjusting their values to the abundances given in table 1 the results are Si IV/ O VI $\simeq$ 0.006, C IV/O VI $\simeq$ 0.12, N V/O VI $\simeq$ 0.036, and S IV/O VI $\simeq$ 0.017. Jenkins (1978b) has found that the average O VI density in the galactic plane is $n(O\ VI) \simeq 2\times10^{-8}$ cm^{-3}. If other highly ionized species are formed in cloud interfaces one would expect to find the following average cloud densities: $n(Si\ IV) \simeq 1\times10^{-10}$ cm^{-3}, $n(C\ IV) \simeq 2\times10^{-9}$ cm^{-3}, $n(N\ V) \simeq 7\times10^{-10}$ cm^{-3} and $n(S\ IV) \simeq 3\times10^{-10}$ cm^{-3}. However, given our lack of knowledge about elemental abundances, the effects of depletion, and the validity of the time dependent calculations, these predictions must be considered quite uncertain.

The addition of time dependent effects to our list of potential problems certainly complicates the study of the highly ionized atoms. Time dependent effects may be important in interface regions as mentioned above or in regions of very low density since collision rates scale as n^2. In the galactic halo where n may approach 10^{-4} cm^{-3} or less, the assumption of time equilibrium should certainly be questioned.

Collisional Ionization in Interstellar Shocks

Highly ionized species are produced in shocked interstellar regions. However, absolute and relative abundance predictions require rather detailed model calculations. Time dependent effects, shock generated ionizing radiation and uncertain grain destruction rates are a few of the serious complications. For recent reviews see McKee and Hollenbach (1980) and McCray and Snow (1979).

The Interfaces of Circumstellar Bubbles

Castor, McCray and Weaver (1975) and Weaver et al. (1977) have studied the structure and evolution of the bubble that is created by stellar winds acting on the interstellar medium surrounding stars with large mass loss rates. These bubbles are expected to contain hot (10^6 K) shocked gas with densities of about 10^{-3} cm^{-3}. The various highly ionized species we are considering could be produced in the interface between the bubble and the surrounding cooler interstellar material. According to Weaver et al. (1977), the expected O VI, C IV, N V, and Si IV column densities in the interface are 10^{13}, 2×10^{12}, 10^{12} and 1.5×10^{11} cm^{-2}, respectively. These numbers are expected to be relatively insensitive to model parameters. If this is true, more than one interface would be required to explain observations of C IV since the IUE detection limit for this ion is about 10^{13} cm^{-2}. However, the interface high ion column densities do scale with the local density to the 9/35 power. Therefore, column densities six times larger than those quoted above would occur for winds interacting with regions with ambient densities of 10^{-3} cm^{-3}.

OBSERVATIONAL RESULTS

In the following sections, recent observational results relating to studies of the highly ionized atomic absorption lines are summarized and the likely origin of the ionization is considered. However, for many of the observational situations considered, it is likely that several different ionization mechanisms are operating simultaneously. This problem is especially serious for those species such as C IV, Si IV and S IV which require less than 54 eV for their production.

Interstellar versus Circumstellar Absorption

A fundamental problem in interpreting interstellar absorption line data is deciding if the observed narrow features relate to the general interstellar medium or to a circumstellar phenomena. Close binaries and Be stars may have circumsystem or circumstellar gas moving at relatively modest velocities. Absorption by this material could be misinterpreted as interstellar. Stars with very large mass loss rates such as the Wolf-Rayet stars may have surrounding shells of material moving at high and low speeds. The low speed material could be confused with general interstellar absorption. Suggestions that such circumstellar absorption is occuring appears in the results of Smith, Willis and Wilson (1980). In a study of 10 Wolf-Rayet stars, they found no apparent relationship between the strength of the narrow high ionization lines and distance or reddening. Observations of γ^2 Velorum (WC8+09I) and γ^1 Velorum (B3III) by Bruhweiler, Kondo and McCluskey (1979, 1980), Sahade, Kondo and McCluskey (1984), and Sahade and Hernandez (1982) provide a very interesting result. γ^1 Vel is about 41" from γ^2 Vel and is very likely a physical companion. For a distance of 480 pc to the γ Vel system (Abt et al. 1976), 41" corresponds to 20,000 AU. Narrow lines of C IV and Si IV near 0 km s^{-1} are found in the spectrum of γ^2 Vel but are not seen in the spectrum of γ^1 Vel. This result suggests that the C IV and Si IV absorption toward γ^2 Vel may occur where the wind merges with the surrounding interstellar medium and this likely occurs within 20,000 AU of γ^2 Vel.

Because of these possible circumstellar-interstellar confusion problems great care must be taken in choosing suitable target stars for interstellar studies. Be stars, stars in close binary systems, and stars with large mass loss rates all potentially have highly ionized gas in their circumstellar environments.

There are cases where the general interstellar origin of the highly ionized species is well established. For example, a number of stars in the halo gas survey of Pettini and West (1982) have radial velocities exceeding 75 km s^{-1} but have strong interstellar absorption near $V_{LSR} \simeq 0$ km s^{-1} (see their Figure 4). IUE high dispersion observations of extragalactic targets also reveal strong Milky Way absorption by highly ionized species near $V_{LSR} \simeq 0$ km s^{-1} even though the target objects have V $\simeq$ 150 to 300 km s^{-1} (Savage and deBoer 1981) or V $\simeq$ 0.16 c (York et al. 1983).

Another approach that can be taken to verify the interstellar origin of a particular absorption line is to look for stationary absorption lines toward objects with variable radial velocity. York (1977) used this technique to prove the interstellar origin of O VI. However, I'm not aware of published

IUE measurements of this type involving C IV, Si IV or N V.

Although there are methods to establish the interstellar origin of the highly ionized species, we should always consider the possibility of circumstellar confusion problems in the sections that follow.

H II Regions Surrounding Hot Young Stars

Black et al. (1980) and Cowie, Taylor and York (1981) suggested that many of their detections of interstellar C IV and Si IV absorption lines could be explained by direct ultraviolet photoionization of gas in the surrounding H II regions. However, H II regions are complex places. Some are known to be sources of X-rays. Some contain rapidly moving gas. Most contain stars with high speed winds. Therefore, most if not all of the various ionization mechanisms listed in Table 1 could affect the state of the highly ionized gas in H II regions. Given the dependence of the expected H II region column densities produced by stellar photoionization on the effective temperature of the target star or stars and on the surrounding gas density (column density ~ $n^{1/2}$), it is not easy to provide a totally convincing demonstration of the photoionization origin of these lines. For example, Jenkins (1981) showed for a large number of stars that the C IV to Si IV column density ratio didn't seem to increase with effective stellar temperature as predicted by the photoionization calculations. Bruhweiler, Kondo and McCluskey (1980) used the large C IV to Si IV column density ratio to rule out the photoionization origin of these lines for a group of 18 stars. While theory and observations strongly indicate that hot young stars are able to produce large column densities of C IV and Si IV by direct ultraviolet photoionization, much additional work will be needed to sort out the relative contributions to the ionization being provided by all the other possible mechanisms.

High ionization absorption lines have been studied in somewhat greater detail for the following nebulae: Orion (Franco and Savage 1982), Carina (Cowie, Hu, Taylor and York 1981); Laurent, Paul, and Pettini 1982; Welsh and Thomas 1982, 1983; and Walborn, Heckathorn and Hesser 1984), M 8 (Welsh 1983), 30 Doradus (deBoer, Koornneef and Savage 1980); Perseus OB 1 (Phillips and Gondhalekar 1981) and Cygnus OB 1 (Phillips, Welsh and Pettini 1984). These studies are providing very significant information about H II region gas kinematics. Such information will help clarify the dynamical consequences of stellar winds and supernova explosions on the surrounding interstellar gas.

H II Regions Surrounding Hot Evolved Stars

Narrow absorption lines of C IV and sometimes Si IV and N V have been detected toward three hot white dwarfs (Bruhweiler and Kondo 1981; Dupree and Raymond 1982; Sion and Guinan 1983). In a fourth case no high ion lines are seen (Malina, Basri and Bowyer 1981). The measurements for Feige 24 by Dupree and Raymond (1982) reveal C IV and Si IV absorption near $V_{Helio} \simeq 0$ km s^{-1} and C IV, Si IV and N V absorption near 83 km s^{-1}. The low velocity absorption likely arises in local interstellar gas photoionized by the white dwarf while the 83 km s^{-1} absorption likely arises in the Feige 24 system. This object provides an excellent illustration of a combination of circumstellar or stellar absorption and interstellar absorption.

The interstellar absorption lines of C IV, Si IV and N V toward white dwarfs seem well described by the photoionization calculations of Dupree and Raymond (1983). Detectable amounts of photoionized C IV are expected if the white dwarfs are in a medium with $n > 0.03$ cm^{-3}. For HZ 43 the upper limits for the high ion absorption implies $n(\text{local}) < 0.03$ cm^{-3}.

Not only do hot white dwarfs create their own highly ionized H II regions which are of interest in their own right, but these stars may also play an important role in creating highly ionized atoms in the general interstellar medium. Estimates of the expected mean interstellar C IV density have been made by Dupree and Raymond (1983). The results depend on the uncertain space density of hot white dwarfs and on the average density of the medium in which the white dwarfs are situated. For $\langle n \rangle \simeq 0.1$ cm^{-3}, the mean C IV density is predicted to lie between 2×10^{-9} and 7×10^{-9} cm^{-3}. These numbers are comparable to the observed mean density (see the section concerning galactic disk gas).

The ultraviolet emission lines from planetary nebulae have been extensively investigated with the IUE (for a brief review see Peimbert 1981). A number of central stars of planetary nebulae have been observed in high dispersion by IUE. Unfortunately, the absorption lines in these data have not received much attention.

Photoionized Gas Near Stellar X-Ray Sources

The two X-ray binary systems observed by IUE in high dispersion are HD 153919 (Dupree et al. 1978) and Vela X-1 = HD 77581 (Dupree 1980). Strong narrow Si IV and C IV absorption is seen toward each system. For HD 153919 the stellar signal near the N V doublet is weak and only an upper limit to the strength of interstellar N V could be established. For HD 77581 there is no continuum near the N V doublet because of the great strength of stellar N V.

HD 153919 is classified as O6 f and may have a surface temperature of about 40,000 K. For such a star, direct ultraviolet photoionization by stellar photons would be expected to produce large column densities of C IV and Si IV. Therefore, it is not clear whether or not the x-ray emission is enhancing the ionization of these species according to the predictions of McCray, Wright and Hatchett (1977).

In the case of the Vela X-1 source, the primary star, HD 77581, is classified as B0.5 Ib. The ultraviolet radiation form such a star might produce Si IV but would not be expected to produce C IV. Dupree et al. (1980) suggest that most of the observed C IV and some of the observed Si IV is due to X-ray photoionization. While this interpretation appears reasonable, it would be valuable to observe targets at a similar distance in directions near to the X-ray source to determine if some of the Si IV and C IV absorption occurs in the general interstellar medium.

Supernova Remnants

Most IUE studies of the physical state of gas in supernova remnants have involved the ultraviolet emission lines (for a review see Raymond 1983). However, important complementary information can be obtained through absorption line studies of stars within and beyond the remnant.

The studies of Jenkins, Silk and Wallerstein (1976) and Jenkins,

Wallerstein and Silk (1984) of the Vela supernova remnant with the Copernicus and IUE satellites illustrate the importance of absorption measurements. In the 1984 paper, IUE observations of absorption lines toward 45 stars in the vicinity of Vela are presented. Over one-third of the stars exhibit high velocity interstellar absorption components with a dispersion in velocities that suggests chaotic motions within the remnant. The high ionization lines of Si IV, C IV and N V are seen at high and low velocity. The high ionization lines at low velocity imply a large (3 to 10x) density enhancement over that found in the general interstellar medium. Jenkins, Wallerstein and Silk (1984) attempted to understand the relative column density ratios of these lines in terms of collisionally ionized gas in conductive interfaces surrounding clouds behind the shock fronts. They found too much Si IV (by a factor of 4) and too little N V (by a factor of 7). They suggested the overabundance of Si IV might be explained by ionization from shock generated ultraviolet radiation. A deficiency of N V compared to the expectations seems to be a very common problem in interstellar studies. Perhaps something is wrong or missing in the atomic rate calculations involving N V. An interstellar nitrogen abundance 2 to 3 tiimes smaller than solar would help reduce the N V discrepancy.

Gas in the Galactic Disk

The density distribution of C IV, Si IV, and N V in the general interstellar medium of the galactic disk is not well determined. This is because of the difficulty of deciding if observed lines arise in stellar H II regions or in the general interstellar medium. A possible solution to the H II region problem involves observing stars cool enough so they do not create their own regions of photoionized C IV and Si IV. According to the calculations of Cowie, Taylor and York (1981), that means stars cooler than about 25,000 K in the case of Si IV and cooler than 30,000 K in the case of C IV. These temperatures correspond to spectral types B1 and B0, respectively. In addition to selecting cooler stars, care must be taken to avoid directions passing near the prominent H II regions surrounding other stars.

Only a few lines of sight have been identified in the literature for which the results likely apply to the general interstellar medium of the galactic disk. These include absorption toward HD 47432 and HD 218915 (Cowie, Taylor and York 1981) and the -10 km s^{-1} absorption toward HD 93205 (Laurent, Paul and Pettini 1982). For these directions the average C IV densities are $9x10^{-9}$, $3x10^{-9}$ and $3x10^{-9}$ cm^{-3}, respectively. In analyzing the Milky Way C IV absorption toward HD 36402 in the Large Magellanic Cloud, Savage and deBoer (1981) estimated a C IV midplane density of about $5x10^{-9}$ cm^{-3} and a Si IV midplane density of about $8x10^{-10}$ cm^{-3}.

The C IV densities reported above aren't too far from the densities expected from the evaporative interfaces of cool clouds embedded in a hot (10^6 K) medium (see earlier section). However, the observed Si IV density is 8 times larger. This suggests that photoionization may be providing a major contribution for that ion. Evaporative interfaces may not be needed to explain the C IV since the estimates of Dupree and Raymond (1983) suggest the observed Si IV and C IV densities could easily be maintained by ultraviolet photons from hot white dwarfs.

The distribution of C IV in halo gas is very patchy. It is quite likely

a similar situation occurs for disk gas. Therefore, measures of only the few lines of sight discussed above do not provide a clear picture of the distribution of this gas. Clearly much more observational work is needed.

Milky Way Halo Gas

The existance of C IV and Si IV in the Milky Way halo at z distances exceeding 1 kpc has been established through observations of extragalactic targets (Savage and deBoer 1979, 1981; York et al. 1983) and from studies of Milky Way halo stars (Pettini and West 1982). The observational situation concerning the much weaker N V doublet is less clear. Fitzpatrick and Savage (1983) claim the marginal detection of Milky Way halo N V toward HD 5980 in the Small Magellanic Cloud. Pettini and West (1982) definitely detected N V toward 2 of 20 stars. In those cases where N V is detected, the N V to C IV column density ratio averages 0.30. For a N V column density detection limit of 3×10^{13} cm^{-2}, this suggests that a C IV column density of 10^{14} cm^{-2} would be required to just begin to see N V. In the Pettini and West survey only 6 of 20 stars have N(C IV) > 10^{14} cm^{-2}. I suspect that N V does generally exist in halo gas, but at a column density somewhat below the IUE detection threshold for most paths so far observed.

The scale height of C IV in the halo appears to be in the range of 2 to 4 kpc. However, the N(C IV) sin b vs z plots of Pettini and West (1982) and deBoer and Savage (1983) imply a very patchy distribution. For a given z the projected column density N(C IV) sin b ranges over a factor of 10. Pettini and West (1982) believe a simple exponential distribution does not describe the C IV density away from the galactic plane. They suggest the density may peak near 1 to 2 kpc. Whether this interpretation is true or not unfortunately depends on our very uncertain understanding of the C IV density in galactic disk gas.

Two fundamental questions relate to the origin of the highly ionized gas in the galactic halo: (1) What holds the gas at such large z distances? and (2) What is the origin of the ionization? In the galactic fountain model of Shapiro and Field (1976) and Bregman (1980), hot (10^6 K) disk gas flows outward, cools, recombines, and returns to the disk as clouds. In this discription, the support is thermal; gas at 10^6 K has a thermal scale height in the galactic gravitational field of 5 kpc. In the galactic fountain model, lines of C IV, Si IV and N V would be formed in the cooling gas associated with the fountain flow. Alternately these particular lines could be produced by EUV photoionization of cooler fountain material. The origin of the EUV might be the extragalactic background or halo stars such as hot white dwarfs or the nuclei of planetary nebulae.

An alternate picture is that of Chevalier and Fransson (1984). In their model, the large z extent of the halo gas is provided by the pressure support of cosmic rays. In such a situation the halo gas can be relatively cool (10^4 K) and still contain C IV and Si IV which are ionized by the extragalactic background. The detailed photoionization calculations by Chevalier and Fransson (1984) and by Hartquist, Pettini and Tallant (1984) suggest that this picture is a viable possibility although the amount of N V predicted for the range of model parameters computed is 10x less than the marginal detection of Fitzpatrick and Savage (1983). However, the degree of ionization in such a photoionized gas would be increased by decreasing the gas

density below the minimum value of 10^{-3} cm^{-3} for which models were run.

As pointed out by Chevalier and Fransson (1984), it is difficult to understand what would prevent their cosmic ray supported galactic halo from converting into a galactic fountain. I suspect the actual situation is a complex combination of a fountain flow with the ionization being provided by thermal ionization in cooling fountain gas and by ultraviolet photoionization from the extragalactic background and hot halo stars.

To begin to resolve some of these questions, space telescope will be particularly valuable. Direct measures of thermal line widths will be possible with the high resolution spectrograph in order to decide between collisional ionization in 10^5 K gas and ultraviolet photoionization in 10^4 K gas. Finally, the high precision photometry possible with the Digicon detectors in the high resolution spectrograph will make searches for the important N V doublet relatively easy.

The Small Magellanic Cloud

High resolution IUE spectra now exist for 10 stars in the SMC. Many of these spectra are found in Savage and deBoer (1981), deBoer and Savage (1980), and Fitzpatrick (1984a). The highest quality data are for HD 5980 (Fitzpatrick and Savage 1983) and Sk 159 (Fitzpatrick 1984b). The interstellar ultraviolet absorption toward the SMC provides information about SMC H II region gas, SMC disk gas, and SMC halo gas. deBoer and Savage (1980) found that the ultraviolet absorption line velocity pattern at SMC velocities for neutral and highly ionized gas was similar to that seen in the Milky Way. This suggested that the SMC may have a gaseous halo similar to that enveloping the Milky Way. Doubt about the reality of an SMC corona or halo was cast by Prevot *et al.* (1980). They observed Sk 159, a B0.5Ia star not expected to produce surrounding photoionized C IV, and found no C IV in the noisy spectrum. Fitzpatrick (1984b) combined three high dispersion spectra of Sk 159 to improve the signal to noise for this important object. The resultant spectrum showed C IV absorption with a column density exceeding 3×10^{13} cm^{-2} near 100 km s^{-1}. C IV absorption at similar velocities (i.e., in the range 100-130 km s^{-1}) is seen toward other SMC stars. These velocities are 30-60 km s^{-1} more negative than expected for the "normal" photoionized nebular component. This gas has a large C IV to Si IV column density ratio similar to that found for Milky Way halo gas. The 100 km s^{-1} absorption may occur in the SMC halo. For additional discussions of this controversial issue see Fitzpatrick and Savage (1984) and deBoer (1984).

The H II region, disk gas, and halo gas confusion problem is particularly severe for C IV because hot stars can create large column densities of photoionized C IV. However, Fitzpatrick and Savage (1983) also found N V absorption between 100 and 200 km s^{-1} toward HD 5980. This ion requires an additional ionization mechanism. Absorption in a hot gaseous halo seems a reasonable possibility, although Table 1 suggests there are many other choices.

The Large Magellanic Cloud

The IUE archives contain high dispersion spectra for 21 LMC O, B and WR stars. Some of these spectra are found in Savage and deBoer (1981) and deBoer

and Savage (1980). The highest quality data are for HD 36402 (deBoer and Nash 1982) and R136a (Savage et al. 1983). As in the case of the SMC, there are major problems associated with locating the spatial region or regions responsible for the complex absorption patterns observed. Thus, the deBoer and Savage (1980) suggestion of an LMC corona or halo has also been criticised (Feitzinger and Schmidt-Kaler 1982). In an on going IUE program, Savage and Fitzpatrick are emphasizing IUE observations of cooler LMC stars, away from regions of nebulosity, in order to minimize the H II region contribution to the high ionization line absorption. Preliminary results for HDE 269599 (B0.5) reveal C IV absorption at LMC velocities even though the object is too cool to produce this ion by direct ultraviolet photoionization.

The detection of N V absorption at LMC velocities toward HD 36402 (deBoer and Nash 1982) reveals that ionization mechanisms other than direct ultraviolet photoionization by population I stars must be operating in the LMC.

Other Extragalactic Objects

High resolution IUE observations have been obtained for a number of extragalactic objects more distant than the SMC and LMC. Some of these data also reveal high ionization absorption. For example, strong Milky Way halo absorption in the lines of Si IV is seen toward 3C273 (York et al. 1983). The strong 3C273 Lyman alpha emission line provided enough flux to record the Milky Way halo absorption, although four 13 hour high dispersion exposures were required. Similar measurements for Mrk 509 (York et al. 1984) have revealed Lyman alpha and C IV absorption systems at z = 0.033297 and 0.034464. These systems are very close to the redshift of the Seyfert nucleus of Mrk 509. The two absorption systems are probably associated with the galaxy. These measurements of faint extragalactic sources with the 0.4 m IUE telescope suggest that the increased spectroscopic capabilities of the Space Telescope will greatly expand our knowledge of the highly ionized gas in and around external galaxies.

TABLE 1

VARIOUS HIGHLY IONIZED INTERSTELLAR SPECIES

SPECIES	λ(Å)	f	IP_{X-1} (eV)	IP_X (eV)	$[n(tot)/n(H)]_\odot$[a]	T_{max}[b] (K)	Sensitivity[c]	POSSIBLE ORIGINS[d]
C IV	1550.762	0.097	47.9	64.5	4.7×10^{-4}	1.0×10^{5}	1.6×10^{-5}	A B C D E F G H
C IV	1548.188	0.194					3.2×10^{-5}	
Si IV	1402.770	0.262	33.5	45.1	3.5×10^{-5}	0.6×10^{5}	2.4×10^{-6}	A B C D E F G H
Si IV	1393.755	0.528					4.8×10^{-6}	
N V	1242.796	0.0757	77.5	97.9	9.8×10^{-5}	1.8×10^{5}	1.6×10^{-6}	B C D E F G H
N V	1238.808	0.152					3.3×10^{-6}	
S IV	1062.672	0.0377	35.0	47.3	1.6×10^{-5}	1.3×10^{5}	3.5×10^{-7}	A B C D E F G H
O VI	1037.627	0.0648	113.9	138.1	8.3×10^{-4}	3.0×10^{5}	1.2×10^{-5}	B C D E F G H
O VI	1031.945	0.130					2.4×10^{-5}	
S VI	944.517	0.210	72.5	88.0	1.6×10^{-5}	2.0×10^{5}	4.0×10^{-7}	B C D E F G H
S VI	933.382	0.426					8.2×10^{-7}	

a) Solar CNO abundances from Lambert (1978), Si and S are from Withbroe (1971). These reference abundances may not be valid for particular lines of sight because of: i) galactic abundance gradients, ii) greater gas phase depletion of certain species such as Si, iii) anomalous abundances in certain interstellar regions such as the halo.

b) T_{max} lists the temperature at which a particular ion reaches maximum abundance assuming conditions of electron collisional ionization balanced by electronic and dielectronic recombination (from Shull and van Steenberg 1982). For Si IV the effects of charge exchange are included according to the calculations of Baliunas and Butler (1980).

c) The quantity listed is the product, $f[n(tot)/n(H)]_\odot [n(ion)/n(tot)] T_{max}$. This is a measure of the sensitivity of a particular line to collisionially ionized gas assuming solar abundances and a uniform distribution of gas temperatures.

d) A number of ionization mechanisms may be responsible for the various species. Some discussed in the literature include:

A) Ultraviolet photoionization by normal population I stars with $50{,}000 \geq T \geq 30{,}000$ K (see Black et al. 1980 and Cowie, Taylor and York 1981).

B) Ultraviolet photoionization by hot white dwarfs (Dupree and Raymond 1983) and the central stars of planetary nebulae.

C) Photoionization by stellar x-ray sources (McCray, Wright and Hatchett 1977).

D) Photoionization by the EUV extragalactic background (Hartquist, Pettini and Tallant 1984; Chevalier and Fransson 1984).

E) Time dependent collisional ionization in the evaporative surfaces of clouds in a hot interstellar medium (McKee and Cowie 1977).

F) Equilibrium collisional ionization (Shapiro and Moore 1976; Shull and van Steenberg 1982).

G) Non-equilibrium collisional ionization (Shapiro and Moore 1976).

H) Collisional ionization in the interface between wind shocked circumstellar bubbles and the cooler surrounding interstellar medium. (Castor, McCray and Weaver 1975; Weaver et al. 1977).

REFERENCES

Abt, H.A., Landolt, A.U., Levy, S.G., and Mochnacki, S. 1976, A.J., 81, 541.
Baliunas, S.L., and Butler, S.E. 1980, Ap.J.(Letters), 235, L45.
Black, J.H., Dupree, A.K., Hartmann, L.W., and Raymond, J.C. 1980, Ap.J., 239, 502.
Bregman, J.N. 1980, Ap.J., 236, 577.
Bruhweiler, F.C., and Kondo, Y. 1981, Ap.J.(Letters), 248, L123.
Bruhweiler, F.C., Kondo, Y., and McCluskey, G.E.R. 1979, Ap.J.(Letters), 229, L39.
Bruhweiler, F.C., Kondo, Y., and McCluskey, G.E.R. 1980, Ap.J., 237, 19.
Castor, J., McCray, R., and Weaver, R. 1975, Ap.J.(Letters), 200, L107.
Chevalier, R.A. and Fransson, C. 1984, Ap.J., (in press).
Cowie, L.L., Hu, E.M., Taylor, W., and York, D.G. 1981, Ap.J., 250, L25.
Cowie, L.L., Taylor, W., and York, D.G. 1981, Ap.J., 248, 528.
deBoer, K.S. 1984 in IAU Symposium No. 108, Structure and Evolution of the Magellanic Clouds, eds. S. van den Bergh and K.S. deBoer (Dordrecht: D. Reidel Pub. Co.), p. 375.
deBoer, K.S., Koornneef, J., and Savage, B.D. 1980, Ap.J., 236, 769.
deBoer, K.S., and Nash, A.G. 1982, Ap.J., 255, 447.
deBoer, K.S., and Savage, B.D. 1980, Ap.J., 238, 86.
deBoer, K.S., and Savage, B.D. 1983, Ap.J., 265, 210.
Dufour, R.J., Shields, G.A., and Talbot, R.J. 1982, Ap.J., 252, 461.
Dupree, A.K., et al. 1978, Nature, 275, 400.
Dupree, A.K., et al. 1980, Ap.J., 238, 969.
Dupree, A.K., and Raymond, J.C. 1982, Ap.J.(Letters), 263, L63.
Dupree, A.K., and Raymond, J.C. 1983, Ap.J.(Letters), 275, L71.
Feitzinger, J.V., and Schmidt-Kaler, Th. 1982, Ap.J., 256, 587.
Fitzpatrick, E.L. 1984a, Ph.D.Thesis (University of Wisconsin).
Fitzpatrick, E.L. 1984b, Ap.J., (in press).
Fitzpatrick, E.L., and Savage, B.D. 1983, Ap.J., 267, 93.
Fitzpatrick, E.L., and Savage, B.D. 1984, "High Ionization Stage Gas Associated with the SMC", (this volume).
Franco, J., and Savage, B.D. 1982, Ap.J., 255, 541.
Hartquist, T.W., Pettini, M., and Tallant, A. 1984, Ap.J., (in press).
Hobbs, L.M., York, D.G., and Oegerle, W. 1982, Ap.J.(Letters), 252, L21.
Hummer, D.G., and Mihalas, D. 1970, JILA Report No. 101, (Boulder: University of Colorado).
Jenkins, E.B. 1978a, Ap.J., 219, 845.
Jenkins, E.B. 1978b, Ap.J., 220, 107.
Jenkins, E.B. 1981, in The Universe at Ultraviolet Wavelengths, ed. R.D. Chapman, (Greenbelt: NASA CP2171) p. 541.
Jenkins, E.B., Silk, J., and Wallerstein, G. 1976, Ap.J.Suppl., 32, 681.
Jenkins, E.B., Wallerstein, G., and Silk, J. 1984, Ap.J.Suppl., (in press).
Kurucz, R. 1979, Ap.J.Suppl., 40, 1.
Kudritzki, R.P. 1980, Astron.Ap., 85, 174.
Lambert, D.L. 1978, M.N.R.A.S., 182, 249.
Laurent, C., Paul, J.A., and Pettini, M. 1982, Ap.J., 260, 163.
Malina, R.F., Basri, G., and Bowyer, S. 1981, Bull.A.A.S., 13, 873.
McCammon, D. 1981, in Phases of the Interstellar Medium, ed. J.M. Dickey (Green Bank: NRAO Publications Division), p. 135.

McCammon, D., Burrows, D.N., Sanders, W.T., and Kraushaar, W.L. 1983, Ap.J., 269, 107.
McCray, R., and Snow, T.P. 1979, Ann.Rev.Astron.Ap., 17, 213.
McCray, R., Wright, C., and Hatchett, S. 1977, Ap.J.(Letters), 211, L29.
McKee, C.F., and Cowie, L.L. 1977, Ap.J., 215, 213.
McKee, C.F., and Hollenbach, D.J. 1980, Ann.Rev.Astron.Ap., 18, 219.
Pettini, M., and West, K.A. 1982, Ap.J., 260, 561.
Phillips, A.P., and Gondhalekar, P.M. 1981, M.N.R.A.S., 196, 533.
Phillips, A.P., Gondhalekar, P.M., and Pettini, M. 1982, M.N.R.A.S., 200, 687.
Phillips, A.P., Welsh, B.Y., and Pettini, M. 1984, M.N.R.A.S., 206, 55.
Prevot, L., et al. 1980, Astr.Ap., 90, L13.
Raymond, J.C. 1983, Adv.Space.Res., 2, 67.
Reilman, R.F., and Manson, S.T. 1979, Ap.J.Suppl., 40, 815.
Rogerson, J.B., et al. 1973, Ap.J.(Letters), 181, L110.
Sahade, J., and Hernandez, C.A. 1982, (preprint).
Sahade, J., Kondo, Y., and McCluskey, G.E. 1984, Ap.J., 276, 281.
Savage, B.D., and deBoer, K.S. 1979, Ap.J.(Letters), 230, L77.
Savage, B.D., and deBoer, K.S. 1981, Ap.J., 243, 460.
Savage, B.D., Fitzpatrick, E.L., Cassinelli, J.P., and Ebbets, D.C. 1983, Ap.J., 273, 597.
Savage, B.D., and Mathis, J.S. 1978, Ann.Rev.Astron.Ap., 17, 73.
Schwartz, D.A. 1979 in X-Ray Astronomy, Proc. of the 21st COSPAR Symposium, ed. W.A. Baity and L.E. Peterson (Oxford: Pergamon Press), p. 453.
Shapiro, P.R., and Field, G.B. 1976, Ap.J., 205, 762.
Shapiro, P.R., and Moore, R.T. 1976, Ap.J., 207, 460.
Sherman, R.D. 1980, Ap.J., 240, 737.
Shull, J.M., and Van Steenberg, M. 1982, Ap.J.Suppl., 48, 95.
Smith, L.J., Willis, A.J., and Wilson, R. 1980, M.N.R.A.S., 191, 339.
Spitzer, L. Jr. 1956, Ap.J., 124, 20.
Sion, E.M., and Guinan, E.F. 1983, Ap.J.(Letters), 265, L87.
Walborn, N.R., Heckathorn, J.N., and Hesser, J. 1984, Ap.J., 276, 524.
Weaver, R., McCray, R., Castor, J., Shapiro, P., and Moore, R. 1977, Ap.J., 218, 377.
Welsh, B.Y. 1983, M.N.R.A.S., 204, 1203.
Welsh, B.Y., and Thomas, C.K. 1982, M.N.R.A.S., 199, 385.
Welsh, B.Y., and Thomas, C.K. 1983, Astrophys.Lett., 23, 103.
Withbroe, G.D., The Menzel Symposium: NBS Spec. Pub. No. 353, ed. K.B. Gebbie (Washington: Government Printing Office).
York, D.G. 1977, Ap.J., 213, 43.
York, D.G., Wu, C.C., Ratcliff, S., Blades, J.C., Cowie, L.L., and Morton, D.C. 1983, Ap.J., 274, 136.
York, D.G., Ratcliff, S., Blades, J.C., Cowie, L.L., Morton, D.C., and Wu, C.C. 1984, Ap.J., 276, 92.

HOT STARS: SIX YEARS OF PROGRESS

Catharine D. Garmany
Department of Astrophysical, Planetary and Atmospheric Sciences, University of Colorado, and Joint Institute for Laboratory Astrophysics, University of Colorado and National Bureau of Standards, Boulder, Colorado 80309

ABSTRACT

Mass loss is known to take place across the H-R diagram, but nowhere is it more pronounced than in the upper left hand corner of that figure. Here, winds from luminous stars peel away a solar mass in a million years or less. The winds of the Of, OB supergiants, and W-R stars have received the most attention because they are so readily studied. Their effect on stellar evolution is significant also. On the other hand, it is the B stars whose variability has been most thoroughly studied with IUE, undoubtedly because historically these stars have been known to vary. This review will concentrate on the current state of our observational understanding of stellar winds, with particular emphasis on how the observations fit various theoretical predictions.

INTRODUCTION

Early rocket observations of hot stars revealed the presence of high ionization stages such as O VI and N V, which are not expected in radiative equilibrium in O and B stars as they require temperatures greater than 10^5 K, compared with photospheric temperatures of 30,000 to 50,000 K. Furthermore, the blue edges of P Cygni profiles revealed terminal velocities greatly in excess of the stellar escape velocity, indicating mass loss (Morton 1967). Thus began the era of stellar winds in hot stars. IUE allows us to observe ultraviolet resonance lines of ions such as C IV, N V and Si IV and these lines are almost always seen as P Cygni profiles. Figure 1 shows the spectrum of an O star from 1000 to 8000 Å, obtained by combining low dispersion IUE data with KPNO IRS data. The P Cygni profile shape depends mainly on the mass loss rate, the velocity of the material as a function of radius, and the change in ionization with radius. More specifically, the strength of the blueshifted absorption indicates the column density of the ion, which is more or less independent of the velocity law. The ratio of emission to absorption, on the other hand, indicates the shape of the velocity law, which more or less independent of the ion column density. The reason for this is that UV resonance lines are primarily scattering lines, so the ratio of emission to absorption depends on the distance of the absorbing material from the stellar photosphere, and hence the velocity law.

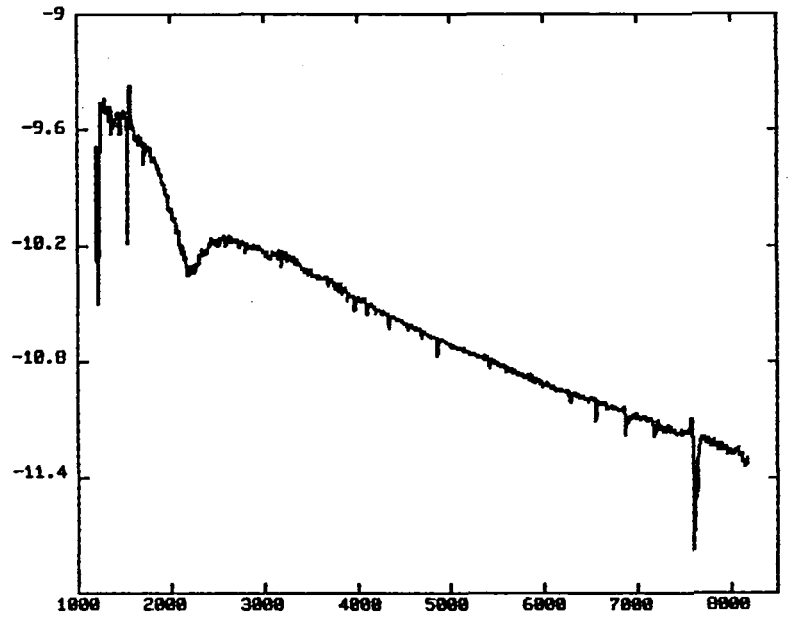

Fig. 1. The spectrum of 9 Sgr, O4V, obtained by combining an IUE low dispersion and a KPNO IRS spectrum. No correction has been made for reddening (Torres, unpublished).

The most widely accepted explanation for these winds is the line radiation pressure model, originated by Lucy and Solomon (1970) and developed further by Castor, Abbott and Klein (1975, hereafter CAK). The envelope of the star is accelerated by momentum transfer from photons to ions due to line absorption. Abbott (1982) has shown that there are sufficient lines in the UV near flux maximum to drive the wind. There are, as would be expected from an initial theory, problems to be addressed. One of the earliest was the source of the anomalously high ionization stages of O VI and N V observed in these stars. Therefore, Cassinelli and Olson (1979) proposed a "corona + cool wind" model, postulating X-rays from the base of the corona as a source of this superionization via the Auger effect. The Einstein satellite observations (Harnden et al. 1979) of X-rays from almost all early stars provided a qualitative confirmation.

A different approach was taken by Lamers and Morton (1976) who proposed that, in addition to line radiation pressure, mechanical energy from the photosphere heats the gas to the required 2×10^5 K in OB stars and produces O VI by collisional ionization. Underhill (1983) has proposed an alternative theory in which the stellar winds are generated in the "mantle," which she describes a low density region and a high density region in suspended magnetic loops of very hot gas which corotate with the star.

MASS LOSS RATES

Line profile models have been computed by Castor and Lamers (1979), and modifications provided by Olson (1981) for excited lines. Although fitting the profiles to the data does not presuppose the mechanism for accelerating and driving the wind, the ionization fraction assumed for the mass loss determination does. This is still an area of some controversy. As luck would

have it, we seldom observe the dominant stage of ionization in the winds of early stars, which are N IV, Si V and C V (Olson and Castor 1981). To compute the ionization balance, it is necessary to observe two lines on different sides of the dominant ion, such as N V and C IV. Olson and Castor find that the wind temperature is about the same for all O stars, implying that the fraction of N V is relatively constant also. On the other hand, Lamers and Snow (1978) calculate the ionization balance for N V and find enormous changes with temperature. This leads to a rather different regime in which the P Cyg lines can be used as mass loss predictors.

Ideally, one would like to compare mass loss determinations from different methods to resolve this issue. This is not easily done, however. Radio observations of free-free emission are the most model independent, depending only on the stellar distance and its flux (Wright and Barlow 1975). They can only be used for stars with the highest mass loss rates, which are generally those with saturated absorption profiles in the UV. Infrared observations of continuum free-free emission have been tried, but recent work by Castor and Simon (1983) and Abbott, Telesco and Wolff (1984) have shown that this method is unreliable. The problem lies in the assumed velocity law, which they find varies greatly from star to star.

There are two basic approaches to understanding the mechanism behind the mass loss. One is to correlate the rates with stellar characteristics such as luminosity, mass, radius, surface gravity, and rotation; the other is to study the wind structure. The underlying question is whether the winds are determined by fundamental stellar parameters or by surface phenomena. Any attempt to correlate mass loss with other stellar parameters requires careful attention to the accuracy of all the parameters involved. The earliest results showed a strong dependence on luminosity, as predicted by the radiation driven wind theory. As more data have accumulated, a variety of studies have explored additional dependences. At present, UV mass loss rates are available for about 100 O and B stars, radio rates for about 15, and IR observations for about 75 stars. This is an important advance over 5 years ago, when the numbers were about a factor of 10 smaller.

Table 1 compares some of the different dependences on mass loss, both theoretical and empirical. In a comprehensive review of the theory of line driven winds, Abbott (1982) has predicted the dependence of mass loss on luminosity, mass, temperature, and metallicity. One of the first quantitative studies of mass loss as a function of more than luminosity alone was by Lamers (1981) who scaled rates from UV, Hα and IR to radio rates. This gave a reasonable range in mass and radius, but questions have been raised about the IR rates. Lamers tried two approaches: mass loss controlled by the star's internal structure vs. mass loss as a surface phenomena; but he could find no clear indication that one was to be preferred over the other. Garmany and Conti (1984) have used a more homogeneous set of data than Lamers, and found no clear improvement from additional parameters, although they note the possibility of an empirical parameterization including the ratio of terminal to escape velocity. This is an area of tantalizing uncertainty: although second-order dependences seem to be present, the errors are large.

Table 1: Mass Loss Parameterization Coefficients

Luminosity	Radius	Mass	$M(1-\Gamma)$	$R/M(1-\Gamma)$	v_∞/v_{esc}	Metal.	Ref.
1.98			-1.03			0.94	1
1.5	2.25	-2.25					2
1.4±0.4	0.6±.1	-1.0±1.0					3
1.7±0.1				0.7±0.1			4
1.6±0.2							5
1.3±0.2					1.2±0.5		5
1.0±0.8	0.8±0.6	0.6±1.2					5

1: Abbott (1982); 2: Andriesse (1979); 3: Lamers (1981); 4: Chiosi and Olson (1984); 5: Garmany and Conti (1984).

An important independent step toward resolving the basic question of how the UV (or wind) spectra are related to fundamental stellar parameters is Walborn's classification of UV spectra (Walborn and Panek 1984b) The large body of IUE data enabled them to select 120 O and early B stars with accurate optical spectral classification and address the question: to what degree do the UV spectra correlate with their optical spectral type? They conclude that both photospheric lines, mainly Fe V and Fe IV, and wind lines, N V and C IV, are very well correlated with the optical spectral type. The implication here is that stellar wind is governed by fundamental stellar parameters.

A very interesting luminosity dependence of the Si IV profile has also been discussed by Walborn and Panek (1984a). They point out that the P Cyg profile of λ1393, 1402 develops from a pure photospheric profile in the main sequence stars to a strong wind profile in the supergiants (see Fig. 2). This has important implications both as a classification criterion and as an astrophysical problem. While C IV and N V are mostly indicative of the wind temperature, Si IV, with an ionization potential near the He II edge, is much more sensitive to the photospheric radiation field. Since there is no way to compute its ionization fraction, it cannot be used to measure mass loss as are other resonance lines. It is interesting to note that the strength of this profile is related to the surface area mass loss. In Fig. 2, the mass loss per unit area for the O6.5I star is three times that of the O6.5V star.

Winds in the Magellanic Clouds

With IUE it is an easy matter to obtain low dispersion spectra of O and luminous B stars in the Magellanic Clouds. With their lower metallicity, the Clouds offer an excellent contrast with galactic stars. If winds in the Clouds are due to radiation pressure, rates of mass loss should be smaller because CNO abundances are lower, and at least among the O stars, these are the driving lines (Abbott 1982). Alternatively, if mass loss is driven by other mechanisms but accelerated by radiation pressure, we expect the same mass loss rates but smaller wind velocities. Hutchings (1982) has discussed some of the most luminous stars in the LMC and SMC and concluded that their

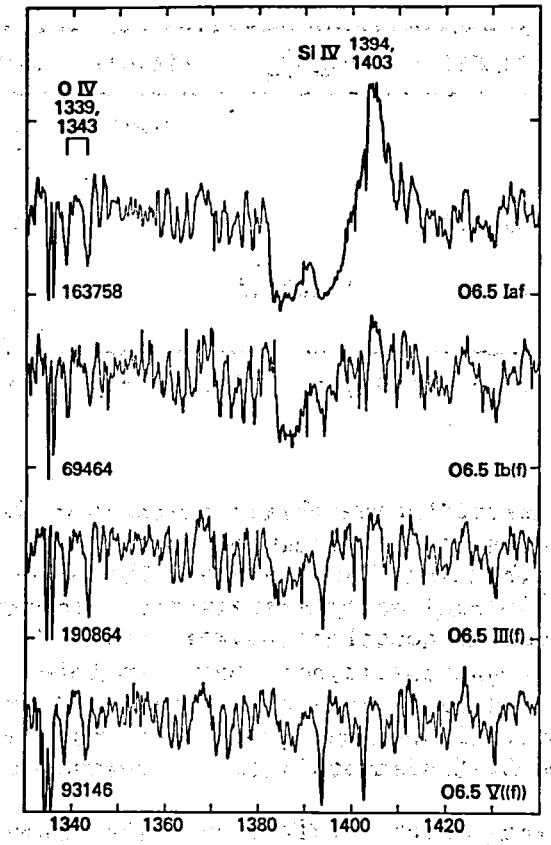

Fig. 2. The development of the Si IV P Cygni profile with luminosity (Walborn and Panek).

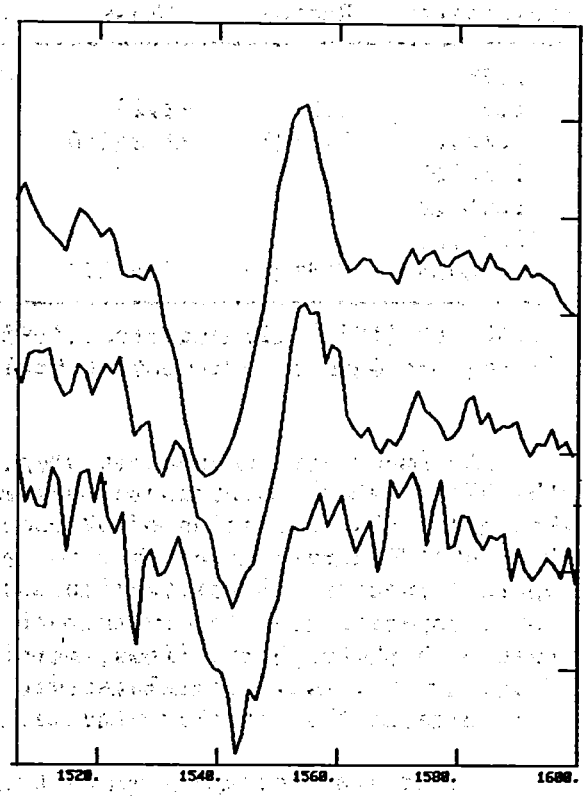

Fig. 3. The C IV line in three O7 III stars. Top: HD 151515 (Galactic), middle: SK-67°38 (LMC), bottom: AV296 (SMC).

wind velocities are lower than in corresponding galactic stars. A similar effect in the SMC alone has been noted by Bruhweiler, Parsons and Wray (1982). One prime difficulty in such studies is the lack of good spectral types for "normal" early stars in the Magellanic Clouds. As a result, many of the stars obsrved with IUE have been classified on the basis of their photometry.

Conti, Massey and I have a program to determine the initial mass function of the O stars in the Clouds, and we are observing O and B stars at classification dispersion with the 4-meter telescope at CTIO. I have observed a number of these stars with IUE and have several preliminary conclusions. The first is that photometry as a means of classifying O stars is not very reliable. An example of this can be seen in Bruhweiler et al., where photometric classification led to the comparison of a galactic O6 star with a Be star, or an O9Ia with a B3I. When we examine spectroscopically similar types, the terminal velocities do not differ very much (Fig. 3). Determining actual mass loss rates is not as straightforward. The modeling techniques used with high dispersion cannot be used on low dispersion spectra, so we must resort to other less accurate mass loss indices, such as the absorption equivalent width suggested by Snow (1979) or the first moment of the profile (Castor, Lutz and Seaton 1981). Comparing these techniques with mass loss determinations from

high dispersion spectra for the same stars shows that the simple method rapidly breaks down as the line approaches saturation. Nevertheless, we can compare the galactic, LMC and SMC stars with low mass loss rates. It appears that there is not much difference between these stars, an unexpected conclusion which we do not yet understand.

WIND STRUCTURE

The study of the structure of the stellar winds is another approach to understanding the mechanism of mass loss. This includes the velocity law, the detection of X-rays from these stars, variability in the wind profiles, and the curious absorption components seen in the wind lines. Many of these observations suggest instabilities in the wind which any theory must explain.

Wind acceleration

The wind terminal velocity, which is easily measured from the shortward edge of the strong wind lines, ranges from 1 to 3 times the stellar escape velocity. Figure 4 shows the ratio of terminal to escape velocity as a function of spectral type, taken from Cassinelli and MacGregor (1983) with additional data from Garmany et al. (1981), and Garmany and Conti (1984). The evolutionary stage of the star is indicated, and it appears that this ratio evolves with the star. Note a selection effect: later than O9 the terminal velocity is not measurable from the P Cygni profile in main sequence and giant stars. The wind theory predicts a relation between the terminal and escape velocity of the form:

$$V_\infty = \left(\frac{\alpha}{1-\alpha}\right)^{1/2} V_{esc} \quad .$$

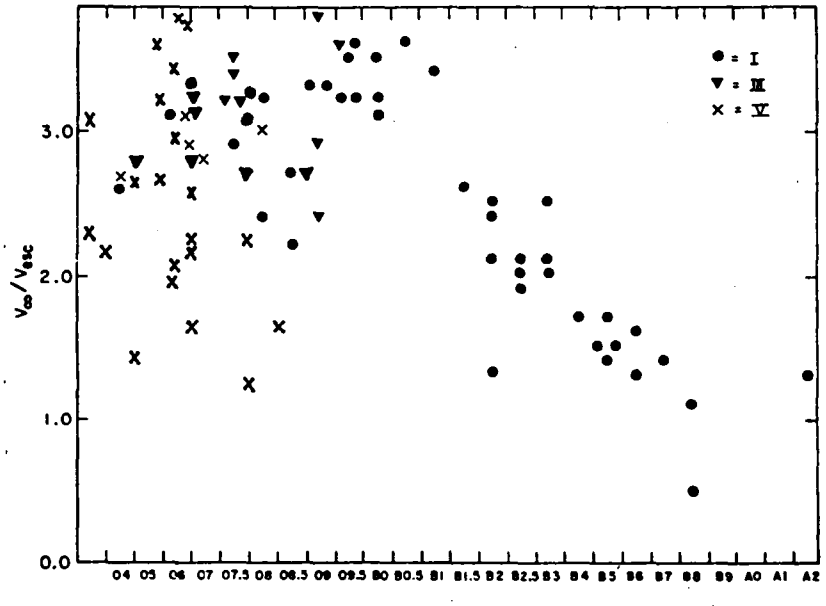

Fig. 4. The ratio of terminal to escape velocity for early type stars of different luminosity classes (adapted from Cassinelli and MacGregor).

The value of α is calculated from the relative contribution of optically thick and thin lines. Abbott (1982) found α to be constant over a broad temperature range and therefore predicted that the winds of OBA stars should conform to a relation $V_\infty = (1.0 - 1.5)\ V_{esc}$. To explain the discrepancy, especially for early O stars, Panagia and Macchetto (1981) have derived a multiphoton scattering model in which $V_\infty \propto T_{eff}^2$. Single photon scattering is sufficient for B supergiants, but multiple scattering is required to explain the observed V_∞ in O supergiants. A more complete calculation has been done by Friend and Castor (1983), who consider randomly spaced overlapping lines and conclude that the terminal velocity is much larger than in the CAK model.

Additional evidence for an evolution of the stellar wind has been found by Abbott, Bohlin and Savage (1982) who pointed out that the ratio of emission to absorption equivalent widths are a factor of 2 smaller in main sequence than in supergiant stars. This indicates a change in the shape of the velocity law in the sense that the material is farther from the star in supergiants than in main sequence stars. A changing velocity law is probably responsible for past inconsistencies between IR mass loss determinations and other methods, since the IR rates are sensitive to the assumed law. The type of velocity law that has been found to fit UV and optical line profiles as well as the IR excess is one of the form:

$$V(r) = V_\infty(1-R_*/r)^\beta$$

where β is generally assumed to be between 0.5 and 2.0. Abbott, Telesco and Wolff (1984) have investigated the problem for stars with both IR and radio observations. They see a trend for the velocity law to become more gradual (β increases) as the temperature decreases, although in their data, this could as easily represent gravity decreasing.

X-rays

That X-rays would be observed coming from O and B stars was predicted by Cassinelli and Olson (1979), who had postulated their existance to explain the anomalously high ionization stages of O and N in terms of Auger ionization. In their model, the X-rays were produced at the base of the corona and the predicted spectrum included little flux below 1 keV. Einstein IPC observations (Cassinelli et al. 1981) confirmed that O and luminous early B stars are X-ray emitters, but there exists significant flux below 1 keV. A number of explanations have been put forth. Most recently, Lucy (1982) has proposed that the X-rays are produced by shocks throughout the wind which result from instabilities in the radiation-driven wind. Cassinelli and Swank (1983) have used the Einstein SSS to make X-ray observations of the belt stars of Orion which fit Lucy's model with X-rays produced by radiation driven shocks. Lucy's theory is attractive because it also explains the broad, deep absorption troughs observed in saturated P Cygni profiles, but not in the atlas of theoretical line profiles computed by Castor and Lamers (1979). In addition, it offers a possible explanation for the narrow absorption components often seen in the wind lines, and discussed in the next section.

Based on the observation of superionized lines of C IV and Si IV in B supergiants, Odegard and Cassinelli (1982) predict that these stars should show considerable X-ray flux, with $L_x/L_{bol} \sim 10^{-8.5}$.

Line Structure and Variability

It was first pointed out by Snow and Morton (1976) from a survey of Copernicus data that the wind lines often show structure. Variously called "narrow components," "shell absorption features," "shell components," and "narrow lines" by different authors, the problem with nomenclature seems to reflect the problem in interpretation. Lamers, Gathier and Snow (1982) have described them more fully: typically they have widths of 100 to 500 km s^{-1}, small compared to the terminal velocity of -1000 to -3000 km s^{-1} of the parent star (see Fig. 5). About 2/3 of the stars in the Lamers et al. sample showed such lines, and about half the 53 stars in a study by Abbott, Bohlin and Savage (1982) had them. Since in most cases there are a small number of observations per star, it is not clear whether a certain percent of the stars show this feature, or whether all stars show these lines a certain percent of the time.

Many types of variability have been reported in early-type stars, and we do not understand how the observations are related. Historically, the Be stars are best known for showing variations in their hydrogen line profiles, although Barker (1983) notes that in a monitoring program, most did not show changes. Perhaps the best known Be star, γ Cas, has been shown by Henrichs et al. (1983) to show narrow components in 2/3 of his 28 IUE spectra. He has proposed that the narrow components represent a time dependent effect of episodic mass loss which is present in all early-type stars. Peters (1982) has also reported variations of this type in other Be stars. Such studies have only been done in a limited way for O stars. The main difference between the O and B stars seems to be that in O stars, the narrow components,

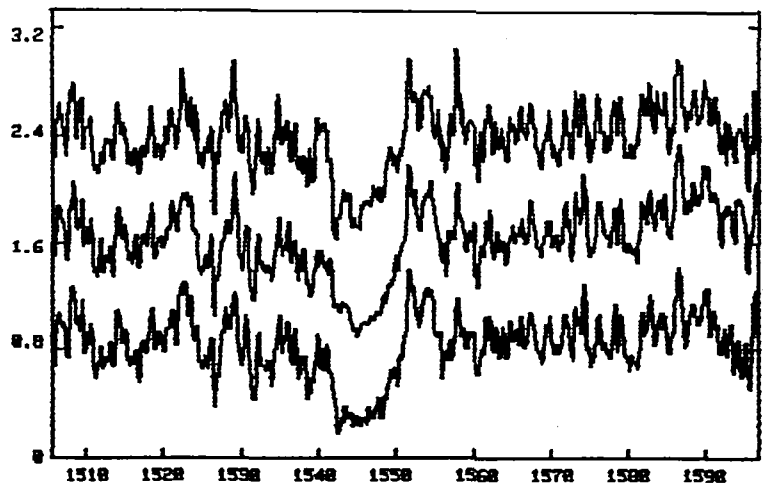

Fig. 5. IUE archive spectra of Zeta Per, B1 Ib, which shows narrow components in C IV whose strength varies with time.

while varying in strength, are fixed in velocity. Variations in the entire P Cygni profile have been observed in some O stars (Grady, Snow and Timothy 1983). Although no short-term variability was found during simultaneous UV and X-ray observations of two OB supergiants by Cassinelli et al. (1983), Snow, Cash and Grady (1981) noted long-term X-ray flux changes in a few stars. In the radio region, Abbott, Bieging and Churchwell (1981) found changes within a timescale of months.

CONCLUSION

Our knowledge of the physics of stellar winds has grown tremendously since the launch of IUE, and we are still far from exploiting the potential of the archival material. The observations have provided food for theoreticians, and although progress has been made, more work is needed.

There is at present no comprehensive theory to explain profile variability. Should we expect the same processes to be at work in an O star and a Be star? Doazan (1982) has discussed evidence for Be stars representing a phase in the life of a B star, so perhaps we should look for a similar phase in O stars. An area in which data are woefully lacking is simultaneous observations in different spectral regions. These would help to define the nature of the profile variations: for example, Gry, Lamers and Vidal-Madjar (1984) predicts Hα variations corresponding to the changes they observed in the narrow components of the Lyman lines if it represents non-symmetric mass loss. Another test would be more simultaneous UV and X-ray observations: if the X-rays are produced at the base of the wind, then X-ray variation should correspond to changes in the absorption profile, while shocks in the outer part of the wind should affect the high velocity part of the profile, including the narrow components (Lucy 1982).

Refinements in the techniques for computing mass loss would allow unambiguous comparisons with the parameterizations predicted by theory. This will require more sensitive profile modeling, as well as a better understanding of the star's fundamental parameters. The potential information from IUE observations of hot stars in the Magellanic Clouds and other galaxies is tremendous. The exposure times with the 0.5-m IUE telescope are comparable to visual observations with a 4-m ground-based telescope, and we are now moving away from studying stars or galaxies, to stars in galaxies.

This work was supported by NASA grant NAG5-78 through the University of Colorado. I would like to thank Drs. D. Abbott and G. Olson for stimulating conversations and clarifications.

REFERENCES

Abbott, D. C. 1982, Ap. J., 259, 282.
Abbott, D. C, Bieging, J. H., and Churchwell, E. 1981, Ap. J., 250, 645.
Abbott, D. C., Bohlin, R. C., and Savage, B. D. 1982, Ap. J. Suppl., 48, 369.
Abbott, D. C., Telesco, C. M., and Wolff, S. C. 1984, Ap. J., in press.

Andriesse, C.D. 1979, Astrophys. Space Sci., 61, 205.
Barker, P. 1983, Pub. A. S. P., 95, 996.
Bruhweiler, F. C., Parsons, S. B., and Wray, J. D. 1982, Ap. J. (Letters), 256, L49.
Cassinelli, J. P., Hartmann, L., Sanders, W. T., Dupree, A. K., and Myers, R. V. 1983, Ap. J., 268, 205.
Cassinelli, J. P., and MacGregor, K. B. 1984, Physics of the Sun, eds. P. A. Sturrock, D. M. Mihalas, T. Holzer, and R. Ulrich, in press.
Cassinelli, J. P., and Olson, G. L. 1979, Ap. J., 229, 304.
Cassinelli, J. P., and Swank, J. H. 1983, Ap. J., 271, 681.
Cassinelli, J. P., Waldron, W. L., Sanders, W. T., Harnden, F. R., Rosner, R., and Vaiana, G. S. 1981, Ap. J., 250, 677.
Castor, J. I., Abbott, D. C., and Klein, R. K. 1975, Ap. J., 195, 157.
Castor, J. I., and Lamers, H. J. G. L. M. 1979, Ap. J. Suppl., 39, 481.
Castor, J. I., Lutz, J. H., and Seaton, M. J. 1981, M.N.R.A.S., 194, 547.
Castor, J. I., and Simon, T. 1983, Ap. J., 265, 304.
Chiosi, C., and Olson, G. L. 1984, unpublished.
Doazan, V. 1982, "B stars with and without emission lines," NASA Monograph Series, p. 285.
Friend, D. B., and Castor, J. I. 1983, Ap. J., 272, 259.
Garmany, C. D., and Conti, P. S. 1984, Ap. J., in press.
Garmany, C. D., Olson, G. L., Conti, P. S., and Vansteenberg, M. E. 1981, Ap. J., 250, 660.
Grady, C., Snow, T. P., and Timothy, G. 1983, Ap. J., 271, 691.
Gry, C., Lamers, H.J.G.L.M., and Vidal-Madjar, A. 1984, Astr. Ap., in press.
Harnden, F. R., et al. 1979, Ap. J. (Letters), 234, L51.
Henrichs, H. F., Hammerschlag-Hensberge, G., Howarth, I. D., and Barr, P. 1983, Ap. J., 268, 807.
Hutchings, J. B. 1982, Ap. J., 255, 70.
Lamers, H.J.G.L.M. 1981, Ap. J., 245, 593.
Lamers, H.J.G.L.M., Gathier, R., and Snow, T. P. 1982, Ap. J., 258, 186.
Lamers, H.J.G.L.M., and Morton, D. 1976, Ap. J. Suppl., 32, 715.
Lamers, H.J.G.L.M., and Snow, T. P. 1978, Ap. J., 219, 504.
Lucy, L. B. 1982, Ap. J., 274, 372.
Lucy, L. B., and Solomon, P. 1970, Ap. J., 159, 879.
Morton, D. 1967, Ap. J., 147, 1017.
Odegard, N., and Cassinelli, J. P. 1982, Ap. J., 256, 568.
Olson, G. L. 1981, Ap. J., 245, 1054.
Olson, G. L., and Castor, J. I. 1981, Ap. J., 244, 179.
Panagia, N., and Macchetto, F. 1981, in IAU Colloquium 59, Effects of Mass Loss on Stellar Evolution, ed. C. Chiosi and R. Stalio (Dordrecht: Reidel), p. 173.
Peters, G. J. 1982, in IUE Symposium, Advances in Astronomy, p. 575.
Snow, T. P. 1979, Mass Loss and Evolution of O-type Stars, ed. P. S. Conti and C. W. H. de Loore (Dordrecht: Reidel), p. 65.
Snow, T. P., Cash, W., and Grady, C. A. 1981, Ap. J. (Letters), 244, L19.
Snow, T. P., and Morton, D. C. 1976, Ap. J. Suppl., 32, 429.
Underhill, A. B. 1983, Ap. J., 265, 933.
Walborn, N., and Panek, R. J. 1984a, Ap. J., in press.
Walborn, N., and Panek, R. J. 1984b, Ap. J., in press.
Wright, A. E., and Barlow, M. J. 1975, M.N.R.A.S., 170, 41.

SOLAR SYSTEM STUDIES WITH THE IUE: 1982 - 1984

John Caldwell
Earth and Space Science Department, SUNY at Stony Brook

ABSTRACT

Planetary observations with the IUE in the last two years are summarized. These include work on the atmospheres of comets and the giant planets; aurorae; rings and circumplanetary environment. Planetary requirements for future Earth-orbital astronomical observatories are also described.

INTRODUCTION

This review includes published papers in the area of planetary science since the previous IUE symposium (NASA CP 2238), as well as several works in progress. It is incremental, not cumulative. It does not represent an exhaustive literature search, but rather a sampling of the most important recent work. Additional references may be found in the papers cited.

Topics summarized below include comet IRAS - Araki - Alcock; the composition of the upper atmospheres of Saturn, Jupiter and Uranus; Saturn's rings; aurorae on Jupiter and Uranus; emissions from the low latitude, upper atmospheric region of Jupiter; and the torus which surrounds Jupiter and includes the orbit of the innermost Galilean satellite, Io.

Finally, those requirements on future space observatories that are unique to planetary studies are described briefly.

COMETS

Comet IRAS - Araki - Alcock (1983d) was the closest Earth-approaching comet of this century, coming within 0.032 AU and permitting the highest spatial resolution of any recent comet. Despite the relatively short notice of the comet's imminent arrival, the IUE observatory was sufficiently flexible to schedule it as a target of opportunity, including the period of closest approach.

This flexibility was magnificently rewarded when A'Hearn, Feldman and Schleicher (1983) discovered emissions from the S_2 molecule near the cometary nucleus. They found more than 10 bands of the B - X system between 2800 and 3100 A. This was the first observation of that molecule in any astronomical object. The discovery was a direct consequence of the very high spatial resolution. In other, more distant comets, the S_2 emitting region would be too small to be observed by the IUE. The derived emission scale length was only 450 km, implying that the S_2 originated in the nucleus itself. Other species observed in this comet, CS and OH, are thought to be dissociation products of coma molecules (CS_2 and H_2O, respectively) and have much larger scale lengths, typically 10^5 km.

The most important question regarding this molecule is whether it is primordial or recently formed. A'Hearn et al. suggest that it may be the result of cosmic ray irradiation, which can penetrate the comet's nucleus and form S_2 from other sulfur-bearing molecules. They propose a test of their hypothesis: short period comets should have much less S_2 than long period ones, because the latter have sufficient time to accumulate the chemical by-products of the cosmic ray energy deposited within their volatile bulk, before these by-products are released to space during the active perihelion phase.

ATMOSPHERIC COMPOSITION OF SATURN, JUPITER AND URANUS

Winkelstein et al. (1983) have modelled the reflectivity of Saturn from 1500 to 3000 A. They agree with the abundances and vertical distributions of C_2H_2 and C_2H_6 derived from Voyager infrared observations, but not with the PH_3 vertical distribution (Courtin et al., 1981). They further require an additional absorber, and suggest that H_2O provides the best fit. If so, this almost certainly requires an external source of oxygen for Saturn's upper atmosphere. Any internal H_2O should be frozen out at levels much too low to be seen in the ultraviolet, where Rayleigh scattering limits photon penetration to the upper few millibars. Saturn's rings are one potential source of oxygen, through trapped particle spattering of H_2O ice.

Wagener (unpublished) has almost completed a similar study for Jupiter. He finds that C_2H_2, C_2H_6, and NH_3 are required, and that trace amounts of other gases including PH_3, H_2O and C_3H_4 (allene) are consistent with the spectrum, although unique identification of these latter species is much more difficult.

Caldwell et al. (1984) have reviewed ultraviolet observations of Uranus and Neptune. Present data are compatible, within calibration uncertainties, with either a clear upper atmosphere on both planets or a thin haze on both. It is probable that whatever the degree of haziness is, it is very similar on both planets. Since infrared observations show clearly that ambient conditions are much different between the upper atmospheres of these two planets, Occam's razor suggests that both are clear.

Caldwell et al. (1984) further claim an apparent secular brightening of Uranus between 1980 and 1982, which is quantitatively consistent with a decrease in C_2H_2 abundance from a mixing ratio of $\sim 3 \times 10^{-8}$ to near zero over that period. However, there is no compelling spectroscopic identification of C_2H_2, because the abundance is certainly small and because the signal to noise ratio is only moderate.

SATURN'S RINGS

Caldwell and Wagener (unpublished) have merged a large number of SWP and LWR spectra to demonstrate that Saturn's rings have a rather flat, low reflectivity (~ 0.02) from 3000 A to 1700 A. The large number of spectra, with a wide range of exposure times, was necessary because of the limited dynamic range of the IUE and the strong decrease in absolute signal level below 3000 A for all objects shining by reflected sunlight.

There is a suggestion of a decrease in reflectivity at 1700 A, which would be expected for H_2O ice and which could contain information on the ring particle size distribution. 1700 A does not represent the absolute limit of IUE sensitivity, because the longest SWP exposure in the series was only 75 minutes. However, the falling Solar flux at shorter wavelengths precludes extension of IUE results much farther.

Holberg (unpublished) has stated that ring reflectivity data from the Voyager UVS instrument show that the reflectivity is also low and flat in the range of that instrument's sensitivity, 600 - 1700 A. This nicely complements the available IUE data, and calls into question the suggestion that the reflectivity may be decreasing right at 1700 A.

Clearly there is potential for learning about the physical characteristics of Saturn's ring particles from such data. Further IUE observations to establish an area of spectral overlap with Voyager would be most useful, and are well within the IUE capability.

AURORAE ON JUPITER AND URANUS

The existence of auroral phenomena on Jupiter has been known for many years. Current research activity in this area consists of monitoring various aspects of the emission in great detail. Skinner et al. (1984) have summarized their latest observations of H I Ly α (1216 A) and H_2 Lyman - and Werner-bands (1600 A). They find that the northern emission is confined within longitudes 120° and 240°, which includes the northern magnetic pole. They cannot differentiate between the magnetotail auroral zone and the Io torus auroral zone as the most probable location of the emission. It is of some interest that other investigators find excess infrared emission from a similar region on Jupiter (Caldwell, Tokunaga and Orton, 1983).

An aurora on Uranus has recently been discovered independently by two investigations with the IUE (Durrance and Moos, 1982; Clarke, 1982). In each case, strong Ly α emission is detected in excess of the geocoronal and interplanetary background. The most plausible explanation is collisional excitation of hydrogen by magnetospheric particles. For example, Rayleigh scattering of Solar Ly α radiation by H_2 in Uranus can be ruled out by the absence of the Raman shifted line at 1280 A. Strong variability is associated with the Uranian aurora.

The cosmogonic significance of this discovery is that Uranus must have a magnetic field. It is now well known that Jupiter and Saturn have such fields. However, the bulk density of Uranus requires that its internal composition be significantly different from those of Jupiter and Saturn, so that it had formerly been possible to speculate that Uranus would not have a magnetic field.

UPPER ATMOSPHERIC EMISSION FROM JUPITER

Skinner et al. (1983) have monitored the brightness of Jovian Ly α emission from late 1978 to early 1982. The primary excitation mechanism is resonance scattering of solar Ly α by H I. They find enhanced emission at the

center of the disk near System III longitude 100° over the entire observation period. The observations indicate no substantial changes in Jovian H I concentration over the period, and disagree quantitatively with Voyager UVS observations.

IO TORUS

Moos et al. (1983) have obtained a high quality SWP spectrum of the Io torus, showing emission lines of S II, S III, S IV and O III. The lines include a pair at 1713.8 and 1729.2 A which have been identified as $^5S_2 - {}^3P_{2,1}$ intercombination doublet of S III. This identification was made before it was observed in the laboratory, but since has been confirmed by P. L. Smith (private communication). This transition, and the one at 1199 A, may be very useful in determining electron temperatures over a wide range in astrophysical plasmas.

FUTURE MISSIONS

As the observing schedule for the IUE moves into its seventh cycle, it is prudent to look ahead to future missions, and to pass on previous experience to those who will build the new spacecraft. Since it is infintely easier to incorporate features into a satellite during its design rather than later, and since planetary observations have their own special requirements, this review will end with a brief summary of what is desirable.

The primary need for planetary work is to be able to track moving targets. However, there is a secondary requirement that is easy to overlook. Because planets are relatively close, they have significant parallax effects. For the case of Mars at opposition, this is at least 40 arc seconds per orbit. It is therefore extremely inefficient to guide on stars for planetary work. The ability to track on the center of light of a bright, extended object like Mars, Jupiter or Saturn would be extremely useful. (Space Telescope will not have this capability, unfortunately, although OAO-A2 did in 1968!) Alternately, the ability to guide on a bright satellite and to offset to specific planetary locations would be appreciated. The offset range should be at least of order tens of arc minutes, to permit observations of whole planetary systems, including magnetospheres, tori and faint satellites. The system should be smart enough to remember that the satellites are moving with respect to the planets, at a known rate.

Venus has always been a problem because previous spacecraft designs have not included the capability to point easily within 45° of the Sun. Certainly it becomes increasingly difficult to approach the Sun, but there is no apparent physical discontinuity at 45°; 40° would be much preferable.

The maximum required tracking rate cannot be specified absolutely. The limiting class of object here is the comets. Since these are probably too diffuse for self-guiding, a different technique will be required, presumably tracking on gyros with appropriate selectable drift rates. It is noted that the maximum apparent rate for comet Halley in 1986 will be 0.2 arc seconds per record of time.

ACKNOWLEDGEMENT Planetary work at Stony Brook has been supported by NASA grants from the IUE since launch. The most important aspect of this support is the training it has provided to several graduate students, including R. Danehy, V. Moore, A. R. Rivolo, R. Wagener and P. Winkelstein. The faculty at Stony Brook who have worked on the IUE, including J. Caldwell, J. Hardorp and T. Owen, are grateful for the opportunity to combine exciting science with the educational process. All planetary scientists appreciate the dedication and enthusiasm of the IUE observatory staff when it comes to solving operational problems that we continually raise because of our perverse insistence on pursuing targets that don't just sit still.

REFERENCES

A'Hearn, M. F., Feldman, P. D., and Schleicher, D. G. (1983). The discovery of S_2 in comet IRAS - Araki - Alcock 1983d. Astropys. J. 274, L99-L103.

Caldwell, J., Tokunaga, A. T., and Orton, G. S. (1983) Further observations of 8 μm polar brightenings of Jupiter. Icarus 53, 133 - 140.

Caldwell, J., Wagener, R., Owen, T., Combes, M., and Encrenaz, Th. (1984) Ultraviolet observations of Uranus and Neptune below 3000 A. NASA CP 0000, in press.

Clarke, J. T. (1982). Detection of variable H Ly α emission from Uranus. Astrophys. J. 299, L105 - L109.

Durrance, S. T. and Moos, H. W. (1982) Intense Ly α emission from Uranus. Nature 299, 428 - 429.

Moos, H. W., Durrance, S. T., Skinner, T. E., Feldman, P. D., Bertaux, J.-L., and Festou, M. C. (1983). IUE spectrum of the Io torus: identification of the $^5S_2 - {}^3P_{2,1}$ transition of S III. Astrophys. J. 275, L19-L23.

Skinner, T. E., Durrance, S. T., Feldman, P. D., and Moos, H. W. (1983). Temporal variations of the Jovian H I Lyman-alpha emission (1979-1982). Astrophys. J. 265, L23 - L27.

Skinner, T. D., Durrance, S. T., Feldman, P. D. and Moos, H. W. (1984). IUE Observations of longitudinal and temporal variations in the Jovian auroral emission. Astrophys. J. 278, 441 - 448.

Winkelstein, P., Caldwell, J., Kim, S. J., Combes, M., Hunt, G. E., and Moore, V. (1983) A determination of the composition of the Saturnian stratosphere using the IUE. Icarus 54, 309 - 318.

ADDENDUM Since this manuscript was written, a preprint by P. S. Butterworth and A. J. Meadows, entitled "Ultraviolet reflectance properties of asteroids" has been received (Icarus, in press, 1984). It describes IUE LWR spectra of 28 asteroids. Absorption features in different classes of asteroids are presented, and compared to available laboratory data. It is suspected that the observed features are due to titanium and iron ions in silicate assemblages. This paper also presents a very readable discussion of the difficulties associated with observing planets by the IUE.

MAGELLANIC CLOUD OBJECTS

J.B. Hutchings
Dominion Astrophysical Observatory

Abstract: In this review, the considerable contributions of IUE to understanding the composition, stellar evolution, interstellar medium, and extinction of the Clouds are discussed and compared with those for the galaxy. Future directions for UV work are suggested.

INTRODUCTION

One of the early surprises of IUE was the discovery that hot stars in the Magellanic Clouds were accessible. There are now some 1000 IUE images of Cloud objects and over 100 papers in print on these data. The research falls into a few main subject areas by numbers of papers, with the principal ones being the hot stars themselves, interstellar extinction studies, cloud halo and ISM, and X-ray sources. These will all be described, but I would like to try to link the different topics with what is probably the single most significant difference between the Clouds and the galaxy — the heavy element abundances - so that is where we will begin. I will also attempt to point to where future work will be needed in each area.

ELEMENT ABUNDANCES

The element abundances in the Magellanic Clouds are of interest to many aspects of research. Most fundamentally, the abundances are a record of the stellar history of a galaxy, and comparison between our own and other galaxies is of great significance. It has also become clear that these abundances affect many ongoing processes in a profound way - principally by affecting the opacity and scattering of radiation. Observed differences between the Clouds and our galaxy in the behaviour of stellar envelopes, stellar mass-loss, interstellar extinction, the determination of absolute fluxes, and strong X-ray source fluxes, are all known examples of where this is important, and they will be dealt with in this review. Other as yet unexplored areas where the effects may be important are novae and their light curves, stellar spectral classification, and stellar evolution in general, including supernovae and compact stellar remnants. To start with, we look at the contribution of IUE to abundance determinations in the Clouds.

It has been noted by many workers over the years that the absorption lines of Cloud stars are weak compared with their galactic counterparts, and generally accepted that this indicates real abundance differences. The UV spectral region contains particularly valuable C lines that the visible region lacks, for this work, as well as many lines vital to the determination of

ionisation fractions in combination with visible region lines. The determination of C abundances has been done by Dufour, Shields and Talbot (1982), and reviewed by Dufour (1984), from H II regions. Their important result is that in the SMC C is depleted (with respect to the galaxy) more than N or O, while in the LMC, N is depleted more than C or O. They argue that N and O are initially generated by massive (>10M_0) star evolution, and C from less massive (4 to 10 M_0) stars. Thus C/N and C/O starts low and rises with time as the less massive stars begin to evolve. Later still, when <4 M_0 stars have evolved, C/N will decrease again, since these stars produce N.

	$12+\log N(X)/N(H)$						
ELEMENT	SMC[a]	LMC[a]	Orion[a]	Sun[b]	PN[c]	SMC-Sun	LMC-Sun
C	7.16	7.90	8.46	8.65	8.93	−1.49	−0.75
N	6.60	6.94	7.48	7.96	8.68	−1.36	−1.02
O	8.05	8.38	8.60	8.87	8.77	−0.82	−0.49
Ne	7.34	7.68	7.79	8.05	8.14	−0.71	−0.37
S	6.61	7.01	7.12	7.23	7.34	−0.38	−0.22
Ar	5.77	6.10	6.27	6.57	6.50	−0.80	−0.47
C/O	−0.89	−0.48	−0.14	−0.22	0.16	−0.67	−0.26
C/N	0.56	0.96	0.98	0.69	0.25	−0.13	+0.27
N/O	−1.45	−1.44	−1.12	−0.91	−0.09	−0.54	−0.53

Table 1. Relative abundances in MCs and galaxy from Dufour et al. (1982).

The situation is summarised in Table 1, and this scenario sets out reasonably clearly the evolutionary history of the Clouds compared with the galaxy. Maran et al. (1982) used the IUE to study planetary nebulae in the Clouds, and obtained interestingly different results. They find C abundances only slightly less than the galaxy, while other elements are depleted by the "normal" amounts. Their finding in other words is that in PN ejecta, C is 40 times the local ISM value in the SMC and 6 times in the LMC. They thus find that at present planetary nebulae are the principal source of C enrichment in the Clouds, and that the C generation processes in Cloud stars are roughly the same as in the galaxy - an important datum for stellar evolution theory. Stecher et al. (1982) discuss the central stars of PN in the Clouds and using IUE fluxes derived (Eddington limiting) masses from the deduced bolometric fluxes. These turn out to be ~ 1 M_0, higher than the 0.6 M_0 generally accepted for galactic PN. They discuss some interesting possible explanations of this. (A further factor, for which there is now some other evidence), is that the Clouds may be closer than the present canonical values.)

These kinds of studies are unique to the far UV and are performed with difficulty with IUE, due to its low sensitivity, low dynamic range and limited photometric accuracy. However, the importance of the results will make the ST spectrographs and other high signal-to-noise instruments very desirable for future work.

INTERSTELLAR EXTINCTION

One of the most spectacular results from IUE has been the study of the UV extinction laws in the Clouds. By means of comparison of reddened and unreddened stars of the same spectral type and from model fitting to stars of known spectral type, it has been found that the UV extinction is different in the two Clouds, and in the galaxy (Koornneef 1982, Morgan and Nandy 1982, Hutchings 1982, Lequeux et al. 1982). The mean extinction characteristics are shown in fig. 1, although there are exceptions in all three galaxies which bridge these differences. The shape of the SMC mean extinction curve is still the subject of some debate and research, but the basic characteristics seem well established. Once again, there is a clear progression from SMC to LMC to galaxy. These results are profound because they show us that the relation between perceived and intrinsic flux in any galaxy cannot be taken for granted, and also that the properties of the interstellar medium are strongly variable between galaxies.

Another aspect of this study has been the determination of gas to dust ratio from the measurement of Lyman α absorption simultaneously with extinction. This shows (Koornneef 1984, Lequeux et al. 1984) that the ratio N_H/E_{B-V} is 17 times the galactic value in the SMC and 4 times in the LMC (fig. 2), thus showing the same sequence evident in the extinction itself. These factors are like the C abundance ratios, rather than Si, O suggesting a connection with graphite. The numbers are probably more reliable than determinations by other methods and instruments. A problem is the separation of foreground Ly α, needing higher resolution.

It has been suggested that the grain sizes are smaller in less evolved galaxies, to account for the far UV differences. More recently, however, Nandy (1984) and Bromage and Nandy (1983) have indicated that the principal difference may be the amount of graphite in the ISM (fig. 3), which links us back once more with the C abundance evolution. Lequeux et al. (1984) reached similar conclusions about the role of graphite. In studies of objects in M33, a galaxy similar in mass and evolution to the LMC, it has been found that an extinction law like the LMC is more appropriate than a galactic one (e.g. Massey and Hutchings 1983). Clearly, future work will need to investigate these differences more deeply, in as many local group galaxies as possible. The present indication is that the extinction curve is strongly linked with the evolutionary state of the galaxy, but it needs quantification and a proper understanding of the local purturbations in each galaxy.

HOT STARS AND STELLAR WINDS

As is well known, the principal OB star stellar wind lines are the UV resonance lines of N V, Si IV, and C IV, and IUE studies of these in galactic stars have been numerous and fruitful (e.g. Hutchings and Von Rudloff 1980; Garmany and Conti 1984). The study of MC supergiants has added significance since the differential distance and reddening effects which plague galactic studies, are largely eliminated. Studies of Cloud stars have revealed a number of differences in the stellar winds compared with the galaxy (Hutchings

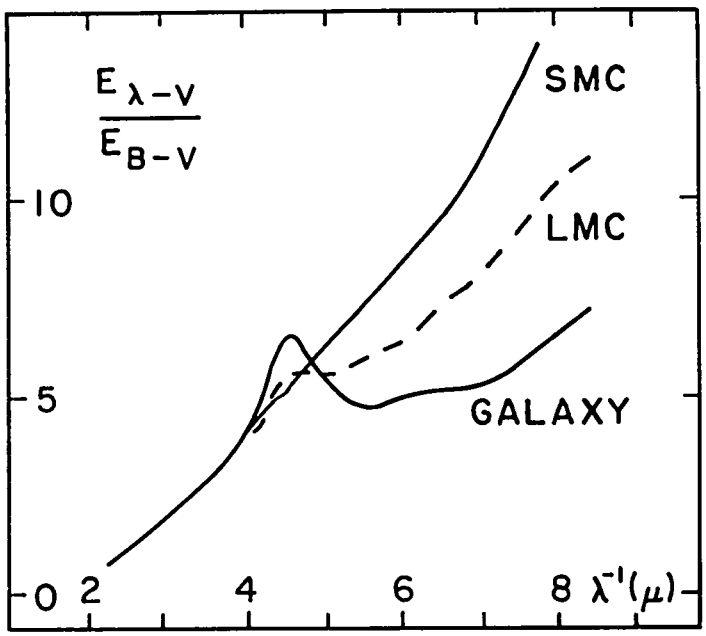

Fig. 1. Mean UV extinction laws, from Lequeux et al. (1984).

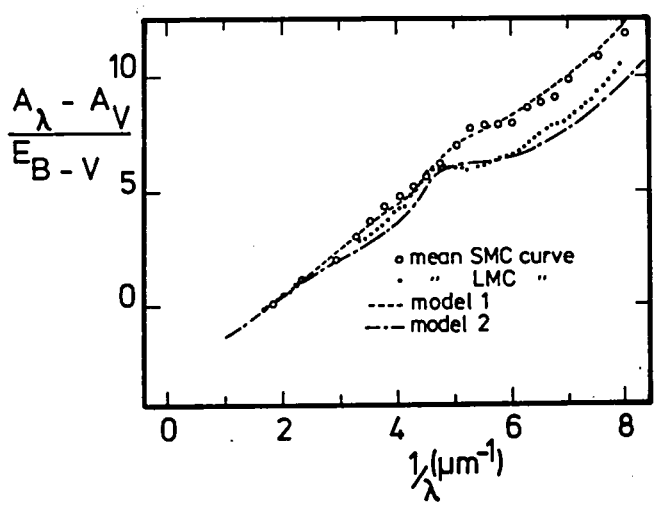

Fig. 2. Model fitting to mean extinction curves (Nandy 1984). Model 1: zero graphite; model 2: 35% galactic graphite.

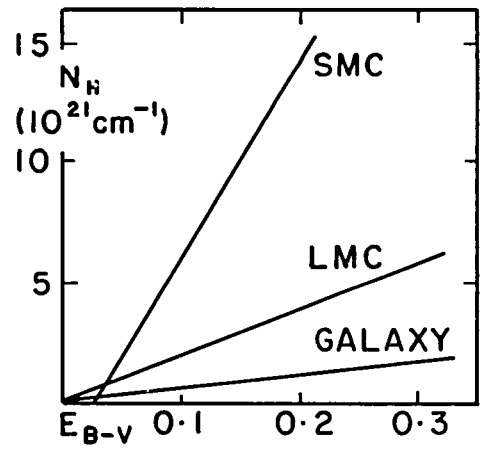

Fig. 3. Mean gas to dust ratio lines, from Lequeux et al. (1984). Diagram covers range of measured values.

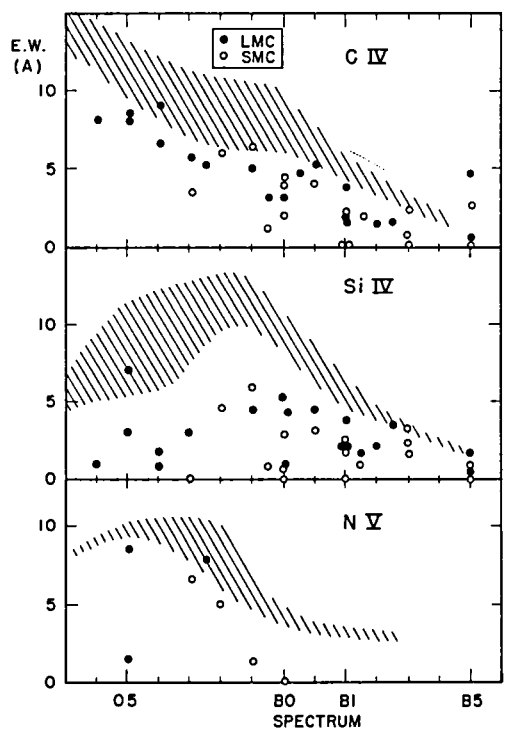

Fig. 4. UV resonance line strengths compared with galactic (hatched areas), from Hutchings (1982).

1982, 1983, Bruhweiler et al. 1982). Figures 4,5 illustrate the differences. Briefly, the resonance lines are weaker and the the terminal velocities of the winds lower in the Clouds than the galaxy, with the SMC being the extreme, as usual. Once again, the effect may be attributed to the heavy element abundance, as it is principally responsible for the radiative opacity which is a major effect in driving hot stellar winds. The exact way in which the winds differ is not understood - for example, the velocity gradients in the visible spectra are larger in the Clouds than the galaxy (Hutchings 1980a) - but the mass-loss mechanisms are not well modelled in the galaxy either. Bruhweiler et al. (1982) suggest that the mass loss rates may be similar in the SMC and galaxy, if the lower C and S abundances somehow balance out the lower line velocities and strengths. However, this actually assumes a greater efficiency if these lines drive the winds, and it seems more likely that all elements are similarly weakly driven. Looking at the W-R stars, Smith and Willis (1983) find that the velocities in these dense winds are similar to galactic ones, and that the abundances are similar to galactic, so that in their (more advanced ?) evolutionary state, the differences may diminish. However, they find that the He II lines are stronger in Cloud WN stars, and the extent of the envelopes is lower.

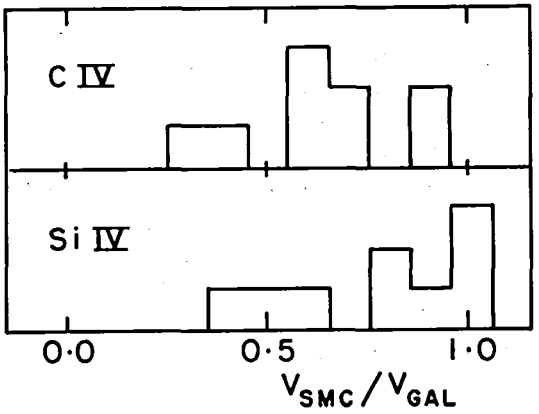

Fig. 5. Resonance line (minimum) velocity ratios SMC/galaxy, from Bruhweiler et al. (1982).

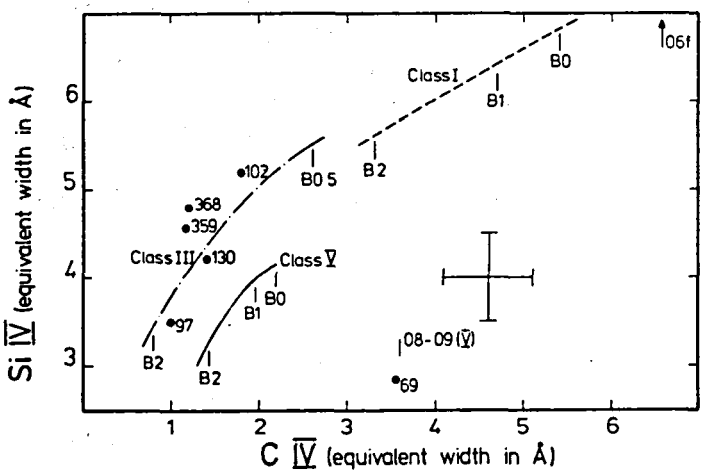

Fig. 6. LMC UV line strengths for giants compared with galactic stars (lines), from Nandy et al. (1983).

Looking at lower luminosity stars, Nandy et al. (1983) find that the resonance line strengths in giants are the same as their galactic counterparts, as are the flux distributions (fig. 6). Thus it may be that only at the highest luminosities do the differences become very apparent. Nevertheless, it is likely that the amount of mass lost from hot stars in the Clouds is considerably less than for their galactic counterparts, and that the evolution of massive stars is significantly different as a result. A further clue may reside in M33 and M31, whose populations of giant H II regions and W-R stars are also different, and suggest a general evolutionary sequence for galaxies which affects the most massive stars. We return to further aspects of this in the X-ray source section. For the future, we will need to study

massive stars in the UV in other galaxies with ST, and also to develop stellar wind models which explicitly embody the initial heavy metal abundance and synthesis in the stars.

There are several individual stars which have been studied in detail with IUE, at both low and high dispersion, and the results have generally been used in conjunction with ground based data in discussing the stars. Stahl et al. (1983), for example derive very high mass loss rates for a group of stars claimed to be like S Dor. Whether these are like galactic counterparts or not is not certain to me at present, mainly because local extinction has prevented the study of such objects in the UV. Kafatos et al. (1983) have studied two peculiar (symbiotic?) stars with IUE. Their results are significant in that, once again, the absolute luminosity of the hot star can be derived, with resulting implications for its mass and evolutionary history. Other extreme objects which have been studied are HD 38489 (Shore and Sanduleak 1983) and HD 34664 (Bensammar et al. 1983). Here, our sample needs to be extended both to other galaxies (the Hubble-Sandage variables) as well as our own galaxy in future UV work.

A final object of exceptional interest has been the apparently super-luminous (supermassive?) star R136a at the centre of 30 Dor (Feitzinger, Hanuschik, Schmidt-Kaler 1983, Moffat and Seggewiss 1983, Savage et al. 1983). The question in essence is whether the flux, (which IUE data show to be hot: > 50000 K) originates in a single star or a compact group of very early O stars. IUE data, in the above references, have been vital in deriving the flux, temperature and mass-loss characteristics of the star(s). The whole question now appears to rely on high resolution spatial imaging, yet to be done definitively (see full discussion in IAU Symp. 108). Whatever the object is, we note that Massey and Hutchings (1983) find similar objects powering similar giant H II regions in the similar galaxy M33. M31 does not appear to contain such objects, again suggesting a global sequence in galaxies.

X-RAY SOURCES

X-ray binaries in the Clouds are not numerous, but scale roughly with the galaxy mass (see Helfand 1984, Hutchings 1984). Nevertheless, they have several special and probably important properties. The cloud binary sources are much more luminous than their galactic counterparts. They also contain the two most rapid X-ray pulsars, strong evidence for luminous disks in massive systems, and two probable black holes in binary systems, in a volume of space which in the galaxy contains less than one. Once again, the single parameter which may be responsible is the abundance, this time affecting the opacity to X-rays. A low opacity to X-rays means that a higher accretion rate is possible on to a compact star, leading to higher luminosity and more rapid spinup of pulsars, as well as the formation of a stable and luminous accretion disk. The possible presence of massive stellar remnants suggests, as in the discussions above, that a history of lower mass-loss together with a collapse which is less opaque to radiation may allow the formation of more massive remnants than in the galaxy, where neutron stars (and supernovae?) are the norm.

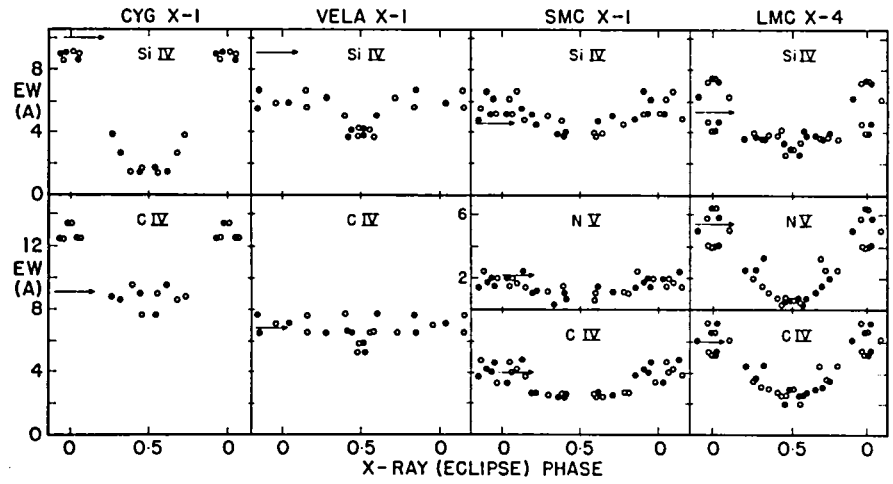

Fig. 7. Phase dependence of UV resonance lines in X-ray binaries in MCs and galaxy. Arrows indicate normal galactic values.

IUE investigations have been made on SMC X-1, LMC X-4, LMC X-1 and A0538-66. In the former two cases (van der Klis et al. 1982), the UV light curves were derived, which enabled modelling of the tidally distorted primary and the light from the disk. In LMC X-4 the data are consistent with precession of a disk on the 30-day period seen in the X-ray intensity. These studies also revealed the ionisation of the stellar winds by the X-rays by the phase dependence of the resonance lines (see also Hammerschlag-Hensberge, Kallman, Howarth 1984). The results are qualitatively similar to the galactic systems (fig. 7), but we need higher signal-to-noise data from future observations to make the important study of the different wind structures and UV photometric behaviour that these systems allow.

The unique variable system A0538-66 has been a fruitful object of IUE study. This system undergoes large optical changes in its 16-day cycle, as well as extended high and low states. Studies by Charles et al. (1983), and Howarth et al. (1983), have shown that the UV flux does not undergo these large changes, so that the effective temperature is lower in high optical states (fig. 8). While we do not get understand the system it is clear that the UV data form a vital part of our study of it. The unique high luminosity in X-rays, high mass-flow and associated optical and UV emitting volume make the understanding of the evolutionary state of this system of great interest. Once again, we look for LMC conditions that may contribute to its unique behaviour.

HALOS

The discovery of the galactic halo by IUE (Savage and de Boer 1979) is now well established by means of UV interstellar absorptions (e.g.C II, Mg II) which are much more sensitive probes than any visible lines. High dispersion studies of MC stars with IUE have also suggested halos associated with these galaxies (de Boer and Savage 1980), but the evidence is less secure. This is because it is difficult to get good data, and because the absorption lines have to be separated from galactic halo and local absorptions around the target stars (e.g. Feitzinger and Schmidt-Kaler 1982). de Boer (1984) gives a

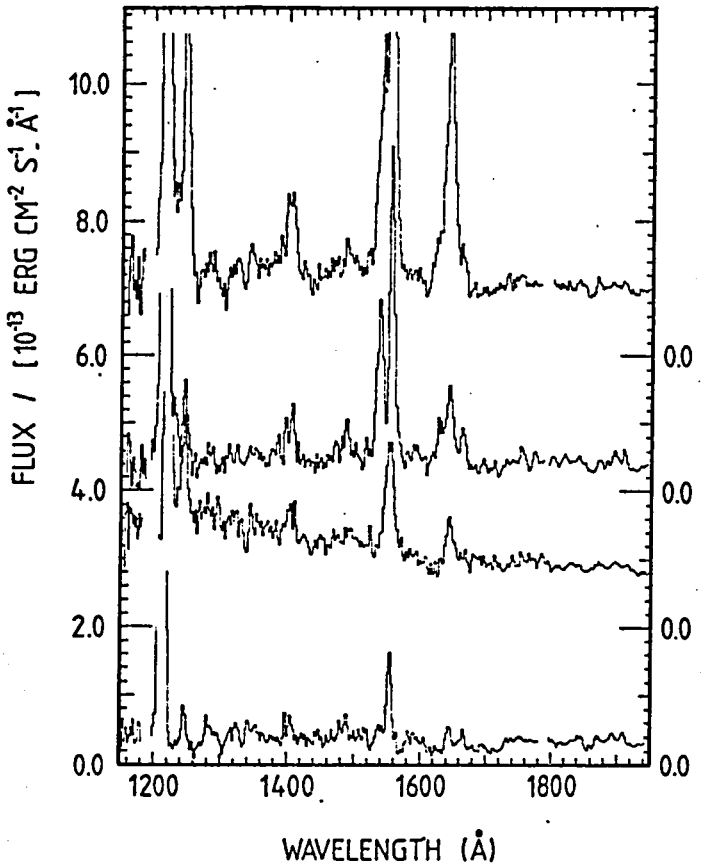

Fig. 8. A0538-66 in various activity states. Note profile, flux, and temperature changes. From Howarth et al. (1983).

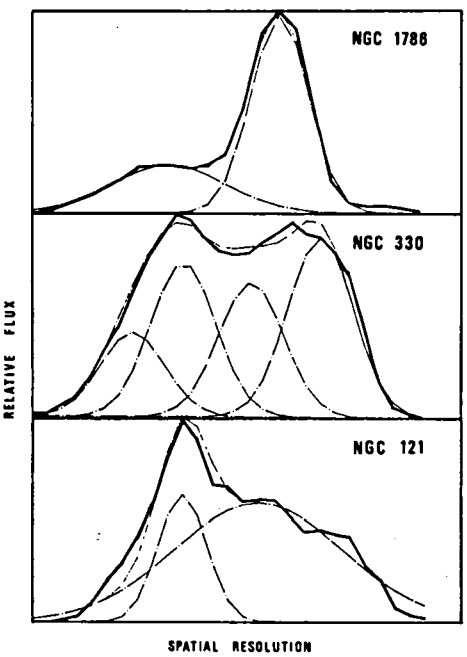

Fig. 10. Cross-sections of IUE spectra of MC clusters, deconvolved into principal components. From Cassatella and Geyer (1984).

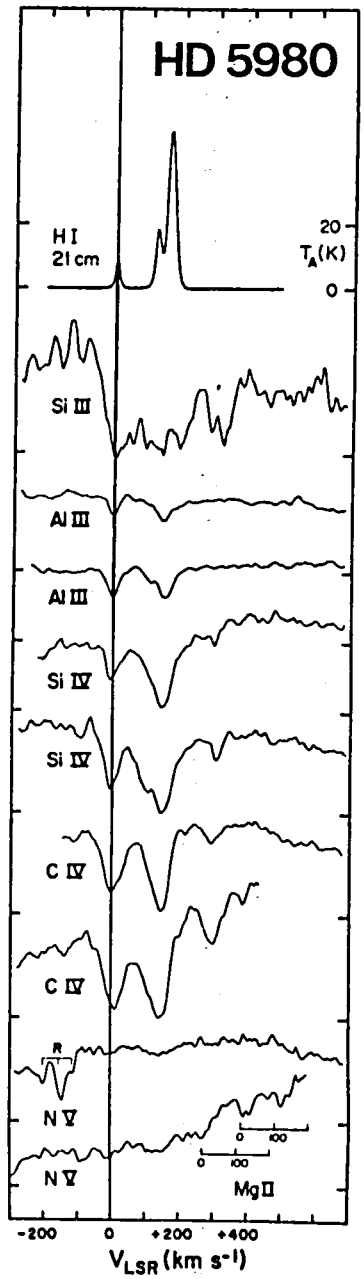

Fig. 9. Interstellar lines in HD 5980, from Fitzpatrick and Savage (1983). Zero velocity component is galactic.

review of the subject, and Fitzpatrick and Savage (1983) give perhaps the best data to date (fig. 9). Table 2 shows that the sharp absorptions in the MC stars are generally larger than for local galactic stars, suggesting that a halo is responsible for the excess. It is of importance to establish the presence or otherwise of these halos since their formation and heating is directly linked to the present stellar wind and supernova activity in the Clouds. There is also the interesting question of whether the halo as a whole rotates more slowly than the stars, as some evidence suggests. Once again, the proper study of the question requires the resolution and signal-to-noise of the Space Telescope HRS.

Table Equivalent Widths for Interstellar CIV Lines in MC Stars and Comparable Milky Way Stars

MC star		Sp. Type	V(star)	V(CIV)	W(1550)	Ref	MW star	Sp. Type	W(1550)	Ref
Sk-67 18	--	O6-7+WN5	272	240:	200:	dBS	HD153919	O6f	90	BKM
Sk-67 5	HD268605	O9.7Ib	294	250:	>150:	dBS	HD213087	B0.5Ib	65	BDHR
Sk-67 104	HD 36402	WC5+OB	315	270	200	dBN	HD113904	WC6+09BOI	80:	BKM
Sk-69 246	HD 38282	WN6	245:	210	230	dBS	HD192163	WN6	320	SWW,1
Sk-71 45	HD269676	O4-5III	229	220	270	GWMN	HD 46223	O4Vf	100	BDHR
Sk-69 243	HD 38268	R 136	245:	215	600	dBS	HD 37022	O6+B0.5V	260	FS,2
Sk 108	R31	O6.5+WN3	129	150	300	dBS	HD 93403	O6f+O7.5	150	BKM
Sk 80	---	O7Iaf+	---	150	280	dBS	HD 57060	O7f	30	BKM
Sk 78	HD 5980	OB?+WN3	---	140	410	dBS	HD190918	WN5+O9.5III	470	BKM,1
Sk 159	---	BOIa	---	170	60	P9	HD152667	BOIa	75	BKM

Table 2. From Koornneef (1984). Note large W values of MC stars, possibly due to halo absorption.

CLUSTERS

As a final section, we look at the efforts to study Cloud globular clusters with IUE (de Boer, 1981; Cacciari et al., 1982; Cassatella and Geyer 1982). These studies have revealed the presence and temperature of hot stars, allowing estimates to be made of their numbers. The absence of extinction suggests that the original cluster gas has either been used up or blown away. Luminosity functions derived for clusters from IUE data have yielded ages in the range 7×10^6 to 8×10^7 years. In some clusters (fig. 10), the spectra of individual stars can be deconvolved, and temperatures derived, which range in general from 12000-30000 K. Bohm-Vitense and Hodge (1984) find LMC type extinction in clusters, and also note the absence of mass loss in LMC stars whose galactic counterparts do show mass loss. These are all important UV studies which will yield significant results on cluster evolution and MC star formation history, and clearly need much future work.

In conclusion, I hope this very superficial report will encourage the pursuit of MC research in the UV. The Clouds appear to form the early part of a sequence in galaxy evolution, which can be traced through the principal local group members. The UV contains much of the vital information in learning about this sequence, and the history of the Clouds themselves.

REFERENCES

Bensammar, S. et al. 1983, A & Ap. 126, 427.
Bromage, G.E., Nandy, K. 1983, M.N.R.A.S. 204, 29P.
Bruhweiler, F.C., Parsons, S.B., Wray, J.D. 1982, Ap. J. 256, L49.
Cacciari, C. et al. 1982, ESA SP-176, p. 519.
Cassatella, A., Geyer, G.H. 1982, ESA SP-176, p. 523.
Charles, P.A. et al. 1983, M.N.R.A.S. 202, 657.
de Boer, K.S. and Savage, B.D. 1980, Ap. J. 238, 86.
de Boer, K.S. 1981, NASA-CP2171, p. 523.
_____. 1984, IAU Symp. 108, Reidel, p. 375.
Dufour, R.J. 1984, IAU Symp. 108, Reidel, p. 353.
Dufour, R.J., Shields, G.A. and Talbot, R.J. 1982, Ap.J. 252, 461.
Feitzinger, J.V., Schmidt-Kaler, T. 1982, Ap.J. 257, 587.
Feitzinger, J.V., Hanuschik, R.W., Schmidt-Kaler, T. 1983, A & Ap. 120, 269.
Fitzpatrick, E.L., Savage, B.D. 1983, Ap.J. 267, 93.
Garmany, C.D., Conti, P.S. 1984, Ap.J. (in press).
Hammerschlag-Hensberge, G. Kallman, T.R., Howarth, I.D. 1984, Ap.J. (in press)
Helfand, D.J. 1984, IAU Symp. 108, Reidel, p. 293.
Howarth, I.D. et al. 1984, M.N.R.A.S. (in press).
Hutchings, J.B. and Von Rudloff, I.R. 1980, Ap.J. 238, 909.
Hutchings, J.B. 1980a, Ap.J. 237, 285.
_____. 1980b, Ap.J. 235, 413.
_____. 1982, Ap.J. 255, 70.
_____. 1984, IAU Symp. 108, Reidel, p. 305.
Kafatos, M. et al. 1983, Ap.J. 275, 584.
Koornneef, J. 1982, A & Ap. 107, 247.
_____. 1984, IAU Symp. 108, Reidel, p. 333.
Lequeux, J. et al. 1982, A & Ap. 113, L15.
_____. 1984, IAU Symp. 108, Reidel, p. 405.
Maran, S.P., Aller, L.H., Gull, T.R., Stecher, T.P. 1982, Ap.J. 253, L43.
Massey, P. and Hutchings, J.B. 1983, Ap.J. 275, 578.
Moffat, A.F.J., Seggewiss, W. 1983, A & Ap. 125, 83.
Morgan, D.H., Nandy, K. 1982, M.N.R.A.S. 199, 979.
Nandy, K. et al. 1983, M.N.R.A.S. 205, 231.
_____. 1984, IAU Symp. 108, Reidel, p. 341.
Savage, B.D. and de Boer, K.S. 1979, Ap.J.230, L77.
Savage, B.D. et al. 1983, Ap.J. preprint.
Shore, S.N., Sanduleak, N. 1983, Ap.J. 273, 177.
Smith, L.J., Willis, A.J. 1983, A & Ap. Suppl. 54, 229.
Stahl, O. et al. 1983, A & Ap. 120, 287.
Stecher, T.P. et al. 1982, Ap.J. 262, L41.
Van der Klis, M. et al. 1982, A & Ap. 106, 339.

Ultraviolet and X-ray Observations of Active Galactic Nuclei: Constraints on Models of the Broad Emission Line Region

Richard Mushotzky
Laboratory for High Energy Astrophysics
NASA/Goddard Space Flight Center

In this talk we will be considering the extensive ultraviolet spectra of broad line active nuclei and the large body of X-ray photometry and spectroscopy of these objects and the constraints that these data place on the photoionization models of the broad emission line region (BLR) of these objects. Many active galactic nuclei, in particular quasars and Seyfert I's, are characterized by strong, broad (full width > 2000 km/sec), emission lines from permitted transitions in abundant elements. In the simplist models these lines originate in clouds located at some characteristic distance from the central ionizing source in a quasi-spherical distribution. While the dynamics of these clouds are quite important we will not consider them here and instead will concentrate on how to derive the observed line strengths and line ratios.

The main inputs into these photoionization models (see Davidson and Netzer (1979) for an extensive review) are:

1) Atomic Physics
2) The continuum spectrum
3) The Cloud Model
4) The global geometry of the region
5) The influence of dust, if any
6) The chemical composition of the gas-that is the metallicity

The main output of these codes are the absolute line strengths and the ratios of these, the "distance" to the clouds, and the general properties of the clouds and the intercloud medium.

Atomic physics, that is the relevant cross sections and reaction rates of the most important processes and the identification of these processes, is perhaps the most crucial input for these models. Unfortunately, at present,

not all of these values are known with sufficient precision. However, sufficient progress has been made that most model builders have been using a consistent set of data (see Mendoza 1983). Thus the relative agreement of the models with the observations is a weak sign that most of the relevant processes and cross sections are understood. It is anticipated that future revisions in the relevant atomic physics will not make a strong change in the modeling results, it must be kept in mind, however that this has happened in the past.

The Continuum

The form of the continuum is perhaps the quantity most susceptible to observation. Of course, it is the interaction of the continuum photons with the ions in the cloud that provides most of the ionization in the broad line region. Thus the continuum is the engine that drives the entire model. There are several distinct regions in which the "ionizing" continuum is observed:

1) The ultraviolet, E<13.6 eV: observed for low redshift objects by IUE and for high redshift objects by ground based observers.

2) The ionizing extreme ultraviolet (XUV) 13.6<E<500 eV: observed over part of this range for high redshift objects by IUE but, for the most part, has to be inferred from observations of lines originating from ions with with high ionization potentials or by continuity arguments between the UV and soft X-ray spectra.

3) The soft X-ray range .5<E<7 keV: observed over the this energy range by a combination of spectrometers on the Einstein observatory and HEAO-1.

4) The "hard" X-ray range E< 7 keV: observed by spectrometers on HEAO-1, in this energy range atomic processes are not very important and the major interactions of photons with ions is through the Thompson cross-section.

X-ray Spectrum

The observed X-ray spectra of broad emission line objects (primarily Seyfert I's) over the energy range E>3 keV (Mushotzky 1984) Rothschild et al. 1983) is quite simple. It is well fit over the range from 3 -100 keV by a power law with mean spectral slope of 0.7 and with a very small dispersion of +/-0.15. There does not seem to exist any dependence of this slope on total luminosity, optical spectral type or radio properties and thus this slope can

be considered to be one of the defining characteristics of broad line active galaxies. For high luminosity objects, log L(x)>43.7 in the 2-10 keV band, this characteristic slope continues down to 0.5 keV (Petre et al. 1984). However lower luminosity objects (Mushotzky 1982, Reichert et al. 1984) show a rollover at lower energies due to the photoelectric absorption of X-rays by "cool", log T<7.5 K, material.

The relationship of the X-ray to "optical" (by optical one typically refers to flux in the 2500-10,000 angstrom range) has been well determined by a wide variety of observers with data obtained from the Einstein observatory (see Kriss 1984 for a recent review). If we use $\alpha(ox)$ a parameter which is related to the logarithmic slope of the mean X-ray to optical fluxes $\alpha(ox)=(\log f(opt)-\log f(x))/\delta \log\nu)$ (Tananbaum et al. 1979) one finds that this quantity is narrowly distributed with almost all the objects having $\alpha(ox)$ between 0.8 and 1.7. However this narrow distribution in $\alpha(ox)$ is misleading because the logarithmic compression "hides" the wide range in the ratio of X-ray to optical luminosities (Reichert et al. 1982). The ratio of luminosities is $\log (L(x)/L(opt)=3.125-2.605\alpha(ox)$. Thus the ratio of X-ray to optical luminosity varies by a factor of over 300.

The Ultraviolet-Optical Spectrum

The nature of the UV continuum is a much more complicated subject. Despite the apparent simplicity, detailed analysis has shown that the form of the continuum in the 500-10,000 angstrom range is quite complicated and not well understood at present. Wu,Boggess and Gull (1983) have noted that the UV continuum is not grossly different from object to object and seems moderately well fit over the entire IUE range by a simple powerlaw. Malkan and co-workers (e.g. Malkan 1983) have fit a model to the IR-UV spectrum of a fairly large sample of active galaxies. They find that most objects require two continuum components to fit the data. A power law of index near 1.2, and an additional component which we will refer to as the "blue bump" (Grandi 1982). These authors feel that the mean spectral index does not vary much from object to object but that the ratio of the blue bump to power law component is quite variable. Green and co-workers (e.g. Bechtold et al. 1984) have found that the spectrum of several high redshift quasars seems to be

considerably steeper than Malkan's mean power law at wavelengths shorter than the Lyman limit. It is not clear at present if this steepening is due to absorption due to intervening hydrogen clouds between the observer and the continuum source, to a steepening of the power law component or to the high frequency exponential roll over of the blue bump.

To considerably confuse the situation detailed studies of several Seyfert I galaxies (such as NGC 4151, NGC 4593, NGC 3783 etc.) seem to show that the slope of the power law in the IUE band is strongly correlated with luminosity, that is the instantaneous luminosity of the galaxy seems to be correlated with the spectral slope, with the steeper spectra being associated with lower luminosity. There is no correlation between the absolute luminosity of a galaxy and the slope of the UV continuum. However there is at present some controversy over whether this effect is real or if real whether it is due to an intrinsic change in the continuum form, to variable reddening, or to a change in the blue bump.

The nature of the blue bump is unclear at present. The present speculation centers around three possible origins, viz. an extremely strong Balmer continuum of rather peculiar shape (see Oke, Shields and Korycansky 1984), a "black body component" due to the accretion disk around a massive black hole or a forest of FeII emission lines (see Netzer et al. in this symposium). It is most likely that the observed component is due to the sum of two or more of these possibilities (or perhaps something else). The detailed data available from IUE on NGC 4151 (Perola et al. 1982) indicates that this blue component does not contribute much to the ionization of CIV and while strongly correlated to the power law continuum sometimes may vary out of phase with it. The Oke et al. results show that the bump is strongly correlated with H β but not with Mg II. IUE data on moderate redshift objects z=0.5+/-.2 where the Lyman and Balmer lines, the strong permitted UV lines and the continuum over a broad band is directly observable will be of great use in understanding the nature of the bump.

Given all these complications most models of the ionizing continuum have used a simple two power law form with a relatively steep, $\alpha \sim 1.2$ UV continuum and a flat, $\alpha \sim 0.7$ x-ray continuum. To avoid over-predicting the soft X-ray flux (Petre et al. 1984) the UV continuum is required to steepen at

some energy greater than 13.6 eV. However the energy at which this occurs and the form of the steepening are poorly determined observationally.

Cloud Model and Geometry

The X-ray data on absorption due to cold material in the line of sight provides unique information on the column density, covering fraction and global geometry of the clouds.

The direct observation in the X-ray of absorption in several objects gives an observed range in the total column density from 2-13 $x10^{22}$ atms/cm^2. This result is in quite good agreement with models developed to "explain" the anomalous Balmer decrement in AGN (e.g. Kwan and Krolik 1981) which require thick clouds of column density greater than 10^{22} in addition to X-ray heating of these deep, warm regions. This agreement, if not fortuitous, indicates that the X-ray absorption is due directly to the clouds responsible for the optical emission lines (and of course that the models developed to explain these lines have some predictive capability).

The fact that some objects do show absorption in the X-ray band indicate that most of the line of sight to the central X-ray source is covered by cloud(s). If this is not circumstantial then this means that the clouds have a large covering factor in these objects. Analysis of relatively large sample of objects (Mushotzky 1982, Reichert et al. 1984) shows that the probability that an object will be absorbed is inversely related to its luminosity. However a detailed analysis of these data (Reichert et al. 1984), in particular explaining why some objects seem to be only "partially covered" (Holt et al. 1981), indicates that this luminosity effect is probably due to the matching of cloud and continuum sizes. That is, the intrinsic cloud size probably is constant from object to object but the continuum source in the lower luminosity sources are small. Thus at low luminosities the projected solid angle to the clouds is the same size, or larger, than the continuum source and when a cloud "gets in the way" we have a total eclipse. For higher luminosity objects a single cloud is too small to occult all the radiation from the large continuum source and the source looks either unabsorbed or partially covered.

The ratio of the strength of the X-ray iron 6.4 keV fluorescent line to the depth of the X-ray Fe K absorption edge optical depth is a measure of the

global geometry of the absorbing region (see Mushotzky et al. 1978). If the line is strong relative to the edge we are probably observing a disklike system face on while if the edge is strong relative to the line the system is edge on. Unfortunately only two objects are bright enough to have had these parameters well determined, Cen-A (Mushotzky et. al. 1978) and NGC 4151 (Holt et al. 1980). In these two systems the data are consistent with a spherical absorbing region.

Dust and Metallicity

The effect of dust on the ultraviolet emission lines is potentially very important. Not only does one have to correct the observed line strengths for the effect of reddening but also correct the form of the continuum. In the UV even a small amount of dust has a very large effect. For E(B-V)=0.1 the flux in Lyman α is changed by a factor of 8 and CIV by a factor of 7. The slope of the spectrum in the ultraviolet is changed by $\delta\alpha = 2.5E(B-V)$. The UV spectrum of Seyfert galaxies and quasars does not evince a strong 2200 A feature which is indicative of dust in our galaxy. However, as demonstrated by the reddening curve in the LMC (Hutchings this symposium) it is not clear that all dust has this feature. More detailed measurements, especially in the infrared wavelengths where silicates and ices show spectral features, will be necessary to determine the amount of dust. In addition if the partial covering models are correct the analysis of the reddening will have to include the effect of light leaking through the holes (Mushotzky 1982). This can be an extremely important effect in the UV; for example the Seyfert II NGC 1068 has a very large amount of dust in the line of sight as determined by IR observations (see Rieke and Lebofsky 1979) but also has a strong UV continuum (Neugebauer et al 1980). Thus in this system the UV light must either originate in a different region from the IR flux or there must be holes.

The metallicity of the gas in the broad line region is poorly determined. As pointed out in Ferland and Mushotzky (1984) since the cooling in the BLR clouds is primarily due to the strong emission lines of the metals (as well has hydrogen) their intensities cannot change greatly in an energy conserving model. Thus from the strength of the emission lines we can only conclude that the clouds must have a metal abundance roughly consistent with solar. X-ray

absorption measurements of the strength of the K absorption lines in AGN can potentially determine the column density of the heavy elements (in particular Fe, Si and S) if the column density is greater than 10^{22}. In the case of NGC 4151 it appears as if the Fe abundance is twice solar. With future X-ray spectroscopy missions, such as OSS-2, it should be possible to determine these abundances in many more objects.

Model Building and Results

In developing the models there have been two general approachs, a constant pressure, and a constant density model. In the these two cases the value of the ionization parameter U is defined differently. In the constant density model the parameter is dimensionally L/nR^2 where L is the luminosity, or number of ionizing photon, n is the density in the cloud and R is the distance of the cloud from the ionizing source. In the constant pressure models (see Kallman and McCray 1982) the ionization parameter is L/R^2P where P is the pressure. As one can see both models have two essentially adjustable parameters once all the other inputs are specified.

Both models can adequately fit the observed AGN spectra with a fair amount of detail (see table in Ferland and Mushotzky 1982). In particular in the constant density models it is found that virtually all the AGN spectra (Mushotzky and Ferland 1984) can be fit with values of log density between 9 and 10.2 and values of log U between -0.5 and -3.0. These models adequately account for virtually all the strong emission lines (but see below) and can explain apparent trends in the data. In particular, the Baldwin effect, the fact that higher luminosity objects have a smaller equivalent width of CIV, appears to be related to a luminosity dependent mean value of U with the higher L objects having a lower value of U (Mushotzky and Ferland 1984). In addition, these models more or less correctly predict the size of the BLR. In the case of NGC 4151 Ferland and Mushotzky (1982) calculated a size of 16 $(n/3x10^9)^{-1/2}$ light days. The observations of Ulrich et al. give a size of 13 light days.

Despite the relative success of these models there still are many difficulties in understanding the broad line regions. First and foremost is the problem of dynamics (Mathews 1982). How do the clouds acquire their high

velocities, are these velocities inflow, outflow, turbulent or rotational? Furthermore the detailed IUE studies of several Seyfert I galaxies show that the line profiles of different lines (e.g. CIV vs. Mg II) are different and change with time. In particular Ulrich et al. (1984) claim that these effects require the existence of several regions of emission of the broad lines. It is also not clear what the detailed geometry of the broad line region is. How are the clouds distributed, what are the shapes of the clouds themselves (pancakes, spheres etc). In addition the field of absorption line spectroscopy of Seyfert galaxies is in its infancy (Penston et al. 1979). It seems clear that in those objects with a large covering fraction, such as NGC 4151, that high resolution absorption line studies of the CIV absorption line will give detailed information on the number of clouds and their sizes relative to the continuum .

In addition to these general problems there still are considerable difficulties in fitting certain lines, in particular the He lines (MacAlpine 1981) and the FeII lines (Netzer et al. this symposium). These two difficulties are rather vexing as the He lines should be easily predictable and the very strong UV lines make the estimates of the total cooling of the deep cool regions where the Hβ lines originate very uncertain. Of course, the nature of the "blue bump" is still very uncertain. If it is related to the lines the photoionization models must be able to account for it.

It seems clear that, at present, we have at least some understanding of the origin of the broad lines in active galaxies and have developed models that, at least computationally, are self consistent and account for many of the observed properties of these objects. However, there is much left to do and many observations are needed to constrain the (more complicated) models that will be developed. While the Space Telescope will be of great use, the monitoring capability of IUE for these variable objects will continue to be very important (see Wamsteker et al. these proceedings). The future of X-ray spectroscopy is much more problematical and hopefully we will not have to wait until AXAF to obtain new results.

Apology : I have not been able in this short paper to truly reference all the excellent work in this field and I apologize to the various workers in the

field for over-referencing my own papers. In such a vast subject ones prejudices have too much room to operate.

Acknowledgements: I would like to thank Gary Ferland and Greg Shields who have taught me what little I know about photoionization models. I also thank Tim Kallman and Dick McCray for very useful discussions. I also thank Yoji Kondo for the opportunity to speak at this symposium.

References

Bechtold, J., Green, R.F., Weymann, R.J., Schmidt, M., Estabrook, F.B., Sherman, R.D., Walhquist, H.D. and Heckman,T.M. 1984, Ap.J. in press
Davidson, K. and Netzer, H. 1979, Rev. Mod. Phys. 51, 715
Ferland, G.J. and Mushotzky, R.F 1982 Ap.J. 262, 564
Ferland, G. and Mushotzky, R.F. 1984 Ap.J. submitted.
Grandi, S.A. 1982 Ap.J. 255, 25
Holt, S.S., Mushotzky, R.F., Becker, R.H., Boldt, E.A., Serlemitsos, P.J., Szymkowiak, A.E. and White, N.E. 1980 Ap.J. Lett 241, L13
Kallman, T.R. and McCray, R.A. 1982 Ap.J. Suppl 50, 263
Kwan, J. and Krolik, J. 1981 Ap.J. 250, 478
Kriss, G.A. 1984 Ap.J. 277, 496
MacAlpine, G. 1981 Ap. J. 251, 465
Malkan,M.A. 1983 Ap.J. 268, 582
Mathews, W.G. 1982 Ap.J. 252, 39
Mendoza, C. 1983 in Planetary Nebulae, IAU Symposium No. 103 D.R. Flower ed.
Mushotzky, R.F. 1982 Ap. J. 256, 92
Mushotzky, R.F. and Ferland, G.J. 1984 Ap. J. in press
Mushotzky, R.F. 1984 in IAU/COSPAR Meeting on High Energy Astrophysics and Cosmology Rojen Bulgaria
Neugebauer G. et al. 1980 Ap.J. 238, 502
Oke, J.B., Shields, G.A. and Korycansky, D.G. 1984 Ap.J. 277, 64
Penston, M.V., Clavel, J., Snijders, M., Boksenberg, A. and Fosbury, R. 1979 MNRAS 189, 45p
Perola, G.C. et al. 1982 MNRAS 200, 293
Petre, R., Mushotzky, R.F., Krolik, J. and Holt, S.S. 1984 Ap. J. in press
Reichert, G., Mushotzky, R.F., Petre, R. and Holt S.S. 1984 in prep
Reichert, G., Mason, K., Thorstensen, J., and Bowyer, S. 1982 Ap.J. 260,437
Rieke, G.H. and Lebofsky, M.J. 1979 Ann. Rev. Astron. and Astrophys. 17, 477
Rothschild, R., Mushotzky, R.F., Baity, W., Gruber, D., Matteson, J. and Peterson, L.E. 1983 Ap.J. 269, 423
Ulrich, M.H. et al. 1984, MNRAS in press
Wu, C.C., Boggess, A. and Gull, T.R. 1983 Ap.J. 266, 28

INTERACTING BINARY SYSTEMS

Jurgen Rahe

Remeis-Observatory, Bamberg
Astronomical Institute, University Erlangen-Nurnberg
Bamberg, Federal Republic of Germany

ABSTRACT

The present paper summarizes the kind of information that has been derived from ultraviolet observations of interacting binary stars and points out problems of current interest. The tasks for observations of close binary systems in the extreme ultraviolet will be discussed in a separate paper.

INTRODUCTION

In view of several recent colloquia, workshops, extensive reviews, and collections of research papers devoted to interacting binary stars, there appears to be little need for another comprehensive review of the properties of interacting binaries as revealed in their ultraviolet spectra. In addition, excellent reviews were given at previous IUE Conferences (Plavec, 1981; Dupree, 1982; McCluskey, 1982; Lambert, 1982; de Loore and Maeder, 1982).

The present paper will therefore only briefly summarize the kind of information that has been derived from ultraviolet observations of interacting binary stars, and point out problems of current interest. Comments for the tasks for observations of close binary systems in the extreme ultraviolet are discussed in a separate contribution. The present paper contains a detailed list of IUE-related papers, with titles which deal with binary star research, and which have been published in the major international astronomical journals since the last IUE Conference, and references to proceedings of meetings devoted to the same subject.

The fact that mass is transferred between the components of close binary systems and lost from the system, as well as the manner in which this is done, is of prime importance to the evolution of close binaries. The last few years have shown a continued strong interest in, and considerable efforts devoted to, the observational and theoretical aspects of this problem.

About 80 IUE related papers dealing with binary star research have been published in the major international astronomical journals in 1982 and 1983; they account for about 20% of all IUE-related publications. In addition, several extended reports or proceedings of international conferences dealing with binaries have been published since 1982.

Recently Observed Properties of Interacting Binaries

From optical photometry and spectroscopy, certain properties of individual components and the presence of circumstellar matter in close binary systems could be derived already at the end of last century. Belopolsky (1893; 1897) detected in Beta Lyrae lines whose Doppler shifts did not follow the motion of either component, and Barney (1923) observed in Algol stationary metallic (Fe, Mg) features which did not show the Doppler shifts of the photospheric lines. A pronounced asymmetry in the radial-velocity curve of the eclipsing binary U Cephei was observed by Carpenter (1930) and Struve (1944), and explained by Struve through "gas streams" within the system. These and subsequent observations, mainly in the ultraviolet spectral range with the Copernicus and especially the IUE satellites, have clearly demonstrated the observational significance of such spectroscopic anomalies. Plasma was observed which for many apparently "normal" binary systems had much higher temperatures than expected from optical observations, and which is generally ascribed to gas streaming from one star to its companion, accretion of matter onto degenerate stars, and considerably enhanced chromospheres and coronae in cooler stars.

In the ultraviolet, multiple emission lines in interacting binaries, i.e., in Beta Lyrae, were for the first time extensively studied by Hack, Hutchings, Kondo, McCluskey, Plavec, Polidan, and others (1975 and subsequent papers). Chapman (1980) reported the first spectroscopic detection of ultraviolet emission lines during the eclipse of Zeta Aurigae. Data on this still mysterious and fascinating binary, and its analysis, belong clearly to the highlights of recent IUE observations.

Zeta Aurigae is the prototype for a group of eclipsing binary systems that consist of a late-type supergiant star and a much smaller, early-type companion. Before and after total eclipse, the light of the companion passes through the extended atmosphere and wind plasma of the supergiant in what is called an atmospheric eclipse.

Chapman (1981) and Ahmad, Chapman and Kondo (1983) have derived a model of the K-star wind, far from the K-star, and its interaction with the B-star. They find a mass loss rate from the K-star of 2×10^{-8} $M_\odot$ yr^{-1}. The rate of accretion by the B-star of material from the K-supergiant is such that the matter accreted in the course of about 10 years is of the order of the total mass of the photosphere of the B-star.

The problem of mass transfer in interacting binaries was during the last several years extensively investigated by several authors. Very detailed studies of a number of different objects have been carried out by Kondo and co-workers; typical examples include Beta Lyrae, U Cephei, UW CMa, and many other systems where especially high resolution IUE spectra reveal the occurrence of mass loss of several 10^{-6} $M_\odot$/year, and loss of angular momentum, often causing a strong period decrease of the order of $\dot{p}/p$ 2×10^{-5}/year.

The expanding gas in Beta Lyrae, e.g., appears to be divided into two regions: a "chromospheric" region with T 10^4K, N_e 10^{12} cm^{-3} which gives rise to the low ionization lines; and a "coronal" region with T 10^5K, N_e 10^{10} cm^{-3} which gives rise to the high ionization lines.

But in spite of such obviously very successful observations and interesting results, I think it is safe to say that the interpretation of the photometric as well as spectroscopic anomalies observed from the ground and in the ultraviolet with the IUE often still present major intriguing problems.

In many binaries, several unusual features are discovered, such as those revealed in the very unusual spectrum of the close binary R Arae, as discussed by Kondo and McCluskey (1983). The outside-eclipse ultraviolet continuum flux varied by more than a factor of 2 in 10 days, and by more than 50 percent within the same orbital cycle. The resonance lines of C II, Si IV, Si II, Fe II and Mg II have P Cygni profiles; their emission component strengths vary with time, while the absorption components reveal both orbital and non-orbital velocity variations. Einstein (HEAO-2) satellite data show this system also to be an X-ray source.

Another very unusual ultraviolet spectrum was reported by Parsons et al. (1983) for HD 207739; it showed abnormally strong and numerous absorption features in the far-UV, and exceptionally strong Mg II emissions. While for R Arae there are as yet no corresponding ground-based observations available, HD 207739 showed very similar phenomena also in the visible spectral range (Kondo, 1984).

Symbiotic stars, Wolf-Rayet binaries and related objects continued to be under close scrutiny, e.g., by Michalitsianos et al. (1982); Sahade et al (1984); Willis (1983); and others; but the complexity of their UV spectra is such that additional observations and interpretations are clearly needed.

Evidence for a high temperature accretion region in Algol-type binary systems was pursued by Peters and Polidan (1984); they observed strong absorption lines of N V, C IV, etc. in the UV spectra of Algol primaries whose photospheric temperatures are much too cool to form such ions.

Anomalies in Zeta Aurigae (Chapman, 1981), Zeta Aurigae-type systems, γ^2 Velorum (Sahade et al., 1984), of UW CMa and other early-type systems (Dupree, Heap, Hutchings, Koch, Plavec, et al.) were interpreted as the effects of winds in these systems.

Winds are considered as the energy source for X-ray emission in massive binaries as a consequence of the interactions of an early-type and a degenerate star (Cyg X-1), of a late type star and a white dwarf (AM Her), or of a normal and a degenerate star (Her X-1).

Special attention is required for systems like Beta Lyrae and Plavec's W Serpentis stars (SX Car, RX Cas, W Ser, U367 Cyg, etc.). According to Plavec (1981), the UV radiation in these systems comes probably from a region which is much smaller than the observed surface and is associated with accretion.

W Serpentis systems have relatively large dimensions, the secondary component is, however, rather small; the outflowing matter has a large angular momentum and forms an accretion disk, similar to the conditions in cataclysmic variables--only that in W Serpentis stars, accretion occurs by a normal B star, not a white dwarf.

A more detailed study of these W Serpentis stars requires, however, additional UV observations, especially at high resolution. Until now, no such high resolution spectrum has been obtained.

Prompted by a growing interest of Western astronomers in binary star research in China, I asked Prof. Shen Liangzhao of Beijing Astronomical Observatory, who is an expert on binary star research in China, for a brief outline of interacting binary star research in China for this meeting. Among other research projects conducted, photoelectric photometry, spectroscopy and radial velocity measurements are carried out with the Beijing 60-cm and the Yunnan 1 m Cassegrain telescopes for short-period eclipsing binaries, with emphasis on W UMa-type stars (Acta Astrophysica Sinica 2, 131; 144, 1982; IBVS No. 2274, 1983; AJ 88, 1679, 1983; etc.); of RS CVn-type binaries; and of long-period binaries during eclipse. The observations are complimented by theoretical studies. I should also point out that a recent report published by the Academia Sinica summarizes astronomical research presently conducted in China.

Until recently, most model computations for the evolution of interacting binaries were carried out under conservative assumptions, e.g., under the assumption that the total mass and the total angular momentum remained the same during the mass transfer phase.

Especially UV observations, however, provided extensive evidence that for a number of binaries where the primary is losing mass, a fraction of the expelled matter leaves the system.

For low-mass systems, calculations including the effects of loss of mass and angular momentum, were carried out by Plavec et al. (1973); for massive systems by de Loore et al. (1979). For massive systems, stellar wind mass losses before the Roche lobe overflow were also taken into account. The evolution of the two components was calculated simultaneously by Helling et al. (1982).

Interpretation of Spectroscopic Anomalies

Although over the years, numerous studies dealt with interaction processes, as well as with the initial conditions leading to mass transfer from one component to the other, the question of mass transfer itself, and a definite identification of escaping mass with spectroscopic anomalies is, however, still not completely and unambiguously solved (see, e.g., Plavec, 1968, Kopal, 1971, 1978, 1983; Paczynski, 1971; McCluskey, 1982). On several occasions, Kopal has commented on the problems that are involved when physical models for interacting binaries are constructed based on photometric and spectroscopic observations; he has enumerated several "caveats" arising in this connection (cf. p. 472 of Kopal, 1978; p. 555 of Kopal, 1981), some of which might also be mentioned in the present paper.

In problems characterized by very many degrees of freedom, as is the case with interacting binaries, it is virtually hopeless to try to arrive at their solution without the support of adequate physical theory.

The phenomena exhibited by close binary systems can only be interpreted in the framework of hydrodynamics (or hydromagnetics) of radiating media, and not particle mechanics. If the motions of atoms or ions which are observed in interacting binaries could be described by collisionless particle trajectories, the density of the gas consisting of such particles would be too low by many orders of magnitude for any kind of observational detection.

One should also remember that the concept of critical Roche equipotential surface as defined conventionally--and used continuously--is of significance only for equilibrium configurations, and becomes physically irrelevant in the presence of motion, or in the presence of a strong field of radiation. Respect should be paid to the Roche lobe whenever it is deserved; but its concept should not be abused and stretched to cases where it no longer applies--such as those involving gas motions, where it is the Jacobi integral which should take its place; or the Bernoulli integral in the case of fluid flow.

A loss or transfer of mass in close binary systems is related with any period changes by equations which are of vector (not scalar) form. In order to specify any period change, one needs to know not only the amount of mass involved in the process, but also the velocity and direction of escape, as well as the region of the star's surface from which the escape may take place.

Finally, before one goes too far speculating on the effects which "shells", "rings", "mass exchange," etc., may produce in the observations, one should address the questions on how, and by which process, could such formations have come into being; if they did, what their lifetime would be; what would maintain them; what would prevent their dissolution; and whether the contemplated formation would be necessary, or only optional, to produce the observed effects.

After these words of caution, we should continue in further pursuit of the goal, to better understand the origin and evolution of close binary systems--strongly supported by IUE and its superb staff, especially Drs. Boggess and Kondo here at Goddard, and Drs. Benvenuti and Wamsteker at Vilspa.

Acknowledgements

It is a pleasure to thank especially Drs. Chapman, Kondo and Kopal for stimulating discussions and contributions.

References

Listed are publications dealing with ultraviolet (mostly IUE) observations of binary stars that have been published in the major international astronomical journals (such as A&A, AJ, ApJ, MNRAS, PASP) since 1982.

Ahmad, I.A., Chapman, R.D., Kondo, Y.: Mg II Profile Variations of Zeta Aurigae. A&A 126, L5, 1983.

Allen, D.A.: The Symbiotic Star H1-36. MNRAS 204, 113, 1983.

Altamore, A., Giangrande, A., Viotti, R.: The Ultraviolet Spectrum of KO Puppis (Boss 1985). A&A Suppl. 49, 511, 1982.

Ayres, T.R. and Linsky, J.L.: Outer Atmospheres of Cool Stars I. HR 1009 at Quadrature, ApJ 254, 168, 1982.

Barney, I.: The Spectrum of Algol, AJ 35, 95, 1923.

Belopolsky, A.A.: Mem. Soc. Spettr. Ital. 22, 101, 1893.

Belopolsky, A.A.: Mem. Soc. Spettr. Ital. 26, 135, 1897.

Blair, W.P., Stencel, R.E., Feibelman, W.A., and Michalitsianos, A.G.: Spectrophotometric Observations of Symbiotic Stars and Related Objects, ApJ Suppl 53, 573, 1983.

Bonnet-Bidaud, J.M., Mouchet, M., Motch, C.: First Ultraviolet Observations of Two New Cataclysmic Variables 1E0643-1648 and 4U1849-31, A&A 112, 355, 1982.

Bradt, H.V.D., McClintock, J.E.: The Optical Counterparts of Compact Galactic X-Ray Sources. Ann. Rev. Astron. Astrophys. 21, 1983.

Budding, E., Kadouri, T.H., Gimener, A.: IUE Observations of Certain Short Period RS CVn-Like Stars, Astrophys. Space. Sc. 88, 453, 1982.

Cardelli, J.A. and Bohm-Vitense, E.: The Interstellar Absorption-Line Spectrum of Mu Ophiuchi, ApJ 262, 213, 1982.

Carpenter, E.F.: U Cephei: An Anomalous Spectrographic Result, ApJ 72, 205, 1930.

Castelli, F., Hoekstra, R., and Kondo, Y.: The Mid-Ultraviolet Spectrum of Epsilon Aurigae, A&A Suppl 50, 233, 1982.

Chapman, R.D., Nature 286, 580, 1980.

Chapman, R.D.: The 1979-80 Eclipse of Zeta Aurigae I. The Circumstellar Envelope, ApJ 248, 1043, 1981.

Chapman, R.D., Kondo, Y., Stencel, R.E.: The Partial Phase of the Eclipse of Epsilon Aurigae, ApJ 269, L17, 1983.

Che, A., Hempe, K., Reimers, D.: A Study of Ultraviolet Spectra of Zeta Aur/VV Cep Systems. II. Mass Loss of Supergiants in Zeta Aur, 32 Cyg, and 31 Cyg, A&A 126, 225, 1983.

Cordova, F.A. and Mason, K.O.: High-Velocity Winds from a Dwarf Nova During Outburst, ApJ 260, 716, 1982.

Cugier, H. and Molaro, P.: High Rotational Velocity of a Region around the Primary of Algol, A&A 128, 429, 1983.

Davis, R. and Hartmann, L.: Constraints of the Inclination and Masses of the HDE 226868/Cygnus X-1 System from the Observations, ApJ 270, 671, 1983.

de Loore, C. and Maeder, A.: Stellar Evolution after IUE: I. Massive Stars during Core Hydrogen Burning and Massive Close Binaries, 3rd Europ. IUE Conf. ESA SP-176, p. 15, 1982.

de Loore, C., Hellings, P., Lamers, H.J.G.L.M.: IAU-Symp. 99, 1982.

Deuel, W., and Nussbaumer, H.: The Evidence for Shell Formation in V1016 Cygni, ApJ 271, L19, 1983.

Dominy, J.F. and Lambert, D.L.: Do All Barium Stars have a White Dwarf Companion? ApJ 270, 180, 1983.

Drechsel, H. and Rahe, J.: On the Ionization and Velocity Structure of Expanding Circumstellar Envelopes, A&A 106, 70, 1982.

Drechsel, H., Rahe, J., Wargau, W., Wolf, B.: The Interacting Early-Type Contact Binary SV Centauri, A&A 110, 246, 1982.

Drilling, J.S. and Schonberner, D.: The Hot Component of KS Persei (HD 30353), A&A 113, L22, 1982.

Dupree, A.K., Hartmann, L., and Raymond, J.C.: Ultraviolet Spectroscopy of Binary Systems in "Close Binary Stars", p. 39, 1980.

Dupree, A.K.: Mass Loss from Cool Stars - Facts, Fads and Fallacies, Adv. UV Astron. 3, 1982.

Eaton, J.A.: Chromospheric Emission of W Ursae Majoris-Type Stars and its Relation to the Structure of Their Common Envelopes, ApJ 268, 800, 1983.

Feibelman, W.A.: Ultraviolet Shell Formation at V1016 Cygni, ApJ 263, L69, 1982.

Feibelman, W.A., and Kaler, J.B.: The Binary Central Star of the Planetary Nebula LT-5, ApJ 269, 592, 1983.

Ferland, F.J., Lambert, D.L., McCall, M.L., Shields, G.A. and Slovak, M.H.: Physical Conditions in the Accretion Disk of V603 Aquilae, ApJ 260, 794, 1982.

Fitzpatrick, E.L.: The Detection of Ultraviolet Photospheric Absorption in the Spectra of Two Wolf-Rayet Stars, ApJ 261, L91, 1982.

Fitzpatrick, E.L., Savage, B.D., Sitko, M.L.: Ultraviolet Visual and Infrared Observations of the WC7 Variable HD193793, ApJ 256, 578, 1982.

Friedjung, M., Andrillat, Y., Puget, P.: The UV Spectrum of the Old Nova HR Del at Different Orbital Phases, A&A 114, 351, 1982.

Friedjung, M., Stencel, R.E., Viotti, R.: Evidence for a Warm Wind from the Red Star in Symbiotic Binaries, A&A 126, 407, 1983.

Greenstein, J.L., and Oke, J.B.: RW Sextantis, A Disk with a Hot, High-Velocity Wind, ApJ 258, 209, 1982.

Hack, M.: IUE Observations of Symbiotic Stars, Adv. UV Astron. 89, 1982.

Hack, M., Hutchings, J.B., Kondo, Y., McCluskey, G.E., Plavec, M.J. and Polidan, R.S.: The Ultraviolet Spectrum of Beta Lyrae, ApJ 198, 453, 1975.

Hamer, D.L., Stickland, D.J., Lloyd, C., Hamer, C.F.W., Pike, C.D., Croft, D.: A Study of the Binary System 58 Persei, MNRAS 204, 927, 1983.

Heap, S.R.: Winds in Close Binary Stars: Assymmetries in the Wind of UW CMa, ApJ, 1984.

Heape, K.: A Study of Ultraviolet Spectra Zeta Aur/VV Cep Systems I. Resonance Line Formation, A&A 115, 133, 1982.

Hellings, P., Vansina, F., Packet, W., Doour, C., de Oreve, J.P., de Loore, C.M.: Pro. IAU Symp. 99, 1982.

Holm, A.V., Panek, R.J., Schiffer, F.H.: Ultraviolet Spectrum Variability of UX Ursae Majoris, ApJ 252, L35, 1982.

Howarth, I.D. and Wilson, B.: A Study of the Low-Mass X-Ray Binary HZ Her/ HER X-1 Using IUE and Optical Data, MNRAS 202, 347, 1983.

Howarth, I.D., and Wilson, B.: HZ Her: The Nature and Origin of the Emission Lines, MNRAS 204, 1091, 1983.

Hutchings, J.B. and Cowley, A.P.: The UV Spectrum of the Symbiotic Binary AR Pavonis During Eclipse Egress, PASP 94, 107, 1982.

Hutchings, J.B., Cowley, A.P., Ake, T.B., and Imhoff, C.L.: The 1982 Ultraviolet Eclipse of the Symbiotic Binary AR Pavonis, ApJ 275, 271, 1983.

Hutchings, J.B. and Massey, P.: IUE Studies of the Wolf-Rayet Binaries HD 186943 and HD 211853 During Eclipse, PASP 95, 151, 1983.

Jameson, R.F., King, A.R., and Sherrington, M.R.: Infrared, Optical and Ultraviolet Observations of TT Ari, MNRAS 200, 455, 1982.

Kafatos, M., Michalitsianos, A.G., Feibelman, W.A.: IUE Observations of the Peculiar Star RX Puppis, ApJ 257, 204, 1982.

Kindl, C., Marxer, N., Nussbaumer, H.: Interpretation of Line Profiles of the Symbiotic Star V1016 Cygni, A&A 116, 265, 1982.

King, A.R., Frank, J., Jameson, R.F., Sherrington, M.R.: Phase-Dependent UV Spectra of UX Ursae Majoris, MNRAS 203, 677, 1982.

Klare, G., Krautter, J., Wolf, B., Stahl, O., Vogt, N., Wargan, W., Rahe, J. IUE Observations of Dwarf Novae During Active Phases, A&A 113, 76, 1982.

Kondo, Y., private communication, 1984.

Kondo, Y., McCluskey, G.E., Wu, C.C.: The Early Type Component in Nu-1 Sagittarii, PASP 94, 647, 1982.

Kondo, Y., Van Flandern, T. C., Wolff, C.L.: On the Clock Mechanism and the Implausibility of the 35 day Precessing Disk in HZ Herculis/Hercules X-1, ApJ 273, 716, 1983.

Kopal, Z.,: Evolution in Close Binary Systems, PASP 83, 521, 1971.

Kopal, Z.,: Dynamics of Close Binary Systems, Reidel, 1978.

Kopal, Z.: Language of the Stars: A Discourse on the Theory of Eclipsing Variables, Astrophys. Space Sc. Library, Vol. 77, 1981.

Kopal, Z.: Gas Streams in Close Binary Systems in Photometric and Spectroscopic Binary Systems, p. 535, E.B. Carling, Z. Kopal, eds', Reidel 1981.

Kudritzki, R.P., Simon, K.P., Lynas-Gray, A.E., Kilkenny, D., Hill, P.W.: LB 3459 - An O-Type Subdwarf Eclipsing Binary System. Non-LTE Analysis of the Primary, A&A 106, 254, 1982.

Lambert, D.L.: Binary Stars: Mass Transfer and Chemical Composition, Adv. UV Astron., 114, 1982.

Landtsheer, A.C. and Mulder, P.S.: IUE Observations of the Eclipsing Binaries TV Cas and YZ Cas, A&A 127, 297, 1983.

Mason, K.O. and Cordova, F.A.: Ultraviolet Spectrophotometry of 2A 1822-371: A Bulge on the Accretion Disk, ApJ 255, 603, 1982.

McCluskey, G.E.: IUE Spectroscopic Investigation of Interacting Binary Systems, Adv. UV Astron. 102, 1982.

McCluskey, G.E. and Kondo, Y.: International Ultraviolet Explorer Observations of the Peculiar Variable Spectrum of the Eclipsing Binary R Arae, ApJ 266, 755, 1983.

Michalitsianos, A.G., Kafatos, M., Feibelman, W.A. and Hobbs, R.W.: Ultraviolet Observations of Four Symbiotic Stars, ApJ 253, 735, 1982.

Michalitsianos, A.G., Kafatos, M., Feibelman, W.A., and Wallerstein, G.: A Brightening of the Symbiotic Variable SY Muscae, A&A 109, 136, 1982.

Nousek, J.A., Pravdo, S.H.: IUE Observations of E1405-451: A New AM Herculis Type Cataclysmic Variable, ApJ 266, L39, 1983.

Nussbaumer, H., Schmutz, W., Smith, L.J., Willis, A.J.: IUE Ultraviolet Spectrophotometry of 15 Galactic Wolf-Rayet Stars, A A Supp 47, 257, 1982.

Nussbaumer, H., Schmutz, W.: The Ultraviolet Variability of the Symbiotic Star HBV 475, A&A 126, 59, 1983.

Oliversen, N.A. and Anderson, C.M.: Observational Studies of the Symbiotic Stars. II. Emission-Line Relative Intensity Variations in CI Cygni, BF Cygni, AX Persei and V1016 Cygni, ApJ 268, 250, 1983.

Paczynski, B., Ann. Rev. Astron. Astrophys. 9, 183, 1971.

Parsons, S.B.: Ultraviolet Spectroscopy of F and G Supergiants with IUE II: The Hot Companions of HR 2786 and HR2859, PASP 94, 642, 1982.

Parsons, S.B.: Ultraviolet and Optical Studies of Binaries with Luminous Cool Primaries and Hot Companions. III. Reticon Radial Velocities, ApJ Suppl 53, 553, 1983.

Parsons, S.B., Holm, A.V., Kondo, Y.: HD 207739: A Strange Composite Star, ApJ 264, L19, 1983.

Peters, G.J. and Polidan, R.S.: Evidence for a High Temperature Accretion Region in Algol-Type Binary Systems, ApJ, 1984.

Plavec, M.J.: Adv. Astron. Astrophys 6 (Z. Kopal ed), 202, 1968.

Plavec, M.J., Weiland, J.L, Koch, R.H.: Energy Distribution in the Strongly Interacting Binary System SX Cassiopeiae, ApJ 256, 206, 1982.

Plavec, M.J.: Far-Ultraviolet Emission Lines in U Cephei: Evidence for a Hot, Turbulent Circumstellar Envelope, ApJ 275, 251, 1983.

Plavec, M.J. and Dobias, J.J.: RW Tauri as a Weak W Serpentis Star, ApJ 272, 206, 1983.

Plavec, M.J.: The Impact of IUE on Binary Star Studies, Universe at UV Wavelengths, 397, 1981.

Reimers, D., and Schroder, K.P.: A Study of UV Spectra of Zeta Aur/VV Cep Stars, IV. System Parameters and Mass-Loss of Delta Sge, A&A 124, 241, 1983.

Ringuelet, A.E., Sahade J., Rovira, M., Fontenla, J.M. and Kondo, Y.: Simultaneous IUE and Ground-Based Observations of V 923 Aquilae, A&A 131, 9, 1984.

Rucinsky, S.M. and Vilhu, O: IUE Observations of W UMa-Type Stars, MNRAS 202, 1221, 1983.

Sahade, J. and Ferrer, O.E.: Ground-Based and IUE Spectral Observations of AU Monocerotis, PASP 94, 113, 1982.

Sahade, J., Kondo, Y, McCluskey, G.E.: Comments on the Ultraviolet Spectrum of Gamma 2 Velorum, ApJ 276, 281, 1984.

Shu, F.H. and Lubow, S.H.: Mass, Angular Momentum, and Energy Transfer in Close Binary Stars, Ann. Rev. Astron. Astrophys. 19, 277, 1981.

Schindler, M., Stencel, R.E., Linsky, J.L., Basri, G.S., and Helfand, .DJ.: UV and X-Ray Detection of 56 Pegasi (KO IIp+WD): Evidence for Accretion of a Cool Wind onto a White Dwarf, ApJ 263, 269, 1982.

Smith, L.J. and Willis, A.J.: UV and Visible Spectrophotometry of Nine LMC Wolf-Rayet Stars, A&A Suppl 54, 229, 1983.

Stencel, R.E. and Chapman, R.D.: The 1979-1980 Eclipse of Zeta Aurigae II. The Emission Spectrum, ApJ 251, 597, 1981.

Stencel, R.E., Michalitsianos, A.G., Kafatos, M. and Boyarchuk, A.A.: Ultraviolet Observations of the 1980 Eclipse of the Symbiotic Star CI Cygni, ApJ 253, L77, 1982.

Struve, O.: The Spectrographic Problem of U Cephei, ApJ 99, 222, 1944.

Szkody, P.: Ultraviolet Comparisons of Normal Outbursts and a Supermaximum in Two Dwarf Novae, ApJ 261, 200, 1982.

Szkody, P. and Shafter, A.W.: A Multiwavelength Study of the Short-Period Cataclysmic Variable V442 Ophiuchi, PASP 95, 509, 1983.

Underhill, A.B.: The Angular Diameters, Effective Temperatures, Radii, and Luminosities of 10 Wolf-Rayet Stars, ApJ 266, 718, 1983.

Van der Klis, M., Hammerschlag-Hensberge, G., Bonnet-Bidaud, J.M., Ilovaisky, S.A., Mouchet, M., Glencross, W.M., Willis, A.J., van Paradise, J., Zuiderwijk, E.I., Chevalier, C.: A Study of Ultraviolet Spectroscopic and Light Variations in the X-Ray Binaries LMC X-4 and SMC X-1, A&A 106, 339, 1982.

Vilhe, O. and Rucinski, S.M.: Period-Activity Relations in Close Binaries, A&A 127, 5, 1983.

Viotti, R., Ricciardi, O., Ponz, D., Giangrande, A., Friedjung, M., Cassatella, A., Baratta, G.B., Altamore, A.: IUE Observations of the High Velocity Symbiotic Star AG Draconis During Active Phase, A&A 119, 285, 1983.

Wargau, W., Drechsel, H., Rahe, J., Vogt, N.: New Evidence of Strong UV Radiation in TT Ari, A&A 110, 291, 1982.

Willis, A.J.: P-Cygni Profiles Observed in the Ultraviolet and Visible Spectra of Wolf-Rayet Stars, MNRAS 198, 897, 1982.

Willis, A.J. and Stickland, D.J.: The Enigmatic Composite System HD 45166 - B8 V + q WR or SdO? MNRAS 203, 619, 1983.

Proceedings of Conferences Dealing with Binary Star Research and Published since 1982.

Photometric and Spectroscopic Binary Systems. Proc. NATO Advanced Study Inst., Maratea, Italy, E.B. Carling, Z. Kopal, eds., Reidel, 1982.

Reports on Astronomy. Transaction IAU Vol. 18A, p. 553-577, Reidel, 1982.

Proc. 18th General Assembly IAU, Patras, 1982. R.M. West, ed., Transactions IAU, Vol. 18B, Reidel, 1982.

Binary and Multiple Stars as Tracers of Stellar Evolution. Proc. IAU Coll. No. 69. Z. Kopal, J. Rahe, eds., Reidel, 1982.

Wolf-Rayet Stars: Observations, Physics, Evolution. Proc. IAU Symp. 99, C. de Loore and A.J. Willis, eds., Reidel, 1982.

Ultraviolet and X-Ray Observations of Close Binaries from Space. Y. Kondo, ed. in Highlights of Astronomy, R.M. West, ed., Vol. 6, p. 637, Reidel, 1983.

Cataclysmic Variables and Related Objects. Proc. IAU Coll. No. 72, M. Livio, G. Shaviv, ed., Reidel, 1983.

Double Stars, Physical Properties and Generic Relations. Proc. IAU Coll. No. 80, B. Hidayat, Z. Kopal, J. Rahe, eds., Reidel, 1984.

Outer Atmospheres of Cool Stars Observed with IUE

S. L. Baliunas

Harvard-Smithsonian Center for Astrophysics
Cambridge, Massachusetts 02138

I. INTRODUCTION

The outer atmosphere of the Sun is a plasma where complex magnetic fields play a prevailing role. The magnetic fields not only govern the morphology but also influence the energy balance throughout the outer atmosphere. The magnetic field varies, in strength and structure, over a wide range of temporal and spatial scales. These variations in the magnetic field of the solar atmosphere produce the myriad of time-variable phenomena labeled "solar activity." The importance of magnetic fields in solar activity is underscored by the wide variety of phenomena controlled by the interplay of magnetic fields, from ephemeral solar flares to the long-term sunspot cycle.

The chromosphere, transition region, corona and solar wind comprise the outer solar atmosphere. The temperature in these outer layers can be vastly hotter than that of the solar photosphere. The elevated temperatures are powered by heating mechanisms that dominate the radiative losses and other cooling mechanisms in these layers (cf. Stein and Leibacher 1974; Linsky 1980; Baliunas 1983). In the quiet Sun, for example, the gradual rise in temperatue through the chromosphere ($5000 \lesssim T \lesssim 20{,}000$K) is partially caused by the damping of short-period acoustic waves generated by the subsurface convective layer (cf. Ulmschneider 1981; Ulmschneider and Stein 1982). The sharp increase in temperature through the transition zone ($20{,}000\text{K} \lesssim T \lesssim 10^6$K) is fueled by the loss of efficient radiators present in the lower chromosphere (for example, H I Ly α, Ca II H and K and Mg II h and k emissions) and by conductive heating downward from the corona. The temperature of the corona ($T \sim 1\text{-}2 \times 10^6$K) is likely maintained by the deposition energy by magnetic mechanisms offset by partial cooling provided by the solar wind and by radiative cooling in the X-ray and extreme ultraviolet spectrum. Such a simplified picture neglects the imperspicuous impact of, for example, magnetic processes which may also be a source of non-radiative heating in the outer solar atmosphere (cf. Stein and Leibacher 1974; Ulmschneider and Stein 1982).

Studies of the outer atmosphere of the Sun and its magnetic fields benefited greatly from ultraviolet and X-ray measurements over the past two decades. The visible face of the solar photosphere and glimpses of the chromospheres available from the ground were augmented by high-spectrum and spatial-resolution observations of the chromosphere, transition region and corona and solar wind available from space-based missions such as Skylab/Apollo Telescope Mount. Theoretical modeling has made great strides in our understanding of the energy balance through the outer solar atmosphere and the mechanisms

powering solar magnetic phenomena.

Fundamental studies of stellar chromospheres of cool stars were accomplished about three decades ago from ground-based observations, primarily of the Ca II H and K emission cores. Stellar activity in the guise of the Ca II H and K cores was noted to be ubiquitous among stars later than about spectral type mid-F. It is reasonable to assume that the impact of magnetic fields on the Sun is similar to that inferred from Ca II emission on other stars. It is also tempting to assume that the mechanisms powering the entire solar atmosphere, not only the chromosphere, are valid for other stellar atmospheres as well. Under the tutelage of solar activity, studies of stellar activity in cool stars burgeoned with the opening of X-ray and ultraviolet windows. The experiments on satellites, for example, SAS-3 and *Copernicus*, along with rocket-borne experiments of the early 1970's, indicated the direction along the road paved by recent satellites such as HEAO-1, HEAO-2 and *IUE*. The *IUE* satellite has opened a window into the ultraviolet spectrum in a variety of cool stars, many of which resemble the solar ultraviolet spectrum, and many of which do not. *IUE* is providing guidelines for theoretical work on atmospheric heating mechanisms which is driven by logical positivism.

In a way similar to the studies of stellar chromospheric Ca II H and K of 30 years ago we seek answers to questions such as: Are the mechanisms exciting the outer solar atmosphere present on other stars? What influences and controls these processes, and in particular, what is the role of the magnetic fields? Ultraviolet observations of cool stars in conjunction with coronal X-ray or ground-based chromospheric measurements, or both, have served both to refine and to define our understanding of stellar activity.

The sensitivity of *IUE* down to a reasonable limiting magnitude put many different stars' ultraviolet spectra at our fingertips. Understanding of stellar activity throughout stellar atmospheres has progressed because we can observe in the ultraviolet particular stars in great detail and many stars in snapshot surveys.

II. RESULTS OF ULTRAVIOLET SURVEYS

The advent of *IUE* provided ultraviolet spectra of stellar chromospheres, transition regions, and winds indicated by features accessible to the range 5×10^3 - 2×10^5K. Figure 1 (upper panel) shows the low-dispersion, short-wavelength spectrum of a dwarf star, ξ Boo A (G8V), with relatively strong chromospheric emission compared to the quiet Sun. The canonical "solar-like transition-region features" such as Si IV (λ1400), C IV (λ1550) and N V (λ1240) indicate the presence of plasmas of temperatures up to $T \sim 2 \times 10^5$K, the temperature of formation of N V, in the dwarf ξ Boo A. There is bright Mg II h and k (λ2800) chromospheric emission in this active star as well. On the other hand, the cool giant β And (MO III), while lacking in observable amounts of high-temperature transition-region material typified by C IV and N V, does show chromospheric emission formed at temperatures less than 20,000K (lower panel, Figure 1). In addition to these two broad categories of short-wavelength *IUE* spectra, namely, the "solar-like" and "non-solar-like" transition-region spectra,

there is a third. The supergiant α Aqr (G2Ib) (middle panel, Fig. 1) possesses not only a "solar-like" transition region with N V, C IV and Si IV, but also evidence of a strong wind in the form of Mg II circumstellar absorption blue-shifted by about -70 km s^{-1}. The supergiant α Aqr is one of the "hybrid" stars. Winds and mass loss will be discussed further below, following an investigation of the parameters governing ultraviolet emission in dwarf stars.

A. Chromospheric Emission in Main-Sequence Stars

Along the lower main sequence, the chromospheric emission strength denoted by Ca II H and K emission is correlated with relative youth and rapid rotation in single stars. It should be noted parenthetically that rapid rotation can be the result of youth or duplicity, a condition inducing rapid rotation by tidal forces in close binary systems. The conclusion that chromospheric emission decays with time for single, main-sequence stars resulted from studies of stars whose ages could be determined, either by membership in galactic clusters or by models of lithium depletion in field stars (Wilson 1963; Skumanich 1972; Duncan 1981). Further, for dwarf stars of a given mass, Ca II chromospheric emission was linearly correlated with rotational velocities (Kraft 1967; Skumanich 1972; Soderblom 1982). The dependence of emission upon rotation and the decay of emission with time led to the conclusion that rotation and emission decreased approximately with a square-root dependence on stellar main-sequence age (Skumanich 1972). Qualitatively, the action of a magnetic dynamo links the stellar magnetic fields and rotation with chromospheric, and presumably coronal emission (cf. Skumanich and Eddy 1981).

With *IUE* the chromospheric indicator provided by the flux in the Mg II h and k emissions can be investigated among main-sequence stars. Two parallel studies of the dependence of Ca II H and K (Noyes *et al.* 1984) and Mg II h and k (Hartmann *et al.* 1984*a*) show the same phenomena controlling both chromospheric indicators. In Figure 2, the total stellar surface flux in Mg II (h + k), normalized by the stellar bolometric luminosity, is plotted as a function of the quantity (τ/P) in main sequence stars. The quantity P is the measured rotation period (Vaughan *et al.* 1981, Baliunas *et al.* 1983*a*), and τ is a function of (B-V) color, or equivalently, the lower main-sequence mass, only. Noyes *et al.* (1984) suggested that τ could represent the convective turnover time for stellar interior models where the mixing-length parameter α = 2 pressure scale heights. The solid line is the vertically-scaled relation for the (Ca II, τ/P) fifth derived by Noyes *et al.* 1984).

As expected, Mg II, as well as Ca II, is not only dependent upon rotation, but also on color, or main-sequence mass. The small scatter for both Mg II and Ca II reveals that both rotation and main-sequence mass, or by inference, convective zone properties, dictate the level of chromospheric emission in dwarf stars. The ratio of the convective turnover time to the rotation period is the inverse of the Rossby number, a parameter fundamental in stellar dynamo theory (cf. Parker 1979). This important result indicates that there is a single determinant of chromospheric activity in lower main-sequence stars that is characterized by the Rossby number and therefore closely linked to dynamo theory.

B. Transition-Region Emission in Main-Sequence Stars

Among the dwarf stars, rapid rotation produces enhanced fluxes in, for example C IV (Hartmann *et al.* 1979; Schrijver *et al.* 1984), the expected result because the transition-region emission is well-correlated with chromospheric fluxes (Hartmann *et al.* 1979; Dupree *et al.* 1979; Ayres *et al.* 1981; Hartmann *et al.* 1982*a*). As a function of age, the cool dwarf stars, from T Tauri stars to the Sun, show a pronounced decay of flux with time (Boesgaard and Simon 1982; Walter *et al.* 1984). The fluxes of the high-temperature species, such as He II, C II, C IV, N V and Si IV, are approximately inversely proportional to age, unlike the chromospheric emissions that show a dependence of fluxes proportional to the inverse square root of time. The different behavior of the chromospheric and transition region fluxes as a function of activity level can be stated alternatively. Figure 3 shows the surface fluxes, relative to those of the quiet Sun, for a variety of stars. The quiet dwarf δ Pavonis has a relative paucity of the transition-region material, while active dwarf stars, whose surface fluxes can be factors of 10-100 above that of the quiet Sun, display an increasing enhancement of high-temperature gas as flux levels increase (Hartmann *et al.* 1979; Ayres *et al.* 1981; Hartmann *et al.* 1982*a*). With greater activity, the emission increases faster in the transition region than it does in the chromosphere.

This behavior was noted for the active portions of the Sun relative to the quiet (Dupree *et al.* 1973) and other active-chromosphere stars observed with *IUE* whose surface fluxes and transition-region pressures are similar to those in the active Sun (Dupree *et al.* 1979; Baliunas *et al.* 1979; Ayres *et al.* 1981; Hartmann *et al.* 1982*a*). Undoubtedly the increased role of conduction in dominating the radiative losses in these higher-pressure transition regions of the active stars causes the relative enhancement of the fluxes of the high-temperature ions, as inferred from the quiet and active Sun (Dupree *et al.* 1973; Baliunas and Dupree 1982).

In dwarf stars, a comparison of the total radiative losses in the chromosphere, transition region and corona suggests that for quiet-chromosphere stars, the chromospheric losses dominate. With increasing activity, the losses throughout the atmosphere increase in a comparable fashion. Hence, the enhancements become largest in the transition region and corona as activity levels progressively increase among stars (Hartmann *et al.* 1982*a*; Hartmann 1983; Hammer *et al.* 1982).

The relative emission measures for the transition region and X-ray measurements agree reasonably well with simple, static "loop" models such as those of Rosner *et al.* (1978; cf. Hartmann *et al.* 1982*a*). Because these loop models explain a range of chromospehric activity in dwarf stars, energy budgeting processes found on the Sun must also behave similarly in other stars.

C. Chromospheric and Coronal Emission in Giant Stars

A survey of F5 III-KO III stars with *IUE* (Simon 1984) reveals that the C IV flux, as a fraction of bolometric luminosity, increases from F5 III to a

maximum at GO III, then sharply declines to limits of detectability at type KO III. The stars earlier than about G2 III are first crossing stars, that is, they are in a state subsequent to departure from the main sequence but prior to ascension to the red-giant branch where helium ignites in the core. The relative increase in C IV fractional emission between F5 III and GO III might be attributed to the development of convective zones that power the chromospheric emission in these stars. In addition, Simon (1984) finds a good correlation between fractional C IV flux and projected rotational velocity. Thus, for giant stars initially exiting from the main sequence, the chromospheric and coronal emission is controlled by the same factors as in main-sequence stars: rotation and depth of the convective zone.

Beyond the spectrum type of late G-giants, however, the sample of giants becomes mixed with second crossing, or post helium flash, stars and the picture of chromospheric and coronal emission becomes murky. One puzzle, however, is apparent among these evolved cool stars. In the Hyades, there are four KO III cluster stars that are presumably homogeneous and coeval. The range in C IV emission is at least a factor of six (see Figure 4) and no obvious macroscopic parameter, such as age or rotation can reasonably account for the discrepancy (Baliunas *et al.* 1983*b*; Böhm-Vitense 1984). Two proposals have been forwarded to account for the range in ultraviolet emission in these stars. For example, the Hyades giants do differ slightly in photospheric effective temperature (but only by as much as about 200K) and a steep dependence of chromospheric heating may exist to produce the wide range of C IV emission (Böhm-Vitense 1984). Alternatively, the giants may have been sampled at random phases of long-term activity cycles analogous to those common in main-sequence stars (Baliunas *et al.* 1983*b*). In either case, the disparity in emission levels in stars thought to be so similar in macroscopic characteristics indicates that a hidden parameter controlling the emission in evolved stars remains to be discovered.

D. Winds and Mass Loss in Evolved Stars

For evolved stars, chromospheric emission is also present, and in addition the extended atmospheres of these stars are cool and can possess strong winds and circumstellar shells. Compared to solar wind, with a temperature of $T \sim 10^6$K, and a mass loss rate, $\dot{m} \sim 10^{-14}$ $M_\odot$ yr^{-1}, the winds in giants and supergiants reach temperatures of only $T \sim 10^4$K with large mass loss rates, $\dot{m} \sim 10^{-6}$ $M_\odot$ yr^{-1} (Linsky and Haisch 1979; Hartmann *et al.* 1982*a*).

These extremes in the winds of cool stars are readily observable in the ultraviolet with *IUE*. On the one hand, the "solar-type" outer atmosphere, showing as it does a temperature rise of over two orders of magnitude from the chromosphere to the wind produces signatures of plasmas accessible from *IUE* from T ~ 5000 to 200,000K. On the other hand, a cool giant star(for example, β And, Fig. 1) lacks observable amounts of these ions and this lack would suggest little gas, if any, exists at temperatures of $T \sim 10^5$K. Spectrum features seen in the ultraviolet in β And are formed at temperatures cooler than about 20,000K. While β And does possess a chromosphere, it does *not* maintain a "solar-like" transition region. The hot transition zones avoid stars in the upper

right of the H-R diagram.

This dichotomy between "solar-like" and "nonsolar-like" outer atmospheres (Linsky and Haisch 1979) is also manifest in the chromospheric Mg II h and k features observed at high-resolution (~ 0.2Å) with the long-wavelength camera of *IUE* (cf. Figure 1). The strong Mg II k (λ2795) emission core of ξ Boo A is symmetric, while that of β And is asymmetric. The deep central reversal of the emission core in β And is caused in part by absorption by interstellar Mg II, but the strong asymmetry, with the blue-shifted emission peak weaker than the red-shifted peak is likely caused by an outwardly-expanding wind at these temperatures. The mass-loss rate in β And is modest, so little circumstellar absorption is apparent. The disappearance of observable hot transition-region material occurs with the appearance of circumstellar shell absorption lines and chromospheric Mg II and Ca II line asymmetries indicating mass loss in the upper-right of the H-R diagram (Reimers 1977; Stencel 1978; Stencel and Mullan 1980).

The possible explanation for this seemingly unbroachable dichotomy of the ultraviolet character of cool outer atmospheres must be examined in light of a new category of ultraviolet spectra: the "hybrid" stars. Also shown in Figure 1, the star α Aqr (G2 Ib) possesses the hot transition-region lines such as Si IV, C IV and N V. The Mg II k line, however, is strongly asymmetric, with the blue peak depressed relative to the red, similar to that of β And and indicative of outflows in the extended atmosphere. In addition there is a strong circumstellar shell, at the relatively cool temperature of Mg II, but blue-shifted by about -70 km s^{-1}, *prima facie* evidence of a strong stellar wind.

The hybrid stars, such as α Aqr (G2 Ib), β Aqr (GO Ib), α TrA (K1 II), θ Her (K3 II), γ Aql (K3 II) and ι Aur (K3 II) (Hartmann *et al.* 1981, 1984*b*; Reimers 1982) provide a link between the hot, rarefied winds similar to that in the Sun, and the cool, dense winds in the cool supergiants. The hybrid stars populate an intermediate domain of modest winds yet these stars maintain a hot transition region with 10-100% solar transition zone surface fluxes.

One proposed explanation of the difference between the solar and nonsolar ultraviolet spectra across the H-R diagram is that wind expansion prevents the atmosphere in cool giants and supergiants from reaching the hot ($T \sim 10^5$K) transition-region temperatures because the wind provides enough cooling via adiabatic expansion (Linsky and Haisch 1979). With the discovery of the hybrid stars, however, an alternative suggestion has developed. Hartmann and MacGregor (1980) propose that stellar winds are driven by Alfven wave dissipation. In luminous stars, the extended density distribution in these atmospheres provides the extra cooling by radiation in order that the terminal velocities of the wind be small, in agreement with observations. The transition-region lines, observed to be quite broad, denote the onset of a warm wind (Hartmann *et al.* 1982*a*). Alternatively, Linsky (1982) proposed that the atmospheres of a hybrid star have two components--one with closed magnetically-confined loops responsible for most of the emission measure at high temperatures of C IV, Si IV and N V, and magnetically open structures analogous to coronal holes where most of the cool gas at Mg II temperatures escapes. The Alfven-wave-driven wind

theory, however, may well be compatible with the observational evidence provided by the hybrid stars and, therefore, may represent the same mechanism by which mass is lost on the Sun. Although the wind process is similar, the low-gravity of the evolved stars drastically alters the outer atmosphere structure. The evidence provided by the hybrid stars and its interpretation in the context of the wave-driven winds is as follows (Hartmann *et al.* 1984*b*).

Variations are evident in the short-wavelength portion of the Mg II emission in α TrA. The changes occur on timescales of a year in the high-velocity wind absorption. Neither the overall flux of the chromospheric Mg II emission nor of the high-temperature fluxes, such as C IV, varies significantly. Thus, variations are caused by the wind, far above the stellar photosphere. Not only the amount of material in the wind but also its velocity is variable. An exposure saturating the chromospheric emission cores reveals faint Mg II absorption in the wind blueshifted by -180 km s^{-1}, close to the escape velocity of the star. A terminal velocity as large as this eases the severe constraints upon wind theory that were previously imposed by observationally-biased low velocities. Such a large outflow velocity may be common among the hybrid stars; however, its discovery may be selected against by the lack of background radiation at these wavelength in these late-stellar photospheres.

The widths of the transition region lines are supersonic, evident from α TrA even in the optically thin transition region lines C III] λ1909 and Si III] λ1892, whose full widths at half-intensity are about 100 km s^{-1} and in the C IV lines about 150-200 km s^{-1}. The deposition of Alfven-driven waves in the transition region could produce mass loss rates of 10^{-9} to 10^{-10} $m_{\odot}$ yr^{-1}, consistent with observed limits (cf. Drake and Linsky 1984). The wave motions may turbulently broaden the transition zone lines to the observed widths. No evidence exists for Doppler shifts larger than 10 km s^{-1} in the high-temperature lines of α TrA. This would be consistent with the large amount of line broadening deposited at the base of the wind. Hartmann *et al.* (1982*b*) show that optically thin line profiles would be broadened nearly symmetrically by such a wave-deposition process. In α TrA, for example, the line widths produced by models of wave deposition can be 140-170 km s^{-1} in C III] and C IV, in reasonable agreement with the observed line widths (Hartmann *et al.* 1984b). Interestingly, the theoretical C IV profile, with only a marginal optical thickness ($\tau \sim 3$), is mildly P-Cygni in character with an apparent "redshift" of about + 8 km s^{-1}.

The overall picture outlined by Hartmann *et al.* (1984b) for the hybrid stars produces a cool, modest wind by a solar-type wind mechanism in stars with an extended density distribution. The turbulence in the high-temperature lines might be provided by the damping of the Alfven waves. These high-temperature lines are formed relatively close to the stellar surface, the acceleration of the wind is much further out in the atmosphere. The waves heat, and the energy is radiated in the extended density distribution of the outer atmosphere. Far out in the wind, recombination of Mg^{++} and Ca^{++} ions cause the blueshifted absorption features. The absorption features are highly variable, suggesting that the far wind is, also. The fluxes of the high-temperature lines do not measurably vary, an indication that although formed in a turbulent re-

gion, the line-forming region is close to the stellar surface. There is no direct evidence that the temperature of the wind is only a few x 10^4K and no hotter. Although no outflow velocities are apparent in the regime of C IV-N V, *IUE* provides no further information with which to probe the proposed interface between the turbulent gas at 2 x 10^5K and the cool, modest wind at 10^4K.

E. Dynamics in Ultraviolet Spectra of Cool Stars

Dynamics apparent from high-resolution spectra show small significant redshifts (less than or about 10 km s^{-1}) of the transition-region lines in slightly higher-gravity stars. In these stars the redshifts are also accompanied by supersonically broad emission lines as observed for the hybrid supergiants. Indeed, in the few high-resolution spectra of evolved stars showing transition-region lines such as β Dra (G2 Ib-II), Brown *et al.* 1984), λ And (G8 IV-III), α Aur (F9 III + G2 III), β Ceti (G9 III) (Ayres *et al.* 1983), the C IV λ1550 and Si IV (λ1400) emissions are broad, for example C IV has a width of up to 120 km s^{-1} in α Aur and 200 km s^{-1} in β Dra. Ayres *et al.* (1983) conclude that the width of these features is *not* caused by opacity effects in the line-forming region; they also suggest that the redshifted velocities are the result of small downflows in magnetically-confined, "loop" regions, as seen on the Sun. Alternatively, the origin of the redshifts may be the result of distortions caused by the deposition of Alfven waves, similar to the suspected line-broadening process in the hybrid supergiants.

III. ATMOSPHERIC INHOMOGENEITIES

Magnetic phenomena observed on the Sun can be sought on other stars. While the surfaces of most stars remain spatially unresolved, the existence of inhomogeneities can be revealed by time-serial observations. Two examples are active areas, associated with starspots, and flares.

A. Active Areas and Starspots

Detailed investigations in the visible and ultraviolet revealed surface inhomogeneities in the active-chromosphere star λ And (Baliunas and Dupree 1979, 1980, 1982). The G8 IV-III component in this 20-day (orbital period) RS CVn-type binary system has strong chromospheric emission and an unseen secondary star. For over 50 years, variations have been noted in the V-passband of up to 30% with a period of about 54 days. These modulations are likely caused by spots, dark in photospheric light, which pass through our line of sight during a stellar rotation period of 54 days. Spectra from *IUE* reveal an anticorrelation of visible light with the strength of the ultraviolet raidation (Figure 5*a*). The appearance of the spotted areas which may cover as much as 30% of the visible hemisphere corresponds to the darkening of the photometric light, and the brightening of the chromospheric and transition-region emissions. The Ca II K emission brightens in concert with the ultraviolet lines. (The flux in Mg II h and k does not measurably vary in the Baliunas and Dupree (1982) studies primarily because the phase coverage of Mg II was not complete.) The

enhancement of the chromospheric and transition region emissions at photometric light minimum are akin to those observed for sunspots and associated solar active regions.

Another RS CVn-type binary, II Peg, with an orbital period of 6.7 d, nearly synchronous with the active KO IV star's rotation period, and χ^1 Ori, a GO V star with a rotation period of 5.1 days were also monitored in the ultraviolet. In II Peg, fluxes of the chromospheric lines including Mg II and the transition region lines increased dramatically as the visual magnitude (monitored with the FES) decreased (Marstad *et al.* 1982). The enhancement of C IV, a factor of five, was the largest among the transition-region lines. The enhancement in the Mg II and other chromospheric lines was less than a factor of two. In absolute terms, however, the radiative losses over the active area in the chromospheric emission are comparable if not slightly larger than those in the transition zone. For II Peg, the shapes of the visible light curve and the ultraviolet flux curves suggest that the photospheric spots cover nearly 30% of the hemisphere while the transition-region inhomogeneity, the active area, is limited to some 6% of the hemisphere (Linsky 1984).

In the study of the behavior of the ultraviolet emission in χ^1 Ori over its rotation modulation phase, Boesgaard and Simon (1984) find a contrast in the transition zone fluxes of factor of about two in C IV. The He II (λ1640) feature and chromospheric Ca II K flux also correlates with the behavior of C IV. Interestingly, significant variations detected in the emission flux of N V, O I (λ1305), C II (λ1335), Si IV and C I (λ1657) do not always correlate with those of C IV. The Mg II emission does not measurably vary, but in terms of absolute losses, the lack of any variation is not troublesome. On χ^1 Ori, then, the picture emerges that low-chromosphere species have contrasts of 3-5 times the quiet regions and can be coincident with the higher-level lines. These regions producing the lower-lying emissions may not be long lived. The most persistent inhomogeneities appear in C IV, possibly in phase over 325 days, and covering some 40% of the hemisphere at maximum emission.

B. Stellar Flares

Ultraviolet spectra from *IUE* of stellar flares provide important constraints for theories of flare mechanisms. Flares in dMe stars are well-documented in visible light, and additional information results from ultraviolet measurements of flares in Proxima Centauri (dM5e, Haisch *et al.* 1983), Gl 867A (dM2e, Butler *et al.* 1981), and EQ Peg B (dM5.5e, Baliunas and Raymond 1984). In addition, flares in the ultraviolet have been detected from active chromosphere stars whose photospheres are hotter than those of the dMe stars and overwhelm the visible light variations present in the flares, for example, in UX Ari (KO IV, Simon *et al.* 1980) and λ And (G8 IV-III) (Baliunas *et al.* 1984). With supplemental X-ray measurements, Haisch (1983) concludes that the stellar flares, observed primarily among the dMe stars, are similar to moderate solar flares in terms of temperatures, inferred loop lengths, emission measures and luminosities, but with shorter decay times compatible with densities about an order of magnitude higher than in solar flares.

The flare observed from λ And (Figure 6) was remarkable in that the enhancement of factors of several in the transition-region lines persisted for over six hours. The energy radiated just in the ultraviolet was in excess of about 10^{35} ergs. The energy present in the ultraviolet is a few orders of magnitude greater than that of the largest solar flares. For this flare, both the Mg II and H I ly α emissions were measured. In Mg II h and k, the energy radiated is five times that of C IV, although the contrast of the increase in C IV is larger than for Mg II. The enormous radiative losses in Mg II and H I Ly α are obscured by the small percent changes in these strong lines. The nonradiative input of energy during the flare is at least comparable in the chromosphere and transition region. The input of this energy in the flaring component of the atmopshere of λ And must be sustained over the duration of the event.

In the dMe stars Gl 867A (Butler *et al.* 1981) and EQ Peg B (Baliunas and Raymond 1984), the ultraviolet flare is also accompanied by the appearance of detectable continuum emission in the wavelength region λλ1700-2000 (Figure 7). The ultraviolet continuum is consistent with models that produce such emission (along with Balmer line emission) in the chromosphere at temperatures near 10^4K (Katsova, Kosovichev and Livshitz 1981).

The ultraviolet fluxes during the flare in EQ Peg B are similar to those either in the thermal phases of large, two-ribbon solar flare where radiative cooling balances thermal conduction or in gas cooling quickly from X-ray emitting temperatures (Baliunas and Raymond 1984).

The ultraviolet observations available from *IUE* are providing information on outer atmospheres of cool stars at a challenging pace. Studies of time variations have revealed atmospheric inhomogeneities, such as the counterparts to active regions and flares. The parameters controlling chromospheric and coronal emission are being sorted out by surveys of ultraviolet emission. Additionally, mechanisms thought to balance the energy budget in the solar atmosphere are being extended and tested across the H-R diagram.

This work is supported in part by NASA grant NAG5-87 to the Smithsonian Institution. I would also like to acknowledge the support of the Langley-Abbot Program of the Smithsonian Institution.

REFERENCES

Ayres, T.R., Marstad, N.C. and Linsky, J.L. 1981, *Ap.J.*, 247, 545.
Ayres, T.R., Stencel, R.E., Linsky, J.L., Simon, T., Jordan, C., Brown, A. and Engvold, O. 1983, *Ap.J.*, 274, 801.
Baliunas, S.L. 1983, *Pub.A.S.P.*, 95. 532.
Baliunas, S.L., Avrett, E.H., Hartmann, L. and Dupree, A.K. 1979, *Ap.J.(Letters)*, 233, L129.
Baliunas, S.L. and Dupree, A.K. 1979, *Ap.J.*, 227, 870.
Baliunas, S.L. and Dupree, A.K. 1980, in *Cool Stars, Stellar Systems and the Sun*, SAO Special Report 389, p. 101.
Baliunas, S.L. and Dupree, A.K. 1982, *Ap.J.*, 252, 668.
Baliunas, S.L., Hartmann, L. and Dupree, A.K. 1983*b*, *Ap.J.*, 271, 672.

Baliunas, S.L., Guinan, E.F. and Dupree, A.K. 1984, *Ap.J.*, in press.
Baliunas, S.L. and Raymond, J.C. 1984, *Ap.J.*, in press.
Baliunas, S.L. *et al.* 1983a, *Ap.J.*, 275, 752.
Boesgaard, A.J. and Simon, T. 1982, in *Cool Stars, Stellar Systems and the Sun*, SAO Spec. Report No. 392, Vol. II, p. 161.
Boesgaard, A.M. and Simon, T. 1984, *Ap.J.*, 277, 241.
Böhm-Vitense, E. 1984, in *Cool Stars, Stellar Systems and the Sun*, eds. S.L. Baliunas and L. Hartmann (New York: Springer), p. 273.
Brown, A., Jordan, C., Stencel, R.E., Linsky, J.L. and Ayres, T.E. 1984, *Ap.J.*, in press.
Butler, C.J., Byrne, P.B., Andrews, A.D. and Doyle, J.G. 1981, *M.N.R.A.S.*, 197, 815.
Drake, S.A. and Linsky, J.L. 1984, in *Cool Stars, Stellar Systems and the Sun*, eds. S.L. Baliunas and L. Hartmann (New York: Springer), p. 350.
Duncan, D.K. 1981, *Ap.J.*, 248, 651.
Dupree, A.K. 1983, in *Solar Wind 5*, ed. M. Neugebauer, NASA Conf. Pub. 2280, p. 229.
Dupree, A.K., Black, J.H., Davis, R.J., Hartmann, L. and Raymond, J.C. 1979, in *The First Year of IUE*, ed. A.J. Willis (London: University College), p. 217.
Dupree, A.K., Goldberg, L., Noyes, R.W., Parkinson, W.H., Reeves, E.M. and Withbroe, G.L. 1973, *Ap.J.*, 183, 321.
Hammer, R., Linsky, J.L. and Endler, F. 1982, in *Advances in Ultraviolet Astronomy: Four Years of IUE Research*, ed. Y. Kondo, J.M. Mead and R.D. Chapman, NASA Conf. Pub. No. 2238, p. 268.
Haisch, B.M. 1983, in *Activity in Red Dwarf Stars*, ed. P.M. Byrne and M. Rodono (Boston: Reidel), p. 255.
Haisch, B.M., Linsky, J.L., Bornmann, P.L., Stencel, R.E., Antiochos, S.K., Golub, L. and Vaiana, G.S. 1983, *Ap.J.*, 267, 280.
Hartmann, L. 1983, *Adv. Space Res.*, 2, 29.
Hartmann, L., Baliunas, S.L., Duncan, D.K. and Noyes, R.W. 1984a, *Ap.J.*, in press.
Hartmann, L., Davis, R., Dupree, A.K., Raymond, J., Schmidt, P.C. and Wing, R.F. 1979, *Ap.J.(Letters)*, 233, L69.
Hartmann, L., Dupree, A.K. and Raymond, J.C. 1980, *Ap.J.(Letters)*, 236, L143.
Hartmann, L., Dupree, A.K. and Raymond, J.C. 1981, *Ap.J.*, 246, 293.
Hartmann, L., Dupree, A.K. and Raymond, J.C. 1982a, *Ap.J.*, 252, 214.
Hartmann, L., Edwards, S. and Avrett, E. 1982b, *Ap.J.*, 261, 279.
Hartmann, L., Jordan, C., Brown, A. and Dupree, A.K. 1984b, *Ap.J.*, submitted.
Hartmann, L. and MacGregor, K.B. 1980, *Ap.J.*, 242, 260.
Katsova, M.M., Kasovichev, A.G. and Livshits, M.A. 1981, *Astrofizika*, 17, 285.
Kraft, R.P. 1967, *Ap.J.*, 150, 551.
Linsky, J.L. 1980, *Ann.Rev.Astr.Ap.*, 18, 439.
Linsky, J.L. 1984, in *Cool Stars, Stellar Systems and the Sun*, eds. S.L. Baliunas and L. Hartmann
Linsky, J.L. and Haisch, B.M. 1979, *Ap.J.(Letters)*, 229, L27.
Marstad, N., Linsky, J.L., Simon, T., Rodono, M., Blanco, C., Catalano, S., Marilli, E., Andrews, A.D., Butler, C.J. and Byrne, P.B. 1982, in *Advances in Ultraviolet Astronomy: Four Years of IUE Research*, ed. Y. Kondo, J.M. Mead and R.D. Chapman, NASA Conf. Publ. No. 2238, p. 554.

Noyes, R.W., Hartmann, L.W., Baliunas, S.L., Duncan, D.K. and Vaughan, A.H. 1984, *Ap.J.*, in press.
Parker, E.N. 1979, *Cosmical Magnetic Fields: Their Origin and Their Activity* (Oxford: Clarenden Press).
Reimers, D. 1977, *Astr.Ap.*, 57, 395.
Reimers, D. 1982, *Astr.Ap.*, 107, 292.
Rosner, R., Tucker, W.H. and Vaiana, G.S. 1978, *Ap.J.*, 220, 643.
Schrijver, C.J., Mewe, R. and Walter, F.M. 1984, in *Cool Stars, Stellar Systems and the Sun*, eds. S.L. Baliunas and L. Hartmann (New York: Springer), p. 166.
Skumanich, A. 1972, *Ap.J.*, 171, 565.
Skumanich, A. and Eddy, J.A. 1981, in *Solar Phenomena in Stars and Stellar Systems*, eds. R.M. Bonnet and A.K. Dupree (Boston: Reidel), p. 349.
Simon, T. 1984, *Ap.J.*, in press.
Simon, T., Linsky, J.L. and Schiffer, III, F.H. 1980, *Ap.J.*, 239, 911.
Soderblom, D.R. 1982, *Ap.J.*, 263, 29.
Stein, R.F. and Leibacher, J.W. 1974, *Ann.Rev.Astr.Ap.*, 12, 407.
Stencel, R.E. 1978, *Ap.J.(Letters)*, 223, L37.
Stencel, R.E. and Mullan, D.J. 1980, *Ap.J.*, 238, 221.
Ulmschneider, P. 1981, in *Solar Phenomena in Stars and Stellar Systems*, eds. R.M. Bonnet and A.K. Dupree (Boston: Reidel), p. 239.
Ulmschneider, P. and Stein, R.F. 1982, *Astr.Ap.*, 106, 9.
Vaughan, A.H., Baliunas, S.L. Middelkoop, F., Hartmann, L., Mihalas, D., Noyes, R.W. and Preston, G.W. 1981, *Ap.J.*, 250, 276.
Walter, F.M., Linsky, J.L., Simon, T., Golub, L. and Vaiana, G.S. 1984, *Ap.J.*, 138, 832.

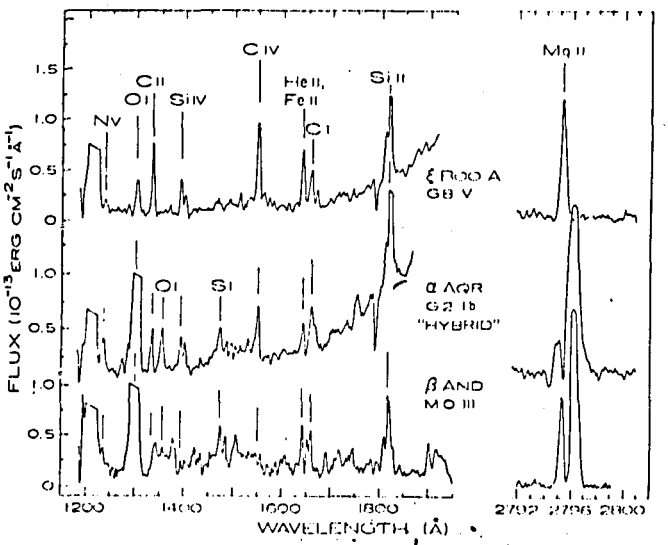

Figure 1 -- *IUE* ultraviolet, short-wavelength spectra (left) and high-resolution Mg II (right) spectra of an active chromosphere dwarf, ξ Boo A, a "hybrid"-atmosphere star α Aqr, and a giant, β And. In the short-wavelength spectra, the presence of high-temperature gas is indicated by N V, C IV and Si IV in ξ Boo A and α Aqr. The star β And shows no observable amounts of these transition-region lines. In α Aqr and β And, the Mg II-k profile suggests mass outflow by the asymmetry of the emission peaks (violet peak weaker than red), and in addition, blue-shifted absorption is present at about -70 km s^{-1} in α Aqr (Dupree 1983, by permission of the author).

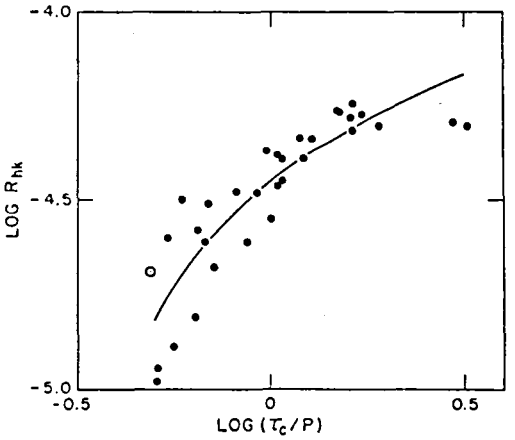

Figure 2 -- Mg II h and k emission, normalized by the stellar bolometric luminosity as a function of τ/P in lower main sequence stars. The rotation period is P, and τ is a function of (B-V), or main sequence mass, alone. The parameter τ is similar to the convective turnover time for α = 2. The Sun is denoted by its symbol "⊙". The solid line is the fit of Ca II emission as a function of τ/P, with a vertical displacement to account for the larger fluxes in Mg II compared to Ca II (Hartmann *et al.* 1984*a*, by permission of the authors).

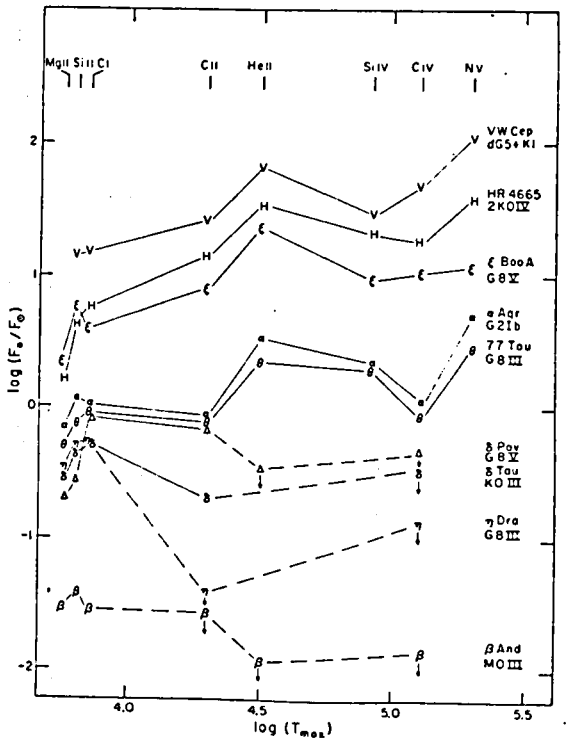

Figure 3 -- Stellar surface fluxes relative to quiet Sun surface fluxes as a function of approximate temperature of formation of ions in a variety of cool stars. Note the paucity of high-temperature material relative to the Sun in, for example, δ Tau. In more active stars, such as VW Cep, the transition-region emission increases faster than the chromospheric fluxes (Hartmann *et al.* 1982*a*, by permission of the authors).

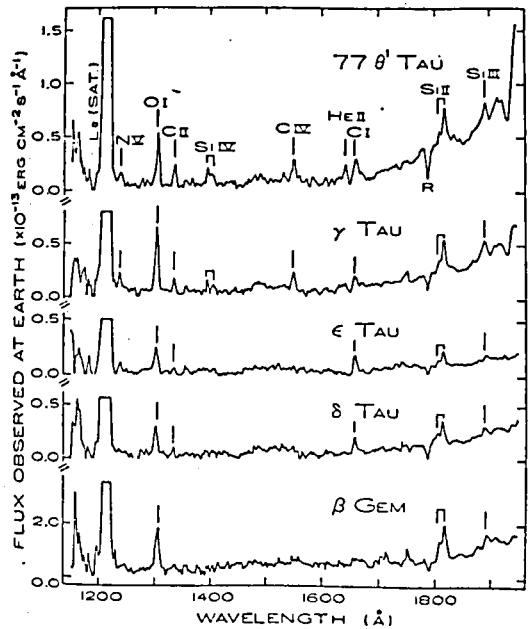

Figure 4 -- *IUE*, short-wavelength, low resolution spectra of the four Hyades giants (KO III) compared to the field star β Gem. Note the presence of high-temperature, transition-region lines (N V, C IV, Si IV) in 77 Tau and γ Tau, which are not detected in ε Tau, δ Tau and the field star β Gem. The presence of high-temperature material in 77 Tau and γ Tau is correlated with increased emission in Ca II and Mg II compared to the other stars (Baliunas 1983*a*, by permission of the authors).

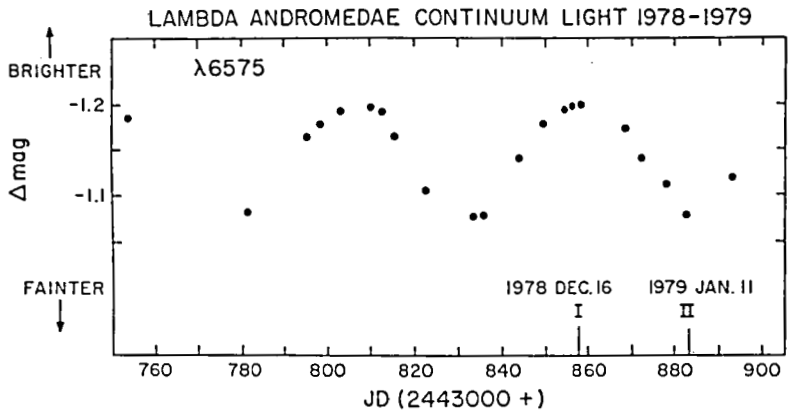

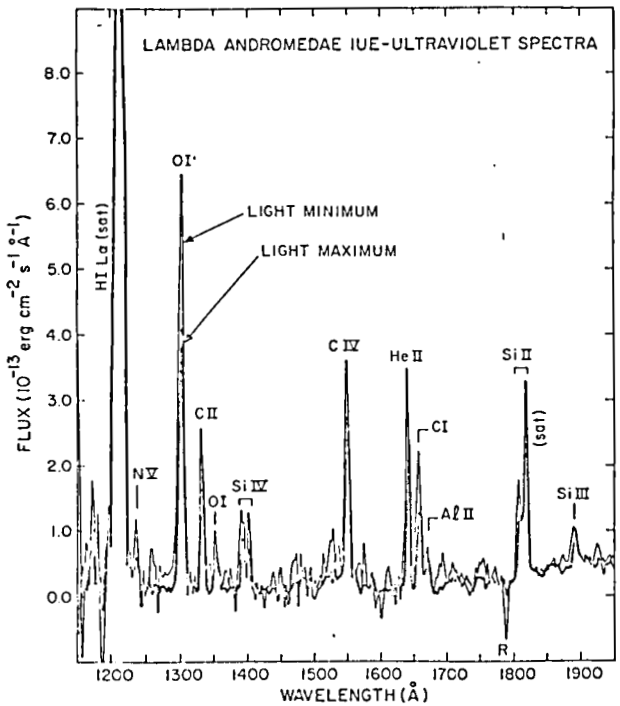

Figure 5 -- (a) The photometric modulation of λ And (G8 III-IV + ?) caused by visibly dark starspot areas during stellar rotation with a period of about 54 days. For the times of maximum and minimum light, marked on the plot, the *IUE*, short-wavelength spectra (*b*) show an anti-correlation of ultraviolet emission with light, similar to the behavior of active regions overlying sunspots on the Sun (Baliunas and Dupree 1982, by permission of the authors).

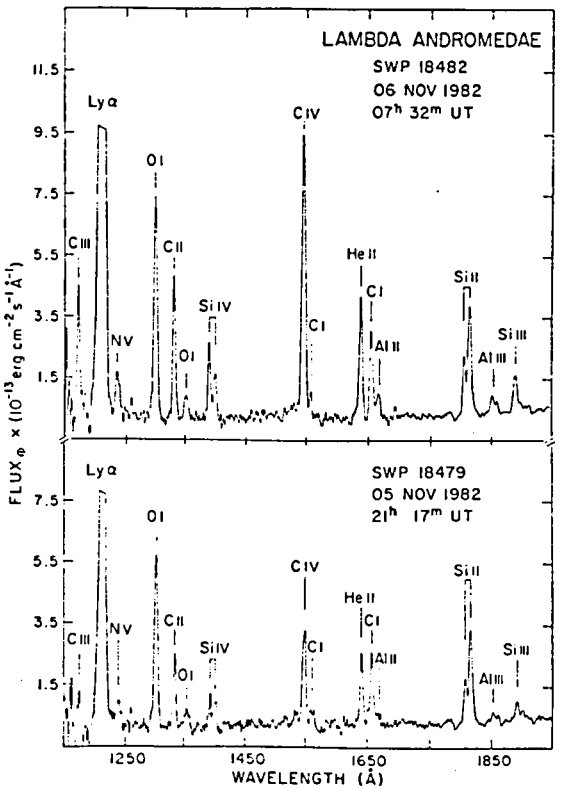

Figure 6 -- *IUE*, short-wavelength spectra during (above) and before (below) a flare lasting over six hours on λ And. The largest enhancement is observed in C IV (Baliunas *et al.* 1984), by permission of the authors).

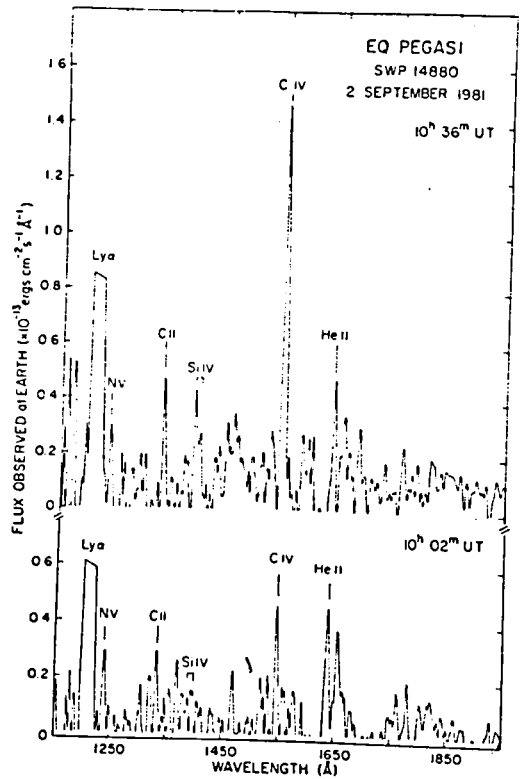

Figure 7 -- *IUE*, short wavelength spectra during (above) and before (below) a flare on EQ Peg (dM4.5e + dM5.5e). Note the appearance of continuous emission (λλ1750-1950) during the flare (Baliunas and Raymond 1984, by permission of the authors).

FUTURE ULTRAVIOLET EXPERIMENTS, INCLUDING FUSE/COLUMBUS

Albert Boggess
Goddard Space Flight Center

Several new facilities for ultraviolet astronomy are under construction or study for launch within the coming decade. These include the Hubble Space Telescope to be launched in 1986 with instruments for spectroscopy, imaging, and photopolarimetry in the ultraviolet; the ASTRO Spacelab payload, also to be launched in 1986 with a similar range of instrumentation; STARLAB, a combined Canadian, Australian and U.S. mission concentrating primarily on imagery; and the Far Ultraviolet Spectroscopic Explorer (FUSE), which has been renamed COLUMBUS. COLUMBUS is currently under study by NASA and ESA as a future joint mission for spectroscopic studies of astrophysical plasmas covering a temperature range from $\sim 10^3$ to $\sim 10^7$K. In order to achieve this objective, the optics should be optimized for wavelengths below 1200 Angstroms, with a total wavelength range from ~2000 to ~100 Angstroms. The operational concept will be based on experience with IUE, but changes in communications techniques since IUE was designed suggest some interesting new approaches to observing.

UV OBSERVATIONS AND RESULTS ON PRE-MAIN SEQUENCE STARS

Catherine L. Imhoff
Astronomy Programs
Computer Sciences Corporation

ABSTRACT

IUE has given us our first good look at the ultraviolet spectra of pre-main sequence objects. This review concentrates on the observations and results obtained for the T Tauri stars and related objects. The T Tauri stars represent a normal phase of pre-main sequence evolution for solar mass stars. As such they provide an invaluable probe of the physical mechanisms involved in star formation and the genesis of stellar magnetic fields and surface activity.

Ultraviolet studies of the T Tauri and related stars have been concentrated in four areas. First, the very strong Mg II emission lines have been observed in order to determine fluxes, line profiles, and variability. Most evidence points to the formation of these strong lines in an extended atmosphere and/or wind. Second, the far-ultraviolet emission lines have been observed to provide diagnostics of the hotter atmospheric regions. The behavior of these lines is very similar to that of the most active late-type stars, lending credence to the belief that many of the T Tauri characteristics are the result of high levels of surface activity. Third, the ultraviolet continuum, which originates largely in the chromosphere, shows potential as a chromospheric diagnostic. Finally, observations of related objects may be used to gain insight into the evolutionary changes occuring during pre-main sequence evolution.

INTRODUCTION

The IUE satellite has proven an extremely useful tool in studies of pre-main sequence evolution. IUE programs that have contributed to our understanding of star formation include studies of young O stars, T Tauri stars, Herbig-Haro objects, Herbig Ae stars, star formation in other galaxies, and the interstellar medium. This review concentrates on the T Tauri stars and related objects.

The T Tauri stars were recognized some time ago as a class of peculiar variable stars (Joy 1945). They are identified through their visual spectra, which are characterized by strong Balmer line and Ca II H,K emission, often Fe II and [S II] emission, a near-ultraviolet excess, veiling of broad photospheric lines of G, K, and M-type spectra, an infrared excess due to dust emission, and irregular variability of most of these characteristics. The broad resonance emission line profiles are

usually interpreted to indicate significant mass loss. However, various scenarios have been used to explain the T Tauri characteristics, including stellar winds, extended gas envelopes, and accretion (see references in Hartmann 1982; also see DeCampli 1981, Hartmann et al. 1982).

The fundamental interest in the T Tauri stars is due to their unique evolutionary status - they appear to represent a normal phase of evolution for roughly solar-mass stars with ages of a few million years. HR diagrams associate the stars with the earliest visible phases of protostellar evolution (Cohen and Kuhi 1979, Stahler 1983). It has been suggested that the T Tauri phase of evolution is associated with the Hayashi phase, i.e. when the star is fully convective (Jones and Herbig 1979).

The fundamental questions that we seek to answer about the T Tauri stars and related objects are these. (1) Why are their spectra and flux distributions so peculiar? (2) Why are the various classes of related objects (T Tauri stars, FU Orionis stars, post-T Tauri stars) so different? (3) What can be learned from these stars about stellar evolution?

The first reported ultraviolet detection of a T Tauri star was not with IUE but with ANS (deBoer 1977). However it is probably fair to say that this field of study did not exist before the lauch of IUE in 1978. A number of researchers have contributed to the study of the T Tauri stars in the ultraviolet. At the end of this paper, a (hopefully) complete list of references is given for IUE observations of the T Tauri stars. A separate list of references is given for papers referred to in the text of this paper. Please note that in the interest of presenting as much material as possible no figures are reprinted in this article; the figures given here are those not otherwise available in published articles.

EARLY IUE RESULTS

The papers describing the observations from the first few years of IUE represent the pioneering results on the T Tauri stars (see references). These early results are summarized here and elsewhere (Gahm 1981, Giampapa 1983, Giampapa and Imhoff 1984).

The primary early result on the T Tauri stars was that they could be detected by IUE! These 11-13 mag G, K, and M stars would not have been detected if it were not for their extreme UV emission.

The second result was the great strength of the Mg II h,k emission lines at 2800 A. (In our first observing run, Mark Giampapa and I never got an LWR exposure short enough to properly expose the MgII line in RW Aurigae!) The surface flux of Mg II in the T Tauri stars is typically 50 times that of the Sun. About 0.1% of the star's bolometric luminosity is emitted in that pair of lines (Giampapa et al. 1981).

Finally, several high-temperature emission lines were identified in

the far-ultraviolet. These include Si IV, C IV, and sometimes He II and N V. The far-UV spectra of the T Tauri stars were found to be quite similar to the spectra of the active late-type stars observed with IUE. In these latter stars, the far-UV emission lines arise in the chromospheres and transition regions of the stars' atmospheres, originating at temperatures of 6000 K to 2 x 10^5 K. The surface fluxes of the far-UV emission lines in the T Tauri stars are around 3 x 10^3 times those of the Sun. These values are as high and higher than for any other late-type stars. The far-UV emission lines contribute another 0.1% to the stellar luminosity for the T Tauri stars (Imhoff and Giampapa 1982a,b). The higher temperature regions of the atmospheres must be produced by in situ heating, not by coronal conduction, to produce this much emission (Cram et al. 1979).

The similarity of the T Tauri UV spectra to those of the active chromospheric late-type stars has provided the strongest evidence to date that the "T Tauri phenomenon" is primarily related to stellar surface activity. Some interesting differences are seen in the UV spectra of the "extreme" T Tauri stars, i.e. the stars showing the greatest line and continuum emission in the visible. Their far-UV spectra show weakened lines of the high temperature lines. The N V and He II emission lines are not seen, although one might argue that this could be an observational problem with noisy data. More convincingly, the C IV line is definitely weakened relative to Si IV. Since C IV is an intrinsically stronger line than Si IV, C IV is virtually always seen as the stronger line in late-type stars. Yet it is weaker than Si IV in a handful of extreme T Tauri stars. We could explain this only if, for some reason, the maximum temperature reached in the star's atmosphere is around the temperature of formation of Si IV, i.e. 8 x 10^4 K. We hypothesized that the mass loss, or stellar wind, in these stars carries away enough energy to inhibit the temperature rise to a coronal region (Imhoff and Giampapa 1980).

FURTHER STUDIES WITH IUE

These early results stimulated a number of investigations of the T Tauri stars with IUE. These have primarily been concerning with refining our understanding of the T Tauri atmospheres by more detailed investigations and extending the observations to a variety of related objects. These results are summarized below.

MgII h,k Emission Lines

The strong Mg II lines have provided us with a useful diagnositic for the T Tauri chromospheres and winds. If the Mg II line is chromospheric in origin, then one would expect it to be variable due to changes in the surface activity and to the rotation of bright "plages" across the stellar disk. However, repeated observations of DG Tauri show no clear variability greater than 10% (Imhoff and Giampapa 1984b). A similar result is found for the extreme T Tauri star RW Aurigae (see Figure 1). The only divergent

value was obtained when the star was particularly active (Imhoff and Giampapa 1984a). The implication of this lack of variability is that the Mg II emission is being produced in an extended region, perhaps in the expanding atmosphere, or wind, of the stars.

Thanks to the strength of the Mg II emission lines, it has proven possible to study them at high dispersion. Ten stars have been observed at high dispersion; about half of these have been published. The line profiles of the Mg II h,k lines are very reminiscent of the those of the other resonance emission lines, such as H-alpha and Ca II H,K. The lines are broad (several 100 km/sec) and appear to be cut by strong blue-shifted absorption. Variability is seen where more than one set of line profiles have been obtained. Interestingly, the variability seems to occur only in the overall strength of the emission and in the blueward absorption (Imhoff and Giampapa 1984a, Jordan et al. 1982). Again this suggests that the Mg II emisson arises in an extended atmospheric region or wind. It is interesting to note that this same result has been obtained for some other active late-type stars (Baliunas, this volume).

Far-ultraviolet Emission Lines

The far-ultraviolet emission lines provide diagnostics of the chromosphere and transition region in the T Tauri atmospheres. Of special interest are the hotter regions of the atmosphere that are accessible only with IUE. (Note: by "transition region", we here refer to an atmospheric region of around 10^5 K. No particular physical mechanism is implied; conduction from a corona is unlikely to produce this region in the T Tauri stars, especially if some of them don't have coronae!)

As many IUE observers know, the IUE spectra are somewhat noisy. The identification of weak features, especially for long integrations where particle "hits" and camera artifacts affect the image, can be difficult. On the other hand, two of the more interesting high-temperature emission lines in the far-ultraviolet, He II and N V, are intrinsically weak compared to C IV and Si IV. Careful reanalysis of a dozen T Tauri spectra shows that the He II and N V lines are definitely detected in only a small proportion of the dozen stars examined (Imhoff and Giampapa 1984b).

One may compare the relative line strengths of the T Tauri stars to those of other active late-type stars. Ayres, Marstad, and Linksy (1981) showed that the emission lines of the late-type stars tend to correlate well with each other. As one progresses to stars with greater levels of surface activity, all the emission lines become stronger but the higher temperature lines tend to be enhanced even more so. For the moderate temperature lines (OI, Si II, C II), the T Tauri stars follow these relations very well, lying just beyond the highest values for the stars examined by Ayres et al. The T Tauri stars diverge, however, for the He II line (thought to be produced by recombination after X-ray photoionization in many late-type stars), the soft X-rays, and for CIV (not plotted separately by Ayres et al.). This divergence occurs even for T Tauri stars

in which He II and the X-rays have been detected, not just the "extreme" T Tauri stars. Thus the relative weakening of the high temperature regions appears to be a general feature of the T Tauri atmosphere. Such effects are also seen in models of a stellar wind and a deep chromosphere (Hartmann, Edwards, and Avrett 1983).

Because of the long integrations involved, studies of the far-ultraviolet variability of the T Tauri stars are limited. The star RW Aurigae has been observed several times since 1978, encompassing periods when the star was particularly active and when it was not. In Figure 2, the far-ultraviolet spectra of RW Aur are shown for four epochs of observation. These are ranked from top to bottom, from most active to least active and from when the star was brightest to when it was faintest. (Most late-type stars are faintest when most active, due to the dark starspots. The T Tauri stars appear to have "bright" spots, or "superplages", with strong chromospheric continuum emission which affects the visual brightness of the stars.) The variations in the lines are more easily followed in Figure 3, where the individual line fluxes are plotted against the visual brightness of the star (in FES counts). The lower temperature lines of C II and Si II increased proportionally with the FES counts, by a factor of 2.5, but the high temperature lines of Si IV and C IV are proportionally much stronger. Figure 4 depicts the dramatic change in the ultraviolet continuum. These spectral changes - enhancement of the high temperature lines, appearance of a UV continuum - resemble strongly the behavior seen in other late-type stars during flares (Baliunas 1983). The primary difference appears to be in time scale. In most late-type stars, flares occur in minutes or at most hours. The level of activity seen in RW Aur in 1979 appeared to persist over a few days. Thus a region of flaring activity, rather than a single flare, may have been involved.

It is clear from a number of lines of evidence that atmospheric motions - winds and turbulence - are very important in understanding the structure of the T Tauri atmospheres. Line profiles for the Balmer lines, Na I D lines, Ca II H,K, and Mg II h,k have been obtained, but all of these lines arise in relatively low temperature regions. A particularly useful observation would be line profiles for the high temperature lines. Since the integration time for these lines in low dispersion is at best 3 hours, few such observations have been attempted. Penston and Lago (1982) have reported one successful observation of the far-ultraviolet emission lines of RU Lupi, another extreme T Tauri star. The lines are relatively broad, about 350 km/sec. The C IV line profiles, though noisy, appear to show blueward emission up to -150 km/sec from the rest velocity.

The UV Continuum

In the T Tauri stars, the ultraviolet continuum seems to be largely produced in the chromosphere (Calvet et al. 1984). This then provides us with a new chromospheric diagnostic. The continuum fluxes may be compared with the newly available model calculations.

Since the UV continuum is relatively easily observed with IUE with integrations of less than an hour, it can be used to study the variability of the stars with reasonably good time resolution and better accuracy than can be obtained with IUE data for single emission lines at low dispersion. Recall that the Mg II lines do not show much variability. However, the UV continuum can show dramatic variability (as seen in Figure 4). We have recently observed several T Tauri stars with IUE in coordination with the photometric monitoring program of Eric Rydgren and Fred Vrba. Our preliminary results indicate that the UV continuum variations matched the visual continuum variations seen over the rotation of the stars. This confirms that the emission arises in the same or related regions of the atmosphere, suggesting that further use may be made of the UV continuum to help us to understand the T Tauri stars.

Related Pre-Main Sequence Objects

In addition to the T Tauri stars, there are several other members of the "pre-main sequence zoo". The objects are generally distinguished by some unique observational characteristics, but ultimately we would like to fit them into the evolutionary scheme of things.

Recent results on bipolar flows, jets, and Herbig-Haro objects indicate that some very energetic events are associated with the earliest stages of evolution of a protostar. The scenario is not yet entirely clear, but these energetic ejection events appear to be associated with the earliest part of the T Tauri phase and even the "pre-T Tauri" phase, when the protostar is still heavily embedded in its natal cloud of dust and gas.

FU Orionis is a pre-main sequence object that brightened by over 5 magnitudes in 1936. A similar nova-like brightening was seen in 1969 in V1057 Cygni. In the latter case, pre-outburst observations indicated that the progenitor was a faint pre-main sequence star with T Tauri characteristics. A statistical analysis by Herbig (1977) showed that in all likelihood such outbursts are quite common during a T Tauri star's lifetime - an outburst every 10^4 years, or 500 outbursts in a lifetime of 5 x 10^6 years. Some confirmation of this idea is found in the expanding shells seen in the Na I D line profiles of several T Tauri stars (Mundt 1982). The nature of the outburst is not well understood (Larson 1980).

We have obtained several spectra of FU Orionis with IUE. Among these are two high dispersion spectra yielding the Mg II emission line profiles. The broad emission components of the h and k lines do not appear particularly remarkable, until one realizes that the emission is nearly all redward of the rest velocity. This does not appear to indicate mass infall, however. Observations of the H-alpha and Na I D lines indicate a very strong stellar wind (Hartmann 1983). Thus the redward emission of the Mg II lines appears to correspond with the emission portion of pronounced P Cygni line profiles. The blueward absorption is not seen because the ultraviolet continuum is very weak in these high dispersion spectra. Thus, after almost 50 years, FU Orionis continues to lose mass in a strong

stellar wind.

The heavily embedded, very young protostars would not appear to be good candidates for IUE observations. An object obscured by 5 magnitudes of visual extinction experiences a factor of about 10^5 attenuation around the C IV line. The Cohen-Schwartz star is such an embedded T Tauri star that has been identified as the source of Herbig-Haro objects 1 and 2. Observations of this star with IUE unexpectedly turned up a weak, extended UV continuum (Bohm and Bohm-Vitense 1982). However Witt and Mundt (1983) have argued convincingly that the weak continuum is due to the Orion reflection nebulosity. Additional IUE observations obtained of the Orion nebula near the star confirm this explanation (Witt 1983).

This result did not deter investigators when the infrared object IRS 8 associated with Herbig-Haro 57 was reported in outburst. Three groups of researchers (Bohm, Bohm-Vitense, Maran, Stecher, Michalitsianos, Kalinowski, and Imhoff) teamed up to obtain a long integration on the short wavelength camera at IRS 8-HH 57. Nothing was detected.

Studies of solar-like main sequence stars have been very successful in finding correlations of stellar surface activity with the age of the star. In addition to earlier work with the Ca II H,K emission lines (e.g. Skumanich 1972), age relations have been found for ultraviolet chromospheric and transition-region lines from IUE data (Boesgaard and Simon 1982, Simon and Boesgaard 1983). Most of the available data are for stars older than 10^8 years. The T Tauri stars have ages around a few million years. Thus there is a gap in our age coverage between the T Tauri stars and the main sequence. Protostars at this stage of evolution (known as "post-T Tauri" stars; Herbig 1973) apparently resemble normal stars in most of their observational characteristics, so few of them have been found. An unexpectedly good method of finding them has been in the X-ray region of the spectrum, where the stars are quite luminous.

A handful of post-T Tauri stars have been observed with IUE. The LWR spectrum of HD 283572 shows a photospheric continuum and weak Mg II emission barely rising above the continuum in low dispersion. The far-ultraviolet spectrum of this post-T Tauri star has been obtained by Walter (1983). As in many other active late-type stars, C IV is the strongest line and He II and N V are clearly seen. Thus in the ultraviolet, this star appears to be intermediate in its characteristics between the T Tauri stars and the young main-sequence stars.

The interesting aspect of all of this is that there is no strong evidence that the known post-T Tauri stars are in fact older or more evolved than the T Tauri stars. If they are placed in the H-R diagram, they fall in a portion of the region occupied by T Tauri stars (albeit at the "bottom" of the convective tracks). The strength of the lithium line, often used as an age indicator, does not distinguish the two groups of stars. If one then hypothesizes that the stars all represent the same evolutionary stage, then one must explain the strong differences among the

stars. It is difficult to explain the higher surface activity of the T Tauri stars with the dynamo effect, since the post-T Tauri stars rotate at least as fast as the T Tauri stars (unless one invokes some other parameter such as convective envelope depth or differential rotation). This question may be expected to keep the pre-main sequence evolution observers and theorists busy for some time.

SUMMARY

Most of the IUE research on the T Tauri stars has focussed on the first of the "big questions" - why are the T Tauri stars so strange? The answer appears to be that they are not so strange. Their UV spectra have demonstrated the similarities of the T Tauri stars to other active late-type stars. The spectral peculiarities seen in the visual appear to be secondary effects produced by the very high level of surface activity evident in the ultraviolet.

The evolutionary questions are more difficult to answer. At present it is not possible to assign a unique age to any given protostar; thus no evolutionary sequence can be reliably constructed from the available data. However, it is tempting to create a hypothetical scenario such as the following. An embedded protostar accretes matter, giving rise to various eruptive events such as FU Orionis-type outbursts and the creation of Herbig-Haro objects and jets. As the circumstellar disk thins, the star becomes visible as a T Tauri star. A high level of surface activity is seen due to strong magnetic fields, which may be primordial and/or produced through a dynamo associated with the deep convective zone and rotation. Waves generated in the convective zone heat and extend the atmosphere, where at the cooler temperature zones emission lines radiate away much of the energy. However at around 10^5 K a wind may carry off a significant amount of the energy. As time goes by the convective zone shrinks, the level of activity decreases, and the atmospheric densities decrease. The non-radiative energy builds up in the atmosphere, which can now reach coronal temperatures. At this point the protostar's atmosphere has become structurally very similar to a main-sequence star.

I would like to thank Mark Giampapa, my collaborator on our IUE studies of the T Tauri stars. In addition, I would like to thank the IUE Project and Observatory personnel for their encouragement and support over the last ten years. This work was performed with the support of NASA contract NAS 5-25774.

REFERENCES: ULTRAVIOLET OBSERVATIONS AND RESULTS ON T TAURI STARS

Appenzeller, I., Bertout, C., Mundt, R., and Krautter, J. 1981, Mitt. Astron. Ges. No. 52, p. 15. "High Resolution IUE Observations of the Mg II Resonance Line in the T Tauri Star S CrA"

Appenzeller, I., Chavarria, C., and Krautter, J. 1981, in the Second European IUE Conference, p. 209. "UV Spectrograms of T Tauri Stars"
Appenzeller, I., Chavarria, C., Krautter, J., Mundt, R., and Wolf, B. 1980, Astron. Ap., 90, 184. "UV Spectrograms of T Tauri Stars"
Appenzeller, I., and Wolf, B. 1979, Astron. Ap., 75, 164. "The Satellite-UV Spectrum of S CrA"
Bertout, C. 1982, in the Third European IUE Conference, p. 89. "T Tauri Stars: Not One But Two Transition Regions"
deBoer, K. S. 1977, Astron. Ap., 61, 605. "Far-UV Observations of T Tau-like Stars" (ANS data)
Brown, A., and Jordan, C. 1982, in Activity in Red Dwarf Stars, IAU Colloq. No. 71, (ed. P. B. Byrne and M. Rodono), p. 509. "Chromospheric Properties of T Tauri Stars Determined from EUV Spectra"
Brown, A., Jordan, C., Millar, T. J., Gondhalekar, P. and Wilson, R. 1981, Nature, 290, 34. "H_2 Emission in the EUV Spectrum of T Tauri and Burnham's Nebula"
Cram, L. E., Giampapa, M. S., and Imhoff, C. L. 1979, Ap. J., 238, 905. "Emission Measures Derived from Far Ultraviolet Spectra of T Tauri Stars"
Gahm, G. F. 1981, in The Universe at Ultraviolet Wavelengths, p. 105. "IUE Observations of Young Variables"
Gahm, G. F., Fredga, K., Liseau, R., and Dravins, D. 1979, Astron. Ap., 73, L4. "The Far-UV spectrum of the T Tauri Star RU Lupi"
Giampapa, M. S. 1983, in SAO Special Report, in press. "Results from Ultraviolet Observations of T Tauri Stars"
Giampapa, M. S., Calvet, N., Imhoff, C. L., and Kuhi, L. V. 1981, Ap. J., 251, 113. "IUE Observations of Pre-Main Sequence Stars. I. Mg II and Ca II Resonance Line Fluxes for T Tauri Stars"
Giampapa, M. S., and Imhoff, C. L. 1984, in Proceedings of the Protostar and Planets Conference II, in press. "The Ambient Radiation Field of Young Solar Systems: Ultraviolet and X-ray Emission from T Tauri Stars"
Giampapa, M. S., Morossi, C., Ramella, M., and Imhoff, C. L. 1981, Bull. A. A. S., 13, 811. "High Resolution, Absolute Flux Profiles of the Mg II h and k Lines for T Tauri Stars" (abstract)
Gondhalekar, P. M., Penston, M. V., and Wilson, R. 1979, in The First Year of IUE (ed. A. J. Willis), p. 109. "The Ultraviolet Spectra of T Tauri Stars"
Imhoff, C. L., and Giampapa, M. S. 1979, in The Universe at Ultraviolet Wavelengths", p. 185. "The Ultraviolet Variability of the T Tauri Star RW Aurigae"
Imhoff, C. L., and Giampapa, M. S. 1980, Ap. J. Letters, 239, L115. "The Ultraviolet Spectrum of the T Tauri Star RW Aurigae"
Imhoff, C. L., and Giampapa, M. S. 1982a, in Advances in Ultraviolet Astronomy, p. 456. "Chromospheres and Coronae in the T Tauri Stars"
Imhoff, C. L., and Giampapa, M. S. 1982b, in SAO Special Report No. 392, II, p. 175. "Far-ultraviolet and X-ray Evidence Concerning the Chromospheres and Coronae of the T Tauri Stars"

Imhoff, C. L., and Giampapa, M. S. 1984a, Bull. A. A. S., 15, 928 (abstract). "The UV Variability of RW Aur"
Imhoff, C. L., and Giampapa, M. S. 1984b, in preparation.
Jordan, C. 1983, Observatory, 103, 129. "Models of T Tau from EUV and X-ray Observations"
Jordan, C., Ferraz, M. C. de M., and Brown, A. 1982, in the Third European IUE Conference, p. 83. "An Analysis of the Ultraviolet Spectrum of T Tauri"
Mundt, R., Appenzeller, I., Bertout, C., Chavarria, C., Krautter, J. 1981, Astron. Ap., 93, 412. "IUE Observations of V1331 Cyg"
Penston, M. V., and Lago, M. T. V. T. 1982, in the Third European IUE Conference, p. 95. "Far UV Line Widths in RU Lupi"
Penston, M. V., and Lago, M. T. V. T. 1983, Mon. Not. R. A. S., 202, 77. "Optical and Ultraviolet Line Profiles and Ultraviolet Line Intensities in the T Tauri Star LHa 332-21"
Walter, F. M., and Brown, A. 1984, Bull. A. A. S., 15, 966 (abstract). "Five Days in the Life of a T Tauri Star: Preliminary Results from a Spectroscopic and Photometric Monitoring Campaign"
Wolf, B., and Appenzeller, I. 1979, in The First Year of IUE (ed. A. J. Willis), p. 100. "The IUE spectrum of the YY Orionis Star S CrA"

REFERENCES: OTHER WORKS CITED

Ayres, T. R., Marstad, N. C., and Linsky, J. L. 1981, Ap. J., 247, 545.
Baliunas, S. 1983, Pub. A. S. P., 95, 532.
Boesgaard, A. M., and Simon, T. 1982, in SAO Special Report No. 392, II, p. 161.
Bohm, K. H., and Bohm-Vitense, E. B. 1982, Ap. J. (Letters), 263, L35.
Calvet, N., Basri, G., and Kuhi, L. V. 1984, in press.
Cohen, M., and Kuhi, L. V. 1979, Ap. J. Suppl., 41, 743.
DeCampli, W. M. 1981, Ap. J., 244, 124.
Hartmann, L. 1982, Ap. J. Suppl., 48, 109.
Hartmann, L. 1983, private communication.
Hartmann, L., Edwards, S., and Avrett, E. 1982, Ap. J., 261, 279.
Herbig, G. H. 1973, Ap. J., 182, 129.
Herbig, G. H. 1977, Ap. J., 217, 693.
Jones, B. F., and Herbig, G. H. 1979, A. J., 84, 1872.
Joy, A. H. 1945, Ap. J., 102, 168.
Larson, R. B. 1980, M. N. R. A. S., 190, 321.
Mundt, R. 1982, in SAO Special Report No. 392, II, p. 181.
Mundt, R., and Witt, A. N. 1983, Ap. J. (Letters), 270, L59.
Simon, T., and Boesgaard, A. M. 1983, in Solar and Magnetic Fields (ed. J. Stenflo), p. 161.
Skumanich, A. 1972, Ap. J., 171, 565.
Stahler, S. W. 1983, Ap. J., 274, 822.
Walter, F. M. 1983, private communication.
Witt, A. N. 1983, private communication.

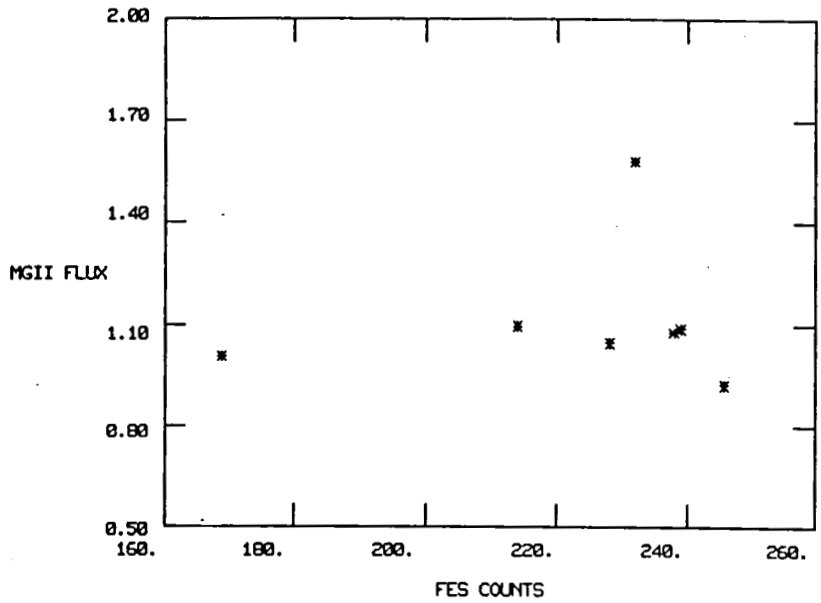

Figure 1. Observed Mg II flux (10^{-11} erg/cm^2/sec) versus visual brightness (FES counts) for several observations of RW Aur.

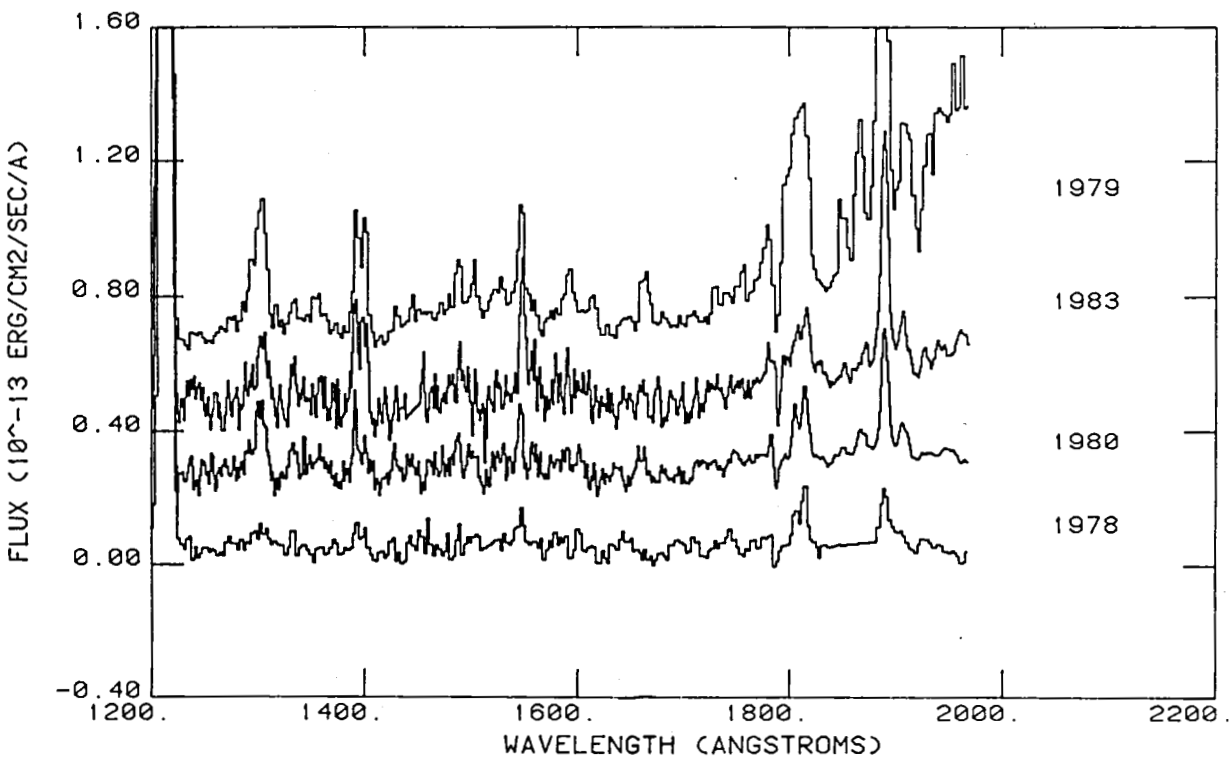

Figure 2. Four SWP spectra of RW Aur, each offset by 0.2 x 10^{-13} in the vertical axis. The strongest emission lines are O I 1300, Si IV 1400, C IV 1550, Si II 1815, and Si III 1892.

Figure 3. Variation of ions formed at various temperatures versus visual brightness for the four SWP spectra of RW Aur.

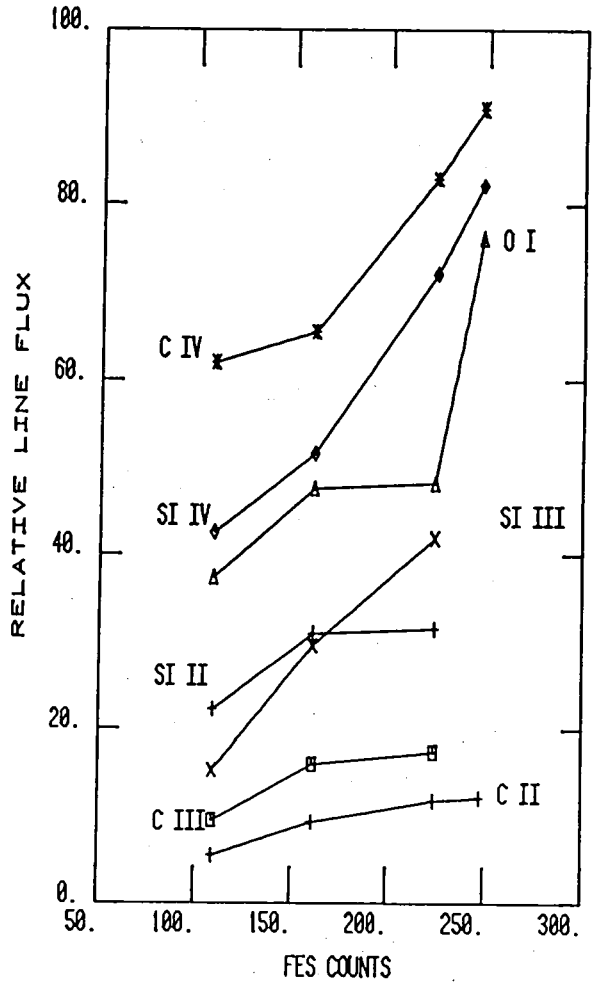

Figure 4. Variation in the UV continuum in RW Aur.

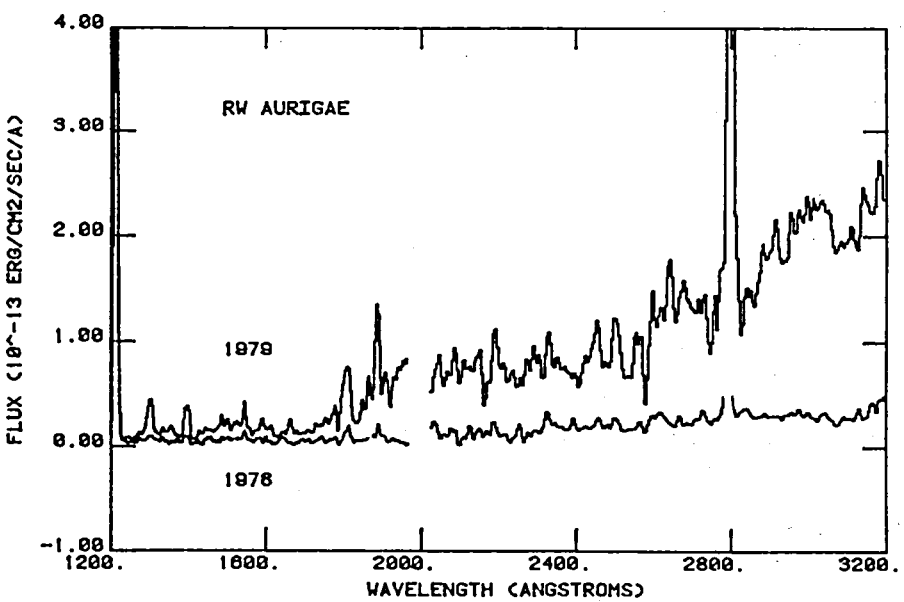

WHITE DWARF STARS AT ULTRAVIOLET WAVELENGTHS

James Liebert
Steward Observatory, University of Arizona

ABSTRACT

Numerous discoveries with the IUE Observatory have stimulated research on most spectroscopic types of degenerate dwarf stars. The hottest helium-rich cases apparently have substantial abundances of certain ions heavier than helium, due most likely to selective radiative acceleration. Hydrogen DA stars show trace abundances at temperatures as low as 20,000 K and provide evidence for modest outflowing winds. Cooler DA stars exhibit mysterious broad features near 1400Å and 1600Å. The element carbon is almost omnipresent in cool helium-rich stars, unless metallic features are seen instead. The carbon is most likely dredged-up by a deep convective envelope. The metals are attributed to interstellar accretion. IUE has played an important role in temperature determinations for helium-rich and magnetic stars. White dwarf components in detached and cataclysmic binaries have been studied extensively with IUE, often for the first time. Among the potential results are mass determinations and information on the photospheric temperature distributions for accreting primaries.

INTRODUCTION

White dwarfs normally show quite dull optical spectra; even with a 4-5 meter telescope and state-of-the-art detectors, only the dominant atmospheric constituent appears. Hydrogen atmosphere cases are classified DA, regardless of temperature; stars showing neutral helium lines are called DB. Stars too cool for the dominant element to be excited generally show no optical features, and are classified DC. The reason for these monoelemental atmospheres is that -- at the high surface gravities -- the lightest element in the envelope floats to the top rather quickly, while heavier elements sink. After all, the physical depth of a white dwarf atmosphere is of order a hundred meters!

Of course, if the foregoing were completely true, I wouldn't have had a Ph.D. thesis derived from detailed optical spectrophotometry (Liebert 1977). There have been three kinds of (nonmagnetic) exceptional white dwarf spectra, all associated with helium-rich atmospheres: (1) Some DB stars show traces of hydrogen, near the limit of detectability; (2) metallic line (DZ) stars show a few metals, but generally no hydrogen or carbon; and (3) the carbon-band white dwarfs generally show no metals or hydrogen. At the time of launch of IUE, nobody understood how these three groups related to each other, or why they were exceptional.

After six years of IUE observations, the vast majority of targetted degenerate stars have revealed ultraviolet spectral features. Generally, only

those white dwarfs too cool and faint for this 0.45-meter telescope retain a strict DC (featureless) spectral type. In the following discussion, several areas of white dwarf research which have been advanced by IUE observations are briefly reviewed. These discoveries are the dominant reason that my earlier review (Liebert 1980) is now out of date.

TRACE ELEMENTS IN HOT WHITE DWARFS

It is logical that the very hottest objects would be among the best candidates for showing multi-element atmospheres. Recently-formed degenerate stars are, of course, less likely to have undergone gravitational diffusion. Moreover, selective radiative acceleration of certain ions having resonance transitions near the star's Planckian radiation peak may result in the suspension or even expulsion of these ions. For unsaturated line transitions, the radiative acceleration depends on T_{eff}^4/A (where A is the atomic mass of the element being considered). Stars with helium-rich atmospheres seemed to be more logical candidates than hydrogen-rich cases for two reasons. First, helium-rich atmospheres generally have higher pressures at a given optical depth, and the resulting increased line widths reduce the effect of saturation on the lines. Secondly, the reduced continuum opacities mean that trace elements are detectable at lower column densities.

Indeed, the very hot pulsating PG1159-035 stars show carbon and probably nitrogen features at optical wavelengths (McGraw et al. 1979; Liebert and Green 1979); a rich variety of ultraviolet metallic features are revealed with the low resolution IUE camera (Wesemael, Green and Liebert 1984). Still, there is a possible discrepancy in temperature estimates for these helium-rich stars. IUE spectra appear to show weak C III, N III transitions, which suggests that $T_{eff} \lesssim 10^5$ K. This is a bit lower than the estimate for the prototype based on the Einstein X-ray detection and the very hot far-UV energy distribution measured with the Voyager detector (Wegner et al. 1982). The supposedly cooler DO star PG1034+001 shows strong N V but no N III features in a high dispersion spectrum (Sion, Liebert and Wesemael 1984). A well-exposed ultraviolet echelle spectrum of PG1159-035 might clear up the problem, showing whether the low ionization features -- if real -- belong to the photosphere. The first heavy element abundance determinations for a helium-rich object -- PG1034+001 -- indicate substantial nitrogen and carbon values -- log (N/He) ~ -2.5 and log (C/He) ~ -2.5 (Sion, Liebert and Wesemael 1984).

For reasons stated earlier, it was more surprising that apparently-photosphere metal features have now been found in some hot DA (hydrogen) white dwarfs, ranging in temperature from about 70,000 K (Feige 24, Dupree and Raymond 1982) to 22,000 K (W1346, Bruhweiler and Kondo 1983). To be sure these transitions of silicon, nitrogen and carbon are quite weak (a few hundred milliangstroms or less) and detectable only with the IUE echelle. Some show radial velocities in agreement with optical H values, though an origin outside the photosphere cannot be ruled out. Others show "shortward shifted" velocities, leading Bruhweiler and Kondo (1983) to argue that there is evidence for modest outflowing winds in DA stars down to T_{eff} ~ 20,000 K. The lack of such features in stars as cool as 40 Eri B (~ 16,000 K) indicates that the radiative acceleration and/or wind processes are no longer operative

at lower temperatures. The first photospheric metal-line calculations for Feige 24 and W1346 indicate abundances of N, C and Si some 1-3 orders of magnitude below solar and with very non-solar relative values (Wesemael, Henry and Shipman 1984). The radiation fields of hot white dwarfs are capable of producing circumstellar Stromgren spheres; their number densities suggest the possibility that they are substantial contributors to the ionization balance of the interstellar medium (Dupree and Raymond 1983).

TRACE ELEMENTS IN COOL WHITE DWARFS

It was not surprising that the cool, helium-rich degenerate stars showing metallic lines at optical wavelengths unveiled a harvest of new lines at IUE wavelengths. Such studies of key stars as by Shipman and Greenstein (1983) and Cottrell and Greenstein (1980) have shown that a simple theory of accretion from an interstellar cloud followed by diffusion does not work. It is still necessary to explain why hydrogen is so effectively screened out (Liebert 1979), and why the heavier metals (Ca, Mg, Fe) are accreted more readily than the CNO species. The recent papers by Alcock and Illarionov (1980) and Truran and Wesemael (1982) lend insight into how a more complicated accretion theory might be made to work -- see also Shipman (1984).

On the other hand, IUE observations have now linked together the cool DC degenerates with those showing molecular carbon (C_2) at optical wavelengths: Both groups exhibit atomic and molecular carbon features at ultraviolet wavelengths. Comprehensive studies summarized by Koester, Weidemann and Zeidler -K.T. (1982), and Wegner and Yackovich (1984) indicate that the features span the range 6,000 - 12,000 K. Koester et al. argued that the trace carbon abundance is due to contamination of the outer helium convection zone by the tail of the equilibrium carbon distribution. Models predicting the amounts of dredged-up carbon by Fontaine et al. (1984) are in rather good agreement with abundance determinations which peak in the stars near 10 - 12,000 K. The abundances are generally low enough that the carbon features may be masked in those stars which accrete from the ISM: The metals supply extra electron donors, which increase the continuum opacity, and hide the carbon.

Despite the absence of sharp metallic or carbon features, it is perhaps the cool DA stars which exhibit the biggest surprises at IUE wavelengths. A fair number of stars show strong, broad or asymmetric absorption dips centered near 1400Å and 1600Å, starting with the discovery of the former in excellent 40 Eri B spectra by Greenstein (1980). Both features appear strongest at temperatures near 10,000 K but have been detected in stars as high as 20,000 K. Tentative explanations include molecular hydrogen transitions (Greenstein 1980), Si II autoionization lines (Sion, Wesemael and Guinan 1984) and bound-free edges of Ca II and Mg II (Wegner 1984a,b). It is possible that the 1600Å feature is related to some seen in Lambda Bootis and other peculiar A stars of lower gravity.

TEMPERATURES AND OTHER STELLAR PARAMETERS

The IUE telescope has proven moderately useful as an ultraviolet photometer for degenerate stars. Temperatures derived for hot helium-rich (DO)

stars from IUE fluxes are sometimes substantially lower than those assigned from He II and He I (optical) absorption features. While questions remain about the accuracy of the IUE flux calibration, the problem arises in only some of the stars; the more likely culprit here is interstellar reddening. Standard ultraviolet extinction curves predicting as much 2200Å "bump" absorption as 1200Å absorption are simply unreliable, especially for these small amounts (Greenberg and Chlewicki 1983). Likewise, temperature assignments for hot DA stars can be made more reliably from hydrogen line strengths.

On the other hand, IUE is playing an important photometric role for hot DB stars in the 20,000 - 40,000 K range. This range represents the broad peak of He I opacity, and the line profiles show remarkably little variation. While it would seem that precise optical photometry (i.e., Stromgren, multichannel) should be accurate enough, there have been numerous instances of systematic errors due to differing photometric systems in use. IUE can therefore play a dominant role in establishing the temperature boundaries of the newly-discovered DB pulsational instability strip (i.e., Winget et al. 1982, 1984; Koester, Weidemann and Vauclair 1983). In Figure 1, I show a fit by Francois Wesemael to the first discovered pulsating DB star GD358, using pure helium, blanketed logg = 8 models from Wesemael (1981). We get a marginally higher temperature estimate (~ 28,000 K vs. 26,000 K) than Koester et al. Curiously, the other displayed DB star (PG0112+10) obviously has a very similar temperature but does not pulsate (Winget 1983, private communication)! Finally, the IUE fluxes severely constrain the temperature of the strange hybrid He, H composition object GD323 to be near those for pulsating DB stars (Liebert et al. 1984).

Ultraviolet spectra and energy distributions from IUE have resulted in drastically altered temperature estimates and composition interpretations for two magnetic white dwarfs. To be sure, the temperature determination for the low field (~ 1.8×10^7 gauss) star Feige 7 was consistent with prior optically-based values and implied a normal white dwarf radius (Greenstein and Oke 1982). However, these authors derived a substantially higher temperature (~ 14,500 K) for the high field magnetic degenerate star Grw+70°8247 by rigorously fitting the extended energy distribution. This would imply an abnormally small radius (~ 0.007 $R_\odot$) and correspondingly large mass. On the other hand, the ultraviolet energy distribution shows evidence for extensive blanketing, especially below 1400Å, which can affect this conclusion. Greenstein (1984) now attributes this blanketing to Ly α absorption, in agreement with Angel's (1979) composition hypothesis for this star. Finally, it should be noted that the IUE fluxes for another strongly-magnetic case, GD229, result in a drastic revision of that star's temperature -- but this time the direction is downwards (Green and Liebert 1981)!

WHITE DWARFS IN BINARY SYSTEMS

Ultraviolet spectroscopy is an invaluable tool for the study of binaries containing a hot white dwarf, both detached systems and cataclysmic variables (CVs). In many cases, IUE has provided the first direct study of a white dwarf component. Examples for detached systems include the DA companion of the G8 IIIp barium star Zeta Cap (Böhm-Vitense 1980), the DO companion to

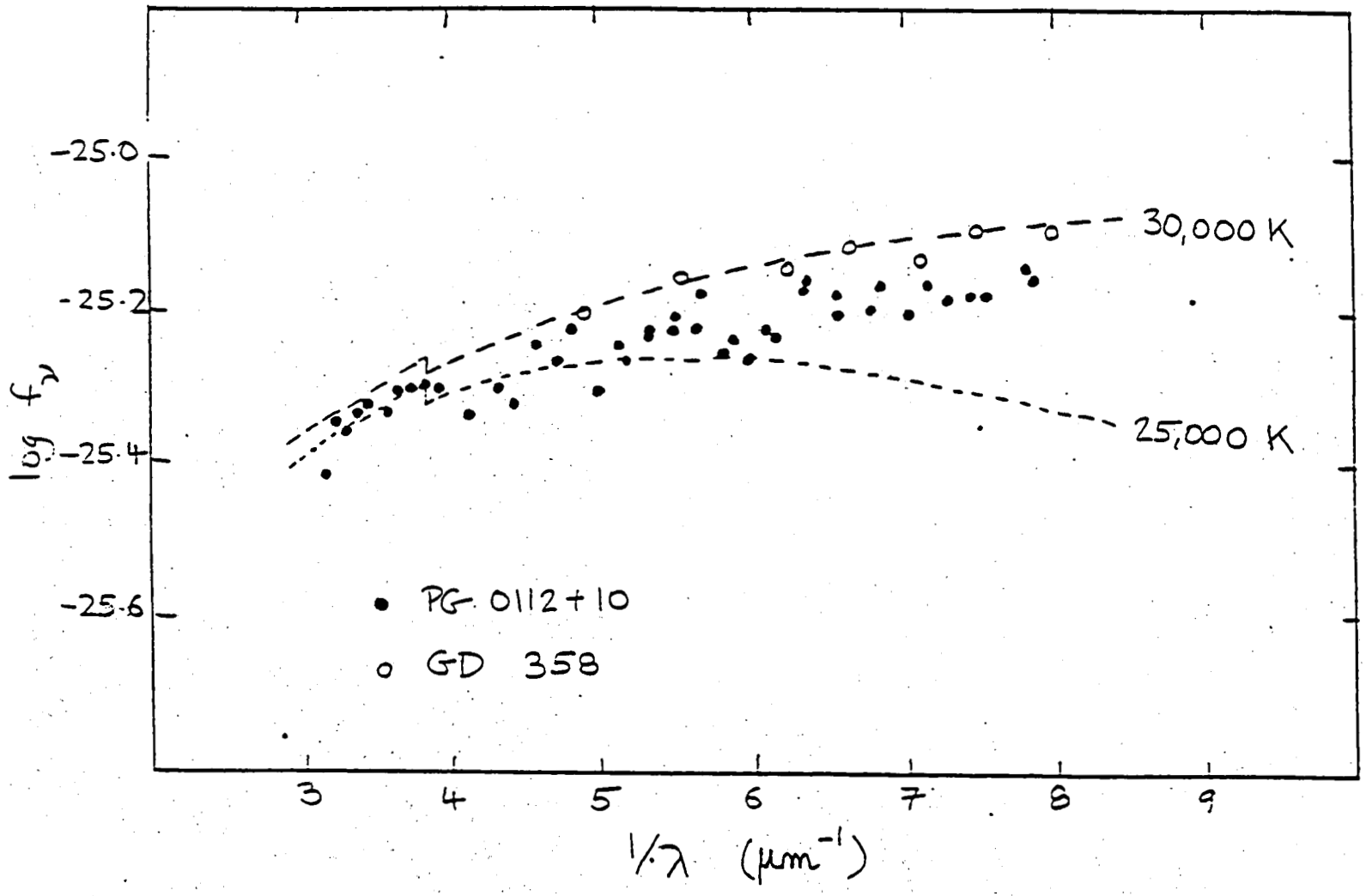
-25.0
-25.2
-25.4
-25.6
log f_λ
30,000 K
25,000 K
PG 0112+10
GD 358
3
4
5
6
7
8
9
1/λ (μm⁻¹)

Figure 1.

HD149499 (Sion, Guinan and Wesemael 1982), and such short-period products of common envelope evolution as the Hyads V471 Tau and HZ9 (Guinan and Sion 1984).

It is often possible to make direct determinations of other stellar parameters besides the temperature. The cool companion's radial velocity provides the systemic reference from which the gravitational redshift and mass of the white dwarf may be estimated from echelle observations. Sion and Guinan (1983) find an implied mass of 0.5 $M_{\odot}$ for HD149499B, the first direct determination for a hot helium star. Moreover, the relative masses at least may be obtained from radial velocity curves for close pairs, generally the cool star is measured with a high-disperison optical spectrograph. Finally, line profile analyses permit gravity determinations by "atmospheric" techniques and comparison to isolated white dwarfs.

CATACLYSMIC VARIABLE PRIMARY STARS

Direct observations of the white dwarf in several CV systems have been possible, for the first time, using IUE. Such observations are both opportunistic and complicated to interpret. The accretion disk generally dominates the energy output at ultraviolet wavelengths. However, some dwarf novae and perhaps all of the diskless AM Herculis objects go into such low accretion states that the white dwarf primary dominates the ultraviolet energy distribution. Important examples include MV Lyrae (Robinson *et al.* 1981), VW Hyi (Mateo and Szkody 1984), and probably U Gem in quiescence (Panek and Holm 1983). All appear to have hot ($T_{eff} \geq 40{,}000$ K) components, though this may be due to selection. In the case of the recent low state of TT Ari (Shafter *et al.* 1984), the spectrum of the white dwarf at optical wavelengths permits a standard photospheric analysis. The star can be classified DAO, yields $T_{eff} \sim 70{,}000$ K, and a He/H ratio not too different from solar, as expected for recently-accreted matter. Moreover, the agreement between optical and IUE temperature determinations leaves no evidence for temperature variations across the surface of the accreting star. This is in contrast to the situation for the magnetic AM Her in its low state. Schmidt, Stockman and Margon (1981) suggested $T_{eff} \leq 22{,}000$ K from their analysis of the magnetic primary's optical spectrum, but Szkody *et al.* (1982) required $T_{eff} \sim 50{,}000$ K to fit the ultraviolet. The obvious answer is that a residual polar hot spot dominates the ultraviolet, while larger, cooler areas of the photosphere dominate the optical light (Liebert and Stockman 1983).

I greatly appreciated many useful discussions with and receipt of information in advance of publication from Ed Sion, Francois Wesemael and Paul Szkody. This work has been supported by various NASA IUE grants and by National Science Foundation grant AST 82-18624.

REFERENCES

Alcock, C., and Illarionov, A. 1980, *Ap. J.*, 235, 541.

Angel, J. R. P. 1979, in *White Dwarfs and Variable Degenerate Stars*, IAU Colloq. No. 53, eds. H. M. Van Horn and V. Weidemann, University of Rochester, New York, p. 313.

Böhm-Vitense, E. 1980, Ap. J. (Letters), 239, L79.
Bruhweiler, F. D., and Kondo, Y. 1983, Ap. J., 269, 657.
Cottrell, P., and Greenstein, J. L. 1980, Ap. J., 238, 941.
Dupree, A. K., and Raymond, J. C. 1982, Ap. J. (Letters), 263, L63.
Dupree, A. K., and Raymond, J. C. 1983, Ap. J. (Letters), 265, L71.
Fontaine, G., Villeneuve, B., Wesemael, F., and Wegner, G. 1984, Ap. J. (Letters), 277, L61.
Green, R. F., and Liebert, J. 1979, in White Dwarfs and Variable Degenerate Stars, IAU Colloq. No. 53, eds. H. M. Van Horn and V. Weidemann, University of Rochester, New York, p. 377.
Green, R. F., and Liebert, J. 1981, Pub. A.S.P., 90, 303.
Greenberg, J. M., and Chlewicki, G. 1983, Ap. J., 272, 563.
Greenstein, J. L. 1980, Ap. J. (Letters), 241, L89.
Greenstein, J. L., and Oke, J. B. 1982, Ap. J., 252, 285.
Greenstein, J. L. 1984, Ap. J. (Letters), 281, in press.
Guinan, E. F., and Sion, E. M. 1984, submitted to A. J.
Koester, D., Weidemann, V., and Vauclair, G. 1983, Astr. Ap., 123, L11.
Koester, D., Weidemann, V., and Zeidler, -K. T., E. M. 1982, Astr. Ap., 116, 147.
Liebert, J. 1977, Ph.D., Thesis, University of California at Berkeley.
Liebert, J. 1979, in White Dwarfs and Variable Degenerate Stars, IAU Colloq. No. 53, eds. H. M. Van Horn and V. Weidemann, University of Rochester, New York, p. 146.
Liebert, J. 1980, Ann. Rev. Astron. Astrophys., 18, 363.
Liebert, J., and Stockman, H. S. 1983, in Cataclysmic Variables and Low Mass X-Ray Binaries, eds. J. Patterson and D. Q. Lamb, Cambridge, Massachusetts, D. Reidel Press.
Liebert, J., Wesemael, F., Sion, E. M., and Wegner, G. 1984, Ap. J., 277, 692.
Mateo, M., and Szkody, P. 1984, Ap. J., in press.
McGraw, J. T., Starrfield, S. G., Liebert, J., and Green, R. F. 1979, in White Dwarfs and Variable Degenerate Stars, IAU Colloq. No. 53, eds. H. M. Van Horn and V. Weidemann, University of Rochester, New York, p. 377.
Panek, R. J., and Holm, A. V. 1983, preprint.
Robinson, E. L., Barker, E. S., Cochran, A. L., Cochran, W. D., and Nather, R. E. 1981, Ap. J., 251, 611.
Schmidt, G. D., Stockman, H. S., and Margon, B. 1981, Ap. J. (Letters), 243, L157.
Shafter, A., Szkody, P., Liebert, J., Bond, H. E., and Grauer, A. D. 1984, submitted to Ap. J.
Shipman, H. L. 1984, Poster Paper, presented at the American Astronomical Society meeting, Las Vegas, Nevada, January 10, 1984.
Shipman, H. L., and Greenstein, J. L. 1983, Ap. J., 266, 761.
Sion, E. M. and Guinan, E. F. 1983, Ap. J. (Letters), 265, L87.
Sion, E. M., Guinan, E. F., and Wesemael, F. 1982, Ap. J., 255, 232.
Sion, E. M., Liebert, J., and Wesemael, F. 1984, submitted to Ap. J.
Sion, E. M., Wesemael, F., and Guinan, D. F. 1984, Ap. J., in press.
Szkody, P., Raymond, J. C. and Capps, R. W. 1982, Ap. J., 257, 686.
Truran, J., and Wesemael, F. 1982, Ap. J., 260, 807.
Wegner, G. 1984a, Preprint on 1400Å Feature.
Wegner, G. 1984b, Preprint on 1600Å Feature.

Wegner, G., Barry, D. C., Holberg, J. B., Forrester, W. T., and McGraw, J. T. 1982, Bull.A.A.S., 14, 914.
Wegner, G., and Yackovich, F. H. 1984, Ap. J., submitted.
Wesemael, F. 1981, Ap. J. Suppl., 45, 177.
Wesemael, F., Green, R. F., and Liebert, J. 1984, Ap. J., in press.
Wesemael, F., Henry, R. B. C., and Shipman, H. L. 1984, Ap. J., submitted.
Winget, D. E., Robinson, E. L., Nather, R. E., and Balachandran, S. 1984, Ap. J., in press.
Winget, D. E., Robinson, E. L., Nather, R. N., and Fontaine, G. 1982, Ap. J. (Letters), 262, L11.

GALAXIES

SUPERNOVA REMNANTS AND THE CARBON ABUNDANCE IN M33

William P. Blair and John C. Raymond

Harvard-Smithsonian Center for Astrophysics

ABSTRACT

We have combined IUE and optical spectral data on a supernova remnant in M33 in order to determine the abundance of carbon in the interstellar gas of M33. We have used new shock model calculations to guide the interpretation and find that a substantially lower value of the ratio C/O than has been assumed previously for M33 may be necessary to explain the data. However, some inconsistencies in the observed and predicted line intensities indicate that the spectra may be partly contaminated by H II region emission or that the preshock gas has been ionized by nearby stars.

INTRODUCTION

Recent improvements in the techniques for calculating shock wave models (Raymond 1979, Shull and McKee 1979, Dopita et al. 1984) have allowed observations of the emission line ratios from supernova remnants (SNRs) to be interpreted in terms of abundances. For all SNRs larger than roughly 5 pc diameter, the supernova blast wave will have swept up many times more interstellar gas than was ejected by the supernova. Hence, this analysis can be used to determine abundances in the interstellar gas. This has been done optically for SNRs in several nearby galaxies, including M31 and M33 (Dopita, D'Odorico and Benvenuti 1980; Blair, Kirshner and Chevalier 1982; Dopita et al. 1984; Blair and Kirshner 1984), with the results from SNRs being compared with results from H II regions to assess the gas phase abundance gradients in these galaxies. One of the uncertainties in the abundance gradient analyses is the unknown abundance of carbon, which has no readily detectable lines in the optical. Previous investigations have had to assume a value for the C/O ratio. Since carbon is an important coolant in both photoionized and shock heated gas, an incorrect carbon abundance can affect the line intensities (and hence abundance estimates) of other elements.

Observations of galactic SNRs with IUE (e.g. Benvenuti et al. 1980; Raymond et al. 1981) have shown that the ultraviolet emission lines of carbon are among the strongest lines in SNR spectra over a wide range of conditions. In addition, the ratio C III] λ1909 / C IV λ1550 is sensitive to shock velocity. During the fifth and sixth years of IUE, we have observed five SNRs in M33 in order to investigate the carbon abundance and determine to what extent the previously assumed abundance of this element may have affected abundance estimates for other elements. Here we will discuss only the observations of M33-8 from the catalog of D'Odorico, Dopita and Benvenuti (1980). In collaboration with S. D'Odorico, P. Benvenuti and M. Dopita, we obtained an 840 minute SWP exposure during an ESA-US1 shift pair. This remnant was chosen for its high surface brightness and low reddening. The remnant has a diameter of about 11 pc and appears to be an isolated emission region on interference filter photo-

TABLE 1

Comparison of M33-8 Observations to Model Calculations

Line	λ	M33-8 F(λ)	M33-8 I(λ)	Model A 90 km/s	Model B 120 km/s
Si IV	1394	}	}	52	25
O IV]	1402	<64	<80	57	245
C IV	1550	336	411	346	547
He II	1640	<46	<56	28	24
O III]	1664	163	197	219	196
Si III]	1892	<40	<50	103	60
C III]	1909	57	70	402	176
[O II]	3727	(520)[a]	543	604	542
[Ne III]	3869	(26)[a]	27	23	17
[S II]	4070	(14)[a]	14.4	21	19
[O III]	4363	(12.5)[a]	12.8	32	27
He II	4686	(12)[a]	12.1	5	4
Hβ	4861	100	100	100	100
[O III]	4959,5007	340	338	413	343
[N I]	5200	<4	<4	23	26
He I	5876	10.3:	10.0:	4	4
[O I]	6300,6364	27:	26:	45	55
Hα	6563	315	300	303	297
[N II]	6548,6584	152	144	153	151
[S II]	6717,6731	197	187	228	225
[O II]	7320,7330	<5	<4.7	39	26
E(B-V)		0.05		---	---
F(Hβ)		1.26 E-14		---	---

[a] Line intensities in parentheses from Dopita et al. (1980).

TABLE 2

Model Parameters and Abundances Relative to Cosmic

Parameter	Model A	Model B	Cosmic Abundances[a]
n_o (cm^{-3})	5	2	---
V_s^o (km s^{-1})	90	120	---
log He	10.93	10.93	10.93
log C	7.70	8.00	8.52
log N	7.56	7.56	7.96
log O	8.42	8.62	8.82
log Ne	7.22	7.52	7.92
log Mg	6.92	7.22	7.42
log Si	6.62	7.22	7.52
log S	7.00	6.90	7.20
C/O	0.19	0.24	0.50

[a] Cosmic abundances by number, from Allen (1973).

graphs.

The observed and reddening corrected line fluxes are listed in Table 1, along with optical data from Dopita et al. (1980; data in parentheses) and Blair and Kirshner (1984). The optical reddening estimates and Hβ flux from Blair and Kirshner (1984) are also shown. Reddening correction has been performed assuming a theoretical ratio of $I(H\alpha)/I(H\beta) = 3.0$ and the extinction curve of Seaton (1979). We note that the comparison of the optical and UV line intensities is only as good as the optical flux calibration (± 35%; Blair and Kirshner 1984).

INTERPRETATION

Qualitatively, the low value of the C III] / C IV line ratio argues for a high shock velocity, and the small C III] / O III] λ1664 ratio implies a C/O ratio considerably smaller than the value of 1/3 previously assumed (Dopita et al. 1980). Table 1 shows two model spectra for shock velocities of 90 and 120 km/s. Preshock densities of 5 and 2 cm^{-3} were assumed to match the densities inferred from the optical [S II] doublet ratio, and the preshock gas was taken to be fully ionized. The models were computed with an updated version of the code used by Raymond (1979) with improved excitation, ionization and recombination rates. The abundance sets used are listed in Table 2. While the agreement between observed and predicted intensities of the strong optical lines is good, and could clearly be improved by modest adjustments to the assumed abundances, two major discrepancies stand out. The C IV/C III] ratio predicted by the 90 km/s shock is far too low to match the observation. The 120 km/s shock does better, though a still higher velocity would be needed to reach the observed value. However, the upper limit on the O IV]-Si IV blend at 1400 Å conflicts with model velocities above 90 km/s. This cannot be avoided by increasing the C to O abundance ratio because of the high observed value of the O III]/C III] intensity ratio. The only apparent way to reconcile the models with the observed spectrum is to appeal to ionization of the preshock gas. The ionization potential of O III coincides with that of He II, while the C III ionization potential is 7 eV lower. Model stellar atmospheres have very deep He II absorption edges, so that the oxygen in an H II region is mostly O III, while the carbon is largely C IV. A slow shock (V_s < 90 km/s) in gas in which the carbon is preionized to C IV would produce the observed large C IV/C III] ratio without producing too much emission at 1400 Å. It might also be possible for radiation produced by the SNR itself to create the necessary ionization state if He II absorbs most of the photons above the O III edge, but this would require a specific evolutionary state for the SNR.

While the strong [S II] doublet suggests a basically collisionally ionized gas, the temperature sensitive line ratios [O II] λλ7320,30/λ3727 and [O III] λ4363/λ5007 are much lower than predicted by the models. While higher velocity shock models do produce lower values for these ratios, the strong upper limit on O IV] λ1400 precludes a high enough shock velocity for this to be a viable explanation. On the other hand, low values of these ratios are typical of photoionized gas. While there is no clear evidence for H II region contamination for this SNR, another M33 emission region has recently been identified as just such a combination: a small diameter SNR embedded in an

H II region (M33-7, see Blair and Kirshner 1984). One could imagine either contamination of the spectrum by H II region emission or photoionization of the shocked gas of the SNR by nearby stars. The observed ratio of the [S II] λ4070/λλ6717,30 lines is close to that predicted by the shock models, suggesting that the [S II] is indeed formed by collisionally ionized gas. Presumably this means that the [S II] emission of the photoionized regions is weak, as is generally observed. One would expect that the lines of [O I], [N I] and He II would also be produced in shocked gas. Their weakness relative to the Balmer lines (when compared with the shock models) suggests roughly equal contributions of shocks and photoionized gas to the Balmer line intensities.

With the exception of the 1400 Å feature, model B does a reasonable job of matching many of the strong emission line intensities. As can be seen from Table 2, the C/O ratio for this model is about half of the cosmic value, while the C III]/O III] line intensity ratio from Table 1 is larger than observed by roughly a factor of 2.5. Hence, it is conceivable that the C/O ratio in M33 has been previously overestimated by a factor of three to five, although a more complete analysis is needed to establish this conclusively. This is large enough to affect the abundance determinations from SNR spectra (cf. Dopita et al. 1984).

SNRs in nearby galaxies are difficult targets for IUE and the uncertainty in the relative calibration of optical and UV data places limitations on the effectiveness of the comparison. The increased sensitivity and resolution of the Faint Object Spectrograph on Space Telescope (Giacconi 1982; Table 1) along with simultaneous UV/optical coverage (1150-7000 Å) will permit many of the M33 SNRs to be observed and will allow a more complete abundance analysis to be performed. This work is supported by NASA grant NAG 5-87 to the Smithsonian Astrophysical Observatory.

REFERENCES

Allen, C.W. 1973, Astrophysical Quantities, (3rd ed.; London: Athlone).
Benvenuti, P., Dopita, M.A., and D'Odorico, S. 1980, Ap. J., 238, 601.
Blair, W.P., and Kirshner, R.P. 1984, Ap. J., submitted.
Blair, W.P., Kirshner, R.P., and Chevalier, R.A. 1982, Ap. J., 254, 50.
Danziger, I.J., Murdin, P.G., Clark, D.H., and D'Odorico, S. 1979, M.N.R.A.S., 186, 555.
D'Odorico, S., Dopita, M.A., and Benvenuti, P. 1980, Astr. Ap. Suppl., 40, 67.
Dopita, M.A., Binette, L., D'Odorico, S., and Benvenuti, P. 1984, Ap. J., 276, 653.
Dopita, M.A., D'Odorico, S., and Benvenuti, P. 1984, Ap. J., 236, 628.
Giacconi, R. 1982, "Science Operations with Space Telescope", in The Space Telescope Observatory, NASA CP-2244, ed. by D.N.B. Hall, p. 1.
Raymond, J.C. 1979, Ap. J. Suppl., 39, 1.
Raymond, J.C., Black, J.H., Dupree, A.K., Hartmann, L.W., and Wolff, R.S. 1981, Ap. J., 246, 100.
Seaton, M.J. 1979, M.N.R.A.S., 187, 73p.
Shull, J.M., and McKee, C.F. 1979, Ap. J., 227, 131.
Smith, H.E. 1975, Ap. J., 199, 591.

COMMENTS ON THE ORIGINS AND VARIATIONS OF CARBON AND NITROGEN IN THE ISM OF GALAXIES AS EVIDENT FROM IUE SPECTROSCOPY OF H II REGIONS

Reginald J. Dufour
Rice University and Dominion Astrophysical Observatory

ABSTRACT

During the last several years IUE observations of UV spectra of galactic and extragalactic H II regions have provided our first good quantitative measurements of gaseous-phase C abundances in the ISM of several galaxies over a broad range of "metallicity". This paper illustrates the observed relative variations of C, N, and O based on IUE and ground-based observations of H II regions and discusses the trends evident using current concepts regarding stellar nucleosynthesis of CNO element group and simple models of galactic chemical evolution.

INTRODUCTION

The first detailed abundance study utilizing IUE observations of the UV spectrum of an H II region was that of the Orion Nebula by Torres-Peimbert, Peimbert, and Daltabuit (1980). They found C/H and C/O to be essentially "solar" in Orion, with no evidence that C varied across the nebula in any manner consistent with the dust distribution, which suggested that depletion of C in dust does not significantly affect the gaseous-phase C abundances obtained at least for the Orion Nebula. Subsequently, Dufour, Shields, and Talbot (1982) reported IUE observations and C abundances for several H II regions in the Large and Small Magellanic Clouds derived through model analyses. They found C/O lower in the LMC by 0.34 dex and lower in the SMC by 0.75 dex compared with Orion. Somewhat surprisingly, the C depletion in the SMC is larger than even N. From the observed C/O and C/N ratios in the Clouds and Orion, they concluded that the nucleosynthetic origins of C are different from O; and that most of the N in the Clouds is the result of primary nucleosynthesis in massive stars, rather than from secondary processing of C. Additional evidence that N/C increases with decreasing C/H in metal-poor extragalactic H II regions has been presented by Gondhalekar (1983), who derived C abundances from IUE UV data on Tol 1924, NGC 2363, NGC 5471, Mkn 59, and NGC 4258.

NEW ANALYSIS OF C ABUNDANCES IN EXTRAGALACTIC H II REGIONS

In a separate paper at this symposium Dufour, Schiffer, and Shields (1984) presented a review of IUE archive data and additional low and high disperison observations of UV emission lines in extragalactic H II regions. To date, largely from C III] measurements, C abundances have been derived in nine extragalactic H II regions or galaxies in addition to the Magellanic Clouds and Orion Nebula (NB: the UV spectra of several other galactic H II regions were observed with the IUE or studied in the archives without any success in measuring any of the UV C lines). The CNO abundance results were summarized in

the previous paper. In this paper the relative variations of C, N, and O derived for the various objects are presented graphically, and some preliminary conclusions are briefly discussed in the context of current ideas regarding stellar nucleosynthesis and galactic chemical enrichment.

RELATIVE VARIATION OF CARBON AND NITROGEN

Figure 1 illustrates the observed variation of N against C in the objects for which C III] has been measured. It is fairly well established that O abundances in a majority of well observed nearby irregular galaxies follow the expectations of the simple "closed box" chemical evolution model with instantaneous recycling and little or no infall (cf. the review by Pagel and Edmunds 1981 and references therein). For such a situation, if N is produced entirely by secondary processing of pre–existing C in stars and ejected into the ISM, then N/H should vary with the square of the C/H abundance. It is clear from Figure 1 that N does not follow such a trend in galaxies for which $12 + \log(C/H) < 8.0$; $\log(N/C)$ *decreases* with $\log(C/H)$ over this range. Aside from the two H II regions in M33 (NGC 604 and NGC 588, for which the optical–to–UV transformation is still suspect), N/H varies as the *square root* of C/H over the metal–poor range. (NB: P. M. Gondhalekar reports in a private communication to the author that the Tol 1924 point in Figure 1, which comes from his 1983 study, is now more firmly established based on additional observations.)

The question as to whether N in galaxies orginates predominantly from primary or secondary nucleosynthesis in stars has received much discussion in the literature during the last few years. Observations of N/O in the H II regions of nearby irregular galaxies suggest that it is roughly constant ($\log(N/O) = -1.5 \pm 0.2$, Talent 1980; also see Figure 1 in Pagel and Edmunds 1981) in systems for which $12 + \log(O/H) < 8.4$, but varies roughtly as the square of O/H in the more metal–rich spirals. Such variation is accountable if N has both primary and secondary origins, such that massive stars produce relatively small amounts of primary N, which is ejected into the ISM via SN II with a yield $y(N) \approx 0.03y(O)$, and less massive stars ($M \leq 5\ M_{\odot}$) produce significant amounts of secondary N, which is ejected into the ISM via planetary nebulae and novae (and/or SN I?). However, both theory and observation are uncertain regarding C dredge–up amounts and how much C is transformed into N in intermediate mass stars during various dredge–up phases of AGB evolution (cf. the excellent review by Iben and Renzini 1983). Such mechanisms would then result in *largely primary* N being ejected by intermediate mass stars; and if the same objects eject most of the C, then $N/C \approx$ constant over the range of C and O. From Figure 1, this may indeed be the situation for evolved systems with $12 + \log(C/H) > 8.0$, but the data are too few to draw any conclusions regarding the variation of N/C in the high metallicity end of the range of H II region abundances (observations of C III] for such objects are usually very difficult due to low ionization levels and particularly low electron temperatures). However, Laird (1984) found C/Fe and N/Fe $\sim$ constant in a majority of galactic field dwarf stars spanning a range of metallicity of almost three orders of magnitude in Fe/H. This result, which is somewhat at odds with ours for the N/C ratio, led him to suggest that the nucleosynthesis of both N and C are predominently primary and arise from the same stars.

RELATIVE VARIATION OF CARBON AND OXYGEN

Figure 2 shows the variation of $\log(O/C)$ verses $12 + \log(C/H)$ for the program H II regions or galaxies. *Over the range of 1.5 dex in* $\log(C/H)$ *it is found that* C/H *varies as the square of* O/H. While this result of C is suprising in the sense that in the simple model it is the variation expected of an element produced as the result of secondary nucleosynthesis

of O or some other primary element, a more likely explanation is that most of the C production and enrichment occurs in lower mass stars than those responsible for the O enrichment.

The expected variation of a primary element produced predominantly in lower mass stars (i.e., SN II, PNe, and novae progenitors) than those which produce most of the O (SN I) following the simple chemical evolution model has been calculated and discussed by Tinsley (1979). Letting her fictitious element Z_1, which is produced in stars between 4 and 6.5 $M_\odot$ (originally intended to represent the "Fe group"), be identical to C, results in the variation of O/C observed in Figure 2 (cf. her Figure 3). To illustrate this, the variation of $\log(O/Z_1)$ verses $12 + \log(Z_1/H)$ from three of her models is shown in the figure, normalized to the values of C and O for Milky Way H II regions. Models 1 and 2 represent simple closed-box models of varying gas exhaustion timescales (or conversely, star formation rates) of 2×10^{10} years in Model 1 and 10^8 years in Model 2. Model 3 is her "extreme infall" model for which the SFR keeps up with infalling gas such that the gas mass remains constant while the total mass of the system grows.

As can be seen from the figure, the O/C data for the galaxies fall between, but along, the variation of O/C against C/H predicted from the slow SFR Model 1 and the high SFR Model 2 or infall Model 3. The data are therefore consistent with the simple model predictions for reasonable SFRs if C is predominantly produced (with Fe) in intermediate mass stars, while most of the O comes from short-lived massive stars. The concept that the nucleosynthetic origins of C and Fe are similar is further supported by the spectroscopic studies of C/Fe in field dwarf stars by Sneden, Lambert, and Whitaker (1979) and Laird (1984), which found C/Fe to be constant and essentially solar amoung stars spanning three orders of magnitude in Fe/H abundances.

REFERENCES

Dufour, R. J., Schiffer, F. H., and Shields, G. A. 1984, paper presented at this symposium.
Dufour, R. J., Shields, G. A., and Talbot, R. J. 1982, *Ap. J.*, **252**, 461.
Gondhalekar, P. M. 1983, *Adv. Space Res.*, **2**, 163.
Iben, I., and Renzini, A. 1983, *Ann. Rev. Astr. Ap.*, **21**, 271.
Laird, J. B. 1984, preprint.
Sneden, C., Lambert, D. L., and Whitaker, R. W. 1979, *Ap. J.*, **234**, 964.
Pagel, B. E. J., and Edmunds, M. G. 1981, *Ann. Rev. Astr. Ap.*, **19**, 77.
Talent, D. L. 1980, Ph. D. dissertation, Rice University.
Tinsley, B. M. 1979, *Ap. J.*, **229**, 1046.
Torres-Peimbert, S., Peimbert, M., and Daltabuit, E. 1980, *Ap. J.*, **238**, 133.

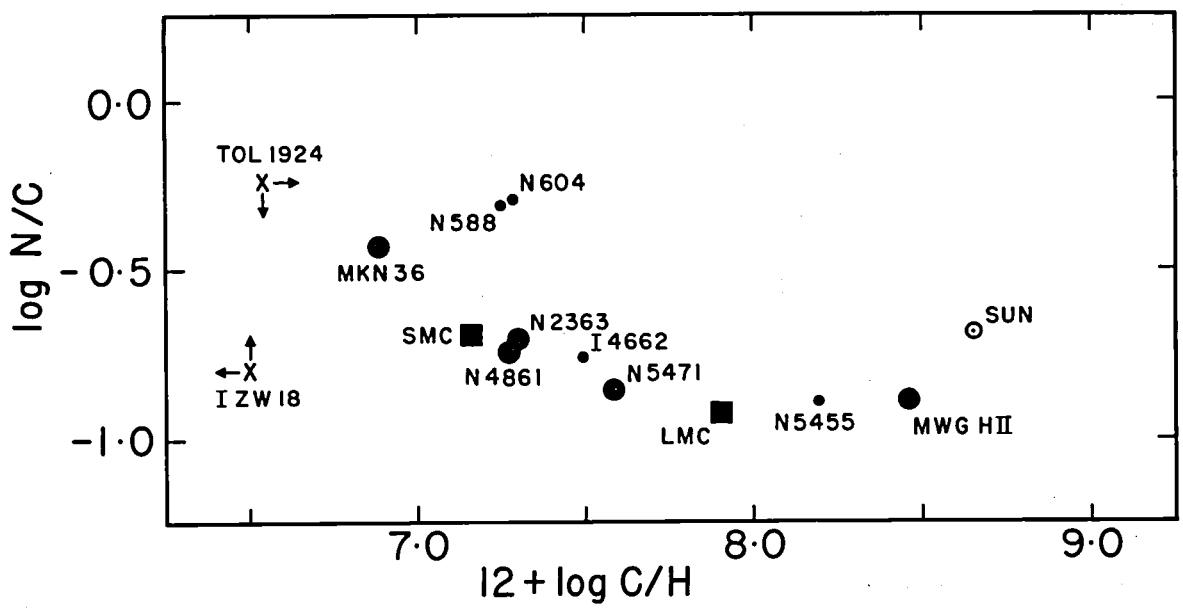

Figure 1 -- Illustration of the variation of the N/C ratio verses C abundance for the program H II regions and/or galaxies. The size of the symbols are proportional to the accuracy for which C/H is believed to be known (cf. Dufour et al. 1984).

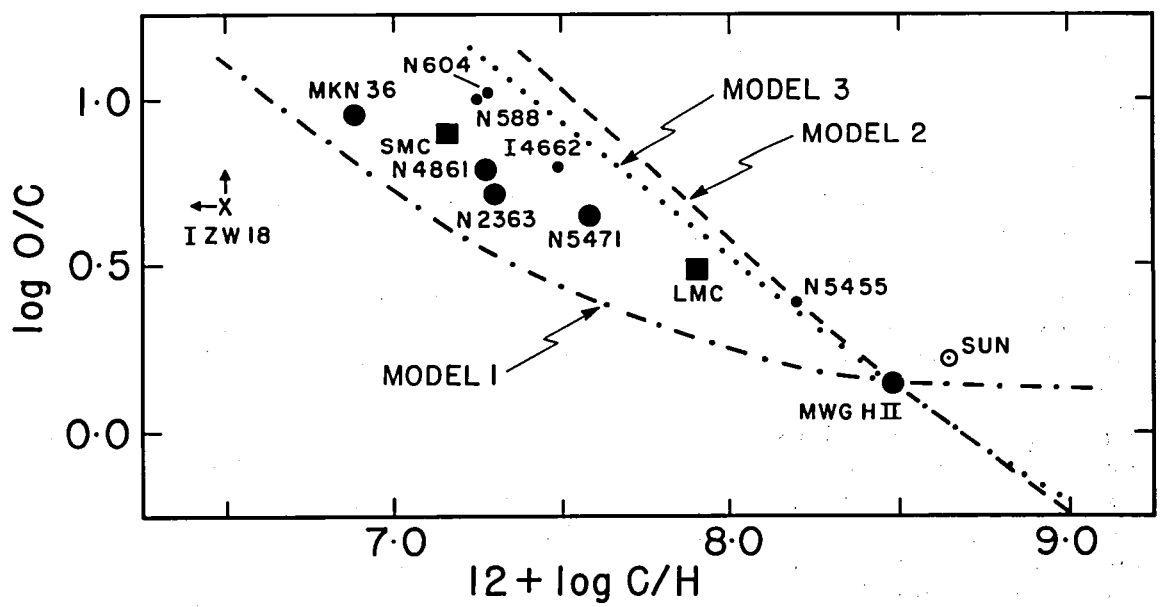

Figure 2 -- Illustration of the variation of O/C verses C abundance for the program objects. Lines represent model predictions by Tinsley (1979).

IUE SPECTROSCOPY OF EXTRAGALACTIC H II REGIONS

Reginald J. Dufour
Rice University and Dominion Astrophysical Observatory

Francis H. Schiffer, III
Computer Sciences Corporation
Space Telescope Science Institute

Gregory A. Shields
The University of Texas at Austin

ABSTRACT

This report summarizes progress made in studying the UV spectra of several prominent extragalactic H II regions with the IUE during the two years since our last report in the Second Goddard IUE Symposium. High dispersion spectra have been obtained of N81 and N66A in the SMC, the 30 Doradus Nebula in the LMC, NGC 2363 in the SBm galaxy NGC 2366, NGC 5471 in M101, and NGC 604 in M33, that are superior in quality to low dispersion spectra in the statistical accuracy and resolution of the nebular emission lines of ions such as C III], Si III], N III], and O III]. These data are combined with ground-based spectroscopy to diagnose physical conditions (temperatures, densities, and ionization) and abundances in over twenty extragalactic H II regions derived from recent IUE low dispersion observations and/or archival spectra are also presented.

INTRODUCTION

The emission line spectrum of H II regions in the ultraviolet contains astrophysically important lines of C II], C III], C IV, Si III], N III], and others, which have no counterparts in the spectral region accessible to ground-based telescopes. The IUE was the first space-borne observatory suited to observing these lines in several of the more prominent galactic and extragalactic H II regions in the sky. A good compilation of the result from IUE low dispersion observations of the UV spectra of extragalactic H II regions and of the publications through 1982 has been given in the form of a spectral atlas by Rosa, Joubert, and Benvenuti (1984).

Because of their relative faintness, most of the IUE observations of extragalactic H II regions have been at low dispersion. While this offers the advantages of highest sensitivity per unit wavelength interval, for most of the objects studied, inclusion of the exciting OB stars in the IUE large aperture results in the H II region spectra being dominated by the stellar continuum rather than the emission lines. This limits exposure times and makes extraction of accurate emission line strengths difficult or impossible for many objects. To get around these problems, we began a program of observing extragalactic H II regions with the IUE at high dispersion in 1982. This paper reports on some of our initial results. By its necessarily brief nature, we must limit this report to a few examples with somewhat

incomplete discussion. The complete results for various objects and a more extensive astrophysical discussion will appear in a series of papers in the *Astrophysical Journal* during 1985.

STATE OF HIGH DISPERSION OBSERVATIONS AND EXAMPLE RESULTS

Long exposure (6—8 hour) high dispersion SWP and LWR (or LWP) spectra have been obtained of N66A and N81 in the SMC, the 30 Doradus Nebula in the LMC, the giant H II region NGC 2363 in the SBm galaxy NGC 2366, NGC 5471 in M101, and NGC 604 in M33. In most cases, the 70x dillution of the underlying stellar continuum at high dispersion resulted in significantly improved detectability and accuarcy of measurement of emission line strengths compared to comparable exposure low dispersion spectra of the same objects.

As an example, in Table 1 we compare the results of a 500 minute high dispersion SWP exposure of NGC 2363 to results obtained from several low dispersion SWP spectra (summed exposure equalled 444 minutes). It is evident that the general agreement between the net fluxes of "strong" lines from both spectra is good (suggesting that the absolute calibration of the SWP high dispersion orders is accurate), but the statistical errors of the line measurements are generally much better at high dispersion (these errors are rms signal-to-noise estimates between the line profile and adjacent continuum uneveness). Moreover, since the velocity resolution of high dispersion is superior to that at low dispersion, weak emission lines can be better detected and measured (or better upper limits set) by fitting a least-squares gaussian profile to a region of the high dispersion spectrum expected to contain the line (where the profile shape and IUE velocity adjusted wavelength can be determined accurately from strong lines such as C III] λ1907/9). Such techniques have proven futile with low dispersion spectra because of the poor wavelength resolution and the sometimes severe blending with stellar absorbtion features. These results lead us to believe that the HRS on the ST may be a better instrument for studying the emission line spectra of distant nebulae than the lower resolution FOS.

Table 1 — Line Measurements for NGC 2363

Wavelength	Ion	— 10^{14} F_λ — SWP 18192 (HD)	Low Dispersion
1393.755	Si IV	5.5 ± 6.3	< 12
1402.769	"	13.2 ± 6.5	} < 10
1406.000	Si IV]	13.1 ± 6.2	
1666.153	[O III]	14.8 ± 5.0	12.8 ± 6.5
1793.800	Ne III	3.6 ± 2.7	< 6
1892.030	Si III]	6.4 ± 1.5	16.2 ± 9.5
1906.680	C III]	33.6 ± 2.6	} 59.4 ± 8.1
1908.734	"	18.0 ± 1.2	

Another advantage of utilizing high dispersion observations of extragalactic H II regions is the additional scientific information provided by the separation of emission line multiplets. Such information is useful for determination of the temperature or density of a nebula, or as a check on values of atomic parameters. An example of this is the C III] λ1906.680/1908.734 pair, for which the ratio is sensitive to the electron density for $10^2 \leq N_e \leq 10^6$ cm^{-3}. Calculations of the λ1909/1907 ratio as a function of electron density

have been made using modern atomic data by Nussbaumer and Schild (1979) for physical situations appropriate to nebulae. For low densities, $N_e \leq 10^2$ cm^{-3}, and temperatures, $T_e \approx 10^4$ ° K, appropriate to H II regions, their calculations suggest that $I_{1909}/I_{1907} \approx 1.5$. By contrast, our high dispersion observations for five H II regions (all with $N_e \leq 10^3$ cm^{-3} from ground based studies) indicate ratios between 1.7 and 1.9. Therefore, either the atomic data (specifically the collision strengths), the calculations, or the calibration of the IUE high dispersion instrumental response is in error. Since these lines have been and are being used in many investigations of emission line objects, resolution of this problem concerning the low density limit ratio of the C III] lines is important.

LOW DISPERSION STUDIES OF CARBON ABUNDANCES

During the past year we have analyzed over a hundred SWP and LWR low dispersion spectra of galactic and extragalactic H II regions with the Goddard RDAF from the archives or, in some cases, obtained as part of our continuing IUE observing program. Emphasis was placed on measuring or obtaining upper limits on the C III] λ1907+1909 flux in H II regions having accurate ground-based spectrophotometry available (or obtained by us at CTIO and/or KPNO) in order to derive C abundances using model analyses. Currently, relatively little information is available on C abundances in the H II regions of galaxies spanning the range of metallicity found from ground-based studies. For the Galaxy, only the Orion Nebula has been adaquately studied in the UV for determination of the C abundance from the UV lines (Torres-Peimbert, Peimbert, and Daltabuit 1980), which was found to be similar to the solar value. Subsequently, Dufour, Shields, and Talbot (1983) have used IUE low dispersion data to determine C abundances in several H II regions of the Large and Small Magellanic Clouds, and found notably lower C/O ratio in the Clouds, particularly the SMC (which has a C/N lower than solar), compared to the sun or Orion. Most recently, Gondhalekar (1983) has reported lower than solar C/N values in several metal-poor systems (Tololo 1924, NGC 5471, and NGC 2363).

Table 2 gives CNO abundances for 13 H II regions or galaxies for which the C abundance was derived from measurements of C III] λ1907+1909 from IUE low dispersion spectra. For objects other than the SMC, LMC, and MWG H II regions (for which the CNO values come from the review by Dufour 1984a), and Tol 1924 (taken from Gondhalekar 1983), the calculation of C abundances (as well as for O and N) followed the model-inferred ionization correction approach of Dufour, Shields, and Talbot (1983). The ground-based data used in the calculations generally come from two or more spectrophotometric investigations with modern spectrometers published in the literature or personal unpublished observations made by the authors. Full details of the observations and physical analysis will be submitted for publication in the near future.

The objects are grouped together in order of the accuracy for which the C abundances are believed to be determined. This accuracy is largely set by how well the UV spectral data could be combined with the optical spectrophotometry. Group A contains the best studied systems, the SMC and LMC, for which the C results are based on three or more H II regions which are in excellent agreement with each other in a given Cloud. Group B contains three "objects" (the MWG H II C abundance is based solely on the Orion Nebula) for which the UV spectra were tied to the optical spectra physically based on multiplet lines of [O III] or [O II] observed in both the UV and optical regions). Group C consists of two objects for which it is believed that the entire emitting region flux is contained within the IUE large aperture and the UV/optical data combined from total fluxes of lines. Group D consists of nebulae for which the UV data were combined to the optical spectra based on a "effective Hβ flux" derived from optical surface photometry extracted to match the shape

and area of the IUE large aperture. Lastly, Group E consists of two O-poor blue-dwarf irregular systems — I Zw 18 and Tol 1924 — for which only limits are to the C III] line and C abundance are known. Formal errors to the abundances are difficult to derive because of the heterogenous mix of data from various sources. However, the O/H abundances should be accurate to ±0.1 dex in most cases, and N/H to ±0.2 dex — except for Group E. C/H abundances are probably accurate to ±0.1 dex for Group A, ±0.2 dex for Groups B and C and ±0.3 dex or worst for Group D. Some of the astrophysical implications of these results are discussed in the paper by Dufour (1984b) at this symposium.

Table 2 — CNO Abundances in H II Regions

		[X] = 12 + log(X/H)				
Group	Nebulae	[C]	[N]	[O]	log(N/C)	log(O/C)
A	SMC	7.16	6.46	8.02	−.70	0.89
	LMC	7.90	6.97	8.43	−.93	0.48
B	MWG H II	8.46	7.57	8.70	−.89	0.14
	NGC 2363	7.30	6.63	8.01	−.67	0.71
	NGC 5471	7.58	6.72	8.22	−.86	0.64
C	NGC 4861	7.27	6.53	8.05	−.74	0.78
	MKN 36	6.88	6.45	7.83	−.43	0.95
D	NGC 604	7.28	6.99	8.30	−.29	1.02
	NGC 588	7.25	6.94	8.25	−.31	1.00
	NGC 5455	8.19	7.31	8.57	−.88	0.38
	IC 4662	7.49	6.73	8.28	−.76	0.79
E	I Zw 18	<6.5	5.71	7.16	> − .8 :	>0.66
	Tol 1924	>6.54	6.31	N/A	< − .23	—
	Sun	8.65	7.96	8.87	−.69	0.22

REFERENCES

Dufour, R. J. 1984a, in "IAU Symp. No. 108: Structure and Evolution of the Magellanic Clouds", eds. S. van den Bergh and K. S. de Boer (Dordrecht: Reidel), in press.
Dufour, R. J. 1984b, paper presented at this symposium.
Dufour, R. J., Shields, G. A., and Talbot, R. J. 1982, *Ap. J.*, **252**, 461.
Gondhalekar, P. M. 1983, *Adv. Space Res.*, **2**, 163.
Nussbaumer, H., and Schild, H. 1979, *Astr. Ap.*, **75**, L17.
Rosa, M., Joubert, M., and Benvenuti, P. 1984, *Astr. Ap. Suppl.*, in press.
Torres-Peimbert, S., Peimbert, M., and Databuit, E. 1980, *Ap. J.*, **238**, 133.

THE USUAL HOT STARS IN UNUSUAL GALAXIES

S. A. Lamb*, J. S. Gallagher†, M. J. Hjellming*, and D. A. Hunter†

ABSTRACT

Two hot amorphous galaxies, NGC 1705 and NGC 1800 were successfully observed with the IUE when we obtained low dispersion, short wavelength data. These spectra, together with new optical data, indicate that the OB stellar content of these systems is quite like that of the normal OB complexes found in spiral and regular Irr galaxies.

INTRODUCTION

Amorphous galaxies form a class of blue, irregular-like galaxies which are remarkable for their lack of distinct OB stellar groups, even though several examples are close enough to be easily resolvable. These systems are a subset of the I0 or Irr II galaxies first described by Holmberg (1958) and were classified by Sandage and Brucato (1979; see also Krienke and Hodge 1974). Basically amorphous galaxies have smooth, elliptical-like optical image properties, but non-interacting members of the class resemble the Magellanic (Im) irregulars in terms of global parameters; i.e. they have low total masses, high hydrogen content, moderate luminosities, and blue colors (e.g. NGC 1800-Gallagher, Hunter and Knapp 1981).

Optical spectra of amorphous irregulars often give evidence of a major intermediate age stellar component indicating that the star formation process has been active for at least the past 10^9 years. Furthermore, we see star formation continuing in these galaxies today. Spatially extended optical emission lines from ionized hydrogen regions show that OB stars with masses of $\geq 15\ M_\odot$ are present, and in some cases the inferred star formation rate is so high that the galaxies must be in comparatively short lived star formation burst phases (cf. NGC 1569-Hunter, Gallagher, and Rautenkranz 1982). Yet in spite of the presence of ionized gas and distinct HII complexes, which albeit tend to blend into one another, individual OB associations are virtually undetectable. Thus, the formation of OB stars in amorphous irregulars is a puzzle which deserves a closer look.

In order to further explore the massive stellar populations in such systems, we have obtained IUE satellite ultraviolet spectra and new optical observations of two amorphous galaxies, NGC 1705 and NGC 1800.

---

*University of Illinois at Urbana-Champaign.
†Kitt Peak National Observatory, operated by Associated Universities for Research in Astronomy, Inc. under contract to the National Science Foundation.

THE ULTRAVIOLET OBSERVATIONS

Short wavelength, low dispersion, large aperture spectra were obtained of NGC 1800 and NGC 1705 with the International Ultraviolet Explorer Satellite on the 14th and 15th May 1983, respectively. SWP #19992 of NGC 1705 is a 240 minute exposure. The continuum level is 220 IUE Data Numbers (DN) and the background is 58 DN. Thus the continuum to background ratio of 4:1 is high enough to allow a detailed analysis of the spectrum. SWP #19983 of NGC 1800 is a 350 minute exposure. Here the continuum level ranges between 200 DN at short wavelengths to 180 DN at long wavelengths. However the high background noise level of 165 DN precludes a detailed analysis of the spectrum, but does allow the general slope of the UV to be established. The extracted spectrum of NGC 1705 with line identifications is shown in Figure 1.

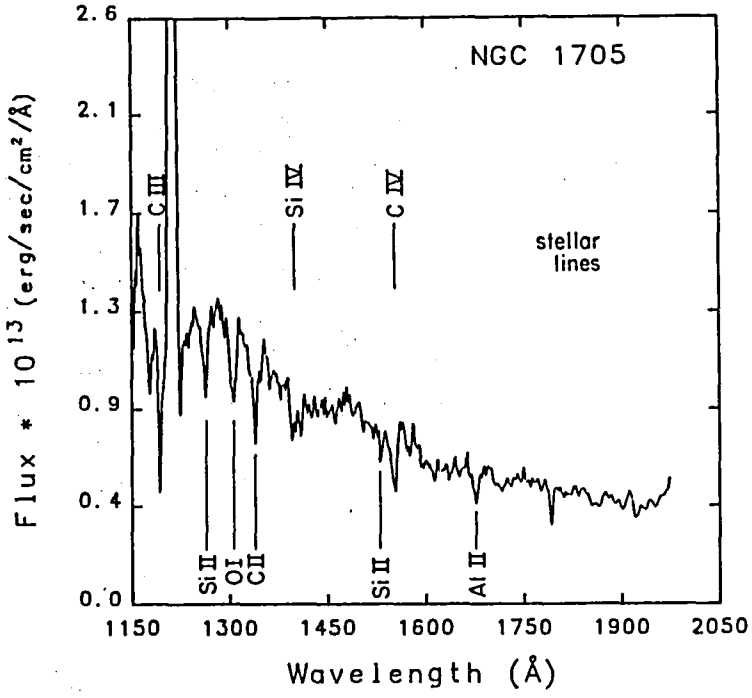

FIGURE 1 - The ultraviolet spectrum of NGC 1705.

PROPERTIES OF THE ULTRAVIOLET SPECTRA

The strong interstellar lines seen in NGC 1705 reflect absorption due to gas within NGC 1705 and in our Galaxy (our spectral resolution is insufficient to resolve these two components for the 640 km s^{-1} redshift velocity of NGC 1705; Lauberts 1982). Since NGC 1705 lies comparatively near the Large Magellanic Cloud (separation of $\sim 20°$), we have used the data presented by Savage and de Boer (1981) to roughly estimate the Galactic interstellar equivalent widths. Results are presented in Table 1, where we also have used the Savage and de Boer LMC data as a guide to interstellar line strengths in hot galaxies, which enables us to classify the origins of the observed absorption lines, most of which are interstellar in origin. The only potentially anomalous result is the great strength of Al II λ1677, which also is seen to be quite pronounced in some H II regions. The presence of strong interstellar lines from within NGC 1705 indicates that the emergent UV energy distribution has been modified by interstellar matter and thus we must rely primarily on stellar spectral features to diagnose the mix of stars responsible for the UV luminosities of these galaxies.

TABLE 1

Absorption Lines in the Ultraviolet Spectrum of NGC 1705

λ_{OBS}(Å)	I.D.	W_λ(total)(Å)	W_λ(gal)[a](Å)	W_λ(1705)(Å)	origin
1178	CIII	1.30	b	--	stellar
1264	SiII	2.94	1.37	1.57	IS
1308	OI,SiII,SiIII	3.12	1.34	1.78	IS
1339	CII,OIV	4.22	1.65	2.57	both
1396-1409	SiIV,OIV	3.43	.38	3.05	stellar
1531	SiII	0.75	.78	.03	
1555	CIV	3.84	.62	3.22	stellar
1571-1576	?	1.44	c	--	
1677	AlII	3.47	1.05	2.42	IS

a) estimates from Savage and de Boer (1981)
b) C III was not within range presented
c) no absorption feature listed

Both the C IV and Si IV blends are likely to originate primarily from stellar photospheres and are approximately equal in strength. This fact immediately excludes dominant presence of very high mass ($\geq$ 30-40 $M_\odot$) stars, as does the absence of strong P Cygni profiles, despite the very blue color of NGC 1705. Also, the UV spectrum (plus optical emission lines) rules out any extreme deficiencies of OB stars in NGC 1705. The strengths of C IV and Si IV are closely matched to those expected for a BO or B1 star in a Magellanic type system, which corresponds to a main sequence star of mass $\sim$ 20 $M_\odot$. This in fact provides a lower bound for the maximum stellar mass. If there is any major abnormality in the upper initial mass function, it must occur only for the most massive stars and is unlikely to be solely responsible for the optical appearance of these galaxies.

A comparison of the IUE spectrum of NGC 1705 with IUE spectra of other blue objects indicates that, in the ultraviolet, NGC 1705 is most similar to the nucleus of M83, which is thought to be in a starburst state (Bohlin et al. 1983). It is also remarkably similar to the composite spectrum of the two blue galaxies NGC 4214 and NGC 4670, with the ratio of the widths of the stellar absorption lines Si IV λ1400 Å and C IV λ1555 Å comparable and approximately equal to one. The IUE spectrum of R 136a, on the other hand, is indicative of a hotter object. However, all of these systems are relatively hot, and interstellar Al II λ1677 Å appears to be a hallmark of hot, gas rich, blue systems.

STRUCTURAL AND EVOLUTIONARY CHARACTERISTICS

Following the approach developed in Gallagher, Hunter, and Tutukov (1984) it is possible to place the star formation histories of these two galaxies on a systematic basis. This has been done by Lamb et al. (1984). They deduce that in NGC 1800 the astration rate has been nearly constant over the past several billion years, although it may have declined slightly over the life-

time average. However the observations suggest that NGC 1705 is in a mild star formation burst phase. New small-aperture optical photometry otained at Cerro Tololo Inter-American Observatory (CTIO), however, suggests that the region observed with the IUE is in a local post-burst phase with weaker emission than the galactic average. This picture is supported by long slit SIT spectra taken with the CTIO 4-m telescope, which detect a major emission region well off of the bright stellar core which contributes heavily to the Hα flux.

All of the available data are consistent with a model for the center of NGC 1705 in which a major star forming event has evolved to the point where the hot stars have largely emerged from their natal gas. This phenomenon is not unique, but is seen in a variety of normal actively star forming galaxies.

The unusual features of the event in NGC 1705 are its smooth high surface brightness, large luminosity, and minimal numbers of surrounding features (e.g. other smaller OB star complexes) which produce little optically resolvable structure. That a small galaxy should support few active star forming centers is not surprising, but that the one should appear to be an unresolved supergiant OB complex is remarkable. We do not know, however, whether the region in NGC 1705 actually is a single coherent OB stellar group or many smaller ones that overlap in the line of sight. Nevertheless, the IUE spectrum shows that the massive component of the stellar population is typical of large star-formation events found in other galaxies (see also Lequeux et al. 1981).

For NGC 1800 more than a single star forming center is involved, as can be seen from the multiple H II complexes detected in echelle spectra obtained by Hunter (1982). These individually appear to be small, but evidently spatially overlap to give rise to the amorphous appearance of NGC 1800 (Sandage and Brucato, 1979; GHK). Since the UV data are of poorer quality, we have less information on the specifics of the hot stellar population mix than in NGC 1705, but again there are no indications of major stellar population anomalies associated with the unusually smooth spatial pattern of star formation.

REFERENCES

Bohlin, R. C., Cornett, R. H., Hill, J. K., Smith, A. M., and Stecher, T. P. (1983) Ap. J. (Lett) 274, L53.

Gallagher, J., Hunter, D., and Knapp, G. (1981) Astron. J. 86, 344.

Gallagher, J., Hunter, D., and Tutukov, A. (1984) Ap. J. in press.

Holmberg, E. (1958) Medd. Lunds. Astron. Obs. II, No. 136.

Huchra, J., Geller, M., Gallagher, J., Hunter, D., Hartmann, L., Fabbiano, G., and Aaronson, M. (1983) Ap. J. 274, 125.

Hunter, D. (1982) Ap. J. 260, 81.

Hunter, D., Gallagher, J., and Rautenkranz, D. (1982) Ap. J. Suppl., 49, 53.

Krienke, O. K. and Hodge, P. (1974) Astron. J. 79, 1242.

Lamb, S., Gallagher, J., Hjellming, M. and Hunter, D. (1984) preprint.

Lauberts, A. (1982) The ESO/Uppsala Survey of the ESO(B) Atlas (ESO).

Lequeux, J., Maucherat-Joubert, M., Dehaweng, J., Kunth, D. (1981) A. A., 103, 305.

Sandage, A. and Brucato, R. (1979) Astron. J. 84, 472.

Savage, B. D. and de Boer, K. S. (1981) Ap. J., 243, 460.

HIGHLY IONIZED GAS ASSOCIATED WITH THE SMALL MAGELLANIC CLOUD

Edward L. Fitzpatrick and Blair D. Savage
Washburn Observatory, The University of Wisconsin-Madison

ABSTRACT

High dispersion IUE spectra of SMC stars are examined to search for evidence of a widespread distribution of highly ionized gas. For all of the stars, absorption by C IV and/or Si IV is found near 160 km s^{-1}, and is attributed to nebular material. In addition, the stars show absorption by the high ion lines in the range 100-130 km s^{-1}. This absorption might indicate the presence of global distributions of these ions, such as a hot phase of the interstellar medium or a halo-like region.

INTRODUCTION

Evidence of widespread C IV and Si IV absorption at large z-distances, in the Galactic halo, was first demonstrated through IUE observations of stars in the Large and Small Magellanic Clouds (LMC and SMC; Savage and de Boer 1979, 1981) and has been confirmed with observations of high latitude Galactic OB stars (Pettini and West 1982). An important issue is whether other galaxies also possess extensive haloes. Such haloes have been suggested as the sources of QSO absorption line systems (Bahcall and Spitzer 1969). de Boer and Savage (1980) found that the ultraviolet absorption line velocity characteristics of SMC neutral and highly ionized gas are similar to those found for the Milky Way. This suggested that some, if not most, of the absorption in the highly ionized gas is occurring in a gaseous halo similar to that surrounding the Milky Way. However, Prevot et al. (1980) argued that the C IV and Si IV lines more likely arise in the nebular environments of the target stars. A recent discussion of this controversial subject is found in de Boer (1984).

In this paper we examine the high dispersion IUE spectra of a number of SMC stars to determine if evidence exists for a global distribution of highly ionized gas (as opposed to "local" or circumstellar distributions). Seven SMC stars are considered here. These stars (and their spectral types) are: HD5980 (OB?+WN3), Sk80 (O7 Iaf+), Sk108 (O6.5+WN3), Sk188 (WO4+O7 III), Sk82 (B0 Ia), Sk159 (B0.5 Ia), and HD5045 (B1-2 I). Interstellar line profiles for most of these stars can be found in Savage and de Boer (1979, 1981), Fitzpatrick and Savage (1983; Paper I), and Fitzpatrick (1984a, 1984b; Papers II and III, respectively). The reduction procedures applied to the data are discussed in Paper I.

DISCUSSION

The C IV $\lambda\lambda$1548, 1550 and Si IV $\lambda\lambda$1393, 1402 interstellar lines for the

stars considered here are shown in Figure 1. For several of the stars, one or more of the lines are affected by a cosmic ray hit in the spectrum or are located in extremely low signal/noise ratio regions and are not shown. Spectra of SMC stars typically show C IV and Si IV absorption in three velocity ranges: near 0 km s^{-1}, near 100-130 km s^{-1}, and near 160 km s^{-1}. The 0 km s^{-1} absorption arises in the Milky Way halo and is not considered here. The 160 km s^{-1} and 100-130 km s^{-1} components are discussed separately below.

a) 160 km s^{-1} Absorption

The strongest C IV and/or Si IV absorption at SMC velocities is seen toward the O and WR+O stars (HD5980, Sk80, Sk108, and Sk188) near 160 km s^{-1}. Among the other three stars in Figure 1, Sk82 and Sk159 show prominant Si IV near 160 km s^{-1}, with weak or absent corresponding C IV. No Si IV or C IV is positively detected in the HD5045 spectrum near 160 km s^{-1}, although the noise level is high. Fitzpatrick and Savage (1984) show that a velocity of 160 km s^{-1} indicates that the lines most likely form in the nebular environments of the stars (which are all similar kinematically). Stellar UV-photoionization is suggested as the dominant production mechanism, although other mechanisms are probably also at work. In particular, the presence of N V absorption at nebular velocities toward the well-observed star HD5980 requires an additional source of ionization.

b) 100-130 km s^{-1} Absorption

The 100-130 km s^{-1} component is most apparent in the C IV lines of Sk159 and HD5045. Its presence is revealed in the spectra of the O and WR+O stars by the asymmetric extension of the strong nebular lines to lower velocities. No 100-130 km s^{-1} component is seen in the Sk82 spectrum, but the most likely indicator of such a component, C IV λ1548, is unfortunately buried in the stellar P Cygni trough. For Sk159 and HD5045, the C IV lines indicate $N(C\ IV) = 3\text{-}4 \times 10^{13}$ cm^{-2} and the weakness or absence of Si IV gives $N(C\ IV)/N(Si\ IV) \geq 10$. Due to the severe blending with the nebular lines, no such measurements can be made for HD5980, Sk80, Sk108, or Sk188. N V absorption in the 100-130 km s^{-1} velocity range, blended with a higher velocity component, is seen in the HD5980 spectrum.

The O and WR+O stars are not suitable targets for an attempt to discriminate between a global and a local/nebular origin for the 100-130 km s^{-1} absorption. The velocity of the feature is 30-60 km s^{-1} more negative than expected for "normal" nebular material; however, high velocity motions are known to exist in the environments of early type stars (e.g., the Carina nebula; Walborn, Heckathorn, and Hesser 1984). Thus any suggestion of a global origin for these lines would be vitiated by the strong possibility of circumstellar or nebular contributions.

The presence of the absorption in the spectra of the B-type supergiants, Sk159 and HD5045, allows the serious consideration of a global distribution of the highly ionized gas. The stars are located in apparently quiescent environments and, while circumstellar/nebular origins cannot be ruled out, a

global origin seems at least as likely. Two types of global distributions suggest themselves - either a truly interstellar distribution (similar to the hot phase of the Milky Way interstellar medium) or a "circum-SMC" distribution (perhaps analogous to the Milky Way halo). Toward the stars considered here, the bulk of the absorption from the neutral interstellar medium occurs in the velocity range 130-140 km s^{-1}. A hot phase would not be expected to mimic exactly the velocity of the neutral material and the 100-130 km s^{-1} velocity is not inconsistent with such an origin. Alternatively, the high ionization absorption might be associated with diffuse low ionization stage absorption seen at about 100 km s^{-1} toward all of the SMC stars observed. It is shown in Paper III that the gas producing this absorption probably lies "above" (i.e., nearer to the Galaxy than) the main neutral interstellar complex. Such a situation is suggestive of the Milky Way halo. Also, the large N(C IV)/N(Si IV) ratio in the Galactic halo ($\sim$ 4-6) is similar to the value in the 100-130 km s^{-1} absorption. A discussion of a possible SMC "halo" is complicated by the fact that both the dynamics and the morphology of the SMC have likely been shaped by gravitational interaction with the Milky Way and the LMC (e.g., Fujimoto and Murai 1984). Thus, a circum-SMC distribution of high and low ionization stage gas might resemble the Milky Way halo in some respects, but the origin of such a distribution might be quite different (Songaila 1981).

In conclusion, examination of the available high dispersion IUE spectra of SMC stars suggests, or at least permits, the existence of a widespread distribution of highly ionized gas. This gas may exist in an SMC halo with properties similar to the Milky Way halo. However, other explanations for the origin of this gas are certainly allowed by the data.

REFERENCES

Bahcall, J.N., and Spitzer, L. 1969, Ap.J.(Letters), 156, L63.

de Boer, K.S. 1984, in IAU Symposium No. 108, Structure and Evolution of the Magellanic Clouds, eds. S. van den Bergh and K.S. de Boer (Dordrecht: Reidel) p. 375.

de Boer, K.S., and Savage, B.D. 1980, Ap.J., 238, 86.

Fitzpatrick, E.L. 1984a, Ap.J., in press (Paper II).

Fitzpatrick, E.L. 1984b, in preparation (Paper III).

Fitzpatrick, E.L., and Savage, B.D. 1983, Ap.J., 267, 93 (Paper I).

Fitzpatrick, E.L., and Savage, B.D. 1984, in preparation.

Fujimoto, M., and Murai, T. 1984, in IAU Symp. 108, Structure and Evolution of the Magellanic Clouds, eds. S. van den Bergh and K.S. de Boer (Dordrecht: Reidel), p. 115.

Pettini, M., and West, K.A. 1982, Ap.J., 260, 561.

Prevot, L., et al. 1980, Astr.Ap., 90, L13.

Savage, B.D., and de Boer, K.S. 1979, Ap.J.(Letters), 230, L77.

Savage, B.D., and de Boer, K.S. 1981, Ap.J., 243, 460.

Songaila, A. 1981, Ap.J., 248, 945.

Walborn, N.R., Heckathorn, J.N., and Hesser, J.E. 1984, Ap.J., 276, 524.

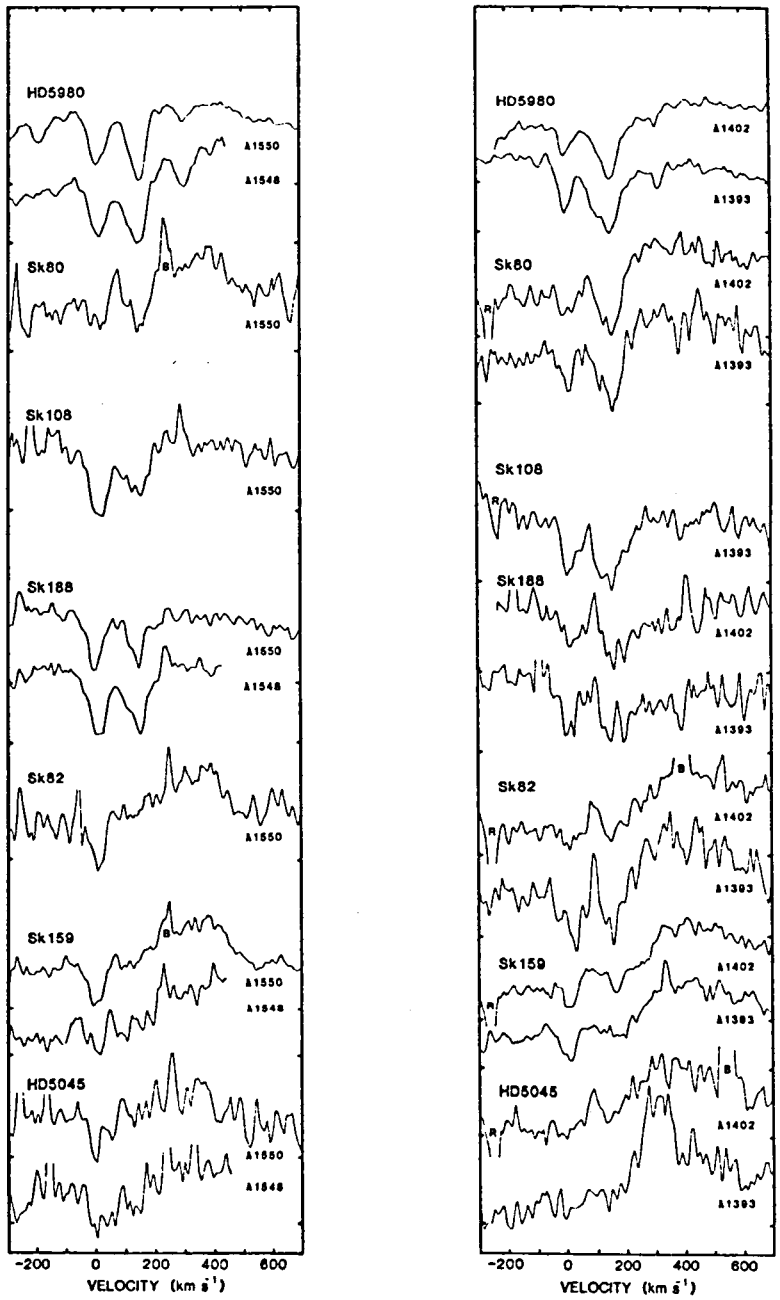

Figure 1 C IV λλ1548, 1550 and Si IV λλ1393, 1402 interstellar line profiles for SMC stars. Spectra are plotted on a net intensity vs. heliocentric velocity scale. Tick marks on the vertical axes indicate the zero levels. "B" denotes either a "hot pixel" or data affected by cosmic ray hits on the detector; "R" indicates a detector reseau mark. The highest quality data are for HD5980 and Sk159, for which 7 and 3 IUE spectra, respectively, have been combined.

GALACTIC ABSORPTION LINES MEASURED FROM THE IUE LOW DISPERSION SPECTRA OF ACTIVE GALAXIES

Chi-Chao Wu - Astronomy Programs, Computer Sciences Corporation
C. J. Blades - Space Telescope Science Institute
A. Boggess - Science Directorate, Goddard Space Flight Center
D. G. York - Department of Astronomy, University of Chicago

ABSTRACT

Galactic absorption lines were detected and measured from the low dispersion spectra of 10 active galaxies. Four of these are at galactic latitudes greater than 60^{o} and the remaining 6 are at latitudes between 20^{o} and 60^{o} and behind high velocity 21-cm clouds. In our galactic absorption line systems, while C II λ1335 is commonly seen, C IV λ1550 is detected with confidence only in high latitude objects and Fairall 9 which has a latitude close to 60^{o} and lies in the general direction of the Magellanic Clouds. The C IV to C II ratio is about one for the high latitude objects; and lower for the low latitude objects. This is consistent with the picture that C IV and C II exist mostly in the halo and disk, respectively. In the quasar absorption line systems, C II is rarely seen while C IV is generally strong. This suggests that the halo of intervening galaxies are large compared to their disk. Therefore, the sight lines to high z QSOs frequently intercept the halo but rarely both the disk and halo of intervening galaxies.

INTRODUCTION

IUE low dispersion observations of active galaxies allow the probe of the galactic disk and halo in many sight lines. The low dispersion data do not have sufficient spectral (velocity) resolution for studying the geometry of the halo from the line profiles, however, they can give reasonably reliable equivalent widths for many ions. The halo of intervening galaxies have been suggested to be the origin of some absorption line systems observed in the spectra of quasistellar objects (for review, see Weymann, Carswell, and Smith 1981). In this report, the absorption line spectra of the disk and halo of our galaxy are compared with those seen in the spectra of high z QSOs. The equivalent widths and line ratios of the detected ions provide important information on the halo of galaxies.

RESULTS

Absorption lines originated in the disk and halo of our Galaxy are readily detectable in the low dispersion spectra of some Seyfert

galaxies and QSOs. Figures 1 and 2 show the absorption lines in the SWP and LWR spectral regions of the Seyfert galaxy Fairall 9. Figures 1 and 2 are the results of combining 12 SWP and 8 LWR images, respectively, after the radiation hits have been removed from the line-by-line data.

Just from the data obtained by two of us (AB and CCW), strong galactic absorption lines were found in the following objects: (1) PG 1116+216, (2) PG 1119+120, (3) Q 1229+204, (4) 3C 273, (5) Akn 120, (6) PG 0803+76, (7) NGC 3783, (8) Mrk 279, (9) Mrk 817, and (10) Fairall 9. The first four are at galactic latitudes greater than 64° and are not known to be behind any high velocity 21-cm clouds. For further discussion, they will be designated as "Pole" objects. Objects (5) - (9) are at galactic latitudes 23° - 54°, and are all behind 21-cm clouds; they will be designated as "Cloud" objects. Fairall 9 is at 59° latitude and behind a 21-cm cloud. It also lies in the general direction of the Magellanic Clouds. The equivalent widths of the absorption lines in the spectra of the Pole and Cloud objects and F9 are given in Table 1 together with HD 5980 in SMC, HD 36402 in LMC (Savage and Jeske 1981) and the absorption line systems seen in the spectra of QSOs PKS 2126-158 (Young et al. 1979) and Q 1756+237 (Turnshek, Weymann, and Williams 1979). In Table 1, if a given species is seen in more than one object, the range of the equivalent width is reported. These equivalent widths were measured only from the spectra taken by ourselves. Si IV 1400 was never reliably identified. However, we have acquired all the active galaxies data from the archive. For a given object, adequately exposed spectra were selected, radiation hits were removed from the line by line data and combined. As shown in Figure 1, Si IV 1400 is present in the spectrum of F9 with the two components resolved.

The following statements can be made based on the comparison of the absorption line spectra for the different sight lines reported in Table 1: (1) The absorption line spectrum seen in F9 is quite similar to that in HD 36402 (LMC), but it is significantly stronger than that in HD 5980 (SMC) and seems to sample gas, at an average, of lower ionization. This may be understood from the fact that F9 is behind a 21-cm cloud which is dominated by low ionization species. (2) The galactic absorption systems (Pole and Cloud) have equivalent widths comparable to some QSO absorption systems. (3) The galactic absorption systems have C IV 1550/C II 1335 < 1. This differs significantly from the QSO absorption systems. Mixed ionization systems which have both the low ionization species like S II, Si II, C II, O I, Al II, Fe II and Mg II and the moderate ionization species like Si IV and C IV are rare among the QSO absorption systems. For example, there are 22 C IV systems in Young, Sargent and Boksenberg (1982) for which the wavelength coverage includes C II, but C II is detected only in 6 of them. Similarly, in the sample of Weymann et al., (1979), C II is present only in 5 out of 30 C IV systems in which it might be seen. In other words, for most QSO absorption systems, C IV 1550/C II 1335 $>> 1$. Even for the mixed systems (e.g., see Table 1), C IV 1550/C II 1335 is generally greater than 1 (Weymann et al., 1981).

We can attempt to reconcile the above observations by making the following arguments: (1) For the galactic absorption systems, most of the C II and other low ionization absorption occurs in the disk, and most of the C IV absorption occurs in the halo. Then our halo is similar to the halo of intervening galaxies in having C IV/C II >>1. (2) Mixed ionization systems belong to the rare sight lines which intercept both the halo and the disk of a galaxy. And it is even more uncommon for a sight line to pass through a neutral cloud which will lead to C IV/C II << 1 as some of our Cloud objects. (3) Since most of the QSO absorption systems do not contain low ionization species, the halo of the intervening galaxies tend to be large compared to their disk.

REFERENCES

Savage, B. D., and Jeske, N. A. 1981, Ap. J., 244, 768.

Turnshek, D. A., Weymann, R. J., and Williams, R. E. 1979, Ap. J., 230, 330.

Weymann, R. J., Carswell, R. F., and Smith, M. G. 1981, Ann. Rev. Astr. Ap., 19, 41.

Weymann, R. J., Williams, R. E., Peterson, B. M., and Turnshek, D. A. 1979, Ap. J., 234, 33.

Young, P., Sargent, W. L. W., and Boksenberg, A. 1982, Ap. J. Suppl., 48, 455.

Young, P., Sargent, W. L. W., Boksenberg, A., Carswell, R. E., and Whelan, J. A. J. 1979, Ap. J., 229, 891.

TABLE 1
ABSORPTION LINE EQUIVALENT WIDTHS (Å)

Line Identification		Pole	Cloud	F9	SMC HD 5980	LMC HD 36402	2126-158 Z_a=2.7685	1756+237 Z_a=1.673
S II	1254	0.3-0.5			0.2	0.2		
Si II + S II	1260	0.6-0.7	0.7	0.7	0.4	0.9	1.1	1.3
OI + Si II	1303	1.2:-1.7	0.8-3.1	1.5	0.4	1.3	1.1	1.3
C II + C II*	1335	0.4:-1.1	0.8-2.4	1.7	0.6	>1.0	1.3	1.3
Si IV	1400				0.3	0.4:	0.7	1.9
Si II	1527	0.9-1.0	1.0-1.5	1.4	0.2	0.8	0.6	1.4
C IV	1550	0.8-1.0	<0.8	0.9	0.7	0.6	1.4	4.0
Fe II	1608	0.7	0.9		0.2	0.3		0.5
Al II	1671	0.7-0.8		0.6	0.3	1.1	0.5	1.3
Fe II	2600	1.5	1.3	1.6	0.4	1.3		
Mg II	2800	1.7	2.6-7.4	3.0	0.7	3.8		

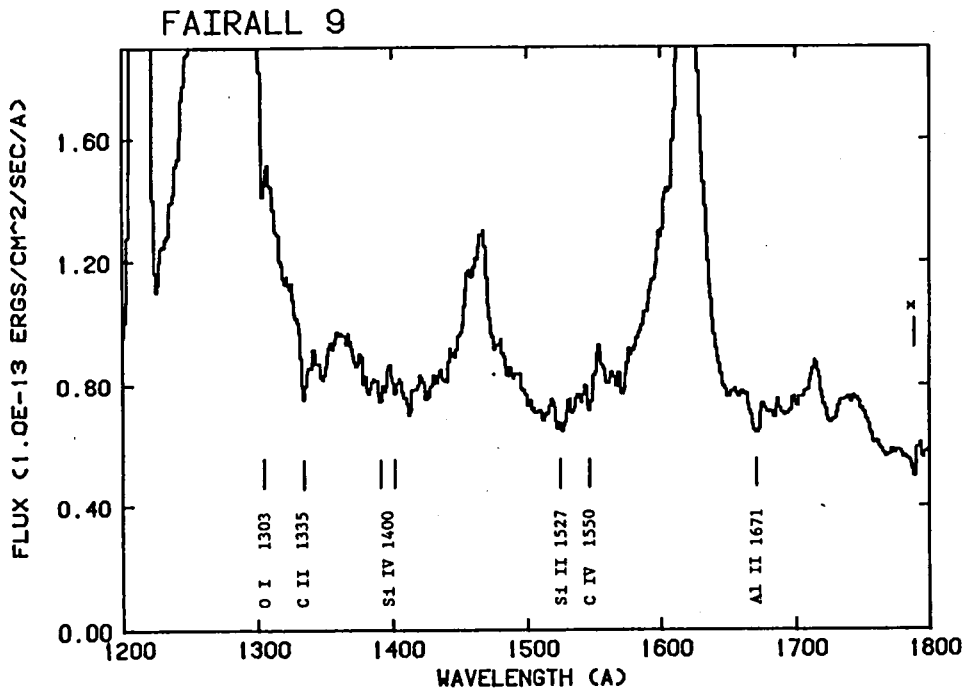

Fig. 1. - SWP spectral region of Fairall 9. Galactic absorption lines are identified. x marks the region affected by reseau.

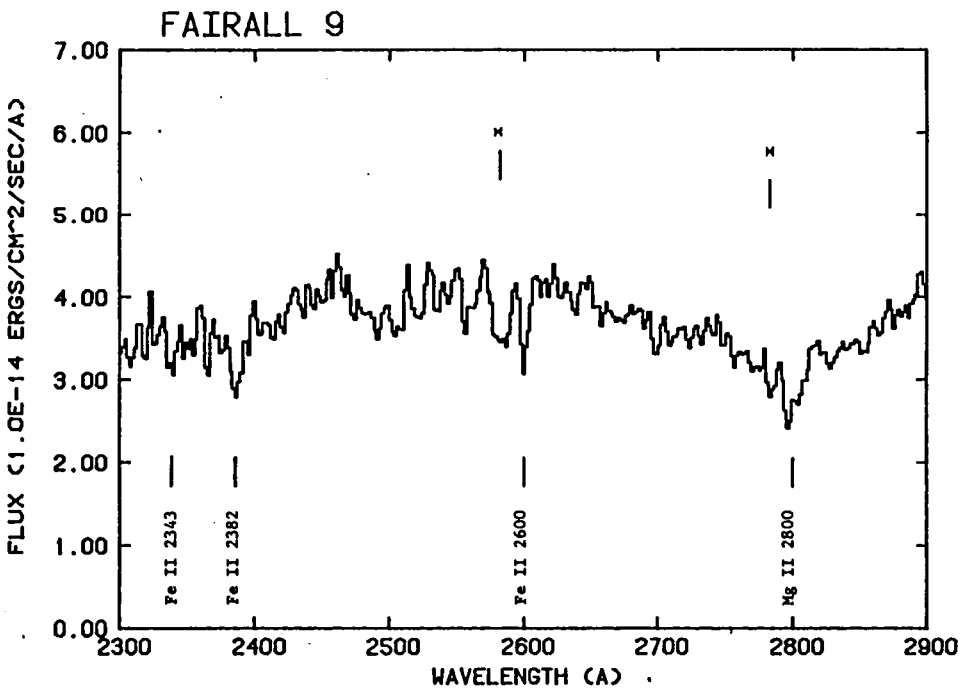

Fig. 2. - LWR spectral region of Fairall 9. Galactic absorption lines are identified. x marks the regions affected by reseau.

STRUCTURE OF THE SEYFERT BROAD LINE REGION AND ABSORPTION REGION OF NGC 4151

G E Bromage[1], A Boksenberg[2], J Clavel[3], M H Demoulin-Ulrich[4], A Elvius[5], M V Penston[2], G C Perola[6], M Pettini[2], M A J Snijders[2], E G Tanzi[7] and M Tarenghi[4]

[1]Astrophysics Group, Rutherford Appleton Laboratory, Didcot, OX11 OQX, UK;
[2]Royal Greenwich Observatory;
[3]Observatoire de Meudon;
[4]European Southern Observatory;
[5]Stockholm Observatory;
[6]Istituto Astronomico dell'Universita, Roma;
[7]Ist. Fis. Cosm. CNR, Milano.

BACKGROUND

We have monitored the Seyfert nucleus of NGC 4151 for six years, including periods of intensive study of the complex variations in the ultraviolet spectrum with IUE, and some co-ordinated optical and X-ray observations. Here we briefly review important IUE results relating to the structure of the Broad Line Region and its physical conditions. Our detailed analyses and results are published in a series of papers, viz: Penston et al 1981 (Paper I: initial IUE results); Perola et al 1982 (Paper II: continuum); Ulrich et al 1984 (Paper III: broad emission lines); Bromage et al 1984 (Paper IV: absorption line region); Snijders et al 1984 (Paper V: atlas and survey). A further paper (VI) on the very low luminosity state of the nucleus, is in preparation. A brief pictorial review of the low-dispersion IUE data and implications can be found in proceedings of the 1982 Madrid IUE Conference (Bromage et al 1982).

Unravelling the complexities of the NGC 4151 IUE spectra to derive the valuable physical information on the BLR has necessarily involved a substantial amount of observing time - for improving signal-to-noise ratios; for observing at high resolution; for establishing timescales of the many variability phenomena; for long-term monitoring; and for the key, intensive following of any outbursts. The main aim of such studies of Active Galactic Nuclei is to derive detailed constraints on radiation mechanisms and physical conditions in the emission region, and hence also constraints on possible central power sources. We would maintain that this can best be achieved by intensive study of a few key AGN's like NGC 4151 - not only with IUE but, a fortiori, with HST and future ultraviolet and X-ray experiments.

RESULTS

The ultraviolet spectrum of NGC 4151 comprises continuum, strong emission lines with different widths, and a rich absorption line spectrum. All components vary (Paper I), with the fastest changes occurring on a timescale of some 5 days. The continuum is most simply represented as a power law together with (at many, but not all, epochs of observation) an additional

component seen as a 'far UV excess'. The power law component hardens as it brightens, with an index of - 3 when the λ2500Å flux is only 5 mJy, and - 1.5 at 20 mJy. This power-law component appears to drive the changes in emission and absorption lines, suggesting that the additional component is weak in the far EUV and thus may be thermal emission - perhaps from an accretion disk in the centre (Paper II).

From the variability timescales and time-lag information for various emission lines, and from their velocity coverage, a partial stratification of the BLR into at least 3 zones is indicated (Paper III). The behaviour is broadly consistent with a black hole/accretion disk scenario with a central mass of $10^{8.0 - 8.5}$ solar masses. The variability data suggest a chain of cause and effect: events are first seen in the 'thermal' continuum component (fuel supply), later in the power law continuum, and last in the emission lines.

Variations in the 'broad' absorption lines seem to derive principally from changes in column densities of absorbing species rather than in velocity dispersions or line profiles (Paper IV). High dispersion profiles and low dispersion doublet-ratios imply a roughly constant effective b-value of some 500 kms^{-1}. The total velocity range is - 1100 to + 100 kms^{-1} approximately (relative to the narrow line region of NGC 4151). Our results suggest a model with large numbers of outflowing absorbing clouds that are almost optically thin. Information collected on space densities (mainly from metastable absorbers), on velocities covered, and on the lack of time lags, together point to most absorption's occurring in a thin shell in the outermost parts of the BLR.

The far-ultraviolet continuum of NGC 4151 has varied by nearly 3 magnitudes during IUE's lifetime. Recently it has been at its lowest recorded UV luminosity, and a large outburst is overdue! Such an occasion would provide a golden opportunity for further unravelling of the BLR structure and constraints on models for the central powerhouse - especially if simultaneous UV and X-ray observations are obtained throughout the outburst.

REFERENCES

Bromage G E et al 1982, ESA SP-176, p 533
Bromage G E et al 1984, MNRAS (to be published) (Paper IV)
Penston M V et al 1981, MNRAS 196, 857 (Paper I)
Perola G C et al 1982, MNRAS 200, 293 (Paper II)
Snijders M A J et al 1984, in preparation (Paper V)
Ulrich M H et al 1984, MNRAS 206, 221 (Paper III)

BROAD EMISSION FEATURES IN ACTIVE GALACTIC NUCLEI

Hagai Netzer, Beverley J. Wills, and D. Wills
Department of Astronomy and McDonald Observatory
The University of Texas at Austin, Austin, Texas 78712

and W. Wamsteker
European Space Agency, Vilspa, Spain

ABSTRACT

We have carried out simultaneous ultraviolet and optical observations of several Seyfert 1 galaxies and QSOs in an attempt to understand some broad emission features between 2000 and 5000 Å. Most of the emission is due to Fe II and Balmer continuum. We have used improved model calculations to estimate the flux in these components and to compare the strengths of the ultraviolet and optical Fe II lines. Our spectral fitting shows that the ultraviolet Fe II lines are much stronger than previously believed. In many cases I(Fe II UV)/I(Fe II opt) > 5 and I(Fe II UV)/I(Mg II λ2798) > 3. Strong ultraviolet Fe II lines are present even in objects showing weak optical Fe II lines. The total flux in Fe II lines sometimes exceeds the Lyman α flux by up to a factor of 2, and there may well be a general "Fe II/Lyman α" problem, with important consequences for the modeling of the broad emission line region in active galactic nuclei.

INTRODUCTION

There has been renewed interest in the study of broad emission features in the spectrum of Active Galactic Nuclei (AGN). In particular, the region between 2000 and 5500 Å has been studied by ground based telescopes, and by the IUE, in an attempt to measure Balmer lines and continuum, as well as many broad Fe II lines. This was not possible to do before the IUE, at least for low redshift objects since the continuum level must be determined from observations over a wide wavelength range.

Thousands of Fe II lines are seen in the above wavelength region. The optical Fe II lines have been known for many years (see Wampler and Oke 1967, Osterbrock 1977, Phillips 1978a, b). They are strong and distinct in most Seyfert galaxies, but weak in some low redshift quasars, and all Broad Line Radio Galaxies. More recently Wills et al. (1980) have shown that the corresponding ultraviolet lines are quite prominent in many quasars. No systematic search comparing the strength of the ultraviolet and optical Fe II lines in Seyfert 1s has yet been published.

Several interesting problems should be addressed: first, it is known that a few Seyfert 1s and most BLRG, do not have strong optical Fe II lines. Is this also true for the ultraviolet multiplets? Second, the total energy in the broad emission features between 2000 Å and 4000 Å have not been measured. This has important implications for AGN models. Third, the continuum shape of GANs cannot be determined until better understanding of the broad features is obtained.

At this meeting we give a short report of a new study of broad emission features in several AGNs. A more extensive observational and theoretical study is given in two other papers (Wills, Netzer, and Wills 1984, and Netzer et al. 1984).

OBSERVATIONS

We have obtained simultaneous ground based and IUE observations of several Seyfert 1s and BLRGs that show weak or no optical Fe II lines. The optical part of the spectrum was observed at McDonald Observatory using the 2.7 m telescope and the IDS detector. We have also obtained ground based observations of intermediate redshift quasars. ($0.5 \leq z \leq 1$) covering the rest wavelength range of 1900 - 5500 Å. Our own and archival IUE data have been used in some cases to supplement our ground based data.

Fig. 1 shows the spectrum of the Seyfert 1 Galaxy Mk290, obtained on July 12, 1983. The long wavelength IUE data joins nicely with the optical spectrum and permits a good estimate of the continuum from 1900 Å to 7500 Å. We have corrected the spectrum for galactic reddening (A_V = 0.11 mag) and for internal reddening (A_V = 0.1), which we found necessary because of a residual 2200 Å feature. The resulting continuum has been fitted by a single power-law continuum, $F_\nu \propto \nu^{-0.59}$. The fit is quite satisfactory for $\lambda \leq 5500$ Å, but steepening of the continuum at longer wavelengths gives some disagreement towards the red end of the spectrum. Since we are only interested in spectral features with $\lambda < 5500$ Å we consider this good enough.

As evident from Fig. 1, the optical Fe II lines in the spectrum of Mk290 are very weak, compared with most other Seyferts (see Osterbrock 1977). The 5300 Å feature (multiplets 48, 49) is nearly absent, and the 4570 Å band (multiplets 37, 38) is no stronger than He II λ 4686. However, an extremely strong 2300 - 2600 Å Fe II feature is clearly seen, similar to that observed in many quasars (Wills et al. 1980). This is demonstrated also in the lower part of the figure, where the power-law continuum has been subtracted from the data.

We have looked at the combined spectra of several other Seyferts (Mk 10, Mk 915), BLRGs (3C390.3) and many quasars and found strong ultraviolet Fe II lines in many cases of weak optical Fe II lines. Part of the data is from the IUE long wavelength camera, which is some cases is too noisy to be used for reliable measurement. The galaxies are discussed by Netzer et al. (1984) and the quasars by Wills, Netzer, and Wills (1984).

MODEL FITTING AND DISCUSSION

Our goal in the present work is to fit all spectral features between 1900 and 5500 Å. For this we have looked into some problems related to AGN models. We have restudied the Fe II problem and found that several important processes have been neglected in the past (Netzer and Wills 1983). Our present Fe II model consists of several thousand lines, and is part of a more general photoionization model calculation. We have aslo calculated the strengths of Balmer lines and continuum, under a variety of conditions

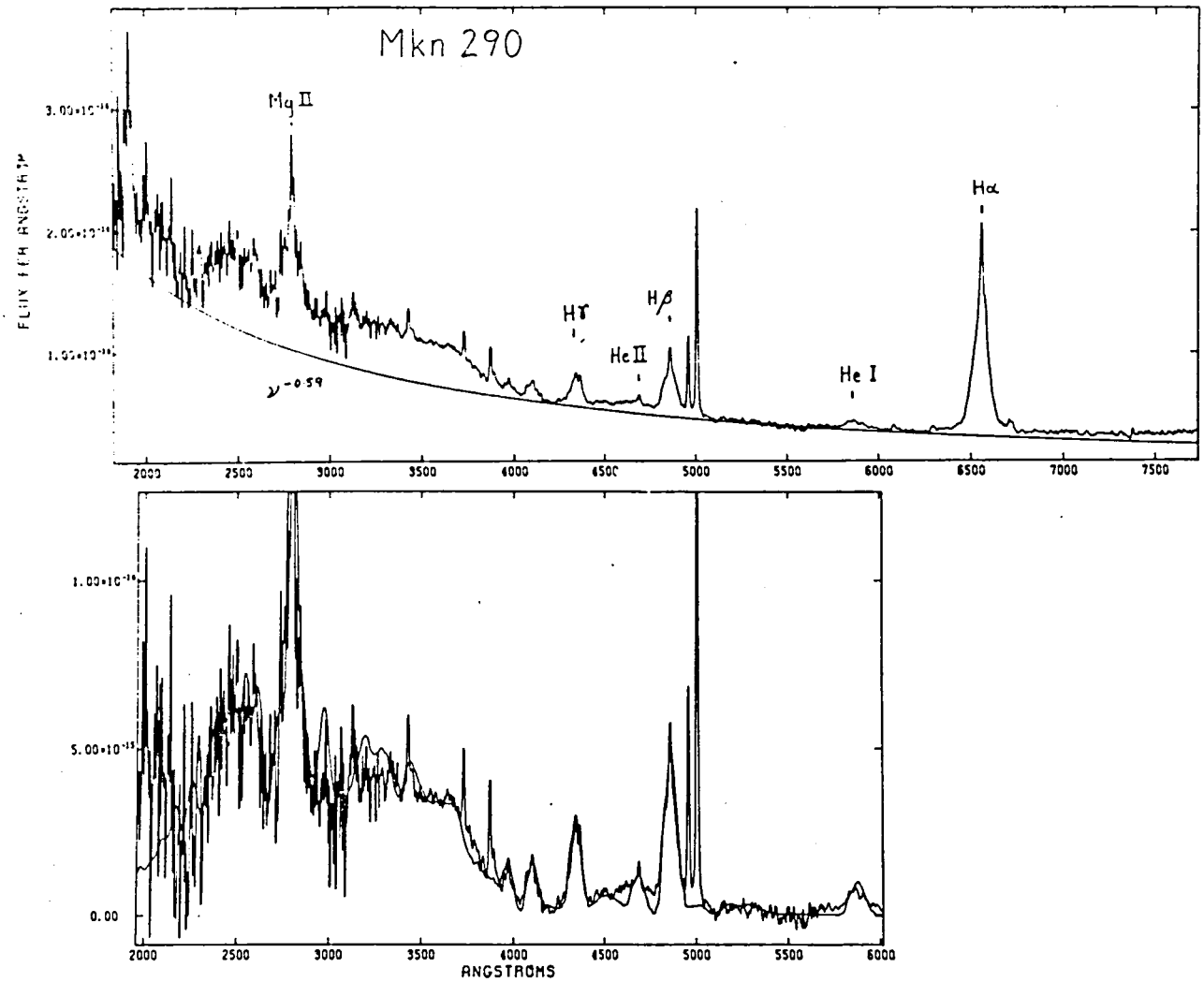

Fig. 1. The combined ultraviolet-optical spectrum of Mk290, obtained on July 12, 1983. Top: The spectrum corrected for galactic and intrinsic reddening, with a power-law continuum fitted. Bottom: Model fitting to the power-law subtracted spectrum. Included are Balmer lines and continuum, Fe II lines, Mg II 2798, He I, He II, and several O III lines.

expected in AGNs' broad line clouds. The new calculations are used to fit the observed data in the wavelength range of interest.

Fig. 1 shows one such model. We cannot describe all the details here, but mention the most important aspects. We found that a good fit can be achieved with the following line ratios: Hα:Hβ:Hγ:Hδ:Hε:Hθ = 3.93:1:0.5: 0.27:0.24:0.15, (Mg II 2798)/Hβ = 1.8, Fe II (2000 - 3000 Å)/Fe II (3500 - 6000 Å) = 10, Fe II (total)/Hβ = 13, Balmer Continuum/Hβ = 8. As seen in

Fig. 1 (solid lines) this model explains quite successfully all the observed features. We should also mention that the model is rather similar to models of other objects showing very weak optical Fe II lines. It demonstrates that ultraviolet lines can be extremely strong even in objects showing very weak optical Fe II lines.

Several of the line ratios mentioned above may force us to change our view of the physcial conditions in AGNs' clouds, especially because of the large intensity of Fe II lines. Although short wavelength IUE data for Mk290 are not available, we can assume that this galaxy is similar to other Seyferts in its Lα/Hβ ratio, i.e.: $5 \leq L\alpha/H\beta \leq 10$. This means Fe II (tot)/Lα ≅ 2! We find similar values for other objects where Lα is directly observed, and present this as a severe problem. Another aspect is the intense Balmer continuum, which is not consistent with present photoionization calculations.

There are several ways to explain the observations. Reddening of lines and perhaps also the continuum is a likely possibility. A high density component ($\sim 10^{11}$ cm^{-3}) and large iron abundance are also possible. This is discussed in detail in Wills, Netzer, and Wills (1984).

REFERENCES

Netzer, H., and Wills, B. J., 1983, Ap. J., 275, 445.

Netzer, H., Wamsteker, W., Wills, B. J., and Wills, D., 1984 (preprint).

Osterbrock, D. E., 1977, Ap. J., 215, 733.

Phillips, M. M., 1978a, Ap. J. Suppl., 38, 187.

_____ 1978b, Ap. J., 226, 736.

Wampler, E. J., and Oke, J. B., 1967, Ap. J., 148, 695.

Wills, B. J., Netzer, H., Uomoto, A. K., and Wills, D., 1980, Ap. J., 237, 319.

Wills, B. J., Netzer, H., and Wills, D., 1984 (preprint).

THE UV SPECTRA OF INTERMEDIATE REDSHIFT QUASARS

A.L. Kinney, P.J. Huggins,
J.N. Bregman, and A.E. Glassgold
Physics Department, New York University

ABSTRACT

A sample of 21 intermediate redshift quasars have been observed with the IUE in order to study their line and continuum properties. Approximately half of these spectra were taken by us and the rest were obtained from the IUE archives. In addition, 18 of the quasars have been observed by the Einstein observatory. These measurements allow us to study the ionizing continuum and the anomalous $L\alpha/H\beta$ ratio in a well defined sample of quasars. Our data also allow us to determine the percentage of the quasar continuum that is covered by gas clouds.

INTRODUCTION

Until the advent of IUE, the UV line and continuum properties were known only for high redshift quasars which suffer the effects of reddening by intervening material. The IUE has enabled us to study the important UV region in low and intermediate redshift quasars, which do not suffer the same contamination effects as their high redshift counterparts. From our sample of spectra of 21 intermediate redshift quasars we have been able to study statistically the UV line and continuum properties, which are reported upon here.

RESULTS

To characterize the continuum spectra, power law fits ($F_\nu \propto \nu^\alpha$) were made to the data over the wavelength range observed, excluding a standard template of regions with known line emission. A power law fit was in most cases an adequate representation of the data. The power law slopes range from -1.65 to 0.29, with a mean of -0.99 ± 0.11.

The IUE observations of this sample of quasars can be combined with observations in the X-ray by the Einstein observatory to try to understand the structure of the ionizing continuum. The average value of the slope from 1200 A to 2 keV (rest frame) for the 16 objects with X-ray detections is $-1.45\pm.03$. For two thirds of these objects we find that extrapolation of the UV continua into the X-ray region pass at least two sigma above the observed X-ray fluxes. In these cases one would expect to see a turnover of the spectra in the extreme UV.

When Baldwin (1977) combined observations of the flux of Hβ of high redshift quasars with Lα observations of low redshift quasars, a very low line ratio was found (Lα/Hβ ~3). This low ratio has been the motivation for much theoretical work (London, 1977, Kwan and Krolik, 1981).

We have here the opportunity to explore this important ratio for an entire sample of quasars. The resulting Lα/Hβ ratios range from 3.3 to 12.3 with a mean value of 8.3±1.4. This is similar to the value of 6.6±0.9 found by Wu, Boggess and Gull (1983) for a sample of 25 Seyfert galaxies.

This sample also allows the estimation of the covering factor. Photoionization models predict that each absorbed ionizing photon results in 0.94 Lyman α photons (Kwan and Krolik, 1981), so that the ratio $N_{L\alpha}/N_{cont}$ is a direct measure of the covering factor. From our data, this ratio is calculated from the observed Lα flux, the flux at 912 Å, and the continuum slopes. The slope is assumed to extend into the extreme ultraviolet to a cutoff at four Rydbergs. For the sample $N_{L\alpha}/N_{cont}$ ranges from 0.04 to 0.47 with a mean of 0.17±0.02.

CONCLUSIONS

We have studied the line and continuum properties of 21 intermediate redshift quasars in the ultraviolet and X-ray wavebands. The main results are: i) The mean UV slope for this sample is -0.99±0.11. ii) The mean slope from 1200 Å to 2 keV is -1.45±0.03. iii) Two thirds of the objects have UV slopes that extrapolate to more than two sigma above the X-ray flux. iv) For 11 objects, the mean Lα/Hβ ratio is 8.3±1.4. v) The covering factor is estimated to be about 0.17.

REFERENCES

Baldwin, J.A., 1977, M.N.R.A.S.,178, 67P.
Kwan, J., and Krolik, J.H., 1981, Ap.J., 250, 478.
London, R., 1979, Ap.J., 228,8.
Wu, C.-C., Boggess, A., and Gull, T.R., 1983, Ap.J., 266, 28.

MULTIFREQUENCY OBSERVATIONS OF BL LAC OBJECTS AND VIOLENTLY VARIABLE QUASARS

Joel N. Bregman, A.E. Glassgold, P.J. Huggins, and A.L. Kinney
Physics Department, New York University

ABSTRACT

We report on the status of our program to obtain simultaneous multifrequency spectra of BL Lac objects and violently variable quasars from the X-ray through radio wavebands. We illustrate the importance of the ultraviolet data in defining the overall shape of optically thin synchrotron emission, its relation to the X-ray emission, and the determination of basic physical parameters of the continuum emitting region.

INTRODUCTION

We have been pursuing a program of obtaining ultraviolet observations of BL Lac objects and violently variable quasars that are simultaneous with observations made in the radio, infrared, optical, and X-ray regions. Eleven sources have been observed in this multifrequency mode, most of them more than once, and a few unusually active sources many times. The general goal of this program is to develop a better understanding of the continuum emission in these sources. In particular, we are concerned with determining the fundamental properties in the nonthermal continuum emitting regions (size, magnetic field, density, bulk motion) and the relationship between the emitting regions which dominate the observed flux in the various wavebands (radio, ultraviolet, X-ray). Here we summarize the progress that we have made in this program.

The approach of obtaining data across as much of the electromagnetic spectrum as is possible requires a variety of instruments on a variety of telescopes. Due to the limitation of telescopes and detectors, nine different telescopes have been used to obtain data from 10^8-10^{18}Hz, which is the range of frequencies that we attempt to sample. It is obviously impossible for one group to obtain all the necessary data, and we are deeply indebted to our collaborators, who have been essential in the success of this project (Table 1).

RESULTS

Due to the limitation of instruments as well as extinction due to the atmosphere and interstellar gas, emission from quasars was conveniently divided up into three spectral regions, which, broadly speaking, are the radio (10^8-10^{11}Hz), the optical (10^{13}-$10^{15.4}$Hz), and the X-ray regions ($10^{16.5}$-10^{18}Hz). Although far-infrared and submillimeter observations are now able to provide data in the gap between the optical and radio regions, it is still useful to consider the three regions separately.

The radio continuum, which is fairly flat in most of our sources, is probably created by several partially optically thick synchrotron sources (e.g. Cotton et al. 1980). The IR-UV continuum, which probably arises from optically thin synchrotron emission, is steeper than the radio continuum. Before data in the far-infrared gap was available, the multifrequency data suggested that the change in slope occurred in the 10^{10}-$10^{12.5}$ Hz region (Bregman et al. 1983, Glassgold et al. 1983, Bregman et al. 1984). Now that data has become available in this far-infrared gap, the region of the spectral turnover can be located with greater accuracy and is near 300 GHz for OJ 287 and 3C 345, and OV-236 (Fig. 1). Because the radio region is known to be optically thick while the optical region is not, it is often suggested that the frequency of the spectral break occurs where the optical depth first reaches unity. If correct, the location of the spectral break region is of fundamental importance to determining the properties of the continuum emitting region.

Because the IR-UV emssion is optically thin synchrotron radiation, its shape yields information on the energy distribution of the electrons responsible for the emission. The slope of the continuum in the infrared and far-infrared region can usually be fit with a single power-law with a slope of about -1, although the slopes range from -0.7 to -1.5 in our sample. Some sources show little or no spectral steepening in the optical and ultraviolet regions (IZw-187; Bregman et al. 1983), some display slow but steady spectral steepening (e.g. OJ 049), while others display extremely rapid steepening in the ultraviolet region (BL Lac and 3C 446). Furthermore, the shape of the IR-UV continuum is generally preserved when the source changes its brightness, although spectral variation is sometimes detected (1156+295, Glassgold et al 1983; 0735+178, Bregman et al 1984).

One of the most common broad-band features seen in the opical-ultraviolet spectrum of non-variable quasars is the 3000 A bump. This feature is generally absent in our sample, with the exception of the BL Lac object IZw-187, which has a weak 3000 A bump (Bregman et al. 1983). We argued that at 3000 A bump in a BL Lac object would be evidence that the bump is not associated with emission line gas, as has been suggested (e.g. Grandi 1982). However, during a subsequent observation of this source, weak optical emission line were discovered that had not previously been detected.

Another feature of interest is the extremely sharp turnover seen in the spectrum of BL Lac and 3C 446. This turnover, which would not have been discovered without ultraviolet observations, is similar in shape to that found in the class of objects known as Red QSOs. The difference is that the turnover occurs in the infrared region for Red QSOs instead of in the ultraviolet region. The turnover has been attributed to an abrupt cutoff in the electron distribution function. The location of the turnover depends not only upon the magnetic field but upon the energy of the electrons, which has proved an elusive property to measure (Bregman et al. 1981, Beichman et al 1981).

The multifrequency spectra can be used to discuss the connection between the IR-UV and the X-ray regions. In our sample, the ultraviolet continuum, when extended to higher frequencies, would nearly always pass below the X-ray datum. This implies that the X-rays are not simply an extension of the IR-UV emission (although IZw-187 is an exception to this rule, Bregman et al. 1983). In the BL Lac object 0735+178 (Bregman et al. 1984), the lack of variation in the X-ray flux during periods of violent variability of the IR-UV continuum suggest that the X-rays are not produced cospatially by a different process. Rather, the X-rays are produced in an entirely different region, possibly by a different process. Whether this behavior is common for this class of objects is the subject of our current program.

We have examined the correlation of the X-ray emission with the optical and radio flux for the sample of sources in which the X-ray flux cannot be an extension of the ultraviolet continuum. We find that the X-ray emission is better correlated with the radio flux than with the infrared, optical, or ultraviolet flux. This is similar to findings by Owen, Helfand, and Spangler (1981) and Zamorani et al. (1981) for differently selected samples.

A comparison of the continuum emission between BL Lac objects and violently variable quasars yields few differences. The spectral shape of 3C 446 is nearly identical to that for BL Lac (although the luminosity is different). Several BL Lac objects (e.g. IZw-187) are very abundant in ionizing photons, so the lack of lines in these sources must be due to a lack of available gas, not a lack of ionizing photons.

The physical conditions in the optically thin emitting region can be determined from the multifrequency spectra if one adopts a model, such as the synchrotron-self-Compton model (e.g. Jones, O'Dell, and Stein 1974). In doing so, we find that the opically thin region has a size between a light week and a few light months, the magnetic field is 0.1 - 100 G, and the Lorentz factor of bulk motion of the emitting plasma is 1-5. The energy of the electrons extends up to about 10 GeV, and the energy densities in electrons, photons, and magnetic field are comparable. By comparing this to VLBI data, we see that the radio emission comes from a larger region of lower magnetic field and where the energy density is nearly entirely in the particles (e.g Kellermann and Pauliny-Toth 1981).

REFERENCES

Beichman, C.A. et al. 1981, Nature, 293, 711.
Bregman, J.N. et al. 1981, Nature, 293, 714.
Bregman, J.N. et al. 1982, Ap.J., 253, 19.
Bregman, J.N. et al. 1984, Ap.J., 276, 454.
Cotton, W.D. et al. 1980, Ap.J., 238, L123.
Glassgold, A.E. et al. 1983, Ap.J., 274, 101.
Grandi, S. 1982, Ap.J., 255, 25.
Jones, T.W., O'Dell, S.L., and Stein, W.A. 1974, Ap.J., 188, 353.
Kellermann, K.I., and Pauliny-Toth, I.I.K. 1981, ARAA, 19, 373.
Owen, F.N., Helfand, D., and Spangler, S. 1981, Ap.J., 250, L55.
Zamorani, G. et al. 1981, Ap.J., 245, 357.

Table 1: Collaborators

Name or Group	Institution	Waveband
Dent, Balonek, O'Dea	U. Mass	radio-mm
Aller, Aller, Hodge	U. Mich	radio
Werner, Rollig	NASA/Ames	submm-IR
Neugebauer	Caltech	IRAS, IR
Rieke, Lebofsky, Rudy, Wisniewski	Steward Obs.	IR-optical
Impey, Williams, Brand	UKIRT, Caltech, RGO	IR
Hackwell	U. Wyoming	IR
Smith, Pollock, Pica, Webb	U. Florida	optical
J.Miller	Lick Obs.	optical
Wills, Wills, Lester	U. Texas	IR-optical
Spinrad	U.C. Berkeley	optical
Henry	U. Michigan	optical
Bregman, Glassgold, Huggins	N.Y.U.	ultraviolet
Ku, Helfand	Columbia U.	X-rays
Tananbaum, Schwartz	C.F.A.	X-rays

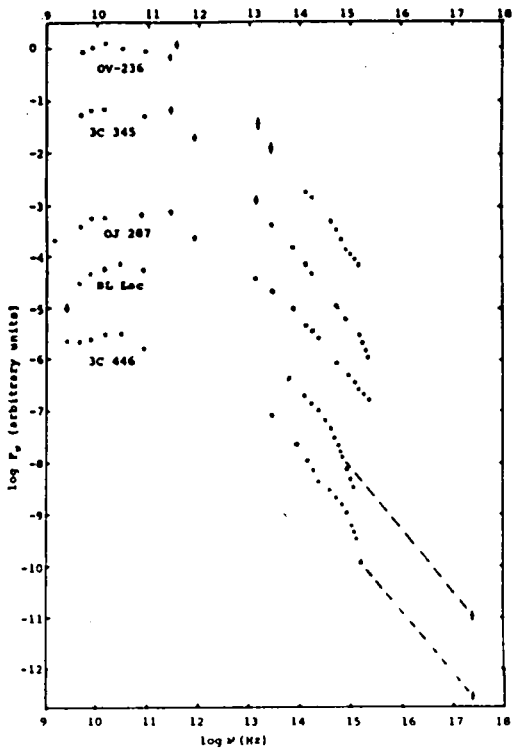

VERY RECENT IUE OBSERVATIONS OF 2 BL LACERTAE OBJECTS

C.M. Urry[1,2], Y. Kondo[2], K.R.H. Hackney[3],
R.L. Hackney[3], S.L. Mufson[4], and W. Wisniewski[5]

ABSTRACT

IUE observations of two BL Lacertae objects, consisting of 2 spectra of 1218+304 and 12 spectra of Mrk 421, are presented. The former object has never been observed with IUE, possibly because it is very faint, but the fact that it is an X-ray source, and a highly variable one, makes it particularly interesting. Mrk 421 has been observed many times with IUE as part of a continuing monitoring program. The present observations indicate an intensity decrease of ~25% on a timescale of one month, with little if any associated spectral change. With one exception, the spectra of these two objects show no discrete features, and the continua are well fit by power law models. The one exception is a long SWP exposure of Mrk 421, from 1984 March 9, which shows a broad emission feature near ~1580 Å. The validity of this feature has not yet been established.

INTRODUCTION

As part of a continuing program of monitoring the broad band spectra of BL Lacertae objects, 1218+304 and Mrk 421 were observed with IUE in January, February, and March of this year (1984). Here we present the IUE data, and where possible, mention the simultaneous coverage in other bands.

1218+304

The BL Lac object 1218+304, first detected with the Ariel V X-ray satellite, was the first BL Lac to be discovered as an X-ray source (Wilson et al. 1979). In the X-ray, it has been seen to vary both in intensity (Wilson et al.) and in spectral shape (Worrall et al. 1981, Urry 1984). It was also detected in the HEAO-1 X-ray All Sky Survey (Piccinotti et al. 1982), and is one of the few extragalactic sources from that survey that has not been observed with IUE. (Because its visual magnitude is ~16, it is one of the faintest objects that can be successfully observed with IUE.)

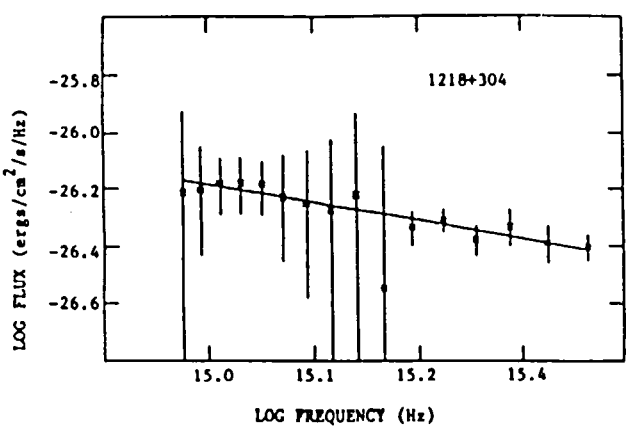

Figure 1. IUE Spectrum of 1218+304

On 1984 February 2, we obtained two images, SWP 22187 (exposed 395 minutes during US 1) and LWP 2733 (exposed 210 minutes during a very low background US 2). The binned data ($\Delta\lambda$~125Å) are shown in Figure 1, with error bars determined from the standard deviation from the mean, and with a line indicating the best fit power law model of the form $F_\nu = (A/10^{26})(\nu/10^{15})^{-\alpha}$ ergs/cm^2/s/Hz, where $A=0.66\pm0.08$ and $\alpha=0.64\pm0.19$. The integrated ultraviolet flux from this object

[1]Johns Hopkins University, now at MIT. [2]NASA/Goddard Space Flight Center.
[3]Western Kentucky University. [4]Indiana University. [5]University of Arizona.

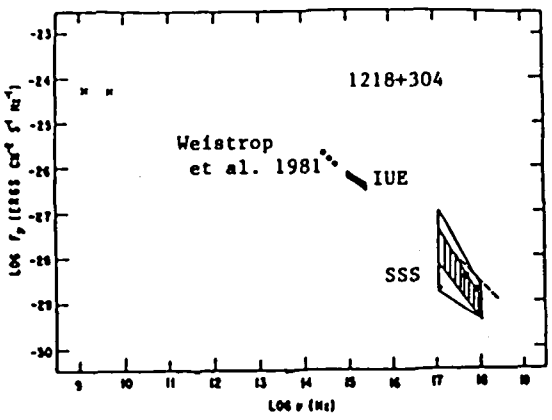

Figure 2. Composite Spectrum of 1218+304

is $(7.2\pm0.9)\times10^{-12}$ ergs/cm^2/s. The composite spectrum, compiled from non-simultaneous data (the simultaneous X-ray, optical, and infrared data are not yet reduced), is shown in Figure 2. Because of the reported variability, it is difficult to comment on this spectrum, beyond saying that it has the typical flat radio-to-optical appearance, followed by a break around 10^{14}-10^{15} Hz, with a steeper spectrum extending smoothly into the X-ray regime. The IUE spectrum seems too flat, flatter than the optical, and we intend to improve the definition of the continuum with a gaussian extraction method, to see if this flat index changes (see Hackney, Hackney, and Kondo, this volume).

Mrk 421

Mrk 421 is one of the brightest BL Lac objects observed with IUE, and has been monitored steadily since the launch of the satellite (Boksenberg et al 1978, Ulrich et al. 1984). The observations discussed here were made on 5 different days: 3 days at the end of January and beginning of February, and 2 days at the beginning of March. The date, image number, and duration of each observation is given in Table 1. In the one month between the two groups of observations, the intensity of Mrk 421 decreased dramatically, confirming it as one of the most variable BL Lac objects. The ultraviolet and optical intensities both decreased by about 20-25% in the space of 4 weeks; there was no obvious variability between the observations that were separated by only a few days. This is illustrated by the light curve in Figure 3, in which we have plotted the ultraviolet and V band fluxes (values taken or adapted from Table 1).

Table 1. Recent IUE Observations of Mrk 421

Date	Image	Length (min)	A	α	F_{uv}	V
1984 Jan 23	LWP 2699 SWP 22082 LWP 2700	75 100 210	6.65±0.12	1.04±0.04	6.01±0.11	13.33
1984 Jan 28	LWP 2711 SWP 22128 LWP 2712	80 33 210	6.35±0.20	1.01±0.07	5.82±0.11	13.34
1984 Feb 2	LWP 2732	90	6.77±0.15*	1.13±0.20*	5.88±0.18*	13.32
1984 Mar 3	LWP 2881 SWP 22398 LWP 2882	80 240 60	5.24±0.18	1.10±0.08	4.61±0.16	13.61
1984 Mar 9	LWP 2915 SWP 22445	95 260	5.04±0.21	1.12±0.08	4.38±0.14	13.60

*Determined from LWP spectrum only, extrapolated where necessary.

For each day's observations, the LWP and SWP spectra were combined (except for the February 2 observation, when only 1 LWP spectrum was taken), and the continuum was fit with a power law of the form given earlier. The parameters A and α are listed in Table 1. In Figure 3, the spectral index determined for each set of spectra has been plotted, and confirming previous findings for this and other BL Lac objects (Urry et al. 1982, Maraschi et al. 1983, Ulrich et al. 1984), we see no evidence for strong spectral variability accompanying the more obvious intensity variability.

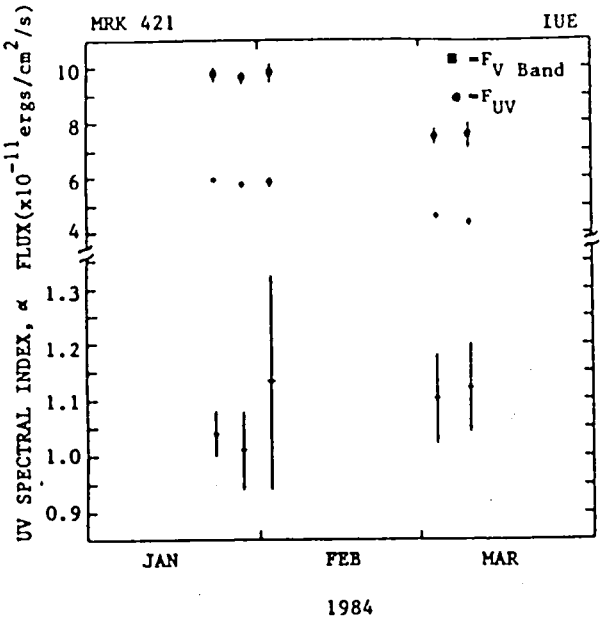

Figure 3. Light Curve of Mrk 421 UV flux, V band flux, and UV spectral index as a function of time.

In each case, the power law model provided a good fit to the data. The details of the simultaneous measurements in other wavebands are not yet available, although we know that the X-ray flux was weak during January and March 1984, relative to previous X-ray observations (Y. Tanaka, private communication). We have assembled a composite spectrum of Mrk 421, shown in Figure 4, from non-simultaneous observations. This figure suggests that like other BL Lac objects, Mrk 421 has a smooth spectrum extending from radio to X-ray frequencies, with a break near 10^{13} or 10^{14} Hz. Detailed analysis of the broad band spectrum will be postponed until the simultaneous observations are assembled.

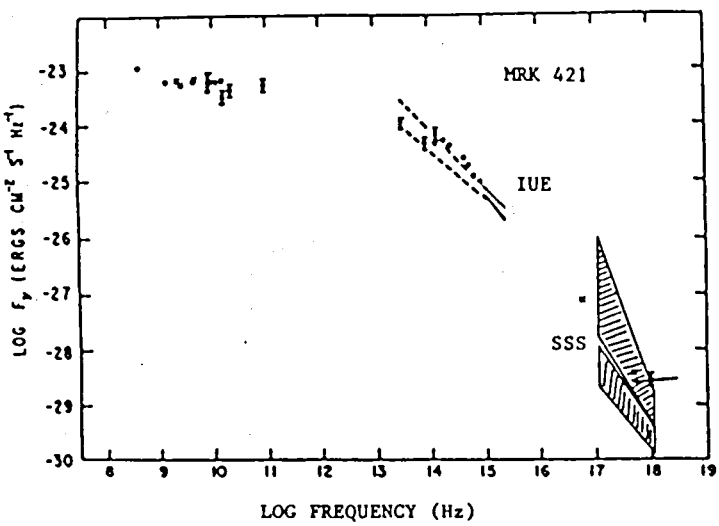

Figure 4. Composite Spectrum of Mrk 421

In the final SWP spectrum of Mrk 421 there is a dramatic, broad emission feature near 1580 Å, with equivalent width 10±1 Å. The 4 SWP spectra are shown in Figure 5. The reality of this feature is in doubt for at least 3 reasons: (1) it was not present in the SWP image obtained 6 days earlier (there is a suggestion of a weaker feature, EW~2 Å, displaced ~5 Å shortward); (2) it may be related to a hot spot in the SWP camera near 1570 Å (Hackney, Hackney, and Kondo 1982); and (3) if it is CIV, it is at a redshift z=0.017±0.002, not the reported [optical] redshift of the galaxy (z=0.0308, Ulrich et al. 1975). However, other facts must also be considered. First, BL Lac objects are highly variable, and Mrk 421,

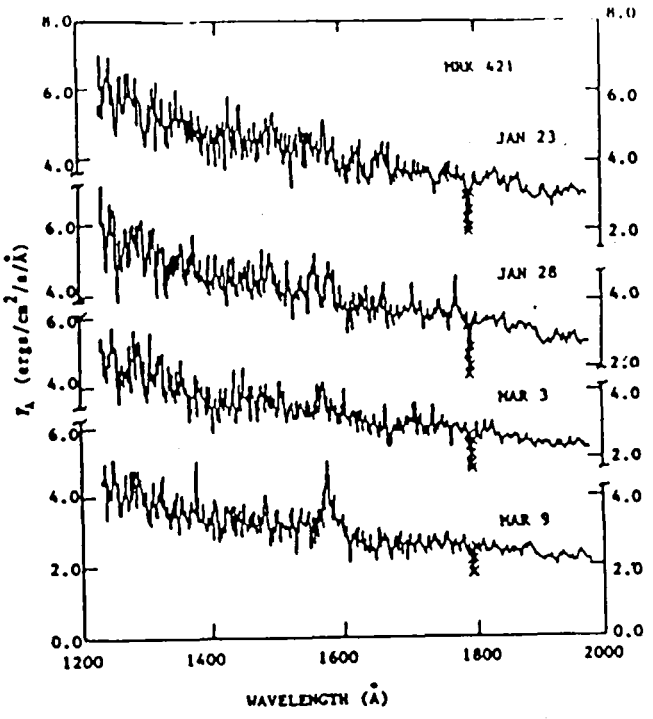

Figure 5. SWP Spectra of Mrk 421

which is one of the most variable, is certainly variable on the timescale of a day. Second, the observed emission feature is broader than a typical cosmic ray hit, and lies directly on top of the spectrum, centered at line 28 (as is the rest of the spectrum). Third, there may be reasons to expect discrete features to be blue-shifted relative to the source frame; in particular, the emission or absorption might arise in a cloud that is moving an a relativistic jet closely aligned with our line of sight, as was suggested to explain the absorption feature seen in the X-ray spectrum of another BL Lac object, PKS 2155-304 (Canizares and Kruper 1984). Further investigation of the validity of this feature, including examination of the photowrites from the IUE observations immediately preceding and following the March 9 observation (to look for spurious emission near 1580 Å); examining reprocessed 110x110 files to determine more precisely the profile and location of the feature in the cross-dispersion direction; and repeating the observations, in the ultraviolet and/or visual bands, will be attempted as soon as possible.

REFERENCES

Boksenberg, A. et al. 1978, Nature, 275, 404.
Canizares, C. R. and Kruper, J. 1984, Ap.J., in press.
Hackney, R. L., Hackney, K. R. H., and Kondo, Y. 1982, in Advances in Ultraviolet Astronomy: Four Years of IUE Research, eds Y. Kondo, J. M. Mead, and R. D. Chapman, (Greenbelt, MD: NASA Conference Publication 2238), p.335.
Maraschi, L., Tanzi, E. G., and Treves, A. 1984, in Proceedings of the COSPAR/IAU Symposium, in press.
Piccinotti, G., Mushotzky, R. F., Boldt, E. A., Holt, S. S., Marshall, F. E., Serlemitsos, P. J., and Shafer, R. A. 1982, Ap.J., 253, 485.
Ulrich, M.-H., Hackney, K.R.H., Hackney, R.L., and Kondo, Y. 1984, Astr.Ap., in press.
Ulrich, M.-H., Kinman, T.D., Lynds, C., Rieke, G., and Ekers, R. 1975, Ap.J., 198, 261.
Urry, C. M. 1984, Ph.D. Thesis, The Johns Hopkins University.
Urry, C.M., Holt, S., Kondo, Y., Mushotzky, R., Hackney, K., and Hackney, R. 1982, in Advances in Ultraviolet Astronomy: Four Years of IUE Research, eds. Y. Kondo, J. Mead, and R. Chapman, (Greenbelt, MD: NASA Conference Pub. 2238), p. 177.
Wilson, A.S., Ward, M.H., Axon, D., Elvis, M. and Meurs, E. 1979, M.N.R.A.S., 187, 109.
Worrall, D., Boldt, E., Holt, S., Mushotzky, R., and Serlemitsos, P. 1981, Ap.J., 243, 53.

COORDINATED MULTIFREQUENCY OBSERVATIONS OF THE BL LAC OBJECTS MRK 180, MRK 421, and MRK 501

S.L. Mufson, Indiana University; D.J. Hutter, Georgia State University; K.R. Hackney and R.L. Hackney, Western Kentucky University; Y. Kondo and C.M. Urry, NASA Goddard Space Flight Center; W.Z. Wisniewski, Lunar and Planetary Laboratory; M.F. Aller and H.D. Aller, University of Michigan

Over the past several years we have been investigating the properties of the three BL Lac objects Mrk 180, Mrk 421, and Mrk 501 using data gathered at ultraviolet, X-ray, optical, and radio wavelengths. These three objects are relatively nearby (z = .046, .031, and .034, respectively) composite systems in which a moderately luminous ($L = 10^{44}$ ergs/s) BL Lac object is found at the core of an elliptical galaxy (Ulrich 1978; Ulrich et al. 1975). These objects have been classified as BL Lacs because of the absence of emission lines in their spectra (Ulrich 1978; Ulrich et al. 1975), their linearly polarized optical continuum emission (Angel and Stockman 1980; Maza, Martin, and Angel 1978), and their flat radio spectra (Kojoian et al. 1976).

In order to understand the processes and conditions occurring within the nonthermal emission region of these BL Lac objects, we have obtained coordinated observations of them at ultraviolet, X-ray, optical, and radio wavelengths (Mufson et al. 1984a; Mufson et al. 1984b). These observations have given us a single epoch snapshot of the continuous spectrum of each object. The ultraviolet observations were obtained by the SWP and LWR cameras on IUE. The X-ray data were obtained by the IPC and the MPC on HEAO-2. The optical photometry consists of broadband BVRI measurements using the 1-m and 1.5-m telescopes of the University of Arizona Mt. Lemmon Observatory. The radio data were obtained with the University of Michigan computer controlled 26-m radio dish. The single epoch data for the three sources are shown in Figs. 1-3. These figures contain in addition archival radio and infrared data. The additional radio data demonstrate that the radio spectra of all the sources are flat.

For each time-frozen spectrum we have computed an inhomogeneous, relativistic jet model (Mufson et al. 1984a; 1984b). Our jet model is a modification of the jet described in Blanford and Königl (1979) and Königl (1981). Our main reason for choosing this model is the growing body of evidence suggesting that highly relativistic jet-like features are common in active galactic nuclei (Kellermann and Pauliny-Toth 1981). In the jets described here, relativistic electrons flow outward with bulk relativistic velocity along a free, conical jet. As they flow outward, the electrons emit synchrotron and self-Compton emission. In Figs. 1-3 we show our best model fits (χ^2/d.o.f. $\lesssim$ 1.5 for all cases) superposed on the data. It is evident that the model spectra fit the data well. It ought to be noted at this conference in particular the importance of the ultraviolet data to these calculations. The ultraviolet is the one spectral region where we are seeing synchrotron emission uncontaminated by galaxy emission, self-Compton emission, or optical depth effects.

A steepening synchrotron emission spectrum from the infrared to the ultraviolet, which is characteristic of relativistic jets (Königl 1981), is present in our model spectra. We can see from the figures that this spectrum, when extrapolated to high frequencies, can account for the X-ray observations. This implies that self-Compton emission is unimportant in these sources. In addition, the superposition of many different synchrotron spectra from different regions along the inhomogeneous jet produces the observed flat radio spectral index, nearly independent of the optical-uv spectral index. One further result of our computations is the relative contribution of galactic and nonthermal emission to the observed optical flux. Figs. 1-3 show that galaxy emission is most important for Mrk 501 and least important for Mrk 421.

We have found from our model fits that the physical structure of all three jets is very similar. The jets differ only in the angle at which they are aligned to the line-of-sight. We find that the relativistic particles all move outward with the same bulk velocity, a result which implies that all three jets have the same opening angle. In addition, the variation of the particle density and magnetic field strength with radius is similar for all three sources. Assuming that the particle density falls like r^{-n} and the field strength falls like r^{-m}, we find that $\langle n \rangle = 1.4$ and $\langle m \rangle = 1.3$, where the averages are taken over the values for the three model jets. For a jet which is free to expand adiabatically, conservation of particle number and magnetic flux predict that $n = 2$ and $m = 1.6$. Since the particle density in the models falls off more slowly than this prediction, particle injection must be occurring along the jet. The magnetic field strength, however, may be conserved along the jet.

Many of the differences observed in these three BL Lac objects can be ascribed to differences in the angle that the jets make with our line-of-sight. Our calculations show that the jet in Mrk 421 is most closely aligned with our line-of-sight ($\theta = 4.^{\circ}6$); the one in Mrk 501 is least closely aligned ($\theta = 23^{\circ}$). Since the jet in Mrk 421 is most closely aligned to the line-of-sight, its Doppler enhancement factor ($\delta = 7.7$) is greatest and its nonthermal radiation is most strongly beamed toward us. This explains why nonthermal emission is such a large fraction of the flux observed from Mrk 421 in the optical. The radiation from the jets is Mrk 180 ($\delta = 1.8$) and Mrk 501 ($\delta = 1.1$) are beamed less, and so galactic emission contributes a larger fraction of the optical flux. In addition, relative jet alignment explains why flux variability is more pronounced in Mrk 421 than it is in the other two sources.

References

Angel, J.R.P., and Stockman, H.S. 1980, Ann. Rev. Astr. Ap., 18, 321.

Blanford, R.D., and Königl, A. 1979, Ap.J., 232, 34.

Kellermann, K.E., and Pauliny-Toth, I.I.K. 1981, Ann. Rev. Astr. Ap., 19, 373.

Kojoian, G., Sramek, R.A., Dickson, D.F., Tovmassian, H., and Purton, C.R., 1976, Ap.J., 203, 323.

Königl, A. 1981, Ap.J., 244, 700.

Maza, J., Martin, P.G., and Angel, J.R.P. 1978, Ap.J., 224, 368.

Mufson, S.L., Hutter, D.J., Hackney, K.R., Hackney, R.L., Urry, C.M., Mushotzky, R.F., Kondo, Y., Wisniewski, W.Z., Aller, H.D., Aller, M.F., and Hodge, P.E. 1984a, Ap.J., in press.

_____. 1984b, in preparation.

Ulrich, M.H. 1978, in Pittsburgh Conference on BL Lac Objects, ed. A.M. Wolfe (Pittsburgh: University of Pittsburgh Press), p. 192.

Ulrich, M.H., Kinman, T.D., Lynds, C.R., Rieke, G.H., and Ekers, R.D. 1975, Ap.J., 198, 261.

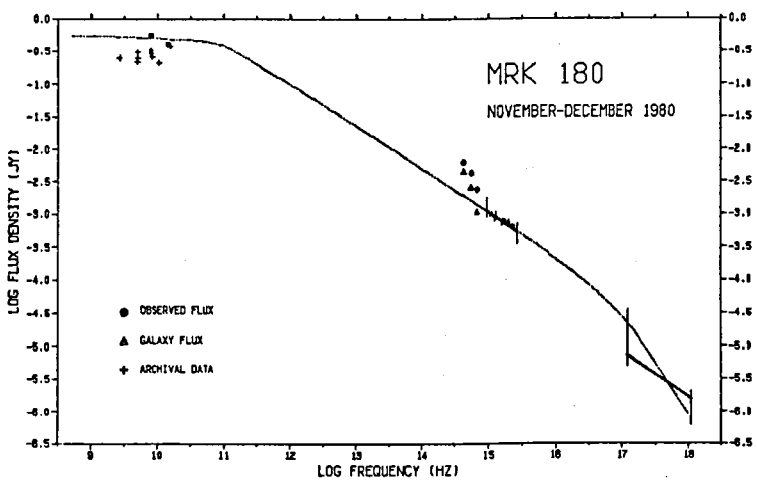

Fig. 1. Coordinated observations and best fit jet model (dashed lines) for Mrk 180.

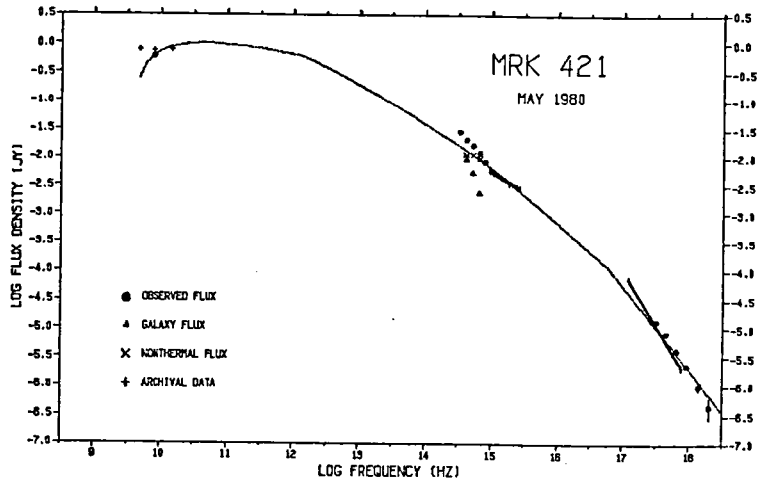

Fig. 2. Coordinated observations and best fit jet model for Mrk 421.

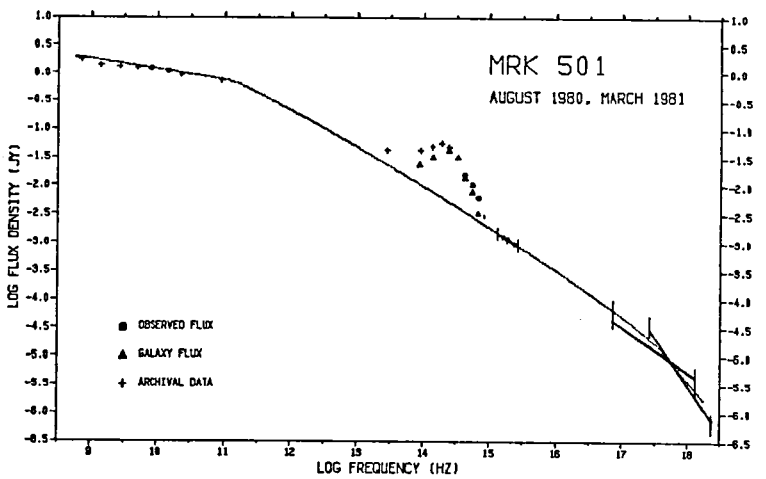

Fig. 3. Coordinated observations and best fit jet model for Mrk 501.

FLUORESCENT EXCITATION OF FE II, MN II, TI II, N I LINES BY C IV, N V, OVI, ... EMISSION LINES IN THE SPECTRA OF SYMBIOTIC STARS & SEYFERT GALAXIES

Daya P. Gilra

SM Systems and Research Corporation, Lanham, Md. 20706

ABSTRACT

Analysis of the published IUE and ground based high resolution spectra of symbiotic stars, particularly RR Tel, shows that the dominant excitation mechanism of Fe II, Mn II, Ti II, N I lines (many of these are left unidentified in the published spectra) is the selective fluorescent excitation of some levels by the strong C IV, N V, O VI, ... emission lines. The same mechanism should work for the excitation of Fe II lines in the spectra of Seyfert galaxies and QSO's whose emission spectra are quite similar to those of symbiotic stars.

The similarities and differences between the fluorescent excitation mechanism reported in this paper and the Bowen's mechanism will be analysed.

A MODEL FOR THE VARIABLE CONTINUUM OF THE SEYFERT I GALAXY NGC 5548

W. Wamsteker, P. Benvenuti, A. W. Harris, A.Talavera
C. Gry, A.Cassatella, B. Hassal, R. Gilmozzi
ESA-ESTEC, Noordwijk, HOLLAND
c/o VILSPA, Madrid, SPAIN

P. Barr
Dept. of Physics & Astronomy, UCL, London, ENGLAND
c/o EXOSAT Observatory
Darmstadt, WEST GERMANY

J. C. Clavel
Observatoire de Meudon
Paris, FRANCE

H. Netzer, B. J. Wills, D. Wills
Astronomy Department, University of Texas,
Austin, Texas

ABSTRACT

The variations of NGC 5548 over the full period of IUE observing until February 1984 are analyzed. The results indicate that the amplitude of the variation is largest at the shorter UV wavelengths. The implications of this wavelength dependence are of importance for the continuum modeling. A fit to a simultaneously obtained UV and optical spectrum in July 1981, based on the Fe II fluorescence model of Netzer and Wills (1983) is shown to give an extremely good match with the data.

INTRODUCTION

The Seyfert I galaxy NGC 5548 has been reported to be variable in the UV (Barr et al., 1983). Line studies based on IUE data have been presented by Boisson and Ulrich (1983) and Gregory et al. (1982). The results presented here are based on data from the IUE Data Base and obtained under our program of simultaneous UV and optical spectroscopy. Athough a considerably larger data set is available, we will here only discuss the combined spectrum of July 1981.

Continuum Variation

In Figure 1 we show the light-curve of NGC 5548 as determined for a continuum window at 1358Å over the period 1978-1984. The large-scale variation seen in Figure 1 has a time scale of approximately 1 year and is very similar to the variation seen in QSO's. Also some indication is present in Figure 1 for variations on a much shorter time scale--of the order of 1-2 weeks--however, the dominant variation appears to be at the larger time scale. Of course, the sampling interval is not sufficiently

short nor regular enough to be able to fully evaluate the importance of short term variations. Some of the data sampled with a short time interval have been taken with relatively short integration times, so that these continuum points have considerably larger errors associated with them. The brightness variation is of similar shape over the whole IUE wavelength range from 1100Å to 3200Å. The amplitude varies as a function of wavelength. At the shorter wavelengths the amplitude is larger than at the longer wavelengths. To illustrate this wavelength dependence, we show in figure 2 the behavior of two logarithmic color indices as a function of the continuum brightness at 1696Å. Figure 2a shows the color index (1446Å-1814Å). Although a slight tendency to get bluer when brighter is indicated, the trend is not very strong. In Figure 2b the logarithmic color index (1446Å-2710Å) is shown. A quite marked and well defined correlation is indicated. These figures illustrate quite clearly the decrease in amplitude with increasing wavelength. Considering that at least part of the flux seen in the UV is represented by a power law spectrum, the data are most easily explained in terms of a non- or, only slightly variable, component in the spectrum whose relative strength with respect to the power law spectrum increases towards longer wavelengths. At longer wavelengths the importance of the Balmer continuum and Fe II increases strongly as has been suggested by various authors (e.g. Netzer and Wills, 1983).

Continuum Fit

Since the short wavelength range shows continuum which is more directly related to the variable component in the spectrum, it is best to match a power law in the SWP range. We can then use the combined optical and UV spectrum to attempt to match the observed data. The optical spectrum used was obtained at McDonald Observatory; both IUE and optical data were obtained between June 28, 1981 and July 3, 1981, so they can be considered as simultaneous. In Figure 3 we show the combined spectrum in a log F_ν - log ν plot (corrected for galactic reddening $E(B-V) = 0.05$ and $z = 0.0174$). A model fit is also shown. The model consists of a power law with $\alpha = -0.5$, Fe II lines (v_t = 20 km/s, Netzer and Wills, 1983), case B Balmer and Paschen continuum at 20,000°K. The lines in the model have not been calculated but are obtained through a Gaussian line decomposition of the data. It can be seen that the model fits the data quite well. The model still left some excess flux at wavelengths >4500Å. This could be allowed for by a small contribution of normal stellar flux (= 2 mJy at 5400Å). The stellar contribution was taken from the M31 observations by Oke et al., (1978). This made the fit rather good. We are aware that this fit is rather crude, e.g., the choice of t = 20,000°K for hydrogen recombination is likely to be too high. However, if the optical depth is considerably higher than is valid for Case B, a similar shaped Balmer continuum would result for a lower temperature.

CONCLUSIONS

The results presented here show that the spectrum of the Seyfert I galaxy NGC 5548 can be fairly well represented by a combination of a single power law continuum, Fe II lines, Balmer lines and continuum and stellar radiation (see also Netzer et al., elsewhere in this symposium). The variability data suggest that the variations in the strength of the power law spectrum are not accompanied by large changes in the spectral index. Apparent spectral index variations can occur due to the difference in relative importance of individual components at different wavelengths.

REFERENCES

Barr, P., Willis, A. J., Wilson, R., 1983, M.N.R.A.S. 203, 201.

Boisson, C., Ulrich, M. H., 1983, ESO preprint, #235.

Gregory, S., Ptak, R., Stoner, R., 1982, Ap. J. 261, 30.

Netzer, H., Wills, B. J., 1983, Ap. J. 275, 445.

Yee, H. K. C., Oke, J. B., 1978, Ap. J. 226, 753.

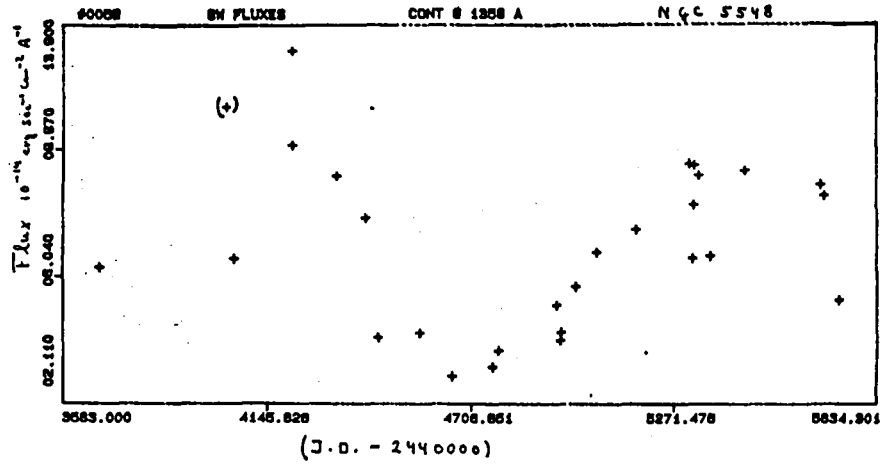

Figure 1 -
The continuum (1348Å-1368Å) variation of NGC 5548 between 1978 and February 1984. The large, long term variation is similar to that seen in QSO's. One observation, clearly affected by instrumental effects, is shown in parentheses. Although some very rapid brightness changes seem to occur, the long term variation appears dominant.

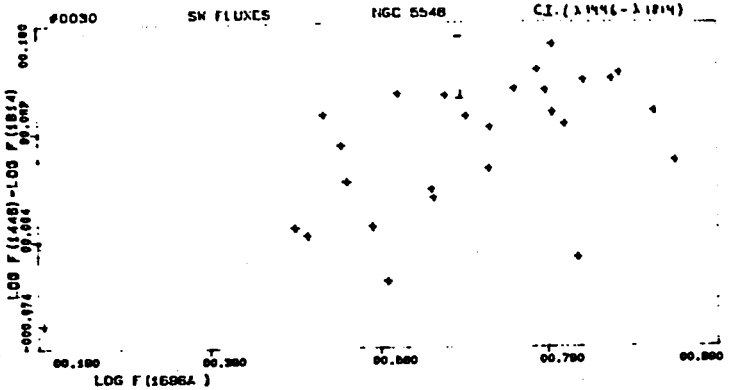

Figure 2a-
The logarithmic color index log ($F_{1446} \div F_{1814}$) is shown as a function of log F_{1656}. The continuum windows were chosen at 1438Å-1455Å, 1687Å-1704Å, and 1808Å-1820Å. Although some dependence of the color index on brightness is indicated, this is only marginally significant.

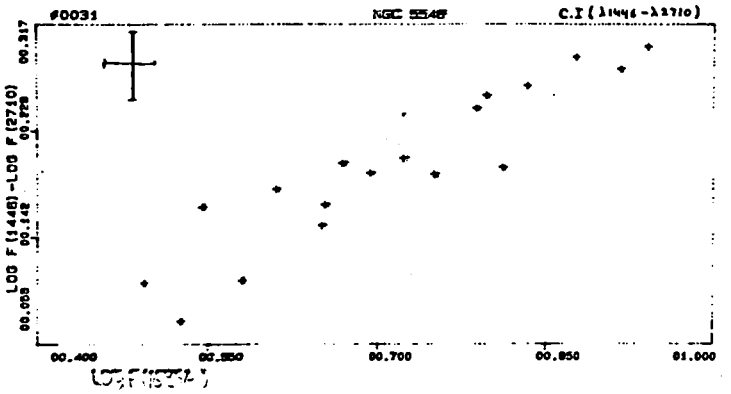

Figure 2b -
Same as Figure 2a, only now the color index is log ($F_{1446} \div F_{2710}$), with the long wavelength window 2896Å-2725Å. In contrast to Figure 2a, here the color index is very closely correlated with the brightness at 1446Å.

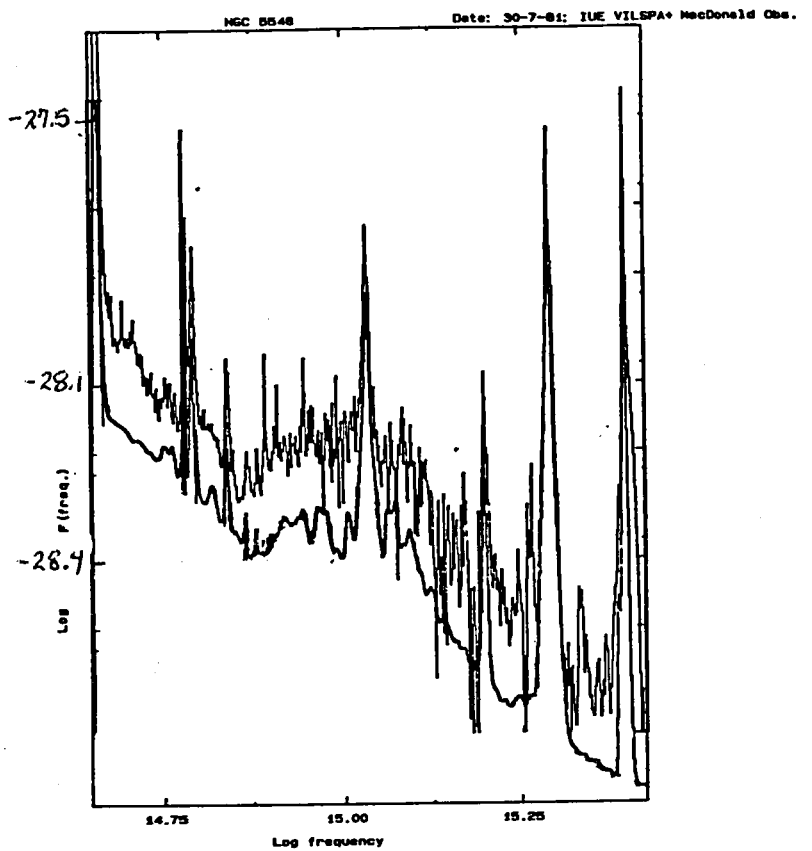

Figure 3 -
The UV optical spectrum of NGC 5548 is shown for July 1981. Somewhat displaced below is shown the model spectrum, which represents the data extremely well. The model consists of a power law $\sim\nu^{-0.5}$. Case B hydrogen recombination at T = 20,000°K, Fe II emission at v_T = 20 km sec^{-1} (Netzer and Wills, 1982), and ~2mJY (at 5400Å) stellar continuum (see also text).

NEBULAE AND CLUSTERS

IUE OBSERVATIONS OF PLANETARY NEBULAE IN THE MAGELLANIC CLOUDS

Stephen P. Maran*, Lawrence H. Aller**,
Theodore R. Gull*, Charles D. Keyes**, and Theodore P. Stecher*
*Laboratory for Astronomy and Solar Physics, NASA/GSFC
**Department of Astronomy, UCLA

ABSTRACT

Four more PN in the Clouds have been observed with IUE (LMC P2, P9, P33; SMC N43). Reliable C abundances were computed for the first time for each PN, and other abundances were calculated from ionization models taking the IUE and earlier groundbased spectra into consideration. P9 has the richest spectrum of any extragalactic PN that we have studied in the UV; three ionization stages of N were detected. We also reobserved three PN (LMC P40; SMC N2, N5) that were studied in 1981, to search for time variations that might be anticipated from the relatively high luminosities and masses that were derived for the central stars of these young, compact objects. For P40, with a derived central star mass of 1.2 M_o, the continuum observations hint at variation of the anticipated type but are not decisive.

DISCUSSION

For procedures adopted, see Maran et al. (1982), Stecher et al. (1982), and Maran et al. (1984) Our 1983 IUE observations of four more planetaries in the Clouds are seen in Figs. 1 and 2. As seen from Fig. 1, P9 has a rich ultraviolet spectrum, with three ionization stages of N. Preliminary abundance calculations (Table 1) show that it is N-rich (the first such PN that we have observed in the Clouds), while LMC P2 and P33 are C-rich and thus their progenitors were carbon stars. Modelling of SMC N43 is in progress. Stecher et al. (1982) derived masses of 1.2 M_o, 0.9 M_o, 1.1 M_o, respectively for the central stars of LMC P40, SMC N2, and SMC N5. The theoretical factor-of-10 fading times since T_{eff} reached 30,000 K vary as $M^{-9.6}$, with t_f = 20 yr for M = 1.2 M_o and 300 yr for 0.9 M_o (Paczynski 1971). The data in Table 2 show no evidence for changes in the strongest two UV emission lines in each of these three PN over two years, although in these dense but optically thin nebulae the emission lines might be expected to closely track changes in the ionizing stellar continuum with negligible delay. As seen from Table 3, the mean ratio (averaged over five wavelength bins) of continuum flux measured in Aug. 1983 to continuum flux measured in May 1981 is 1.05 $\pm$ 0.07, consistent with no change. However, in the shortest wavelength bin (where the flux is dominated by the star, according to Stecher et al. 1982), there is an apparent 16% decrease over two years, while in three other bins (where the flux is mainly due to the nebular recombination continuum), there were apparent increases of 6%, 11%, and 18%. Looking at these results, we cannot avoid noting that if the central star were fading rapidly, as anticipated if M = 1.2 M_o, the flux in the shortest wavelength bin (arising from the star itself) would decrease in agreement with the observations, while flux in the longer wavelength bins would at first increase, thanks to increased recombination due to the reduction in ionizing radiation. However, to determine whether we can be confident in the significance of apparent continuum changes at the observed levels (even at 16% and 18%, surely not at 6%) we would need to inspect

repeated long exposure observations of the same nebula, made at the same epoch. Such observations are not available, nor are pairs of long exposure 1981 and 1983 continuum observations of N2 and N5. It would be desirable to monitor P40, N2, and N5 photometrically in H-beta.

REFERENCES

Maran, S. P., Aller, L. H., Gull, T. R., and Stecher, T. P. 1982, Ap. J. (Letters), 253, L43.

Maran, S. P., Gull, T. R., Stecher, T. P., Aller, L. H., and Keyes, C. D. 1984, Ap. J., in the press (May 15, 1984).

Paczynski, B. 1971, Acta Astr., 21, 417.

Stecher, T. P., Maran, S. P., Gull, T. R., Aller, L. H., and Savedoff, M. P. 1982, Ap. J. (Letters), 262, L41.

Table 1: Chemical Abundances

	P9	P2	P33
He	11.23	11.06	11.08
C	7.74	8.75	8.77
N	8.40	7.74	7.65
O	8.02	8.24	8.43
Ne	7.54	7.42	7.65
S	6.84	6.59	6.72
Ar	6.35	6.02	6.20

Table 2: Stability of Emission Line Fluxes Over Two Years

	P40	N2	N5
C III]	0.995	0.89	1.04
C IV	0.92	1.06	0.92

Tabulated: (1983 flux)/(1981 flux).

Table 3: Ultraviolet Continuum Fluxes at Two Epochs

Wavelength Bin angstroms	May 1981 erg cm^{-2} s^{-1} A^{-1}	August 1983 erg cm^{-2} s^{-1} A^{-1}
1800 - 1880	2.20×10^{-15}	2.34×10^{-15}
1760 - 1840	2.26×10^{-15}	---
1680 - 1760	2.46×10^{-15}	2.74×10^{-15}
1360 - 1440	2.70×10^{-15}	3.18×10^{-15}
1260 - 1340	2.80×10^{-15}	2.41×10^{-15}

Mean change, (1983 Flux)/(1981 Flux) in Table 3 = 1.05 $\pm$ 0.07.
No reddening corrections applied to data in Table 3.

FIGURE CAPTIONS

Fig. 1: Low dispersion, short wavelength ultraviolet spectrum of LMC P9. The top spectrum is a 30-min exposure, taken with the target slightly off center in the large entrance aperture. The center spectrum is a 72-min exposure, taken with the target centered in the aperture. At the bottom is an exposure-weighted average of the two upper spectra.

Fig. 2: Low dispersion, short wavelength IUE spectra of three planetary nebulae in the Magellanic Clouds. Top: SMC N43, 33-min exposure. Center: LMC P33, 70-min exposure. Bottom: LMC P2, 150-min exposure.

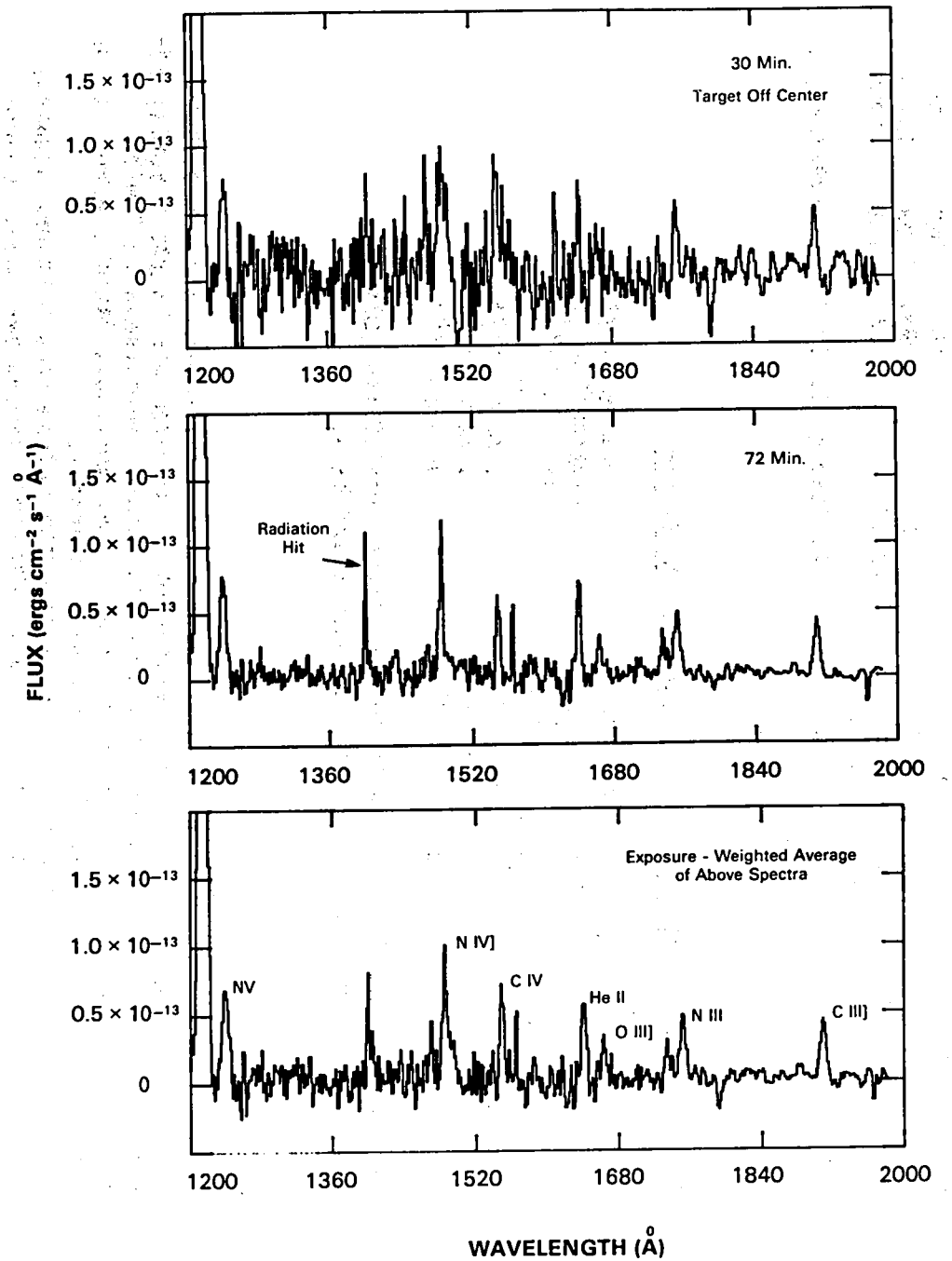

ULTRAVIOLET SPECTRA OF PLANETARY NEBULA

P9

IN THE LARGE MAGELLANIC CLOUD

OBTAINED WITH
INTERNATIONAL ULTRAVIOLET EXPLORER
1983 JULY 9

SHORT WAVELENGTH SPECTROGRAPH

LOW DISPERSION CAMERA

($\Delta\lambda = 6$Å)

PROCESSED AT IUE
REGIONAL DATA ANALYSIS FACILITY
NASA — GODDARD SPACE FLIGHT CENTER

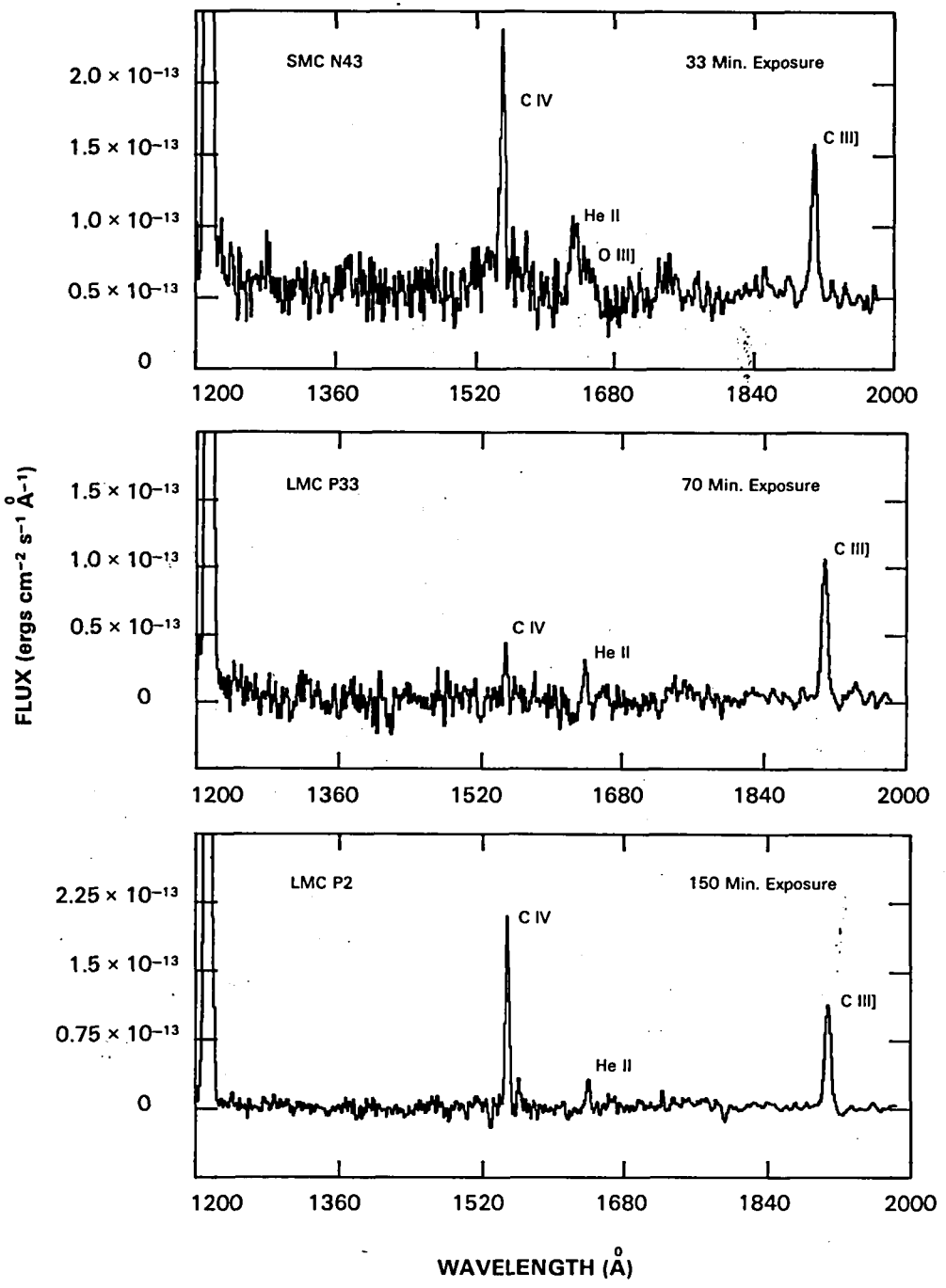

ULTRAVIOLET SPECTRA OF PLANETARY NEBULAE IN THE MAGELLANIC CLOUDS

OBTAINED WITH
INTERNATIONAL ULTRAVIOLET EXPLORER
1983 JULY

SHORT WAVELENGTH SPECTROGRAPH

LOW DISPERSION CAMERA

($\Delta\lambda$ =6Å)

(S.P. MARAN, L.H. ALLER,
T.R. GULL, T.P. STECHER)

1983 OBSERVATIONS OF THE ECLIPSING NUCLEUS OF THE BIPOLAR PLANETARY NEBULA NGC 2346.

Walter A. Feibelman
NASA-GSFC, Laboratory for Astronomy and Solar Physics, Greenbelt, MD.

and

Lawrence H. Aller
Astronomy Department, University of California, Los Angeles, CA.

ABSTRACT.

We present IUE data of the eclipsing nucleus of NGC 2346 obtained at 3 phases of the 1983 observing season. At $\phi = 0.02$ a highly asymmetric C IV emission line is seen, but the He II line has a gaussian profile with a slight suggestion of an inverse P Cygni character. The stellar continuum in the 1200-1950A region and high excitation emission lines argue for a hot subdwarf component in the binary nucleus.

INTRODUCTION

The single-lined spectroscopic binary nucleus of the bipolar planetary nebula NGC 2346 was found by Kohoutek (1982) to show deep eclipses in late 1981. Searches of Harvard plate material by Schaefer (1983) and Sonneberg material by Luthardt (1983) indicate that no eclipses took place between the years 1897 and 1981. The relatively bright visible central star has been known to be of spectral type A5 V, which is insufficient to ionize the nebula; an unseen hot companion was therefore suspected as the source of excitation. A considerable amount of confusion has arisen for the orbital elements from conflicting values of photometric vs. radial velocity measurements.

For the present discussion, we adopt the period of 15.991 days and t_o = 2443126.0 from Méndez, Gathier and Niemela (1982) but add that the following comments of our IUE observations should be viewed as a preliminary report pending further confirmation of ground-based photometry and spectroscopic studies, possibly augmented by infrared observations. The radial velocity period remained constant at slightly less than 16 days, but the shape of the light curve changed drastically during the interval 1981 to 1983 and presumably is still changing. Both the maximum and minimum values have steadily decreased and the minimum has become extremely broad (Méndez *et al.* 1982; Kohoutek 1983). A spherical dust cloud model for this behavior was proposed by Méndez *et al.* (1982) but requires some modification.

1983 IUE OBSERVATIONS

We obtained low dispersion IUE spectrograms of the nucleus and of the nebula at three phases of the 16-day period during the 1983 observing season, as summarized in Table 1. Our original intent was to obtain a high dispersion spectrogram at maximum light, based on the prediction by Méndez *et al.* (1982) that the eclipses of the binary system should cease by March or April of 1983,

but this was not the case. In fact, the entire light level of the system continued to decline so that when our first observation was made on April 17, 1983, the IUE guidance system locked onto the center of light which was of nebular origin, thus resulting in a spectrum of the nebula; the faintness of the nucleus thus precluded obtaining a high dispersion spectrum. We then used blind offsets to the coordinates of the central star(s) and obtained stellar spectra originating primarily from the hot companion since the contribution of the A-type star shortward of 1600A is essentially zero. At the time of observation we were unaware that the shape of the light curve had drastically changed from the one published by Kohoutek (1982) to that of Kohoutek (1983). This broadening of the minimum, however, explains the discordant point of our 1982 "light curve" (Feibelman and Aller, 1983). The progressive decline of the maximum continued during the 1983 observing season, as indicated by Marino, Williams and Walker (1984) who were no longer able to detect the peaks of the light curve which had become fainter than $m_v = 14$. A minor complication for our observing program arose from the fact that the planned observation at maximum on May 12 was "bumped" by one day due to the priority given to Comet IRAS-Araki-Alcock. All observations were taken through the large (10" x 20") entrance aperture and include some nebular contribution to the He II line for the flux shown in Table 1.

DISCUSSION AND RESULTS.

From the fluxes of the stellar C IV line given in Table 1 it is seen that its intensity was maximum near $\phi = 0.02$. We interpret this to be in agreement with the prediction of Méndez (1983) that the brightness of the exciting hot star should be at maximum at the same time when the brightness of the A-star is near minimum, and viceversa. We indicate our observations at 3 phases by vertical lines in Fig 1, which is adopted from Méndez *et al.* (1982) with the addition of Kohoutek's (1983) latest data adjusted to the orbital elements of Méndez *et al.* (1982). Fig. 2 shows the asymmetric C IV emission line profile at $\phi = 0.02$ which suggests a blue shifted component that may be due to a stellar wind or gas stream. The asymmetry is largest at this phase. The He II line, shown in Fig.3 for the same phase, is a mixture of stellar and nebular emission (determined from the photowrite image) and has a gaussian profile with a slight suggestion of an inverse P Cygni profile. If real, this would signify inflow of material at $\phi = 0.02$. A nearby reseau mark may have contributed to the absorption feature but is not seen at other phases. A more detailed analysis of this and other emission lines to deconvolve the stellar and nebular components is planned for the near future. The narrow stellar continuum is clearly seen on the photowrite throughout the SWP range. The spherical dust cloud model proposed by Méndez *et al.* (1982) explains some of the observed characteristics of this strange system but requires some modifications, as was already suggested in the footnote added by Méndez *et al.* (Astr. Ap., 119, corrected version of 116, L5) since the eclipses did not stop in the spring of 1983. The progressive reddening of the nucleus shown by Kohoutek's (1983) plot of m_v vs (B-V) supports the dust cloud model. The stellar continuum evident on the present SWP spectrograms, the emission of C IV, He II and N V, together with the estimate of a minimum mass of 0.32 M_o and an upper limit of 0.45 M_o for the companion determined by Méndez and Niemela (1981) suggest a hot subdwarf with T_{eff} in the range of 60,000-100,000K and unusually low mass as the exciting star of NGC 2346.

Table 1.
1983 IUE OBSERVATIONS OF NGC 2346.

Date,1983	Image	Expos.(min)	Phase [a]	F(1550)[b]	F(1640)[b]	Remarks
April 17	SWP 19740	150		1.7	7.0	nebula
"	LWR 15756	25				nebula
"	SWP 19741	105	0.836	<1.0*	12.8	nucleus
"	LWR 15757	75				high rad.
April 20	SWP 19768	165	0.020	3.9	10.8	nucleus
May 13	SWP 19967	180	0.496	3.1	9.6	nucleus
"	LWR 15928	120				nucleus

[a] phases are based on orbital elements of Méndez et al.(1982), t_o = 2443126.0 and P = 15.991d, and are not compatible with those of Kohoutek (1982,1983) or the ones used by FA derived from them. The phase shown refers to the midpoint of the exposure for the respective SWP images of the nucleus.

[b] Flux in units of 10^{-13} ergs cm^{-2} sec^{-1}; these are observed values, not corrected for reddening, because of the uncertain differential extinction of star and nebula.

* Low value may be due to poor signal to noise ratio.

REFERENCES.

Feibelman, W.A., and Aller, L.H. 1983, Ap.J., 270, 150. (FA).

Kohoutek, L. 1982, IAU Inf. Bull. Var. Stars, No. 2113.

————————.1983, M.N.R.A.S., 204, 93P.

Luthardt, R. 1983, IAU Inf. Bull. Var. Stars, No. 2360.

Marino, B.F., Williams, H.O., and Walker, W.S.G. 1984, IAU Inf.Bull.Var. Stars, No. 2467.

Méndez, R.H., 1983 (private communication)

Méndez, R.H., Gathier, R., and Niemela, V.S. 1982, Astr. Ap., 116, L5, (corr. in Astr. Ap. 119).

Méndez, R. H., and Niemela, V.S. 1981, Ap.J., 250, 240.

Schaefer, B.E. 1983, IAU Inf. Bull. Var. Stars, No. 2281.

FIGURE CAPTIONS.

Fig. 1. Radial velocities and B_J magnitudes adopted from Méndez et al. (1982) and Kohoutek (1982, 1983). In the upper panel, the open squares indicate velocities obtained from December 1976 to February 1981; the 10 filled squares are velocities obtained in March-April 1982, connected by a dashed line. In the lower panel, the filled squares are B_J magnitudes measured by Kohoutek in January-February 1982. The open squares are B_J magnitudes measured by Gathier in March-April 1982. The lowest light curve is from Kohoutek (1983) but adjusted for the orbital elements of Méndez et al. (1982). The vertical lines indicate the phases at which 1983 IUE data were obtained.

Fig. 2. The stellar C IV line at ϕ = 0.02.

Fig. 3. The He II line at ϕ = 0.02; the *'s represent the data points, with a computer-generated gaussian profile superposed (solid line).

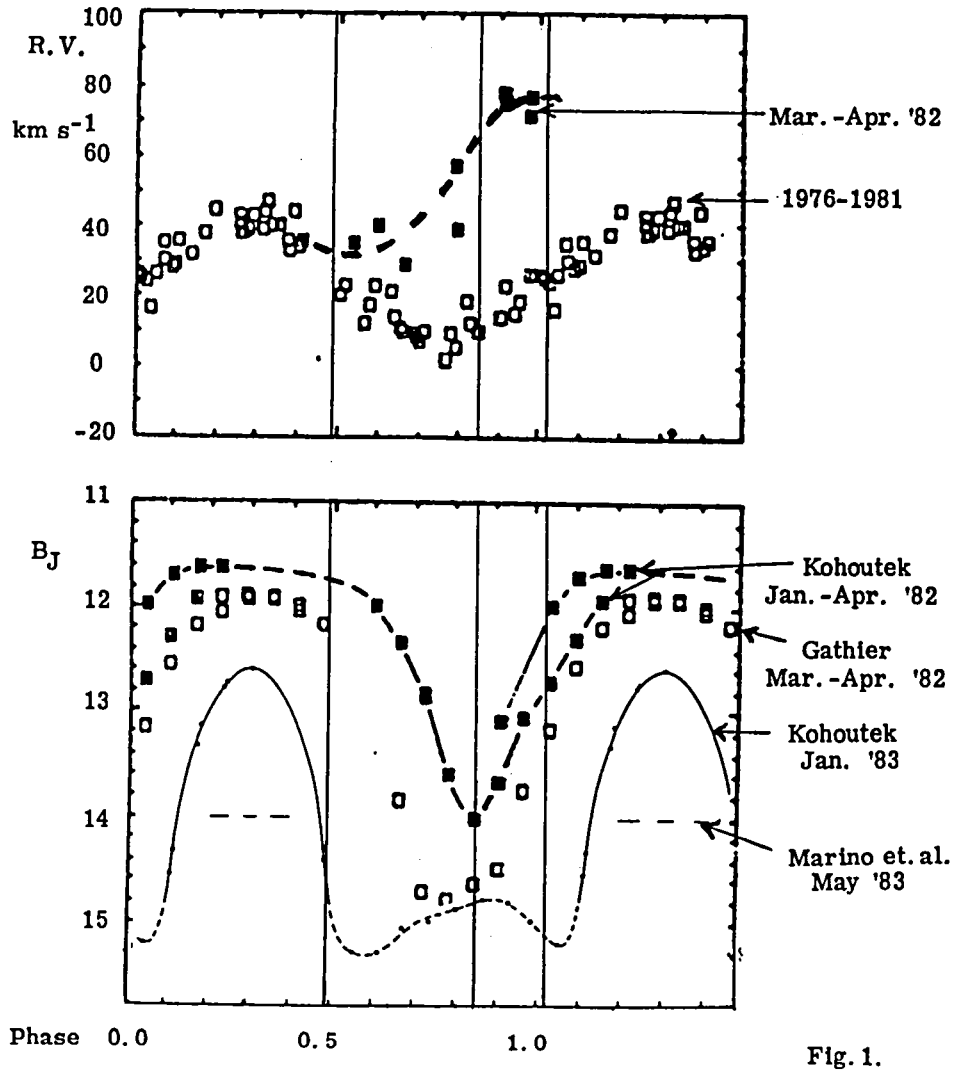

Fig. 1.

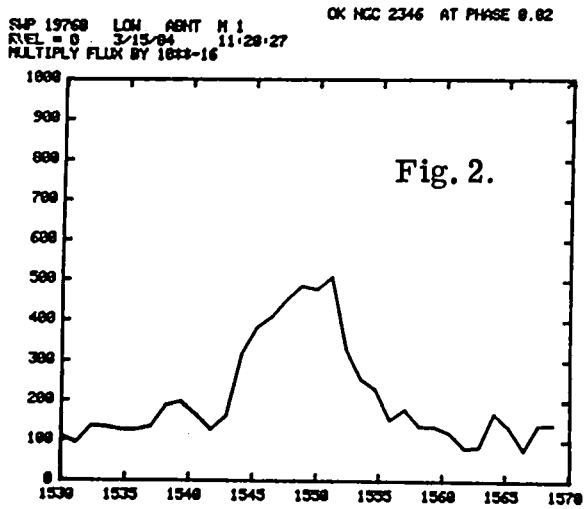

Fig. 2.

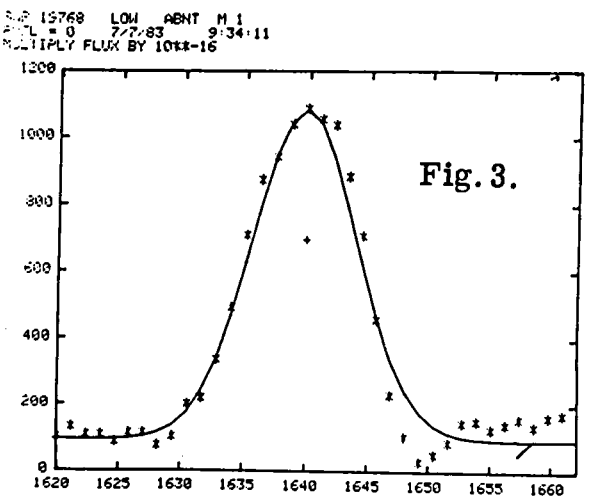

Fig. 3.

IUE OBSERVATIONS OF THE "JET" EMISSION FEATURE IN R AQUARII

by

A.G. Michalitsianos
J.M. Hollis

Laboratory for Astronomy and Solar Physics
NASA-Goddard Space Flight Center

and

M. Kafatos
Department of Physics
George Mason University

Abstract

IUE low dispersion observations of the "jet" emission feature in the symbiotic variable R Aquarii were obtained over the course of two years. A comparison SWP λλ1200-2000 spectra obtained of both this feature and the central UV star indicates significant differences exist between these emission regions; Si III] λ1893 which is prominent in the central star is virtually absent in the "jet". Based upon analyses of UV and optical emission line spectra, the spectral properties of the feature suggest it is a highly excited tenuous region $\sim 10^4$ cm^{-3} characterized by prominent forbidden nebular line emission.

1. Introduction

The composite emission object R Aquarii embodies a number of characteristic properties that distinguish it from other peculiar emission stars. The visual spectrum (M7 + pec) indicates the presence of a cool Mira variable in close association with a hot unresolved ionizing source of radiation that appears to be responsible for the high excitation nebular emission observed. Encircling this spatially unresolved ionized region is an extended ring-like filamentary nebula that subtends ~1 arcmin on either side of the central object. Spectra obtained by Merrill (1935,1950) indicate that R Aquarii continues to exhibit sporadic outbursts which he characterized as a "simmering nova"; from 1928 to 1935 the optical spectrum exhibited a strong blue continuum, and P-Cygni structure in the hydrogen lines dominated the normally strong molecular features and absorption continuum formed in the extended atmosphere of the 387-day period Mira.

2. Observations

Positioning of the large 10x20" entrance aperture of IUE was facilitated by high spatial resolution (~1 arcsec) 6-cm VLA radio maps (Kafatos et al. 1982) (Fig. 1). A comparison between low dispersion ultraviolet spectra obtained with IUE of the central ionized region and "jet", slit positions B and A, respectively (Fig. 2), that significant differences exist between these regions. Most striking is the absence or comparative weakness of Si II λ1808 and Si III] λ1892 emission in the feature, while C III] λ1909 is prominent in both regions (Michalitsianos

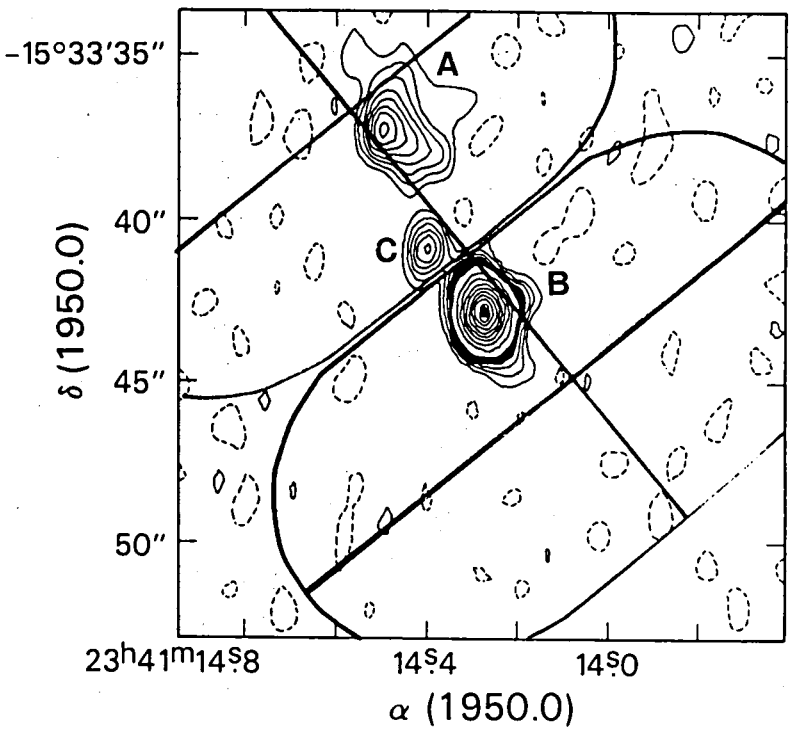

Fig. 1

and Kafatos 1982). From initial observations of the "jet" obtained with IUE, the apparent weakness or absence of silicon in the feature probably reflects a low abundance. More recent IUE observations, however, reveal the presence of very weak emission from the Si III] λλ1883,1892 multiplet. Usually seen in very low density objects such as planetary nebulae such as NGC 7662 Harrington et al. (1982), the appearance of Si III] λ1883 emission is another indication that the prevailing densities in the feature are quite low, i.e. $>10^4$ cm^{-3}-the density in the compact nebula that surrounds the central system is $n_e \sim 10^5$-10^6 cm^{-3} Michalitsianos et al. (1980). Accordingly, the comparative weakness of silicon in the feature is probably due to a combination of low abundance and very low electron densities. Additionally, IUE observations indicate that the overall UV continuum and line intensity level have continued to increase over ~1 year! The appearance of the C IV λλ1548,1550 doublet in IUE spectra of the "jet" suggests that the feature is extended (~3") and is not completely co-spatial with the continuum. In particular, the continuum which appears to originate from a point source coincident with the peak radio contours of VLA 6-cm maps, whereas the high excitation C IV lines appear extended spatially. This structure could reflect optical depth effects in the line and continuum, in which the region of peak radio emission in the feature coincides with the greatest electron densities $\sim 10^5$ cm^{-3}, which gradually decline if we proceed in a direction across the feature.

The Feature A appears to have enhanced emission in low excitation species; the C II] λ1335 and O I λ ~1300 lines are particularly strong in the feature. The continuum in the λλ1200-2000 range in the "jet" appears to rise with decreasing wavelength; the UV continuum of the central ionized region is independent of wavelength over this region.

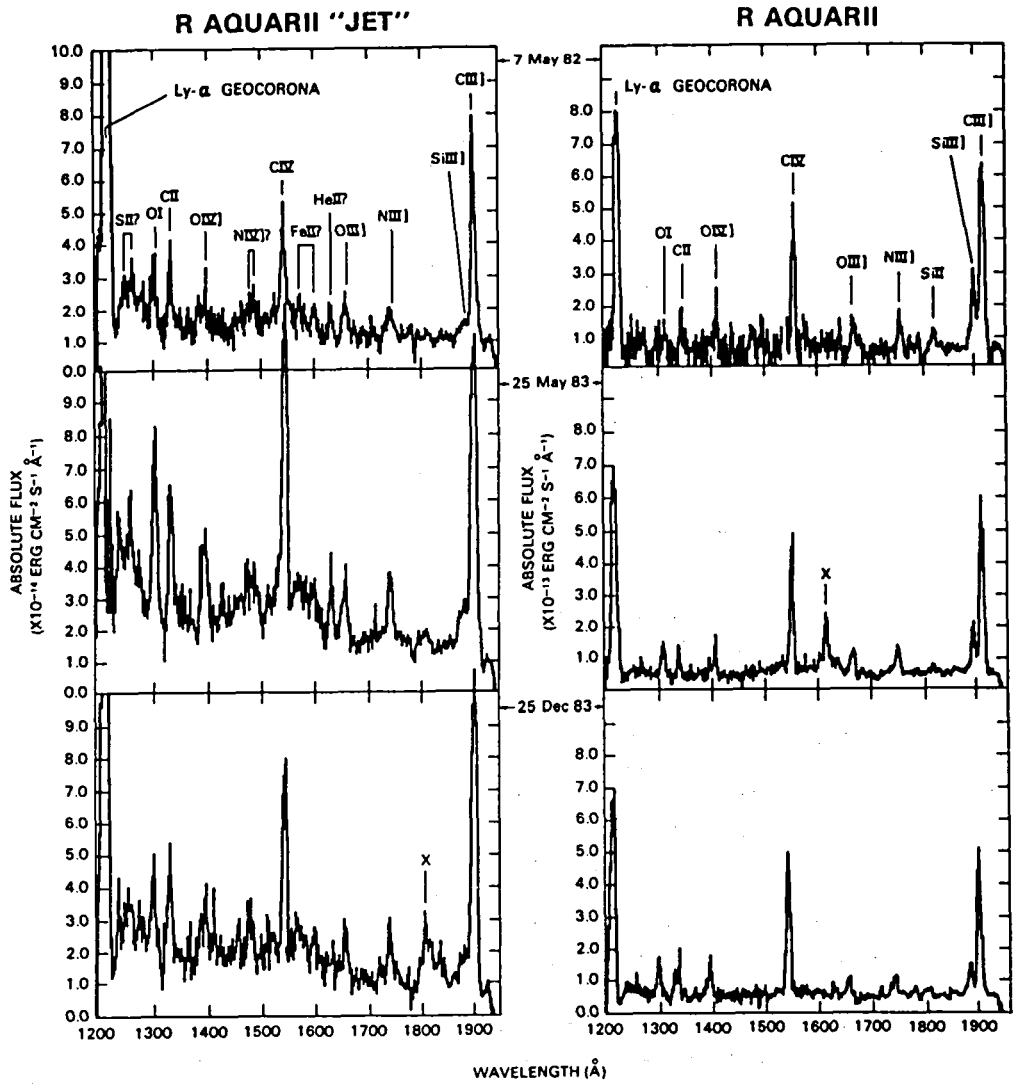

Fig. 2

The wavelength dependent continuum in the "jet" is possibly explained by blends of low excitation lines which combine to form a pseudo-continuum that is most pronounced above Lyman-α. For example, strong unidentified lines at λ1250.5 and λ1259.5 in the "jet" are possibly attributed to S II emission (Michalitsianos and Kafatos 1982). Difficulties in analysing the UV continuum properties of the R Aquarii system are further compounded by circumstellar absorption. Brugel et al. (1982) recently found that the general level of absorption in the central object has declined from a value of E_{B-V} = 0.65 in 1977, to values around 0.40±0.05 and 0.15±0.05 in 1979 and 1982, respectively. This could support the model of an obscuring dust cloud having partially eclipsed the Mira variable (Willson et al. 1981). This is further coinsistent with Whitelock et al.(1983) who find evidence from (JHKL) infrared photometry for a partial eclipse of the Mira in 1975-78 having occurred by an obscuring dust cloud.

The absolute UV flux intensity and general ionization level in the feature appears lower in comparison to the ultraviolet emission from the

central unresolved region. The "jet" appears to have enhanced emission in low excitation species; the C II] λ1335 and O I λ ~1300 lines are particularly strong in the feature. The continuum in the λλ1200-2000 range in the "jet" appears to rise with decreasing wavelength; the UV continuum of the central ionized region is independent of wavelength over this region. et al.1980).

Overall, the UV spectrum of the feature exhibits a wide range of excitation. The high degree of spatial structure evident in VLA radio maps suggest that material expulsion is directed outwards, similar to that observed in Herbig-Haro objects. For example, the extended CO structure seen in the infrared in Herbig-Haro objects has been interpreted as a strong stellar wind channeled into bi-polar flow from an accretion disk (cf. Snell et al.1980). Continued monitoring of the UV spectral emission of the feature are planned during the 7th IUE observing year, which will provide a three year data base for investigating the temporal UV emission properties of this unique object.

References

Brugel, E.W., Cardelli, J.A., Szkody. P. and Wallerstein, G. 1983, Ap.J., in press.

Harrington, J.P., Seaton, M.J., Adams, S. and Tutz, J.H. 1982, MNRAS, **199**, 517.

Kafatos, M., Hollis, J.M. and Michalitsianos, A.G. 1982, Ap.J. (Letters), **267**,L103.

Merrill, P.W. 1935, Ap.J., **81**, 312.

_____. 1950, Ap.J., **112**, 514.

Michalitsianos, A.G., Kafatos, M. and Hobbs, R.W. 1980, Ap.J., **237**, 506.

Michalitsianos, A.G. and Kafatos, M. 1982, Ap.J. (Letters), **262**, L47.

Snell, R.L., Loren, R.B. and Plambeck, P. 1980, Ap.J.(Letters),**239**,L17.

Wallerstein, G. and Greenstein, J.L. 1980, P.A.S.P., **92**, 275.

Whitelock, P.A., Feast, M.W., Catchpole, R.M., Carter, B.S., Roberts G. 1983, S.A.A.O. preprint.

Willson,L.,Garnavich,P., Mattei, J.A. 1981,Inf.Bull.Var.Stars, no. 1961.

THE CHANGING ULTRAVIOLET SPECTRUM OF HERBIG-HARO OBJECT NO. 1

K.H. Böhm, E. Böhm-Vitense
University of Washington, Seattle
and
E.W. Brugel
University of Colorado

ABSTRACT

IUE spectra of H-H1 taken in March 1982 and December 1983 show steady qualitative changes of the short wavelength emission line spectrum. Earlier IUE studies (in 1979 and 1980) had shown the typical "high excitation object" ultraviolet spectrum with the CIV 1550 and the CIII] 1909 lines being very strong. These line fluxes have steadily decreased and are presently not detectable on a 4-1/2 hour exposure. While the spectrum looked very similar to that of H-H2 in 1980, it now gives more the impression of the spectrum of a low excitation H-H object with a possible presence of fluorescent lines from the H_2 Lyman bands.

INTRODUCTION

Ultraviolet spectra of Herbig-Haro (H-H) objects (cf. Ortolani and d'Odorico 1980, Böhm, Böhm-Vitense and Brugel 1981, Brugel, Shull and Seab 1982, Böhm-Vitense et al. 1982, Schwartz 1983a) show emission lines and continua or quasicontinua. In view of the rather low optical brightness and the moderately large color excess of these objects, their ultraviolet brightness is surprisingly large. Nevertheless, the number of H-H objects observable with IUE is small. It is, however, surprising that among the objects observed so far in the ultraviolet there seemed to be two distinct classes: 1) objects showing relatively high ionization with CIV 1550 and CIII] 1909 being the strongest lines (H-H1, H-H2, H-H32); and 2) objects showing almost only fluorescent lines of the H_2 Lyman bands (H-H43, H-H47) (see Schwartz 1983a). The membership in class 1 or 2 is correlated with the property of being a "high excitation" or "low excitation" object (cf. Dopita 1978, Böhm, Brugel and Mannery 1980) in the optical range. It is surprising that, until recently, we had seen only these two types of "extreme" cases and no "intermediate" ultraviolet spectra.

Why is all this important? During the last few years more and more evidence for the interpretation of H-H objects in terms of high velocity gas-dynamic processes has accumulated (cf. Herbig and Jones, 1981, 1983). The interpretation of the optical spectra by studying their formation in the cooling regions of plane shocks (cf. Dopita 1978, Raymond 1979) or of bow shocks (cf. Hartmann and Raymond 1984, Choe, Böhm and Solf 1984) has been fairly successful. On the other hand, the simultaneous interpretation of optical and UV spectra in terms of shock wave models has caused considerably more problems (cf. Schwartz 1983b, Böhm 1983) and the question remains whether in the ultraviolet we see only the line formation which is to be

expected for the models which (approximately) explain the optical spectra or whether more sophisticated models are needed.

Recent observations of qualitative changes in the ultraviolet emission line spectrum of H-H1 which we shall describe below show some new and unexpected aspects of this problem. We emphasize that the spectrum changes are qualitative, so that they cannot be due to (reasonably moderate) uncertainties of the spectrophotometric accuracy.

THE OBSERVATIONS

Our results are based on a comparison of the early IUE observations of H-H1 to our recent observations in March 1982 and December 1983. In the early observations Böhm et al. (1981) and Ortolani and d'Odorico (1980) both found a CIII] flux of 330 (if $F_{H\beta} = 100$) and a CIV flux of 416 (Böhm et al. 1981) or 232 (Ortolani and d'Odorico 1980). Both groups also detected and measured the flux in NIII] 1747/1754 (Bohm et al.: 188, Ortolani and d'Odorico: 315). We cannot easily decide whether the differences of the order of 40% which occur for the CIV and NIII] lines are due to measurement problems or whether they indicate already a time change. This, however, is of no great importance for the following. The earlier measurements of H-H1 showed especially in the CIV 1550 and CIII]] 1909 line fluxes (relative to H_β), a great similarity to the values which were later found for H-H2.

With the measurements of March 22, 1982, it became clear that a drastic time change had occurred in H-H1 (see Figure 1). CIV 1550 was barely detectable, CIII] 1909 weak. A strong line at $\lambda \sim 1489$ A had appeared and dominated the spectrum. This may be the 1489.6 fluorescent H_2 line or the NIV] 1486 line or a blend of both.

An even more drastic change had occurred when we observed H-H1 on December 14, 1983. Of the "standard" emission lines which are known to occur in "high excitation" H-H objects, only NIII 1750 remains. An outstanding feature seems to be a broad "emission band" in the range 1440 A $\lesssim \lambda \lesssim$ 1560 A. It is possible that a considerable part of the flux in this band is a consequence of the clustering of fairly strong fluorescent H_2 lines in this wavelength range which are not clearly recognizable because the spectrum is faint and noisy. In Figure 1 we have marked the positions of the five strongest fluorescent lines. We have numbered them according to their strength in H-H43 (Schwartz 1983a, b) with 1 being the strongest and 5 the relatively faintest line. The maximum in the H-H1 distribution occurs near 1505 A, which is the wavelength of the strongest H_2 fluorescent line in the low excitation H-H object H-H43. The line 3 (1446 A) seems to be clearly present.

We conclude from the observations presented in Figure 1 that the ultraviolet (SWP) spectrum of H-H1 has definitely changed drastically since 1980, when we saw a spectrum similar to the UV spectrum of H-H2. The CIV 1550 and CIII] 1909 emission line fluxes had declined considerably already by March 1982 and are now undetectable on a 4-1/2 hour exposure.

DISCUSSION

We believe that the present investigation is of considerable importance for the shock wave interpretation of Herbig-Haro objects. The shock wave interpretation (Schwartz 1975) undoubtedly has been the fundamental recent breakthrough with regard to our understanding of H-H objects. But it is also true that the easily convincing interpretations are mostly restricted to the optical part of the spectrum. The combination of optical and ultraviolet observations lead to some apparent contradictions (cf. Böhm 1983) which, however, can be overcome to some extent (Schwartz 1983b).

The present observations of time variations point towards a more fundamental problem. During the time interval 1980-1983, during which these drastic changes in the ultraviolet have been observed, no drastic changes have been noticed in the optical part of the spectrum. In January 1982 Solf and Böhm have taken high resolution Coude spectra of a number of H-H objects, including H-Hl. They clearly show that, e.g., the flux ratio of [OIII] 5007/H (which is very sensitive to the shock conditions; cf. Shull and McKee 1979) has practically not changed.

The shock wave theory of H-H objects has been so successful in explaining different aspects of optical observations that we feel that it must be basically correct. The drastic changes in the ultraviolet must then mean that either a more sophisticated shock wave theory contains some aspects which are not yet understood and which lead to strong changes in the UV but not in the visual spectrum or that the shock wave interpretation is not the only relevant aspect of a complete theory of H-H objects. The situation would be especially complicated if it is confirmed that H-Hl does indeed make a transition from a high excitation to a low excitation object in the UV.

REFERENCES

Böhm, K.H. 1983, Rev. Mexicana Astr. Ap. 7, 55.
Böhm, K.H., Böhm-Vitense, E. and Brugel, E. 1981, Ap.J. (Letters) 245, L113.
Böhm, K.H., Brugel, E.W. and Mannery, E. 1980, Ap.J. (Letters) 235, L137.
Böhm-Vitense, E., Böhm, K.H., Cardelli, J., Nemec, J. 1982, Ap.J. 262, 224.
Brugel, E.W., Shull, J.M. and Seab, C.G. 1982, Ap.J. (Letters) 262, L35.
Choe, S.U., Böhm, K.H. and J. Solf 1984, submitted to Ap.J. (Letters).
Dopita, M.A. 1978, Ap.J. Suppl. 37, 117.
Hartmann, L. and Raymond, J.C. 1984, Ap.J. 276, 560.
Herbig, G.H. and Jones, B.F. 1981, A.J. 86, 1232.
Herbig, G.H. and Jones, B.F. 1983, A.J. 88, 1040.
Ortolani, S. and d'Odorico, S. 1980, Astr. Ap. 83, L8.
Raymond, J.C. 1979, Ap.J. Suppl. 39, 1.
Schwartz, R.D. 1975, Ap.J. 195, 631.
Schwartz, R.D. 1983a, Ap.J. (Letters) 268, L37.
Schwartz, R.D. 1983b, Rev. Mexicana Astr. Ap. 7, 27.
Shull, J.M. and McKee, C.F. 1979, Ap.J. 227, 131.

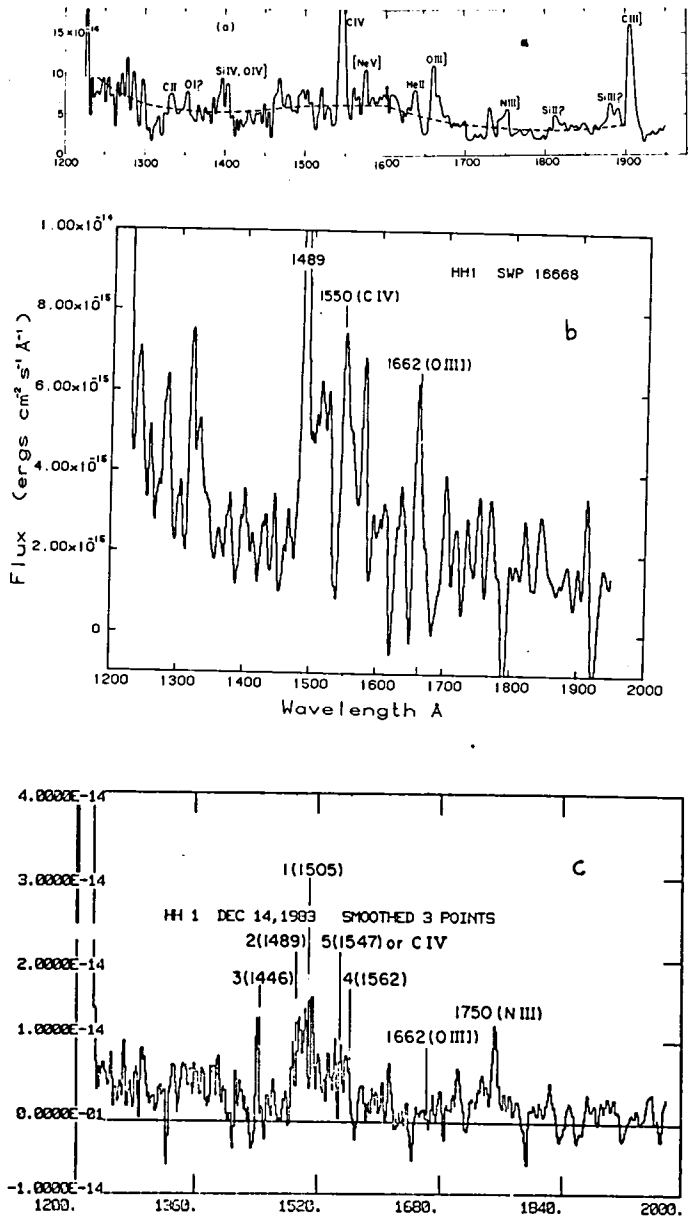

FIGURE CAPTIONS

Figure 1: Comparison of the SWP spectrum of H-H2 (to which the spectrum of H-H1 was practically identical in 1980) (a) to the SWP spectrum of H-H1 in March 1982 (b) and in December 1983, (c). Figure a is corrected for reddening, Figures b and c are uncorrected. Note the different abscissa scales in (a), (b) and (c). In spite of these shortcomings of this way of presentation, we can clearly recognize the change of CIV 1550 and CIII] 1909 from being the strongest emission lines in 1980 to becoming undetectable in December 1983.

SHORT-WAVELENGTH OBSERVATIONS OF HH-2H and HH-24A

Edward W. Brugel and J. Michael Shull
Laboratory for Atmospheric and Space Physics
University of Colorado, Boulder

ABSTRACT

There still remains some debate about the exact origin of the very blue optical and ultraviolet continuum in Herbig-Haro objects. We Believe that there is reasonably good evidence for a two-photon continuum in HH-2H. It has recently been suggested that there is a significant contribution to the uv continuum from scattered light in the general Orion region. We present evidence from spatially resolved IUE spectra which indicate the continuum and emission line fluxes have the same spatial distribution. A very low ultraviolet extinction is indicated based upon an enhanced two-photon origin for the uv continuum. A recent observation of HH-24A shows an interesting absence of high excitation emission lines and a weak continuum.

INTRODUCTION

Ultraviolet observations of Herbig-Haro objects have lead to several new insights, as well as new enigmas. The initial uv observations of HH-1 (Ortolani and D'Odorico 1980; Bohm, Bohm-Vitense and Brugel 1981) presented two interesting problems - (1) the continuum seemed to increase monotonically to shorter wavelengths out to 1216A; (2) the uv line spectrum corrected for standard IS extinction, indicated an ionization which was considerably too high to be compatible with the shock-wave parameters deduced from the optical forbidden line spectrum. This difficulty with the emission line, uv-optical incompatiblity is of course very dependent upon the reddening correction as applied in the uv where it is least understood.

It has also been discovered that the uv spectra of the low excitation objects, HH-43 and HH-47 (Schwartz 1983) are significantly different than those of HH-1 or HH-2H. These objects are characterized by a prominent continuum which has an apparent turnover at approximately 1500A indicative of enhanced two-photon radiation. In addition, there is a complete absence of high excitation uv lines (e.g. CIV 1549A; CIII] 1909A), yet surprisingly strong flourescent lines of molecular hydrogen are seen.

The first IUE observations of HH-2H were presented by Bohm-Vitense, et al. (1982) and contained two SWP spectra with a total exposure time of 560 minutes. An additional single exposure of 430 minutes was obtained (Brugel, Shull and Seab 1982) with improved signal-to-noise, which provided evidence of the two-photon nature of the uv continuum in these shock excited nebulae.

RESULTS: New observations of HH-2H

Herbig-Haro object No. 2H is the observationally brightest HH object in the ultraviolet and it has received the most observing time. We have obtained two additional spectra, thus there are now five SWP images with a total exposure time of 1750 minutes (29.1 hours). There remains some debate concerning the interpretation of the ultraviolet spectrum. The first topic of dispute is the continnum. Mundt and Witt (1983) have suggested that a large fraction (35% for the flux at 1500A) of the observed short wavelength continuum is not formed within the HH object but rather is scattered light seen in the general Orion region. One way to test this hypothesis is to compare the spatial distribution of the continuum flux with that of the emission lines, which are believed to be formed in situ. Of course, this comparison will lead to viable conclusions only if the flux in the emission lines does not fill the entire IUE aperture.

A spatial representation of the flux in the continuum was constructed by adding the uncalibrated flux from 1230-1600A in each of the 55 spatially resolved line-by line spectra and then subtracting the flux due to the known emissions in this spectral region. The CIV doublet at 1550A was used as representative of the spatial distribution for the emission line flux; the wavelength interval used was 1540-1560A. To compare these line-by-line distributions, the fluxes were scaled so that the background levels were equal. This is illustrated in figure 1. It is apparent that the spatial distribution is larger that a point source but it definitely does not fill the aperture. In addition, the continuum flux very closely follows the extent of the emission line. We conclude that the observed continuum and the emission lines are associated phenomena, and that there is no conclusive evidence for a scattered light contribution to the observed continuum.

We maintain that the best explanation for the observed uv continuum (Brugel, Shull and Seab 1983) is collisionally enhanced H^{o} two-photon emission, as theoretically suggested for the far uv (Shull 1982) and the blue continuum (Dopita, Binette and Schwartz 1982). All the available short wavelength data for HH-2H is shown in figure 2. The continuum flux has been averaged over approximately 50A wide bins and the bins have been chosen to

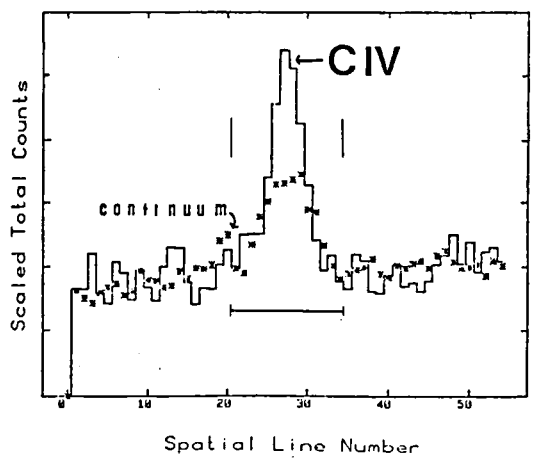

Figure 1

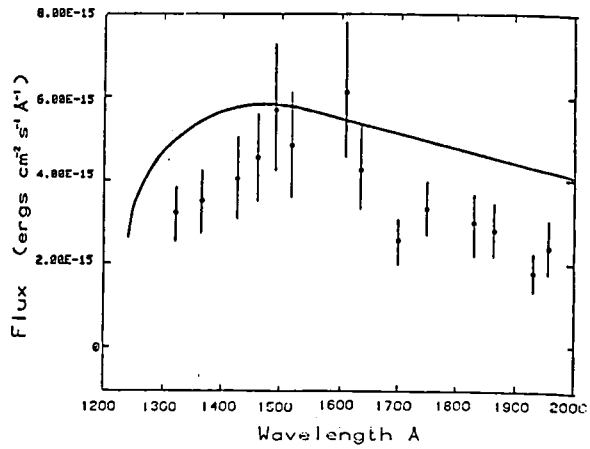

Figure 2

exclude any obvious emission lines. There still remains the "unresolved" problem of possible contributions due to weak unidentified emission lines; this problem will remain unresolved until higher dispersion observations become possible. A semi-empirical two-photon continuum is also plotted in figure 2; this curve is based upon the theoretical (Spitzer and Greenstein 1951) two-photon energy distribution normalized to the observed reddening corrected optical continuum at 4500A (Bruel, Bohm and Mannery 1982, Dopita, Binette and Schwartz 1982). Thus this curve represents an upper limit to the intrinsic ultraviolet two-photon continuum emitted by HH-2H. Since this "intrinsic" curve is only slightly greater than the observed uncorrected data, it is apparent that the degree of ultraviolet extinction is not large. Correcting the emission lines with this much smaller than average IS extinction greatly reduces the disprepancy between the uv and optical line strengths, in terms of a single set of shock parameters.

In light of the recent discovery of dramatic variabity in the uv emission line strengths of HH-1, we have re-examined all five spectra of HH-2H. We do see differences in line strengths from one spectrum to another and these differences can be as large as 50%. Nonetheless, it is not possible to ascertain any pattern to these differences or to convince oneself that they are real variations.

HH-24A

A single 540 minute SWP exposure of HH-24A was obtained on 11 Nov 1983. This object was chosen because of its uniquely large optical continuum polarization (Schmidt and Miller 1979) and its strong continuum relative to its emission lines (Brugel, Bohm and Mannery 1982). This short wavelength spectrum is shown in figure 3. With the possible exception of OIII 1661A, there is an absence of high excitation lines as is also seen in the low excitation nebulae HH-43 and HH-47. However, HH-24A does not possess a low excitation optical line spectrum. There is also no indication of an

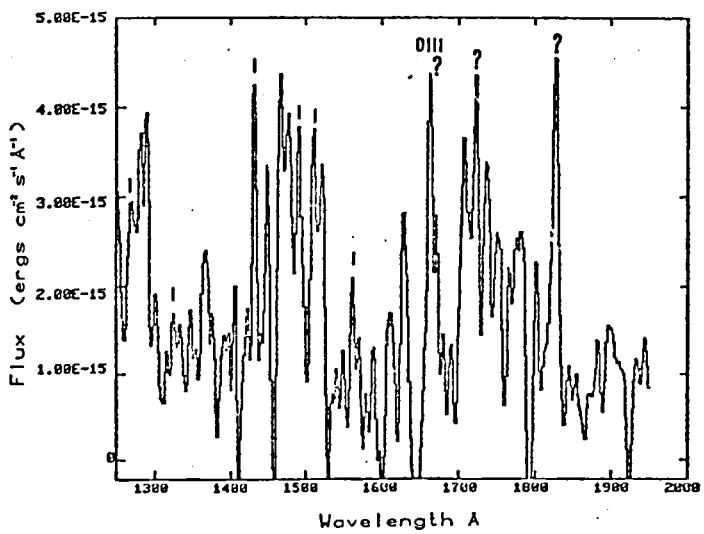

Figure 3

identifible two-photon continuum which appears prominent in HH-43 and HH-47. A few of the known H_2 lines appear to be present, there are also some lines which are not seen. The weakness of this spectrum prevents any definite assertion that molecular is definitely detected. It should be noted that this object has an E(B-V) = 0.71, as determined by the optical emission line spectrum. It is possible that the region in which the uv lines are formed is totally obscured by the large ultraviolet extinction, though these regions can be seen at longer optical wavelengths. Perhaps the observed uv radiation comes from scattering in the outter most part of the nebula. Extreme variability in the uv lines cannot be excluded as recently seen in HH-1 (Bohm, Bohm-Vitense and Brugel 1984).

REFERENCES

Bohm,K.H., Bohm-Vitense,E. and Brugel,E.W. 1981, Ap. J. Lett., 245, L113.
Bohm,K.H., Bohm-Vitense,E. and Brugel,E.W. 1984, in preparation.
Bohm-Vitense,E., Bohm,K.H., Cardelli,J.A. and Nemec,J.M. 1982, Ap. J., 262, 224.
Brugel,E.W., Bohm,K.H. and Mannery,E. 1981, Ap. J., 243, 874.
Brugel,E.W., Shull,J.M. and Seab,C.G. 1982, Ap. J. Lett., 262, L35.
Dopita,M.A., Binette,L. and Schwartz,R.D. 1982, Ap. J., 261, 183.
Mundt,R. and Witt,A.N. 1983, Ap. J. Lett., 270, L59.
Ortolani,S. and D'Odorico,S. 1980, Astr. Ap., 83, L8.
Schmidt,G.D. and Miller,S.S. 1979, Ap. J. Lett., 234, L191.
Schwartz, R.D. 1983, Ap. J. Lett., 268, L37.
Shull,J.M. 1982, in Regions of Recent Star Formation ed. R.S. Roger and P.E. Dewdrey (Dordrecht:Reidel), pp. 91-105.
Spitzer,L. and Greenstein,J. 1951, Ap. J., 114, 407.

DUST IN THE REGION OF HERBIG-HARO OBJECTS: THE CASE OF NGC 1999

J. A. Cardelli and K. H. Böhm
Astronomy Department, University of Washington

ABSTRACT

We have used observations of the reflection nebula NGC 1999 (taken at a small offset angle) and its illuminating star V380 Ori to examine the properties of dust in the region of Herbig-Haro objects H-H 1 and H-H 2. The ratio of nebular intensity to stellar flux is fairly flat in the uv and is remarkably similar to that for NGC 7023/HD 200775 for small offset angles. If reflected light represents a strong contribution to the continua of H-H objects, then our results seem to rule out geometries in which this reflection arises from forward scattering of light from imbedded T Tauri stars. In addition, we have examined the extinction to V380 Ori and find it similar to the curve for HD 200775, both of which are lower than the average galactic extinction curve in the uv. This seems to justify the use of extinction curves like θ Ori for correcting the observations of H-H objects, particularly H-H 1 and 2, for reddening.

INTRODUCTION

It has been an accepted reality for quite some time that the properties of dust in regions of star formation, particularly extinction by dust, tend to deviate from the galactic average. As a consequence, the analysis of the intrinsic properties of astrophysical objects associated with this dust has become difficult. A good example of this concerns the study of Herbig-Haro objects. In addition to the problems of extinction correction, some uncertainty must be assigned to the origin of the observed continuum in some of these objects. There has been some debate over the past few years as to whether H-H continua arise from scattered light (Strom, Grasdalen and Strom 1974, Strom, Strom and Kinman 1974) or arise by some internal process such as two-photon radiation by hydrogen (Brugel, Shull and Seab 1982, Böhm 1983).

In an attempt to understand the properties of dust in the region of H-H 1 and H-H 2, we have chosen to examine the properties of the nearby reflection nebula NGC 1999 and its illuminating star V380 Ori. At a distance of about 500 pc (Herbig 1960), NGC 1999 lies about 0.29 pc from H-H 1. Because V380 Ori is a Herbig Ae star and consequently a young object, its association with this general region of star formation seems reasonable. In addition, since the reddening to V380 Ori ($E(B-V)\sim0.40$) is similar to that of H-H 1 and 2, it seems plausible to assume that the dust associated with NGC 1999 could be similar to the dust associated with the nearby H-H objects.

OBSERVATIONS AND REDUCTIONS

We have obtained low resolution observations of NGC 1999 using both the short and long wavelength cameras of IUE. In addition, we have extracted several images of V380 Ori from the IUE archives. The nebular observations

were obtained at an offset angle of 15" east of V380 Ori with the aperature oriented in a N-S direction. The data for both cameras were reasonably good with the exception of the range 1900-2300 Å where the data are fairly noisy.

For such a small offset angle, one must consider, in general, contamination of the nebular observations by instrumentally scattered light originating from the illuminating star (Witt, Bohlin and Stecher 1982). However, the relatively high surface brightness of the nebula (Warren-Smith 1983) coupled with the faintness of V380 Ori (m_V~10.3) makes this unlikely (Witt, private communication). More likely is the contamination of the stellar observations by nebular light. Normal stellar images generally show no flux outside of a spatial width of 3-5 pixels. However, flux for V380 Ori increases by about 15% if the spatial width of the spectrum is increased from 5-9 pixels. To determine the wavelength dependence of this contamination, we compared the spatially summed 5 line (pixel) reduction with a single line through the image center and a small aperature observation. The latter two, which we considered to suffer from the least nebular contamination, show the same wavelength dependence. In comparison, however, the 5 line spectrum (normalized at 3000 Å) shows an increasing excess flux below 3000 Å (to a maximum of about 20% at 1300 Å). Since we are only interested in the normalized wavelength dependence of nebular to stellar light, we have used the above results to correct our stellar observations for nebular contamination.

RESULTS

Figure 1 shows a plot of the ratio of nebular intensity (I) to stellar flux (F) in the uv normalized in the region 2900-3100 Å. Also plotted is the data for NGC 7023/HD 200775 at an offset angle of 22".5 taken from Witt, Bohlin and Stecher (1982). As indicated, the ratio of nebular to stellar light for both nebulae is remarkably similar. In addition, the reddening for V380 Ori (E(B-V)~0.40) is quite similar to that of HD 200775 (E(B-V)=0.44) and indicates that both stars are imbedded. This seems to imply that conditions giving rise to the scattering of radiation (i.e. small angle scattering) are similar in both nebulae. The above similarities seem even more significant when you consider similar plots as in figure 1 for the Pleiades (Witt, Bohlin and Stecher 1982) which arise by light scattered from stars with small reddenings (stars that are not imbedded). Such plots rise steeply towards shorter wavelengths and appear to be the result of predominantly large angle scattering.

We have also made an attempt to determine the extinction towards V380 Ori. Herbig (1960) and Mendoza (1968) assign V380 Ori a spectral type of A0 - A2 based on the underlying absorption spectrum in the visual. The uv data seem to infer types B9 - A0 (type A1 proved defficient in flux below about 1700 Å). Figure 2 shows the resulting curve for V380 Ori found using E(B-V)=0.40 (an appropriate average from the literature) and an A0 V comparison star (main sequence stars were used because they were readily available from the IUE Spectral Atlas; Wu et al. 1983). Also shown is the curve for HD 200775 (Walker et al. 1980) and the average galactic extinction curve of Seaton (1979). Comparison of V380 Ori with a B9 V and a B9.5 III gave similar results to type A0 V throughout except at the shorter wavelengths where the extinction more closely followed the Seaton curve. In light of the similarities between

NGC 1999/V380 Ori and NGC 7023/HD 200775 shown in figure 1, we find the qualitative agreement in figure 2 satisfying. Also, the extinction to both of these stars seems to exhibit the same type of anomalous extinction often seen in regions of star formation (Snow and Seab 1980, Bohlin and Savage 1981).

With regard to the problem of continuum formation in H-H objects, we conclude the following. Because of the agreement between NGC 1999 and NGC 7023 discussed above, we find it tempting to imply that the analysis for NGC 7023 (Witt et al. 1982, Witt, Bohlin and Stecher 1982) also applies to NGC 1999. For NGC 7023 they find that the phase function changes from strongly forward scattering ($g \sim 0.6$-0.7) in the visual to nearly isotropic ($g \sim 0.25$) at 1400 Å. If this applies in general to situations of small offset angles from an imbedded illuminating source, then such a geometry must be ruled out for H-H 1 and 2 and possibly H-H objects in general. For typical T Tauri stars, it does not seem possible that such a geometry could result in the steeply increasing continua (see figure 1) towards shorter wavelengths observed in many H-H objects (Böhm, Böhm-Vitense and Brugel 1981, Böhm, Böhm-Vitense and Cardelli 1982, Brugel, Shull and Seab 1982).

Finally, our tentative extinction results for V380 Ori (figure 2) seem to imply that the dust in the region of H-H 1 and 2 is similar to other regions of star formation that also show peculiar (lower than average) extinction. As such, it seems to add justification towards the use of extinction curves like θ Ori (Bohlin and Savage 1981) instead of the average galactic curve (Seaton 1979) to correct observations of H-H objects (particularly H-H 1 and 2) for reddening.

REFERENCES

Bohlin, R. C. and Savage, B. D. 1981, Ap.J. 249, 109.
Böhm, K. H. 1983, Rev. Mexicana Astron. Astrofis 7, 55.
Böhm, K. H., Böhm-Vitense, E. and Brugel, E. 1981, Ap.J. (Letters) 245, L113.
Böhm, K. H., Böhm-Vitense, E. and Cardelli, J. A. 1982, in Advances in Ultraviolet Astronomy, ed. Y. Kondo, J. M. Mead and R. D. Chapman, NASA, p.223.
Brugel, E. W. , Shull, J. M. and Seab, C. G. 1982, Ap.J. (Letters) 262, L35.
Herbig, G. H. 1960, Ap.J. Suppl. 4, 337.
Mendoza, E. E. 1968, Ap.J. 151, 977.
Seaton, M. J. 1979, MNRAS 187, 73P.
Snow, T. P. and Seab, C. G. 1980, Ap.J. (Letters) 242, L83.
Strom, S. E., Grasdalen, G. L. and Strom, K. M. 1974, Ap.J. 191, 111.
Strom, K. M., Strom, S. E. and Kinman, T. D. 1974, Ap.J. (Letters) 191, L93.
Walker, G. A. H., Yang, S., Fahlman, G. G. and Witt, A. N. 1980, Pub.A.S.P. 92, 411.
Warren-Smith, R. F. 1983, MNRAS 205, 349.
Witt, A. N., Bohlin, R. C. and Stecher, T. P. 1982, in Advances in Ultraviolet Astronomy, ed. Y. Kondo, J. M. Mead and R. D. Chapman, NASA, p. 401.
Witt, A. N., Walker, G. A. H., Bohlin, R. C. and Stecher, T. P. 1982, Ap.J. 261, 492.
Wu, C. C. et al. 1983, The IUE Spectral Atlas, in IUE NASA Newsletter, No. 22.

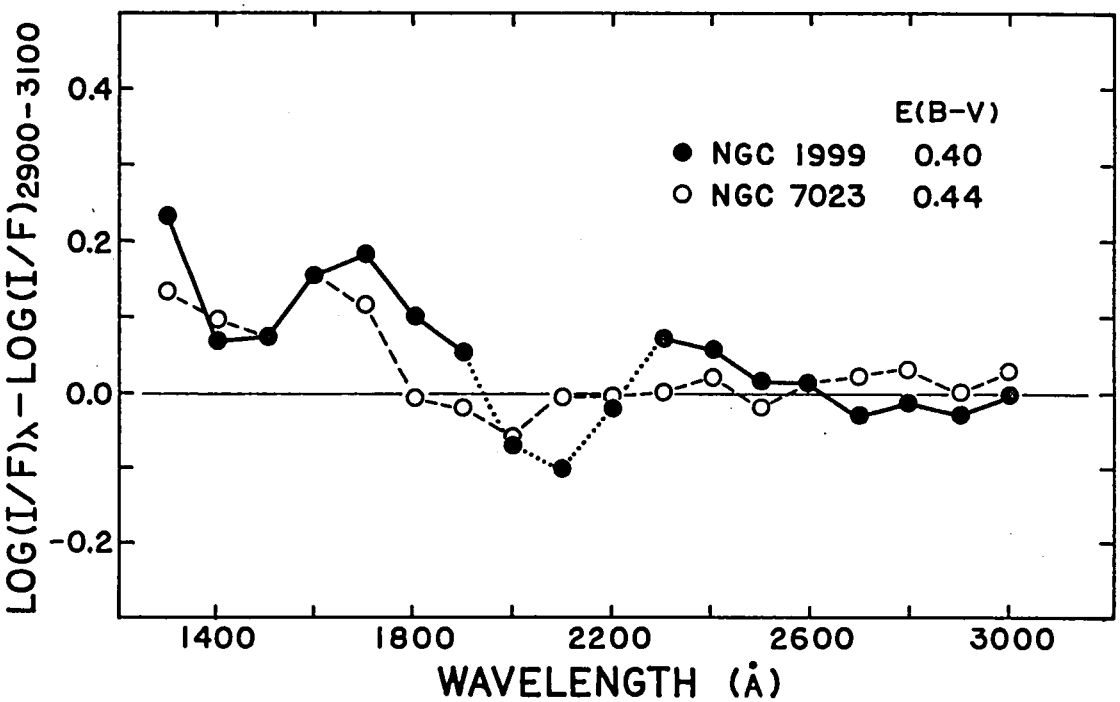

FIGURE 1: The ratio of nebular intensity (I) to stellar flux (F) normalized in the region 2900-3100 Å for NGC 1999/V380 Ori (solid curve) and NGC 7023/HD 200775 (dashed curve). The dotted portion of the NGC 1999/V380 Ori curve represents uncertain (noisy) data.

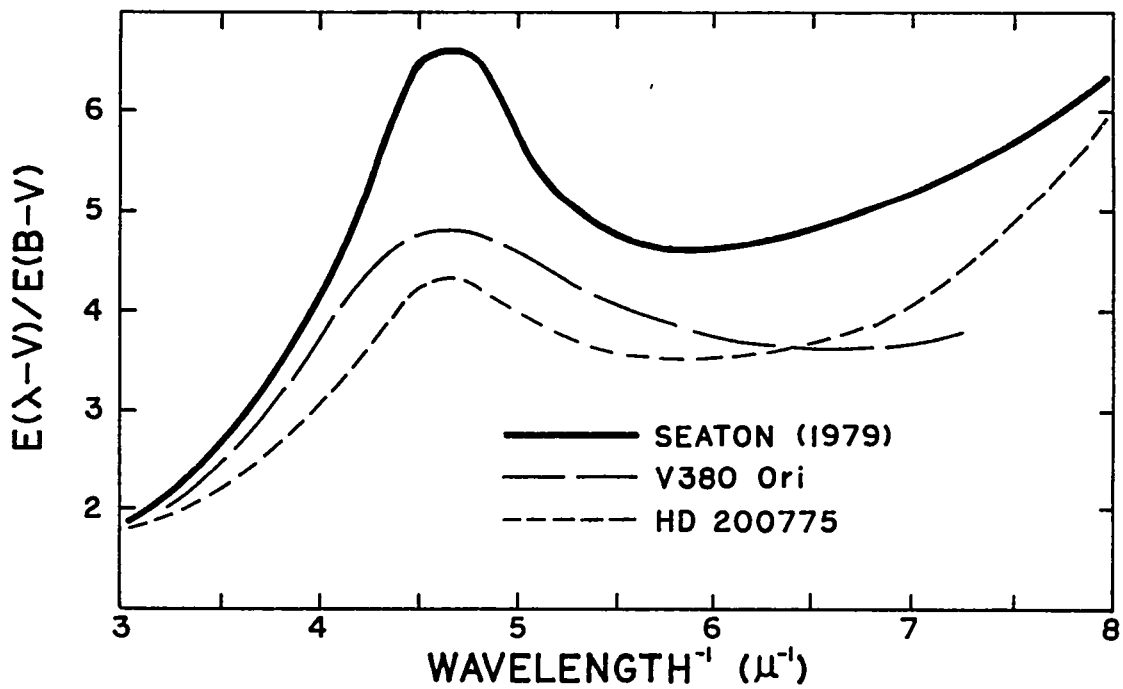

FIGURE 2: The smoothed extinction curves for V380 Ori (long dashes) and HD 200775 (short dashes) compared to the average galactic extinction curve of Seaton (1979; solid curve).

IUE Observations of Blue Horizontal Branch Globular Clusters and UV-Bright Stars

Bruce M. Altner
Applied Research Corporation

Brian Holton and Terry A. Matilsky
Rutgers University

ABSTRACT

Recent theoretical attempts to understand the later evolution of Population II stars have met with some success in accounting for the positions of UV-bright stars in globular cluster color magnitude diagrams. In particular, model calculations have been published which suggest the existence of two distinct sub-classes of UV-bright star, based on their luminosity above the horizontal branch (HB). IUE observations of individual UV-bright stars in several globular clusters do indeed show a separation into two luminosity groups, with more than half of the stars belonging to the high luminosity class. Whereas spectra of resolved hot sources found in the cores of seven clusters lead us to believe that they are also UV-bright stars, unlike the stars outside the core they fall mostly in the low luminosity group. Further observations are planned to extend these results to more clusters.

INTRODUCTION

The UV-bright region in a globular cluster color magnitude diagram is usually defined as that brighter than the HB and redward of the red giants. UV-bright stars are found preferentially in clusters with predominantly blue HBs (i.e., BHB clusters; Harris, Nemec and Hesser, 1983). In addition, hot, luminous stars have been found to be present in the cores of some clusters, as first shown by Dupree, et al. (1979). Since it would take almost 1000 red giants to equal the brightness of a single BHB star at 1500 A (Code, 1982), SWP images taken through the large aperture can easily distinguish these hot stars from the cooler sources that dominate cluster observations in the optical bands.

UV-bright stars are considered to be Population II objects in one of the following stages:

- Evolved off the zero-age HB; in this stage the star is burning helium in the core and hydrogen in a shell just outside the core. The color of the star depends critically on its envelope mass and chemical composition (only small differences are expected in the mass of the He core).

The low mass ($0.5M_\odot \leqslant M \leqslant 0.6M_\odot$), low metallicity stars which inhabit the blue end of the HB in the temperature range $4.1 \leqslant \log T_{eff} \leqslant 4.3$ eventually evolve into UV-bright stars somewhat redder and about 1 magnitude brighter than their zero-age loci. Such stars are known in the literature as supra-HB stars (Zinn, 1974). Since the more massive ($0.65M_\odot \leqslant M \leqslant 0.8M_\odot$) HB stars evolve directly onto the asymptotic giant branch (AGB) from their positions at the red end, only BHB stars contribute to populating the supra-HB domain;

- Evolved off the AGB; as with the first giant branch, thermal pulses and rapid mass loss characterize evolution off the AGB. Such stars are powered via a double shell structure, with the H burning shell providing 90% of the luminosity. Such a configuration, however, is unstable, and post-AGB evolution is rapid. Calculated model tracks are consistent with the presence of a small number of hot, very bright stars several magnitudes above the HB (Sweigart, Mengel and Demarque, 1974). Evidence that mixing might be important at this stage is suggested by lines of He at or greater than the level of Population I abundances in such stars as Barnard 29 in M13, I33 in M10 and Von Zeipel 1128 in M3 (Strom and Strom, 1970).

OBSERVATIONS

In Figure 1 we have plotted the relative SWP fluxes of several UV-bright stars, all found well outside the cores of their respective globular clusters. The data has been averaged in 50 A bins, corrected for interstellar reddening and scaled to the distance of NGC 6397 to facilitate comparison. Also plotted are the recently discovered hot object in M5 (Bohlin, et al., 1983), K 648, the planetary nebula in M15 and, to represent the level of the BHB in this wavelength range, one of the two stars found in the core of M13 by de Boer and Code (1981). The stars appear to fall into two luminosity groups; about 1 magnitude above the HB for the lower group and almost 3.5 magnitudes above the HB in the higher luminosity group at 1600 A. Not shown in Figure 1 is the star K 559 in M15 which almost exactly overlaps the M5 source.

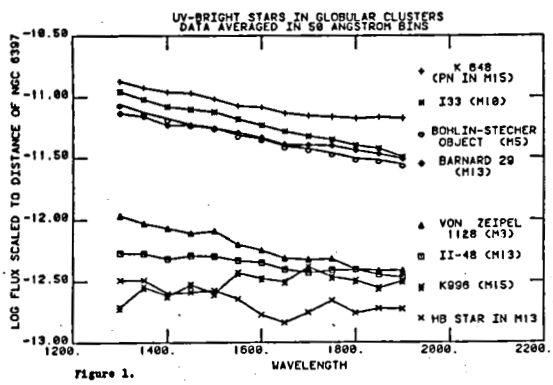

Figure 1.

These values are consistent with those reported by Strom and Strom (1970) with the major exception being that Von Zeipel 1128 was one of the brightest stars in their sample and here it seems to be among the supra-HB stars. A study of 9 UV-bright stars far outside the core in ω Cen by Norris (1974) found 6 of the 9 to be in the high luminosity group.

In order to discuss the sources found in the cores of the clusters it is necessary to resolve them spatially, for, as shown in Figures 2 and 3, the flux distribution in the large aperture clearly indicates multiple sources. Figure 2 is included as an example of an "easy" case: two stars are obviously present and we confirm the result of de Boer and Code (1981) that the two have very similar spectra. Figure 3 is an example of the opposite extreme: even at the short wavelength end the sources are blended and are difficult to resolve by simple inspection. For such cases we employ an interactive least squares fitting scheme which assumes a gaussian point spread function. In this way the flux distribution in Figure 3 has been "resolved" into 3 sources. The source profiles and their sum (plus background) are shown in Figure 4. In a similar manner multiple, overlapping sources were resolved in M15, M2, M30, M92 and NGC 6752. It should be noted in Figure 4 that the derived FWHMs are still slightly broader than the instrumental point spread function (FWHM = 5".4 at 1400 A). Thus, the fluxes derived from this fitting procedure are upper limits. Figure 5 shows many (for clarity, overlapping sources have not been plotted) of the resolved stars found by this procedure. Again, the HB star in M13 is included for comparison. No gap is immediately apparent, as it is in Figure 1. The stars labeled M92 A, M70 A and NGC 6752 are between 1.2 and 0.7 magnitudes above the HB star at 1600 A while the very brightest source, the star in M15 is about 2.3 magnitudes above the same star at 1500 A, in line with the value found by Gursky and Davis (1980). The most interesting comparison occurs when the range of log flux values in Figure 5 is compared to that in Figure 1. We note that most of the core stars, with the possible exception of the one in M15, would fall in the lower luminosity group of Figure 1.

DISCUSSION

Sweigart, Mengel and Demarque (1974) pointed out that the luminosities of the post-AGB tracks are very sensitive to the total mass of the model. The most massive stars reach the highest luminosities before reaching the turnoff point that leads, ultimately, to the white dwarf cooling curves. Since HB stars of all but the smallest masses eventually reach the AGB, any intrinsic mass spread along the zero-age HB should result in a luminosity spread among the post-AGB UV-bright stars.

That almost all of our core sources seem to be supra-HB stars, whereas one might expect massive stars in the core of dynamically relaxed systems, might be due to the small number of stars accomodated by the IUE aperture and the very rapid (10^5 years) timescale for post-AGB evolution compared to HB lifetimes (10^8 years) and supra-HB lifetimes (10^7 years). In this view, the brighter group of stars might be in the core but are so rare that the 10 X 20 arcsecond IUE aperture would have to be precisely pointed to find them. Alternately, it just may be that for the HB and post-HB stars the cluster cores are <u>not</u>

dynamically relaxed, and that therefore the most massive stars are not in the cores at all. Clearly, more data is needed before these results are fully understood. A much better way to look at these relative luminosities, of course, would be to construct log ($L/L_\odot$) versus log T_{eff} diagrams, but so far fits to model atmospheres have been hampered by the ubiquitous, broad absorption feature centered at 1600 A. Until the problem of this "dip" is solved, reliable temperature determinations will elude us.

This work was partially supported by NASA grant NAG 570. We acknowledge the help of the National Space Science Data Center in obtaining archival spectra of clusters and UV-bright stars used in this study.

REFERENCES

de Boer, K. and Code, A. 1981, Ap. J. (Letters), 243, L33.
Bohlin, R., Cornett, R., Hill, J., Smith, A., Stecher, T. and Sweigart, A. 1983, Ap. J. (Letters), 267, L89.
Dupree, A., Hartmann, L., Black, J., Davis, R., and Matilsky, T. 1979, Ap. J. (Letters), 230, L89.
Gursky, H. and Davis, R. 1980 in Highlights of Astonomy, 5, 231, P. Wayman, ed.
Harris, H., Nemec, J. and Hesser, J. 1983, Pub. A.S.P., 95, 256.
Norris, J. 1974, Ap. J., 194, 109.
Strom, S. and Strom, K. 1970, Astr. Ap., 8, 243.
Sweigart, A., Mengel, J. and Demarque, P. 1974, Astr. Ap., 30, 13.
Zinn, R. 1974, Ap. J., 193,593.

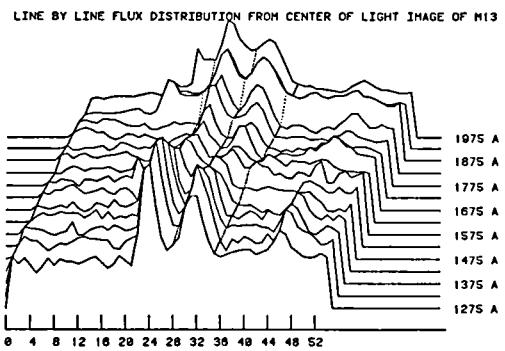

Figure 2.

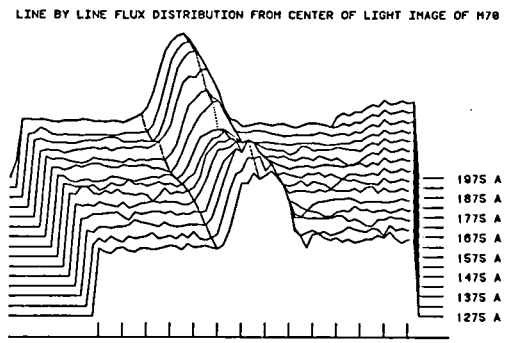

Figure 3.

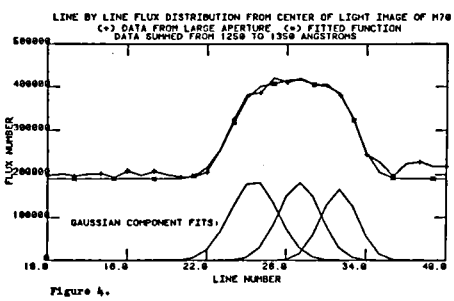

Figure 4.

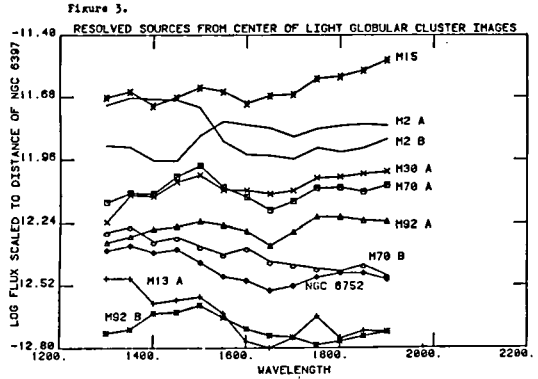

Figure 5.

A SEARCH FOR YOUNG STELLAR CHROMOSPHERES IN NGC 2264

Theodore Simon
Institute for Astronomy, University of Hawaii

ABSTRACT

Pre-main-sequence stars in the galactic cluster NGC 2264 were observed with IUE to search for ultraviolet chromospheric and transition region (TR) emission lines. Fifteen cluster members of spectral type A-K, ranging in age from 1 to 10 million years, and 4 other stars in the direction of the cluster were observed at low resolution. Chromospheric emission was detected only in the faint Hα emission-line star NX Mon (W 79); its Mg II surface flux, $F_{Mg} \approx 1 \times 10^8$ ergs cm^{-2} s^{-1}, is comparable to that observed for very active T Tauri stars. Upper limits on chromospheric and TR line emission of the remaining stars are an order of magnitude below the surface fluxes and normalized fluxes, f_L/ℓ_{bol}, of T Tau stars and of the chromospherically-active Ae star HR 5999. These upper limits are comparable to the emission-line strengths of solar-type stars in the Hyades and UMa clusters and of the youngest field stars. The bright pre-main-sequence stars in NGC 2264 therefore have weaker chromospheres and TRs than do the T Tau stars, but it is uncertain whether their activity levels are intermediate between those of the T Tau and older stars, as would be expected if chromospheres steadily decline with age.

INTRODUCTION

The chromospheric emission of solar-type main-sequence stars in the nearby field and in nearby open clusters like Ursa Major and the Hyades is inversely correlated with age. According to Skumanich (1972), the strength of the emission in the cores of the Ca H-K lines declines with the square root of age for stars older than ~0.1 Gyr. Similar power laws have been derived for UV chromospheric and TR lines (Simon and Boesgaard 1983), except that the high-temperature lines decline more steeply with age than do the low-temperature lines. For very young stars the chromospheric activity-age relation may be more complicated than this; there are major difficulties in interpreting the UV (and X-ray) observations of pre-main-sequence T Tau stars in terms of surface activity and in placing these stars on the activity-age relations of the older stars.

This paper reports on a search for chromospheric activity in the brightest pre-main-sequence stars in NGC 2264. This cluster has been the subject of numerous modern photometric and spectroscopic studies, starting with Herbig's (1954) census of faint emission-line stars. Members of the cluster have been identified from their proper motions by Vasilevskis et al. (1965). NGC 2264 has a normal main sequence populated from O6 to B9, but many of the cooler members lie in a band above and parallel to the ZAMS (Walker 1956). These stars are still gravitationally contracting toward the main sequence; from a comparison with isochrones, Strom et al. (1971) derived ages for these stars of 1 to 10 million years.

OBSERVATIONS

Nineteen stars were selected from Walker (1956) and Vasilevskis et al. (1965). Fifteen stars of spectral type A-K are bona fide members, 2 are probable foreground stars. Most lie above the main sequence, a few are close to or below the ZAMS, and 7 are rapid rotators (Vogel and Kuhi 1981) expected to show intense dynamo action and chromospheric emission. Low-resolution spectra were obtained with the SWP and LWR cameras, usually under low noise conditions, with exposure times of 5 to 240 min. The spectra were well exposed for the hot stars but underexposed for some faint cool stars. The FES magnitudes agree with published V band photometry, except for 2 stars where the identification of the IUE target is now suspect.

Examples of spectra are presented in Figures 1 and 2. Detection limits for integrated emission-line fluxes are $2 \times 10^{-14} - 4 \times 10^{-13}$ ergs cm^{-2} s^{-1}. No stellar chromospheric lines were detected in the 1200-2000 Å spectral region. In the long exposures of a few stars (e.g., W 92), nebular emission fills the large aperture. Stellar emission lines are present in the 2000-3200 Å spectra of W 90, an Ae star located below the main sequence, and W 79 (= NX Mon), a ~16th mag Hα emission-line star. The other stars have normal absorption line spectra. The emission lines of Mg II and Fe II (UV62 and UV63) in the spectrum of W 90 most likely arise in the CS envelope of this star. The variable Mg II emission of NX Mon might be chromospheric. The optical spectrum is heavily veiled (Herbig 1954), indicating an extremely thick chromosphere or a very extensive CS shell. The average surface flux in Mg, $F_{Mg} = 1.6 \times 10^{8}\ r_*^{-2}$ dex $(0.8\ A_V) = 5 \times 10^{7}$ ergs cm^{-2} s^{-1} if I assume a radius $r_* = 2\ r_o$ and an interstellar extinction correction, $A_V = 0.25$ mag. This surface flux is comparable to the intrinsic (reddening-corrected) surface fluxes of the most active T Tau stars in star-forming regions like Tau-Aur, and is an order of magnitude larger than the flux of young solar-type field stars (e.g., χ^1 Ori), 30 times the quiet-Sun value, and ~100 times the quiescent surface flux of nearby active dMe flare stars.

DISCUSSION

In order to assess the present results we need to consider what levels of activity observed by IUE in nearby young stars could be detected at the distance of this cluster. The 2σ detection threshhold (for cool stars) was ~4×10^{-14} ergs cm^{-2} s^{-1}. Scaled to 800 pc, the observed emission-line fluxes of only the most active pre-main-sequence stars would be detected, and then only for the Mg II lines. Corrected for extinction, the intrinsic surface fluxes of the strong lines of nearly all the T Tau stars observed to date would be detected easily; if the stars in NGC 2264 are post-T Tau stars whose CS envelopes have been cleared away to reveal intense surface activity, these fluxes would be observable. The Mg flux of young solar stars like χ^1 Ori, however, would be an order of magnitude below this detection limit and their C IV emission would be 1000 times too faint to be detected. The emission from dMe stars would fall short by 2-6 orders of magnitude even during flares. For hot stars the detection limit was 4×10^{-13} ergs cm^{-2} s^{-1} because of their

strong continuum emission. The Mg II and C IV lines of the Ae star HR 5999 (Tjin A Djie et al. 1982) are just barely detectable at 800 pc.

At the distance of NGC 2264, interstellar absorption lines might be strong enough to mask completely any chromospheric emission features. The interstellar Mg II lines in high-dispersion IUE spectra of S Mon have an EW = 0.75 Å and coincide with the radial velocity of the cluster. Equally strong interstellar lines of C II, C III, and O VI are present in Copernicus spectra of S Mon (Shull 1980). To estimate whether the interstellar lines would obliterate stellar chromospheric emission in Mg II, we can use the line width-luminosity relation (Weiler and Oegerle 1979). This relation predicts that late-type cluster members intrinsically brighter than 16th mag would have Mg lines broader than the interstellar features, and interstellar absorption would typically remove half the intrinsic stellar line emission. For NX Mon, 90% of the stellar emission may be masked, but the amount of obscuration depends on the (unknown) v sin i of the star. Since the line widths of T Tau stars are observed to be up to ~3 times wider than the predicted widths, the extinction correction appropriate to NX Mon is probably smaller.

For 10 cluster stars whose bolometric luminosities are known, we derive normalized Mg II line flux upper limits, $f_{Mg}/\ell_{bol} < 5 \times 10^{-5} - 1 \times 10^{-4}$. These limits are 20-40 times smaller than the normalized intrinsic fluxes of T Tau stars and comparable to those of χ^1 Ori and the Hyades dwarfs. The C IV normalized fluxes of the cluster stars, $f_{C\ IV}/\ell_{bol} < 3 \times 10^{-5}$, are an order of magnitude below the T Tauris, lying between them and the young solar-type stars. We also use the Barnes-Evans relation to convert from upper limits on f_L to upper limits on F_L. The limit for F-K stars, $F_L < 5 \times 10^6$, is a factor of 10 below the T Tau stars and lies between them and χ^1 Ori. The upper limit for the A-type stars in NGC 2264, $F_L < 4 \times 10^7$, is slightly below the T Tau intrinsic fluxes. In summary, the pre-main-sequence stars in NGC 2264 exhibit weaker UV chromospheric activity than do various T Tau stars (RW Aur, AS 205, RU Lup, etc.), but the comparison with nearby field and cluster stars is inconclusive.

REFERENCES

Herbig, G. H. 1954, Ap. J., 119, 483.
Shull, J. M. 1980, Ap. J., 238, 560.
Simon, T., and Boesgaard, A. M. 1983, in Solar and Stellar Magnetic Fields, ed. J. O. Stenflo (Dordrecht: Reidel), p. 161.
Skumanich, A. 1972, Ap. J., 171, 565.
Strom, K. M., Strom, S. E., and Yost, J. 1971, Ap. J., 165, 479.
Tjin A. Djie, H. R. E., The, P. S., Hack, M., and Selvelli, P. L. 1982, Astr. Ap., 106, 98.
Vasilevskis, S., Sanders, W. L., and Balz, A. G. A. 1965, A.J., 70, 797.
Vogel, S. N., and Kuhi, L. V. 1981, Ap. J., 245, 960.
Walker, M. F. 1956, Ap. J. Suppl., 2, 365.
Weiler, E. J., and Oegerle, W. R. 1979, Ap. J. Suppl., 39, 537.

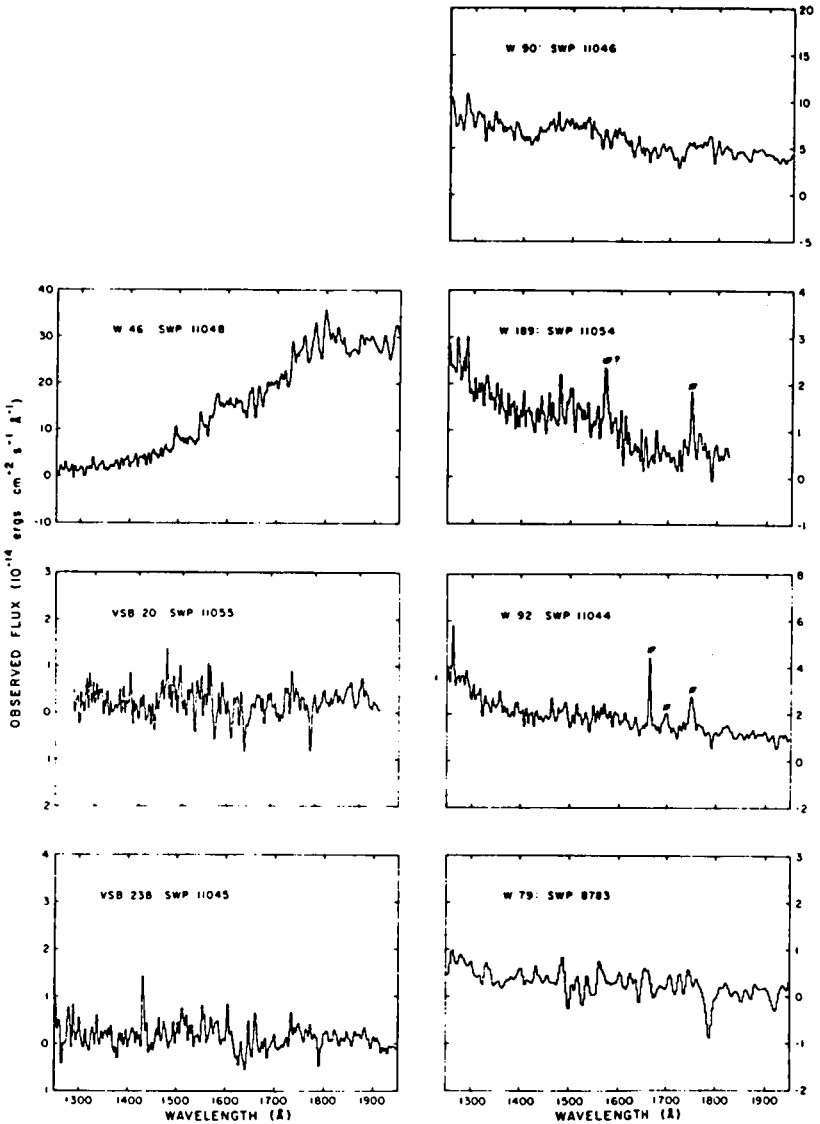

Figure 1 - SWP spectra

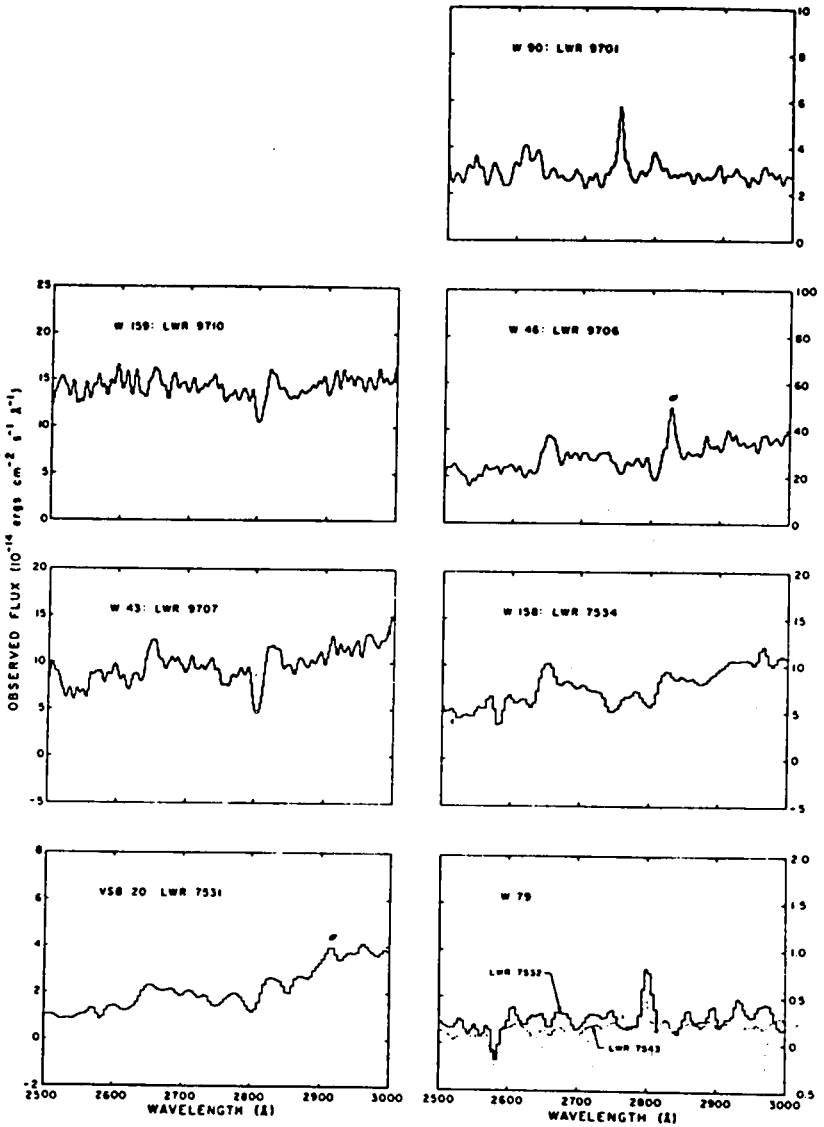

Figure 2 - LWR spectra

THE UV EXTINCTION LAWS IN TWO VERY YOUNG CLUSTERS, NGC 6530 IN THE GALAXY AND NGC 2100 IN THE LMC

Erika Böhm-Vitense, Paul Hodge and Don Boggs
University of Washington, Seattle

ABSTRACT

We have studied the UV extinction for a number of O and B stars in the galactic cluster NGC 6530. We also have studied the extinction law for several stars in the LMC cluster NGC 2100. We find distinct differences for different stars in the same cluster. In NGC 6530 we see a correlation of the extinction law with T_{eff} or with position in the cluster. In NGC 2100 the 2200 A absorption appears to be much stronger in the center of the cluster.

We have also studied the interstellar gas line absorption for the stars in NGC 6530. No correlation with the variations in the UV extinction law has been found so far.

INTRODUCTION

It is well known that the interstellar UV extinction law may vary from place to place in the galaxy (see, for instance, Savage and Mathis 1979, Meyer and Savage 1981, Massa, Savage and Fitzpatrick 1983). Variations are believed to be related to differences in grain size. Some dependence on spectral type of the star has been suggested by Massa and Conti (1981). In our studies of the position of the NGC 6530 stars in the HR diagram, a careful determination of the UV extinction law emerged as a byproduct. In the following we report our results.

THE OBSERVATIONS

These studies relied heavily on archival data. Several of our program stars had been observed previously by different observers for various programs. These existing observations were supplemented by our own observations when necessary. The European observations were generally less noisy than the ones taken on this side of the Atlantic, which were taken during US2 shifts with large background radiation.

DETERMINATION OF EFFECTIVE TEMPERATURES

Color excesses E(B-V) were determined from the UBV color measurements of Walker (1957) and Chini and Neckel (1981). Unfortunately, their U-B colors show some systematic but unexplained differences. From the theoretical relations between different colors, using the UV and visual data and effective temperatures, it became obvious that the U-B colors are most sensitive to T_{eff} and therefore suited best for the determination of T_{eff}. The uncertainty in the U-B colors is therefore rather unfortunate. After

the best possible determination of T_{eff}, we determined the ratio of the measured UV fluxes to the model atmosphere fluxes of Kurucz (1979). The differences in magnitudes were interpreted as interstellar extinction. With the E(B-V) determined from the UBV colors, the $(A_\lambda - A_V)/E(B-V)$ could be determined as a function of wavelength. Small corrections to the originally determined T_{eff} were then applied in order to match the average galactic extinction law for $\lambda > 2600$ Å.

THE UV EXTINCTION LAWS IN NGC 6530

In Figure 1 we compare the $(A_\lambda - A_V)/E(B-V)$ values as a function of wavelengths as measured for the different stars in NGC 6530. The curves are arranged in order of T_{eff} of the stars. We see distinct changes in the A_λ for $\lambda < 1900$ Å. In Figure 2 we show a schematic plot with the positions of the stars with respect to the center of the cluster. It turns out that the hottest stars are also those which have the largest distance from the center of the cluster. It is therefore possible that we actually see a dependence of the UV extinction on the distance from the cluster center. The stars in the center of the cluster show the smallest extinction for $\lambda < 1900$ Å.

Small variations in A_λ are also seen for 2300 Å $< \lambda <$ 2600 Å. We presently have no explanation for these variations. The bump strength at 2200 Å is, however, very similar for all the cluster stars.

The angular size of the region studied here is less than 1° in each dimension, which corresponds to less than 35 pc, at the cluster distance of about 2000 pc.

THE CORRELATION OF UV EXTINCTION WITH INTERSTELLAR GAS ABSORPTION IN NGC 6530

If the observed variations in the UV extinction law are due to the destruction of small grains in the cluster interstellar material we might perhaps see a correlation of the depletion of heavy elements with the variation of the extinction law. So far we have looked at interstellar lines of Fe, Si, Mn, and Mg. No such correlation has been found so far. We are continuing our studies.

INTERSTELLAR EXTINCTION IN THE LMC CLUSTER NGC 2100

In a separate note in this volume Ch. Proffitt will report on our extinction determination for NGC 2100 in the LMC. Here we only want to point out that in this cluster again we find variations of the extinction over the surface of the cluster which has a diameter of about 30 pc. Figure 3 shows the observed energy distributions for our program stars. There is little (B20) or no indication of the 2200 Å absorption band due to interstellar extinction in the spectra of the program stars. In Figure 3 we also show energy distributions from images obtained by Geyer and by Cohen for the whole cluster. Geyer obtained the image placing the center of the cluster in the center of the large entrance aperture of the IUE

spectrograph. We do not know the exact position of the image taken by Cohen. For these two spectra the dip due to the 2200 Å absorption is clearly present. It then appears that in this populous young cluster the material which causes the 2200 Å extinction is concentrated near the center while very little of this material is found in the outer regions. This situation is very different from what we find in the galactic cluster NGC 6530.

REFERENCES

Altena, W.F. van, and Jones, B.F. 1972, Astron. Astrophys. 20, 425.
Chini, R., and Neckel, Th. 1981, Astron. Astrophys. 102, 171.
Kurucz, K. 1979, Ap.J. Suppl. 40, 1.
Massa, D., Savage, B.D. and Fitzpatrick, E.L. 1983, Ap.J. 266, 662.
Massa, D., and Conti, P.S. 1981, Ap.J. 248, 201.
Meyer, D.M. and Savage, B.D. 1981, Ap.J. 248, 545.
Savage, B.D. and Mathis, J.S. 1979, NN. Rev. Astr. Astrophys. 17, 73.
Walker, M.F. 1957, Ap.J. 125, 636.

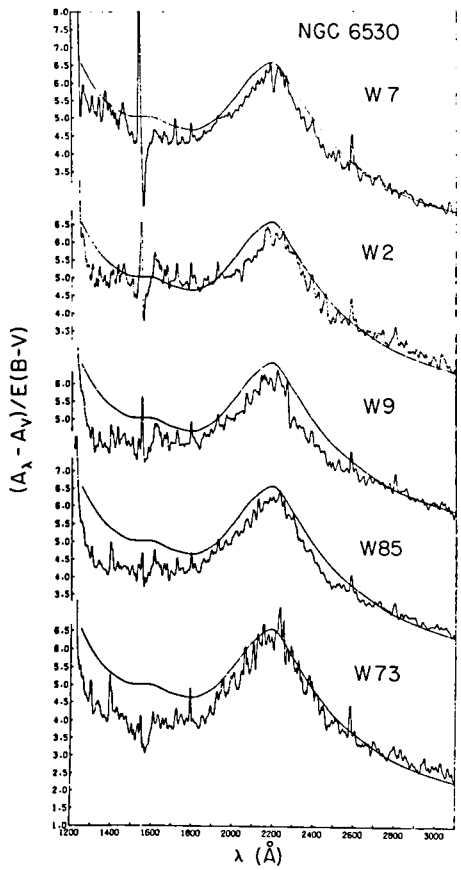

Figure 1. The UV extinction laws derived for the different stars in NGC 6530. The hottest stars are at the top; the coolest ones at the bottom. The Walker numbers of the stars are given

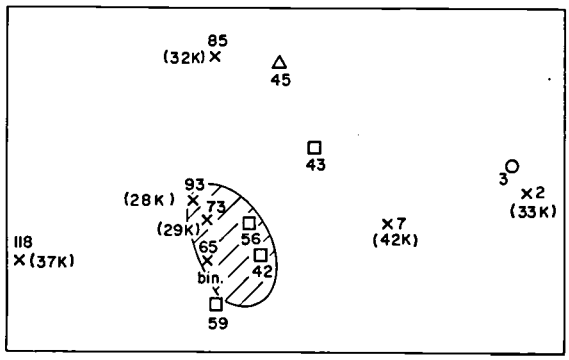

Figure 2. Positions of our stars relative to the cluster center.

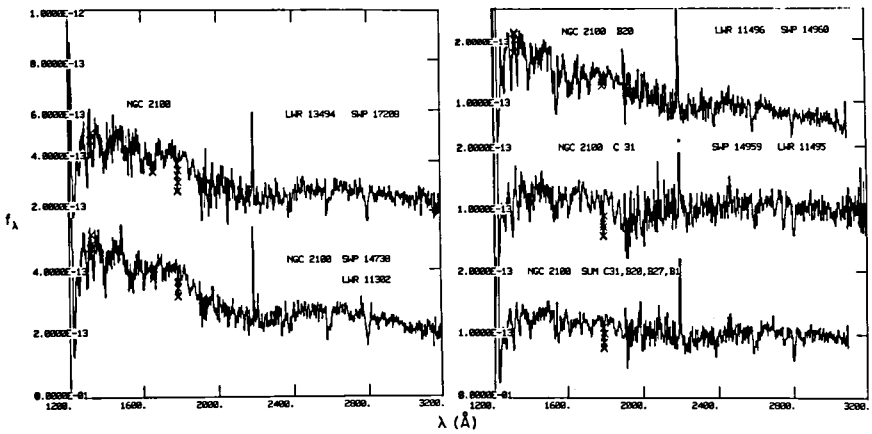

Figure 3. Energy distributions f_λ [erg/cm^2/sec] obtained for our program stars in the LMC cluster NGC 2100 are shown as a function of wavelength on the righthand side. On the lefthand side the energy distributions f_λ [erg/cm^2/sec] for the cluster NGC 2100 obtained by Geyer (SWP 14738, LWR 11302) and by Cohen (SWP 17208, LWR 13494) are shown as a function of the wavelength λ.

ULTRAVIOLET STUDIES OF THE YOUNG POPULOUS CLUSTER NGC 2100 IN THE LMC

Erika Böhm-Vitense, Paul Hodge and Charles Proffitt
University of Washington, Seattle

ABSTRACT

Stars in the populous young cluster NGC 2100 were observed with IUE in the low resolution mode. Color excesses, effective temperatures and luminosities were determined for eight stars in the cluster. A comparison of observed and model atmosphere energy distributions shows that the Nandy et al. (1981) average LMC extinction curve does not give good matches for the cluster stars. For most of the cluster stars no hump in the extinction at 2200 A is observed and too little flux is observed between 1400 and 2000 A.

We find masses between 15 and 30 solar masses for our stars and an age of about 6×10^6 years. Two stars, B27 and C1, may have an age of up to 12×10^6 years.

INTRODUCTION

In the LMC there are a number of blue clusters, whose appearance resembles globular clusters. They lack galactic counterparts. Apparently, small populous clusters are still forming in the LMC. NGC 2100, near the 30 Doradus region, is one of these. Previous studies of this cluster in the B and V bands were published by Robertson (1974) and Westerlund (1961), and indicated an age of about 7×10^6 years, but the scatter in the observations was large and the reddening poorly determined. With better UBV photometry and low resolution IUE spectra, better values for the reddening, effective temperature and luminosity of stars in this cluster can be obtained, and the interstellar extinction in the ultraviolet can be studied.

THE OBSERVATIONS

UBV Colors

Photoelectric UBV colors of our eight program stars were obtained in 1984 with the 0.9m reflector at CTIO. These and some earlier photoelectric measurements kindly provided by J. Nemec (1982) are listed in Table 1. The values agree rather well. For the sake of consistency, only the 1984 observations are used in the following discussions. Since an 11" diameter entrance aperture had to be used, the colors of the stars close to the center of the cluster (B27, B20 and C7) may be affected by background starlight.

IUE Observations

Both short (1200-1950 A) and long (1950-3000 A) wavelength low resolution spectra of each of the program stars were obtained with IUE. Most of the observations were made using blind offsets from B1 and we must be aware of the possibility that some light may have been lost because of incorrect centering of the star in the entrance aperture. For two of our program stars, C13 and C14, the observed ultraviolet flux levels are inconsistent with the UBV data. We therefore do not use the IUE data for these two stars in the following discussions.

DETERMINATION OF THE EFFECTIVE TEMPERATURES

If the intrinsic colors and surface gravity of a star are known, its effective temperature can be determined. Theoretical unreddened UBV colors and visual to 2912 A colors were obtained from Kurucz's (1979) model atmospheres (Table 5B). (The UV line absorption in these models was corrected for a reduced metal abundance of [A/H] = -0.5 appropriate for the LMC.) The appropriate surface gravity to be used to determine the unreddened colors was derived from the position of the star in the HR diagram and the evolutionary tracks of Brunish and Truran (1982). A distance modulus of $m_V - M_V = 18.6$ was used.

For the two stars, C7 and B20, whose UBV colors are uncertain because of background contamination, only the f(2912)/f(V) versus B-V diagrams were used. For the other stars both color-color plots give consistent results.

From the dereddened colors and magnitudes, the effective temperatures and luminosities are determined using model atmospheres. The results are listed in Table 2 and the H-R diagram is plotted in Figure 1.

THE ULTRAVIOLET SPECTRA

With the values for the color excesses and temperatures determined above we can correct the observed energy distribution for interstellar extinction using Nandy's (1981) average LMC extinction curve. We assume that 0.05 of the reddening is due to our galaxy and use Seaton's (1979) average galactic extinction law for the correction. We can then compare the dereddened energy distributions with model atmosphere energy distributions. The spectra for B27 and C7 are both better fit with higher temperatures than derived from the color-color plots. The spectra and best fit model atmosphere energy distributions are plotted in Figure 2.

For most of the stars, except B20, we seem to have overcorrected for the 2200 A feature. Also, between 1400 and 2000 A the spectra show strong absorption features not present in the models. Either the models overestimate the flux at these wavelengths (see Koornneef and Code 1981, Llorent de Andres, et al. 1981), or the extinction in the cluster is larger at these wavelengths than found by Nandy for the average LMC extinction. If the model energy distributions in Figure 2 are assumed to be correct, the

extinction laws can be determined from a comparison of the ratios of the observed to model atmosphere energy distributions. The results are shown in Figure 3. The absorption bump around 1600 A is clearly visible in all stars and its strength does not seem to be well correlated with effective temperature. We are thus inclined to attribute most of this absorption to interstellar extinction rather than to absorption features in the stars.

THE AGE OF NGC 2100

B20, C31 and B1 (and also C7 if the higher temperature found in Section IV is used) seem to lie very close to a single mass track of about 25M with very little spread in age. This corresponds to an age of about 6×10^6 years. The positions of the other stars in the H-R diagram are less accurately determined, but may indicate a slightly larger age. The position of C1 corresponds to an age of 12×10^6 years. Perhaps this star is not a cluster member, or it may represent the initial phase of star formation in the cluster and its larger association of stars (Westerlund 1961).

REFERENCES

Brunish, W.M. and Truran, J.W. 1982, Ap.J. Suppl. 49, 447.
Koornneef, J. and Code, A. 1981, Ap.J. 247, 860.
Kurucz, R. 1979 Ap.J. Suppl. 28, 73.
Llorent de Andres, F., Morales, C., Ruizde Arbol, J.A., Perez Mollu, J. 1981, Astron. Astrophys. 100, 138.
Maeder, A. 1981, Astron. Astrophys. 102, 401.
Nandy, K., Morgan, D.H., Willis, A.J., Wilson, R., Gondhalekar, P.M. 1981, Mon. Nat. R. Astr. Soc. 196, 955.
Robertson, J.W. 1974, Astron. Astrophys. Suppl. 15, 261.
Seaton, M.J. 1979, Mon. Not. R. Astr. Soc. 187, 73p.
Westerlund, B. 1961, Upp. Ast. Obs. Ann. 5, 1.

Table 1

	Hodge			Nemec	
	V	B-V	U-B	V	B-V	U-B
B1	11.84	+0.12	-0.55	11.72	+0.13	-0.57
B20	13.50	-0.03	-1.04	13.66	-0.05	-0.98
B27	12.13	+0.14	-0.31	12.08	+0.17	-0.28
C1	11.90	+0.22	+0.00			
C13	13.83	-0.04	-0.82			
C14	15.32	-0.09	-0.92			
C31	12.57	+0.04	-0.77	12.63	+0.05	-0.74

Table 2

Star	From log (f_{2912}/f_V) vs. B-V T_{eff}	log g	E_{B-V}	M_V	log L/L_o	From (U-B) vs. B-V T_{eff}	log g	E_{B-V}	M_V	log L/L_o
C7	30,000	3.5	.32	-4.63	4.93					
C14						30,000	3.5	.20	-3.93	4.66
B20	27,500	3.0	.23	-5.88	5.34					
C13						23,500	3.0	.20	-5.42	5.03
C31	19.300	2.5	.23	-6.78	5.37	20,000	2.5	.24	-6.81	5.42
B1	15,300	2.0	.26	-7.61	5.52	15,000	2.0	.27	-7.64	5.49
B27	12,500	2.0	.25	-7.28	5.17	11,000	1.75	.20	-7.12	4.99
C1	9,200	1.5	.22	-7.41	4.97	8,500	1.3	.20	-7.22	4.83

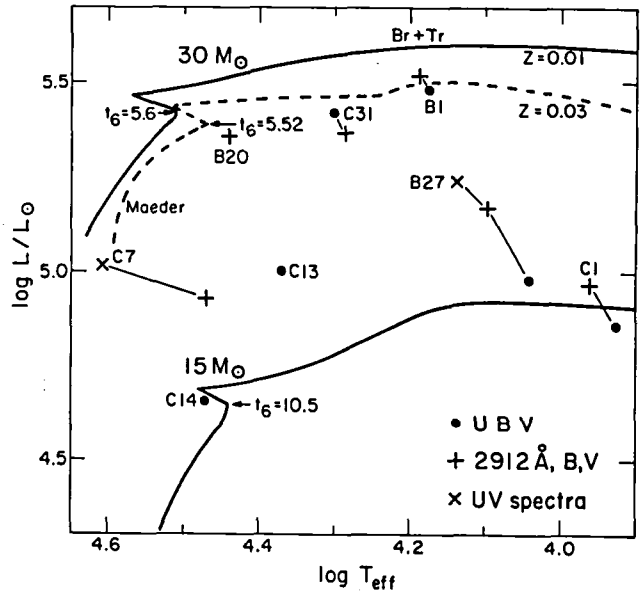

Figure 1. The H-R diagram for NGC 2100, 15 and 30 solar mass model evolutionary tracks from Brunish and Truran (1982) and a 30 solar mass model track from Maeder 1981 are shown.

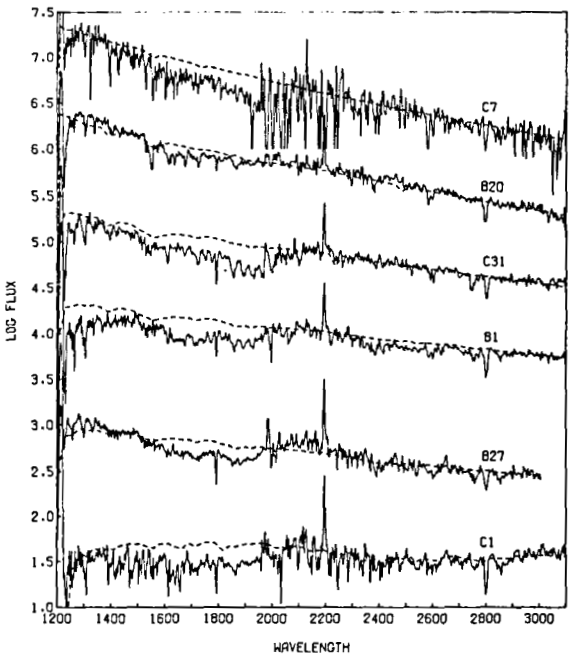

Figure 2. Comparison of dereddened IUE spectra to Kurucz model atmosphere energy distributions.

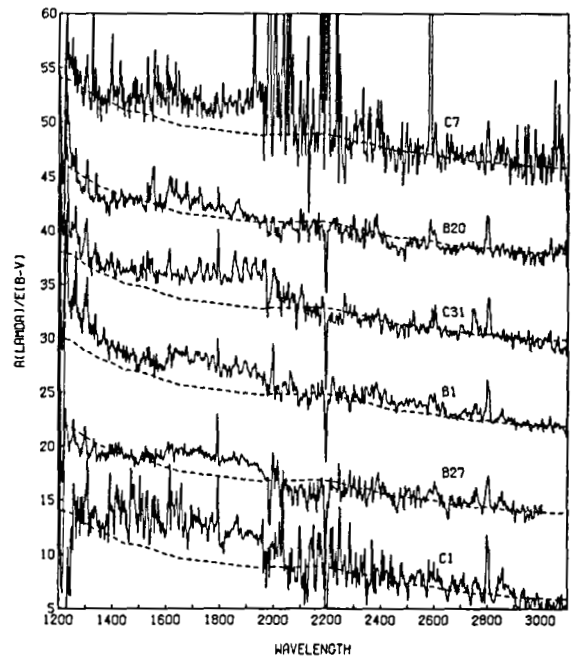

Figure 3. LMC reddening curves derived assuming model atmosphere energy distributions as shown in Figure 1. Galactic reddening with E(B-V) = 0.05 and Seaton's 1979 average galactic reddening curve was assumed.

INTERSTELLAR MEDIUM

IUE OBSERVATIONS OF INTERSTELLAR LINES

Daya P. Gilra
SM Systems and Research Corporation, Lanham,Md.

For the study of interstellar lines about 350 spectra of about 40 stars were obtained from the IUE Vilspa data bank and analysed. The preliminary results are :-

1) Ihave discovered lines due to interstellar Germanium,Gallium,and Krypton. These elements are much less depleted than the iron group elements (it is possible that they are almost undepleted). These are all with atomic number greater than 30. This discovery will have important bearing on the general depletion problem in interstellar gas.

2) Several intercombination lines of Fe II and several Ni II lines have been discovered. With the observations of the intercombination lines the column densities can be easily derived since the lines are on the linear part of the curve of growth.

3) There is a qualitative difference between the lines of highly ionized species such as C IV, Si IV arising in H II regions on the one hand and those arising in interstellar medium where no H II region can be traced. The H II region lines are considerably narrower. In both cases, however, multiple components are seen. Many of these components have no counterparts in the Si II or C II lines.

4) There is a probable detection of one Fe I line. On the other hand 6 Mg I lines have been detected (many for the first time). Apart from the much higher depletion of Fe, the ratio Fe I / Fe II is much lower than the Mg I / Mg II ratio.

5) An apparently unsuccessful attempt was made to detect interstellar lines from highly metastable levels of excited terms. Specifically, no line was detected from the Mg $I\,^3P_0$ level (life time= 10^{12} seconds.) This fact combined with the strength of the lines from the ground level of Mg I also has important bearing on the ionization and recombination processes in interstellar space.

6) A search for molecules other than $C^{12}O$ and $C^{13}O$ was apparently unsuccessful. Two " forbidden" $C^{12}O$ bands were also observed. HD 147889, the heavily reddened star in the Rho Oph cloud shows the strongest CO lines.

7) Several instrumental effects, such as, the background problem, the fixed pattern noise, the instrumental resolution, and the wavelength calibration were also studied.

OBSERVATIONS OF MG I AND MG II IN THE LOCAL ISM

F. Bruhweiler[1], W. Oegerle[2], E. Weiler[3], R. Stencel[3], and Y. Kondo[4]

ABSTRACT

We have used high quality IUE data combined with that acquired by Copernicus to study the Mg II/Mg I ionization balance in the local interstellar medium within 50 pc of the Sun. The high resolution, high signal-to-noise Copernicus data reveal, in three stars, weak interstellar Mg I features at 2852 A. High quality IUE data for interstellar Mg II near 2800 A were acquired by coadding high dispersion images and incorporating an observing technique that minimized the effects of camera fixed-pattern noise. The results are in agreement with the local cloud model as presented previously by Bruhweiler. The Mg I and Mg II column densities are used to place constraints on the physical conditions of the interstellar gas near the Sun.

INTRODUCTION

Recent studies of the local interstellar medium (LISM) (Bruhweiler and Kondo 1981, 1982a, 1982b; Bruhweiler 1982) based primarily on IUE data show the Sun is embedded in and near the edge of a rather diffuse cloud with a total column density of $(1\text{-}2)\times10^{19}\text{cm}^{-2}$. However, in directions away from the cloud core lies the pervasive, extremely low density ($n\sim10^{-2.5}\text{cm}^{-3}$), high temperature ($T\sim10^{5.5}\text{K}$) gas with no evidence of additional clouds within at least 50 pc for the lines of sight studied.

If the Sun is indeed embedded in and near the edge of the local cloud, then the gas in the immediate vicinity should be quite warm ($T\sim8{,}000$:K; McKee and Ostriker 1977).

Since neutral magnesium originates primarily in the interstellar medium through dielectronic recombinations near 10^4K, significant amounts of Mg I would be present in any warm gas near the Sun. Thus, Mg I might be useful as a tracer for the warm neutral and ionized gas components (WNM and WIM) discussed by McKee and Ostriker (also see York 1983).

OBSERVATIONAL DATA

We present IUE and Copernicus data corresponding to the interstellar lines of Mg I and Mg II (Mg I 2852; Mg II 2795, 2802 A) for five B and A stars within 40 pc of the Sun. All the Mg I data presented were acquired using the spectrometer aboard Copernicus. The Mg II data presented were obtained by both the IUE and Copernicus.

Although the Copernicus data is of high resolution, and in most cases higher signal-to-noise than that obtained with the IUE, Copernicus data obtained with the near-UV detectors have large charged particle backgrounds.

1 Department of Physics, Catholic University of America
2 Space Telescope Science Institute
3 NASA/ Headquarters
4 NASA/ Goddard Space Flight Center

This background can in some cases far exceed the stellar signal. Techniques, developed to correct for this background (Weiler 1978), have proven quite successful when the background levels are comparable or less than the stellar signal. This is a negligible problem in the case of Mg I, where the expected and observed features are weak and on the linear portion of the curves-of-growth. However, the Mg II features can be quite strong and approaching saturation. Since each member of the Mg II doublet is scanned seperately and have seperate background corrections applied, any errors in the background subtraction might be magnified in deriving the Mg II column densities.

The IUE data is of lower resolution than Copernicus data and of limited signal-to-noise. However, background subtraction is no problem near 2800 A where the echelle orders are widely spaced and the interorder signal can be reliably measured. To achieve good signal-to-noise in IUE data, one must choose exposure times which maximize the signal-to-noise for specific features. When interstellar lines are in troughs of photospheric features, one must overexpose the stellar continuum. Also, the signal-to-noise can be improved by coadding data from multiple IUE images (Bruhweiler and Kondo 1982b). Yet, the detector fixed-pattern noise limits the increase in signal-to-noise, when IUE images acquired during a single observing session are coadded. For images significantly seperated in time, the thermal behavior of the IUE camera (Thompson, Bohlin, and Turnrose 1982) effectively uncorrelates the fixed-pattern noise and does not seriously limit the improvement in signal-to-noise when images are coadded. One can artificially uncorrelate the fixed-pattern noise by taking repeated images in a short time period with the target positioned at different locations in the 10"x22" aperture. During the data reduction process, the spectral data can be aligned and coadded with the desired results. This technique was applied in acquiring the IUE spectral images for α Gru. (See Figures 1 and 2.)

RESULTS

A comparison of the IUE and Copernicus results for Mg II in Table 1 shows excellent agreement. Although the comparisons are limited, the agreement, especially for α Gru, implies that the background corrections for the Copernicus data are quite good. The nine individual measurements of the Mg II interstellar lines in the three IUE images (Mg II 2802 is in echelle orders 82 and 83) yielded a maximum deviation of 8 mA. This suggests that the co-added equivalent widths for α Gru have an accuracy on the order of 3 mA. The IUE results suggest that for a b-value on the order of 4.5 km s^{-1} (typical of those found here), reliable column densities can be obtained for interstellar features with equivalent widths $\lesssim$ 170 mA. For larger b-values and more observations, this limit might be pushed to larger equivalent widths. These results show that useful interstellar data can be obtained with the IUE, providing care is taken in collecting, reducing, and analyzing the data. The apparent disagreement in the case of α PsA is most likely due to the very high background level in the Copernicus data. Kondo et al. (1978) cautioned that their Copernicus results on α PsA were highly uncertain due to the high background level for that star. In contrast, the background level for the other Copernicus observations were equal to or less than the local continua for the Mg I and Mg II interstellar features. (See accompanying Figures and

Table 1.)

Backscattering results for H I Lymanα and He I 584 A imply a neutral hydrogen number density near the Sun of n(H I)=0.04-0.06 and that (N(H II)/N(H I)) $\approx$ 1.5 (Weller and Meier 1981). From Table 1, we adopt (N(Mg II)/N(Mg I))=500. By substituting $\Gamma' = 8\times10^{-11}$ s^{-1} (de Boer et al. 1973) and the total recombination rate of $\alpha_T(T)$ (Shull and Van Steenburg 1982) into the ionization equation, $N(Mg\ II)/N(Mg\ I)=\Gamma'/n_e\alpha_T(T)$, we find that T = 7,500 - 10,000 K, in the local solar vicinity. This result compares favorably with the 9,000 - 15,000 K deduced by Weller and Meier. The absence of Mg I toward α PsA, when combined with limits on n (Bruhweiler and Kondo 1982b) indicates much lower temperatures. More detailed results of this work will appear elsewhere.

REFERENCES

de Boer, K.S., Koppenaal, K., and Pottasch, S.R. 1973, Astr.Ap., 28, 145.

Bruhweiler, F.C. 1982, 'Advances in Ultraviolet Astronomy: Four Years of IUE Research,' ed. Y. Kondo, J.M. Mead, and R. Chapman, CP-2238, p.125.

Bruhweiler, F.C. and Kondo, Y. 1982a, Ap.J., 259, 232.

_____. 1982b, Ap.J. (Letters), 260, L91.

Kondo, Y., Talent, D.L., Barker, E.S., Dufour, R.J., and Modisette, J.L. 1978 Ap.J. (Letters), 220, L97.

McKee, C.F. and Ostriker, J.P. 1977, Ap.J., 218, 148.

Shull, M. and Van Steenburg, M. 1982, Ap.J.Suppl., 48, 95.

Thompson, R.W., Bohlin, R.C., and Turnrose, B. 1982, Astr.Ap., 107, 11.

Weiler, E. 1978, Ap.J.,

Weller, C.S. and Meier, R.R. 1981, Ap.J., 246, 386.

TABLES AND FIGURES

TABLE 1

SUMMARY OF MAGNESIUM DATA*

Star	Equivalent Width(mA)			Column Density(cm^{-2})	
	Mg II 2795	Mg II 2802	Mg I 2852	N(Mg II)	N(Mg I)
αCMa	71	47	$\leq$1.5	3.3×10^{12}	$\leq1.1\times10^{10}$
α Gru	161.7±3 (3)	146.7±3 (3)		6.1×10^{13}	
	170+14	153+11	12.5	5.4×10^{13}	9.8×10^{10}
α Eri	312 (1)	297 (1)			
	292	266	29.5	1.35×10^{14}	2.4×10^{11}
α Lyr	105 (2)	102 (2)			
	120±22	100±31	22	8.1×10^{13}	1.9×10^{11}
α PsA	183 (4)	162,157 (4)		4.0×10^{13}	
	133:	127:	$\leq$2.5		$\leq1.8\times10^{10}$

*The ratios given in each row are the IUE value over the Copernicus value. Numbers in parentheses are the number of IUE images used to get the result. Notes for individual objects are given below:

αCMa= This direction is away from cloud core, hence the low Mg I and Mg II column densities.

αLyr=IUE data have very low exposure levels for local continuum for IS lines. Photospheric features are quite sharp(v sin i =17 km/s). Interstellar and photospheric features likely not completely resolved.

αPsA= Very high Copernicus background level,(background/local continuum)=15. IUE data from Bruhweiler and Kondo 1982b.

Figure 1. Coadd Mg II data for three IUE images of α Gru. Corrections for echelle ripple have been applied. Data were normalized after coadding images. The smooth curve is a Gaussian fit to the broad spectral features of α Gru.

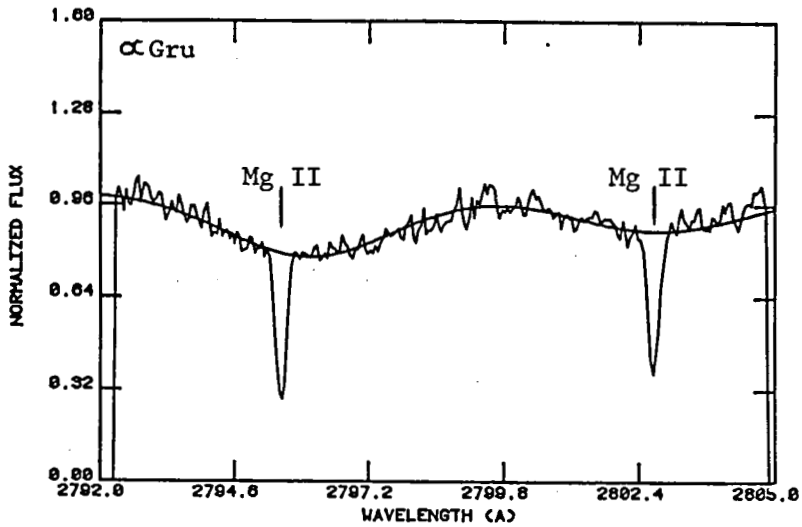

Figure 2. Rectified Continuum for Mg II Interstellar Lines. The IUE data in Fig. 1 are divided by the Gaussian fit. Deviations of ±5% from unity are noted, which correspond closely to ±2 σ deviations over most of the displayed data.

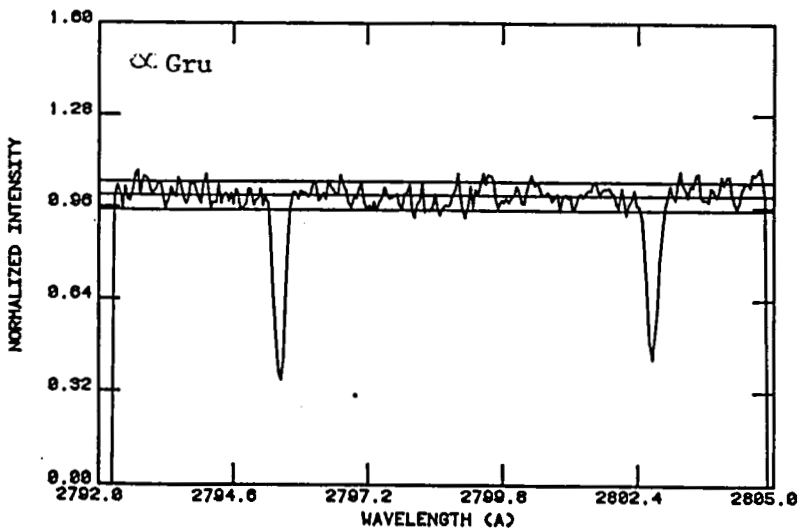

Figure 3. Interstellar Mg I in Copernicus Data showing Interstellar Mg I in α Gru.

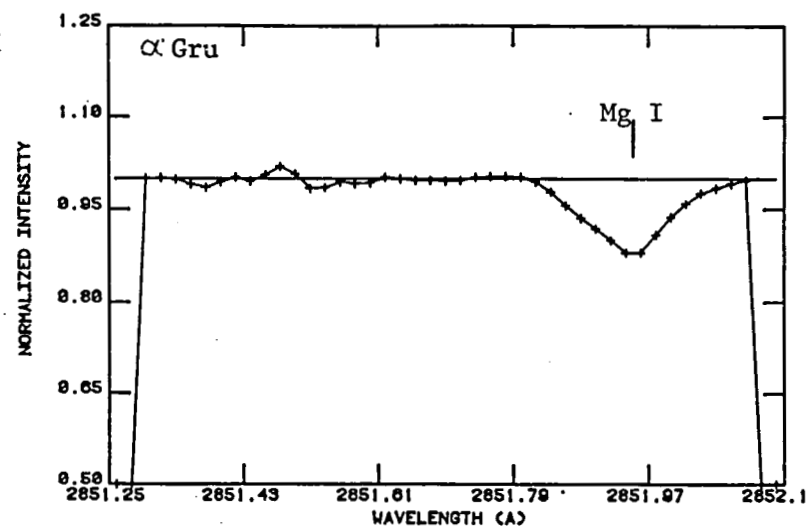

THE DEPENDENCE OF INTERSTELLAR ELEMENT DEPLETIONS ON MEAN SPACE DENSITY

Alan W Harris* and Gordon E Bromage
Astrophysics Group, Rutherford Appleton Laboratory, UK

Cecile Gry*
Astronomy Division, ESTEC

*(IUE Observatory, ESA, Apartado 54065, Madrid, Spain)

ABSTRACT

Correlations of interstellar gas-phase depletions with hydrogen column density N(H), and with mean line-of-sight space density $\bar{n}(H) = N(H)/r$, are investigated for 14 elements. For the 6 most depleted elements, correlations with $\bar{n}(H)$ are clearly stronger than with N(H). In general, the survey supports the proposal that depletion is mainly governed by density-dependent processes. It also suggests that depletion occurs in relatively low density gas as well as in dense clouds.

INTRODUCTION

Investigations of absorption by interstellar gas in the sight-lines to many stars have been carried out with the Copernicus and IUE satellites. Moreover, the total amount of archived data now enables surveys to be made of absorption by particular elements in a large number of sight-lines, with a wide distribution of galactic co-ordinates, column densities, and so on.

Two of the most interesting trends in these data, of relevance to theories of grain formation and gas-grain interactions, are the correlations of gas-phase depletion with element condensation temperature and with mean space density. The more volatile elements are less depleted; and depletion increases with space density (see: Savage and Mathis 1979 for a review and references to original work). There is now increasing evidence (Savage and Bohlin 1979, Phillips et al 1982, Murray et al 1984, Harris et al 1984) of good correlations between depletions of several elements such as Fe, Ca, Al, Mg, and the mean line-of-sight space density $\bar{n}(H) = N(H)/r$, where N(H) is the total H column density ($2N(H_2) + N(HI)$) and r is the sight-line length. We report here on detailed investigations of these trends, via surveys of the two volatile elements Zn and Cl using IUE and Copernicus data, and via a general survey of depletions and $\bar{n}(H)$. These surveys are described in more detail elsewhere (Harris et al 1983, 1984; Harris and Bromage 1984).

ZINC AND CHLORINE

Both zinc and chlorine are volatile, and early Copernicus results suggested they were both undepleted. Zinc is particularly suitable for study with IUE.

The main conclusions from the zinc study (Harris et al 1983, 1984) are that the element is only very slightly depleted (0.2 dex) and that the abundance is essentially independent of N(H) and $\bar{n}$(H). For example, the linear correlation coefficient for abundance versus log $\bar{n}$(H) is only 0.24 and the slope of the best fit is only 0.08 dex per order of magnitude change in $\bar{n}$(H). Indeed the abundance of zinc is so invariant that Harris et al (1983) suggested the element can be used as a rather reliable tracer of metallicity in the interstellar medium.

However, chlorine behaves differently. Harris and Bromage (1984) have demonstrated the completely unexpected result that the chlorine abundance shows a marked decrease with increasing $\bar{n}$(H). It seems that chlorine adheres to dust grains rather more readily than was previously thought.

GENERAL SURVEY: RESULTS

Bearing in mind the earlier demonstration of a strong correlation of depletion wi th $\bar{n}$(H) by Savage and Bohlin (1979) for highly-depleted Fe, together with our detailed results for Zn and Cl, we undertook a general survey using published data. We investigated the correlations of depletion with both N(H) and $\bar{n}$(H). The data sources are given in Harris et al (1984). The main results are summarised in Table 1, where the elements are listed in order of decreasing mean depletion. For the 6 most heavily depleted elements, the correlation with $\bar{n}$(H) is clearly the stronger one. This is surprising if depletion only occurs in dense clouds, since N(H) would then be the more realistic density indicator. Thus our results are consistent with a more homogeneous distribution of depleted gas.

Table 1

Species	Mean depletion (dex)	Correlation coefficient (linear) for abundance versus: (a) log N(H)	(b) log $\bar{n}$(H)
Ca II	3.2	.60	.87
Ti II	2.1	.70	.91
Fe II	1.9	.48	.75
Si II	1.0	.36	.43
Mg II	1.0	.79	.88
Cl I + II	0.5	.73	.85
P II	0.5	.78	.81
Ar I	0.3	.71	.71
C II	0.3	.50	.44
S II	0.2	.68	.64

Table 1 (Continued)

Species	Mean depletion (dex)	Correlation coefficient (linear) for abundance versus: (a) log N(H)	(b) log $\bar{n}$(H)
Zn II	0.2	.37	.24
N I	0.1	.26	.12
O I	0.1	.35	.15
D I	(?)	.23	.09

CONCLUSIONS

For heavily depleted elements, the correlation of depletion with $\bar{n}$(H) is clearly stronger than with N(H), whilst for Zn, N, O and D there is virtually no correlation with either quantity. No evidence is found for any significant depletion of deuterium. The two volatile elements Zn and Cl behave rather differently, with Cl being significantly depleted.

In general, the results support the proposal that depletion is mainly governed by density-dependent processes (grain accretion and/or sputtering). They also suggest that depletion occurs in relatively low density gas as well as in dense clouds.

In conclusion it should be emphasised that our surveys described above are but preliminary steps, in that they mainly use integrated line-of-sight parameters. The trends revealed are both exciting and tantalising. We eagerly await the next generation of far-ultraviolet astronomy experiments to probe the sight-lines to distant objects at higher spectral resolution than IUE, and at shorter wavelengths than either IUE or the HST.

REFERENCES

Harris A W, Bromage G E and Blades J C, 1983, MNRAS 203, 1223.
Harris A W and Bromage G E, 1984, MNRAS, in press (RAL-84-004).
Harris A W, Gry C and Bromage G E, 1984, Ap J, in press (RAL-84-013).
Murray M J, Dufton P L, Hibbert A and York D G, 1984, Ap J, in press.
Phillips A P, Gondhalekar P M and Pettini M, 1982, MNRAS 200, 687.
Savage B D and Bohlin R C, 1979, Ap J 229, 136.
Savage B D and Mathis J S, 1979, Ann Rev Astron Astrophys 17, 73.

HIGH-VELOCITY INTERSTELLAR GAS IN THE LINE-OF-SIGHT TO HD 50896

Joy N. Heckathorn
Computer Sciences Corporation

Robert A. Fesen
University of Colorado

ABSTRACT

Using high-dispersion IUE spectra, we have discovered a large interstellar shell structure in the line-of-sight to the Wolf-Rayet star HD 50896. Blue-shifted interstellar absorption lines indicative of high-velocity gas are present in the spectra of four B stars located up to 2° away from HD 50896 and at a distance of 1000-1400 parsecs, suggesting a linear diameter for the structure of at least 40 parsecs. These high-velocity components, present only in the low ionization lines and exhibiting nearly cosmic abundances, can be interpreted as a heretofore unknown and extremely old supernova remnant. The existence of such a supernova remnant potentially associated with HD 50896, a runaway Wolf-Rayet star believed to have a compact companion, implies that HD 50896 may be a binary in its second Wolf-Rayet phase of evolution.

INTRODUCTION

Wolf-Rayet stars are generally believed to evolve from either massive single O stars or from binary systems containing massive O stars. The scenario for binary stars is that two OB stars undergo mass transfer through stellar winds and Roche Lobe overflow of the primary to produce a Wolf-Rayet star and an OB star (de Loore, 1981). The Wolf-Rayet star then becomes a supernova, leaving a neutron star. Assuming the system remains bound, the remaining OB star then evolves into a Wolf-Rayet star by means of mass transfer and may also ultimately undergo a supernova explosion.

Although a crucial test of this evolutionary theory would be to find objects in the second Wolf-Rayet star phase of evolution, no Wolf-Rayet star has been associated with a known supernova remnant. This is perhaps not surprising since the maximum lifetime for a supernova remnant to be detectable via either radio or optical emission is 10^5-10^6 years, which is less than the predicted time between the supernova explosion and the beginning of the Wolf-Rayet stage for the secondary (de Loore, 1982). However, the column densities of the cool dense shell in

such an old supernova remnant (SNR) should be sufficient to be detected in absorption with IUE. HD 50896 is one of six known runaway Wolf-Rayet stars and is believed to have a compact companion (Firmani, et al., 1980). Also, it is well below the galactic plane (b=-10°) allowing less confusion in detection of any high-velocity shell structure. It is therefore a prime candidate for the second Wolf-Rayet star stage of binary evolution having an associated, highly evolved SNR.

OBSERVATIONS

High dispersion IUE spectra of HD 50896 show high-velocity components in the low-ionization interstellar lines (Smith, et al. 1978). We have observed eight B stars at high dispersion within 2° of HD 50896. Four of these stars (see Table 1) were found to show high velocity components of the same low-ionization interstellar lines that appear in the spectra of HD 50896. These low ionization lines are MgII, C II, Si II, Al II, Fe II, and O I. The spectra of the most distant target, HD 51285 at 2.9 kpc, show 2 distinct high-velocity components at -115 and -80 km/sec, both of comparable strength (Fig. 1). HD 50896, HD 51854, and HD 50646 generally show only a component at -80 km/sec. However, an additional weak component at -100 km/sec is present in Mg II in the spectra of HD 50896. This is consistent with the earlier, higher resolution Copernicus data (Shull, 1977). The spectra of HD 51038 differs from the others in that only the component at -100 km/sec is present, with equivalent widths 30-50% of the equivalent widths in the high-velocity components of the other stars.

DISCUSSION

We believe we have detected a large, expanding shell-like structure, the near side having a radial velocity of approximately -115 km/sec and the far side having a radial velocity of about -80 km/sec with respect to the main interstellar component at +36 km/sec. The data indicate that: 1) The star HD 51285 is behind the structure we have detected, and that the near and the far sides are approximately equally dense in this line of sight, 2) The stars HD 50896, HD 51854 and HD 50646 are probably also background to the structure, but in these cases, the front side of the structure is much less dense than the back side and the components are blended, and 3) HD 51038 may be within the structure, because it shows only the higher velocity component. Based on these conclusions, the distance to the shell would be about 1.1 kpc, its radius at least 20 parsecs, the radial velocity of the medium in which the shell is moving -90 to -95 km/sec with respect to the main component, and the expansion velocity of the shell itself 15-20 km/sec.

An alternate interpretation of these observations might be that all the high-velocity components arise in the front side of the shell structure, representing filaments moving at velocities ranging from -80 to -115 km/sec. The back side, being at a greater z distance, may be much less dense than the front side, and possibly undetectable. In this case, the expansion velocity of the shell would be greater than 15-20 km/sec, but the distance estimate would be approximately the same.

The parameters of the shell we have detected appear consistent with those of an old supernova remnant. No star in the field could have sufficient stellar wind to produce an interstellar bubble of this magnitude, other that HD 50896, which appears to be outside the shell. Also, the shifted components are present only in the low ionization lines and the expansion velocity is low, as would be expected for an very old SNR (Woltjer, 1972). If HD 50896 was in fact the OB companion to the star which caused the SN explosion, it would have moved well outside the SNR (to a distance of approximately 200 parsecs from the center of the remnant) when the Wolf-Rayet phase began after about 6×10^6 years (de Loore, 1982), based on a radial velocity of 36 km/sec. It therefore appears a viable possibility that HD 50896 is related to the old supernova remnant we have detected.

CONCLUSIONS

In summary, a large interstellar structure at least 20 parsecs in radius and expanding at 15-20 km/sec has been detected in the line-of-sight of HD 50896 by means of interstellar absorption lines in the IUE spectra of field stars. This structure may be the remnant left by the supernova explosion caused by the companion to HD 50896. If this scenario is correct, HD 50896 would then represent the second Wolf-Rayet stage of the evolution of a massive OB binary.

REFERENCES

de Loore, C.,1981: Effects of Mass Loss on Stellar Evolution, ed. C. Chiosi and R. Stalio (D. Reidel), 405.

de Loore, C., 1982: Wolf-Rayet Stars: Observations, Physics, Evolution, ed. C. de Loore and A.J. Willis (D. Reidel), 343.

Firmani, C. Koenigsberger, G., Bisiacchi, G., Ruiz, E. and Solar, A., 1978: Mem. Soc. Astron. Ital., 49, 453.

Smith, C., Willis, A.J. and Wilson, R., 1980: Mon. Not. R. Astron. Soc., 191, 339.

Shull, J.M., 1977: Astrop. J., 212, 102.

Woltjer, L.,1972: Ann. Rev. Astr. Ap., 10, 129.

TABLE 1

Object	Spectral Type	Distance	Shifted Component Present?
HD 51285	Be	2.9	yes
HD 51854	B2 IV	1.6	yes
HD 50896	WN5	1.4	yes
HD 50154	B3 V	1.2	no
HD 50646	B1 V	1.1	yes
HD 51038	B3 V	1.1	yes
HD 49233	B5	0.9	no
HD 51283	B1 III	0.8	no
HD 52596	B3 V	0.6	no

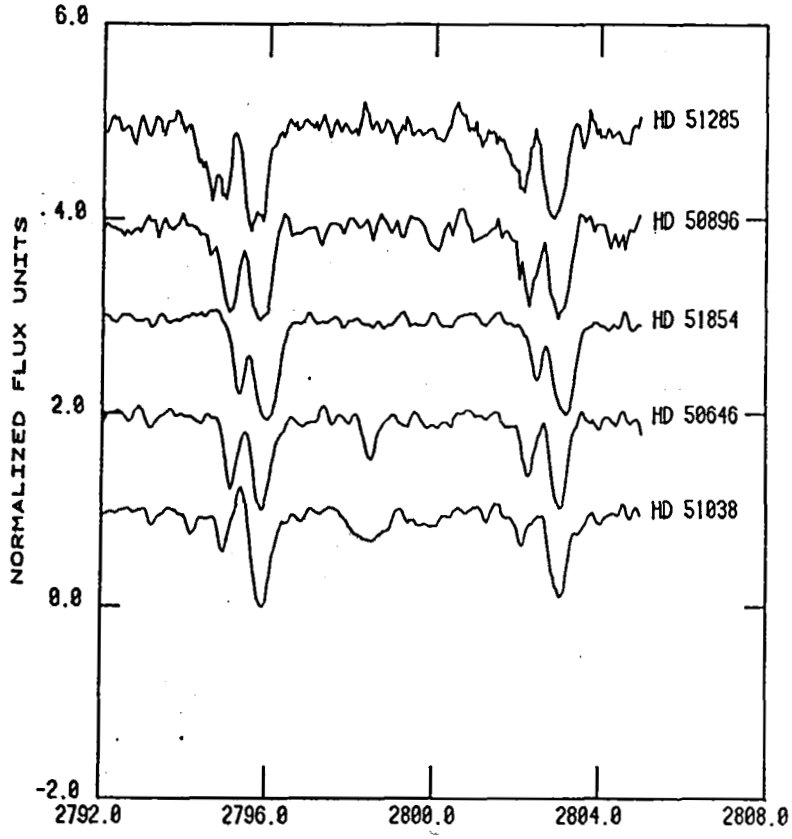

Figure 1: Montage of IUE spectra in the region of the Mg II lines for HD 50896 and 4 stars that show the presence of high-velocity components.

The Variation of Galactic Interstellar Extinction in the Ultraviolet

A. N. Witt, Univ. of Toledo; R. C. Bohlin, STSI;
and T. P. Stecher, GSFC

The interstellar extinction in the UV ($3.25\ \mu^{-1} \leq \lambda^{-1} \leq 8.0\ \mu^{-1}$) has been determined from IUE spectra for 29 reddened early-type stars by use of the pair method. The star sample was selected on the basis of highly deviant ratios of the strength of the λ4430 Å diffuse interstellar absorption feature to color excess E(B-V) (15 stars) and on the basis of association with reflection nebulae (9 stars). The incidence of peculiar extinction curves among this sample as measured by significant deviations from the mean galactic extinction law is near 70%. Deviations in the strength of the λ2175 Å extinction bump appear to occur independently of deviations in the rise of the far-UV extinction at λ1250 Å in about 35% of the stars. On the average, stars associated with dense interstellar clouds exhibit weaker UV extinction in the $\lambda < 2500$ Å range than do stars observed through low-density diffuse clouds, if normalized to constant E(B-V). At λ1250 Å this difference between the averages of the two groups amounts to 27%, measured in units of the average galactic extinction per unit E(B-V) at λ1250 Å, but wide dispersions are evident for both groups.

The average galactic extinction in the UV for diffuse cloud stars, measured by E(1250-V)/E(B-V) and E(2160-V)/E(B-V), was found to be distinctly higher than the galactic average based on the mean galactic extinction law of Savage and Mathis. The average strength of the 2200 Å extinction bump was found to be the same for both types of cloud environment and to agree with the previous galactic average.

Earlier claims by other authors regarding regional variations of UV extinction characteristics dependent on position in galactic longitude or on location within the Perseus arm are supported by our results.

A detailed account of the work will be published in the April 15, 1984, issue of the Astrophysical Journal. Material support was provided by the National Aeronautics and Space Administration through grants NAG 5-167 and NAGW-89.

INTERSTELLAR EXTINCTION IN THE NUCLEUS OF H PER *

A. Magazzu[1] and *R. Stalio*[2],[3]

(1) SISSA-ISAS, Trieste; (2) Osservatorio Astronomico, Trieste; (3) National Solar Observatory, Tucson

We construct the extinction curves in the direction of four early-B main sequence stars located in the nucleus of h Per: BD+56°501, BD+56°510, Oo 929 and Oo 936 (Oo numbers are from Oosterhoff, 1937), and compare them among each other and with the extinction curves derived from eight stars of the same general area but lying at different distances. UBV photometry and low dispersion optical and ultraviolet (IUE) spectroscopy were used to derive these curves. The results of this study can be summarized as follows:

(a) The interstellar reddening law in the line of sight of the four h Per stars is constant. This result, together with the constant color excess found by Crawford et al. (1970) for a larger sample of member stars, indicates that there is no appreciable gradient in the properties of the dust particles within the nucleus itself, contrary to what was suggested by Wildey (1964).

(b) The same curves agree well with the curves derived from stars located in the region of the Perseus arm surrounding the cluster. This indicates that the interstellar medium in h Per has the same properties as the medium outside the cluster; thus the high energy radiation and mass fluxes produced by the very large number of hot star populating h Per do not affect the properties of the dust particles.

(c) There is a rather smooth decrease of the extinction per unit distance with increasing height from the galactic plane which is consistent with the expected lower column densities of the interstellar medium at higher galactic latitudes and suggests the absence of any enhancement in the Perseus arm.

References

Crawford, D. L., Glaspey, J. W., Perry, C. L.: 1970, *Astron.J.*,75,822

Oosterhoff, Ph. T.: 1937, *Ann.Leiden*,17, 1

Wildey, R. L.: 1964, *Astrophys.J.Suppl.*,8, 439

* Paper submitted to Astronomy and Astrophysics.

HOT STARS

CORONAL EFFECTS ON THE WINDS OF EARLY-TYPE STARS

Wayne L. Waldron

Applied Research Corporation
and
Bartol Research Foundation, University of Delaware

ABSTRACT

The X-ray emission from early-type stars can be a dominant factor in determining the ionization structure of a stellar wind. Using a base coronal model, the UV resonance lines of N V, Si IV, and C IV are calculated by subjecting them to changes in the coronal emission measure, coronal temperature, and mass loss rate. The calculations predict that a unique behavior is present in the variations of these line profiles. This suggests that it would be possible to distinguish which quantity was responsible for the variation. A preliminary search for this predicted variability, using the high-resolution SWP data from the IUE archives, has been conducted for several stars.

INTRODUCTION

One of the present unsolved problems concerning the atmospheres of early-type stars is determining the source and location of the X-ray emission. Models developed to explain the X-ray emission suggest that radiatively driven shocks occuring in the stellar wind may produce the observed X-rays (Lucy and White 1980), or that coronal zones located at the base of the stellar wind may be responsible (Cassinelli and Olson 1979; Waldron 1984). It is quite possible that both processes may contribute to the observed X-rays. However, Waldron (1984) has shown that the base coronal model alone can be very successful in reproducing the observed IPC X-ray spectra for early-type stars.

Variability in the UV lines of early-type stars has been known for several years. Recently, variability in the X-rays has also been detected for several early-type stars (Snow et al. 1981; Cassinelli et al. 1983). The variability in the UV and X-rays both have time scales ranging from hours to years. Waldron (1984) noticed that small changes in the coronal properties of a base coronal zone can produce significant changes in the total wind structure (i.e., velocity, ionization). These changes should be reflected in the UV resonance lines and may provide a useful diagnostic in the understanding of UV line variability.

MODEL UV RESONANCE LINES

Using the base coronal models of Waldron (1984), model P-Cygni line profiles of N V, Si IV, and C IV are calculated by subjecting them to changes in the coronal emission measure, EM_c, coronal temperature, T_c, and mass loss rate, $\dot{M}$. The models were calculated assuming a single component of the doublet. Therefore, only the absorption side of the P-Cygni profile is appropriate in comparing with the observations, and are shown in Figure 1 for the star ϵ Ori (B0Ia). The curve labeled 2 corresponds to the base coronal model that gives

the best fit to the observed X-rays. The other curves represent changes in EM_c and $\dot{M}$ by ±10% and T_c by ±25%. In each case, while one quantity was varied, the other two quantities were held fixed at their values indicated by curve 2.

Several interesting features are illustrated in Figure 1: (1) The C IV line remains saturated, while significant changes can occur in the N V line at high velocities, and the Si IV line at low velocities. (2) Changes in T_c or $\dot{M}$ produce the same effect in all 3 lines, except that a larger change in T_c (±25%) is needed to produce an equivalent effect by a smaller change in $\dot{M}$ (±10%). (3) An increase/decrease in EM_c (Fig. 1a) produces the same effect as a decrease/increase in T_c (Fig. 1b) or $\dot{M}$ (Fig. 1c). (4) However, the Si IV line has a unique behavior that provides a way to distinguish which quantity was responsible for the change. For an increase in EM_c, the Si IV absorption becomes stronger at high velocities, and weaker at low velocities. Correspondingly, a decrease in T_c or $\dot{M}$ produces weaker absorption at both high and low velocities in Si IV. (5) Another important result is shown in the N V line when $\dot{M}$ is increased, in that the strength of the absorption decreases contrary to what one would normally expect. The reason for this effect is that by increasing $\dot{M}$, the absorption of X-rays by the wind becomes stronger, and the ionic abundance of N V decreases.

These characteristic features are directly related to the strength of the X-ray flux throughout the stellar wind and the resultant velocity and ionization structures. A detailed discussion of this UV variability and the corresponding variability in the X-rays is currently in preparation for publication elsewhere.

OBSERVATIONS AND SUMMARY

A preliminary search for this predicted variability focused on stars which are known or suspected X-ray variables. The high-resolution SWP data were obtained from the IUE archives and reduced at the Goddard Space Flight Center reduction facility. The spectra were normalized to their respective continuum values, and the wavelength scales were converted to a normalized velocity scale. The uncertainties in the flux are approximately ±10%.

The results of 2 stars are shown in Figure 2. The first thing to notice is that for both stars, the C IV lines are essentially unchanged and the N V, Si IV lines do indicate variations as suggested by the models. For ϵ Ori, between the dates indicated by curve 1 and 2, the variations in N V and Si IV may have been produced by an increase in T_c or $\dot{M}$ (decrease in absorption in N V at high velocities; increase in absorption in Si IV at both high and low velocities). For δ Ori, the change indicated by curve 1 and 2 in N V and Si IV is suggestive that a decrease in EM_c may have occured (decrease in absorption in N V at high velocities; and for Si IV, a decrease in absorption at high velocities and a increase at low velocities). However, for both stars the variations are marginally close to the uncertainties in the flux.

Similar results have been detected in a few other stars, but the statistics are currently to weak to make any kind of definitive statement on

whether the predicted variations have been observed. It is planned to continue searching for these systematic variations in the N V and Si IV lines, and develop other models for a broader range of stars.

This work was supported in part by NASA grant NAG5-344 at the Bartol Research Foundation.

REFERENCES

Cassinelli,J.P., Hartmann,L., Sanders,W.T., Dupree,A.K., and Myers,R.V. 1983, Ap.J.,268,205.
Cassinelli,J.P., and Olson,G.L. 1979, Ap.J.,229,304.
Lucy,L.B., and White,R.L. 1980, Ap.J.,241,300.
Snow,T.P., Cash,W., and Grady,C.A. 1981, Ap.J.(LETTERS),244,L19.
Waldron,W.L. 1984, Ap.J.,282 (in press).

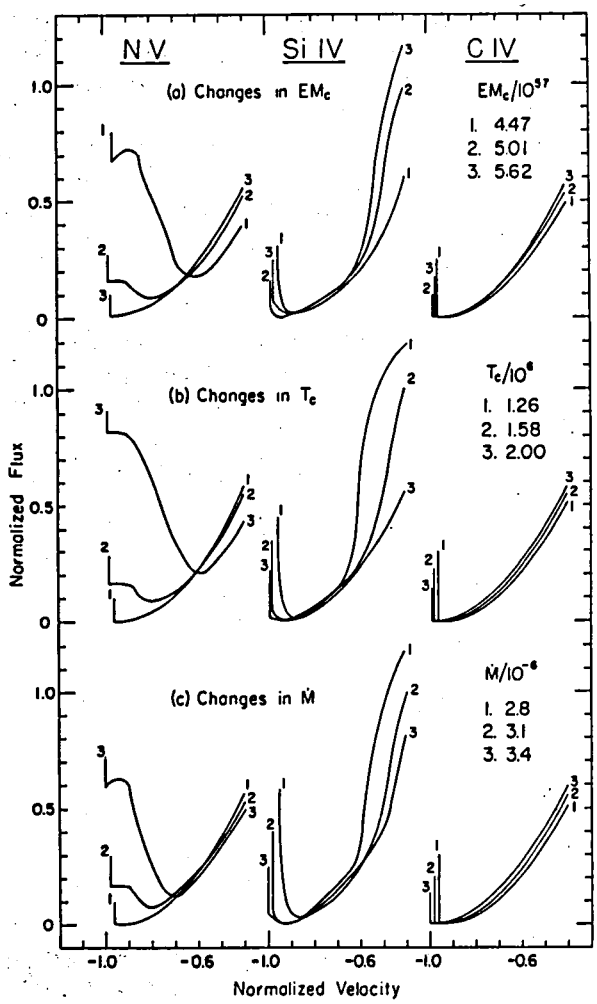

Figure 1. Model P-Cygni absorption features for ϵ Ori are shown for the resonance lines of N V, Si IV, and C IV.

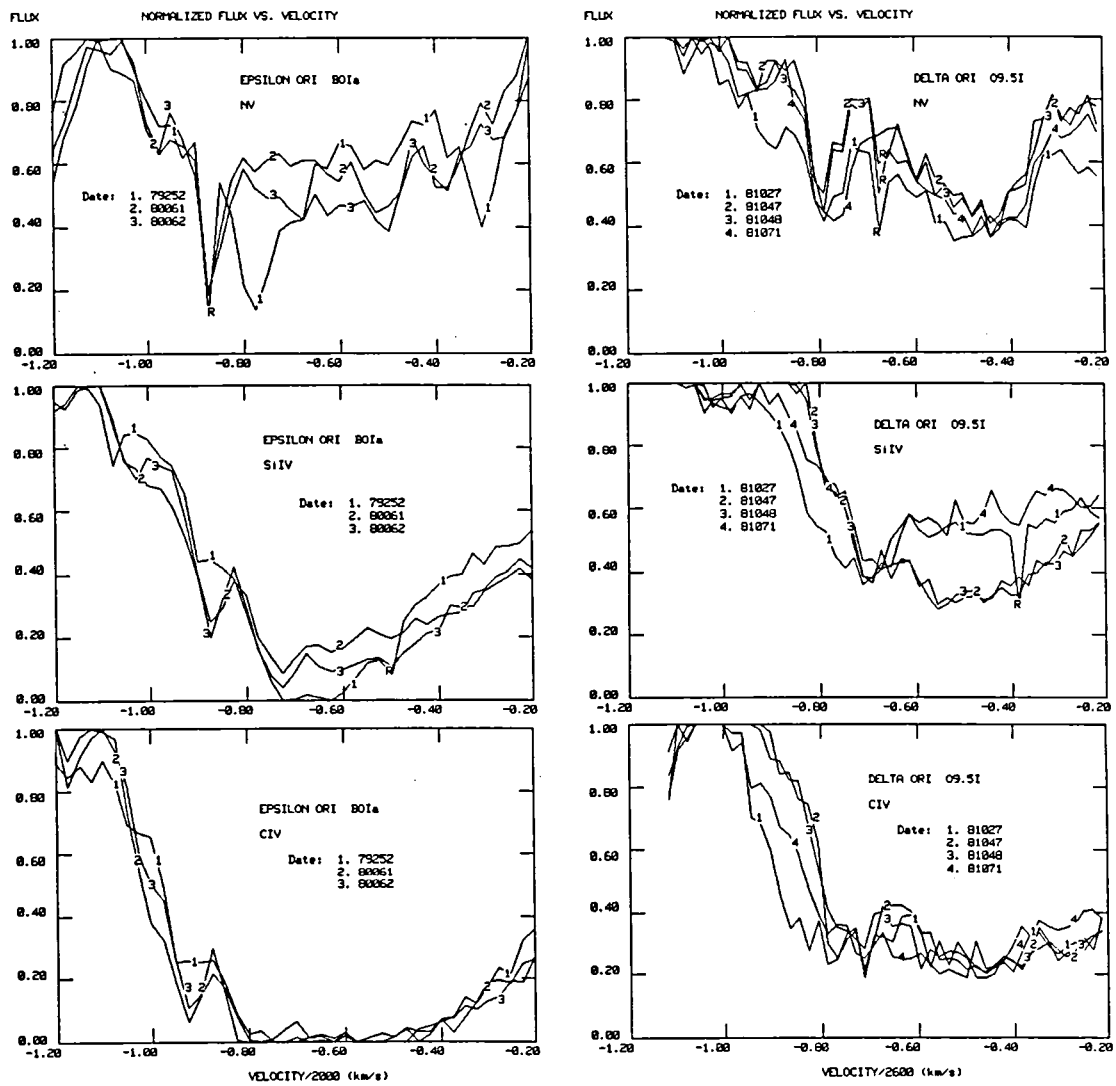

Figure 2. Observational data showing the P-Cygni absorption features for ϵ and δ Ori. The dates of the observations are indicated in each figure.

SUPERIONIZED SPECIES AND WINDS IN LOW LUMINOSITY B AND Be STARS

Paul K. Barker, J. M. Marlborough, and J. D. Landstreet
Department of Astronomy, University of Western Ontario

ABSTRACT

High dispersion IUE spectra have been obtained of 72 luminosity class III-V Be stars and 82 luminosity class IV-V normal (no Hα emission) B stars, with the objects in each group distributed at random in projected rotational velocity and spectral type. For normal B stars, the C IV λλ1548,50 resonance doublet is observed only at type B2 or earlier, whereas C IV can occur as late as B9 among the Be stars. In both groups of stars the average C IV equivalent width is greatest at the earliest spectral types, and decreases rapidly in strength toward later types; however, at each spectral subtype a large range of C IV equivalent widths exists. From B0 to B2 the average C IV equivalent width is about a factor of two higher for Be stars than for normal B stars. For the Be stars there is no correlation between the equivalent widths of C IV absorption and Hα emission. Neither normal B nor Be stars show any clear correlation between C IV equivalent width and projected rotational velocity v sin i. C IV emission is definitely present in only two Be stars; this is is sharp contrast to the magnetic stars in this spectral region, which frequently show C IV strongly in emission above the continuum.

INTRODUCTION

In previous investigations (Snow 1981, 1982; Marlborough and Peters 1982; Slettebak and Carpenter 1983) it has been demonstrated that the resonance doublets of "superionized" species such as N V, C IV, and Si IV may be present in the UV spectra of near main sequence Be stars. These species often show extended shortward absorption and asymmetry, indicative of high velocity (∿1000 km/s) mass loss via a stellar wind. On the other hand, the Balmer emission lines in the optical spectra of Be stars apparently arise from an envelope whose expansion velocity is less than ∿100 km/s. Clearly one wishes to understand the relationships, if any, between the stellar winds and emission envelopes of Be stars, and between the stellar winds of Be and normal B stars.

Because relatively few Be stars have been observed in the prior studies--and even fewer normal B stars--a survey of superionized species has been carried out with IUE in a large sample of normal B and Be stars. Contemporaneous ground based observations of Hα were made with the University of Western Ontario intensifier-dissector-scanner (Barker 1983a,b).

RESULTS

This paper presents preliminary results of the survey, for the C IV doublet and Hα. The program stars, and their distribution in spectral type and v sin i, are shown in Figure 1. Note that there is a shortage of Be stars at moderate and low v sin i, as well as a lack of moderate and high v sin i B stars, for the earliest spectral types. Among Be stars, C IV can occur at much later spectral types than for normal B stars.

Figure 2 shows the measured C IV absorption equivalent widths; at each spectral subtype there is a large range of equivalent widths, and the average C IV strength decreases rapidly toward later types. There is a significant difference between the Be and normal B stars in that not only does C IV occur for later types among the Be stars, but also the average C IV equivalent width from B0 to B2 is about a factor of two higher for Be stars than for normal B stars. Figure 2 also shows that there is no obvious correlation between C IV equivalent width and v sin i in either group of stars. Note that the apparent excess of normal B stars with strong C IV at low v sin i arises because the normal B stars show C IV only for types B2 and earlier, and there is a short-

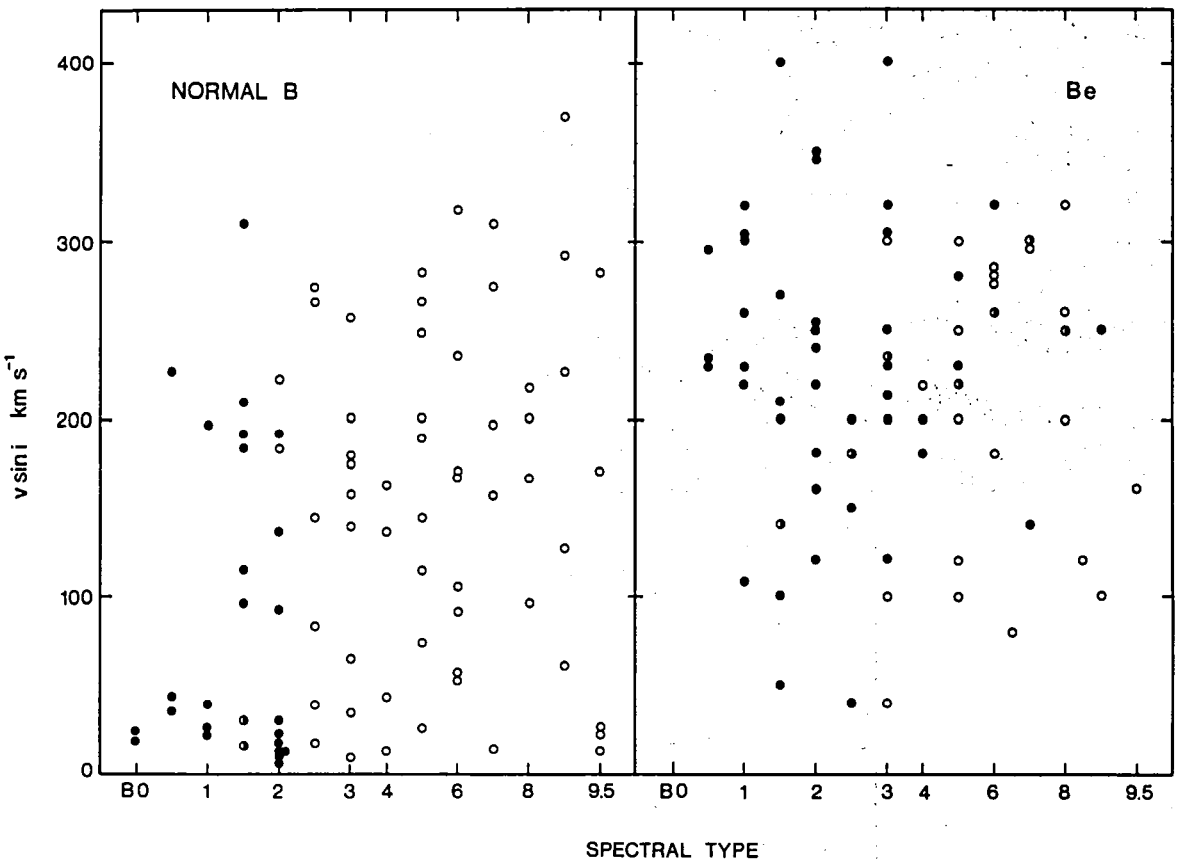

Figure 1.--The distribution in spectral type and v sin i of the normal B and Be stars surveyed. Filled circles mark those stars in which C IV λλ1548,50 is definitely present; half-filled circles represent objects in which C IV may be present; open circles locate stars with no identifiable C IV.

age of high v sin i normal early B stars in the sample. Similarly, the superficial lack of low v sin i Be stars with strong C IV may reflect only the scarcity of low v sin i Be stars in general. The luminosity class III Be stars tend to have the strongest C IV at each subtype, but the class III stars are scattered throughout the C IV/v sin i diagram.

Figure 3 demonstrates the complete lack of any correlation between the equivalent widths of C IV absorption and Hα emission among the Be stars. Thus, if there is any strong physical relationship between the stellar winds and Balmer emission envelopes of Be stars, it is not discernible in a "snapshot" survey such as this.

In the sample drawn from the 100 brightest northern Be stars, there are only two instances of definite C IV emission. However, the magnetic helium-strong stars in this spectral region (some of which do show weak Hα emission, and thus are magnetic Be stars) frequently have quite strong C IV emission above the continuum, from their magnetospheres and winds (Barker et al. 1982). Thus the distribution of circumstellar material around magnetic Be stars is

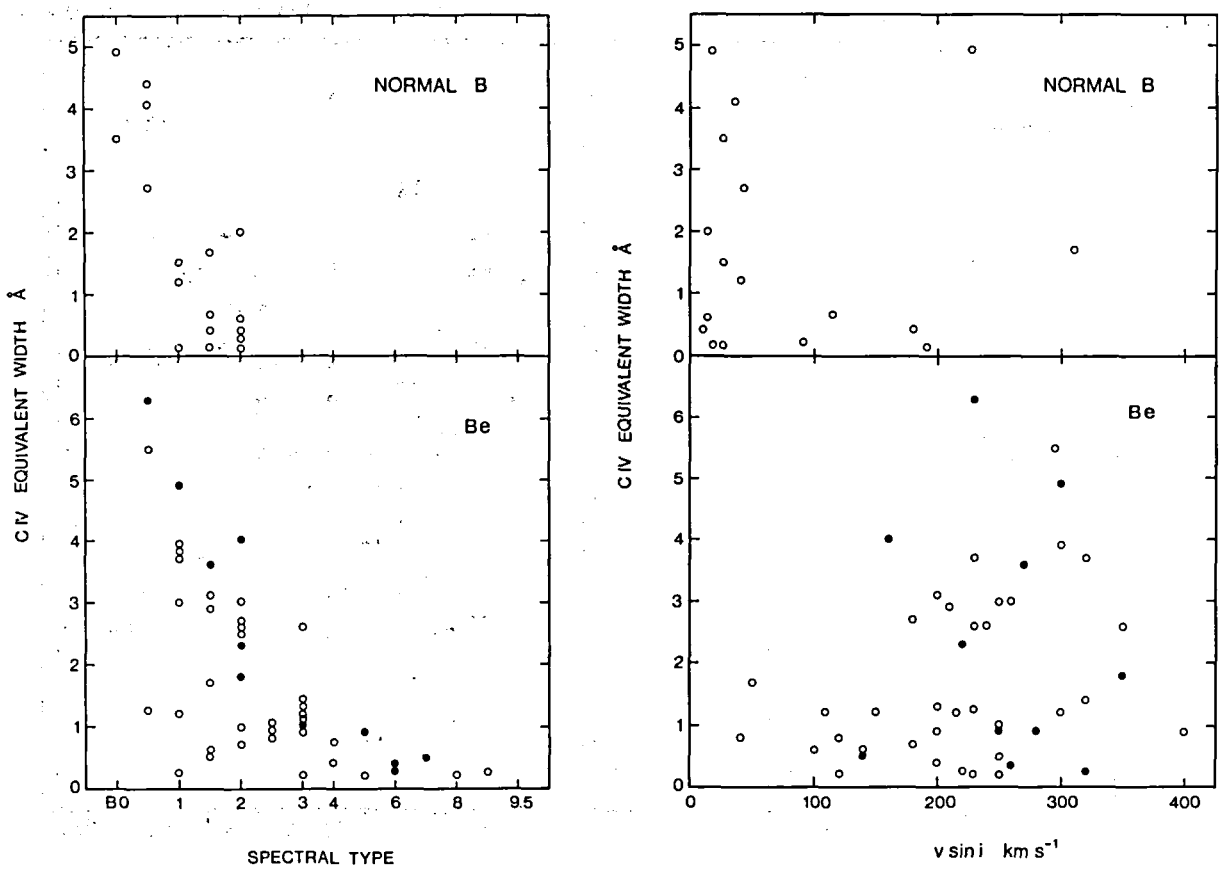

Figure 2.--Left panel shows the dependence upon spectral type of C IV equivalent widths measured in normal B and Be stars. Right panel shows the lack of correlation between C IV equivalent width and v sin i for both groups of stars. In both panels, filled circles identify the luminosity class III Be stars.

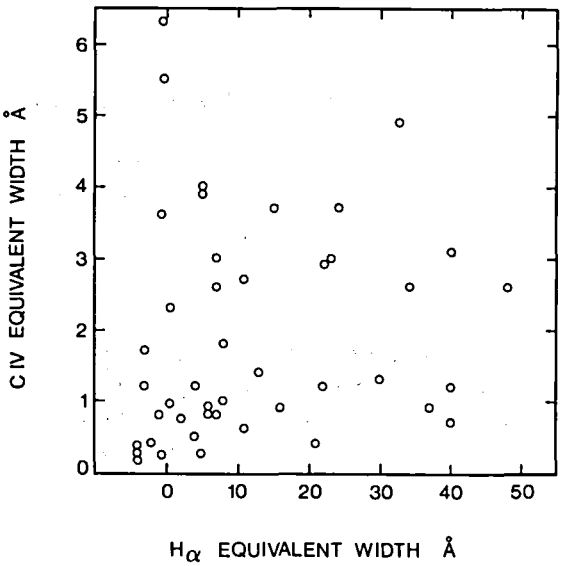

Figure 3.--The lack of correlation between the equivalent widths of C IV and Hα for Be stars. The Be stars with no C IV feature are also distributed randomly with respect to Hα emission strength.

likely to be significantly different from that around ordinary Be stars.

Future analysis of the large data base acquired during this survey will include examination of other superionized features such as Si IV, determination of terminal velocities and mass loss rates, and comparison with synthetic spectra in order to evaluate the effects of, for example, the blending of several Fe III lines with C IV. Multiple observations of more than half the sample will permit study of variability in Be and B stellar winds; a few repeatedly observed objects will further allow a search for any dynamic relation between C IV and Hα.

The contribution of the World Data Center A in supplying archival IUE data is acknowledged. This work was supported by the Natural Sciences and Engineering Research Council of Canada.

REFERENCES

Barker, P.K. 1983a, A.J., 88, 72.
-- -- -- --. 1983b, Pub. A.S.P., 95, 996.
Barker, P.K., Brown, D.N., Bolton, C.T., and Landstreet, J.D. 1982, in Advances in Ultraviolet Astronomy: Four Years of IUE Research, ed. Y. Kondo, J.M. Mead, and R.D. Chapman (NASA CP-2238), p.589.
Marlborough, J.M., and Peters, G.J. 1982, in IAU Symposium 98, Be Stars, ed. M. Jaschek and H.-G. Groth (Dordrecht: Reidel), p.387.
Slettebak, A., and Carpenter, K.G. 1983, Ap.J. Suppl., 53, 869.
Snow, T.P. 1981, Ap.J., 251, 139.
-- -- -- . 1982, Ap.J. (Letters), 253, L39.

STELLAR WINDS IN THE YOUNG GALACTIC CLUSTER NGC 6530

Erika Böhm-Vitense and Paul Hodge
University of Washington, Seattle

ABSTRACT

We have studied line profiles for O stars on or close to the main sequence in the young galactic cluster NGC 6530. P Cygni profiles are seen for $T_{eff} > 36000K$. Different stars show, however, different lines and different outflow velocities. The degree of ionization in the wind appears to depend on T_{eff}.

INTRODUCTION

It is well known that for early-type stars mass loss rates generally increase with increasing luminosity of the stars (Lamers 1981, Gathier, Lamers and Snow 1981). For given luminosities supergiants appear to have larger mass loss rates than main sequence stars. Since along the main sequence the luminosity decreases with decreasing T_{eff}, mass loss rates decrease when going down the main sequence. Mass loss for main sequence stars stops to be observable around spectral types BO. We still do not understand which mechanism starts the flow. We believe that once the flow has started, radiation pressure will accelerate it, though we also do not know how the observed momentum can be transferred from the photons to the wind. We also do not understand what causes the high degree of ionization in the winds, though X-rays from thin hot coronae have been suggested (Cassinelli and Olson 1979) as ionization sources for OVI. Since stellar winds die in a more or less continuous way, when we go down the main sequence we may be able to learn something about the ionization mechanism when studying systematic changes of ionization along the main sequence. Unfortunately, we cannot observe the OVI lines with IUE, which show the highest degree of ionization, but we can observe NV, NIV, CIV, HeII, SiIV, SiIII, CII, SiII.

For the stars in NGC 6530 we have the advantage to know that they are all on or close to the main sequence. We know they all have about the same age and chemical composition. The only free parameter is T_{eff} or L. Rotation could perhaps enter.

We have looked at the profiles of "wind" lines for stars in NGC 6530 with different T_{eff}. In the following we shall describe our results. We must admit that we do not yet understand them, but they look interesting anyhow.

THE OBSERVATIONS

High resolution spectra for our program stars were obtained either from the data bank or by us, if no spectra were available. The quality of some of our spectra suffered from high background radiation. In Figure 1 we reproduce the line profiles of the NV (1240 A) and the CIV (1550 A) lines for stars with different T_{eff}. NV (χ_{ion} (NIV) = 47.4) line profiles indicating its presence in winds is only seen for the hottest stars, 9 Sgr and W118. (W numbers are from Walker 1957.) HeII is only seen in the wind of W 118, which is a spectroscopic binary but may also be the hottest star in the cluster. It is interesting to note that the NIV line at 1718.5 A shows a P Cygni profile only for W7 = 9 Sgr. Even W118 does not show any indication of its presence in the wind, even though the NV and CIV lines are strong in the wind. For the cooler stars the CIV P Cygni emission disappears first, and then also the shortward extended wings. For W9 with $T_{eff} \sim 33000$K, no indications of a stellar wind are seen any more in the CIV line.

For the coolest stars like W73 ($T_{eff} \sim 30000$K) the CIV line looks like it has some shortward emission (see Figure 3). For this star we observe an extended shortward wing for the SiIV line 1393.75 which is not seen in the wind for any of the other stars (nothing is seen in the 1403 line). For this star we also see a blueward extended wing (vel $\sim$ 100 km/sec) for a narrow SiII line at 1808 A, which looks almost like an interstellar line. This line must be formed at a large distance from the star. It might then indicate that for this star the wind velocity is decreasing outward. The velocity seen in the SiIV line is less than the escape velocity.

For W93, also with $T_{eff} \sim 30000$K, the HeII, 1640 A, line and the CIV, 1550.8 A line show longward extended wings, extending to about 750 km/sec, which is about the free fall velocity for this star (see Figure 4).

We wonder whether for those stars close to the temperature when the wind dies, the wind may never reach escape velocities and may actually return to the star.

Of course, there may be higher velocity material which is optically too thin to be observable. The profile of the SiII line is certainly puzzling.

Generally, it seems that for decreasing T_{eff} the degree of ionization in the wind seems to decrease.

REFERENCES

Cassinelli, J.P., Olson, G.L. 1979, Ap.J. 229, 304.
Lamers, H.J.G.L.M. 1981, Ap.J. 245, 593.
Gathier, K., Lamers, H.J.G.L.M. and Snow, T.P. 1981, Ap.J. 247, 173.
Walker, M. 1957, Ap.J. 125, 636.

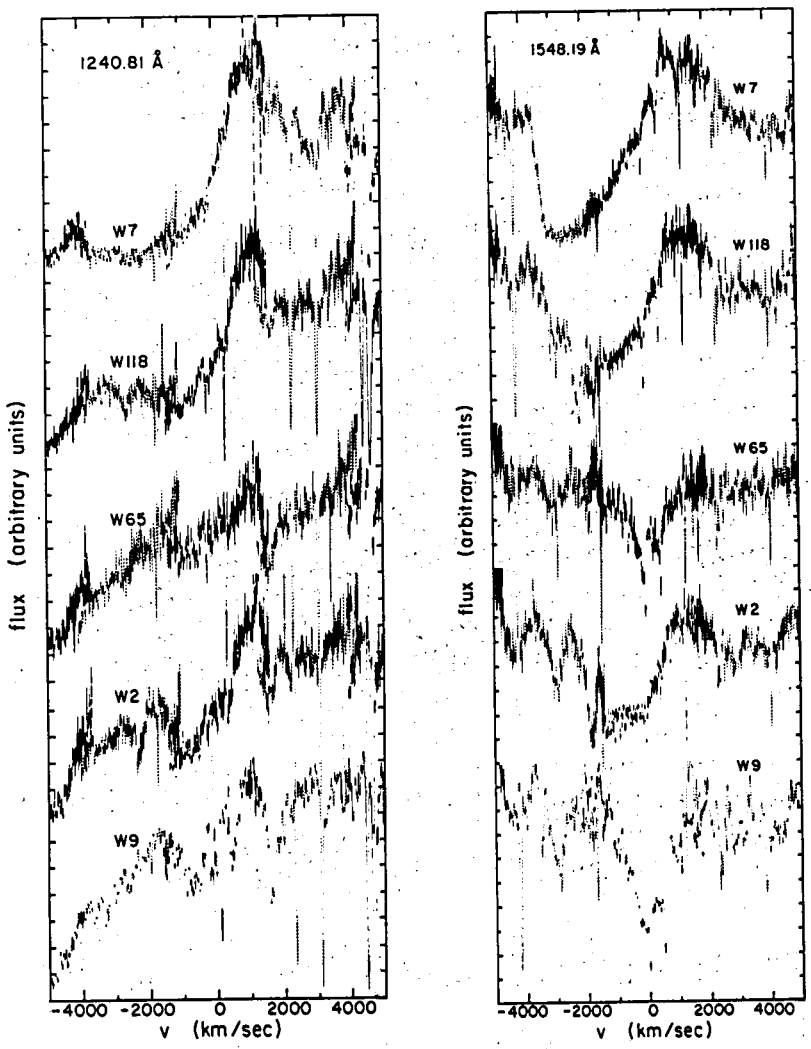

Figure 1. NV (1240 A) and CIV (1548 A) line profiles for stars in NGC 6530. The hottest stars are in the top line, the cooler stars at the bottom.

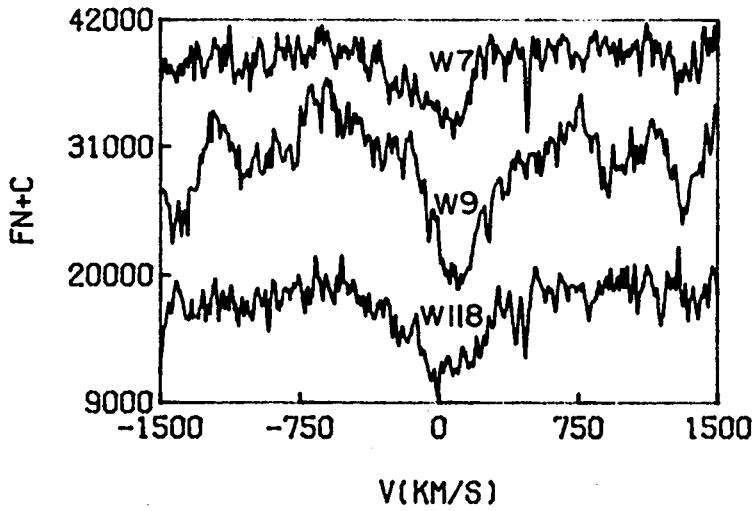

Figure 2. Line profiles for the HeII line at 1640 A.

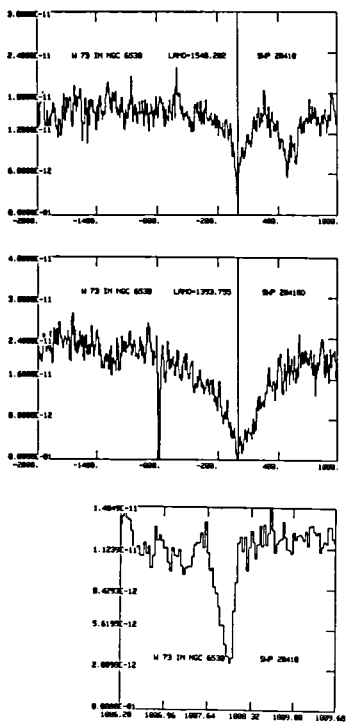

Figure 3. Line profiles in the star W73 with $T_{eff} \sim$ 30000K.

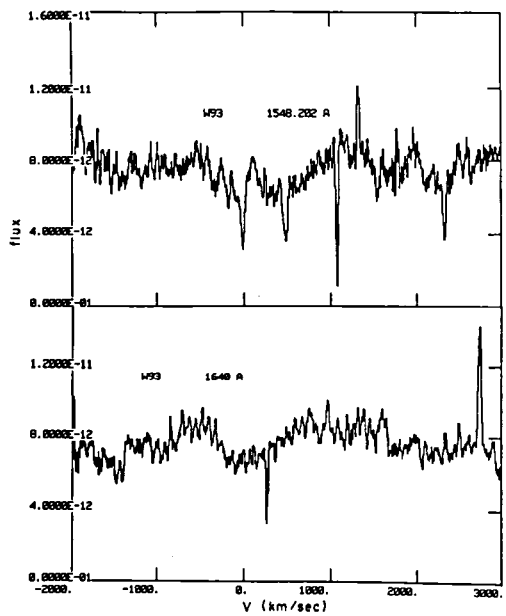

Figure 4. The CIV (1548 A) and the HeII (1640 A) line profiles in the star W93 show longward extended wings.

MAIN SEQUENCE B STARS WITH STRONG WINDS

D. Massa and B.D. Savage
Washburn Observatory, University of Wisconsin

INTRODUCTION

Aside from MK classifications, very little spectroscopic work has been carried out on distant main sequence B stars in either the visual or the UV. We obtained low resolution IUE observations of BO-2V stars in several young open clusters as part of a project to derive the UV extinction to the clusters. The aim of this study was to use the extinction found from the B stars to deredden the cluster O stars. In the process, it became obvious that the BO-2V stars in the nuclear cluster of Sco OB1, NGC 6231, had very unusual UV spectra. This discovery prompted us to obtain a high dispersion IUE spectrum of one of the peculiar NGC 6231 B stars, BD-41°7719.

OBSERVATIONS

Low resolution IUE spectra of the NGC 6231 B stars are presented in Fig. 1. Most of the program star spectra lie outside the 2-dimensional classification grid defined by the standards given by Wu et al. (1983). The CIV absorption in the spectra of HD326330, BD-41°7724, BD-41°7743, BD-41°7719 and BD-41°7727 is stronger than in any of the standards. The spectra of BD-41°7730, BD-41°7736 and Braes 1017 are also considered peculiar This is because the wavelength of the maximum depth of their CIV absorption is significantly shorter than any of the standards. BD-41°7719 (whose low dispersion spectrum is shown in Fig. 1) was observed at high dispersion. Its spectrum is remarkably similar to normal B1V stars except for the resonance lines of SiIV and CIV.

ANALYSIS

The model fits shown in Figure 2 use Olson's (1982) model for doublet formation in a stellar wind. It is obvious that BD-41°7719 has a much larger mass loss rate than normal B1V's although its CIV profile is still unsaturated. Furthermore, the wind of BD-41°7719 must accelerate very quickly. This is because its CIV profile shows little evidence for reemission by the wind even though there is substantial wind absorption. The model fit implies a mass loss rate of at least $4 \times 10^{-9} M_{\odot} yr^{-1}$ with a terminal velocity of 2,300 km/s. The lower limit for the mass loss rate was obtained by assuming that the CIV doublet furnishes all of the acceleration to the wind at high velocity. The parameters of the model fit can then be used to determine a minimum mass loss rate (see Lamers and Rogerson 1978).

DISCUSSION

Throughout the discussion, we assume that all the B stars with peculiar

UV spectra (see Fig. 2) also have strong winds. In a separate, but related, study we found that several of the O stars in NGC 6231 have abnormally large UV color temperatures. When the positions of all the peculiar cluster stars are plotted on the sky, a very interesting pattern emerges (see Fig. 3).

We now consider some likely causes for the strong B star winds.

Age - Their positions in the HR diagram of the cluster indicate that they are main sequence stars (see Garrison and Schild 1979).

Rotation - This explanation seems unlikely since none of the program stars are Be stars and their H beta photometric indices are normal.

Magnetic Fields - The argument against this origin is that the cluster contains very few stars with the spectral peculiarities normally associated with strong atmospheric magnetic fields (Garrison and Schild 1979).

Chemical Composition - An overabundance of carbon is certainly the most straightforward interpretation of both the strong wind and photospheric absorption of CIV in the spectrum of BD-41°7719. Walborn (1976) found a large number of chemically peculiar OB supergiants in Sco OB1 and noted a tendency for them to concentrate near NGC 6231. The fact that the main sequence O and B stars do not have MK peculiarities does not conflict with this interpretation because abundance anomalies of about 5 times solar will not be detected by MK classifications of these stars (Baschek and Scholz 1974).

There are also theoretical reasons to expect that unsaturated wind lines should be very sensitive to abundance anomalies. The reason is that metalic lines furnish the force responsible for radiatively driven stellar winds. Consequently, mass loss rates scale, roughly, as abundance. Furthermore, the optical depth of an overabundant ion in the wind also scales as its abundance. The net result is that the absorption of a wind line due to an overabundant element has an abundance squared dependence - one power from the increased mass loss rate and one power from the enhanced number of the element per unit mass in the wind.

All of these factors lead us to conclude that the peculiar spectra of the main sequence B stars in NGC 6231 are the result of an overabundance of carbon (and possibly other elements) in their atmospheres. Quantitative analysis shows that an enhancement of about 3-5 times solar is sufficient to explain the observations.

It is remarkable that the peculiar stars are concentrated in such a small region of space (Fig. 3). This suggests that small scale chemical inhomogeneities can develop within a molecular cloud complex either before or during the process of star formation and that the UV color temperatures of O stars may also be related to abundances.

REFERENCES

Baschek, B. and Scholz, M. 1974, Astr. Ap., 30, 395.
Garrison, R.F. and Schild, R.E. 1979, A. J., 84, 1020.
Lamers, H.J.G.L.M. and Rogerson, J.B. 1978, Astr. Ap., 66, 417.
Olson, G.L. 1982, Ap. J., 255, 267.
Walborn, N.R. 1976, Ap. J., 205, 419.
Wu, C.-C., et al. 1983, IUE NASA Newsletter, No. 22.

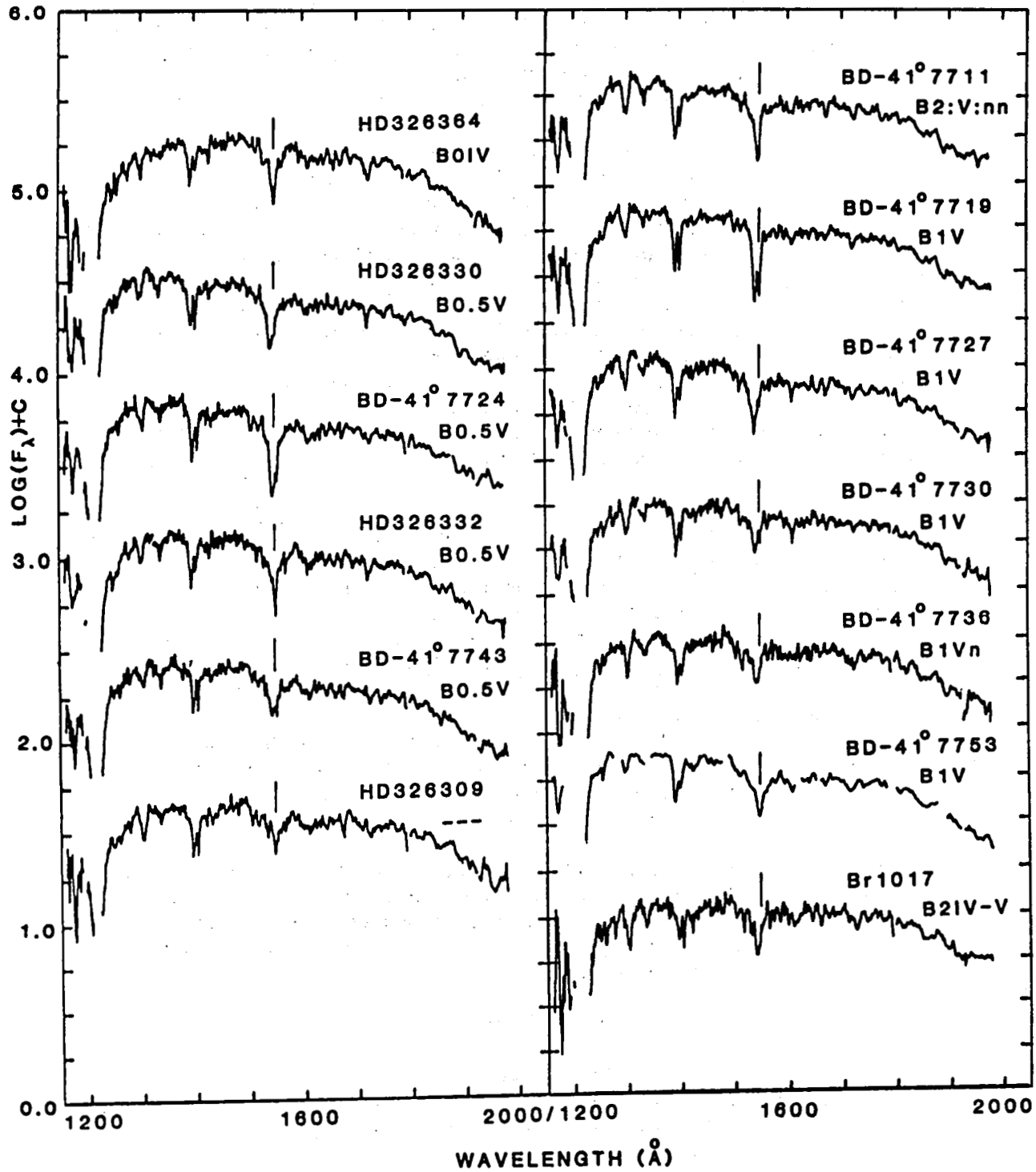
6.0
5.0
4.0
3.0
2.0
1.0
0.0
LOG(F$_\lambda$)+C
HD326364
B0IV
HD326330
B0.5V
BD-41°7724
B0.5V
HD326332
B0.5V
BD-41°7743
B0.5V
HD326309

BD-41°7711
B2:V:nn
BD-41°7719
B1V
BD-41°7727
B1V
BD-41°7730
B1V
BD-41°7736
B1Vn
BD-41°7753
B1V
Br1017
B2IV-V
1200
1600
2000/1200
1600
2000
WAVELENGTH (Å)

Figure 1

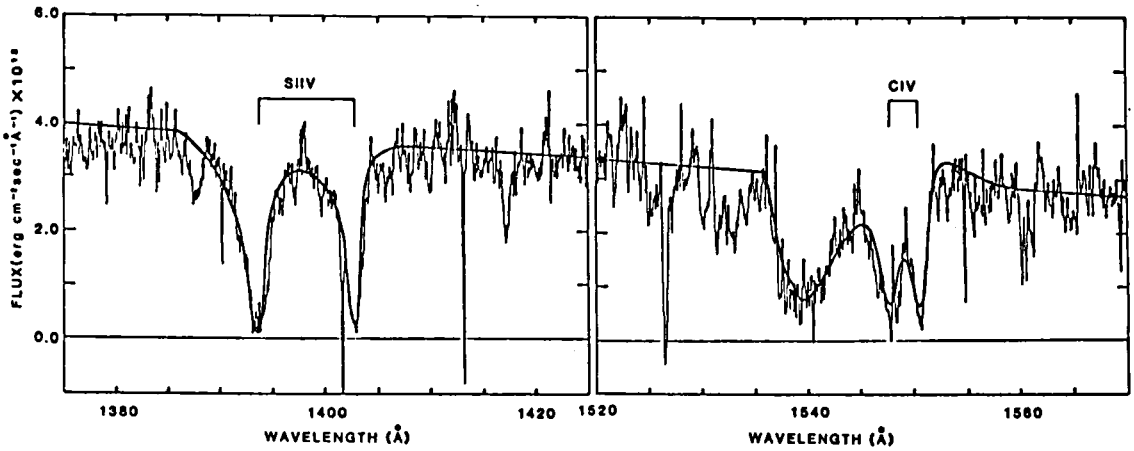

Figure 2

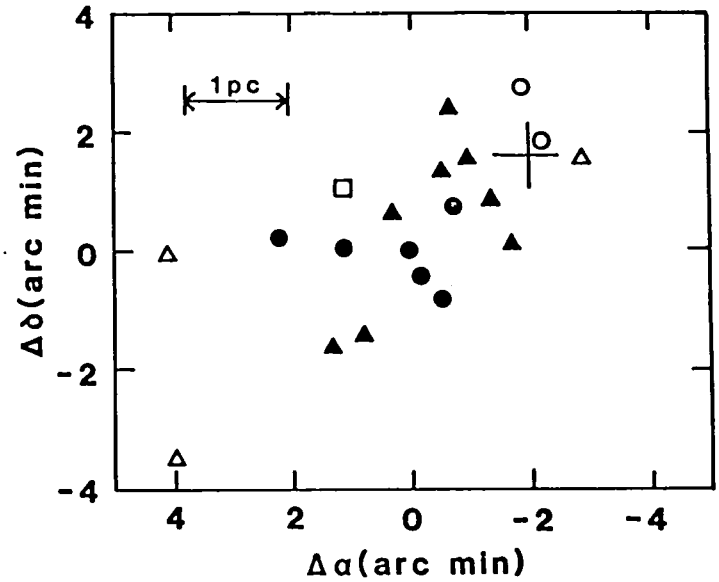

Figure 3. Distribution on the sky of NGC 6231 stars observed with IUE. The figure is centered on HD 152248 which defines the centroid of the O and early B stars in the cluster. The cross denotes the cluster centroid determined from star counts. Symbols represent the following: square - WC star; open circles - O stars with normal UV continua; filled circles - O stars with large UV color temperatures; open triangles - BO-2V stars with normal UV line spectra(HD 326309 and HD 326364 are beyond the boundaries of the figure); filled triangles - BO-2V stars with peculiar UV line spectra. A clustering of the peculiar stars is apparent.

IUE AND ESO OBSERVATIONS OF THE P CYG STAR AG CARINAE AND ITS RING NEBULA*

R. Viotti[1], A. Altamore[2], M. Barylak[3]
A. Cassatella[3], R. Gilmozzi[3], C. Rossi[2]

1. Istituto Astrofisica Spaziale, CNR, Frascati, Italy
2. Istituto Astronomico, Università La Sapienza, Roma
3. Astronomy Division, ESTEC, Villafranca, Madrid, Spain

ABSTRACT

From the study of the optical and ultraviolet spectrum of the P Cyg variable AG Car, we conclude that this high luminosity ($M_{bol} \cong -8.3$), high mass loss star is a massive object evolving towards the WR region after a cool supergiant phase. Like in other superluminous stars, the large photometric and spectroscopic variations are attributed to flux redistribution of the stellar radiation due to structure variations of the expanding atmosphere.

INTRODUCTION

AG Car (HD94910) is a variable P Cyg star surrounded by a small ring nebula. For its peculiarities, this star close resembles the category of the high luminosity variable stars, including the galactic η Car, the Hubble-Sandage variables, and the LMC stars S Dor and R 71.
The nature of these objects is still matter of controversy. Their high luminosity and large mass outflow suggest that they are massive stars undergoing a rapid evolutionary phase. The study of these stars could therefore be a tool to clarify the nature of the superluminous stars, and to investigate the structure and time variability of their atmospheric envelopes.

AG Car is known for its large photometric (from V=6 to 8.5)and spectroscopic variability. Caputo and Viotti (1970) found that the equivalent spectral type is variable from AlI to BOI, close resembling P Cyg at minimum, and S Dor at maximum (cf. Wolf and Stahl 1982). In addition the star is characterized by a strong IR excess suggesting the existence of an intense stellar wind (Bensammar et al. 1981). This result is confirmed by the mass loss rate of 3×10^{-5} $M_{\odot} y^{-1}$ derived by Wolf and Stahl (1982) from the H_{β} profile.
More recently, Whitelock et al. (1983) found large variations of the IR flux, being stronger and redder at visual maximum, and suggest a mechanism of shell ejection in 1980. The high resolution UV spectrum is described in detail by Johnson (1982). Like P Cyg, AG Car displays a UV spectrum dominated by FeII absorptions shifted by -200 km s^{-1} and faint emission components.

---

* Based on observations with IUE collected at the Villafranca Satellite Tracking station of ESA, Madrid, Spain, on archive IUE images, and on spectroscopic observations obtained with the 1.5m telescope and with the CAT-CES system of the European Southern Observatory (ESO) at La Silla, Chile.

OBSERVATIONS

Low resolution UV spectra of AG Car and of its nebula were obtained with IUE in 1981 August, when the star was near maximum (V=6.2), and in 1983 June, when it was at minimum (V=7.2). Figure 1 shows that between 1981 and 1983 the UV flux of the star has largely decreased in the LW region, but in the meantime the far-UV flux was more intense at minimum, indicating a temperature increase of the continuum. This result indicates that the observed large luminosity variations could be attributed - as also suggested by the IR photometry and optical spectroscopy discussed above -, to flux redistribution at different wavelengths due to temperature and density variation of the extended atmospheric envelope of AG Car.

In order to verify this point, we have measured the dereddened energy distribution of AG Car in different epochs using the archive IUE images and the IR photometry of Whitelock et al. (1983). The fluxes were corrected for an interstellar extinction of $E(B-V)=0.60 \pm .05$, as derived from the intensity of the 2200 A band and the Ly_{α} line. The UV flux shortwards of the IUE range was derived using a Kurucz (1979) model atmosphere to fit the visual-to-UV energy distribution, as shown in Figure 2.
For an assumed distance of 2500 pc, the bolometric magnitude of AG Car during 1978 to 1982 remained nearly the same ($M_{bol}=-8.2/-8.5$) in spite of the large optical and UV variability.

The optical spectrum of AG Car is characterized by prominent H emissions. In 1984 February we have obtained the very high resolution ($R=10^5$) H_{α} profile using the CES/RETICON system of the 3.6m ESO telescope at La Silla, fed by the 1.4m auxiliary telescope. The H_{α} profile of AG Car shows a strong central peak flanked by extended wings, probably produced by electron scattering, and by a blue shifted absorption with a sharp edge indicating a terminal wind velocity of about -200 km s^{-1}. This value is lower than the terminal velocity of -320 km s^{-1} derived from the UV line profiles of FeII and MgII, probably because the lines are formed at different depths of the expanding envelope.
We have also found large variations of the optical and UV line profiles. For instance, H_{α} during some epochs displayed a double absorption component (cf. Bensammar et al. 1981).

One of the major peculiarities of AG Car is its ring nebula which is probably formed by matter ejected by the star $\sim$4000 years ago.
The LWR images taken in 1981 and 1983 show a spectrum of the nebula very similar to that of the star, except for some FeII emission features. Viotti et al. (1984) found that the star/nebula flux ratio is nearly independent on λ, and suggest that the nebular continuum is probably due to scattering of starlight by dust particles.
Figure 4 shows the optical spectrum of the nebula obtained in 1983 February with IDS at the 1.5m ESO telescope. Also in this case we can identify prominent low excitation emission lines (H, [NII], [SII]) formed in the nebula, and a rather strong continuum which is attributed to scattered starlight.

CONCLUSIONS

Our optical and UV observations shows that AG Car is a luminous P Cyg star with variable structure of the expanding envelope causing the observed spectroscopic and photometric variations, while its bolometric magnitude probably

remained constant. In this respect AG Car close resembles the LMC variables S Dor and R71 (cf. Wolf and Stahl 1982). Also in the case of ηCar the present bolometric luminosity (mostly emitted at IR wavelengths) is close to the luminosity of the star during the light maximum of last century, the observed large luminosity fading being caused by the formation of the dust envelope (cf. Andriesse, Donn and Viotti 1978).
Also the large luminosity variations observed in the Hubble-Sandage variables could be attributed to variation of their wind structure and, in some cases to dust formation, although it is difficult to say whether they are also associated to large changes of the mass outflow rate.

The presence of dust grains in the AG Car nebula would imply that either like in ηCar, dust has been condensated during the explosive phase 4000 years ago, or that dust was present in the atmospheric envelope of the star during a previous short, high mass loss phase. We therefore conclude that most probably AG Car is a post-MS massive star moving back towards the WR region after a cool-supergiant, high mass loss phase, in agreement with the theoretical evolutionary scenario (cf. Chiosi et al. 1978).

REFERENCES

Andriesse, C.D., Donn, B.D., Viotti, R. 1978, Mon. Not. R. A. S. 185, 771.
Bensammar, S., et al. 1981, IAU Coll. 59, C. Chiosi, R. Stalio (eds.),p.67.
Caputo, F., Viotti, R. 1970, Astron. Astrophys. 7, 266.
Chiosi, C., Nasi, E., Sreenivasan, S.R. 1978, Astr. Astrophys. 63, 103.
Johnson, H.M. 1982, Ap.J. Suppl. Ser. 50, 551.
Kurucz, R.L. 1979, Ap.J. Suppl. Ser. 40, 1.
Viotti, R., Cassatella, A., Ponz, D., The, P.S. 1984, in preparation.
Whitelock, P.A., et al. 1983, Mon. Not. R. A. S. 205, 577.
Wolf, B., Stahl, O. 1982, Astr. Astrophys. 112, 111.

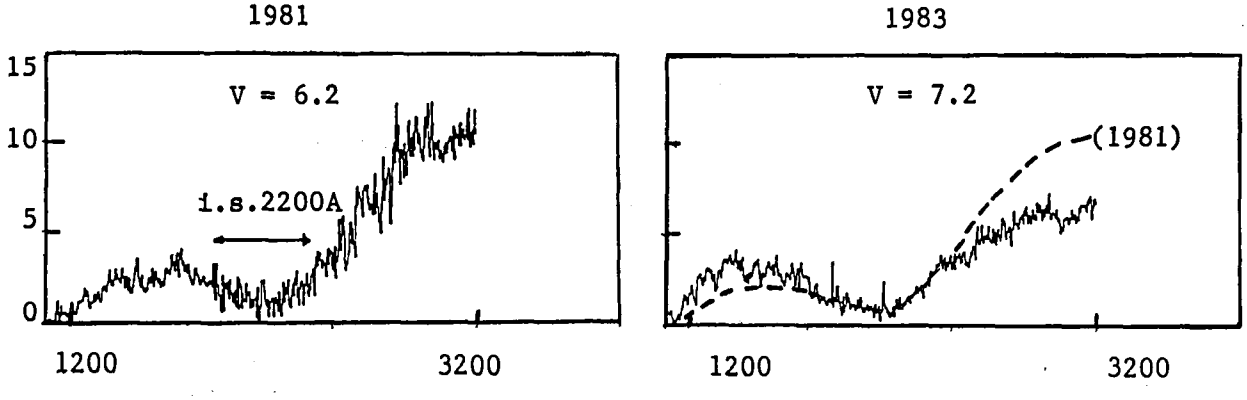

Figure 1. The low resolution IUE spectrum of AG Car in 1981 August and 1983 June. Ordinates are observed fluxes in 10^{-12} erg $cm^{-2}s^{-1}A^{-1}$. The interstellar 2200 A band is indicated.

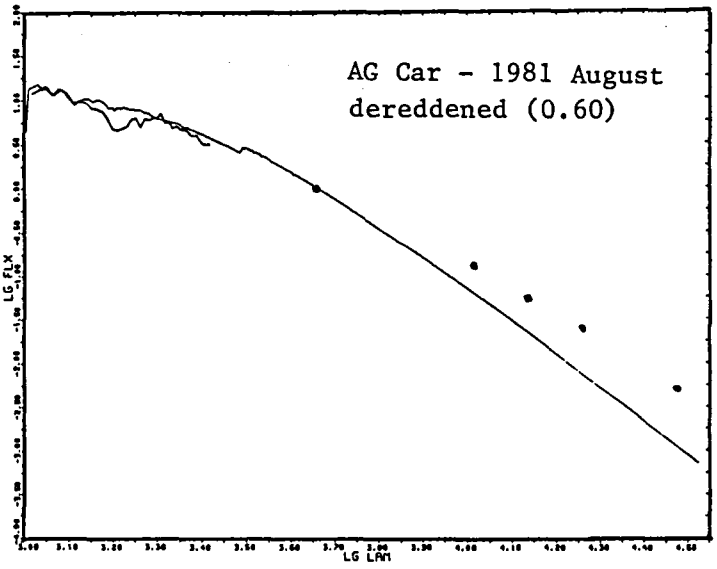

Figure 2. The energy distribution of AG Car from 1200 A to 3.6 μm in 1981, corrected for E(B-V) = 0.60. V is from the IUE FES. The visual and UV is compared with a Kurucz model atmosphere with T=16000K.

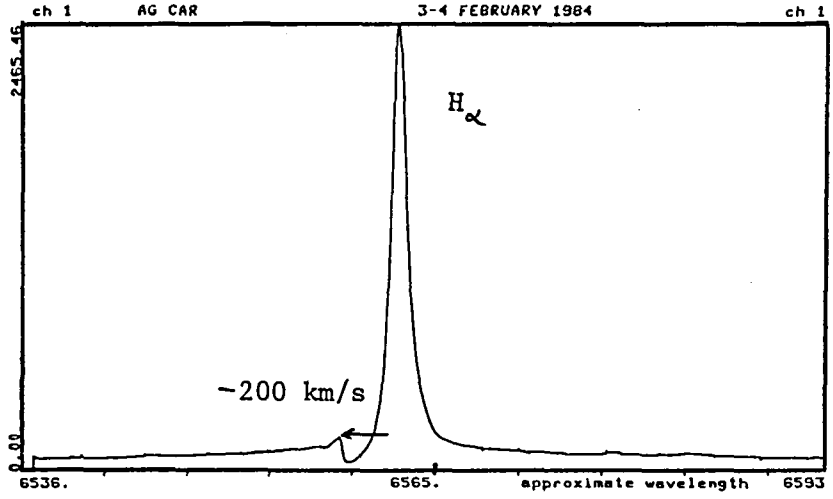

Figure 3. The high resolution H_α profile of AG Car in 1984 February obtained with the ESO CAT/CES system. Note the blue shifted absorption and the broad wings.

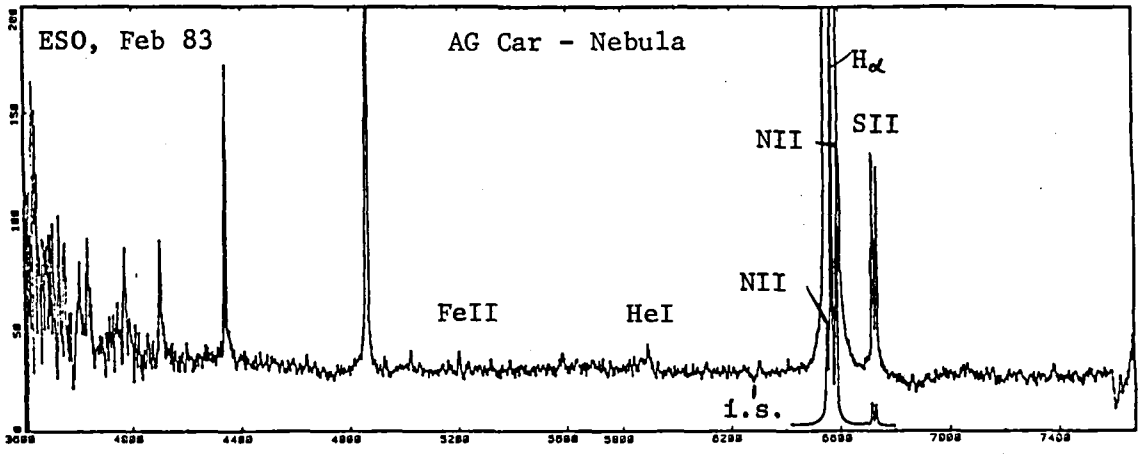

Figure 4. The IDS (1.5m ESO telescope) spectrum of the ring nebula of AG Car. Ordinates are fluxes in 10^{-14} erg $cm^{-2}s^{-1}A^{-1}$ for a 4x4 arcsec aperture.

COORDINATED ULTRAVIOLET AND VISUAL OBSERVATIONS OF ω ORIONIS 1982-1983

C.A. Grady, George Sonneborn, Chi-Chao Wu,
Astronomy Program, Computer Sciences Corporation

Daniel P. Hayes,
Department of Astonomy, Columbia University

E.F. Guinan,
Astronomy Department, Villanova University

Paul K. Barker,
Astronomy Department, University of Western Ontario

and

H.F. Henrichs
Astronomical Institute, University of Amsterdam

ABSTRACT

Coordinated IUE high dispersion and visual observations of ω Orionis (HD 37490, B2 IIIe) in 1982-1983 covering periods of both low and high B-band linear polarization have shown that line profile variability seen in the ultraviolet resonance lines of Si IV and C IV is not correlated with the visual continuum polarization state of the star. Variations in the visual colors and continuum fluxes are correlated with the amount of linear polarization. Hα emission strength variations are only weakly correlated with the polarization activity. The variation seen in C IV and Si IV is consistent with density perturbations propagating through the wind acceleration zone. The observed data are interpreted as indicating that the stellar wind is latitudinally separated from the continuum scattering envelope.

INTRODUCTION

It is now well established that some of the better studied Be stars are characterized by visual line profile and continuum light variations, as well as by ultraviolet line profile variability. The relation between the various formation zones is still unclear. We present results of a coordinated program of ultraviolet and visual observations of the bright Be star ω Orionis (vsini=160 km/s (Slettebak 1982)). Data for this study was obtained between 1982 August 14 and 1983 April 27.

VISUAL DATA

During the study period Omega Ori went through two distinct episodes of increased B-band linear polarization (Figure 1). The first, and weaker event was centered on JD 244 5318. The main event began no later than JD 244 5367, reached maximum strength by JD 244 5379, and then decreased gradually until the end of the study

period. The morphology of the main event is similar to previous episodes reported by Hayes (1980) and Hayes and Guinan (1984). When the observed data are plotted in the Stokes parameter (Q–U) frame, the data can be least squares fit to a straight line with a standard deviation of only 0.025 percent. The visual polarization data allow two important inferences to be made about this star. First, the intrinsic polarization denotes a non–negligible scattering optical depth, and hence an asymmetric distribution of scatterers in an extended atmosphere or envelope. The colinearity of the data in the Stokes parameter (Q–U) frame implies that the scatterers have an axially symmetric distribution.

A limited number of visual photometry and Balmer line profile spectra were obtained during the study period. These showed that the continuum light increased during the polarization episodes, and appeared to follow the behavior of the polarization. The star also became redder during the episode. This is similar to results reported by Hayes and Guinan (1984). H α emission was observed throughout the study period, and appears to have increased slightly by the end of 1983 April. Hα line profiles taken before and during the polarization episode, show that essentially identical line profiles can occur during both polarization low and high states. This suggests at most a weak correlation between Hα emission and the linear polarization.

ULTRAVIOLET DATA

Three resonance lines, Si III, Si IV and C IV show high velocity absorption from the stellar wind. As noted by Peters (1982) the lines are characterized by asymmetric absorption profiles with an enhanced absorption "narrow component" of the type reported by Snow (1977), and Lamers et al. (1982) in O stars. During the study period, the centroid velocities of the narrow components were the same in all three ions in any given image, but varied from image to image. Multiple absorption components are sometimes observed in both Si IV and C IV.

During the study period both Si IV and C IV showed significant variation. The largest variations in absorption depth relative to the continuum were observed in C IV between −400 and −700 km s^{-1}. Similar changes were observed in Si IV. In addition to changes in the maximum absorption depth, Si IV and C IV also showed changes of up to a factor of 1.5 in the overall absorption equivalent width (see figure 3). These changes are significant at the 2.5 sigma level. The narrow component radial velocity and absorption depth are anticorrelated (see figure 4). The linear relation between the centroid velocity and the absorption depth, which is proportional to the column density, is similar to the result of Henrichs, et al. (1983) for γ Cas. The absorption components become more pronounced with respect to the underlying profile as the ionization potential of the species increases, in agreement with the observations of Lamers et al. (1982) for O stars. Most of the line profile variation in ω Ori appears to be due to variations in distribution in radial velocity, and strength of these components.

DISCUSSION

The visual and ultraviolet data present very different views of the envelope of ω Ori. From the visual data alone, the picture which emerges is of episodic increases in the number of electron scatterers, aligned presumably in a disk. Hayes and

Guinan (1984) have suggested that these events represent the morphology of mass loss episodes. If this were true, a correlation between the visual activity and the ultraviolet wind might be expected. This is not observed. In addition no strong correlation between the continuum variability and the Balmer line activity is observed. The lack of any clear-cut correlation between the continuum polarization and the Balmer line features is understandable since the Balmer lines are expected to be formed further from the photosphere, although, still primarily in the equatorial plane (Fuhrenlid and Young, 1980). A less pronounced correlation of Balmer line emission and linear polarization was also observed in a previous polarization episode (Hayes and Guinan 1984). A likely explanation for the lack of correlation reported here is that the region giving rise to the continuum polarization is radially separated from the Balmer line formation zone. The wind acceleration zone observed in the ultraviolet resonance lines may in turn be latitudinally separated from the polarization, continuum light, and Balmer line formation zones, since model calculations for B stars (see Slettebak, et al, 1980) predict that the equatorial zones which are distended by the rotation are also considerably cooler that the regions producing detectable polarization. Under such a scenario, the wind occurs at high latitudes, while the radially separate electron scattering, and Balmer line formation zones occur in the equatorial plane.

REFERENCES

Fuhrenlid, I., and Young, A. 1980, *ApJ.* **240,** L59.
Hayes, D.P. 1980, *P.A.S.P.*, **92,** 661.
Hayes, D.P. and Guinan, E.F. 1984, *ApJ.* (in press).
Henrichs, H.F., Hammerschlag-Hensberge, H., Howarth, I.D., and Barr, P. 1983, *ApJ.*, **268,** 807.
Lamers, H.J.G.L.M., Gathier, R.L., and Snow, T.P., Jr. 1982, *ApJ.* **258,** 186.
Peters, G.J. 1982, *ApJ.* **253,** L33.
Snow,T.P., Jr. 1977, *ApJ.* **217,** 760.
Slettebak,A. 1982, *ApJ. Suppl.*, **50,** 55.
Slettebak, A., Kuzma, T.J., and Collins, G.W, Jr. 1980, *ApJ.* **242,** 171.

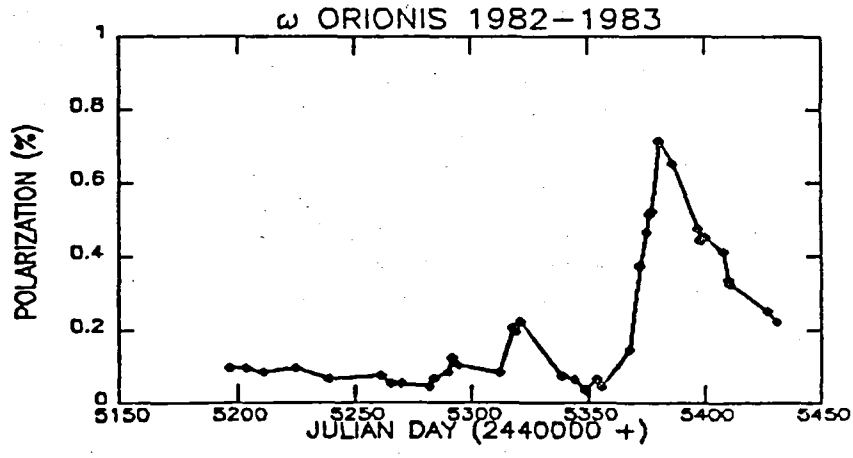

Figure 1: B-band intrinsic stellar polarization of ω Ori plotted as a of time.

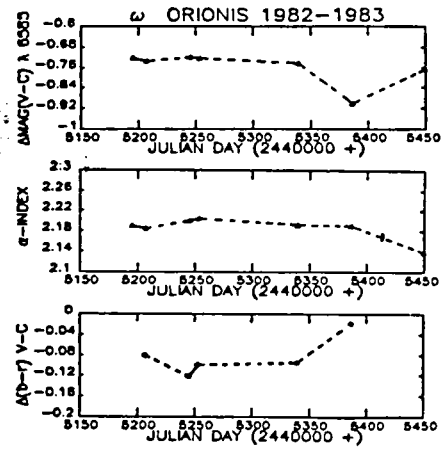

Figure 2: Visual Photometry of ω Ori. The photometric data consist of intermediate band (λ 6585) continuum observations, narrow band (Hα) data (where larger negative values indicate stronger emission), and color indices derived from λ 4530 and λ 6585 observation

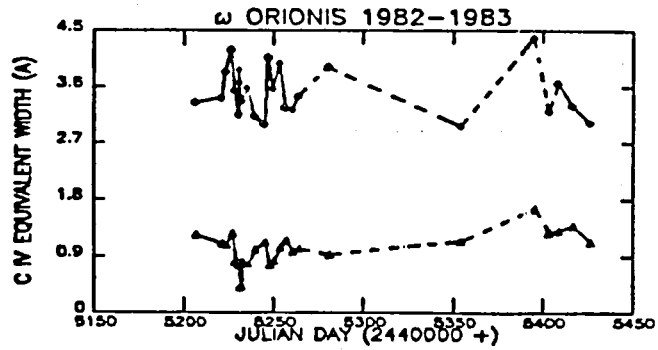

Figure 3: C IV absorption equivalent width as a function of time.

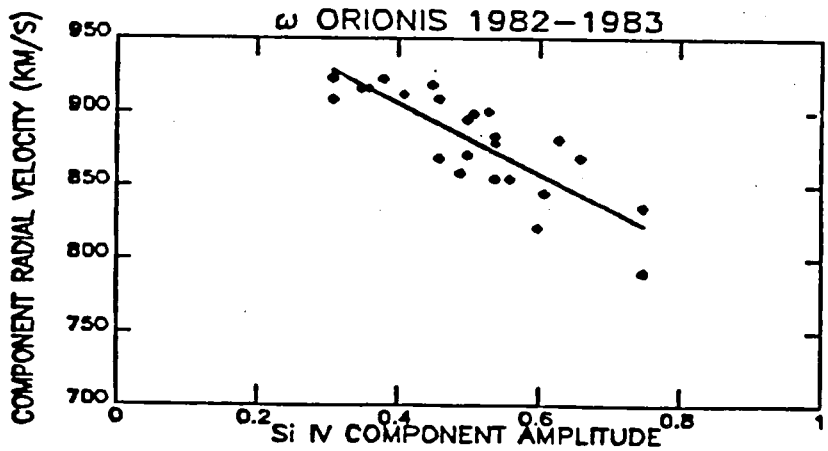

Figure 4: Anticorrelation of Si IV narrow absorption component depth and centroid radial velocity.

THE SPECTROSCOPIC ANTICS OF S 18/SMC

Steven N. Shore[1,2] and N. Sanduleak[1,2]
Warner and Swasey Observatory,
Case Western Reserve University

and

D. A. Allen
Anglo - Australian Observatory

ABSTRACT

We present optical (3600 - 10000 A) and IUE (1200 - 3200 A) observations of the peculiar, luminous early-type supergiant star S 18/SMC which cover the period 1981 - 1983. This is supplemented by objective prism and high dispersion studies from 1967 - 1980. The HeII 4686 line is variable in the optical, with HeII 1640, CIV 1550 and NV 1245 also variable. FES magnitude data suggest that the photometric variations are less than $0^m.1$. P Cygni profiles are observed on the hydrogen lines to H9, and HeI, FeII, [FeII], NIII, and weak SiII are seen in the optical spectrum. The red CaII lines are strong in 1983. There is no evidence for a red companion. The UV spectrum is dominated by emission lines of nitrogen. The variations show a striking similarity to HBV475, and the UV spectrum and derived N enhancement is quite similar to Sanduleak's star in the LMC. We present evidence for a nitrogen overabundance of a factor of the order of 70, and discuss a preliminary stellar wind model for the star.

INTRODUCTION

Attention was first called to S 18/SMC by Henize (1956) on the basis of its hydrogen emission, while interest in the star was aroused by the observation of strong HeII 4686 variations by Sanduleak (1974). At the time, it was called a symbiotic. The line varies from invisibility on objective prism plates to a strength about the same as $H\beta$. It was studied by Azzopardi et al. (1981), who obtained a low dispersion optical spectrum that showed P Cygni profiles on the hydrogen lines, and no evidence for photospheric absorption lines. Graham (1974, unpublished) has confirmed the variations of HeII 4686 using nova patrol objective prism plates. The star was included in the survey by Shore and Sanduleak (1982, 1984) of the most luminous early-type emission line stars of the Magellanic Clouds, and it was this survey that first found the strong variations of the UV emission lines of NV, CIV and HeII. Having now several years of data, we here will attempt to piece together a picture of the physical nature of this remarkable star.

OBSERVATIONAL MATERIAL

Optical spectra have been obtained using several instruments. Only

one published optical spectrum exists (Azzopardi et al. 1981). This was obtained in 1978. Almost at the same time, a spectrum was obtained using the Boksenberg device at AAT at similar resolution (June 1978). This latter spectrum covers 3600 - 7000 A, while the ESO spectrum does not include the Hα and HeI 6678 lines. Two additional spectra, one obtained at the AAT using the Faint Object Spectrograph with a CCD detector (Oct. 1983) and one from CTIO using the 1m Yale telescope and CITS system with IIIaJ plate at 121 A mm^{-1}, have been secured. Both cover the red region, with the AAT spectrum going from 5000 - 10000 A and the CTIO spectrum covering 3600 to 7000 A (see table 1 for journal of observations). The last three-mentioned spectra are calibrated, the one from ESO is density only.

All ultraviolet spectra have been obtained with the SWP camera of IUE. An LWR spectrum was also obtained, but will not be discussed in this paper (other than to mention that there is no strong emission and no 2200 A bump observed in this wavelength region). The spectra cover 1981 - 1983.

FES magnitudes were obtained at the time of each IUE exposure. The average magnitude was about 13.5, with no variation greater than $0^m.1$ being observed, despite the marked changes seen in the UV spectrum. There is no published photometric history for this star.

OBSERVED SPECIES

Hydrogen: Balmer emission is seen to H9, P Cygni profiles being present, and weak absorption seen to H 10 or H 11. Paschen lines are observed to P 14. There is emission in the Paschen continuum observed on the Oct.1983 spectrum. P Cygni structure is weak on Hα , and quite marked on all but the June 1974 spectrum, on all higher Balmer lines.
Helium: Neutral helium is observed on all spectra, with HeI 5875, 6678 and 7065 among the strongest emission lines in the spectrum. HeII 4686, 5411 and 8237 are observed in the optical, with HeII 1640 being one of the most variable and overall strongest lines in the UV. The HeII 4686 is variable on a timescale of about one month, while the HeII 1640 is variable on a timescale likely shorter than 3 months.
Carbon: Weak CIII] 1910 is present on all UV spectra. CIV 1550 is strong and variable on the same timescale as HeII 1640. No CII is seen in emission in either the UV or optical.
Nitrogen: The nitrogen spectrum in this star is very rich. All stages from NIII - NV are observed. Since no forbidden lines are seen, it is not a surprise that NII is not observed. NIII 4640, 1751, NIV 1487,1718 and NV 1245 are all observed. NV is the most variable line in the UV, with changes of more than a factor of two in equivalent width observed.
Oxygen: OI 1304 and [OI] 6300 are present, the latter being extremely weak. OIII] 1667 is present on all SWP spectra.
Silicon: SiII 5958-79 is present, but weak, in Oct.1983. SiIII] 1895 is present on all UV spectra, with about the same strength as CIII] 1910. The SiIV 1400 line is diffuse and probably variable, but present on all of the UV spectra. Its profile is quite similar to that observed in Sanduleak's star in the LMC (Kafatos et al. 1983).
Calcium: No CaII H and K emission is detected in the optical spectra. The CaII lines at 8491, 8542 and 8662 are quite strong on the Oct.1983 spectrum.

Very weak [CaII] 7291-7324 emission is also present.
Iron: A rich permitted FeII spectrum is present. Only [FeII] 4277, 4287 and 4414 are weakly present in the June 1974 and Dec. 1983 spectra.
Argon: Weak [ArV] emission is observed in the Oct.1983 red spectrum.
Chlorine: Weak [Cl III] 5550 is observed in the Oct. and Dec. 1983 spectra.

RESULTS AND DISCUSSION

The steepness of the Balmer decrement is similar to a number of other stars which we have observed (Shore, Sanduleak and Chu 1984,in prep.) The average of 7 stars is 4.4 ± 2.5, for those stars with strong emission, and the wind stars show the steeper decrement. The highest Balmer line gives a terminal velocity of the order of 1200 km s^{-1}, similar to the velocity width of the UV lines (see Shore and Sanduleak 1984). Despite the large variations of the higher excitation lines, the HeI and H lines are quite constant in relative intensity, although there are suggestions that the equivalent widths of the Balmer lines are quite variable. Some of this may be due to differences in instrumentation. The CaII red system is quite strong, looking much like a chromosphere. There is no evidence, to 1μ, for a red component in the system, so it would appear that these lines arise in the wind itself. It is clear that S 18 is not a symbiotic of any conventional sort, and the emission lines and P Cygni profiles would lead to the conclusion that it is a single, extremely luminous, mass-losing star.

The model we have derived in similar in many ways to S 134 (= HD 38489; Shore and Sanduleak 1983). From the CIII]1910/CIV 1550 ratio, we get $C^{+3}/C^{+2} \sim 0.9$ (Kaler et al. 1976)(using for reference $T = 2\times10^4$K, e.g. Shore and Sanduleak 1984) . The NIII]1751/CIII]1910 ratio can then be used to give an N/C ratio (Davidson et al. 1983) which we find to be $N/C \gtrsim 7.0$. Using Maran et al.(1982) for abundances of SMC HII regions, we find a nitrogen enhancement of about 70x. This is remarkably similar to that found for the LMC star Sanduleak's star by Kafatos et al.(1983), to which the UV spectrum of S 18 bears a striking resemblence. Using the CIII 1910, CIV 1550 and SiIV 1400 lines, we derive $P_e \gtrsim 10^{15.5\pm0.5}$ (from Cook and Nicolas 1979) so that $n_e \gtrsim 10^{11}$ cm^{-3} (±0.8 dex, assuming T from 10000 to 40000 K). This accounts for the extreme weakness of the forbidden line spectrum. The mass loss rate agrees with the analysis by Shore and Sanduleak (1984), being about $10^{-5}M_\odot yr^{-1}$. It is most interesting to note that while the variations of this star resemble the well known symbiotic HBV475, its spectrum is quite like an LMC star not known to clearly be a binary (Sanduleak's star). In fact, it is striking to notice that two stars which began life with presumably different chemical makeup have wound up looking so very much alike. This should prove useful for models of nucleosynthesis in massive stars.

A more complete account of the full observational data is now in preparation.

We thank the IUE staff, especially K. Feggins and R. Bradley, for their kind help and quick and sure work. SNS and NS were guest observers with IUE on program NAG 5-179 during 1981 through 1984.

REFERENCES
Azzopardi,M.,Breysacher,J. and Muratorio,G. 1981,Astron.Ap., 95, 191.
Cook,J.W. and Nicolas,K.R. 1979,Ap.J., 229,1163.
Davidson,K.,Walborn,N.R. and Gull,T.R. 1982,Ap.J.(Letters),254,L47.
Henize,K.G. 1956,Ap.J.Suppl.,2, 315.
Kafatos,M.,Michalitsianos,A.G.,Allen,D.A. and Stencel,R.E.1983,Ap.J.,275,484.
Kahler,J.B.,Aller,L.H.,Czyzak,S.J.,Epps,H.W. 1976,Ap.J.Suppl.,31,163.
Maran,S.P.,Aller,L.H.,Gull,T.R. and Stecher,T.P. 1982,Ap.J.(Letters),262,L41.
Shore,S.N. and Sanduleak,N. 1982,in Adv.in UV Astron.(NASA CP 2238)p.602.
———————————. 1983, Ap.J., 273, 177.
———————————. 1984, Ap.J.Suppl., in press.

1. Guest Investigator, IUE Observatory
2. Visiting Astronomer, Cerro Tololo Interamerican Observatory

Table I: Journal of Observations

1978 June	AAT	10A resolution 3600-7000A	(DAA)
1978 July	ESO	114 A/mm 3600-6000A	(Azzopardi et al. 1981)
1981 July	IUE	SWP 14463, LWR 11058	(SNS,NS)
1981 Sept	IUE	SWP 15122	(SNS,NS)
1982 March	IUE	SWP 16599	(SNS,NS)
1983 March	IUE	SWP 19731	(SNS,NS)
1983 Oct.	AAT	FOS/CCD 4A resol.5000-10000A	(DAA)
1983 Dec.	CTIO	121A/mm IIIaJ 3600-7000 A	(SNS)

Table II: UV Line Equiv.Widths (A)

Spectrum	NV1245	SiIV1400	CIV 1550	NIII1751	HeII 1640	NIV1487
SWP 14463	152.0	69.9	46.0	30.8	120.5	------
SWP 15122	297.0	----	34.3	14.2	98.3	41.9
SWP 16599	114.2	23.7	12.6	14.2	70.5	27.5
SWP 19371	72.4	----	28.3	8.8	115.3	21.8

Table III: Optical Line Equivalent Widths (A)

Spectrum	Hα /Hβ	Hβ /Hγ	HeI4471	HeI5875	HeI6678	HeII4686	Hβ
June 78	4.9	3.8	3.4	25.0	5.5	33.5	170.0
Oct 83	---	---	---	25.8	16.8	----	40.0
Dec 83	4.4	3.7	1.5	9.9	5.5	15.4	61.5

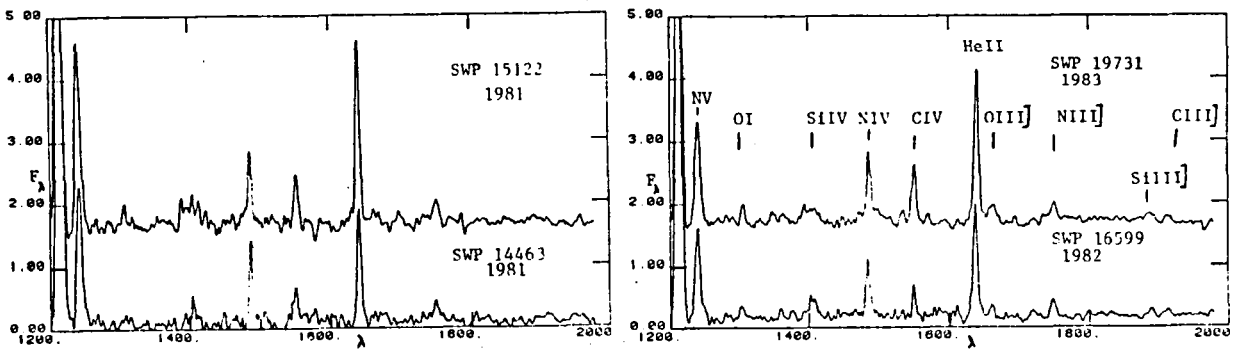

AN EPISODIC RED-WING STRUCTURE OF SiIV, λ1394Å, IN γ CAS

V. DOAZAN, G. SEDMAK, R. STALIO, R.N. THOMAS, A.J. WILLIS
Paris and Trieste Observatories, Institut d'Astrophysique Paris, University College London

ABSTRACT

IUE observations of γ Cas obtained in January 1983 show the conspicuous presence of a red-wing structure in the SiIV, λ1394A, resonance line in γ Cas. The λ1403A, shows a much less enhanced trace of the same effect. A comparison between 1983 IUE spectra with previous-ones obtained in 1980 show that in January 1983 the red absorption wing is strongly depressed relative to the 1980 profile where the red feature was absent. We conclude that this red wing feature is in absorption rather than in emission. This same wing-structure is suggested on 1982 IUE spectra. It has also been remarked by Marlborough et al (1978) on 1976 Copernicus observations, but these authors identify it as an emission feature. Combining long-term variations of γ Cas in the visual, summarized in two preceding papers, with published far UV data, we note that this red feature seems to occur preferentially at epochs where the V/R ratio of the violet and red emission peaks at Hα is less than one. We suggest that these two characteristics, visual and far UV, are linked to the flow-deceleration in the outer-atmosphere.

I. BACKGROUND

FarUV observations have caused a profound new orientation in Be-star studies. Visual observations alone characterized the Hα emission-envelope, whose existance defines a Be-star, as : quite variable, most-strikingly exhibited in the B-normal, Be, Be-shell phases for a single star ; very extended (5-50 photospheric radii) ; significantly colder than classical photospheric modeling would predict ; usually expanding at less than 100 km/s, although some observations of some stars at some phases suggest infall motions. But in a superficially-conflicting configuration, far UV and X-ray observations establish the universal presence in Be and B-normal stars of low-lying, superhot, rapidly-expanding, chromospheric-coronal regions. These rapid expansion velocities are highly variable in a given star, and can differ significantly among "similar" stars, reaching values as high as 2000km/s for a B main-sequence star. Any Be-star model must take into account the presence of these two kinds of regions. The precise relative geometry, and especially its time-variability, and the physical relations among these simultaneously-observed superhot and supercool regions are not yet unambiguously-clear. We need long time-baseline

panspectral, studies, especially of stars observed to exhibit different phases ---Be, Be-shell, B-normal. Because of the large number of Be stars which exist, in the B-normal as well as Be and Be-shell phases, a random sampling of such stars at random phases is not adequate to clarify the general physical picture of a Be star, and its time-variability. We need a more systematic approach to choosing stars and phases for detailed study. We stress that the observed time-scales of such variability are all much smaller than evolutionary times ; so they relate to the dynamical structure of the subatmosphere, atmosphere, and local environment of the star, not to an evolutionary change in a quasi-thermal structure. And we stress that apparently there are a large variety of such time-scales: in both intervals between significant changes in structural configuration, and in speed with which a given change occurs (Doazan and Thomas, 1983 ; Doazan, 1983).

Because Be stars are unambiguously identified only in the visible, and because one would assume that observational trends must exist between associated changes in hot and cold structures, it is most useful to try to use "well-studied" stars to identify "visual indicators" which might warn of, even though not sufficing to predict the precise observeable details of, those structural changes which are reflected throughout the whole spectrum. Then, simultaneous spectral studies of those stars, at those phases of such change, will provide valuable informatin for diagnosing the physics of Be stars. We have used such indicators from reasonably-detailed visual studies of such stars as γ Cas, 59 Cyg, θ CrB, 88 Her to select those stars, at those phases, where simultaneous studies in the several spectral regions might provide illuminating results. Such an approach has given us a preliminary broad picture of the general atmospheric structure associated with a monotonically outward-expanding, although variably accelerated and decelerated, flow ---based on sequences of observed blue-displaced spectral features. These combine to produce a picture of both atmospheric, and local environmental, structure associated with such mass-flux from the star (Doazan, 1982, Thomas, 1983 ---this latest monograph is available, on request, at this Goddard meeting.).

The present communication is a preliminary part of our 3rd paper in a series devoted to the study of γ Cas, the first-identified Be star, and the one for which we have the longest baselines of observations in the visual, far UV, and X-ray spectral regions. Papers I and II (Doazan et al., 1983, 1984) summarized, and discussed, the visual observations, and the several models proposed to interpret them. Here, we try to put into focus a preliminary result on a red-wing structure in the resonance line, λ1394A, of the SiIV resonance doublet. To a first approximation, this structure, which is variable, appears to be associated, empirically, with the behavior of the V/R ratio in Hα. Although the existance of the Hα envelope requires simply a mass-flow, the details of its structure appear to be linked to the self-interaction of a <u>variable</u> mass-flow which, in the postcoronal regions, produces a

deceleration of the flow. Thus, a link between a characteristic of the Hα envelope, and a red-wing, rather than blue-wing, structure of a line coming from an ion which is just marginally-superionized in this star, is important for Be-star modeling.

II. THE OBSERVATIONS :

The observations were made with IUE at the Madrid (VILSPA) station, at high dispersion, in the short wavelength, with the large aperture, and an exposure time of 9sec. Data analysis was done at the Computing Center of the Trieste Observatory.

A comparison of the SiIV resonance doublet, λ1393.8 and λ 1402.8, between two observing epochs : May, 26 1980 (SWP9130) ; January 27, 1983 (SWP19097) is shown in Figure 1. These two spectra show striking differences in two aspects : (1) the pattern of the several line-components of the doublet structure ; (2) the profiles of each of these components.

(1) In May 1980 there were two strong line-components for each member of the doublet ---almost equal in central intensity but differing significantly in width. The broadest components were violet-displaced by some 150km/s ; the narrowest were violet-displaced by some 1300km/s. In January 1983, one could again identify two line-components for each member of the doublet : The small-displaced lines retained their 1980 depths positions, while the large-displaced lines had decreased strongly their depths and their displacement had substantially decreased to some -950km/s. Such variable appearance of a high-velocity component of the SiIV doublet has been discussed in the literature (Henrichs, et al, 1980, 1983) in terms of "puffs" of high-velocity material moving through the outflowing gas. We have suggested it more likely marks a variability in particle concentration at nearly the same location in an outflow, where the observed velocity of a given ion reflects the T_e-structure of the accelerated-decelerated velocity field (Doazan, et al 1980).

But turning to (2), the profiles of the several components, one finds a prominant, differential, change in red-wing structure of the low-velocity component in 1983 over that in 1980. It is most pronounced in the λ1394 component of the doublet ---whose f-value is some 30% larger than the λ1403 component, where, however, the effect is also detectable. At first glace, one has the alternatives of a red-displaced emission peak, or a red-displaced, by about 150km/s, absorption minimum. Superposing the 1980 and 1983 profiles, however, one notes that the structure is more nearly a significant drop in the red-wing intensity. The blue wings, and absorption minima, match fairly well at the two epochs. Much depends, of course, on where one draws the continuum. Alternatively, one can mimic the phenomenon as the absorption-center in 1983 being slightly red-shifted relative to 1980, and a broader absorption profile. The observeable differential effects are smaller, for the λ 1403

components, but describable with the same alternatives.

Searching the literature, we find another example of the same phenomenon. Marlborough, et al (1978) remarked the same effect in a January 1976 Copernicus observation, again in the λ1394 component, which they identify as probable emission in the line core. They reference Slettebak and Snow (1978) as exhibiting other examples of the same phenomenon in the cores of both, of the low-displaced components of the doublet.

III. DISCUSSION

Because of the increased strength in the λ1394A SiIV component, with the larger f-value, it is tempting to regard this red-wing structure as a radiative-transfer effect accompanying a slight red-displacement of the absorption-wavelength in some atoms contributing to that low-displaced component of the doublet. A similar configuration has been suggested for the solar CaII resonance doublet (Thomas, 1972). We note that there are two atmospheric regions which can contribute to such a low-velocity component of SiIV : that in the low atmosphere, in the rise to chromosphere-corona ; and that in the outer-atmosphere, just after the deceleration in the post-corona. Because the appearance of this component accompanies a weakening of the high-velocity component, it is tempting to interpret this as a shift in the optical-depth location of the deceleration : that in 1983 occuring closer to the star. This would decrease the extent of the high-velocity, preshock component : and increase the extent of the past shock component. We do not push this suggestion further, here, until we have analyzed all our data.

We also note that if we look at the epochs of all these observations on the "long-term variability" chart for γ Cas, shown in Doazan (1982) and Doazan, et al (1983, Paper I), reproduced here as Fig2, there is a suggestion that they occur at epochs when the V/R ratio is <1 for the Hα emission. Possibly unjustifiably, we can attempt to answer why there should be such a correlation, by noting that twice during the spectacular episode of variation for γ Cas (1932-42), the occurrence of shell spectra coincided with such transitions in V/R. Indeed, it was from observing the occurrence of such V/R fluctuations that a shell-phase has been expected to occur in recent years for γ Cas. IF one interprets the cooling, and formation of narrow, deep absorption components in the shell phase as implying a strong increase in local particle concentration in the Hα envelope ---then V/R is an "indicator" of such density increase, even though we do not yet understand the underlying physics. In which case, occurrence of V/R fluctuations can also indicate a density increase, but one not large enough to produce the shell phase. Again, further speculation, until the basis for the effect is demonstrated quantitatively, is unwarranted. We only emphasize the possibility that we have found, here, an observational approach to demonstrating a deceleration in the flow,

also, changes with phase of the star.

References

Doazan, V., Selvelli, L., Stalio, R., Thomas, R.N., 1980, Second European IUE Conf., ESA-SP-157, p.145.

Doazan, V., 1982, The B Stars With and Without Emission Lines, A.B. Underhill and V. Doazan eds., NASA SP-456.

Doazan, V., 1983, in Effects of Mass-Loss on the Local Stellar Environment, Second Trieste Workshop, R. Stalio and R.N. Thomas eds.

Doazan, V. and Thomas, R.N., 1983, in Rapid Variability in Early-Type Stars, ed. P. Harmanec.

Doazan, V., Franco, M., Rusconi, G., Sedmak, G., Stalio, R., 1983, Astron. Astrophys. 128, 171.

Doazan, V., Franco, M., Rusconi, G., Sedmak, G., Stalio, R., 1984, Astron. Astrophys. Suppl. 55, 1

Henrichs, H.F., Hammerschlag-Hensberge, G., Lamers, H.J.L.M., 1980, in Second IUE European Conf., ESA-SP-157, p.146.

Henrichs, H.F., Hammerschlag-Hensberge, G., Howarth, I.D., Barr, P., 1983, Astrophys.J. 268, 807

Marlborough, J.M., Snow, T.P., Slettebak, A., 1978, Astrophys. J. 224, 157

Slettebak, A., Snow, T.P., 1978, Astrophys. J. Lett. 224, L127.

Thomas, R.N., 1972, Solar Physics, 27, 303.

Thomas, R.N., 1983, Stellar Atmospheric Structure Patterns, NASA-SP-471.

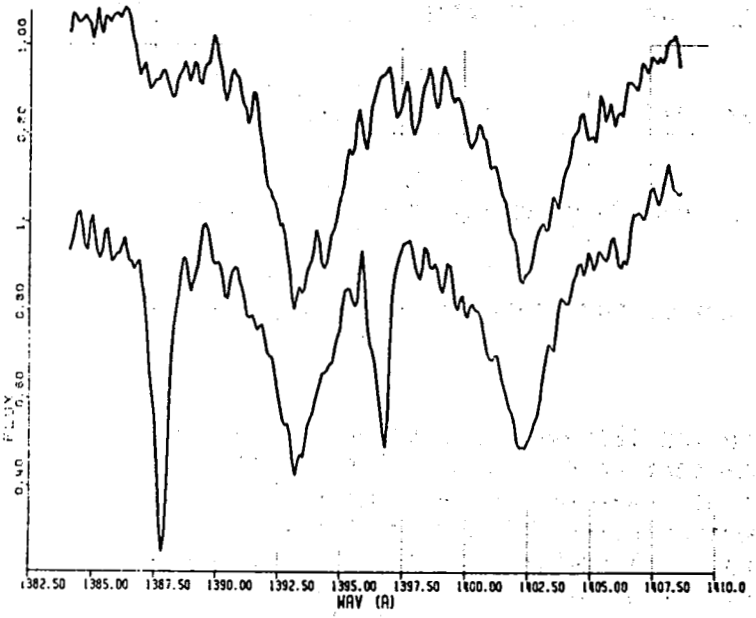

Fig. 1 - The SiIV resonance lines of γCas.
Top, in January 27, 1983. Bottom, in May 26, 1980.

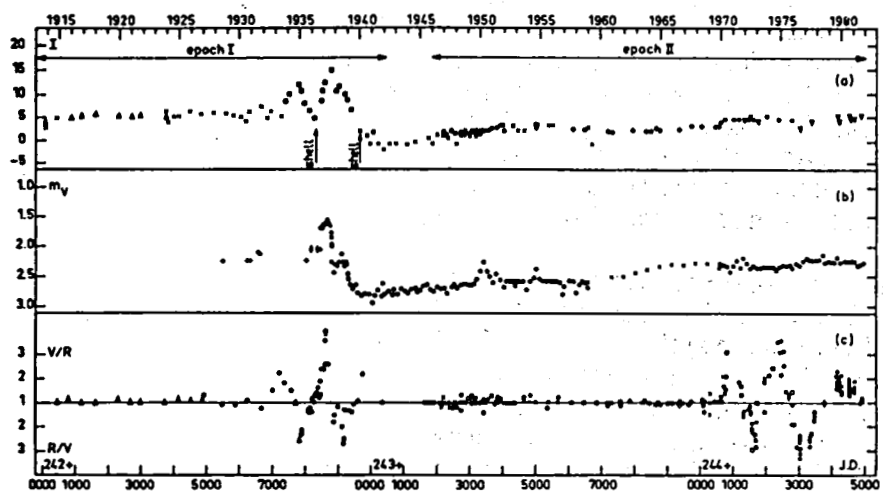

Fig. 2 - The long-term variations of γCas in the visual region. (a) Intensity variations of the Balmer emission lines. (b) Light variations. (c) V/R variations of the first Balmer lines. From Doazan et al. 1983.

IUE AND VOYAGER OBSERVATIONS OF VERY HOT O-TYPE SUBDWARFS

J. S. Drilling
Department of Physics and Astronomy, Louisiana State University

J. B. Holberg
Lunar and Planetary Laboratory, University of Arizona

D. Schönberner
Institut für Theoretische Physik, Universität Kiel

ABSTRACT

We have observed 12 newly-discovered subdwarf O stars with IUE and have obtained complementary observations of two of these with Voyager 1. We find that these stars all have effective temperatures of at least 60,000 K and that they occupy a region in the H-R diagram between the hottest white dwarfs and the central stars of planetary nebulae, i.e. that they are the hottest known O-type subdwarfs. We present evidence that the abundances of H, He, C, N, and possibly Fe vary widely from star to star. We believe that these stars represent the state of evolution immediately preceding the white dwarf state, and that the abundance differences are due to diffusion and convective mixing in surface layers.

Drilling (1983) has recently discovered 12 hot, relatively bright subluminous O stars ($V < 13$) during a spectroscopic investigation of non-emission OB+ stars from the Case-Hamburg surveys and their extension to $b = \pm 30°$ for $\ell = \pm 60°$. These surveys cover more than 13 times the area of the SGP survey of Slettebak and Brundage (1971), from which most of the sdO's included in the recent study of Hunger et al. (1981) were selected, but Drilling's sample was expected to include only the hottest and/or helium-rich stars since only the weakest-lined O and B-type stars were investigated.

We have used low-resolution (6Å) IUE spectra covering the wavelength range 1200-3200 Å to place these stars in the H-R diagram of Figure 1. We determined E(B-V) using the Seaton (1979) reddening law to nullify the 2200 Å feature, and in all cases $E(B-V) < 0.25$. Effective temperatures were then determined using R, the ratio of the total flux between 1240 and 1945 Å to that between 1945 and 3120 Å. This quantity is dependent on effective temperature and is nearly independent of the color excess for a variety of different reddening laws.

In order to calibrate R against temperature, we chose four hot stars from the IUE data center with reasonably well-known temperatures, gravities, and compositions (see Table 1). Because R is dependent on composition, we calibrated it against the color temperature, T_{BB}, rather than against effective temperature. This is the temperature of the black body which best fits the flux distribution between 1200 and 3100 Å of our model atmosphere corresponding to the published values of effective temperature, gravity, and composition. We then estimated the compositions of our subdwarf O stars from

visual spectra (Drilling 1983) and assigned to each star the effective temperature of the model whose UV flux best matches that of a black body with temperature T_{BB}. The effective temperatures range from 60,000 K to over 100,000 K, and are consistent with the appearance of the visible spectra. Because these 12 stars all lie near the Galactic plane, we have also been able to derive absolute visual magnitudes from the color excesses and apparent magnitudes (Drilling 1983) using the color-excess-distance relations of FitzGerald (1968), Lucke (1978), and Nandy et al. (1978). The absolute magnitudes range from 1.5 to 8, and are consistent with the surface gravities indicated by the visible spectra.

It is seen that our objects occupy a previously empty region of the H-R diagram which is bounded by the central stars of planetary nebulae, the hottest white dwarfs, and cooler subdwarf O stars. We believe, in fact, that they represent a funneling together in the H-R diagram of two different kinds of evolutionary tracks. Those stars which lie in or near the region of central stars in the H-R diagram are post-AGB objects which are evolving according to the evolutionary theory of Schönberner (1979, 1983). The rest of the stars shown in Fig. 1 are descendants of the extended horizontal branch. A typical evolutionary track, for a 0.5 $M_\odot$ helium core surrounded by a 0.01 $M_\odot$ envelope of normal composition (Caloi 1972), is shown by the dotted curve. Such an evolutionary scheme is not only able to account for the distribution of the sdO's in Fig. 1, and for the much greater space density of sdB's indicated by the survey of Carnochan and Wilson (1983), but is also able to explain the observed variations in the H/He abundance ratio as a consequence of convection and gravitational settling in surface layers (Michaud et al. 1983, Winget and Cabot 1980, Wesemael et al. 1982).

We have also observed two of these stars, LSE 21 and LSIV +10°9, in the wavelength range 912 - 1200 Å at 25 Å resolution using the ultraviolet spectrometer on board Voyager 1 (Broadfoot et al. 1977, Broadfoot et al. 1981). These spectra are displayed in Fig. 2 along with low resolution IUE spectra for 6 of the stars and UBV photometry for LSE 21 and LSIV +10°9 (Drilling 1983). The following calibrations were employed: Holberg et al. (1982) and Holberg and Polidan (1983) for the Voyager 1 data, Bohlin and Holm (1980) for the IUE data, and Hayes (1979) for the UBV photometry. All fluxes have been corrected for interstellar absorption using the law of Savage and Mathis (1979) extrapolated to $A_\lambda/E(B-V) = 17.72$ at $\lambda = 912$ Å. The model atmospheres mentioned above are also shown in Fig. 2 for the stars observed with Voyager 1, and there is an indication that we have underestimated the effective temperatures of the hottest stars. In fact, the slope of the continuum of LSE 21 is indistinguishable from a model of infinite temperature, and soft X-ray observations of this object would be highly desirable.

The low-resolution UV line spectra are consistent with the H/He ratios indicated by the visible spectra, in that the helium-rich objects tend to have stronger HeII $2 \rightarrow \infty$ HeII $3 \rightarrow \infty$, and weaker Lyman absorption, than the normal and helium-poor objects. The IUE spectra also indicate large variations in the N/C abundance ratio from star to star. For example, LSE 153 and LSE 259 have strong NV and CIV lines, whereas LSE 263 has a strong NV but only a weak CIV absorption. On the other hand, LSIV +10°9 has the strongest CIV line of all 12 objects, whereas NV is invisible. All four of these objects lie in the

same part of the H-R diagram and all four are helium-rich. Three of the four objects of highest luminosity show evidence of mass loss. LSS 2018 and LSE 125, which have been found to possess planetary nebulae, have blueward displaced NV absorptions, and in LSE 259, P-Cygni profiles of NV and CIV are present. The blueward shifts correspond to wind velocities of 1900 to 2400 km/sec. Finally, many of these stars show considerable line-blocking shortward of 1600 Å, and high-resolution IUE spectra obtained for six of them show that this is due to numerous absorption lines of FeV and FeVI.

This work was supported in part by NASA Grant Nos. NAG 5-71 and NAGW-147, and by NSF Grant Nos. AST-8018766 and INT-8219240.

Table 1

Star	T_{eff}	n(He)/n(H)	T_{BB}	R	Ref.
HD 49798	47,500	1.0	58,000	2.30	Kudritzki and Simon, 1978
BD +75°325	55,000	1.5	63,000	2.50	Kudritzki et al. 1980
HZ 43	62,500	< 0.001	97,000	3.10	Auer and Shipman, 1977
NGC 7293	105,000	0.01	145,000	4.00	Bohlin et al. 1982 Mendez et al. 1983

REFERENCES

Auer, L. H., and Shipman, L. H. 1977, Astrophys. J. Letters 211, L103.
Bohlin, R. C., Harrington, J. P., and Stecher, T. P. 1982, Astrophys. J. 252, 635.
Bohlin, R., and Holm, A. 1980, IUE Newsletter No. 10, p. 37.
Broadfoot, A. L., et al. 1977, Space Sci. Rev. 21, 183.
Broadfoot, A. L., et al. 1981, J. Geophys. Res. 86, 8259.
Caloi, V. 1972, Astron. Astrophys. 20, 357.
Carnochan, D. J., and Wilson, R. 1983, M.N.R.A.S. 202, 317.
Drilling, J. S. 1983, Astrophys. J. 270, L13.
FitzGerald, M. P. 1968, Astron. J. 78, 983.
Hayes, D. S. 1979, Problems of Calibration of Multicolor Photometic Systems, ed. A. G. D. Philip (Dudley Obs. Reprint No. 14), p. 297.
Heber, U., Hunger, K., Jonas, G., and Kudritzki, R. P. 1983, Astron. Astrophys. in press.
Holberg, J. B., Forrester, W. T., Schemansky, D. E., and Barry, D. C. 1982, Astrophys. J. 257, 656.
Holberg, J. B., and Polidan, R. S. 1983, Bull. American Astron. Soc. 15, 968.
Hunger, K., Gruschinske, J., Kudritzki, R. P., and Simon, K. P. 1981, Astron. Astrophys. 95, 244.
Kudritzki, R. P., and Simon, K. P. 1978, Astron. Astrophys. 70, 653.
Kudritzki, R. P., Gruschinske, J., Hunger, K., and Simon, K. 1980, Proc. Second Year IUE Conference, Tubingen.
Lucke, P. B. 1978, Astron. Astrophys. 64, 367.Mendez, R. H., Kudritzki, R. P., and Simon, K. P. 1983, IAU Symposium No. 103, 343.
Michaud, G., Vauclair, G., and Vauclair, S. 1983, Astrophys. J. 267, 256.

Nandy, K., Thompson, G. I., Carnochan, D. J., and Wilson, R. 1978, M.N.R.A.S. 184, 733.
Paczynski, B. 1971, Acta. Astr. 21, 1.
Savage, B. D., and Mathis, J. S. 1979, Ann. Rev. Astron. Astrophys. 17, 73.
Schönberner, D. 1979, Astron. Astrophys. 79, 108.
Schönberner, D. 1983, Astrophys. J. 272, 708.
Seaton, M. J. 1979, M.N.R.A.S. 187, 73P.
Slettebak, A., and Brundage, R. K. 1971, Astron. J. 76, 338.
Sweigert, A. V., and Gross, P. G. 1976, Astrophys. J. Suppl. 32, 387.
Wesemael, F., Winget, D. E., and Cabot, W. 1982, Astrophys. J. 254, 221.
Winget, D. E., and Cabot, W. 1980, Astrophys. J. 242, 1166.

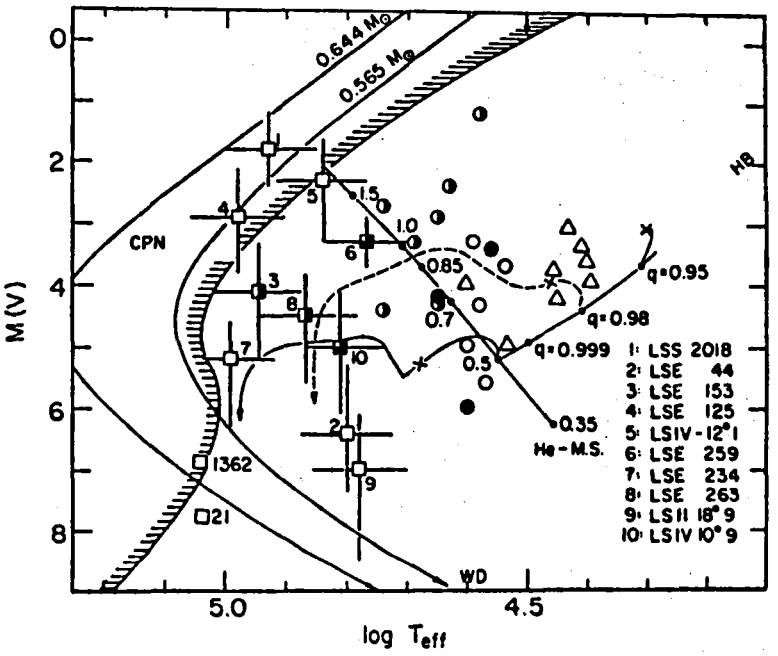

Figure 1. H-R diagram with the central star region (CPN) to the left of the shaded line, the helium main sequence (Paczynski 1971), the extended horizontal branch (q), and the loci of our objects (squares). The evolutionary paths of post-AGB models of 0.565 and 0.644 M_0 are from Schönberner (1979,1983), and that of a 0.5 M_0 pure helium star is from Paczynski (1971). The central helium-burning phase of an EHB model with M_0 = 0.5 M_0 and q = 0.95 (Sweigert and Gross 1976) is also shown. The (estimated) evolution of a 0.5 M_0 EHB star with q = 0.98 is marked by a dashed line. The crosses indicate the termination of central helium burning. The sdO's (circles) from Hunger et al. (1981) and sdB's from Heber et al. (1983) are also displayed. The n(He)/n(H) ratios are indicated as follows: open symbols: normal or helium-poor; half filled: helium-rich; three-quarters filled: probably extremely helium-rich; filled: extremely helium-rich.

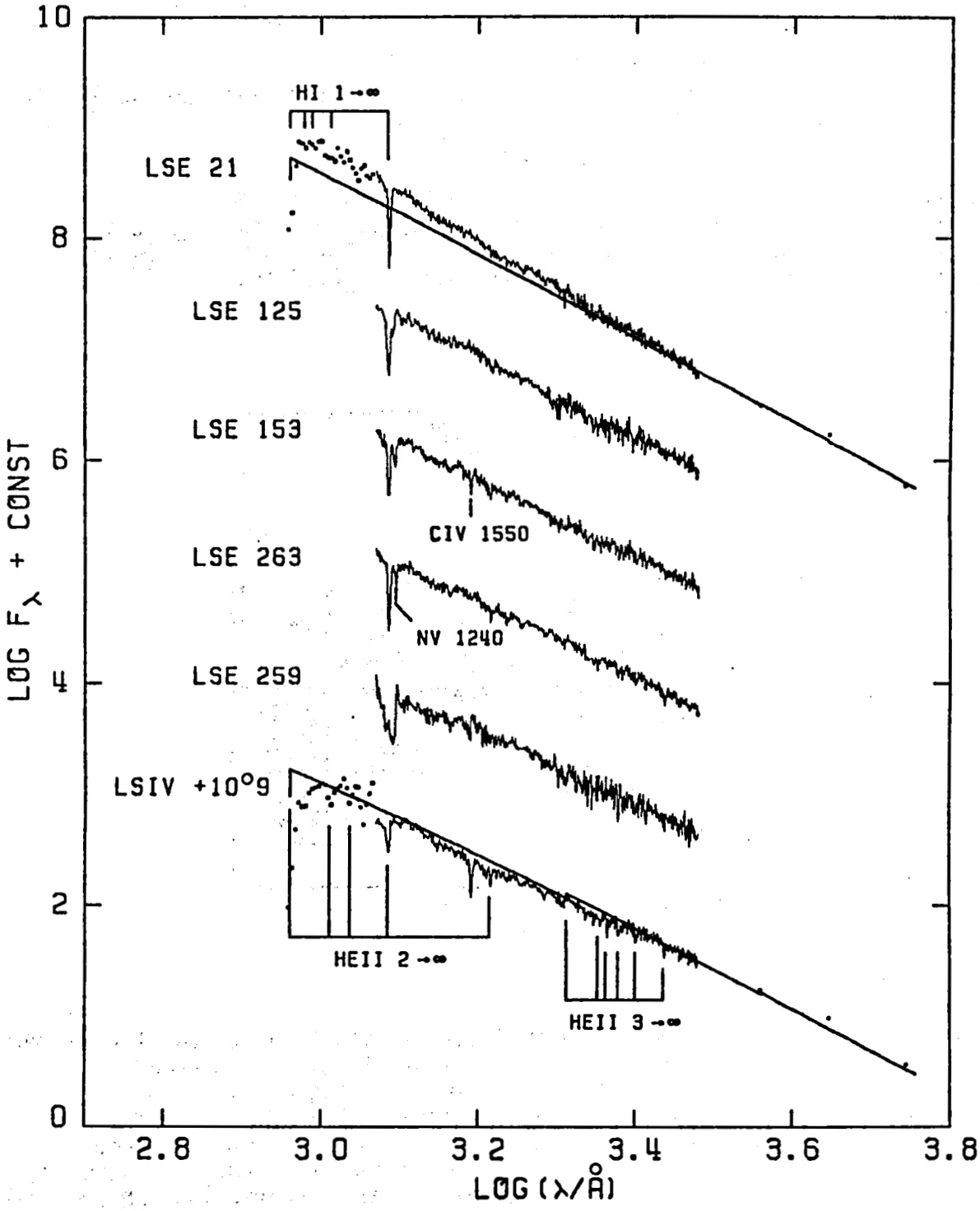

Figure 2. De-reddened spectra of 6 very hot O-type subdwarfs between 912 and 5500 A. The spectrum of LSE 21 is compared to a model atmosphere with T_{eff} = 100,000 K, log (g) = 8, and n(H)/n(He) = 0.1. That for LSIV +10°9 is compared to a model with T_{eff} = 65,000 K, log (g) = 6, and n(He)/n(H) = 1. In all cases, the points represent Voyager 1 and UBV observations, and the solid curves represent IUE observations and model atmosphere calculations.

ANALYSIS OF HIGH-DISPERSION IUE SPECTRA OF SUBDWARF B STARS

R. Lamontagne, F. Wesemael, G. Fontaine
Département de Physique and Observatoire du mont Mégantic
Université de Montréal
and
E.M. Sion
Department of Physics, Arizona State University
and
Department of Astronomy, Villanova University

ABSTRACT

High-dispersion IUE spectra of the subdwarf B stars UV 1758+36 and Ton S-227 are presented. These spectra are characterized by the presence of a large number of photospheric low- and medium-excitation lines from numerous ions. The lines of C, N, and Si are used in conjunction with LTE metal line calculations to derive preliminary abundances for these elements. These results are compared and contrasted with those obtained for the hotter OB and O subdwarfs.

INTRODUCTION

Abundance analyses of hot subdwarfs based on high-dispersion, far-ultraviolet observations from the IUE constitute a powerful tool for the study of these stars, as abundance differences between various classes of subdwarfs will, ultimately, have to be interpreted either in terms of different initial conditions, or as the logical consequence of physical processes (such as convection or element diffusion) operating along a single evolutionary track. The initial studies of high-dispersion IUE spectra of hot subdwarfs have underscored the usefulness of such observations by revealing an ultraviolet spectrum very rich in metal lines (Baschek, Kudritzki, and Scholz 1980; Gruschinske et al. 1980; Rossi et al. 1980; Simon et al. 1980; Bruhweiler, Kondo, and McCluskey 1981; Baschek et al. 1982 hereafter BKSS; Baschek, Höfflich, and Scholz 1982, hereafter BHS; Heber et al. 1982). These investigations have already revealed some interesting patterns. Silicon, for example, has been suggested to be in solar abundance in the hot sdO stars, but strongly deficient in the intermediate-temperature OB subdwarfs.

In order to further study abundance trends in hot B subdwarfs, we have observed UV 1758+36 (V=11.4) and Ton S-227 (V=11.8) with the IUE satellite. A preliminary analysis of these ultraviolet spectra is presented here, together with our initial estimates of the abundance of the astrophysically important C, N, and Si ions.

OBSERVATIONS

High-dispersion IUE spectra of UV 1758+36 and Ton S-227 were obtained with the SWP camera on 1983 August 12 (SWP 20668) and 1983 October 25 (SWP 21362) respectively. The exposure times were 225 m and 210 m respectively. Our radial velocity measurements from these images are in fair agreement with published values obtained from optical spectra (v=-44 km s^{-1} for UV 1758+36; v=+84 km s^{-1} for Ton S-227).

The observed spectra display numerous low- and medium-ionization absorption lines. This is illustrated in Figure 1 where we show the region around 1300 Å in UV 1758+36. The separation between interstellar and photospheric components is eased by the large stellar radial velocity although, in the case of UV 1758+36, the ISM lines were also found to be displaced by a rather large velocity (v_{ISM}=-38±1 km s^{-1}), thus rendering the separation considerably more difficult than anticipated. The identification of photospheric C, N, and Si features was performed by comparing the laboratory wavelengths of Kelly and Palumbo (1973) with those measured on our spectra shifted to the laboratory frame. In general, a wavelength coincidence to better than 0.1 Å was required for identification. We find no evidence, at this stage, for P Cygni profiles (e.g., Hamann et al. 1981) or for line velocity structure (e.g., Bruhweiler and Dean 1984) in the spectra of these two objects.

Because of the numerous absorption lines present in the ultraviolet spectra of B subdwarfs, we found no truly objective way to set the continuum for equivalent width measurements. The procedure we have adopted consists of fitting a spline through each order, using typically 12-15 visually chosen points per order to define collocation points. All our measurements incorporate an empirical correction to correct for improper background subtraction below ~ 1400 Å. As a check, we have used our method to measure equivalent widths of several lines in the high-dispersion images of the sdOB stars HD 149382 and Feige 66. A comparison of these measurements with those of BKSS and BHS shows average differences of ~ 20% -with our widths being generally, but not consistently, lower than those of these authors (who used the standard IUE background correction procedure).

ABUNDANCE DETERMINATIONS

Preliminary abundances for the C, N and Si ions in the atmosphere of UV 1758+36 and Ton S-227 were obtained by performing LTE metal line calculations for two model atmospheres with the following parameters: T_e=32,500 K, log g= 5.25, He/H=1.7x10^{-2} for UV 1758+36 (Giddings and Dworetsky 1978); and T_e=34,000 K, log g=6.0, and He/H=5x10^{-3} (Heber et al. 1984) for Ton S-227. A microturbulent velocity ξ=5 km s^{-1} was adopted for all abundance determinations. This value is consistent with that determined in the OB subdwarf HD 149382 by BKSS, and with the upper limits in three subdwarf O stars of Simon et al. (1980).

The carbon abundance determination is based on the presence of three ionization states (CII, CIII, and CIV). The CIII λ1176 line in our objects is contrasted with that in the two OB subdwarfs studied by BKSS and BHS in Figure 2. We believe our final abundance to be quite reliable, although the error bars do reflect a tendency for CII λ1324 to yield somewhat larger abundances than the CIII, CIV features. The nitrogen determination is also based on three ionization states (NIII, NIV, and NV), and is thus reasonably secure. The values given represent an average based on 5-7 features. The silicon abundance is based exclusively on the absence of Si IV λ1400 in the spectra of both stars (see Fig. 3), which yields rather stringent limits.

Our preliminary abundances are summarized in the table, where we also list those values determined from IUE spectra for the hotter OB and O subdwarfs. We find both the carbon and silicon abundances to be much less than solar, while nitrogen appears normal. The silicon abundance, in particular, appears

quite different from that in the sdO stars, and also from that determined from optical and low-dispersion ultraviolet data in other sdB stars (Baschek and Norris 1970; Baschek, Sargent, and Searle 1972; Heber et al. 1984); it is consistent, however, with that determined in two OB subdwarfs by BKSS and BHS. Clearly, these preliminary investigations suggest that the heavy element abundances in hot subdwarfs may well display considerable variations from star to star. This points toward a need for further high-dispersion IUE studies, coupled with abundance analyses, of these objects.

This work was supported in part by the NSERC Canada, the NASA grant NAG 5-343, and the NSF grant AST 81-17177.

REFERENCES

Baschek, B., Höfflich, P., and Scholz, M. 1982, Ast. Ap., 112, 76 (BHS).
Baschek, B., Kudritzki, R.P., and Scholz, M. 1980, in Proceedings of Second European IUE Conference, ESA SP-157, p. 319.
Baschek, B., Kudritzki, R.P., Scholz, M., and Simon, K.P. 1982, Ast. Ap., 108, 87 (BKSS).
Baschek, B. and Norris, J. 1970, Ap.J. Suppl., 19, 327.
Baschek, B., Sargent, W.L.W., and Searle, L. 1972, Ap.J., 173, 611.
Bruhweiler, F.C. and Dean, C.A. 1984, Ap.J. (Letters), 274, L87.
Bruhweiler, F.C. and Kondo, Y. 1982, Ap.J., 259, 232.
Bruhweiler, F.C., Kondo, Y., and McCluskey, G.E. 1981, Ap.J. Suppl.,46, 255.
Giddings, J.R. and Dworetsky, M.M. 1978, M.N.R.A.S., 183, 265.
Gruschinske, J., Hunger, K., Kudritzki, R.P., and Simon, K. 1980, in Proceedings of Second IUE Conference, ESA SP-157, p. 311.
Hamann, W.R., Gruschinske, J., Kudritzki, R.P., and Simon, K.P. 1981, Ast. Ap. 104, 249.
Heber, V., Hamann, W.R., Hunger, K., Kudritzki, R.P., Simon, K.P., and Mendez, R.H. 1982, in Proceedings of Third European IUE conference, ESA SP, p. 297.
Heber, U., Hunger, K., Jonas, G., and Kudritzki, R.P. 1984, Ast. Ap., 130, 119.
Kelly, R.L. and Palumbo, L.J. 1973, Atomic and Ionic Emission Lines below 2000 Angstroms (NRL Rept., No. 7599).
Rossi, L., Viotti, R., Darius, J., and D'Antona, F. 1980; in Proceedings Second European IUE Conference, ESA SP-157, p. 323.
Simon, K.P., Gruschinske, J., Hunger, K., and Kudritzki, R.P. 1980, in Proceedings Second IUE Conference, ESA SP-157, p. 305.

METAL ABUNDANCES IN HOT SUBDWARF STARS

Star	Type	Abundances[1]			Reference
		ϵ C	ϵ N	ϵ Si	
UV 1758+36	sdB	$6.7^{+0.6}_{-0.3}$	7.6±0.4	<1.9±0.6	a
Ton S-227	sdB	$4.8^{+1.0}_{-0.5}$	7.8±0.5	<3.1	a
HD 149382	sdOB	6.6±0.3	8.0±0.3	<2.3±0.6	b
Feige 66	sdOB	6.4±0.3	8.2±0.3	<2.3±0.6	c
Feige 110	sdOB	3.1±0.5	$7.8^{+0.4}_{-1.2}$	...	d
HD 49798	sdO	7.9	10.0	8.3	e
HD 127493	sdO	7.7	9.6	8.4	e
BD +75°325	sdO	8.1	9.8	8.3	e
Sun	...	8.5	8.0	7.5	...

References - a) This work; b) Baschek et al. (1982); c) Baschek, Höfflich, and Scholz (1982); d) Heber et al. (1982); e) Simon et al. (1980).

[1] $\epsilon_Z \equiv 12 + \log (N(Z)/N(H))$

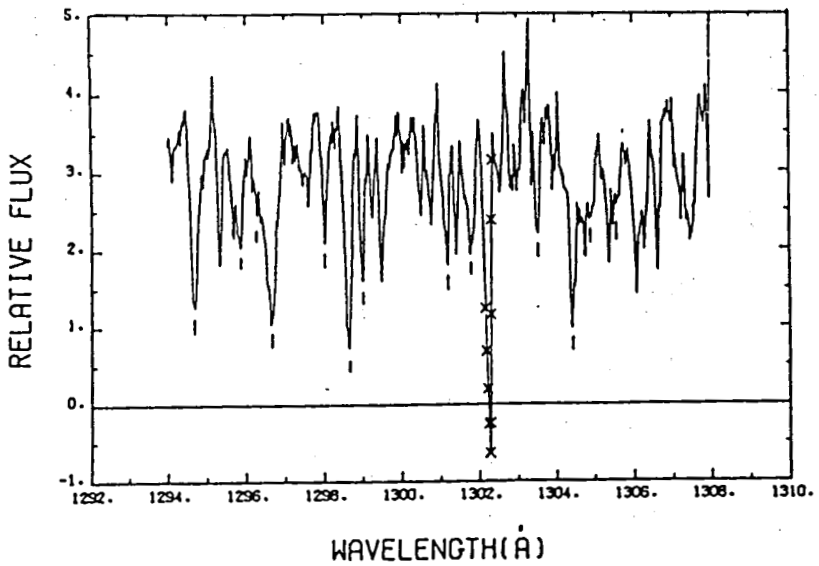

Fig. 1 - The region around 1300 Å in UV 1758+36. Tick marks indicate features with a preliminary identification.

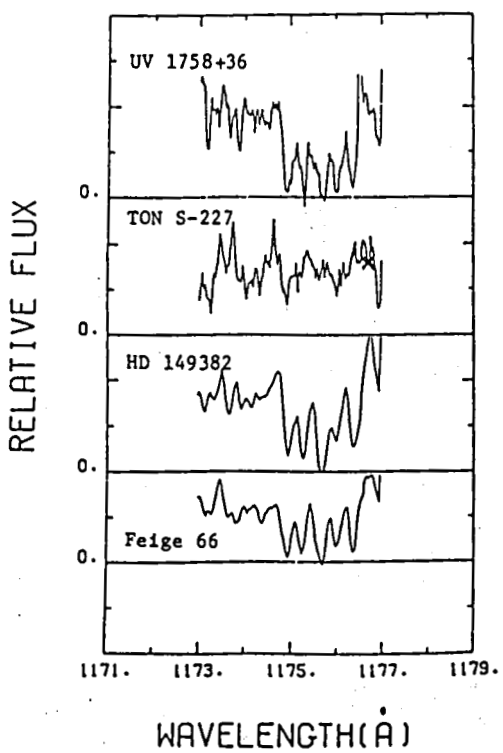

Fig. 2 - The CIII λ1176 complex in two sdB stars (top) and two sdOB stars (bottom).

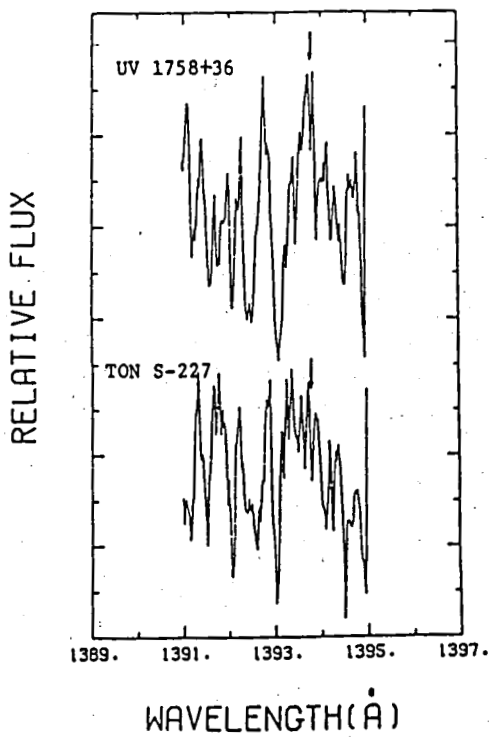

Fig. 3 - The region around 1393 Å in our program stars. The arrows indicate the expected location of the Si IV λ1393 component.

MASS DISTRIBUTION AND EVOLUTIONARY SCHEME FOR CENTRAL STARS OF PLANETARY NEBULAE

Sara R. Heap, Goddard Space Flight Center
and
Harry G. Augensen, Widener University

I. INTRODUCTION

Nearly all investigators agree on the general scheme for the late stages of evolution of stars having low or intermediate masses. According to this scheme, a star ascends the asymptotic giant branch all the while losing mass via a strong stellar wind. At some point, the star enters a brief "superwind" phase, during which the planetary nebula is formed, and the remnant central star then evolves toward its final fate as a white dwarf.

Implicit in this scheme is a funneling process whereby stars with a wide range in initial mass get skinned down below the Chandrasekar mass limit (1.44M⊙) for white dwarfs. Iben and Renzini (1983) have built evolutionary models that account for mass-loss by red-giants by means of a semi-empirical formula devised by Reimers (1975):

$$\dot{M} = \eta * 4.E\text{-}13\ L/g/R\ M\odot \text{ per year.}\quad (L, g, R \text{ in solar units}).$$

They compute a mass-funneling (Figure 1) which at least qualitatively approximates observational evidence (Weidemann 1981).

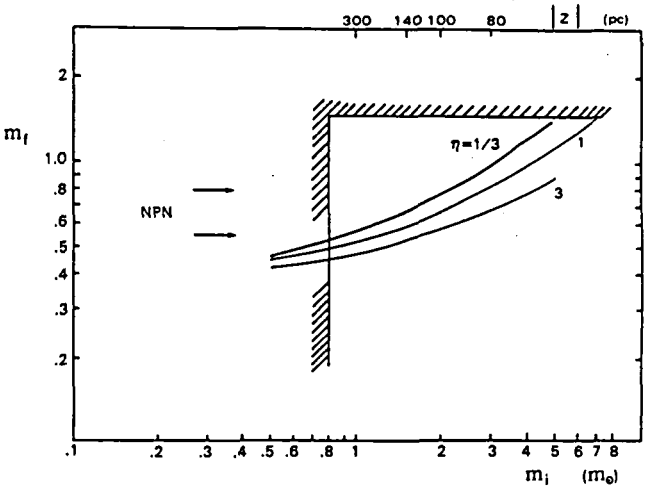

Figure 1. Relation between initial mass (mi) and final mass (mf) for three values of η. The range in the masses of nuclei of planetary nebulae observed with the IUE is indicated by "NPN".

What remains controversial is just what the value of η is (assuming, perhaps naively, that the Reimers formula is valid). The answer to this question has important implications for stellar evolution. The value of η is thought to be about one but uncertain by a factor of three or so. If η is as low as one-third, then stars initally more massive than 5M$_\odot$ become neutron stars, and stars less massive than 5M$_\odot$ become white dwarfs; if η is as high as three, then the critical mass dividing these two end-points of evolution is 8M$_\odot$.

In this talk, we present new estimates of the initial mass and final mass of central stars of planetary nebulae, and we argue for a low value of η.

II. THE MASS DISTRIBUTION OF CENTRAL STARS

We inferred the (final) masses of central stars from their positions on an evolutionary diagram, which plots optical stellar magnitude vs. kinematic age, as indicated by the radius of the nebula (Rneb). This type of plot (Figure 2) is an extraordinarilly sensitive mass-analyzer. The sensitivity results from the facts that: i) the main effect of stellar evolution is optical fading of the central star, and ii) that the rate of fading is an extremely strong function of mass. This method of evolutionary plots was first devised and applied by Schoenberner (1981), but we have added a new twist: we used IUE data to derive the stellar absolute magnitude at 1300 Å. The reasons why we used IUE fluxes for this diagram are that they form an internally consistent and remarkably reliable set of photometric data. More importantly, they offer the greatest possible discrimination of the star against the surrounding nebula. This contrast enhancement afforded by the far-ultraviolet allowed us to broaden our observing sample to include stars embedded in small, bright nebulae.

At the time when we started this study, there were about 65 planetaries whose IUE spectra showed the definite presence of a hot central star, and so we used this set as our observing sample. The spectra of the IUE sample are as diverse as central stars in general: there are white dwarfs, Wolf-Rayet stars, Of, O, and sdO stars, and stars with apparently continuous spectra. In other ways, the sample is somewhat biased: the stars are among the apparently brightest of central stars, and their galactic distribution tends more toward a halo population than does that of planetaries as a whole.

Figure 3 shows an evolutionary plot of ultraviolet stellar magnitude versus observed nebular radius, corrected for variable expansion velocity and for the effects of optical thickness (R'neb). The superposition of a theoretical mass-age grid onto the evolutionary diagram indicates that all the central stars in the IUE sample have masses in the range, 0.55 to 0.75 M$_\odot$. This mass range is even more restricted than that of white dwarfs

(Koester et al. 1979)! Evidently a central star more massive than $0.75M_\odot$ evolves so quickly that it becomes a faint white-dwarf beyond the reach of IUE before we recognize that a nebula has even been formed. A central star less massive than $.55M_\odot$ evolves away from the red-giant branch so slowly that the nebula has disappeared from view long before we recognize the stellar remnant as a hot planetary nucleus. Perhaps, many of the field sdO stars are central stars that have outlived their nebulae.

III. IMPLICATIONS FOR STELLAR EVOLUTION

With such a narrow distribution in stellar mass, you might not expect to distinguish mass-effects within the sample. Nevertheless, that is exactly what you see. If you divide up the IUE sample according to population type (using height above the galactic plane and deviation from circular velocity as population indicators) you find (Figure 3) that the halo-prone central stars have lower masses than do the disk-prone central stars. Evidently, the mechanism for mass-loss in red-giants is so finely tuned that, regardless of population type and initial mass of the precursor, the final remnant mass falls neatly into a slender mass range with the high-mass (disk-type) progenitors producing slightly more massive central stars than the low-mass (halo-type) progenitors.

What are the progenitors of planetaries? To answer this question, let's go back to Iben and Renzini's graph (Figure 1) relating initial mass to final mass. We have an estimate of the average mass of central stars in the IUE sample. We also have an estimate of their average initial mass from their galactic distribution and from Schmidt's (1963) calibration of the galactic Z - initial mass relation. What we find is that the higher-mass central stars ($\sim .7M_\odot$) are concentrated in the galactic disk and derive from stars with initial masses of $\ddot{\sim}1.4M_\odot$, while the low-mass central stars ($\ddot{\sim}.55M_\odot$) belong to the old-disk or halo populations and derive from stars with initial masses of $\ddot{\sim}1.0\ M_\odot$ or less. Armed with this information, we can read off the value of η directly from Figure 1. Depending on whether we treat the IUE sample as a homogeneous group or take into account their distribution in population type, we get an η between a third and a half. This value for η implies that white dwarfs have progenitors whose masses were $5M_\odot$ or less.

Iben,I. and Renzini, A., 1983, Illinois Astr. Preprint 82-2.
Koester,D. et al. 1979, Astr. Ap., 76, 262.
Reimers,D. 1979, in Problems d'Hydrodynamique Stellaire, Liege
Schmidt, M. 1963, Ap. J., 137, 758.
Schoenberner, D. 1981, Astr. Ap., 103, 119.
Weidemann,V. 1981, in Effects of Mass-Loss on Stellar Evolution, Reidel: Dordrecht.

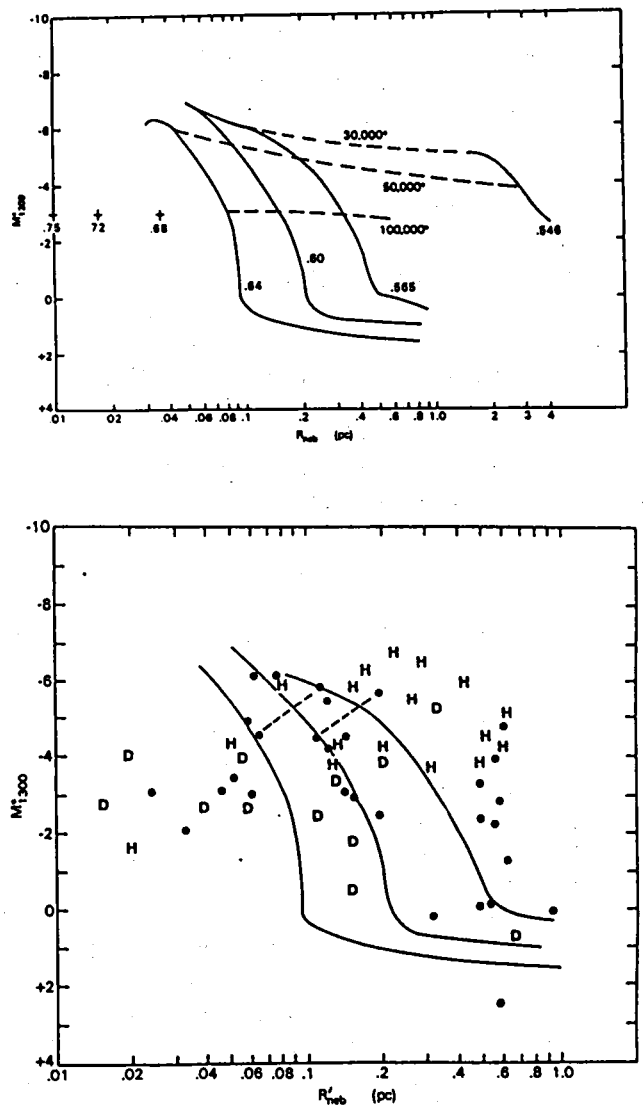

Figure 2. Mass-age grid for planetary nuclei. The ordinate is absolute stellar magnitude at 1300 Å. The abscissa is nebular radius in parsecs. Lines of constant mass are shown as solid lines; constant stellar temperature as dashed lines.

Figure 3. Evolutionary plot for planetary nuclei. Halo-, intermediate- and disk-type stars are indicated by H, •, and D, respectively. Dots connected by dashed lines indicate objects whose distances were computed both on the assumption of an optically thick (lower left dot) and optically thin (upper right dot) nebula.

THE CENTRAL STAR OF NGC 40.

Luciana Bianchi[1] and Michael Grewing[2]
(1) Osservatorio Astronomico di Torino, Italy
(2) Astronomisches Institut Tübingen, W.Germany

ABSTRACT

We present in this paper high and low resolution IUE observations of the central star of the planetary nebula NGC 40. From consideration of the 220.0nm interstellar extinction feature we determine the reddening towards NGC 40 to be E(B-V)=0.50. The continuum distribution is best fitted with a blackbody emission with Temperature between 80000 and 100000K. Comparison with existing model atmospheres for WR stars is also discussed.

The line spectrum is dominated by strong emission lines from different ionization stages of C. From the high resolution spectrum we saw that almost all the emission line flux is of stellar origin, as all the lines are extremely broad. P Cygni profiles of the CIV and SiIV resonance lines and of HeIIλ1640 indicate an expanding wind with a terminal velocity of V_∞=-1800 Km/s.

INTRODUCTION

As part of a general program to study the detailed ionization structure of planetary nebulae, we obtain UV spectrophotometry of central stars and of offset positions in extended planetary nebulae. The UV data are an important complement to the optical observations (CCD direct imaging through interference filters and IDS and CES spectroscopy): UV low dispersion spectra allow a very good determination of the reddening, and to study the central star and nebular con= tinuum distribution. From high resolution data the mass loss from the central star can be determined, which is an important parameter in the evolutionary models for PN's, and several emission lines can be resolved, which are good indicators of Temperature and Density.

In this paper we discuss the UV spectrum of the central star of NGC 40: BD+30-3639. The star was classified as WC8 by Hiltner and Shild (1966). This spectral type was the confirmed by several authors.For a review of the previous optical and UV observations of the star and the nebula we refer to Grewing and Bianchi(1984), hereafter GB84.

THE ULTRAVIOLET DATA

The IUE observations

We obtained low and high resolution spectra of the nucleus of NGC 40 with the IUE SWP and LWR cameras. We also used data available from the IUE archive, and combine them with our data. Details of the data, and discussion of the observations offset the nucleous can be found elsewere (GB84).The low resolution spectrum (combination of several images) is shown in Fig.1.

Extinction and distance

In the literature very different values are quoted for the reddening of NGC 40, from E(B-V)=0.20 to 0.82. From the strength of the 220.0nm dip we derive E(B-V)=0.50±0.05, assuming that the continuum distribution is smooth over the range. We can in fact exclude any contribution from the nebular continuum, as the spectra are not extended, and the nebular continuum observed in offset positions is almost two orders of magnitude fainter that the stellar flux. A detailed discussion of previous determinations of E(B-V) and of the uncertainties of the various method used is given in GB84. Our value of 0.50 is in agreement with determinations based on the ratio Radio/H_β flux (E(B-V)≤0.65, Cahn and Kaler,1971; E(B-V)=0.50, Cahn,1976; E(B-V)=0.45, Pottash et al.,1977) and based on the Balmer line measurements by Clegg et al.(1983):E(B-V)=0.45 and 0.51. However Balmer line ratios can give very different results, since NGC 40 is very inhomogeneous (e.g. Cahn,1976, finds E(B-V)=0.20).

Based on ANS data, Pottasch et al.(1978) find E(B-V)=0.38. We can see from our spectra that the CIII λ 2297 line is very strong, which was included in the ANS band centered at 2200Å. This explain the discrepancy of the results by Pottasch et al. Also based on UV data, Benvenuti et al.(1982) quote E(B-V)=0.40 and Clegg et al.(1983) infer E(B-V)=0.34. These values however leave the 220nm bump strongly undercorrected.

From our value of E(B-V)=0.50, we derive a distance for NGC 40 of d=980pc, by comparison with stars of known distance and reddening within 2°from the position of NGC 40. This value is in agreement with previous determinations, except for values based on the angular expansion velocity.

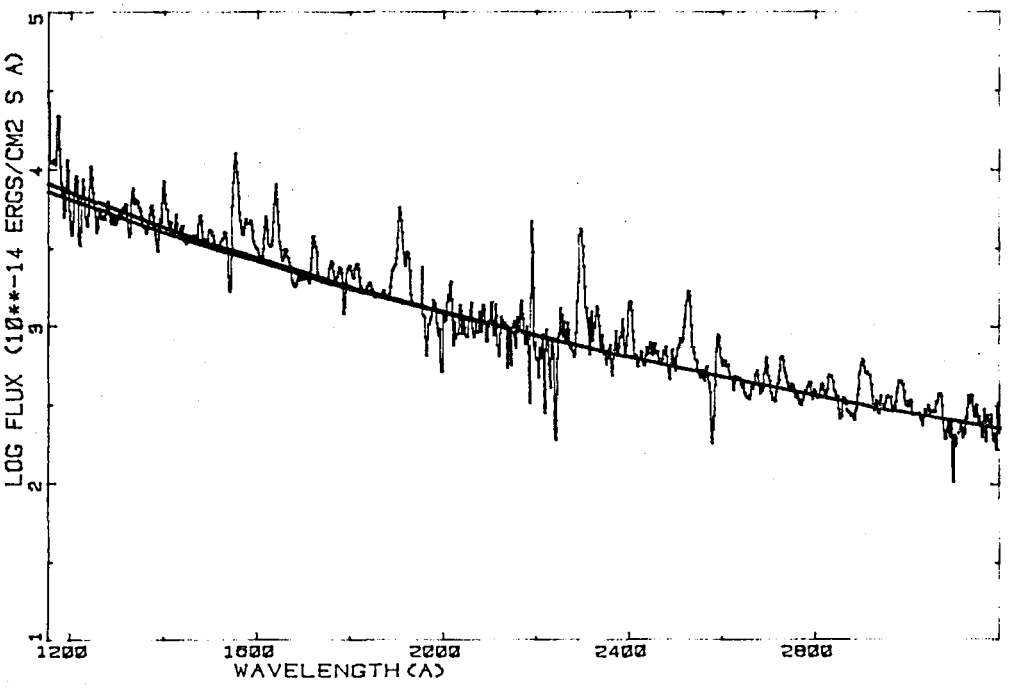

Fig.1. The SWP+LWR spectrum, dereddened with E(B-V)=0.50 is compared with blackbody distributions for T=80000K and T=100000K.

Temperature and luminosity

In Fig.1 we show a blackbody fit to the dereddened spectrum for T=80000K and T=100000K. Such a high temperature is in agreement with the theoretical predictions; in fact, on the basis of evolutionary calculations, WN and WC stars are expected to have temperatures around 90000K (Vanbeveren, 1980). Early optical studies (e.g. Kuhi,1966,1968) indicated that WR continua are very hot, however much lower values (T=30000 to 70000K) are often quoted in the literature. The discrepancies are not surprising, since in WR stars effective temperature, color temperature and excitation temperature are not simply related, and the color temperature depends on the wavelength at which it is determined, due to the influence of the "extended continuum" which can significantly modify the emergent flux.

Comparison of existing models for WR stars show that stars with very different Teff can have the same distribution of the emergent flux, depending on the extent of the dense atmosphere. All the models are cooler than our observed spectrum. Maybe the nucleus of NGC 40 does not have a very extended dense envelope, to "flatten" the emergent flux. This seem to be supported by the density values derived from the CIII lines relative intensities (see GB84).

Determinations of T based on energy-balance methods (OIII/OII ratio,e.g. Köppen and Tarafdar,1978; Zanstra method, e.g.Harmann and Seaton,1966) give low values, around 30000K. This may be due to the fact that NGC 40 is optically thin.

From the blackbody fits shown in Fig.1 we derive, using our value of the distance d=980pc, a radius of the emitting nucleus of R=0.45 and R=0.53 $R_\odot$ for T=80000 and T=100000K respectively. This value is typical for a WR PN nucleus.

The line spectrum

A table with line identifications and absolute fluxes is given in GB84. We show in Fig.2 some portions of the high resolution spectrum, to illustrate the fact that the emission lines from all ionization stages of C observed are stellar, having a width of more than 1000 Km/s. Nitrogen lines are almost absent, as in most WC stars. The resonance doublets of CIV and SiIV, and HeII λ1640, show P Cygni profiles characteristic of WRs, with very high emission/absorption ratio. They indicate that the envelope is expanding with a terminal velocity of -1800Km/s. We are in the process of fitting these profiles with theoretical calculations, to determine the mass loss rate (results will be published elsewhere).

REFERENCES

Benvenuti,P.,Perinotto.M.,Willis,A.,1982,IAU Symp. N99,p.453
Cahn,J.H.,1976,Astron.J.,81,407
Cahn,J.H.,Kaler,J.B.,1971, Ap.J. Suppl.,22,319
Grewing,M., Bianchi,L.,1984, preprint
Hartmann,R., Seaton,M.,M.N.R.A.S.,132, 15
Hiltner,W., Schild,R., 1966, Ap.J.,143, 770
Koppen,J., Tarafdar,S.P.,1978, A.A.,69,363
Kuhi,L.V.,1966, Ap.J.,143,753
Kuhi,L.V.,1968,in "WR stars",Gebbie and Thomas eds.,U.S.Govt.printing off.,p.110
Pottasch,S.,Wesselius,P.,Wu,C.,van Duinen,R.,1977, A.A., 54, 435
Vanbeveren,D., 1980,IAU Symp. N.88, p.169

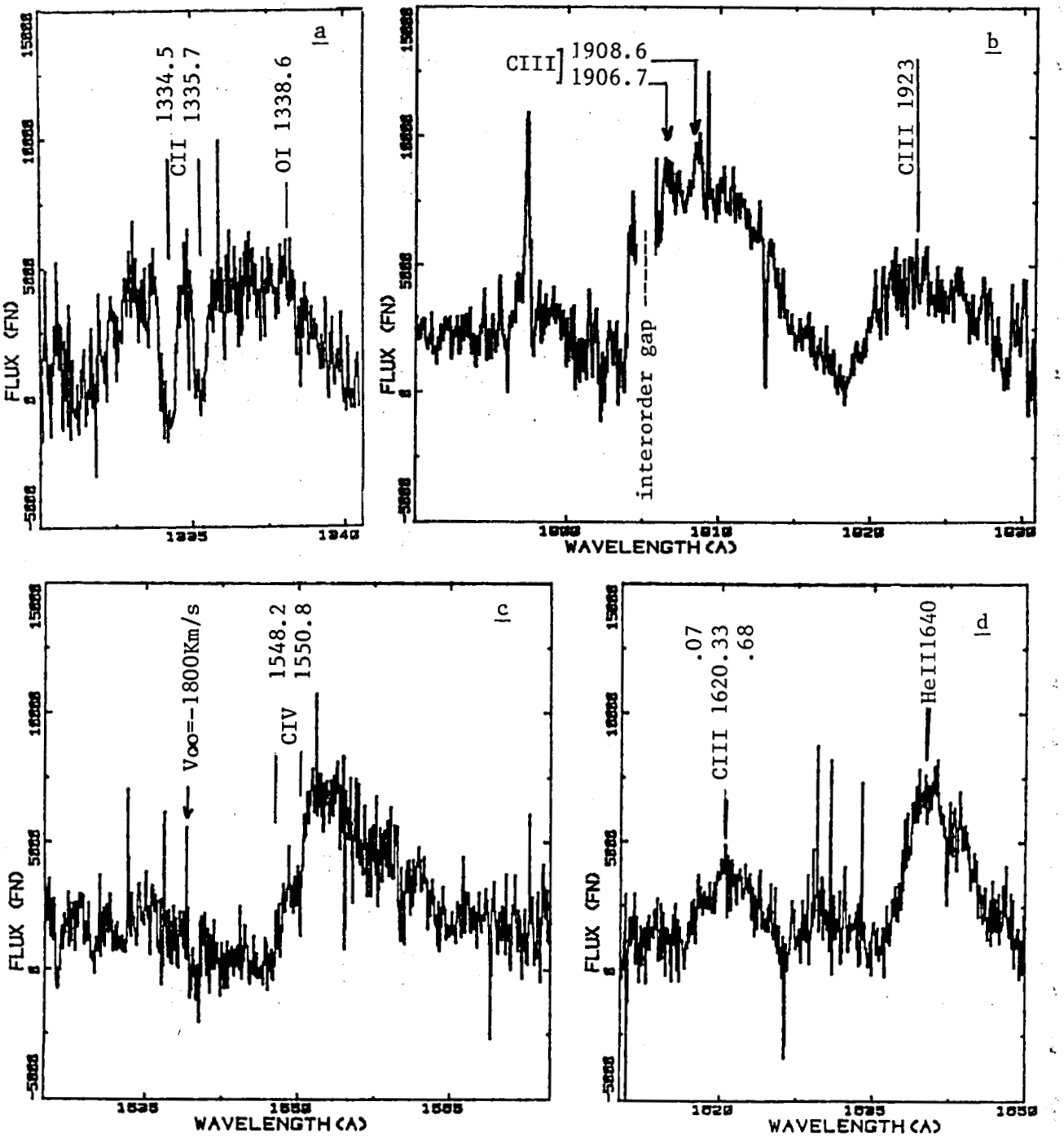

Fig.3 . Some portions of the high resolution spectrum of NGC 40's nucleus are shown. In a and b :the doublets of CII(1)1335 and CIII] 1908 are blended, due to the extreme broadening of the stellar lines. On top of the CIII stellar emission the two narrow nebular components are visible (indicated with arrows). In c and d the P Cygni profiles of CIV(1) and HeII are shown.

WHITE DWARFS

FURTHER INVESTIGATIONS OF MASS LOSS PHENOMENA IN HOT WHITE DWARFS AND O SUBDWARFS

Frederick C. Bruhweiler
Department of Physics
Catholic University of America

ABSTRACT

Previous IUE studies have found sharp, shortward-displaced absorption features in two DA white dwarfs (Bruhweiler and Kondo 1981, 1983) and in three O subdwarfs (Bruhweiler and Dean 1983) indicative of mass loss. Anomalous abundances and the presence of subordinate lines, especially in the case of the DA white dwarf, 2111+49, rules out an interstellar origin for these features. Continued analysis of new and archival data has added one DA white dwarf and possibly two O subdwarfs to the growing list of subluminous stars displaying these features. One, possibly both, of these new O subdwarfs are of extreme low luminosity, intermediate between normal O subdwarfs and the hot white dwarfs. These observations provide evidence that a single mechanism is responsible for the unusual features seen in O subdwarfs and DA white dwarfs.

INTRODUCTION

High dispersion IUE data have revealed at least six hot white dwarfs to display absorption features of heavy elements. In two DA white dwarfs, G191-B2B and 2111+49, sharp, shortward-dispalced absorption features are seen, which are formed in an expanding halo, which further implies that these white dwarfs are undergoing mass loss (Bruhweiler and Kondo 1981, 1983). These features appear "interstellar-like" and an interstellar origin for these features has been proposed (Dupree and Raymond 1983). However, such an interpretation is in sharp conflict with most of the observed data. This is especially true for the "silicon" white dwarfs, W1346 and 2111+49 (Bruhweiler and Kondo 1983). In the case of 2111+49, only shifted features of Si III and Si IV are seen; this includes the strong 3P-3P^{o} subordinate lines of Si III near 1300 A. The observed presence of only Si in 2111+49 and W1346 implies very unusual abundances. Either the unusual abundances in the Si white dwarfs, or the appearance of subordinate lines in 2111+49 is enough to rule out an interstellar origin for these lines.

We have extended our search of shortward-displaced features to the higher luminosity O subdwarfs, possible evolutionary progenitors to white dwarfs. We have specifically studied the spectral regions bracketting the resonance doublets of N V (1240 A), C IV (1550 A), and Si IV (1400 A). Preliminary inspection has revealed shortward-displaced features in BD+28^{o}4211, BD+75^{o}325 and HD 128220 B (Bruhweiler and Dean 1983). Features are found to be both transient, lasting on the order of months or less before fading away, and persistent, remaining relatively constant in strength and velocity over at least nine months. Whether the features seen in O subdwarfs are manifestations of a similar process occurring in the white dwarfs is not clear.

OBSERVATIONS

We present sample results obtained in our continuing program to search for, and hopefully, ultimately explain the presence of displaced sharp-lined features in hot subluminous stars. We briefly present recent results for one DA white dwarf and two O subdwarfs below.

a. The DA White Dwarf GD 071

We have utilized the exceptionally good interval wavelength scale of the SWP camera (Thompson, Bohlin, and Turnrose 1982) to aid in searching for weak shifted features. Instead of analyzing the spectral data in the wavelength frame, we convert all data to the velocity frame with the transformation $v = c(\lambda-\lambda_{lab})/\lambda_{lab}$ where c is the speed of light and λ_{lab} is the laboratory wavelength of the transition of interest. Examining data in the velocity frame has proven quite valuable in confirming the existance of weak, shortward-displaced features in O subdwarfs (Bruhweiler and Dean 1983).

Figure 1 shows the results for the high-dispersion image SWP 22023, which displays the spectral regions around the stronger transitions of the resonance doublets of N V, C IV, and Si IV in GD 071. This figure reveals what can be interpreted as a spectral component in all three ions. These features are very weak, and the interpretation may at first appear questionable. However, the continua of hot DA white dwarfs are flat and featureless, except in rare instances where a few spectral lines are found. Thus, we can coadd the spectral-velocity information in Figure 1, such that any velocity components would be greatly enhanced. Figure 2 shows the results of coadding the data in Figure 1. Analysis performed on another high-dispersion image (SWP 18273) of GD 071 yielded identical results. Both images were in excellent agreement and a velocity component at $V_o = +36$ km s^{-1} is unmistakable. The measurements yielded a σ less than 4 km s^{-1}. This derived velocity compares to $V_\odot = 63\pm19$ km s^{-1} determined for the photospheric Balmer lines (Trimble and Greenstein 1972), and $V_\odot = 11\pm3$ km s^{-1} for the interstellar lines. The evidence suggests that these are halo lines formed in the gravitational potential well, above the more gravitationally red-shifted photospheric Balmer lines of the white dwarf. Alternatively, the halo might be expanding, and similar to what is observed for G191-B2B and 2111+49.

b. The O Subdwarfs LS II 18°9 and LSE 21

The IUE spectra of the two unusually hot, and likely low luminosity O subdwarfs LS II 18 9 (T_{eff}= 60,000 K; log $(L/L_\odot)$ = 1.1 +0.6/-0.8) and LSE 21 (T_{eff}= 120,000 K; log $(L/L_\odot) \sim 1.7$) (Schönberner and Drilling 1984) reveal shortward-skewed profiles for the lines of the N V doublet at 1240 A (Figure 3). Weak Fe VI photospheric features are expected at -30 and -34 km s^{-1} from the N V photospheric lines. Yet, they should be too weak and too sharp to account for the observed asymmetries. Since O subdwarfs typically show extensive Fe IV, V, and VI line blanketing in the UV (Bruhweiler, Kondo, and McCluskey 1981; Dean and Bruhweiler 1984), we cannot rule out other photospheric contributors. Nonetheless, these observations are consistent with shortward-displaced N V, either arising in a low terminal velocity wind or in discrete velocity components on the order of -70 to -125 km s^{-1}. If this interpretation is correct, then these extreme low luminosity O subdwarfs may

link to the mass loss phenomena seen in O subdwarfs to that seen in the hot DA white dwarfs.

One can speculate that a common mechanism is responsible for these features, possibly akin to that which produces planetary nebulae. Or, one can alternately speculate that the appearance of sharp, shortward-shifted features in relatively unevolved O and B stars (Lamers et al. 1982; Peters 1982) may suggest that there is a universal mechanism producing these features in all hot stars regardless of luminosity. (More detailed results will be presented elsewhere.)

REFERENCES

Bruhweiler, F.C., and Dean, C.A. 1983, Ap. J., 274, L87.
Bruhweiler, F.C., and Kondo, Y. 1981, Ap. J. (Letters), 248, L123.
_____. 1983, Ap. J., 269, 657.
Bruhweiler, F.C., Kondo, Y., and McCluskey, G.E. 1981, Ap. J. Suppl., 46, 255
Dean, C.A., and Bruhweiler, F.C. 1984, Ap. J. submitted.
Drilling, J.S., Holberg, J., and Schönberner, D. 1984, Preprint.
Dupree, A.K., and Raymond, J.C. 1984, Ap. J. (Letters), 275, L71.
Lamers, H.J.G.L.M., Gathier, R., and Snow, T.P. 1982, Ap. J., 258, 186.
Peters, G.J. 1982, Ap. J. (Letters), 253, L33.
Schönberner, D., and Drilling, J.S. 1984, Ap. J., In Press.
Thompson, R.W., Turnrose, B.E., and Bohlin, R.C. 1982, Astr. Ap., 107, 11.

FIGURES

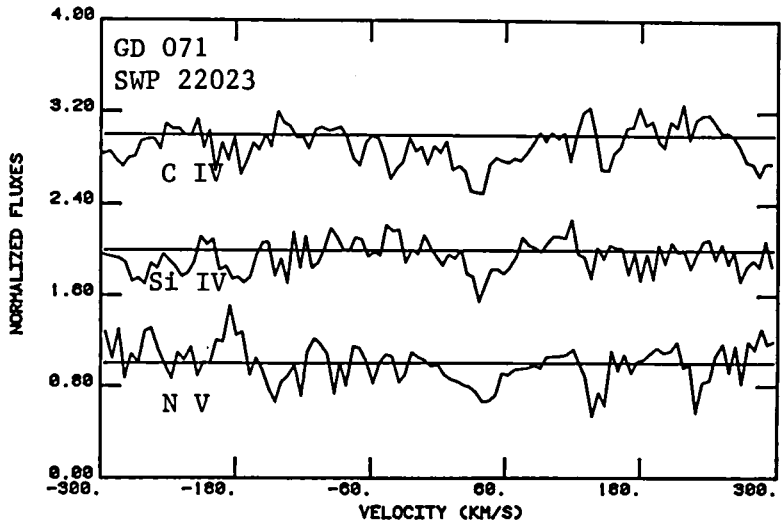

Figure 1. The spectral regions of N V, Si IV, and C IV in GD 071. The regions around the stronger line of each resonance doublet is displayed. The spectra have been normalized for display purposes. Possible weak features near -40 km s^{-1} are evident as indicated.

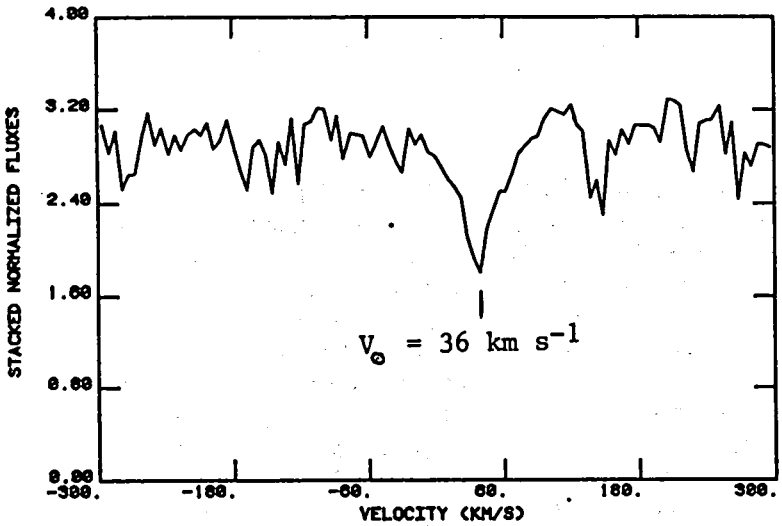

Figure 2. The coadded spectral-velocity information. The spectra in Fig. 1 are coadded. A definite velocity component appears at +36 km s^{-1}. The component at 130 km s^{-1} is an artifact and not real.

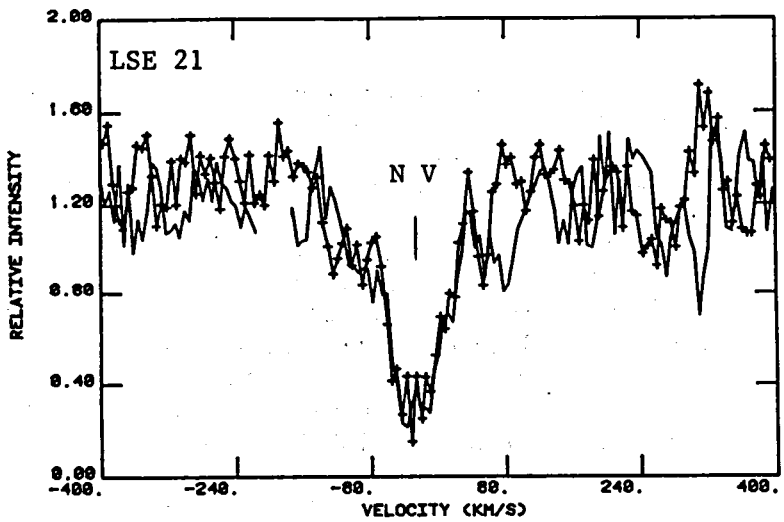

Figure 3. N V in LSE 21. A shelf or asymmetry is seen in the shortward wing of the N V profile. The stronger, shorter wavelength line of the N V doublet is represented by (+).

IUE SPECTROPHOTOMETRY OF THE HOT HELIUM-RICH PG1159 DO DEGENERATES

Edward M. Sion[1], James Liebert[2], Sumner Starrfield[3], and F. Wesemael[4]

ABSTRACT

The PG1159 degenerates represent the hottest spectroscopic subgroup of DO stars. Their optical spectra are characterized by broad HeII (λ4686) absorption and several transitions of CIV, NIII and CIII. High resolution MMT scans reveal central emission reversals. The discovery of complex, non-radial pulsations in four members of the class underscores the need for accurate temperatures, gravities and abundances for these objects. We have obtained low resolution IUE spectra of four PG1159 stars, PG1151-029, PG1424+535, PG1520+525 and an additional image of PG1159-035 as well as an optical ultraviolet spectrum of PG2131+066. Our IUE (SWP) spectra suggest the presence of numerous metallic absorption features of CIII (λ1426-29), NIII (λ1345=48), SiIV (λ1394, 1402), SIII (λ1294-1303) CIV (λ1550), NV (λ 1240) and a few unidentified features. The metal absorption lines and HeII (λ1640) have equivalent widths of a few angstroms. IUE/Optical energy distributions are considered. Tentative identifications of CIV absorptions and possibly, weak OVI features in our optical ultraviolet reticon spectra suggest a probable link to the subluminous Wolf-Rayet OVI planetary nuclei. The PG1159 DO degenerates are the hottest known ($T_e \gtrsim 10^5$K), high gravity ($\log g \gtrsim 7$) objects.

INTRODUCTION

The PG1159 stars appear to represent the hottest spectroscopic subgroup of DO stars with two cooler subgroups being characterized on the basis of their spectra by PG1034+001 and PG0108+101 on the one hand and the coolest DO stars: HZ21, Lanning 14 and HD149+99B on the other. The critical scientific importance of the PG1159 stars is multi-fold: (1) they may represent the hottest fully or near fully degenerate stars known (Wesemael, Green and Liebert 1984, hereafter WGL) with $\log g \gtrsim 7$ and $T_e \gtrsim 10^5$K. Knowing how hot a fully degenerate star can be is of fundamental importance in determining the final evolutionary connection between the hottest white dwarfs and the subdwarf O stars, planetary nebulae nuclei and other types of very hot subluminous stars; (2) the discovery of complex, non-radial pulsation modes in the proto-type, PG1159-035, by McGraw et al. (1979) and the subsequent discovery of pulsations in three more members of the class underscores the need for accurate temperatures, gravities, and abundances for this new kind of pulsating star. Pulsation computations by Starrfield, Cox, Hodson and Pesnell (1983) have established a new hot instability strip, where partial ionization of oxygen and carbon can drive pulsations; (3) these very hot helium-rich DO stars may be the immediate progenitors of the virtually pure helium DB white dwarfs; (4) in contrast to the excitement generated by the discovery of weak (∿50-300 mA) metal absorption features in hot white dwarf IUE echelle spectra (cf. Bruhweiler and Kondo 1981; Sion and Guinan 1982; Dupree and Raymond 1982), the PG1159 stars exhibit a rich metal absorption line spectrum whose equivalent widths are a few Angstroms! Thus the PG1159 degenerates present a critical test of diffusion theory and radiative acceleration in hot helium-rich high gravity atmospheres.

OPTICAL CHARACTERISTICS

The optical spectra of these objects are characterized by a broad absorption trough at λ4640-4690 A whose red end is dominated by HeII (λ 4686) and blue end is blanketed by several transitions of CIV, NIII, and CIII with the biggest contributor usually being CIV (λ4658). A typical spectrum is shown in figure 1. Note the central emission reversals in CIV and HeII which are an additional hallmark of these objects. The emission is blue shifted with respect to the absorption centers of CIV and HeII. We also note that in sdO stars, which are presumably lower in gravity, the blends are not observed and the absorption lines are sharper. We also obtained the first optical ultra-violet reticon spectrum of a PG1159 star, PG2131+066. We tentatively identify an absorption feature at λ3687 as CIV (multiplet no. $6h^2\ H^0\text{-}9i\ ^2I$), a transition observed in some WC Wolf-Rayet stars in emission. This identification is greatly strenthened by the existence of the CIV λ4658.4 blend with HeII (λ4686). We note in passing that highly tentative identifications of weak OVI lines at λ3434, λ3811, as well as the CIV λ3934 blend, if correct, would suggest that PG2131+066 is linked to the OVI planetary nuclei (cf. Heap 1975; Kaler and Shaw 1984) but it is cooler and has a higher gravity.

ULTRAVIOLET ENERGY DISTRIBUTION AND LINE SPECTRA

We have obtained low resolution IUE spectra of four "PG1159" stars during April 1983 and December 1983, three of which had no previous IUE spectra. Our short wavelength spectra reveal, in some or all of the stars, numerous metallic absorption features of CIII (λ1426-29), NV (λ1240), SiIV (λ 1394, 1403), CIV (λ1550), NIII (λ 1345-78) and HeII (λ1640) as well as a few unidentified features. We present a summary of our suggested UV line identifications in table 1. It is possible that a few of the weaker low excitation features could have an interstellar origin. Also, there are problems with the NIII (λ1350) identification due to an uncertain wavelength coincidence and the absence of NIII at λ1750, a transition having a much greater oscillator strength. An OIV identification may be more plausible but the wavelength coincidence is even worse. If the identifications of CIII, CIV, NIII and NV are correct and these features originate in the stellar photosphere, then the effective temperature is constrained to be 10^5K or slightly higher (see WGL). A crude gravity determination for the proto-type (fitting the red wing of HeII λ4686)yielded log g = 7 . Our long wavelength spectra are quite noisy but weak HeII Paschen lines may be present. The strongest UV feature in PG1151-029, PG1424+535 and PG1520+435 is the λ1350 absorption tentatively identified as NIII.

In figure 2 we present the IUE and optical multi-channel spectrophotometric energy distributions. The energy distributions of PG1151-029, PG1525+525 and PG1424+535 are quite similar to other members of the subgroup and are very close to the Rayleigh-Jeans Limit. Observations of PG1159-035 with the UV spectrometer on board the Voyager 2 spacecraft provide additional EUV flux points but still no temperature discrimination.

DISCUSSION

The "PG1159" DO spectroscopic subgroup now includes eight members, of which four: PG1159-035, 2131+066, 1707+427 and the planetary nucleus K1-16 are known to pulsate. One other object PG1151-029 was a null detection for pulsations (Winget 1984) while the others have not yet been observed.

There can be little doubt that the PG1159 DO stars are the hottest known ($T_e \geq 10^5$K), high gravity (log g $\geq$ 7) objects. The presence of the CIV features in the optical ultraviolet spectra, if they are correctly identified, would point to an extended atmosphere structure for these objects, similar perhaps to subluminous Wolf-Rayet central stars, but with higher gravity. In order to fully understand their pulsation properties, and the edges of the hot instability strip, a still more accurate knowledge of their gravities, surface temperatures, and metal abundances is required. This work is now in progress using our UV line information, newly computed abundances together with optical spectra and a forthcoming high dispersion IUE echelle observation of PG1159-035 itself.

It is a pleasure to thank Dr. Anne Cowley for a useful discussion of the absorption feature at λ3689. This work has been supported by NASA grant NAG5-343, NSF grants AST81-17177, AST83-14788, AST82-24324 and the NSERC Canada.

REFERENCES

Bruhweiler, F., and Kondo, Y. 1981, Ap. J. (Letters), 263, L63.

Dupree, A.K. and Raymond, J.C. 1983, Ap. J. (Letters), 263, L63.

Heap, S.R. 1975, Ap. J., 196, 195.

Kaler, J. and Shaw, R.A. 1984, Ap. J., in press.

McGraw, J.T., Starrfield, S.G., Liebert, J. and Green, R.F. 1979, in White Dwarfs and Variable Degenerate Stars, IAU Colloq. No. 53, eds. H.M. Van Horn and V. Weidemann, University of Rochester, New York, p. 377.

Starrfield, S.G., Cox, A.N., Hodson, S.W. and Pesnell, W.D. 1983, Ap. J. (Letters), 268, L27.

Sion, E.M. and Guinan, E.F. 1982, Ap. J. (Letters), 265, L87.

Wesemael, F., Green, R.F. and Liebert, J. 1984, Ap. J., in press (WGL).

Winget, D. 1984, private communication.

[1]Dept. of Physics, Arizona State Univ. and Villanova Univ.
[2]Steward Observatory, University of Arizona
[3]Dept. of Physics, Arizona State Univ.; Theoret. Div., Los Alamos Nat. Lab.
[4]Dept. de Physique and Observatoire du mont Megantic, Universite de Montreal

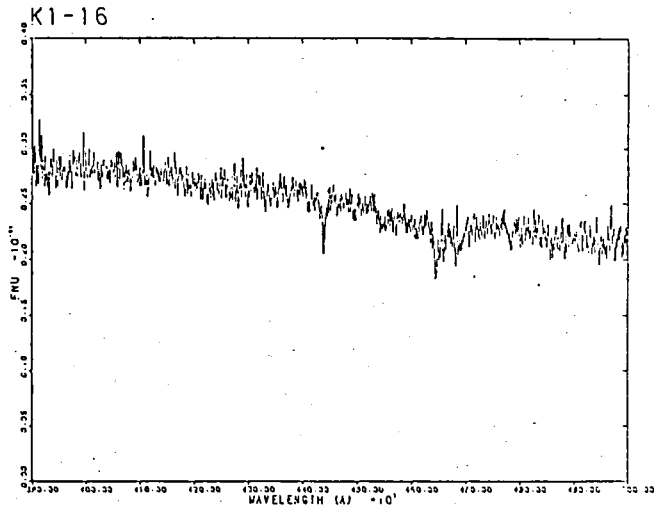

Figure 1. Steward 2.3 m PC Reticon spectrum of the PG1159 star, K1-16 showing CIV (λ4441), and HeII λ4686 (+ CIV λ4658.4).

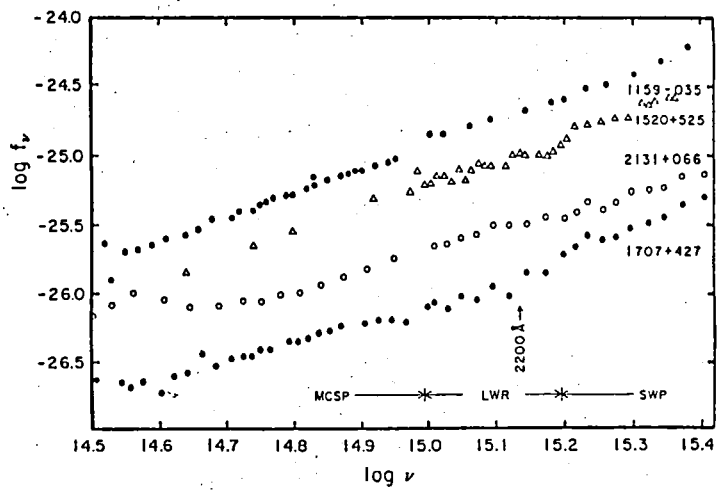

Figure 2. Energy distributions for four of the PG1159 objects. The ranges of the multi channel scanner (MCSP), and of the IUE LWR and SWP are indicated.

TABLE 1
PG1159 UV Line List (SWP Range)

1159-035	1707+427	2131+006	1151-029	1525+525	1424+535	Sugg. ID
x	1237	1239	1240	x	x	NV
(1300, 1315)	1310	1312	x	(1300)	x	blends? Si/III?
1351	1348	1350	1352	1350	1350	NIII?
x	(1368)	1370	x	x	x	?
1400	x	x	x	x	x	SiIV
(1455)	1450	x	x	1460	x	?
1547	1546	1548	x	1550	1549	CIV
x	1580	1583	1590	x	x	OIV?
1639	1637	1637	1639	1640	1640	HeII

Self-Consistent Recalibration of IUE and Determination of Hot DA White Dwarf Effective Temperatures

David S. Finley, Gibor Basri, Stuart Bowyer

Astronomy Department, University of California, Berkeley

ABSTRACT

Using low dispersion short and long wavelength camera observations we have analyzed the spectra of over twenty stars identified as DA white dwarfs, with temperatures in the range 20,000 to 70,000 K. In addition to the IUE data, we have collected all other available data on these stars from which temperature estimates may be made. We compared the observed IUE fluxes with the FUV fluxes predicted by using the observed V magnitudes and temperatures obtained from non-IUE data. These comparisons indicate a need to revise the overall IUE calibration by ~ +10% in F_λ. We computed the appropriate correction as a function of wavelength, and applied this correction to the measured IUE fluxes. We then obtained temperatures with significantly more accuracy than is achievable with optical photometry.

I. Introduction

We initiated an observing program two years ago to obtain spectra of a number of DA white dwarfs with IUE. This was motivated to a large extent by our upcoming EUV all-sky survey with the EUV Explorer, which is likely to detect large numbers of hot white dwarfs. We began by taking low and high dispersion IUE spectra of known DA's with the objective of determining T_{eff} and N_H for these objects. With these parameters, one can predict EUV detectability in the various bandpasses. Additionally, since EUV fluxes are a strong function of T_{eff}, N_H, and photospheric chemical composition, the FUV data will serve as an additional constraint on these quantities.

Our initial expectation of straightforwardly deriving temperatures on the basis of IUE fluxes was not borne out by the results. We found large discrepancies between measured and expected fluxes. As a result, we had to rederive the absolute photometric calibration for IUE before we could proceed with the analysis of our stars. We will show here the magnitude and nature of the IUE calibration errors, the means by which we corrected for these errors, and will then present our results for the stars we analyzed. Finally, we will discuss some further consequences of the current state of the IUE calibration, and describe some of the improvements that may be achieved by using our recalibration.

II. Observations and Data Reduction

The program stars are as follows: WD0050-332, WD0549+158, WD0651-020, WD1031-114, WD1620-391, and WD2309+105. The spectra were taken in May and October of 1982.

The data were analyzed by means of Basri's white dwarf model atmosphere code (Martin *et.al.* 1982). This is based on Auer's linearization method, and implements hydrogen line blanketing in LTE. The models generated have log g = 8, n(He)/n(H) = 1×10^{-5}. The effects of other helium abundances within the DA range of $< 10^{-3}$ upon the FUV fluxes are minimal.

The analysis was performed as follows. First, we obtained monochromatic colors for the star and a particular model. We have that

$$c_s(\lambda_i) = -2.5 \times log[f(\lambda_i)/f(\lambda_V)]$$

while

$$c_m(\lambda_i) = -2.5 \times log[H(T_{eff},\lambda_i)/H(T_{eff},\lambda_V)]$$

where the subscripts s and m refer to the star and the model, respectively, and $\lambda_V = 5490$Å. Then the stellar-to-model color difference is just

$$\Delta c(\lambda_i) = c_s(\lambda_i) - c_m(\lambda_i)$$

The obvious criterion for having a match of model and stellar effective temperatures is that

$$\sum[\Delta c(\lambda_i)] = 0.$$

We then proceeded to obtain effective temperatures for these objects, using the procedure described above. In addition to our program stars, we also analyzed spectra for HZ43 and G191-B2B which we had obtained from the archives.

III. Discussion

The results obtained were surprising. First, there were large systematic differences as a function of wavelength between the model fluxes and the IUE fluxes (~20 %). This is shown in Figure 1a, where we have plotted the stellar-to-model color difference as a function of wavelength for three typical stars; this color difference is calculated in the manner outlined in Section II, then

smoothed with a 21-point running boxcar mean to filter out random noise. Secondly, the temperatures obtained from fitting the IUE flux were all substantially lower than the temperatures derived from optical photometry and other measures (such as EUV photometry, ANS data, Balmer or Lyman line profile fitting). As can be seen in Figure 2a, in which we have plotted the temperature derived from uncorrected IUE fluxes *vs* the temperature derived for each star from the available non-IUE data, the trend is for the FUV/optical temperature difference to increase with increasing temperature. (Note the two different results for HZ43, for the different published values of m_V). The origin of the discrepancy is pointed out by the lower curve, which shows which temperatures would be deduced from the FUV data as a function of the true temperature if the IUE flux were systematically 10% low. Hence, this difference is most likely due to an error in the IUE calibration.

Given such an error, which makes 55,000 K objects appear to be 40,000 K, the obvious desirable course of action is to obtain a correction factor which would bring the IUE flux in line with that predicted by the optical data and the models. DA white dwarfs represent the best available means of performing a calibration in the FUV. They are nearby (<100 pc.) and hence generally unreddened, their FUV flux consists of a pure continuum, and the physics of high gravity pure hydrogen atmospheres is better known than for any other stellar type. Shipman (1979) estimates that the models predict the emergent flux to ~2% accuracy. This correction factor could be obtained by taking a large sample of observations, predicting fluxes for each star, finding the difference between the predicted and actual fluxes, and averaging these differences together. The correction obtained should be very accurate, because although the flux predictions for individual objects have some random error due to observational uncertainties, the averaging procedure will cause these random errors to cancel out when many different objects are utilized.

Toward that end, we obtained more spectra from the archives in order to enlarge our time base and improve the statistical significance of the results. Data were obtained for WD's 0004+330, 0136+351, 0346-011, 0644+375, 1254+223, 1615-154, and 2111+498. We then obtained temperatures for the objects. We preferentially used the multichannel data from Greenstein (1984), with our model predictions of MC colors (*i.e.*, (u-v)). For objects without MC data, we used the Greenstein data set to obtain the correlation between (u-v) and the appropriate Johnson or Stromgren colors to get (U-V) or (u-y) *vs.* T_{eff}. Next, uncorrected flux comparisons were made for the stars. Results for all stars were similar to those previously pointed out in Figure 1a. Note that the smoothed color differences for the lower two spectra, from the same time period, match very closely, which points up the instrumental origin of the variations with wavelength. The top spectrum is from a somewhat earlier period, and is significantly different from the other two. This is due to the changing sensitivity of IUE with time (Sonneborn & Garhart, 1983).

With the individual differences as a function of wavelength in hand for 14 observations of 13 objects (two observations of WD2309+105 were used), we then performed an averaging. For determining the wavelength dependence, we used the 9 highest quality, low-noise SWP+LWR spectra. Due to the changes in sensitivity with time, and the changeover in 1980 to the new extraction scheme, the objects were grouped into three time periods: late 1979, mid 1981, and mid 1982. The raw corrections for each time period were then made by averaging together the differences obtained for the stars within that group. Next, the appropriate "zero-shift" normalization had to be applied to the raw corrections. The magnitude of the normalization at each epoch was computed by calculating the wavelength-averaged mean color difference for all 14 observations:

$$<\Delta c_\lambda> = \sum[\Delta c(\lambda_i)].$$

These individual offsets were then corrected for the known sensitivity change with time, and their mean found. The individual corrections were then normalized such that the variations of the corrected spectra from the mean offset were minimized.

In Figure 1b, we show the *corrected* stellar-to-model color differences, calculated and displayed in the same manner as in Figure 1a. After applying the correction, the match between the models and the corrected fluxes is extremely good: the previous large-scale variations of ~0.3 mag are reduced to small-scale differences of at most ~0.05 mag after smoothing. The RMS variation of the unsmoothed corrected fluxes relative to the models is typically 0.05 mag (5%). The error in the zero point for the corrected fluxes is expected to be small. The individual stellar to model mean offsets have a 1σ error of $\pm$ 0.06 mag, due to the optical color uncertainty of $\pm$ 0.03 mag. With 13 objects being averaged together, the formal error in the correction is $1/\sqrt{13}$ the individual errors, or ~0.02 mag. A conservative estimate would be that the random error is < 0.04 mag. The RMS variation in the wavelength-averaged mean color differences for the entire group is ~0.05 mag, which is within the $\pm$ 0.06 mag expected to result from the ± 0.03 mag uncertainty in the optical colors.

Our final results are displayed in Figure 2b, where we have plotted optically determined temperatures *vs* temperatures obtained from the corrected IUE fluxes. A comparison of Figures 2a and 2b shows that our photometric recalibration of IUE does indeed produce agreement between the different temperature determinations. Some points on the individual objects should be noted. WD2309+105 was observed twice: at epoch 1979.9, and epoch 1982.4. The success of compensating for the changing sensitivity is evident in that the temperatures derived from the two different observations agree quite well. We thus find that 2309 is the currently known DA white dwarf which is nearest in temperature to HZ43. For the latter, however, the uncertainty in its V magnitude (due to the 3" separation between it and its companion M star) renders rather uncertain the fitting of the FUV continuum. Our present estimate of its effective temperature is based on matching the FUV slope, since matching the flux level relative to m_V gives the wrong slopes at either of the published values of m_V. WD1254+223 has been detected by Einstein in X-rays, as reported by Kahn *et.al.* (1984). Our temperature of 40-46,000 K is in agreement with their value of 40-44,000 obtained by fitting the H_β profile. WD0346-011 is also an X-ray source; in this case, though, our FUV (SWP only) temperature of 36-40,000 K is significantly lower than Kahn's 45-50,000 K (again, based on H_β). The

lack of an LWR spectrum prevents us from obtaining an independent reddening estimate; assuming that the higher temperature is correct, the reddening would amount to E_{B-V} = 0.01-0.02 mag. Our analysis confirms that G191-B2B is the hottest known DA white dwarf. Our temperature for it is 67,000 ± 8,000 K. This higher temperature significantly alleviates the mass problem for G191. At 55,000 K and with the nominal parallax distance of 48 pc, this star's radius would be that of a 0.21 solar mass dwarf. Taking our upper limit of 75,000 K and the minimum distance of 43 pc. raises the derived mass to 0.38 solar masses, which is just below the 0.4 solar mass theoretical lower limit.

IV. Further Ramifications of Results Obtained

Beyond the improvement in the situation of the stars we have directly examined, other effects will also result from the IUE calibration correction we are proposing. Among WD's, there had remained a problem with Sirius B. Martin *et.al.* (1982) reported that fitting model atmosphere fluxes to the data from optical to X-ray produced an acceptable fit everywhere but in the FUV, where the IUE data appeared to be systematically ~15% low. Our correction will significantly reduce that anomaly. Still in the realm of white dwarfs, there have been other IUE observations made of mixed composition WD which may have stratified atmospheres, and of cool He WD which appear to have significant FUV absorption by metals. Our enhancement of the photometric accuracy of IUE is sufficient to make reanalysis of such objects in order to obtain improved constraints on the physical conditions in their atmospheres a worthwhile option.

There is also another effect of our proposed recalibration which is of general significance. We have displayed in Figure 3 the correction curves which we derived for the three epochs our observations were clustered around. The correction is formed from the average of the color differences for the different observations, as defined above the figure. Hence the correction is applied as follows:

$$f_\lambda(true) = f_\lambda(nominal) \times 10^{0.4C_\lambda}$$

Note that our correction curves have a pronounced peak at ~2200 Å of ~ 0.27 mag, corresponding to a 22% dip in the nominal fluxes. (We reemphasize that the stars used in obtaining the correction have nearly zero reddening). An observer who has taken recent spectra, and who took the IUE calibration at face value, would assume that an intrinsically unreddened star actually was reddened by ~ 0.08 mag, on the basis of the depth of the 2200 Å "feature". This would correspond to ~ 0.7 magnitudes of extinction at 1400 Å.

V. Conclusions

By analyzing a portion of the available IUE data from hot DA white dwarfs, we have been able to derive a correction which substantially improves the photometric accuracy of the IUE data. This correction has been used by us to calculate effective temperatures for these stars which are more accurate than those based on optical photometry. Our improvement in the photometric accuracy of IUE may help resolve some of the outstanding issues involving non-DA white dwarfs. Our results show that observers should be cautious in their interpretation of large and small scale features seen in low dispersion spectra at even the 20% level (as shown by Figure 1a). Finally, it has come to our attention that a corrected calibration of IUE is now in the process of being done. We suggest that the existing data base of IUE spectra of DA white dwarfs would be useful for revising the absolute photometric calibration.

References

Greenstein, J. L. 1984, *Ap. J.*, **276** ,602.

Martin, C., Basri, G., Lampton, M., and Kahn, S. M. 1982, *Ap. J. (Letters)*, **261** ,L81.

Shipman, H. L. 1979, *IAU Colloquium 53,* in *White Dwarfs And Variable Degenerate Stars,* ed. H. M. Van Horn and V. Weidemann (Rochester: University of Rochester Press), p. 86.

Sonneborn, G. and Garhart, M. 1983, *NASA IUE Newsletter No. 23,* p. 23.

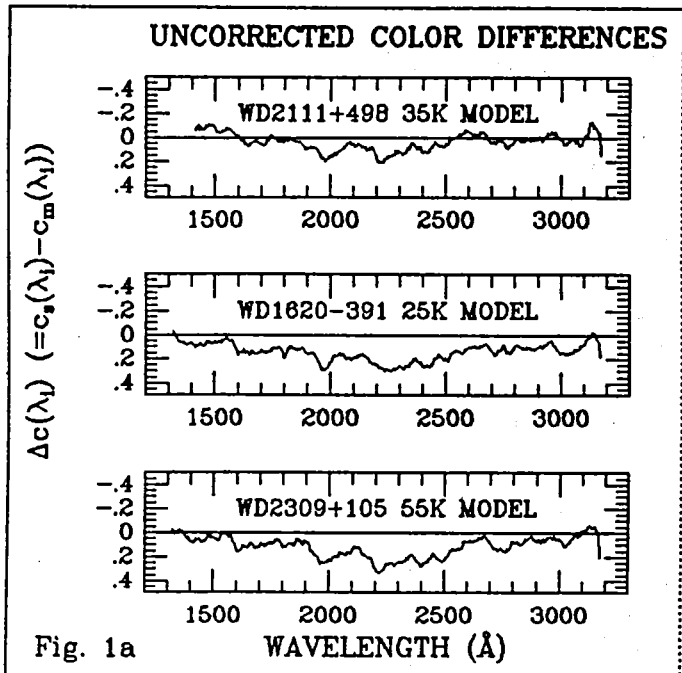

Fig. 1a

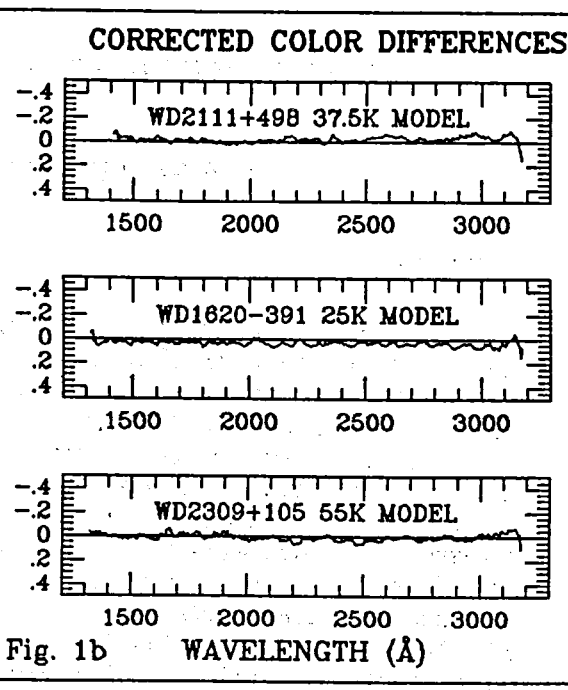

Fig. 1b

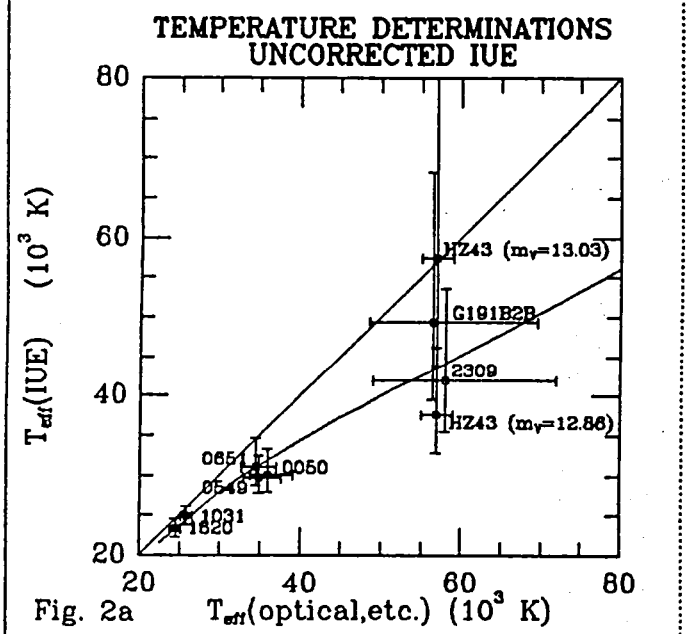

Fig. 2a

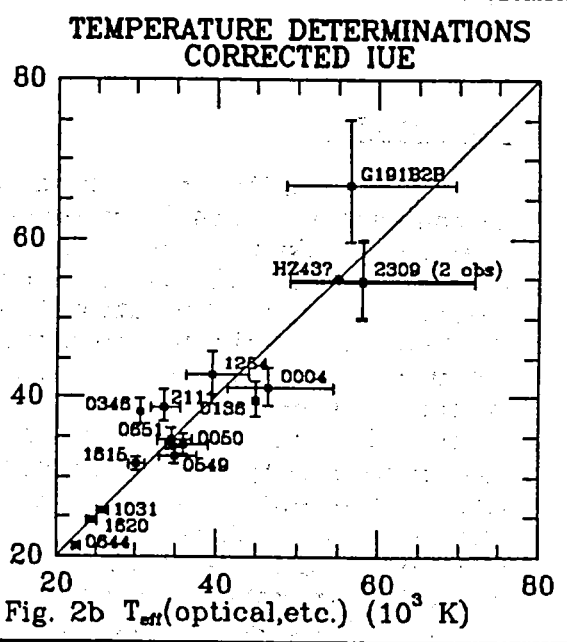

Fig. 2b

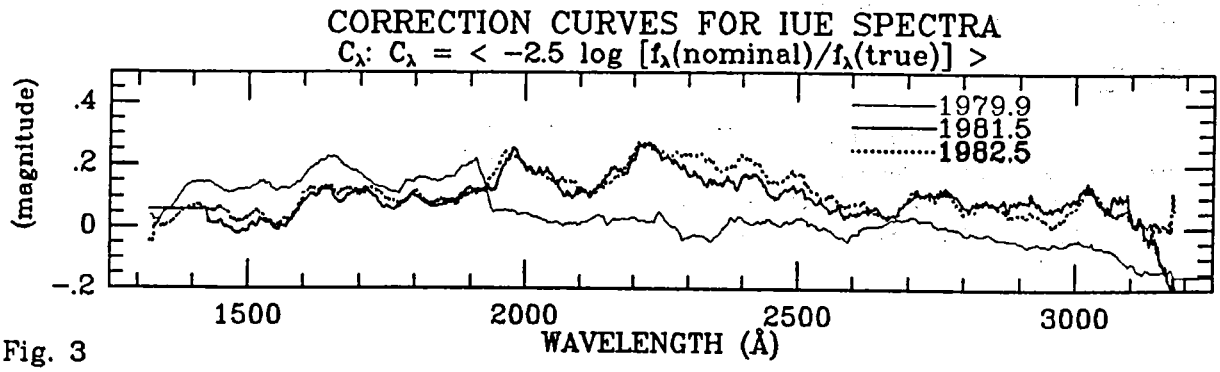

Fig. 3

CARBON, SILICON, AND OXYGEN IN THE WHITE DWARF STAR GD 40

Harry L. Shipman
Physics Department, University of Delaware

ABSTRACT

An IUE spectrum of the metal-rich DB white dwarf star GD 40 shows no unequivocal spectral features in the range of the SWP camera (1200-2000 A). This wavelength region contains resonance lines of many common elements: H I, C I, C II, Si II, and O I. Upper limits to the abundances of H, C, Si, and O are derived from model atmosphere calculations. These limits, combined with the detection of Ca II, Mg II, and Fe II, conflict with the predictions of diffusion theories, which have been widely invoked to explain the presence of metals in the spectra of the He-rich white dwarf stars. The upper limit to the C abundance indicates that the C abundances in He-rich white dwarfs peak at a temperature of about 12,000 K. This paper concludes with some comments about how future missions can contribute to further understanding of the chemical compositions of white dwarf stars.

INTRODUCTION

White dwarf stars show an amazing variety of chemical compositions, in contrast to stars in other parts of the HR diagram. About two-thirds of the white dwarf stars have hydrogen dominated atmospheres, with He present, if at all, at the level of He/H $\sim$ 1/10,000 or less. About one third have helium dominated atmospheres, where the He/H ratio is reversed: He/H $\gtrsim$ 10,000, (these are spectral types DB, DC, and DQ). The metal abundances in the He-rich stars vary enormously; for example, log [Ca/He] varies from -6 in GD 401 to -11 in Van Maanen 2. Another important new factor is the variation in the carbon abundance in the cooler He-atmosphere DQ stars (Wegner and Yackovich 1984; Koester, Weidemann, and Zeidler-K.T. 1983, and references therein). What causes the compositions of white dwarf photospheres to vary so widely? Some answers may come from the star GD 40. It is the hottest DB star to show metals, and IUE and optical spectra at longer wavelengths show Ca, Fe, and Mg features (Shipman, Greenstein, and Boksenberg 1977; Shipman and Greenstein 1983). An IUE SWP spectrum of this object was obtained on July 5 1983.

RESULTS

The SWP spectrum showed no unambiguous spectral features. An ambiguous, 1.5 sigma feature at the right wavelength for O I 1302 is not regarded as real at this time. Upper limits to the abundances were calculated using an LTE spectrum are as follows, given as limits to log

[X/He]: H-(-5.5), C-(-6.7), O-(-7.5), Si-(-6.7). These abundance limits are determined from the non-visibility of Lyman alpha, C I 1657, C II 1335, O I 1302, and Si II 1265. These are the strongest resonance lines of these elements expected in this spectral region. For Lyman alpha, only the line wings (1260-1400 A region) were used for the fit.

DISCUSSION

For the past decade or so, it has generally been thought that the heavy elements seen in stars like GD 40 come from accretion from the interstellar medium. These elements diffuse through the stellar photosphere with slightly different velocities, but if they are accreted in solar proportions, the ratios of one element to another do not depart by more than a factor of 2-3 from the solar value (see Fontaine and Michaud 1979, Vauclair, Vauclair, and Greenstein 1979, Muchmore 1984 for recent articles on this topic). Were this to be the case, the metal abundance of all species, relative to the solar abundance, should be about the same. Figure 1 shows that both C and O should be present at a level of 0.01 times the solar abundance, while the upper limits derived from this investigation are 1-2 orders of magnitude lower.

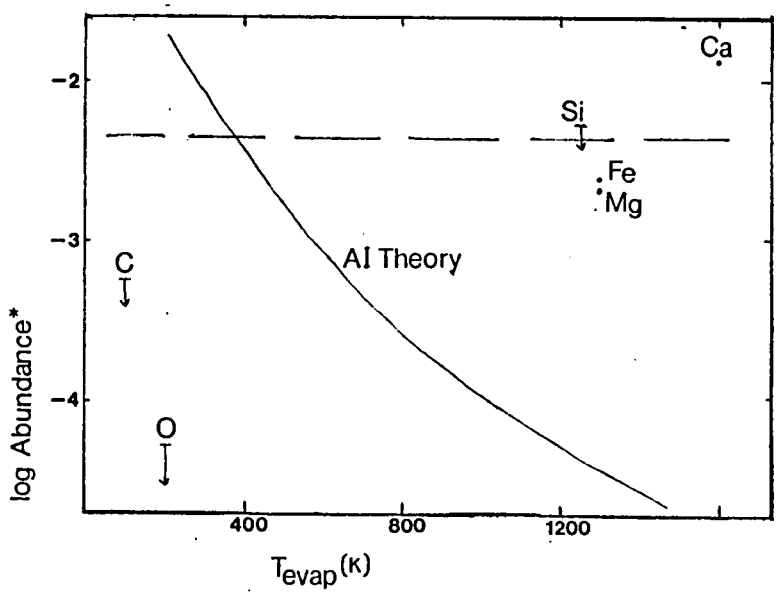

Figure 1. Element abundances in GD 40 plotted against evaporation temperature. The dashed line shows, roughly, the predictions of simple diffusion theories; "Al theory" refers to the proposal by Alcock and Illarionov (see text).

However, events in the circumstellar environment could alter the composition of the material considerably from the solar value. Alcock and Illarionov (1980) suggest that, since much of the heavy elements in the ISM are in the form of grains, that the volatile elements should be evaporated in a circumstellar H II region and should accrete preferentially. The solid curve indicates the functional relationship predicted from their scheme. It fits the data even worse than a simple theory, which would be a straight line across the graph.

Another outstanding question regarding the chemical composition of white dwarf stars has to do with the abundance of carbon in the DC and DQ stars. Wegner, using the IUE, has investigated the carbon abundance of a variety of stars and shows that log [C/He] is about -6 for the coolest temperatures, 7,000 K, and it rises to -2 at 12,000 K (Wegner and Yackovich, 1984). With GD 40 having log [C/He] < -6.7, this functional relationship must turn over at T(eff) = 12,000 K, as has been recently predicted by a theoretical calculation in which C is seen as being dredged up from below by the penetration of the He convection zone to the stellar core (Fontaine et al. 1984, Wesemael et al. 1984).

PROSPECTS FOR THE FUTURE

Since the topic of this conference is "the future of ultraviolet astronomy," it is appropriate to include a few words about how future instruments, specifically ST and FUSE/COLUMBUS, can assist in understanding the problem addressed in this paper: why do white dwarf stars have such peculiar and variable chemical compositions? These two instruments will give us photon counting detectors, higher spectral resolution, much greater aperture (in the case of ST) and somewhat greater aperture with an extension to shorter wavelengths (in the case of FUSE). The range of elements and ionization stages will be considerably greater when these missions fly. In particular, the short wavelength capability of FUSE/COLUMBUS is a real plus.

One general class of theories for the origin of the heavy elements in white dwarf stars is the class of accretion/diffusion theories, in which the heavy elements come from the interstellar medium. Different theoretical schemes (see references above) predict various behaviors of the abundances of different elements as a function of variables which can include evaporation temperature of grains incorporating these elements and stellar effective temperature. Because of its limited spectral resolution, photometric accuracy, and collecting area, IUE can only measure lines of the strongest elements in the brighter white dwarf stars. ST and FUSE/COLUMBUS can probe a greater variety of less abundant elements and ions in fainter stars, probing any possible relation between element abundances, evaporation temperatures, and temperatures of the star (or any other parameter). Specifically, Ar and N, two elements which have very low condensation temperatures, can only be observed by FUSE since the

resonance lines of Ar I, N I, and N II lie in the 900-1200 A spectral region. The short-wavelength capability of FUSE/COLUMBUS can also help at the high-temperature end by measuring resonance lines of highly excited ions like N III, O VI, S II, and Fe III.

The range of problems relating to the late stages of stellar evolution which ST and FUSE/COLUMBUS can probe goes considerably beyond the question of chemical composition considered here. For example, these projects, especially FUSE/COLUMBUS, can determine temperatures for hot white dwarfs or pre-white dwarfs and unscramble the mess at the left hand side of the HR diagram. UV measurements of the accretion disk spectra in interacting binaries could be particularly exciting. Thus FUSE/COLUMBUS and ST can solve many problems in the white-dwarf field which go beyond those described in this short paper.

SUMMARY

Upper limits to the abundances of C, Si, O, and H in the He-rich DBZ4 star GD 40 are derived from IUE observations. These upper limits, combined with the abundances of Ca, Mg, and Fe derived by Shipman and Greenstein (1983), are inconsistent with both simple diffusion theories and more complex ones. The relationship between the carbon abundance and temperature in the He-rich DB and DQ stars reaches a maximum near 12,000 K, agreeing with a recent theoretical prediction (Fontaine et al. 1984, Wesemael et al. 1984).

This research was supported by NASA (NAG 5-348) and by the NSF (NSF AST 81-15095 and 83-43067).

REFERENCES

Alcock, C., and Illarionov, A. 1980, Ap. J. 235, 541.
Fontaine, G., and Michaud, G. 1979, Ap. J. 231, 826.
Fontaine, G., Villeneuve, B., Wesemael, F., and Wegner, G. 1984, preprint.
Koester, D., Weidemann, V., and Zeidler-K.T., E.-M. 1983, Astr. Ap. 116, 147.
Michaud, G., Fontaine,.G., and Charland, Y. 1984, Ap. J. in press (May 1, 1984).
Muchmore, D. 1984, Ap. J. in press (March 15, 1984).
Shipman, H.L., Greenstein, J.L., and Boksenberg, A.. 1977, A.J. 82, 480.
Shipman, H.L., and Greenstein, J.L. 1983, Ap. J. 266, 761.
Wegner, G., and Yackovich, F. 1984, preprint.
Wesemael, F., Fontaine, G., Villeneuve, B., and Wegner, G. 1984, Bull. AAS 15, 983.

ANALYSIS OF WHITE DWARF LYMAN α PROFILES

J. B. Holberg
Lunar and Planetary Laboratory, University of Arizona

and

F. Wesemael
Département de Physique and Observatoire du mont Mégantic
Université de Montréal

ABSTRACT

Through the use of a doubly exposed large and small aperture SWP image it is possible to obtain Lyman α profiles for white dwarfs which are relatively free from geocoronal Lyman α contamination. For DA white dwarfs the analysis of both wings of these broad profiles yields well-determined temperatures and useful constraints upon surface gravity. Two examples of such an analysis are discussed, and the results compared with temperatures determined from Voyager far UV (912-1150 A) fluxes.

INTRODUCTION

For hot DA white dwarfs, the relatively broad HI Lyman α (Lyα, 1216 A) profiles which can be observed by IUE offer the promise of being a reliable means of estimating effective temperatures and, at the same time, providing useful constraints on surface gravity. The usefulness of IUE Lyα profiles as temperature indicators in white dwarfs has been recognized by numerous authors including, Greenstein and Oke (1979), Böhm-Vitense *et al*. (1979), Greenstein (1980), and Sion, Wesemael, and Guinan (1983), among others. These authors have all either concentrated upon the red wing of Lyα or have counseled caution in acceptance of the IUE blue wing data. The principle reason for reduced confidence in the blue wing is the strong instrumental sensitivity gradient and resulting uncertainty in the relative calibration of the last 50 A (1150-1200 A) of SWP data. To this calibration uncertainty can be added well known problems with contamination of the core of the Lyα profile with geocoronal Lyα emission and the reseau at ~1190 A in the SWP large aperture images. In this paper we discuss how these difficulties can be overcome.

IUE LYMAN ALPHA PROFILES

As is well known, substantial improvements in the appearance of Lyα profiles result if SWP spectra are obtained through the small aperture. The chief advantages are a substantial reduction in geocoronal contamination and an absence of the annoying reseau. The principle disadvantage of a small aperture image is the loss of absolutely calibrated fluxes. This disadvantage can be almost entirely overcome if a double exposure of the object is made through both large and small apertures. The small aperture fluxes can then be normalized to the large, placing them on an absolute scale. The resulting improvement in Lyα profiles is illustrated in Figure 1 where we show the

result of such a double exposure for the DA white dwarf WD 0050-33 (GD 659). In Figure 1 the small aperture fluxes were adjusted to those of the large by application of a single scaling quantity.

The question of the reliability of fluxes in the blue wing of Lyα can be addressed by considering observations made with the Voyager 1 and 2 ultraviolet spectrometers, which are sensitive over the range 500-1700 A. For hot stars fainter than magnitude 7 the useful range of Voyager is generally restricted to wavelengths shortward of 1150 A. This is due to a combination of low long wavelength sensitivity and scattering from the strong interplanetary Lyα emission line. Even though white dwarf Lyα profiles are not observable with Voyager the remainder of the Lyman series are and this affords a valuable means of complementing IUE observations below 1150 A. To date we have observed nine of the brighter hot white dwarfs with Voyager. In Figure 2 we display the complementary nature of Voyager and IUE (small aperture) with observations of the white dwarf CD -38° 10980. As illustrated by the model atmosphere comparison shown in Figure 2 the Voyager and IUE blue wing fluxes are remarkably compatible. The absolute calibration applied to the Voyager fluxes is that of Holberg et al. (1982) while the IUE calibration is that of Bohlin and Holm (1980).

DISCUSSION

There exist two DA white dwarfs, CD -38° 10980 and WD 0050-33, which have suitable SWP (large/small aperture) images and complementary Voyager observations. We shall briefly discuss our analysis of the Lyα profiles for both of these stars. CD -38° 10980 currently possesses the best Voyager and IUE data as well as a useful variety of ground based observations. In order to investigate this star in detail we have computed a small 3 x 3 grid of model atmospheres covering 24,000-26,000 K in temperature and log g = 7.5-8.5 in surface gravity. These pure H models are extensions of those of Wesemael et al. (1980) and use the unified broading theory of Vidal, Cooper and Smith (1973). Similar models specifying emergent fluxes over the range 950-3200 A were employed in the Voyager observations of Sirius B (Holberg, Wesemael, and Hubený 1984).

A complete discussion of the CD -38° 10980 data will be presented elsewhere. Here we are principally concerned with the analysis of the IUE Lyα profile. The IUE Lyα profile (1150-1350 A) shown in Figure 2 was compared with our grid of model atmospheres in the following manner. We used visual photometry (V = 11.00, Wegner 1973) to establish the apparent solid angle of the star. Emergent model fluxes were scaled by this solid angle and compared with the absolute IUE fluxes. Best fitting models were determined by computing a χ^2 for a large number of models interpolated within our 3 x 3 grid. The best fitting model was found to correspond to a temperature of 24,700 K and a gravity of log g = 8.1. Applying the same procedure to the Voyager data alone one obtains a similar result; 24,600 K and log g = 8.1. The relationship of these two results is shown in Figure 3 where we also show results of a similar analysis of the observed Balmer α profile of CD -38° 10980. The contours shown in Figure 3 represent contours of equal χ^2. As can be seen all three results independently indicate good general agreement. The comparison model (24,700 K and log g = 8.0), shown in Figure

2, represents a best fit to all the available data on CD -38^{o} 10980. The important properties of Lyα profiles in this temperature range can be seen in Figure 3. First, the sensitivity to temperature is evidenced by the narrowness of the Lyα contour. Second the vertical alignment of the Lyα contour demonstrates a lack of correlation between temperature and gravity. This latter aspect was also noted by Greenstein and Oke (1979). A final important observation which can be made from Figure 3 is that the temperature and gravity dependence of Lyα and Balmer α profiles are near orthogonal. Thus, joint analysis of Lyman and Balmer α profiles affords an excellent means of estimating two important atmospheric parameters, effective temperature and surface gravity.

At present our grid of model atmospheres has not been extended to cover WD 0050-33. Therefore, in our discussion of this star we have fixed the surface gravity at log g = 8 and considered models varying only in temperature. Initially we ignore the Voyager data and consider the fit of the models to the absolute IUE fluxes (1150-1350 A) shown in Figure 1. The only constraint applied to the models is that they satisfy the observed visual magnitude of WD 0050-33 (V = 13.36, Wegner 1973). Subject to this constraint, the best fitting model had a temperature of 39,000 K. Treating the 912-1150 A Voyager data in a similar manner yields nearly identical results (T_{eff} = 38,500 K). In Figure 4 we compare the best fit Voyager model (T_{eff} = 38,500 K and log g = 8) to the IUE Lyα profile. It should be noted that for this preliminary exploration of the temperature dependence of the model profiles we have not smoothed the models to the 6 A IUE spectral resolution, hence the sharp core shown in the model (Fig. 4). In the future it is planned to extend this type of analysis to include additional DA white dwarfs.

CONCLUSIONS

We have demonstrated that it is possible to obtain reliable Lyα profiles including both red and blue wings, for white dwarfs using large and small aperture SWP images. Considerable confidence can be lent to the blue wing fluxes by consideration of Voyager observations shortward of 1150 A. Finally we have shown that the results obtained by a systematic analysis of the entire Lyα profile are consistent with independent measures of temperature and gravity and that Lyα profiles offer a sensitive means of estimating effective temperatures.

REFERENCES

Bohlin, R.C., and Holm, A. 1980, IUE Newsletter No. 10, p. 37.

Böhm-Vitense, E., Dettman, T., and Kapranidis, S. 1979, Ap. J. (Letters), 232, L189.

Greenstein, J.L. 1980, Ap. J. (Letters), 241, L89.

Greenstein, J.L., and Oke, J.B. 1979, Ap. J. (Letters), 263, L63.

Holberg, J.B., et al. 1980, Ap. J., (Letters), 242, L119.

Holberg, J.B., Wesemael, F., and Hubený, I. 1984, Ap. J., in press.

Sion, E.M., Wesemael, F., and Guinan, E.F. 1984, Ap. J., in press.

Vidal, C.R., Cooper, J., and Smith, E.W. 1973, Ap. J. Suppl., 25, 37.

Wegner, G. 1973 M.N.R.A.S., 163, 381.

Wesemael, F. Auer, L.H., Van Horn, H.M., and Savedoff, M.P. 1980, Ap. J. Suppl., 43, 159.

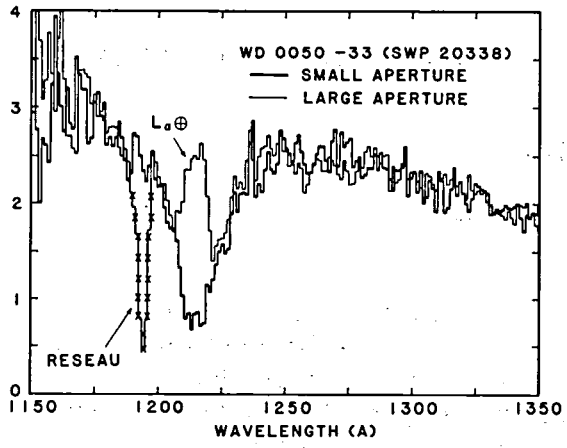

Fig. 1.—A comparison of the large and small aperture Lyα profiles of WD 0050-33. The small aperture fluxes have been scaled by 1.62 in order to normalize them to those of the large aperture. Note the presence of the strong geocoronal Lyα (⊕) feature and the reseau in the large aperture profile. Flux units are 10^{-13} ergs/cm² sec A.

Fig. 2.--A comparison of the Lyman series region of the spectrum of CD -38° 10980 with Voyager 2 (λ < 1150 A) and IUE (λ > 1150 A). The continuous curve represents the model atmosphere discussed in the text. Between 1150 and 1250 A the IUE fluxes are derived from small aperture data. Longward of 1250 A large aperture fluxes are used. Flux units are 10^{-11} ergs/cm² sec A.

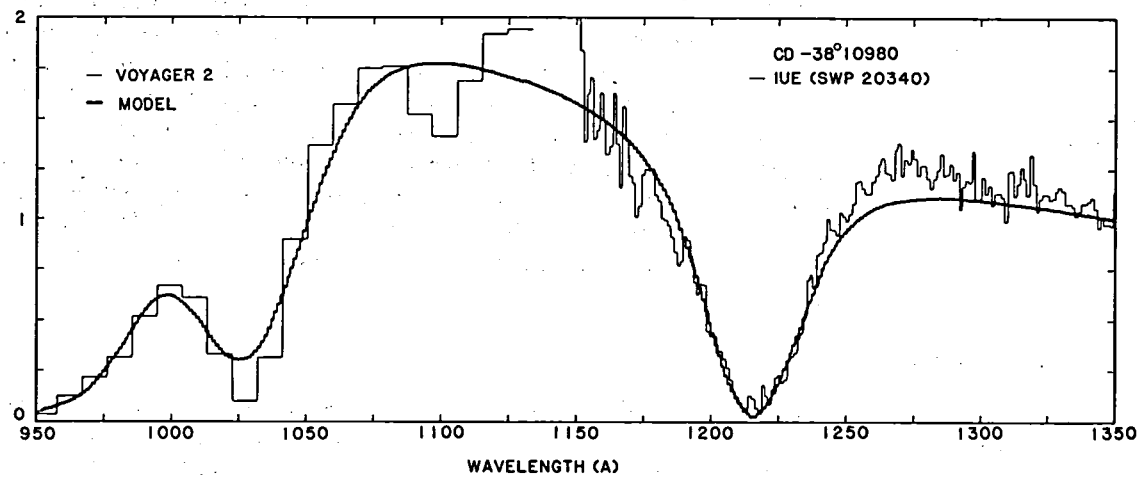

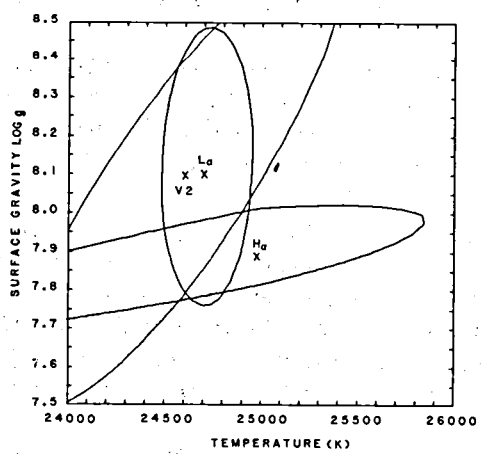

Fig. 3—Contours showing the regions in the temperature-gravity plane which best fit the Voyager (V2), IUE Lyα profile (Lα) and Balmer α (Hα) profile data for CD -38° 10980. Lyα profiles exhibit good temperature discrimination while the Balmer α profile is most sensitive to gravity.

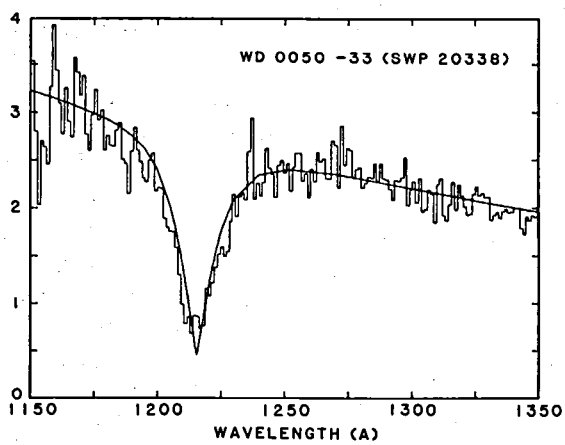

Fig. 4.--The Lyα profile of WD 0050-33 compared with the log g = 8.0 model atmosphere which best fits the Voyager 1 912 to 1150 A data. As discussed in the text, no adjustment of surface gravity was attempted in fitting the Lyα profile nor were the models convolved with the spectral resolution of the SWP. Flux units are 10^{-13} ergs/cm² sec A.

A SEARCH FOR WHITE-DWARF COMPANIONS OF SUBGIANT CH STARS

Howard E. Bond
Department of Physics and Astronomy, Louisiana State University
and
Space Telescope Science Institute

ABSTRACT

Subgiant CH stars are F- and G-type subgiants and dwarfs showing enhanced carbon and *s*-process abundances at their surfaces. Their low luminosities are difficult to understand in the context of standard stellar-evolution theory. One possible hypothesis is that subgiant CH stars are the former secondary components of binary systems in which processed material was transferred from a red-giant carbon-star primary; the former primary would now be an optically invisible white dwarf. However, *IUE* spectra of 21 subgiant CH stars have failed to reveal any of the predicted white-dwarf companions. Together with the distribution of these objects in the HR diagram, the observations suggest that subgiant CH stars are former red giants that, evolving as single stars, have undergone violent mixing events that returned them to the vicinity of the main sequence. Nevertheless, many subgiant CH stars (and their probable descendants, the barium and CH stars) are long-period spectroscopic binaries. Our results are compatible with the conclusion that the unseen companions are generally unevolved red dwarfs. Apparently the primary components of such wide binaries are, for some as yet unknown reason, predisposed toward violent mixing.

INTRODUCTION

Barium stars and CH stars are red giants whose surfaces show enhanced abundances of carbon and the *s*-process elements (such as Sr, Y, Zr, and Ba). (For a recent review, see McClure 1984*a*.) The overabundant elements are believed to be synthesized by nuclear reactions (helium burning and neutron captures) that can only occur deep in stellar interiors. One of the outstanding problems in stellar astrophysics is to account for the presence of core material at the surfaces of these stars.

Subgiant CH stars are a more recently discovered class of F- and G-type stars lying on or near the main sequence, but having carbon and *s*-process enhancements similar to those of CH and barium red giants (Bond 1974; Sneden and Bond 1976; Sneden 1983). It has been suggested that subgiant CH stars are the immediate progenitors of the CH and barium stars (Luck and Bond 1982; Bond and Luck 1983).

Two plausible explanations for the origin of subgiant CH stars (and hence of barium and CH stars) are (1) that they are members of close-binary systems in which the more-massive star became a red-giant carbon star and transferred processed material to its companion's surface before becoming an optically invisible white dwarf; or (2) that they are evolved single stars that have undergone mixing events violent enough not only to mix processed material to the surface, but to mix enough hydrogen into the stellar core to reduce the luminosity significantly.

At first glance, the binary hypothesis appears more likely, since ground-based observers have discovered that many barium and CH stars (and even several subgiant CH stars) are long-period single-lined spectroscopic binaries (McClure *et al.* 1980; Griffin and Griffin 1980; McClure 1983, 1984*a*,*b*). Furthermore, *IUE* has revealed a white-dwarf companion of the brightest barium star, ζ Capricorni (Böhm-Vitense 1980).

The case for additional examples of Ba II stars with degenerate companions is less convincing. It has been reported that two "mild" barium stars, ζ Cygni and ξ^1 Ceti, have hot subluminous companions (Böhm-Vitense 1980; Böhm-Vitense *et al.* 1983); however, short-wavelength observations of stars this bright must be corrected for a considerable contribution from scattered light in the SWP camera (Clarke 1981) before any definite conclusions can be reached. Dominy and Lambert (1983) obtained *IUE* spectra of five other classical and mild Ba II stars without finding any evidence for hot companions. Finally, the K0 II star 56 Pegasi, which has a quite conspicuous hot companion (Schindler *et al.* 1982), has sometimes been considered to be a mild barium star, but a high-dispersion abundance analysis by Luck (1977) failed to confirm any barium characteristics.

IUE OBSERVATIONS

The binary hypothesis for the origin of subgiant CH stars implies that they should have white-dwarf companions (the remnants of the former red-giant primary stars). To test this hypothesis, we obtained low-dispersion *IUE* spectra for a total of 19 subgiant CH stars (most of which had been found on objective-prism plates by the writer during the past several years). The *IUE* archive also contains short-wavelength spectra (obtained by E. Böhm-Vitense) for two further subgiant CH stars, bringing the total number observed by *IUE* to 21.

Although the program stars have visual magnitudes of 7-10, they are actually at smaller distances than 3rd-magnitude ζ Cap (since they have much lower luminosities). Thus they provide the ideal proving ground for a test of the hypothesis of degenerate companions of late-type peculiar stars.

RESULTS

Fig. 1 shows a typical *IUE* observation, in this case of the 7.8-mag subgiant CH star HD 182274 (which has recently been found to have a variable radial velocity by McClure 1984*b*). A 90-min SWP exposure and a 2-min LWR exposure have been combined to show the spectrum from 1250 to 3200 Å. (The abrupt reduction in the noise level below 1950 Å is due to the much longer duration of the SWP exposure.) As can be seen, scattered light is not a problem in an SWP exposure of this length on a 7th-mag star.

The *IUE* observations of HD 182274 show only the ultraviolet tail of the F-type star; there is no trace of a white-dwarf companion. The limits that can be placed on any such low-luminosity component are the following. From an analysis of coudé spectrograms of HD 182274, Luck and Bond (1982) derived an effective temperature of 6000 K and a surface gravity that leads to an absolute magnitude $M_V = +4.8$ (for an assumed mass of 1 $M_\odot$). Since $V = 7.8$, the distance modulus is $m - M = 3.0$ ($d = 40$ pc).

Consider a typical DA white dwarf, 40 Eridani B, which has an effective temperature near 17,000 K and a distance of 4.8 pc. Greenstein's (1980) *IUE* observations show a flux of 1.1×10^{-11} erg cm^{-2} s^{-1} Å^{-1} at wavelengths near 1500 Å. Scaling 40 Eri B to the larger distance of HD 182274, we would expect a flux of 1.5×10^{-13} erg cm^{-2} s^{-1} Å^{-1} at 1500 Å. Such a companion is clearly ruled out by Fig. 1. Of course, HD 182274 could have a cooler low-luminosity companion that would escape detection; we can only rule out degenerate companions hotter than about 12,000 K.

None of the 21 subgiant CH stars that have been observed by *IUE* have shown any evidence for white-dwarf companions.

DISCUSSION

Before definitively ruling out the binary hypothesis for the origin of subgiant CH stars, we must consider the fact that white dwarfs gradually cool. A faint companion of a subgiant CH star that has cooled to an effective temperature similar to, or lower than, that of its primary could never be detected in the ultraviolet. As just described, we can only rule out companions hotter than about 12,000 K for a typical subgiant CH star. The cooling time to such a temperature is about 10^9 years (*e.g.* Lamb and Van Horn 1975). Thus if, for example, every subgiant CH star has a white-dwarf companion, and if these white dwarfs have ages spread uniformly between zero and the age of the galactic disk (say 5×10^9 years), then only 20% of them would be detectable with *IUE*. (This is actually a lower limit to the expected percentage, since the calculation ignores the time required for the former primary to evolve to the red-giant stage.)

Among the 21 subgiant CH stars that have been observed with *IUE*, we would therefore expect to have detected at least four white-dwarf companions. Since, in fact, none were detected, significant doubt is cast upon the binary mass-transfer hypothesis.

Further support for regarding subgiant CH stars as mixed stars, rather than contaminated ones, comes from their positions in the HR diagram. The mass-transfer hypothesis would lead to the expectation that, since the subgiant CH star is merely an innocent bystander, it could lie at any random location along the main sequence. In fact, however, subgiant CH stars are found only in the vicinity of the turnoff for old disk stars (Luck and Bond 1982). This is just what would be expected if subgiant CH stars are low-mass old-disk stars that have recently returned to the vicinity of the main sequence.

There remains, however, the disturbing ground-based evidence that many Ba II, CH, and probably subgiant CH stars are long-period spectroscopic binaries. Our *IUE* observations strongly suggest that the unseen companions are usually unevolved K or M dwarfs (although ς Cap shows that the companion can occasionally be a white dwarf). This conclusion may imply that some binary-star mechanism more exotic than simple mass transfer is responsible for the presence of processed material at the surfaces of these stars—perhaps tidally induced mixing, although it would seem that any tidal effects in such wide binaries must be insignificant. Alternatively, it may be that mixing and binarism are both symptoms of some common cause; *i.e.*, whatever it is that predisposes certain low-mass stars toward violent internal mixing tends to occur only in members of wide binaries.

It thus appears that subgiant CH stars may provide a tantalizing hint of an unexpected and important new property of binary systems.

The writer thanks R. E. Luck for useful discussions, and acknowledges financial support through NASA grant NAG 5–197.

REFERENCES

Böhm-Vitense, E. 1980, *Ap. J. (Letters)*, **239**, L79.
Böhm-Vitense, E., Nemec, J., and Proffitt, C. 1983, preprint.
Bond, H. E. 1974, *Ap. J.*, **194**, 95.
Bond, H. E., and Luck, R. E. 1983, *Bull. A.A.S.*, **13**, 810.
Clarke, J. T. 1981, *IUE Newsletter*, No. 14, p. 143.
Dominy, J. F., and Lambert, D. L. 1983, *Ap. J.*, **270**, 180.
Greenstein, J. L. 1980, *Ap. J. (Letters)*, **241**, L89.
Griffin, R., and Griffin, R. 1980, *M.N.R.A.S.*, **193**, 957.
Lamb, D. Q., and Van Horn, H. 1975, *Ap. J.*, **200**, 306.

Luck, R. E. 1977, *Ap. J.*, **212**, 743.
Luck, R. E., and Bond, H. E. 1982, *Ap. J.*, **259**, 792.
McClure, R. D. 1983, *Ap. J.*, **268**, 264.
_____. 1984*a*, *Pub. A.S.P.*, **96**, 117.
_____. 1984*b*, *Ap. J. (Letters)*, in press.
McClure, R. D., Fletcher, J. M., and Nemec, J. M. 1980, *Ap. J. (Letters)*, **238**, L35.
Schindler, M., Stencel, R. E., Linsky, J. L., Basri, G., and Helfand, D. J. 1982, *Ap. J.*, **263**, 269.
Sneden, C. 1983, *Pub. A.S.P.*, **95**, 745.
Sneden, C., and Bond, H. E. 1976, *Ap. J.*, **204**, 810.

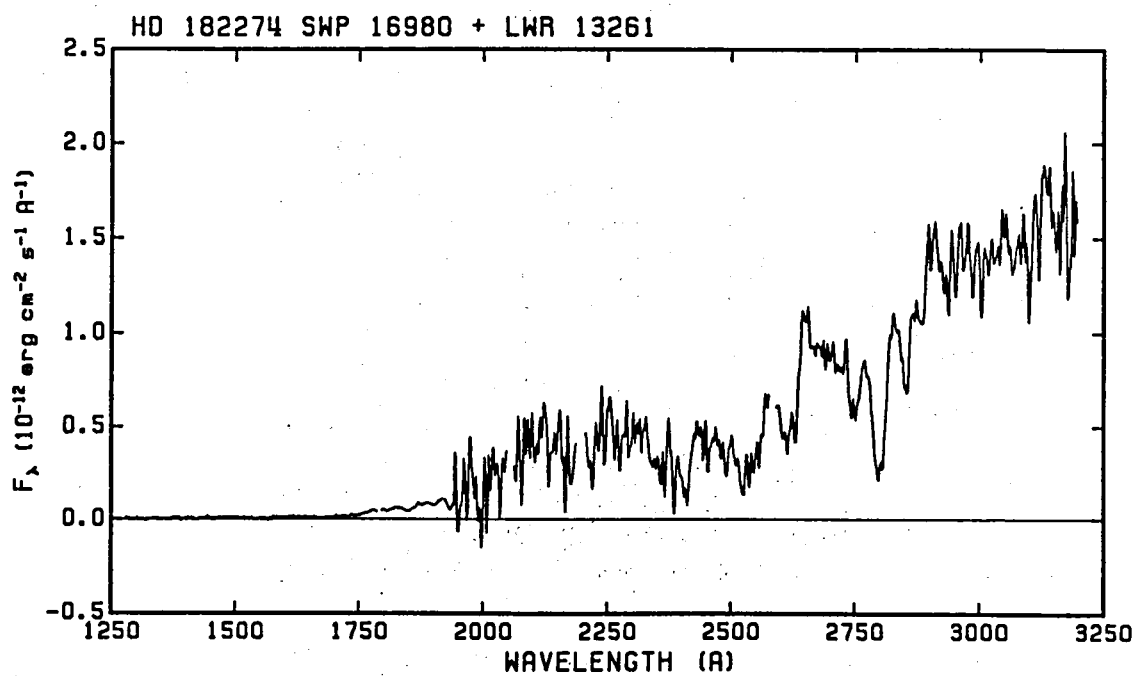

Figure 1
IUE spectrum of the subgiant CH star HD 182274.
There is no evidence for a hot companion.

THE WHITE DWARF COMPANION OF THE MILD BA STAR ξ^1 Cet

Erika Böhm-Vitense and Charles Proffitt
University of Washington, Seattle
and
Hollis Johnson, Indiana University, Bloomington

ABSTRACT

The mild Ba star ξ^1 Cet was found to have a hot companion. The absolute intensities and the relative energy distribution shows that it is a DA white dwarf with broad absorption bands around 1400 and 1650 A. The temperature is determined to be T_{eff} = 13000 $\pm$ 1000K.

INTRODUCTION

McClure, Fletcher and Nemec (1979) found that all Ba stars show radial velocity variations, indicating their binary nature. These results were confirmed by McClure (1983) when radial velocity variations were also found for some mild Ba stars. Subsequently, white dwarf companions were detected for the Ba star ζ Cap (Böhm-Vitense 1980), the mild Ba stars ζ Cyg (Böhm-Vitense 1980, Lambert 1982) and 56 Peg (Schindler et al. 1982). We now also observed a white dwarf companion for the mild Ba star ξ^1 Cet. In the following we will describe its properties.

THE OBSERVATIONS

A short wavelength low resolution 4^h exposure was taken of ξ^1 Cet, a mild Ba star with m_v = 4.4, which indicated the presence of a faint companion much hotter than ξ^1 Cet. Assuming that in the UV the relative energy distribution of the Ba star is similar to the one seen for ε Vir, we scaled the ε Vir energy distribution to the same visual magnitude as ξ^1 Cet and subtracted this scaled energy distribution from the one observed for ξ^1 Cet. In this way we obtained the energy distribution for the companion shown in Figure 1. Since the energy distribution of ξ^1 Cet probably does not correspond exactly to ε Vir, the fluxes in the wavelength region $\lambda >$ 1800 A are very uncertain. Some broad absorption bands around 1400 and 1650 A are seen. Similar bands have been observed for several DA white dwarfs with $T_{eff} \approx$ 12000 $\pm$ 2000K (Greenstein 1980, Wegner 1982, Koester 1983). The origin of these bands is presently not known, but I understand that studies are underway at several places.

ATMOSPHERIC PARAMETERS FOR THE ξ^1 Cet COMPANION

D. Koester kindly provided us with model atmosphere energy distributions for DA white dwarfs in the appropriate range of T_{eff} and with log g = 8. In Figure 1 we reproduce model energy distributions for T_{eff} = 12000K and 13000K, which fit rather well at the shorter wavelengths except that some emission seems to be present around 1300A in the ξ^1 Cet spectrum.

THE MASS OF THE ξ^1 Cet COMPANION

With T_{eff} assumed to be known from the relative energy distribution the absolute intensity of the observed flux will give us the radius of the star if the distance is known. With the atmospheric parameters for the Ba star ξ^1 Cet as determined by Pilachowski (1977) we can get a consistent picture if ξ^1 Cet has a mass of 2.5 M_o and $M_v \approx 1$. This gives us the distance and a radius for the companion which fits the radius of a white dwarf of M = 0.7 M_o if T_{eff} = 12000 and M = 0.8 M_o if T_{eff} = 13000°K.

REFERENCES

Böhm-Vitense, E. 1980, Ap.J. (Letters) 239, L79.
Dominy, J.E. and Lambert, D. 1983 Ap.J. 290, 180.
Greenstein, J. 1980 Ap.J. 241, L89.
Koester, D. 1983, private communication.
Lambert, D. 1982, in "Advances in Ultraviolet Astronomy", NASA Conference Publication No. 2238, p. 114.
McClure, K.D., Fletcher, J.M., and Nemec, J.H. 1980, Ap.J. Letters 238, L35.
McClure, R.D. 1983, Ap.J. 268, 264.
Pilachowski, C.A. 1977, Astron. Astrophys. 54, 465.
Schindler, M., Stencel, K.E., Linsky, J.L., Basri, G.S., Helfand, D.J. 1982, Ap.J. 263, 269.

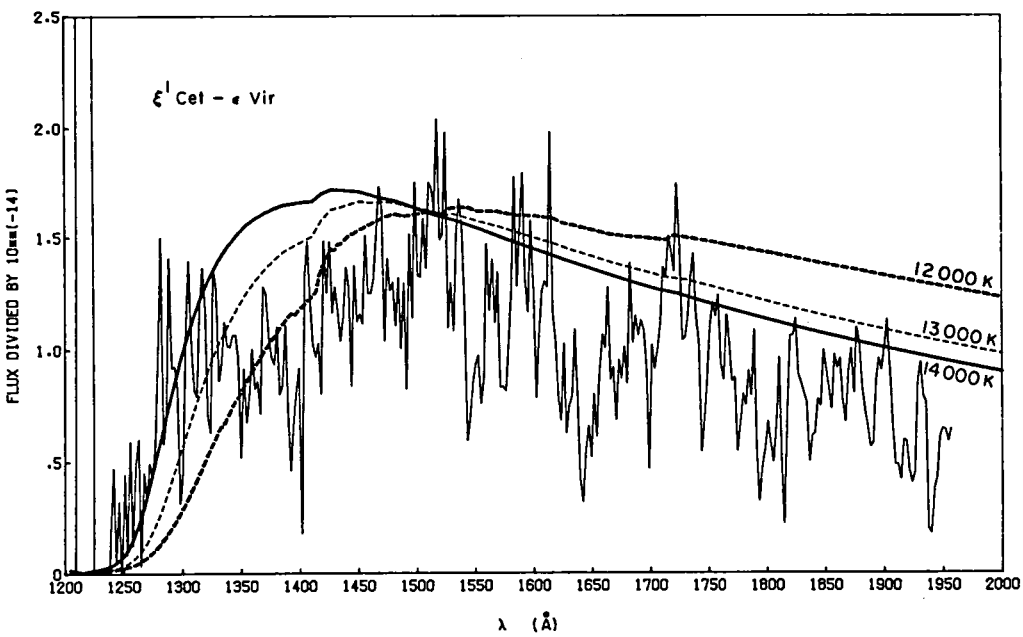

Figure 1. The energy distribution of the ξ^1 Cet companion is compared with model atmosphere energy distributions of DA white dwarfs with log = 8.0, which were kindly provided to us by D. Koester (1983).

VARIABLE STARS

The Outburst and Long Term Behavior of the Triple Period Cataclysmic Variable TV Col

Paula Szkody and Mario Mateo
Department of Astronomy, University of Washington

ABSTRACT

We have analyzed 48 of our IUE spectra and 16 archival spectra of the cataclysmic variable TV Col obtained over a 4 year period in order to study variability associated with the orbital period of 5.49^h, the photometric period of 5.19^h and a longer beat period of 4.024 days. Both the short and long timescale trends are probably complicated by random variability. The most extreme event occurred in November, 1982 when TV Col underwent an unprecedented 2 magnitude continuum outburst in the UV and optical with large increases in the high excitation lines of HeII 1640 and NV 1240. The only repetition timescale apparent from all the data appears to be the 4 day beat period. The flux distributions from UV through 2.2μ can usually be represented by a power law with $F_\lambda \alpha \lambda^{-2.3}$ and a black body component with T near 10000K.

INTRODUCTION

TV Col (= 2A0526-328) has been identified as a DQ Her type cataclysmic variable with an asynchronously rotating white dwarf (Hutchings et al 1981). There are 3 periods known to be present; a spectroscopic orbital period of $5^h29^m11^s$ and photometric modulations of about 30% amplitude at $5^h11^m29^s$ and 4.024 days (Motch 1981). Hutchings et al suggested that these periods can be produced by an accretion column attached to a magnetic white dwarf which is rotating slower than the orbital period. Radiation from this column can illuminate a part of the accretion disk or secondary as it rotates once every 4 days with respect to the binary orbit.

Previous IUE observations (Mouchet et al 1981) have shown a continuum flux distribution that may be fit by a power law ($F_\lambda \alpha \lambda^{-2.3}$) plus a 9000K black body. In November, 1982, we observed TV Col with IUE at low dispersion and with ground based optical coverage at CTIO during 4 consecutive US2 shifts in order to study the changes in the 2 components associated with the 3 known periods. However, during this time, TV Col underwent an unprecedented outburst of 2 magnitudes which ruined the coverage of the 4 day phenomena but enabled a new study of the variability associated with this object. We have since obtained all existing data from the archives on this object in order to compile the long term behavior. This includes 48 of our spectra and 16 others from April 1980 through Sept 1983. Eliminating the 21 spectra obtained during and immediately following the night of the outburst left us with 25 SWP spectra and 17 LWR spectra. Seventeen pairs of combined SWP + LWR spectra taken from 8 separate shifts were able to be used to construct flux distribution fits.

RESULTS

The Continuum Fits

With the exception of 4 spectra, all pairs of SWP + LWR + optical continua could be adequately represented by a 2 component fit of a power law and a black body. The addition of infrared flux points J, H, K (1.25-2.2μ) did not change this fit, indicating that the secondary star is of little importance. An example of this fit is shown in Figure 1. Although we cannot imply that this type of fit is the only one possible or that it actually represents the temperatures of the components involved, it is apparent that whenever a long wavelength distribution is available (SWP + LWR and especially the optical), a one component model is not adequate. The SWP essentially samples the hotter component and the LWR and optical samples the cool component. The range of α's of our fits were -3.77 to -2.31 and the range in BB temperature of the cool component were 7193 to 13770 °K. Table 1 gives the mean values and deviations for all the data as well as for the individual nights of Nov 21 and 24, 1982 when entire single orbits were covered.

The Outburst

Previous to Nov. 1982, TV Col had remained at a steady V=14 mag state. On the night of Nov. 22, the UV and optical continuum rose by almost 2 magnitudes during a 30 minute timescale and remained at a higher than normal state (V=13.5) the following night. The continuum fits showed a steepening of the power law distribution and an increase in T of the longer wavelength source. The UV line fluxes increased dramatically (by factors of 63 for HeII, 13 for NV and 9 for CIV), with P Cygni features present at the maximum of the outburst (Figure 2). The timescales and intensity of the outburst are consistent with an accretion event occurring very close to the inner disk surface (Szkody and Mateo, 1984).

The Periodic Variability

After eliminating the large outburst event and the night following, we plotted individual continuum points throughout the SWP and LWR spectra on the 3 known periods. An example of the total fluxes (converted to F_λ magnitude units) is shown in Figure 3. It is apparent that random variability dominates any consistent variation on photometric or spectroscopic periods but the 4 day beat period variation is evident. Generally, the SWP shows a smaller range of variation from the mean (0.18 mag) than the LWR (0.35 mag), implying a greater amount of change in the cool component (hot spot?) rather than the hot component (overall disk?). The phase of the 4 day variation is consistent with the ephemeris given by Hutchings et al (1981). On the nights of Nov. 21 and 24, 1982 when individual orbits were covered, there is a trend for higher fluxes around photometric phase 0.2 and lower fluxes near phases 0.7-0.8, but even on 2 consecutive orbits the peak to peak variation is on the order of 0.2 mag. In general, the cool black body component temperature increases and the alpha index steepens as the total fluxes increase, in the same manner as occurred during the large outburst. In order to resolve these dependencies, future observations will have to be made over several single orbits.

TV Col epitomizes the difficulties encountered with cataclysmic variables in general. The domination of random variability, the occurrence of unexpected outbursts and the need for simultaneous long wavelength coverage means that observations must be conducted at several wavelengths simultaneously and that combining different orbits for greater signal/noise or phase coverage is not practical.

We acknowledge the help of the IUE operators and staff throughout the course of several runs and Dr. John Hutchings for providing some of the archival data.

REFERENCES

Hutchings, J.B., Crampton, D., Cowley, A.P., Thorstensen, J.K., and Charles, P.A. 1981, Ap. J. 249, 680.
Motch, C. 1981, Astr. Ap. 100, 277.
Mouchet, M., Bonnet-Bidaud, J.M., Ilovaisky, S.A. and Chevalier, C. 1981, Astr. Ap., 102, 31.
Szkody, P. and Mateo, M. 1984, Ap. J. 280, in press.

Table 1 - Continuum Fits

	Mean α	σ	Mean T (°K)	σ	N
All Data	-2.61	0.37	10210	1560	17
Nov. 21, 1982	-2.41	0.06	10378	470	5
Nov. 24, 1982	-2.47	0.04	9916	540	5

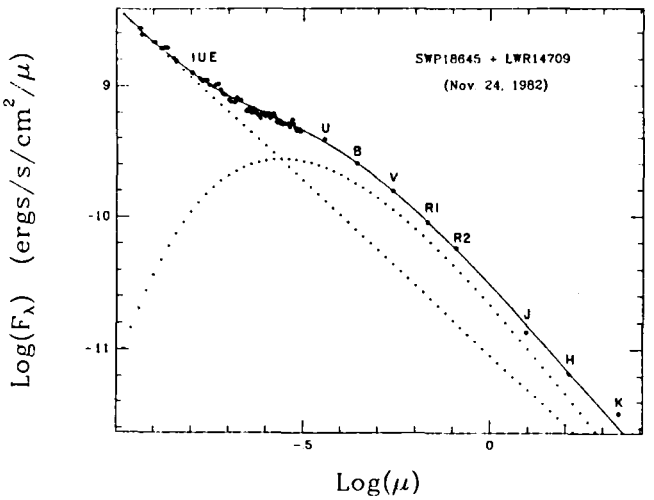

Fig.1 The continuum flux distribution of TV Col. Points are data, dotted lines are a 10500K BB and a power law of α=-2.6 and the solid line is the sum of the 2 components.

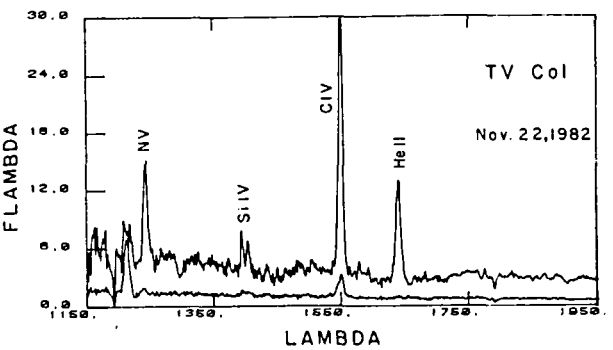

Fig.2 The normal (bottom) and outburst (top) SWP spectra.

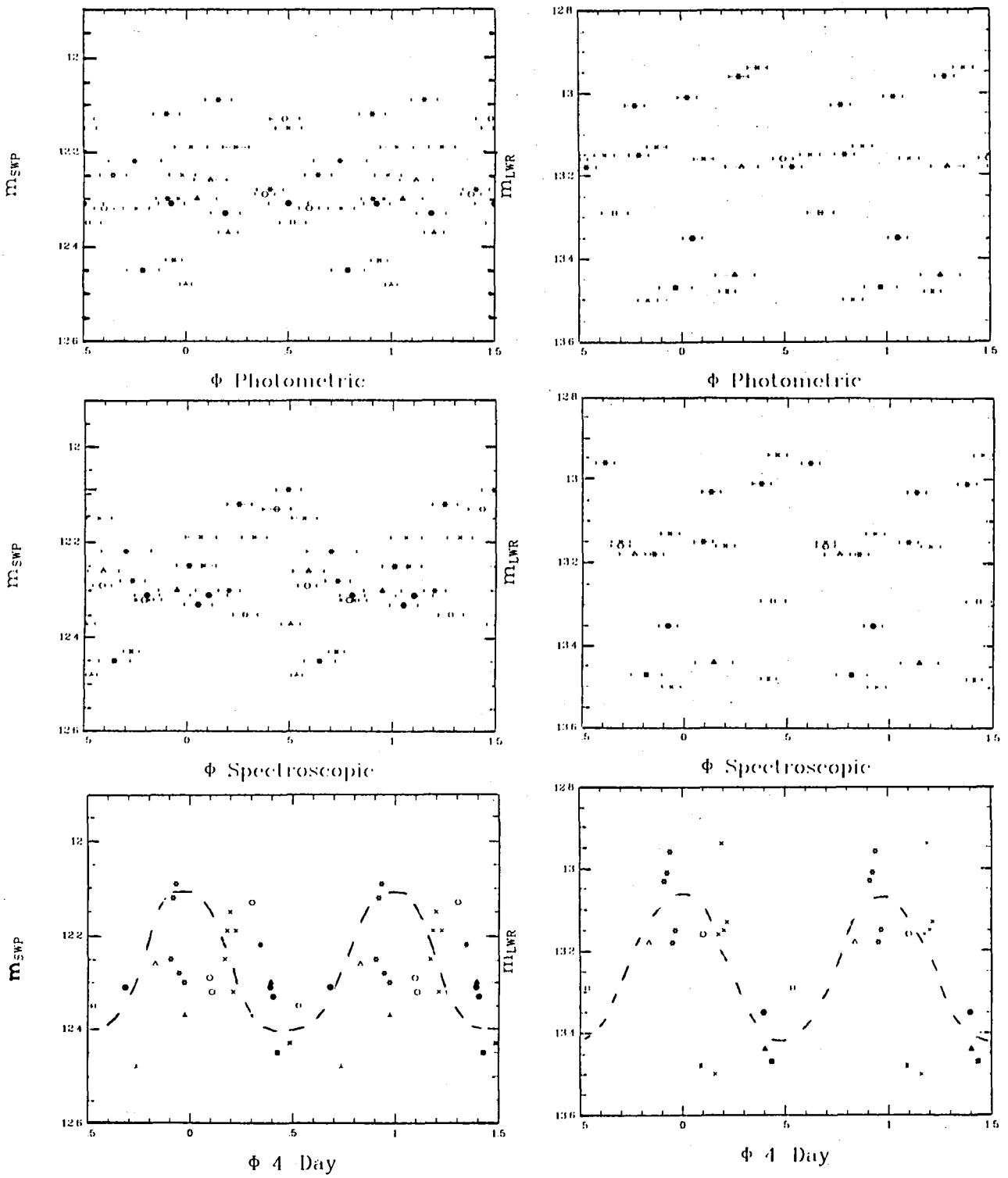

Fig.3 The available SWP and LWR magnitudes folded on the 3 known periods. Each day is represented by a given symbol.

P CYGNI PROFILES IN HL CMa

J.C. Raymond

Harvard-Smithsonian Center for Astrophysics

ABSTRACT

The C IV doublet in spectra of the dwarf nova HL CMa shows strong P Cygni profiles during the late rise, peak and decline from outburst maximum. Very high velocity emission wings are seen in some spectra. The N V, Si III and Si IV lines generally show blueshifted absorption with very weak emission components. Models of the ionization state of the wind provide a basis for discussion of the wind geometry.

INTRODUCTION

P Cygni profiles indicating high velocity winds and substantial mass loss rates are observed in spectra of some dwarf novae in outburst (e.g. TW Vir, Cordova and Mason 1982), nova-like variables (e.g. LSI 55° - 8, Guinan and Sion 1982), and ex-novae (e.g. HR Del, Hutchings 1980). Neither driving force nor wind geometry is yet understood. HL CMa (1E0643-1648) is well suited for study of winds in dwarf nova outburst because it has strong C IV P Cygni profiles, it has frequent outbursts (roughly every 15 days, Chlebowski, Halpern and Steiner 1981), and it is fairly bright. The orbital period is 0.2145 days (Wargau et al. 1983), but it is not precisely enough known to phase spectra from different outbursts. The white dwarf mass is close to 1 solar mass, and the inclination angle is near 45° (Hutchings et al. 1982). From the probable detection of TiO bands in the spectrum at minimum and the absolute magnitude of the secondary which would fill its Roche lobe at the known orbital period, J. Patterson estimates a distance of 120 pc. Accretion disk models (Tylenda 1981) then imply mass transfer rates of 2×10^{15} g/s at minimum and 4×10^{16} g/s at maximum.

OBSERVATION

Over 20 SWP spectra of HL CMa were obtained at various stages of outburst. Most used the Large Aperture, but a few Small Aperture spectra provide an absolute wavelength scale and Ly α absorption profiles. Thanks to J. Mattei and the AAVSO, one spectrum was obtained during the rise, shortly before maximum light. Figure 1 shows the average of nine of the SWP spectra. Individual spectra show fairly similar C IV profile shapes, though the equivalent widths vary by a factor of two. The terminal velocity is 4000 - 5000 km/s, which is similar to TW Vir (Cordova and Mason 1982). The N V line is stronger and the Si IV line weaker than in TW Vir, implying a more highly ionized wind (Kallman 1984). A few of the spectra show C IV P Cygni emission at high velocities, and one of the spectra at minimum shows a pure emission C IV line whose asymmetric profile suggests emission from a wind even at minimum. The N V and Si IV lines show very weak or absent P Cygni emission components.

Figure 2 shows the equivalent widths of the emission and absorption components of the C IV line at various outburst phases. The continuum flux at 1485 Å used as a measure of the system's brightness is closely correlated with the FES magnitude, but the correction to the FES magnitude for scattered light from Sirius makes the optical brightness less accurate. Each point is an average of 2 to 4 spectra, some of the averages including substantial variations between sequential spectra. The unfilled circles show the equivalent widths from the rise phase spectra. The relatively small equivalent widths during rise show that either the mass loss rate or the C IV ionization fraction was substantially smaller just before maximum (though the terminal velocity was unchanged). A smaller mass loss rate might be expected if the inner disk development is delayed by a day or so in comparison with the optical light (Hassall et al. 1981) and the wind is powered by the boundary layer. On the other hand, the wind is likely to be overly ionized by the boundary layer emission, so that the C IV ionization fraction might be expected to drop as the boundary layer develops.

MODELS

It is not obvious whether the wind originates from the disk or in or near the boundary layer. So far we have computed absorption profiles for spherically symmetric winds originating near the white dwarf. These profiles are unusual because the continuum emission originates in the disk and because most of the continuum near 1500 Å originates at 3 to 15 times the white dwarf radius. This means that the wind is nearly at its terminal velocity throughout the region responsible for the absorption lines. Therefore, the velocity structure of the absorption lines reflects the geometry rather than the velocity structure of the wind, and the line of sight velocity is close to the projection of the terminal velocity onto the line of sight. A typical profile for a mass loss rate of 10^{-10} solar masses per year, an inclination angle of 45°, a C IV ionization fraction of 0.1, and the "standard" velocity law for stellar winds ($v_{max}(1-r_*/r)^{1/2}$) is shown in Figure 3. The C IV ionization fraction is nearly constant throughout the wind, since both the ionizing flux and the density fall off as r^{-2} for $r >> r_*$. The absorption profile clearly fails to match the observations.

A further problem is that the boundary layer luminosity and temperature inferred from the white dwarf mass and the mass transfer rate (Pringle 1977) ionize the wind far too effectively. For a mass loss rate of 10^{-10} solar masses per year (or 1/4 the mass transfer rate), the C IV ionization fraction is only 1.4×10^{-5}. At $T_{BB} = 1.7 \times 10^5$ K, a model atmosphere flux distribution would increase this by 30% compared with the blackbody distribution used. Since the ionization fraction is proportional to the density (and therefore mass loss rate), a mass loss rate ten times the mass transfer rate would be needed to produce C IV optical depths near unity. Kallman (1984) also found that blackbody boundary layer emission predicted theoretically could not account for the observed ionization state of the TW Vir wind. There are several plausible ways to get more C IV in the wind. One is to assume that the boundary layer lies in the plane of the disk, so that the ionizing flux is proportional to the $\cos\theta$. This gives substantial C IV densities near the disk.

Models for spherical mass distributions with the $\cos\theta$ ionizing flux dependence still require a mass loss rate comparable to the mass transfer rate. For 45° inclination the model profiles have minima near 1.0 and 0.7 v_{max} which might conceivably be identified with the double minima in Figure 1. Another way to increase the C IV is shock compression in the wind similar to the shocks in the radiation pressure driven winds of early-type stars (Lucy and White 1980). These shocks could compress the gas and increase the C IV ionization fraction by factors like 100. A third possibility is that part of the inner disk shadows the outer disk from the boundary layer emission. A limitation on the assumption is that boundary layer emission is observed from SS Cyg at a high inclination angle. A great deal more work will be needed to construct plausible models of the flow pattern for winds originating from the disk and to compute the emission profiles of the winds.

This work has been supported by NASA grant NAG5-87.

REFERENCES

Chlebowski, T., Halpern, J.P., and Steiner, J.E. 1981, Ap. J., 247, L35.
Cordova, F.A., and Mason, K.O. 1982, Ap. J., 260, 716.
Guinan, E.F., and Sion, E.M. 1982 in "Advances in Ultraviolet Astronomy: Four Years of IUE Research", Y. Kondo, J.M. Meade and R.D. Chapman eds., p 465.
Hassall, B.J.M., et al., 1981, M.N.R.A.S., 197, 275.
Hutchings, J.B. 1980, P.A.S.P. 92, 458.
Hutchings, J.B., Cowley, A.P., Crampton, D., and Williams, G. 1981, P.A.S.P., 93, 741.
Kallman, T. 1984, preprint
Lucy, L.B., and White, R.L. 1980, Ap. J., 241, 300.
Pringle, J.E. 1977, M.N.R.A.S., 178, 195.
Tylenda, R. 1981, Acta Ast. 31, 127.
Wargau, W., Bruch, A., Drechsel, H., and Rahe, J. 1983, Astr. and Ap., 125, L1.

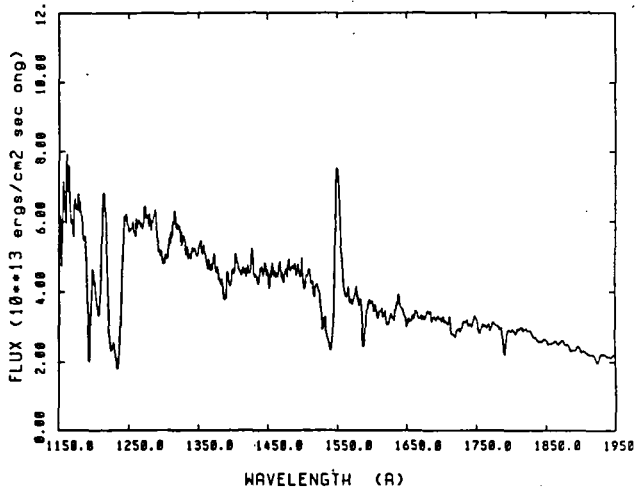

Figure 1.

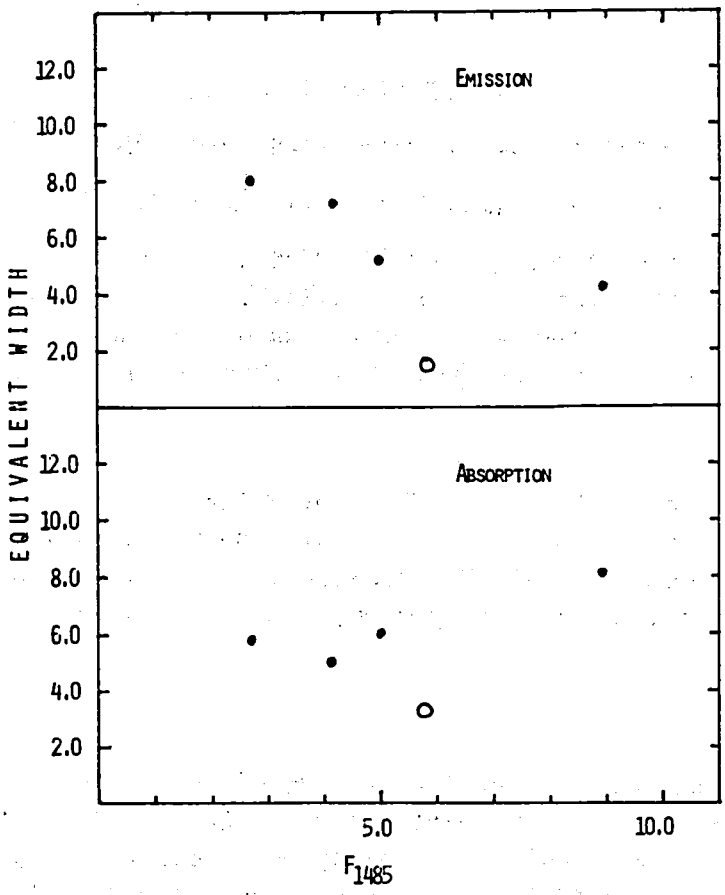

Figure 2.

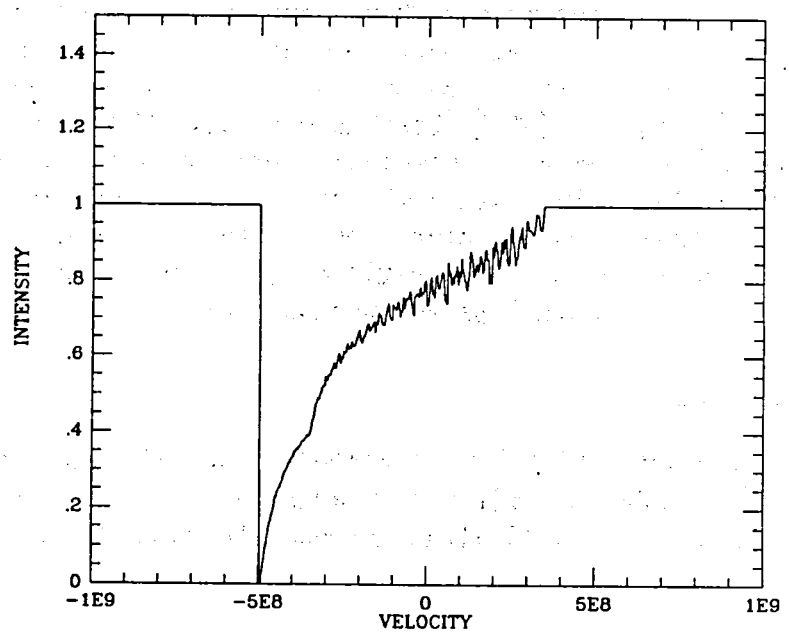

Figure 3.

NEW RESULTS ON PU VUL*

M. Friedjung[1], M. Ferrari-Toniolo[2], P. Persi[2]
A. Altamore[3], A. Cassatella[4], R. Viotti[2]

1. Institut d'Astrophysique, CNRS, Paris, France
2. Istituto Astrofisica Spaziale, CNR, Frascati, Italy
3. Istituto Astronomico, Università La Sapienza, Roma
4. Astronomy Division, ESTEC, Villafranca, Madrid, Spain

ABSTRACT

We analyze coordinated UV and IR observations of the nova-like variable PU Vul made during the 1983 September active phase. A reddening of E(B-V) = 0.49 is obtained, while the 1980 fading is attributed to absorption by dust formed in the interactive binary system, containing an active warm component and an M giant.

INTRODUCTION

PU Vul is a nova-like variable discovered by Y. Kuwano (Kozai 1979) which underwent a large gradual luminosity increase from B=12-13^m to V=8^m.9 in 1978-79. During 1980 a large luminosity fading occurred, followed by a recovery to the present stage, about 0.5 mag brighter than in 1979 (Belyakina et al. 1982, Kolotilov and Belyakina 1982, etc.). The spectral type during the bright phases was that of an F supergiant (Gershberg et al. 1982, Iijima and Ortolani 1984), while at minimum this warm spectrum disappeared, and a red continuum with strong TiO bands typical of an M5 giant emerged, with narrow emission lines of H, NaI, [NII], and [OIII] (Gershberg et al. 1982). Emission lines of H, [OII] and [OIII] were recently observed by Purgathofer adn Schnell (1983) in 1983 September, probably indicating the occurrence of an active phase of PU Vul. It is therefore of particular interest the fact that during the same period we organized coordinated ultraviolet (IUE) and infrared (TIRGO) observations with the aim of investigating the nature of this peculiar object.

---

* Based on observations with IUE collected at the Villafranca Satellite Tracking Station of ESA, Madrid, and on archive IUE images, and on infrared photometry obtained with the Italian National Infrared Telescope (TIRGO) at Gornergrat.

OBSERVATIONS

Fig.1 shows the low resolution LW IUE spectrum of PU Vul observed in 1983 September compared with the previous spectrum obtained in 1982 August. The spectrum resembles that of a late A-early F giant or supergiant without clear evidence of emission lines. A large flux variation took place between 1982 and 1983, while the visual magnitude was nearly the same, in agreement with the active phase found by Purgathofer and Schnell (1983). The ultraviolet energy distribution of PU Vul appears redder than in normal A-F stars. By comparison with the A7III star θ Tau (V=3.41, E(B-V)=0.06) we derived for PU Vul a preliminary estimate for the i.s. extinction of $E(B-V) = 0.49 \pm 0.02$, with a wavelength dependence close to the standard one.

PU Vul was observed at the Italian National Infrared Telescope (TIRGO) at Gornergrat on 1983, September 15 using the helium-cooled Ge bolometer of the Istituto Astrofisica Spaziale, Frascati. The IR magnitudes were:

$K = 6.09 \pm .12 \quad L = 5.53 \pm .15 \quad M = 4.01 \pm .26 \quad N > 3.5$

The K and L fluxes are close to those of Bensammar et al. (1980) taken in 1979 April during the first bright stage of PU Vul (V=8.89). These values have to be compared with the value of K=6.4 found by Belyakina et al. (1982) in 1980 October, when PU Vul was near the deep minimum(V=13.45). These results show that the IR flux only slightly varied during minimum, in spite of the large optical variations.

The ultraviolet-to-infrared energy distribution of PU Vul in 1983 September is shown in Fig.2. The visual magnitude of V=8.53 was derived from the FES IUE counts. The energy distribution corrected for $E(B-V) = 0.49$ is also given in the figure. The optical-ultraviolet energy distribution can be fitted with a normal late-A giant spectrum. An IR excess is present below 2-3 micron which could be attributed to the faint M star and/or to dust emission. The exact value of the excess is difficult to be determined because of the uncertainty on the true energy spectrum of the warm star, and of the variability of PU Vul as discussed below.

DISCUSSION

We have measured the ultraviolet flux of PU Vul in line free regions during 1979-83, using the archive IUE spectra collected at VILSPA and GSFC. Fig.3 shows the UV light curve of PU Vul compared with the visual light curve as derived from the AAVSO Circulars. For completeness, also the infrared (K) magnitudes are shown in the figure. As already noticed by Holm and Wu (1980), the UV flux began to decrease well before the optical fading. Also after the end of the visual minimum, the UV flux continued to increase without large changes of the visual luminosity.

In addition, preliminary examination of archive IUE spectra of 1979 April 19 and 1980 May 5 suggests that the fading on the latter date may be accounted for by an additional absorption with a law similar to the interstellar one and a supplementary E(B-V) of 0.5. The 1980 October infrared magnitudes may similarly be compatible with an additional E(B-V) of 1.3. A similar idea was used to interpret optical observations by Yamashita et al. (1982).

These results clearly indicate that PU Vul is an interactive binary system containing an active warm component, a giant M star, and varying quantities of dust which can absorb light from both components. Dust condensation then occurred in spring 1980 and cleared in 1981. This star may be related to the D (dust) type symbiotics. Excluding the minimum, its spectral evolution recalls the early phases of RR Tel, and a final fading may soon occur after the present active phase.

REFERENCES

Belyakina, T.S., et al. 1982, Soviet Astronomy 26, 1.
Bensammar, S., Friedjung, M., Assus, P. 1980, Astr. Astrophys. 83, 261.
Gershberg, R.E., et al. 1982, Soviet Astronomy 26, 3.
Holm, A.V., Wu, C.-C. 1980, IAU Circular 3471.
Iijima, T., Ortolani, S. 1984, Astr. Astrophys. in press.
Kolotilov, E.A., Belyakina, T.S. 1982, Inf. Bull. Var. Stars No.2o97.
Kozai, Y. 1979, IAU Circular 3344.
Purgathofer, A., Schnell, A. 1983, IAU Circular 3859.
Yamashita, Y., Maehara, H., Norimoto, Y. 1982, Pub. Astr. Soc. Japan 34, 269.

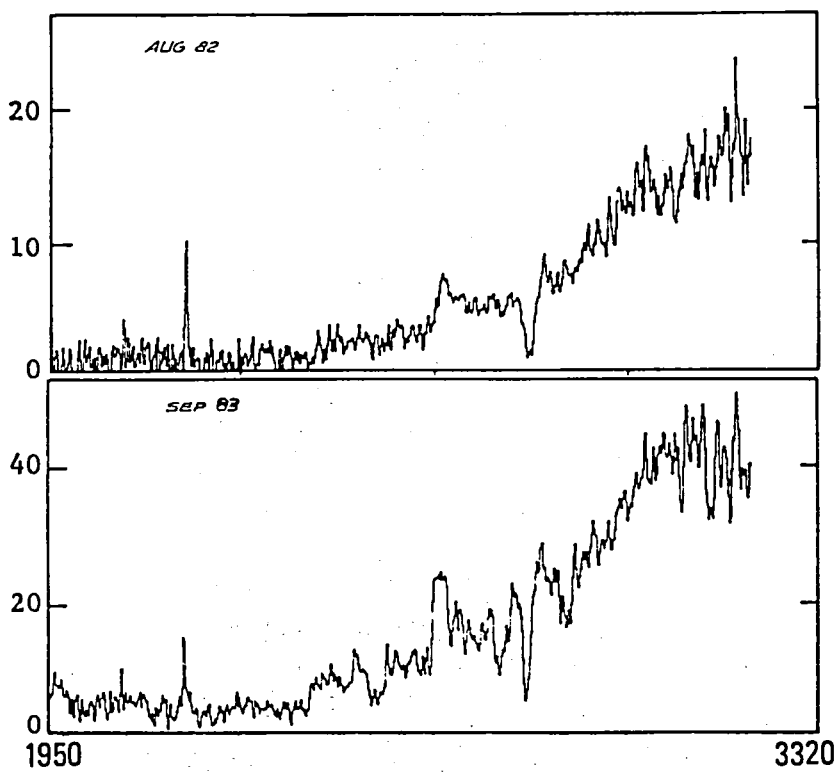

Figure 1. The low resolution LWR spectrum of PU Vul in 1982 and 1983.

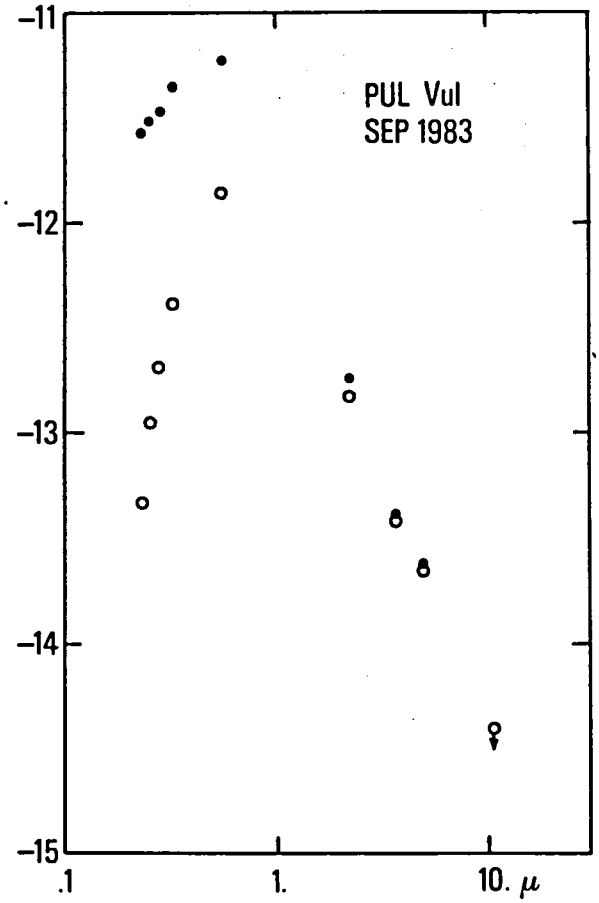

Figure 2. The ultraviolet-to-infrared energy distribution of PU Vul in 1983 September. Open circles: observations; filled circles: data corrected for E(B-V) = 0.49.

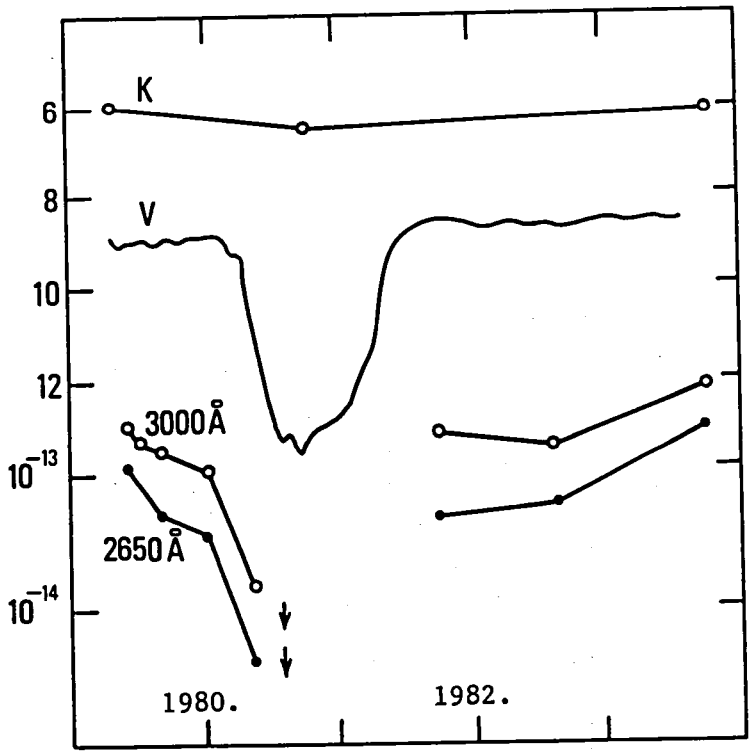

Figure 3. The infrared (K), visual, and UV (3000 and 2650 A) light curve of PU Vul during 1979 to 1983. The large minimum is attributed to dust formation.

THE ABUNDANCES OF THE ELEMENTS -CARBON TO SILICON- IN NOVA CORONA AUSTRINA 1981

Sumner Starrfield
Department of Physics, Arizona State University
and Theoretical Division, Los Alamos National Laboratory

Robert E. Williams
Steward Observatory, University of Arizona and M.P.I., Garching

Warren M. Sparks
Applied Theoretical Physics Division, Los Alamos National Laboratory

Susan Wyckoff
Department of Physics, Arizona State University

James W. Truran
Department of Astronomy, University of Illinois

Edward P. Ney
Department of Astronomy, University of Minnesota

ABSTRACT

We observed Nova Corona Austrina 1981 systematically over a period of seven months with the IUE satellite. These spectra cover the range 1150-3200 A, and are mostly at low dispersion. The emission lines identified in the low dispersion spectra cover a range in ionization potential from about 8 ev (Mg II) to about 80 ev (N V). Line emission fluxes and widths have been measured in all spectra. Several months after maximum visual light, high ionization forbidden lines of sodium, magnesium, and aluminum appeared and then declined over a period of two months. The abundances deduced from these lines imply that nitrogen, oxygen, neon, sodium, magnesium, and aluminum are all enhanced with respect to helium while carbon is not. The observations of this nova, plus the observations of Nova Cygni 1975 and Nova Aquila 1982, imply that some fraction of novae contain white dwarfs that have undergone non-degenerate carbon burning prior to entering a close binary-nova phase of evolution.

INTRODUCTION

Low dispersion spectra of Nova Corona Austrina 1981 were obtained over the interval from April 1981 to November 1981. The spectral scans were all reduced at Goddard Space Flight Center using the R.D.A.F. to obtain flux calibrated spectra and integrated line fluxes were determined for all emission lines. As is usually the case for novae in the decline phase of visual

light, the spectra show only the presence of very broad emission lines formed by high velocity ejecta. Nova CrA 1981 displayed a number of UV emission features that have not previously been seen in any astronomical object (Williams, et al. 1984: hereafter, W84). For these lines we have attempted to make identifications which are consistent with the presence of well known species. The line identifications and detailed analyses of the spectral changes with time are presented elsewhere (W84). Here we are only concerned with the abundance results and the very important implications of these results.

OBSERVATIONS AND ANALYSIS

On May 25, 1981, the spectral evolution of this nova underwent its first significant change with the appearance of emission lines which we attribute to forbidden lines from highly ionized species. The strength of these lines increased through June 1981 and then began to decline. They disappeared into the continuum in August 1981. During this same period the CNO resonance lines maintained roughly the same strength relative to each other. Since virtually all of the possible transitions from the lowest excited levels to the ground state of moderately to highly ionized lines of neon, aluminum, and magnesium, are found in the spectrum, we are quite confident in these identifications. We note that this behavior is similar to that of Nova V1500 Cygni 1975 which was discovered, from observations in the near IR, to have highly ionized "coronal" forbidden lines from some of these same elements about one month after the peak of the outburst (Grasdalen and Joyce 1976).

The abundance ratios, by number, that we determine for the ejected gas, using the spectra obtained in June 1981, are as follows: C/N=0.070; N/O=0.77; Ne/N=1.45; Al/Mg=0.41; Si/Al=0.71; Mg/Ne=0.036; and N/He=0.075. Since, several stages of ionization are observed at the same time for neon, magnesium, and aluminum, this improves our confidence in the abundance determinations. Figure 1 shows the relative abundance distribution plotted for the above elements and normalized to He=1. The solar abundance distribution is plotted on the same figure for comparison. The enhancement found for these nuclei is striking and unusual! The only hydrogen emisssion accessible at IUE wavelengths is Ly-α and it is strongly affected by scattering from the interstellar medium and geo-coronal emission. One optical spectrum, obtained shortly after outburst, shows emission features, including Hα, characteristic of a nova in decline.

The most surprising feature of our IUE spectra is the extreme enhancement of neon, sodium, magnesium, and aluminum with respect to helium and carbon. Although CNO enhancement is now regularly reported for novae studied with modern techniques (c.f., Starrfield 1984), only marginal enhancements of neon (in novae) have been reported previously (Ferland and Shields 1979; Williams and Gallagher 1979). On the contrary, in Nova CrA 1981

we find neon to be more abundant than carbon, nitrogen, or oxygen and the enrichment with respect to helium is a factor of 100. Another nova which showed similar abundances and, therefore, supports this analysis is Nova Aql 1982. Snijders, et al. (1984) have found that the neon abundance in the ejected gas was roughly equivalent to that of helium implying an enhancement of $\sim 10^3$.

DISCUSSION

The accepted model for the classical nova outburst involves the accretion of hydrogen-rich material onto a C/O white dwarf until a thermonuclear runaway ensues in the accreted material (see Starrfield 1984 and references therein). Carbon and oxygen nuclei are mixed up from the core into the envelope, by some unknown mechanism, and serve as catalysts to increase the strength of the outburst. Both predictions and observations confirm that carbon, oxygen, and nitrogen are enhanced in ejecta of typical novae. (The enhancement of nitrogen is produced by the CNO reactions with carbon and oxygen.) However, the enhancements of neon, aluminum, and magnesium relative to CNO, observed in Nova CrA 1981, cannot be accounted for within the framework of the current nova theory if the degenerate star is a C/O white dwarf. Both thermonuclear runaway studies and nucleosynthetic calculations show that only under the most extreme conditions can any CNO nuclei be processed to magnesium or aluminum and under these same conditions the most likely product is iron (Wallace and Woosley 1982; Truran 1984). Unfortunately, it was not possible to determine an iron abundance for Nova CrA 1981. In Nova Cygni 1975 it was solar (Ferland and Shields 1978).

Since the white dwarf must be the origin of the enhanced material, then a more likely possibility is that it is an O/Ne/Mg white dwarf and that it is this material which has been mixed up into the accreted envelope. The next nuclear burning stage that occurs in a star, after helium burning, is carbon burning which produces oxygen, neon, and magnesium. We note that it has recently been suggested that stars with a main sequence mass of $\sim 10 M_\odot$ to $\sim 12 M_\odot$ can evolve through carbon burning and become O/Ne/Mg white dwarfs (c.f.; Nomoto 1983; Iben 1982; Law and Ritter 1983). If we assume that the binary system of Nova CrA 1981 contains such a white dwarf, then it remains only to perform nucleosynthetic calculations to determine if hot hydrogen burning in an O/Mg/Ne mixture can produce the observed abundance ratios. We have recently evolved an accretion sequence with only oxygen enhanced and found that a fast nova resulted. These calculations show that during the evolution to the runaway that a fraction of the oxygen, initially present in the envelope, is burnt to carbon and it is this carbon which causes the fast nova outburst (Starrfield, Sparks, and Truran 1984, in preparation).

Therefore, we suggest that the white dwarf components of Nova CrA 1981, Nova Aql 1982, and possibly V1500 Cyg consist of O/Ne/Mg white dwarfs (see also Law and Ritter 1983). These

systems were probably formed from initially very widely separated binaries with a large main sequence mass. Hot hydrogen burning then converted the initial mixture to those nuclei enhanced in the ejected gas: N, O, Ne, Na, Mg, Al, and Si.

Finally these results strongly imply both that core material is being dredged up into the envelope and that the mass of the white dwarf decreases as a result of the outburst.

We are pleased to acknowledge valuable discussions with Arthur Cox, Icko Iben, Jim MacDonald, and Rick Wallace. S. Starrfield thanks Drs. George Bell, Stirling Colgate, and Michael Henderson for the hospitality of the Los Alamos National Laboratory. This research was supported in part by National Science Foundation Grants to Arizona State University (AST81-17177 and AST83-14788) and the University of Illinois (AST83-14415) and by the DOE.

REFERENCES

Ferland, G.J., and Shields, G.A. 1978,Ap.J.,226,172.
Grasdalen,G.l., and Joyce,R.R. 1976,Nature,259,187.
Iben,I. 1982,Ap.J.,259,244.
Law,C.Y., and Ritter,H. 1983,A. and A.,123,33.
Nomoto,K. 1983,preprint.
Snijders, M.A.J., et al. 1984,submitted to MNRAS.
Starrfield, S. 1984, in The Classical Nova, ed M. Bode and A. Evans(New York:Wiley) in press.
Truran, J.W. 1984, Ann. Rev. Nuc. Science, in press.
Wallace, R.K., and Woosley,S.E. 1981,Ap.J. Supp.,45,389.
Williams, R.E., and Gallagher, J.S. 1979,Ap.J.,228,487.
Williams, R.E., et al. 1984, submitted to MNRAS.

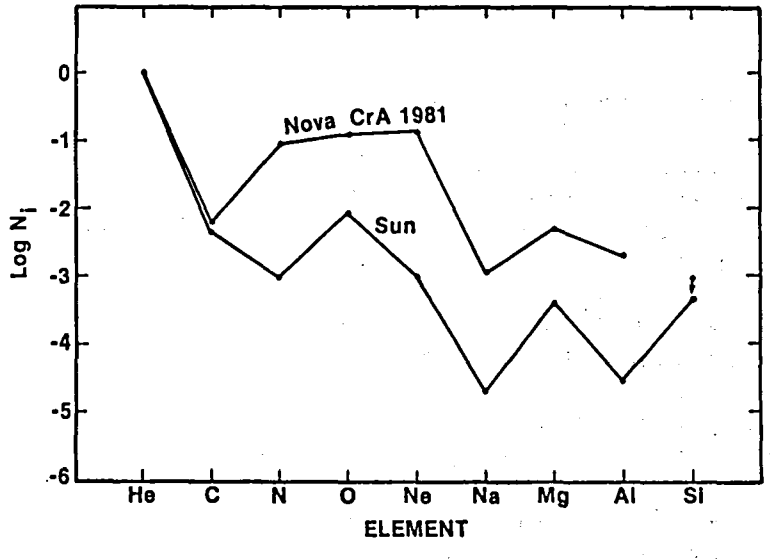

Figure 1. The logarithm of the abundances, by number, of the elements that we were able to analyze for both Nova CrA 1981 and the Sun.

HYDRODYNAMIC SIMULATIONS OF RECURRENT NOVAE

Sumner Starrfield
Department of Physics, Arizona State University
and Theoretical Division, Los Alamos National Laboratory

Warren M. Sparks
Applied Theoretical Physics Division, Los Alamos National Laboratory

James W. Truran
Department of Astronomy, University of Illinois

Edward M. Sion
Department of Physics, Arizona State University
and Villanova University

ABSTRACT

We have continued our simulations of the 1979 outburst of the recurrent nova U Scorpii. We have used a Lagrangian, hydrodynamic computer code which now incorporates accretion in the evolution to the outburst. We computed three evolutionary sequences in an attempt to understand the very rapid outburst and short recurrence time of this most unusual nova. It is now possible to reproduce the CNO composition of the ejected material, the light curve, the amount of ejected material, and the kinetic energy of the ejecta. The best sequence that we studied involved accretion of solar rich material onto a $1.38M_\odot$ white dwarf at a rate of 1.6×10^{-8} $M_\odot$ per year.

INTRODUCTION

It is now commonly accepted that the classical nova outburst is the result of a thermonuclear runaway (hereafter:TNR) in the accreted hydrogen rich envelope on a white dwarf in a close binary system. A recent review of both the observational and theoretical evidence leading to this claim will soon appear in print (Bode and Evans 1984). In our own studies (see Starrfield 1984) we have shown that if enough material is accreted by the white dwarf and that if this material is enhanced in CNO nuclei, by some process as yet unknown, then a fast nova outburst will occur.

However, a recent IUE study of the recurrent nova, U Sco, has found some very surprising results (Williams, et al., 1981; hereafter W81). First, the amount of mass ejected during the outburst was only $\sim 10^{-7}$ $M_\odot$, at least a factor of 10^3 smaller than for a classical nova. Second, the CNO nuclei were not enhanced above solar in the ejecta even though the outburst was extremely rapid. Third, an optical study of the outburst found that the

ratio of hydrogen to helium was ~0.5 by number (Barlow, et al. 1981). Finally, recent quasi-static studies of accreting white dwarfs have implied that recurrence times as short as that of U Sco (30 yr and 46 yr) cannot be produced as a result of a TNR on even the most massive white dwarfs (MacDonald 1983).

These results could imply that the outburst of U Sco was not a TNR event but was caused by some other process (c.f., Webbink 1976). In order to investigate this question, we have performed three studies of accretion onto white dwarfs. We have used the published results (W81; MacDonald 1983) to define the initial conditions for each of these sequences. We utilized massive, luminous, white dwarfs in order to shorten the time to outburst. We also assumed an evolved secondary, since the accretion disc in U Sco is very helium rich, in order to enhance the mass transfer rate. Finally, we did not enhance the CNO nuclei in order to agree with the observations of U Sco. The program and method of solution will be described elsewhere (Starrfield, Sparks, and Truran 1984; hereafter: SST).

RESULTS

We calculated three evolutionary sequences with a $1.38M_\odot$ white dwarf. Each of our models consists of 95 zones with a hard core inner boundary that has a radius of 1.148×10^8 cm and a surface mass fraction of 2.7×10^{-2} $M_\odot$. Model 1 had a luminosity of $0.1L_\odot$ and we began the evolution with an accretion rate of 1.6×10^{-8} $M_\odot$ yr^{-1}. Model 2 had a luminosity of $0.01L_\odot$ and an accretion rate of 1.6×10^{-9} $M_\odot$ yr^{-1}. Model 3 was evolved with the envelope initially in place and in thermal and hydrostatic equilibrium. It had the same envelope mass as was accreted during the evolution of model 2 and was used to compare the evolutionary results with and without accretion.

Model 1 required 32.7 yr of evolution to reach the peak of the outburst. Over this time period it accreted 5.2×10^{-7} $M_\odot$ of hydrogen rich material. This very short evolution time agrees quite closely with the recurrence times observed for U Sco and is only a factor of 3 longer than the average recurrence time of T Pyx. A TNR results from this evolution and the shell source reaches a peak temperature of 2.23×10^8 K and a peak rate of energy generation of $\sim 1.3 \times 10^{14}$ erg gm^{-1} sec^{-1}. A convective region forms just above the shell source and by the time of peak temperature has caused the luminosity at the surface to reach $\sim 3 \times 10^4$ $L_\odot$. Since the radius of the white dwarf is still small, the effective temperature exceeds 10^6 K and the object would be observed as a fast, soft, X-ray transient source. Figure 1 shows the variation in the temperature of the core-envelope interface as a function of time at the peak of the outburst. Figure 2 shows the bolometric and visual light curves during the outburst. The rapid rise and fall in the visual output from the nova are caused by the decrease and later increase in the effective temperature.

This sequence ejects ~3.0 x 10^{-8} $M_\odot$ of material moving with velocities from ~300 km sec^{-1} to ~3000 km sec^{-1}, in good agreement with the observations of U Sco. After about one year of evolution past the peak of the runaway, the non-escaping material (94% of the accreted material) has retreated to ~2 x 10^9 cm and is falling back onto the white dwarf at a speed of ~0.2 km sec^{-1}. We find, therefore, that the mass of the white dwarf grows as a result of a nova outburst on a 1.38$M_\odot$ white dwarf.

Model 2 took 1570 yr to reach the peak of the runaway and by this time had accreted 2.5 x 10^{-6} $M_\odot$, in excellent agreement with the calculations of MacDonald(1983). Peak temperature in this sequence is 3.4 x 10^8 K and peak energy generation is 1.8 x 10^{14} erg gm^{-1} sec^{-1}. The peak surface luminosity is ~4 x 10^4 $L_\odot$ and the effective temperature has a maximum value of 1.3 x 10^6 K early in the runaway. This sequence ejects ~2 x 10^{-7} $M_\odot$ at rather low speeds: ~60 km sec^{-1} to ~300 km sec^{-1}. The light curve is given in Figure 3. As in the last sequence, a major fraction of the accreted material is burnt to helium and falls back onto the white dwarf so that the mass of the white dwarf also increased during this evolution.

Model 3, evolved for comparison purposes, had the envelope in place so that no accretion occurred during the evolution to runaway. We find that the evolution time to peak temperature (3.5 x 10^8 K) is only 10 yr and that peak energy generation is 1.5 x 10^{14} erg gm^{-1} sec^{-1}. Both of these values are in good agreement with model 2. In fact, the rest of the evolutionary behavior is very similar to that of model 2 enhancing our claim that our studies with the envelope in place are valid representations of studies with accretion included. A light curve for this model is give in Figure 4.

DISCUSSION

We have found that a simulated nova outburst can occur as a result of a TNR on a very massive white dwarf. Our mass accretion rates were equal to, if not greater than, the values predicted for mass transfer from an evolved secondary as is the case for U Sco and T CrB. The shortest time scale to runaway that we found, 32.7 yr, is in excellent agreement with the observed recurrence times for U Sco. The amount of mass ejected during the outburst, ~10^{-7} $M_\odot$ is also close to the value found for U Sco.

The models reported in this paper showed that mass ejection and a nova light curve occurred without the CNO nuclei being enhanced in the accreted envelope. This is in contrast to our studies of TNR's on lower mass white dwarfs where it was found that CNO enhancement was required to produce a fast nova outburst. The cause of this difference is that the steady burning luminosity on a massive white dwarf (Paczynski 1971) is approximately equal to the Eddington luminosity which facilitates ejection by radiation pressure. We also found that the mass of

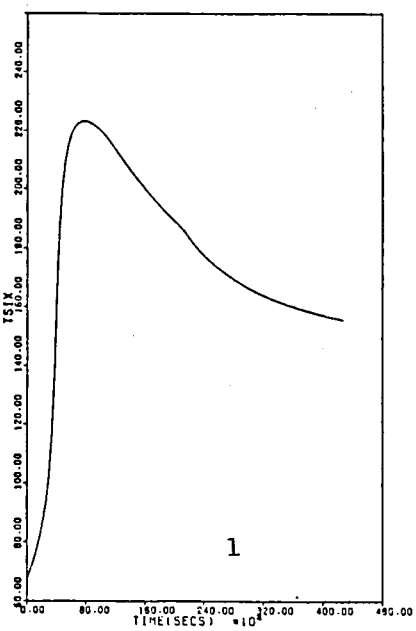

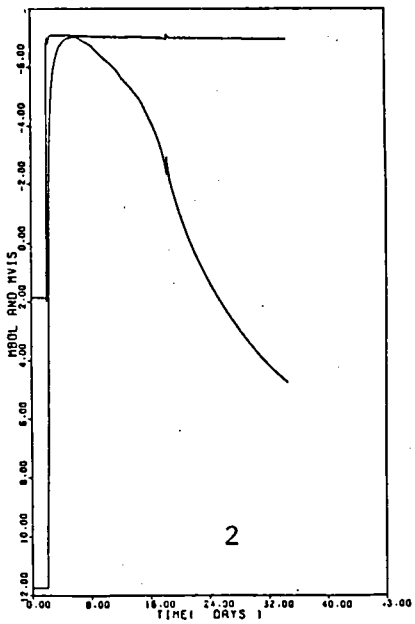

Figure 1. The temperature at the composition interface as a function of time for model 1 near the peak of the outburst.
Figure 2. The light curve for model 1 as a function of time. The upper curve is M_{bol} and the lower curve is M_v.

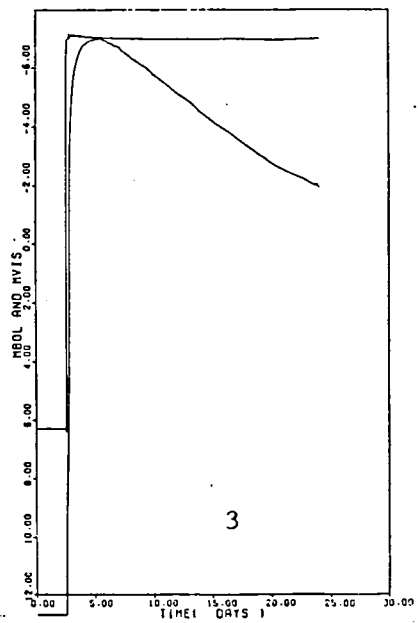

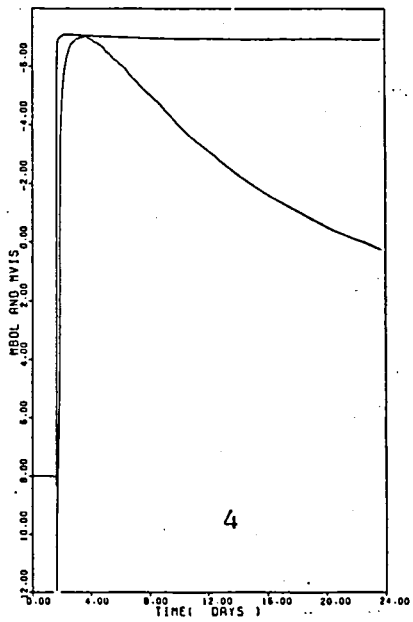

Figure 3. The light curve for model 2 as a function of time. The upper curve is M_{bol} and the lower curve is M_v.
Figure 4. The light curve for model 3 as a function of time. The upper curve is M_{bol} and the lower curve is M_v.

the white dwarf increases as a result of the nova outburst. This is also in contrast to our studies at lower mass where the mass of the white dwarf decreases as a result of the outburst (Starrfield, Truran, and Sparks 1981). At the accretion rate that we used, it will take the white dwarf component in U Sco less than 10^7 yr to reach and exceed the Chandrasekhar limit. This star is, therefore, well on its way to undergoing an SN I explosion.

Finally, our comparison sequence demonstrated close agreement with the accretion sequence although the time scale to runaway was shorter. This implies that our previous studies done with the envelope initially in place are completely valid representations of the evolution. We can continue to use quasi-static studies to determine the value of the envelope mass to use for a given white dwarf mass and luminosity and be quite confident in the evolutionary results.

We are pleased to acknowledge valuable discussions with Drs. Arthur Cox, Stirling Colgate, Jim MacDonald, Robert Williams, and Rick Wallace. S. Starrfield thanks Drs. George Bell, Stirling Colgate, and Michael Henderson for the hospitality of the Los Alamos National Laboratory and a generous allotment of computer time. This research was partially supported by National Science Foundation Grants to Arizona State University (AST81-17177 and AST83-14788) and the University of Illinois (AST83-14415) and by the DOE.

REFERENCES

Barlow, M. J., et al. 1981, MNRAS, 195, 61.
Bode, M. and Evans, A. (ed.) 1984, The Classical Nova, (New York: Wiley), in press.
MacDonald, J. 1983, Ap. J., 267, 732.
Paczynski, B. 1971, Acta Astr., 21, 417.
Starrfield, S. 1984, in The Classical Nova, ed. Bode and Evans., in press.
Starrfield, S., Sparks, W.M., and Truran, J.W. 1984, preprint.
Starrfield, S., Truran, J.W., and Sparks, W.M. 1981, Ap. J., 243, L27.
Webbink, R. 1976, Nature, 262, 271.
Williams, R.E., Sparks, W.M., Gallagher, J.S., Ney, E.P., Starrfield, S., and Truran, J.W. 1981, Ap. J., 251, 221.

THE UV EXTINCTION OF HR 5999

J. H. Hecht, Space Sciences Laboratory, The Aerospace Corporation

A. V. Holm, T. B. Ake, III, C. L. Imhoff, N. A. Oliversen and G. Sonneborn
Computer Sciences Corporation

ABSTRACT

The irregular Ae variable HR 5999 has been observed by IUE during a period of minimum light ($7.4 \leq Mv \leq 7.7$). By comparing these spectra with spectra of the star taken five years previously near maximum light ($Mv \sim 6.9$) we have obtained a UV extinction curve. The shape of the curve as a function of wavelength does not resemble other extinction curves. A possible cause of the extinction could be 110 nm graphite particles in the star's atmosphere along our line of sight. It is proposed that this star is intermediate as a dust producer between other Ae and T Tauri stars, whose variability appears to be due to spotting, and R CrB variables where dust production is the cause of the light extinction.

INTRODUCTION

The Ae star HR 5999 is irregularly variable between $6^m.8$ and $8^m.0$ with a period on the order of one month. It has been the subject of numerous studies over the past 15 years (Thé et al., 1981) which have concluded that the star is surrounded by dust (Thé et al., 1982); that the variability is caused by the formation of dust not by changes in the star's surface temperature or radius (Tjin A Djie and Thé, 1978); and that some activity at the surface is triggering the dust formation (Tjin A Djie and Thé, 1982). Thus, this star affords the opportunity both to study the dust formation process and to calculate a true dust extinction curve without having to use the standard star comparison method. In both these regards it is similar to the R CrB variables (Hecht et al., 1984).

RESULTS

After notification by Dr. F. Bateson of New Zealand that the star had faded, we observed it on 6/2/83 ($M_{FES} = 7.6$, SWP 20133, LWR 16060), and on 8/31/83 ($M_{FES} = 7.4$, SWP 20861-20863, LWR 16706/07). It had also been observed earlier at $M_{FES} = 7.6$ on 8/28/82 (SWP 17790, LWR 14027). Unfortunately, only our 8/31/83 spectra were well exposed over the entire wavelength range. For comparison we used spectra taken near maximum ($M_{FES} = 6.9$) on 5/10/78 (SWP 1514, LWR 1465) and on 5/18/78 (SWP 1511, LWR 1569). The extinction is proportional to $\log_{10} (F_{max}/F_{min})$, where F_{max} is the flux near maximum light, and F_{min} is the flux at minimum when the star is obscured by dust (Hecht et al., 1984). An extinction spectrum is shown in Fig. 1 which uses the 8/31/83 spectra for F_{min} and the 1978 spectra for F_{max}. It resembles neither the normal curve nor other peculiar extinction curves. In particular while the bump position is near the normal interstellar position at

2200 Å, the extinction at 1600 Å is much less than at 2800 Å. Thus, the shape is more extreme than that of θ ORI (Massa et al., 1983) and approaches that of the dereddened Herschel 36 (Hecht et al., 1982). However, the latter curve is dissimilar to Fig. 1 from 2200-2800 Å.

The extinction for the well-exposed parts of the 6/2/83 spectra is similar to Fig. 1 in that the peak is near 2200 Å but it has an even steeper decline to 1600 Å. The 1982 extinction spectrum is much flatter than Fig. 1 from 1600 to 2200 Å with, if anything, more extinction at 1600 Å than at 2200 Å.

DISCUSSION

Dust Material

While both carbon bearing and oxygen bearing materials have been proposed for the 2200 Å feature (see Massa et al., 1983 or Hecht et al., 1984) our calculations show that only graphite particles of near 110 nm radius give a reasonable fit to Fig. 1. Interestingly, both the calculation and data indicate that there is a second peak between 1200 and 1600 Å. While our present observations are too noisy to confirm this, future well exposed spectra could determine if (1) the continuum extinction showed this second peak consistent with the graphite hypothesis, and (2) whether the hot shell emission lines of OI(1304) and CIV(1550) showed more or less extinction than the continuum. In addition simultaneous IR and UV observations could help identify the particles. The graphite identification would be more likely if the 10 μ silicate feature was not seen at the same time as the 2200 Å feature.

Dust Formation

The short term (several days) variability of other Ae and T Tauri stars has recently been attributed to surface spotting presumably associated with magnetic fields (Herbst et al., 1983). This might be happening part of the time in HR 5999 since the 1982 extinction curve shows flatter extinction in the UV, with an increase towards 1600 Å. This would be expected if part of the star's surface were spotted. However, some of the time dust formation must be triggered, perhaps by magnetic cooling (Wdowiak, 1983), or by formation in the cool post shock-front of ejected gas (Fadeyev, 1983). Both have been proposed for R CrB variables. If the gas is ejected below the escape velocity of the star, and expansion velocities for HR 5999 appear to be below it (Bessel and Eggen, 1972), then after the initial event the dust could re-evaporate and the star would return to normal magnitude.

Another class of dust producing variables, the R CrB stars, are hydrogen deficient, have long term variability, and eject amorphous carbon dust at greater than escape velocity. Thus HR 5999, which has substantial atmospheric hydrogen and perhaps forms graphitic carbon, may be intermediate between the short-term variable, non dust-producing T Tauri stars, and the long-term variable, dust-ejecting R CrB stars.

REFERENCES

Bessell, M. S. and Eggen, O. J. 1972, Ap. J. 177, 209.
Fadeyev, Y. A. 1983, Ast. Sp. Sci. 95, 357.
Hecht, J., Helfer, H. L., Wolf, J., Donn, B. and Pipher, J. L. 1982, Ap. J. 263, L39.
Hecht, J. H., Holm, A. V., Donn, B. and Wu, C. C. 1984, Ap. J. (accepted).
Herbst, W., Holtzman, J. A. and Kalsky, R. S. 1983, A. J. 88, 1648.
Massa, D., Savage, B. D., Fitzpatrick, E. L. 1983, Ap. J. 266, 662.
Savage, B. D. and Mathis, J. S. 1979, Ann. Rev. Astr. Ap. J. 17, 73.
The, P. S. et al., 1981, Astron. Astrophys. Suppl. Ser. 44, 451.
Tjin A Djie, H. R. E. and The, P. S. 1978, Astron. Astrophys. 70, 311.
Tjin A Djie, H. R. E. and The, P. S. 1982 "Proceedings of the Third IUE Conference," Madrid, ESA SP-176, p. 113.
Wdowiak, T. J. 1983, Ap. J. (submitted).

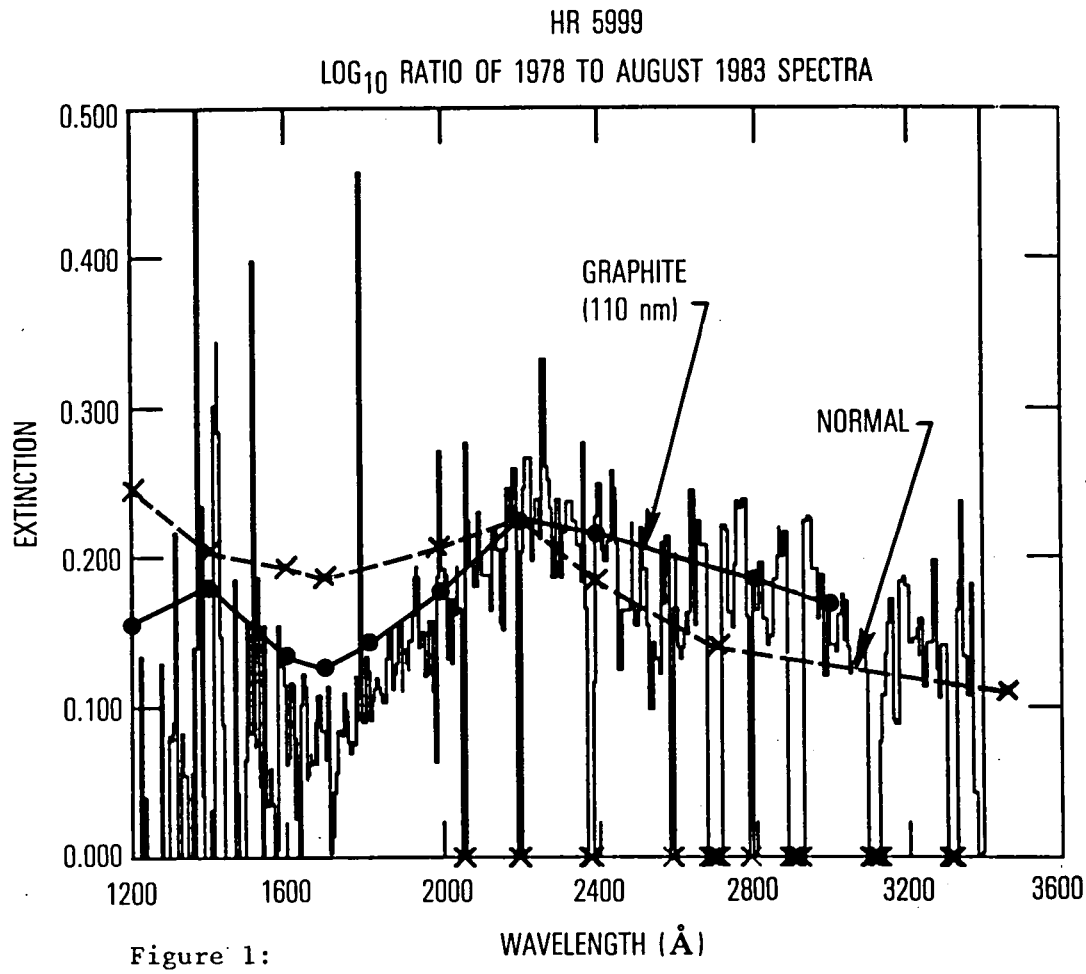

Figure 1:

Full line curve is the extinction for HR 5999 using August 1983 and 1978 spectra for F_{min} and F_{max} respectively.

●——●——● is a calculated extinction curve for 110 nm graphite particles.

X---X---X is the normal interstellar extinction curve (Savage and Mathis, 1979) normalized to the graphite peak at 2200A.

Variability of Ultraviolet Emission Lines in the Carbon Star TX Psc

John H. Baumert
Computer Sciences Corporation
and
Hollis R. Johnson
Astronomy Department, Indiana University

ABSTRACT

During the course of our study on the R and N stars we have obtained multiple observations of the carbon star TX Psc. We report here the probable time variations of the Mg II 2800 Å line and possible variation of the C II 2325 Å line in the spectra of this object.

I. OBSERVATIONS

The N-type carbon star TX Psc (NO;C6,2) ranks along with Y CVn as the brightest carbon star in the sky. It is an irregular (Lb) variable with V ~ 5. Four low-resolution, long-wavelength (1900-3300 Å) spectra have been obtained with IUE over a 26-month period. The spectra, exposure times, and dates are: (1) LWR 11843 (120 minutes) on 25 October 1981; (2) LWR 14062 (90 minutes) on 31 August 1982; (3) LWR 16373 (180 minutes) on 19 July 1983; (4) LWP 2511 (300 minutes) on 27 December 1983. The spectra were converted to a flux scale using the absolute calibration of Bohlin and Holm (1980).

II. LINE IDENTIFICATION

The spectra of TX Psc as observed on 25 October 1981 and 31 August 1982 are shown in Figure 1. The features we are concerned with in this report are those near 2800 Å and 2325 Å.

The Mg II resonance lines at 2795.5 and 2802.7 Å are well known diagnostics of chromospheric activity in late-type stars. At our low resolution (~ 6 Å) the h and k lines are blended together as one line. This feature is easily recognizable in all four of our spectra.

An issue of particular importance is the identification of the relatively strong feature at 2325-35 Å. The reason for its importance is that if it is attributed to C II, it becomes the line of highest excitation or ionization in the chromosphere and therefore sets rather relatively severe constraints on any chromospheric model for these stars (Avrett and Johnson 1983). The only plausible candidates for producing this strong feature are Fe II (UV 2), Fe II (UV 3), Ni II (UV 11), and C II (UV 0.01). We consider each of these in turn.

We note that Fe II multiplets (UV 1), (UV 4), (UV 5), (UV 62), and (UV 63) are detected but multiplets (UV 2) and (UV 3) are either marginally detected or not seen at all. The difference apparently arises from the density of lines within the multiplet. Those multiplets detected are dense multiplets with all lines packed within 20-30 Å (except for (UV 62, 63), which are spread over 40 Å). All have noticeable line clumps. On the other hand, (UV 2) and (UV 3) are spread over 50-80 Å and there are no line clumps. Even the strongest groups of lines in these latter multiplets (at 2343-44, 2381-83, and 2404-11 Å) are either absent or very weakly detected. We can therefore be assured that any contribution of Fe II multiplets (UV 2) and (UV 3) to the peak at 2325-35 Å is negligible.

Ni II multiplet (UV 11) has its strongest lines at 2316, 2302, and 2297 Å. There is certainly no evidence for these lines because the emission tends to rise rather sharply between 2320 and 2325 Å on the different spectra with relatively little or no emission shortward of that. Apparently then, Ni II does not contribute to the peak at 2325 Å.

A feature at this wavelength is seen in all late-type giant stars as can be seen in the ultraviolet spectral atlas (Wu et al. 1983). There its identification is certain since there is no possibility that any other features could be that strong and since high resolution spectra show it to be C II beyond any doubt. We are therefore forced to conclude that the same feature which is present in TX Psc and in almost all N-type carbon stars observed to date is also attributable to the C II intercombination line.

III. LINE FLUXES AND THEIR VARIATION

The Mg II and C II fluxes are shown in Table 1. We estimate that the errors for the C II fluxes is approximately 50% while the Mg II fluxes for the observation of 27 December 1983 may be underestimated by a factor of 4-6.

As is apparent from the table, the flux in the ionized magnesium line varies by at least a factor of 3 and perhaps as much as 25 depending on the value of the overexposure assigned to the December 1983 exposure. The flux in the ionized carbon line varies by a factor by about 50% although this may be within the uncertainty in the observations.

If Mg II is the major source of radiative cooling in the chromosphere of TX Psc, we must conclude that the cooling rate varies by the same rate as the emission flux seen in the line; that is, by at least a factor of 3. It appears that such a variation could have interesting consequences for theories of chromospheric heating and energy balance.

Table 1
Emission Line Fluxes

Spectrum Number	Mg II 2800 Å		C II 2325 Å	
	peak flux*	integrated line flux**	peak flux*	integrated line flux**
LWR 11843	2.43	25.1	1.04	11.1
LWR 14062	0.74	5.5	0.74	8.1
LWR 16373	1.57	20.9	0.83	10.2
LWP 2511	1.56+	22.2+	1.11	10.0

*units 10^{14} $f_{\lambda o}$ (ergs/cm^{2}sÅ) **units 10^{14}f (ergs/cm^{2}s)
+lower limit; line saturated

The only attempt of which we are aware to model a chromosphere for a cool carbon star are those of de la Reza (1984) and Avrett and Johnson (1983). These workers attached various chromospheric models to a photosphere for the star from the models of Johnson (1982) with the parameters (3000/0.0/solar except C; C/O = 1.05), which are close to those for the star TX Psc (Johnson et al. 1982). The authors find that a chromospheric model can be found with the following properties and draw the following conclusions: (1) The Mg II line at 2800 Å can be produced in approximately (though slightly less than its observed strength, while (2) no emission is observed in the Balmer Alpha line of hydrogen, which is not observed in these stars (Yamashita 1972, 1975). To do so the authors are forced to consider a boundary temperature of 2000 K. The identification of the emission at 2325 Å with C II sets a much more severe constraint upon the chromosphere and careful studies of the consequences of this identification will be fruitful.

The authors acknowledge NASA Grants NSG 182-5 for IUE observations and NSF Grants AST 7913149 and 82-058-00 under which model atmospheres for these stars were computed and some of the line identifications were carried out.

REFERENCES

Avrett, E. H. and Johnson, H. R. 1983, in Proc. Third Cambridge Conf. on Cool Stars, Stellar Systems, and the Sun, ed. S. L. Baliunas and L. Hartmann (New York: Springer Verlag).
Bohlin, R. and Holm, A. 1980, NASA IUE Newsletter, No. 10, p. 37.
De la Reza, R. 1984, in preparation.
Johnson, H. R. 1982, Ap. J., 260, 254.
Johnson, H. R., O'Brien, G. T. and Climenhaga, J. 1982, Ap. J., 254, 175.
Wu, C. -C., et al. 1983, NASA IUE Newsletter No. 22.
Yamashita, Y. 1972, Ann. Tokyo Astr. Obs., 13, 169.
_____ 1975, Ann. Tokyo Astr. Obs., 15, 47.

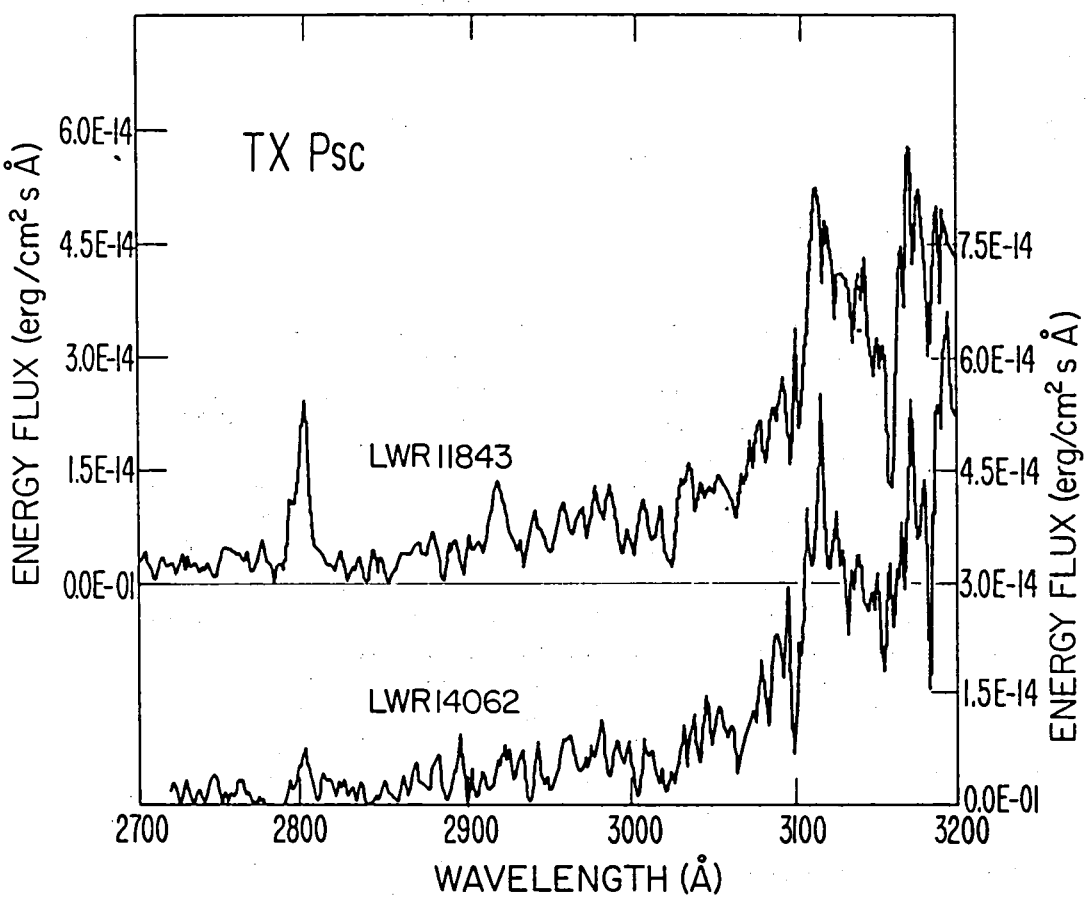

Figure 1. Spectra of TX Psc taken 10 months apart show a factor 3 variation in the peak flux of the Mg II line near 2800Å.

TEMPORAL UV EMISSION FROM THE PECULIAR STAR RX PUPPIS

M. Kafatos
Department of Physics
George Mason University

A.G. Michalitsianos
Laboratory for Astronomy and Solar Physics
NASA Goddard Space Flight Center

John Brugioni
Department of Physics
George Mason University

ABSTRACT

We have monitored the peculiar emission star RX Puppis with the International Ultraviolet Explorer in low and high dispersion. The ultraviolet spectrum of RX Puppis is characterized by strong permitted and intercombination emission lines similar to that observed in slow novae and symbiotic stars. The absolute emission fluxes of most lines appear to have increased since the first year of observations, during which the resonance doublet of C IV λλ1548,1550 increased by approximately 14 percent. During this period the intensity ratio of the C IV I(λ1548)/I(λ1550) typically had values less than unity, and thus exceeded the optically thick limit. Over the several years of observations following maximum UV emission, the doublet ratio appears to be approaching values ~1. C IV doublet ratios <1 could be explained by P-Cygni structure in the λ1550.7 line, in which the broad absorption component deminishes emission at λ1548.2 during ejection. This would imply expansion velocities >500 km s^{-1}. The high dispersion line profile structure in both permitted and intercombination lines appear generally complex and time dependent. We present a description of our IUE data and suggest that the temporal nature of the line profile structure is consistent with an ejection event having occurred.

I. Introduction

RX Puppis displays a rich emission line spectrum that features intense emission from He II, [Fe VII], [Ne V] and other emission lines from ions with >100 eV ionization potential. The high dispersion UV spectrum in the SWP λλ1200-2000A wavelength range has been described previously by Kafatos et al. (1982). In addition to strong high excitation emission lines observed in the optical and UV, RX Puppis is also characterized by strong infrared emission (Swings and Allen 1972)

that is variable in the 1-4μm range (Feast et al. 1977). Feast et al. attribute the infrared variability to the presence of a Mira-type variable, although Klutz, et al. (1978) discounted the presence of an M giant. However, Barton et al. (1978) find from 1.9μm absorption the presence of water vapor (H_2O) which they find is suggestive of a T_{eff} ~2400K Mira variable in the system; Whitelock and Catchpole (1982) find a 580-day period for the Mira.

The emission lines of N IV] λ1489, C IV λλ1548,1550, He II λ1640, O III] λλ1660,1666, N III] λ~1750, Si III] λ1892 and C III] λ1909 all exhibit intensity variations over the course of the four year observing program. In high dispersion IUE spectra these emission lines exhibit multiple component structure. The C IV resonance double exhibits the most complicated line profile structure, as evident in Figure 1. In each of the broad doublet emission lines we have identified seven individual narrow emission components which blend to form the extended profile. In Table 1 we show the wavelengths individual emission components found in

Table 1

Emission Components Identified in C IV

λ_o=1548.2A	λ_o=1550.7A
1547.7	1550.3
1548.1	1550.7
1548.3	1550.9
1548.4	1551.1
1548.6	---
1549.3	1551.9
1549.8	1552.3

each of the doublet lines. The average velocity separation of the individual emission components that combine to form the line profile is $\Delta v \sim 62$ km s^{-1}. Only one C IV component is identified shifted blueward with respect to λ_o. IUE data obtained on 22 March 81 probably coincides closely with the time of maximum emission because the respective absolute fluxes now appear to be approaching initial values measured in 20 Sept 80. The dominant brightening in C IV and other emission lines generally occurred at their respective rest wavelengths. The redward displaced components have had more moderate intensity enhancements compared to emission at their respestive rest wavelengths. Observing time for all our observations did not permit a very deep high dispersion SWP exposure in order to detect structure in the far wings of the emission lines nearer the continuum. Similar temporal behavior is also evident in other emission lines as well, such as He II, O III], N III], Si III] (see Figure 1b), although the number of emission components are fewer and the line profile structure is not as complex as C IV.

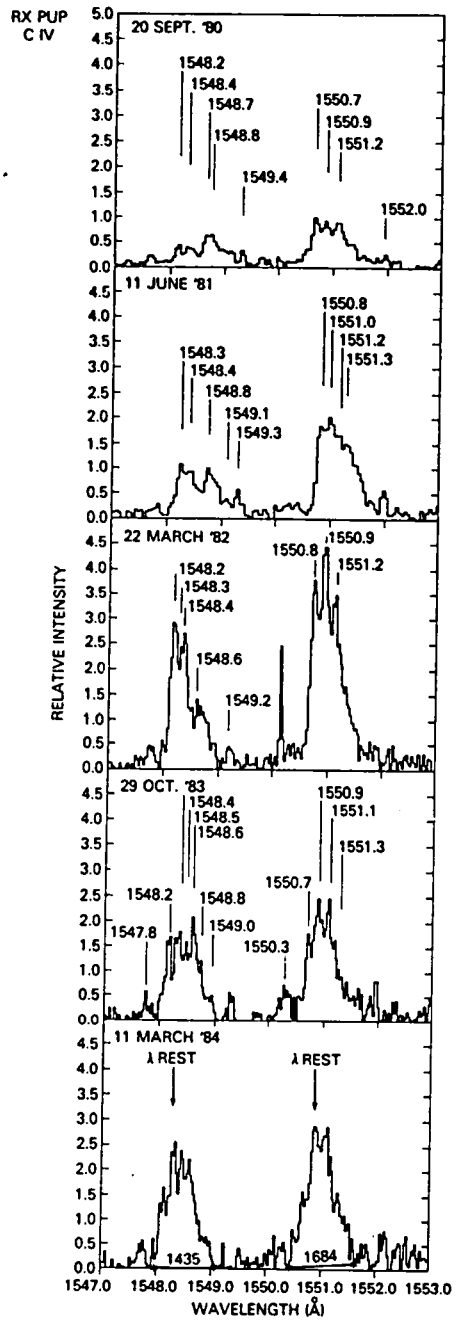
RX PUP
C IV
20 SEPT. '80
1548.2
1548.4
1548.7
1548.8
1549.4
1550.7
1550.9
1551.2
1552.0
11 JUNE '81
1548.3
1548.4
1548.8
1549.1
1549.3
1550.8
1551.0
1551.2
1551.3
22 MARCH '82
1548.2
1548.3
1548.4
1548.6
1549.2
1550.8
1550.9
1551.2
29 OCT. '83
1548.4
1548.5
1548.6
1547.8
1548.2
1548.8
1549.0
1550.3
1550.7
1550.9
1551.1
1551.3
11 MARCH '84
λ REST
λ REST
1435
1684
RELATIVE INTENSITY
WAVELENGTH (Å)

(a)

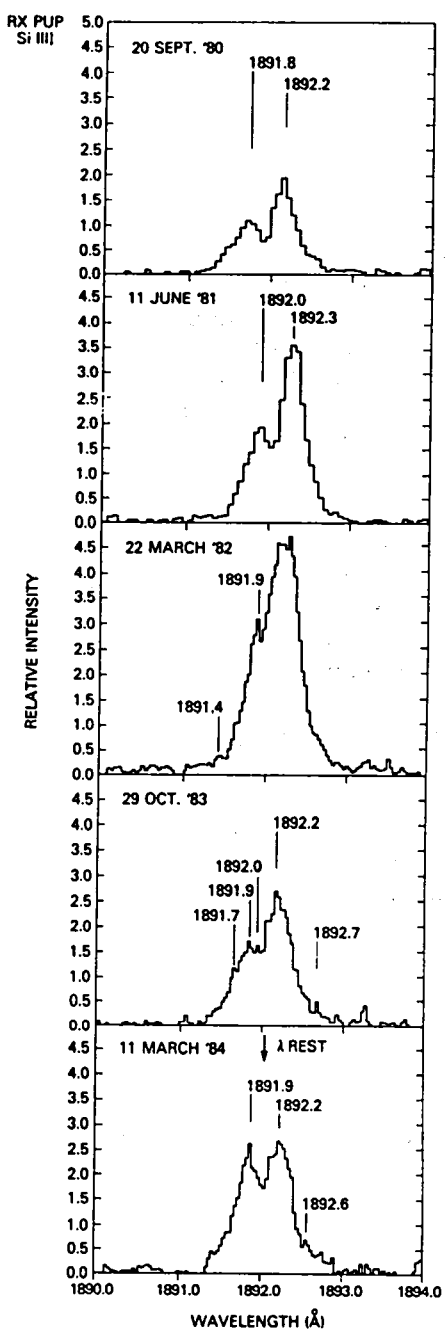
RX PUP
Si III]
20 SEPT. '80
1891.8
1892.2
11 JUNE '81
1892.0
1892.3
22 MARCH '82
1891.9
1891.4
29 OCT. '83
1892.2
1892.0
1891.9
1891.7
1892.7
11 MARCH '84
λ REST
1891.9
1892.2
1892.6
RELATIVE INTENSITY
WAVELENGTH (Å)

(b)

Figure 1

The overall intensity of the C IV doublet in RX Puppis is unusual because the λ1548 line is generally weaker than the λ1550 line i.e. $I(\lambda1548)/I(\lambda1550) < 1$; it thus exceeds the optically thick case. This is reminiscent of the C IV doublet ratio observed in a similar systems such as AG Pegasi by Keyes and Plavec (1982). They attribute the ratio $I(\lambda1548.1)/I(\lambda1550.7) \lesssim 1$ to the broad P-Cygni absorption component of the λ1550 line that absorbs emission at λ1548. This would imply shell expansion velocities of ~500 km s^{-1}. From Figure 1a, it is evident that the C IV doublet ratio $I(\lambda1548)/I(\lambda1550)$ was considerably less than unity during epochs when the general line intensities of C IV lines (as well as other permitted and intercombination lines) were near maximum. With the continued decline in line intensity emission, the C IV doublet ratio now appears to be approaching values around unity (see Figure 1a, 11 March 1984). Therefore, it appears that maximum enhancement in the UV line emission coincided with a mass ejection event. This is consistent with the temporal behavior of the emission line intensity ratios of the C IV doublet, if the expanding shell produced broad P-Cygni structure that substantially affected emission at λ1548. RX Puppis likely underwent a slow outburst in which the material ejected from the object took place on a dynamical timescale of ~1 to 2 years. It is further interesting to note that if ~500 km s^{-1} is representative of the ejection velocities from the system, that the hot star in the system resembles more a main sequence type star. From the range of parameters calculated by Kafatos et al. (1982) for the secondary in the system, a main sequence size star would favor a model for the component of T_{eff} = 40,000K, $R_*/R_\odot$ = 0.88 and $L_*/L_\odot = 1.7 \times 10^3$ with an E_{B-V}=0.7. Analysis of IUE and optical data continues in order to develop a model for the complex kinematic behavior of the nebular emitting gas in this object.

References

Barton, J.R., Phillips, B.A. and Allen, D.A. 1979, M.N.R.A.S., **187**, 813.

Feast, M.W., Robertson, B.S.C. and Catchpole, R.M. 1977, M.N.R.A.S., **179**, 499.

Kafatos, M., Michalitsianos, A.G. and Feibelman, W.A. 1982, Ap.J., **257**, 204.

Keyes, C.D. and Plavec, M.J. 1980, "The Universe at Ultraviolet Wavelengths" ed. R.D. Chapman (NASA Proc. Conf. #2171), p. 443.

Klutz M., Simonetto, O. and Swings, J.P. 1978, Astron. and Astrophys., **66**, 283.

Swings, J.P. and Allen, D.A. 1972, Pub. Ast. Soc. Pacific, **84**, 523.

Whitelock, P.A. and Catchpole, R.M. 1982 "The Nature of Symbiotic Stars" eds. M. Friedjung and R. Viotti (D. Reidel Pub. Co.-Holland), p. 207.

THE FADING OF R CORONAE BOREALIS

A.V. Holm[1], J. Hecht[2], C.-C. Wu[1], and B. Donn[3]
1 Computer Sciences Corporation
2 The Aerospace Corporation
3 NASA Goddard Space Flight Center

ABSTRACT

We obtained IUE spectra of R CrB near the beginning of one of its infrequent minimum. These spectra show major changes in the apparent spectrum. We attempt to identify new features and to interpret the overall change in the continuum in terms of an obscuring cloud model.

THE OBSERVATIONS

At the end of August 1983 the variable star R CrB started a descent to minimum (Fig. 1). IUE low dispersion spectra were obtained during the evening of Aug 31/Sept 1, during Sept 2, and during the evening of Sept 8/9. Figure 2 shows the ultraviolet spectra observed on Sept 1 and on Sept 8.

For reference, we also show a reference spectrum of R CrB at maximum light with identifications for the strong absorption features (Holm and Wu 1982). This spectrum represents the average of five observing runs between 1978 Dec 25 and 1980 April 30. The pulsational phase (Fernie 1983) of the reference observations is uncertain, but there clearly are phase dependent differences. The observed range at maximum light is less than 0.3 mag in the optical; at 1800 A it is 1.2 mag.

THE SPECTRA

Our observations show major changes in the appearance of the ultraviolet spectrum of R CrB during the descent to minimum. In the Sept 1 spectrum many of the absorption features were filled in; only the Mg II and Al I features were still strong. By Sept 8, more changes have occurred in the apparent spectrum. Mg II has acquired a strong emission core. The Al I feature has disappeared. In addition, a number of new features are seen. The two most prominent are an apparent absorption feature at 2650 A with an equivalent width of 18 A and a broad feature covering the 2980 A to 3050 A region with an equivalent width of 15 A. The Sept 2 spectrum is not illustrated in this paper; it generally resembles that of Sept 1, but is 0.6 mag fainter overall and shows weakly the features that are strong in the Sept 8 spectrum.

Are there plausible identifications of these new features? For the 2980–3050 A feature we considered both the (0–4) band of the Fox–Herzberg system of C_2 (Fox and Herzberg 1937) and an absorption complex seen in stars with spectral types around K0 (Wu et al. 1983). Unfortunately both proposed identifications encounter problems. The absence of the Fox–Herzberg (0–3) band at $\lambda\lambda$2855–2903 weakens the

argument for C_2. Likewise, the structure within the R CrB feature does not match the K0 spectrum details. We do not propose an identification for the 2650 A feature.

The C II 1335 A emission remained constant at about 9.0E-14 ergs/cm^2/s on Sept 1 and Sept 8. This flux is the same as at maximum light (Holm and Wu 1982).

To put these apparent spectral changes into perspective, we point out that during the early stages of a typical minimum many optical emission lines of neutral and once ionized metals are seen (Herbig 1949, Payne-Gaposchkin 1963). Most of these lines gradually fade and leave an absorption spectrum similiar to the spectrum at maximum.

EXTINCTION

The next stage in our analysis was to compare the spectra obtained during the descent to minimum with the reference spectra to attempt to define the extinction characteristics of the obscuring material.

There was a substantial interval between when the reference spectra were taken and the descent to minimum. To derive a correction for the LWR's wavelength-dependent degradation of sensitivity (e.g. Sonneborn and Garhart 1983), we compared five standard star spectra from Dec 1978 with four from Aug 1983. Figure 3 shows the filtered and binned degradation function. We divided the R CrB observations by this function to correct them to a common epoch.

Figure 4 shows the derived extinction. On Sept 1 nowhere was the UV extinction greater than the visual and it only reached the visual level at a few wavelength ranges. Everywhere else the star showed a UV excess relative to the visual. This excess was especially strong at wavelengths where the reference spectrum showed strong absorption. This result is consistent with the filled in appearance of the lines in the spectra. On Sept 8, the situation had changed a little. The UV had become relatively fainter than the visual from 1940 to 2300 A and at the 2650 A and 2980-3050 A features discussed above. But the UV excess still persisted over wide wavelength bands.

Neither of these curves show a 2400-2500 A bump such as observed for RY Sgr during its recovery from the 1978 minimum (Holm, Wu, and Doherty 1982; Hecht et al. 1984).

DISCUSSION

Can these observations be interpreted without recourse to large and peculiar changes in the underlying star? We believe so. First we point out that the Sept 1 spectrum is not compatible with that of any normal star because the absence of Fe II absorption at 2600 A is inconsistent with the strong Mg II absorption. We discuss qualitatively below how an obscuring cloud can produce the observed spectrum.

We take the following scenario for the life cycle of an R CrB minimum. First a cloud of carbon grains (Loreta 1934; O'Keefe 1939) forms more or less along our line of sight near the star. The cloud grows either by expansion, by new condensation, or both until it totally eclipses the star. As it continues to expand it gradually

becomes optically thin, allowing the observer to see a recovery to maximum light.

The observed initial absence of any ultraviolet extinction greater than that in the visual implies that the star was partially occulted by an optically-thick cloud. This is consistent with the above scenario since the grains constituting this cloud must form in dense, cool gas.

The ultraviolet excess may be interpreted in two ways. First, it might be emission from the cloud of gas from which the dust cloud condensed. Second, it might be radiation from unocculted regions of the stellar atmosphere. The former interpretation is unlikely because the carbon grains will not condense until the gas temperature falls far below the level required to produce the Mg II emission seen on Sept 8. The latter interpretation is similar to that proposed by Hartmann and Apruzese (1976) to explain the optical spectrum. Our model differs from theirs in that we consider that the ultraviolet excess might come from three sources: from a true chromosphere where most of the emission lines arise, from an extended region where the resonance lines of C II, Mg II, Ca II, and Na I arise, and from wavelength-dependent differences in the photospheric limb darkening. This last source requires a brief explanation. Because of the transparancy of a helium atmosphere, we expect that limb darkening will be strong in R CrB's optical continuum. But limb darkening will not be as strong where line blanketing restricts the physical depth to which the observer can see. Thus, if an expanding cloud is centered on the stellar disk, the continuum will fade systematically faster than the line blanketed wavelength range.

The apparent absorption features at 2650 A and at 2980-3050 A may be due to a relative absence of emission.

Confirmation of this picture will require high resolution spectra during the early stages of a descent to minimum and low dispersion spectra at fainter visual magnitudes. The IUE is capable of obtaining such data, but the next minimum may not occur until the IUE mission is complete and it is necessary to use Space Telescope.

REFERENCES

Böhme, D. 1983, Info. Bull. on Variable Stars No. 2442.
Fox, J.G., and Herzberg, G. 1937, Phys. Rev. *52*, 638.
Hartmann, L., and Apruzese, J.P. 1976, Ap.J. *203*, 610.
Hecht, J., Holm, A.V., Donn, B., and Wu, C.-C. 1984, Ap.J. in press.
Herbig, G.H. 1949, Ap.J. *110*, 143.
Holm, A.V., Wu, C.-C., and Doherty, L.R. 1982, Publ. A.S.P. *94*, 548.
Holm, A.V., and Wu, C.-C. 1982, in "Advances in Ultraviolet Astronomy: Four Years of IUE Research", ed. Y. Kondo, J.M. Mead, and R.D. Chapman, NASA CP-2238, p. 429.
Loreta, E. 1934, Astr. Nach *254*, 151.
O'Keefe, J. 1939, Ap.J *90*, 294.
Payne-Gaposchkin, C. 1963, Ap.J. *138*, 320.
Sonneborn, G., and Garhart, M.P. 1983, NASA IUE Newsletter No. 23, p.23.
Wu, C.-C., et al. 1983, NASA IUE Newsletter No. 22, p. 1.

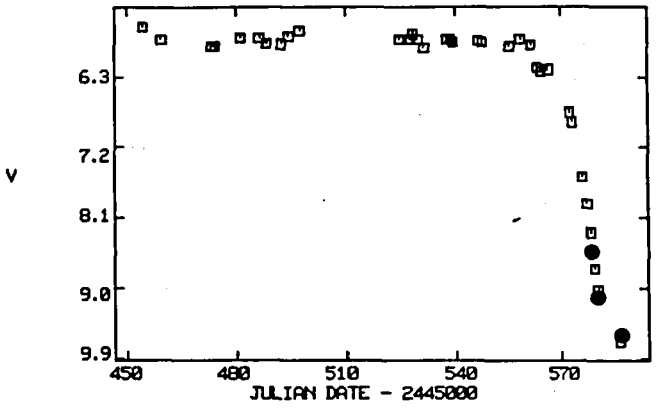

Figure 1 – Visual light curve of R CrB from Böhme (squares) and from the IUE's FES using (B–V)=+0.6 in the color term (filled circles).

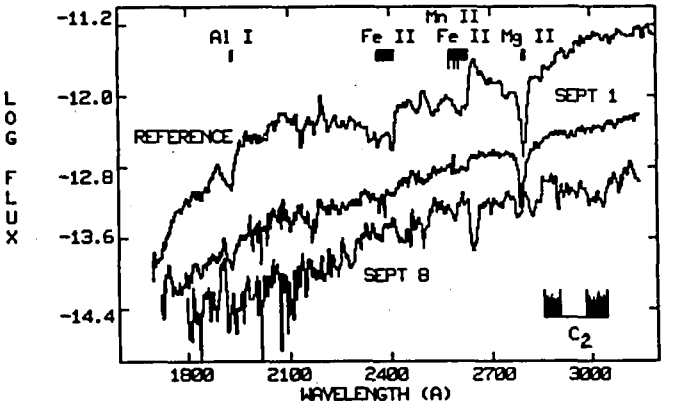

Figure 2 – R CrB spectra during the descent to minimum (Sept 1 and Sept 8) and at maximum. The wavelengths of strong atomic absorption features are indicated above the spectra; those of the Fox–Herzberg (0–3) and (0–4) bands of C_2 are indicated below the spectra.

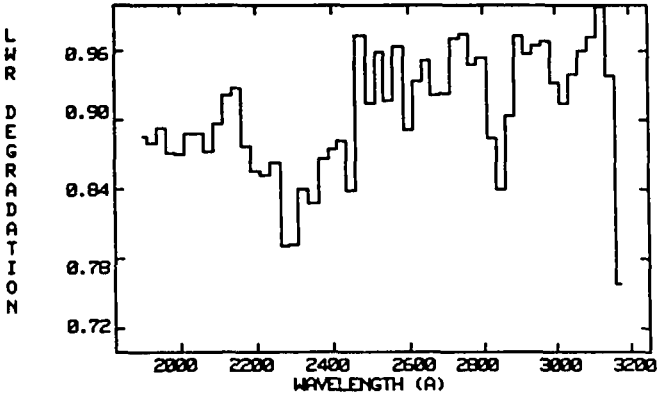

Figure 3 – The LWR camera's sensitivity degradation between Dec 1978 and Aug 1983 as derived from observations of standard stars.

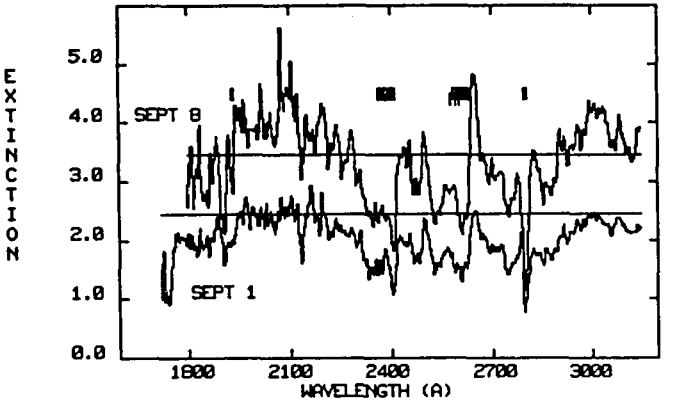

Figure 4 – The extinction derived from the spectra of Sept 1 and Sept 8 relative to the reference spectrum; the horizontal lines represent the visual extinction. Wavelengths of the strong absorption features in the reference spectrum are indicated above the curves.

OBSERVATIONS OF RR LYRAE AND X ARIETIS WITH THE IUE SATELLITE

J. T. Bonnell
Astronomy Program, University of Maryland

R. A. Bell
Division of Astronomical Sciences, NSF

ABSTRACT

Seven low-dispersion spectra of RR Lyr and 11 of X Ari were obtained with the LWR camera of IUE. RR Lyr was also observed in the low-dispersion mode with the SWP camera (9 spectra) and in the high-dispersion mode with the LWR camera (3 spectra). The observed fluxes have been compared with fluxes calculated using synthetic spectra and angular diameters determined by Manduca et al. (1981) from photometry at longer wavelengths. The observed fluxes for RR Lyr were found to be significantly fainter than the computed ones. RR Lyr was also found to be 0.4 magnitudes fainter at 2200A and 2500A during minimum light than it was during previous ultraviolet observations with the ANS satellite. It is suggested that both these differences are due to the star's secondary cycle (the Blazhko effect). One of the high-dispersion exposures made near maximum light was deep enough to reveal the cores of the Mg II h and k lines. No emission was observed and a strong interstellar absorption component was present. Emission features were also generally absent from the SWP spectra. An excellent agreement between observed and calculated fluxes was found for X Ari for which no Blazhko effect has been observed.

INTRODUCTION

The accurate determination of absolute magnitudes of RR Lyrae stars is important in the matter of establishing the astronomical distance scale. Recent work in this field has exploited the dependence of stellar surface brightness and color index on effective temperature (e.g. Barnes and Evans, 1976) to determine stellar angular diameters. Manduca et al. (1981) have used model atmospheres and synthetic spectra to interpret VR photometry of RR Lyr and X Ari and derive their angular diameters. The angular diameter curves combined with relevant radial velocity curves allow the derivation of the radius and absolute magnitude at any phase.

IUE observations of these stars are an important independent test of the angular diameters derived from photometry at longer wavelengths.

OBSERVATIONS AND CALCULATIONS

The observations were made from January 25 through 28, 1980 and cover essentially one primary pulsation cycle for both stars. The high dispersion spectra of RR Lyr were taken near maximum light. Fluxes were derived from the

low dispersion observations made with the large aperture based on the May 1980 calibration (Bohlin and Holm). These fluxes were then averaged within 50A bins and combined with a phase computed for midexposure to produce the observed light curves. Bad data points were eliminated from the averages. To allow a convenient comparison of the calculated and observed light curves, phase zero was taken to be maximum light.

The model atmospheres were taken from Manduca et al. with supplementary models constructed using the computer program MARCS (Gustafsson et al., 1975). Surface fluxes for the models were computed using the SSG program (Bell and Gustafsson, 1978) and averaged within the relevant bins. A metal abundance parameter, [A/H], of -1.0(-2.0) was used for RR Lyr(X Ari). The resulting fluxes were reddened using the average ultraviolet extinction curve of Savage and Mathis (1979) and E(B-V) = 0.016(0.153) for RR Lyr(X Ari) following Manduca et al. These fluxes were then combined with the derived angular diameters to generate the calculated light curves. Examples of the light curves are illustrated in the figures, the solid lines represent the calculated curves and the open circles the observed fluxes.

DISCUSSION

The computed fluxes for RR Lyr are significantly brighter than the observed ones, being roughly 50% too bright during minimum light. In order to determine the relative contribution of errors in angular diameter to this difference, the observed fluxes for individual observations were ratioed to the observed flux in the bin centered at 2400A and compared to the calculated fluxes ratioed to the calculated flux at 2400A. The differences arising from this comparison are independent of the angular diameters. The calculated flux ratios were also found to be insensitive to the adopted surface gravities. The observed differences in the flux ratio comparison for RR Lyr suggest that errors in the assumed reddening, stellar temperatures and computed line blocking cannot totally account for the differences in the observed and calculated light curves. The observed IUE fluxes were also compared to observations of RR Lyr made with the ANS satellite reported by Bonnell et al. (1982) by appropriate binning of the IUE fluxes into the ANS bandpasses centered at 2200A and 2500A and the use of the relative calibrations (Bohlin et al., 1980). The IUE observations indicate that the star was 0.4 mag fainter at minimum light than during the ANS observations. The Manduca et al. angular diameters reproduce the ANS light curves significantly better than the IUE ones. These results indicate that these angular diameters were not relevant to the star during the IUE observations. This problem is most likely related to the star's secondary cycle (Blazhko effect). In the course of RR Lyr's secondary cycle the V magnitude is known to vary by at least 0.2 mag at minimum light (Preston et al., 1965).

During maximum light LWR high dispersion observations of RR Lyr were attempted. An exposure time of 1.25 hours in the large aperture was necessary to record the cores of the Mg II h and k lines. No emission was detected and strong interstellar absorption features were present. In addition, the line profiles appear to be asymmetric when compared to synthetic ones computed

assuming a constant photospheric velocity. During the exposure it is estimated that the stellar temperature changed by 400K and the photospheric velocity varied between +20 and -25 km/sec relative to the center of mass, making the interpretation of the profile uncertain. An inspection of the low dispersion observations for emission features indicates that they are generally absent, with the possible exception of two weak emission peaks corresponding to the Al III resonance lines at 1854A and 1862A which are visible in an SWP observation made at phase 0.38 corresponding to a T_{eff}/log(g) of 6200/2.5.

Uncertainties in the analysis of X Ari are greatly reduced by the absence of an observed Blazhko effect, and the observed and calculated light curves agree well. The observed fluxes usually match the calculated curves to within 10% at minimum and maximum light. Only small systematic differences are apparent in the sense that the calculated fluxes are slightly higher than the observed fluxes at minimum light in the longer wavelength light curves. The observed and calculated flux ratios also agree well between 1900A and 3000A. This indicates that the angular diameters used are accurate and confirms the results obtained by Manduca et al.

CONCLUSION

The ability of the model atmospheres and synthetic spectra to match ultraviolet observations of these stars indicates that the parameters of these stars derived by Manduca et al. from the interpretation of VR photometry using spectrum synthesis techniques are valid. Difficulties encountered in the analysis of the IUE observations of RR Lyr are believed to be due to the star's secondary cycle.

REFERENCES

Barnes, T.G., and Evans, D.S. 1976, M.N.R.A.S., 174, 489.

Bell, R.A., and Gustafsson, B. 1978, Astr. and Ap. Suppl., 34, 229.

Bohlin, R.C., and Holm, A.V. 1980, IUE Newsletter No. 10, 37.

Bohlin, R.C., Holm, A.V., Savage, B.D., Snijders, M.A.J., and Sparks, W.M. 1980, Astr. and Ap., 85, 1.

Bonnel, J., Wu, C.-C., Bell, R.A., and Hutchinson, J.L. 1982, Pub. A.S.P., 94, 910.

Gustafsson, B., Bell, R.A., Eriksson, K., and Nordlund, A. 1975, Astr. and Ap., 42, 407.

Manduca, A., Bell, R.A., Barnes, T.G., Moffett, T.J., and Evans, D.S. 1981, Ap. J., 250, 312.

Preston, G.W., Smak, J., and Paczynski, B. 1965, Ap. J. Suppl., 12, 99.

Savage, B.D., and Mathis, J.S. 1979, Ann. Rev. Astr. and Ap., 17, 73.

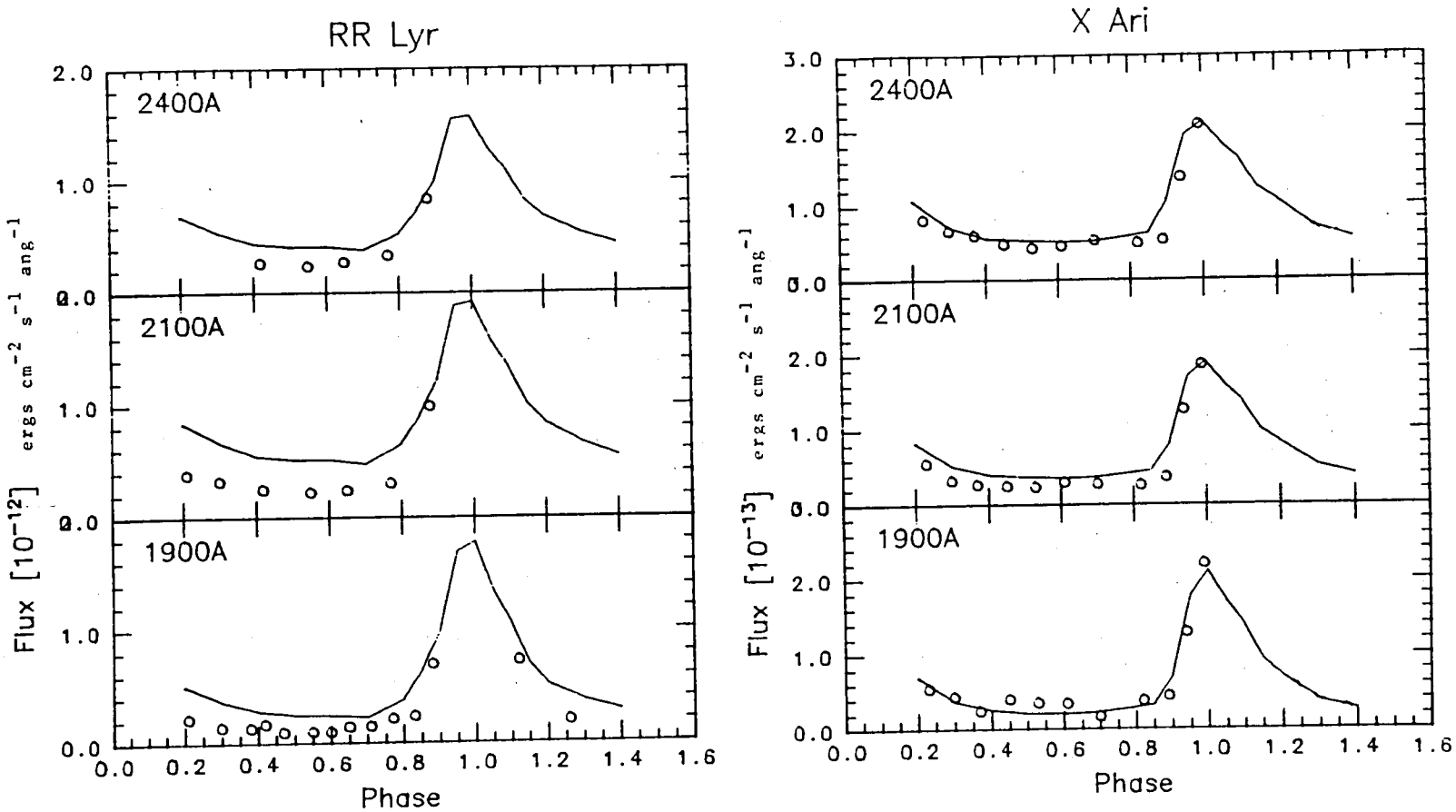
RR Lyr
2400A
2100A
1900A
Flux [10^-12] ergs cm^-2 s^-1 ang^-1
Phase
X Ari
2400A
2100A
1900A
Flux [10^-13] ergs cm^-2 s^-1 ang^-1
Phase

ATMOSPHERIC PROPERTIES OF RU LUPI DERIVED FROM HIGH- AND LOW-RESOLUTION IUE SPECTRA

A. Brown,[1] M. V. Penston,[2] R. Johnstone,[2] C. Jordan,[3]
N. P. M. Kuin,[3] M.T.V.T. Lago,[4] B. Gross[1] and J. L. Linsky[1,5]

[1]JILA, Univ. of Colorado and National Bureau of Standards, Boulder, CO 80309.
[2]Royal Greenwich Observatory, Hailsham, East Sussex, UK.
[3]Department of Theoretical Physics, University of Oxford, UK.
[4]Grupo de Matematica Applicada, Porto, Portugal.
[5]Staff Member, Quantum Physics Division, National Bureau of Standards.

ABSTRACT

High- and low-dispersion IUE spectra of the pre-main sequence star, RU Lupi, have been obtained using both the SWP and LWR cameras. Strong P Cygni line profiles are seen in Mg II and Fe II emission lines, indicating that the lines are formed in the stellar wind of RU Lupi. An increase in transition region line widths is seen with increasing temperature, which cannot be due solely to opacity broadening, thus indicating that kinematic broadening mechanisms (e.g. flows and turbulence) are dominant. The transition region density is $\sim 3 \times 10^{10}$ cm^{-3} derived from the Si III λ1892/C III λ1909 line ratio. The status of our atmospheric modeling of RU Lupi is discussed.

INTRODUCTION

The T Tauri stars are pre-main sequence (PMS) objects which show many chromospheric phenomena in their most extreme form. IUE has allowed the study of a number (~30) of these stars at low dispersion but high dispersion spectra have proved difficult to obtain even for the Mg II resonance lines, which generally need several hours of exposure time. RU Lupi shows the strongest observed chromospheric and transition region (TR) emission lines of all PMS stars and we have therefore studied this star extensively at high and low dispersion with IUE.

RU Lupi is among the most extreme of the T Tauri stars in that emission from its expanding atmosphere dominates its photospheric radiation in both the UV and optical spectral regions. Lago (1982) has constructed an atmospheric model for RU Lupi based on its optical spectrum and Penston and Lago (1982) have discussed earlier IUE observations of this star.

IUE OBSERVATIONS

We have obtained spectra of RU Lupi during the period 1983 April 15-16. These spectra include both high dispersion (SWP 19736, 755 min; LWR 15755, 416 min; LWR 15746, 40 min) and low dispersion (SWP 19739, 120 min; LWR 15745, 25 min; LWR 15754, 8 min) exposures. These data have been combined with earlier spectra, particularly the high-dispersion image SWP 14980 (316 min), in order to investigate the UV spectral properties of RU Lupi.

The low-dispersion SWP spectrum of RU Lupi is shown in Fig. 1 and the observed line fluxes derived from this spectrum, $F_{\oplus}$, are given in Table 1. The flux, F_{corr}, corrected for interstellar absorption (A_V = 0.6 mag; Cohen and Kuhi 1979), using the mean interstellar extinction curve of Savage and Mathis (1979) is also given. Profiles of the stronger SWP emission lines are shown in Fig. 2. These profiles are obtained from the addition of images 19736 and 14980 weighted by the relative exposure times. It seems likely that the line fluxes in the later exposure were somewhat lower. Line widths (FWHM) were derived for several lines and are given in Table 1. Figure 3 shows the LWR spectral region containing the UV1 multiplet of Fe II.

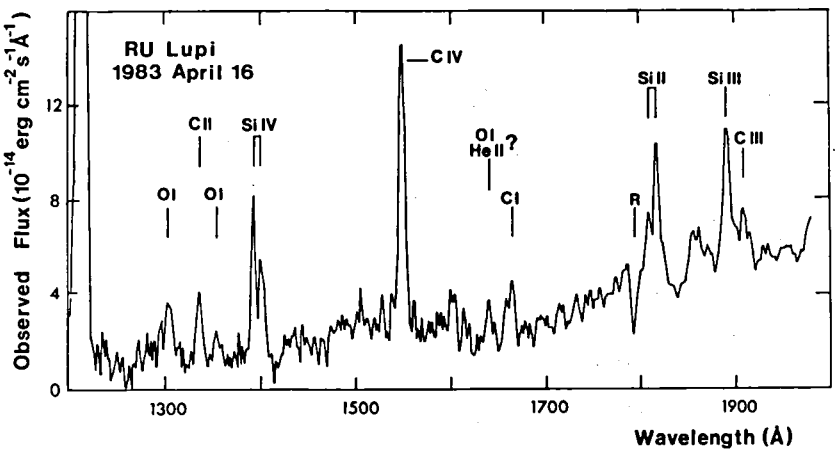

Fig. 1. The low dispersion spectrum (SWP 19739) of RU Lupi. The more prominent emission lines are identified. The line near 1660 Å, identified as C I, includes a significant flux from the O III intersystem lines at 1661 and 1666 Å. Reseaux are marked by 'R.'

Table 1: RU Lupi Emission Line Fluxes and Widths

Ion	λ (Å)	$F_{\oplus}$ (10^{-13} ergs cm^{-2} s^{-1})	F_{corr} (10^{-12} ergs cm^{-2} s^{-1})	Δλ (Å)
N V	1240	≤0.5	≤0.3	
S I	1296	0.9	0.5	
O I	1304	2.2	1.2	
C II	1335	2.0	1.0	
O I	1356	1.1	0.6	
Si IV+O IV	1397	6.3	3.0	0.95 (λ1394)
Si II	1529	≤6.1	≤0.4	
C IV	1549	9.5	4.2	1.05 (λ1548)
He II, O I	1640	1.2	0.5	
C I	1657	1.2	0.5	
O III	1663	1.9	0.8	
Si II	1814	5.8	2.4	0.76 (λ1808)
Aℓ III	1858	2.2	0.9	
Si III	1892	4.7	2.0	0.99
S I	1900	1.1	0.5	
C III	1909	1.4	0.6	
S I	1915	0.7	0.3	
C II	2325	7.5	3.8	
Aℓ II	2670	6.3	2.1	
Mg II	2800	≥69	22	

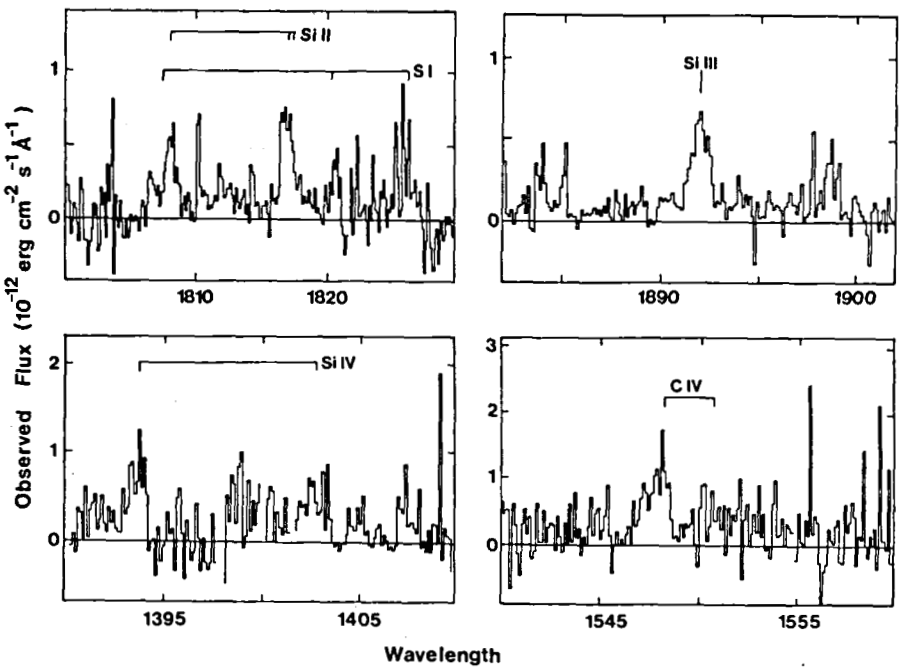

Fig. 2. High dispersion line profiles obtained from the summation of two SWP images of RU Lupi. Bright noise spots were removed from SWP 14980 by reprocessing the image with a median filter set with a suitable threshold. The expected positions of certain emission lines are indicated.

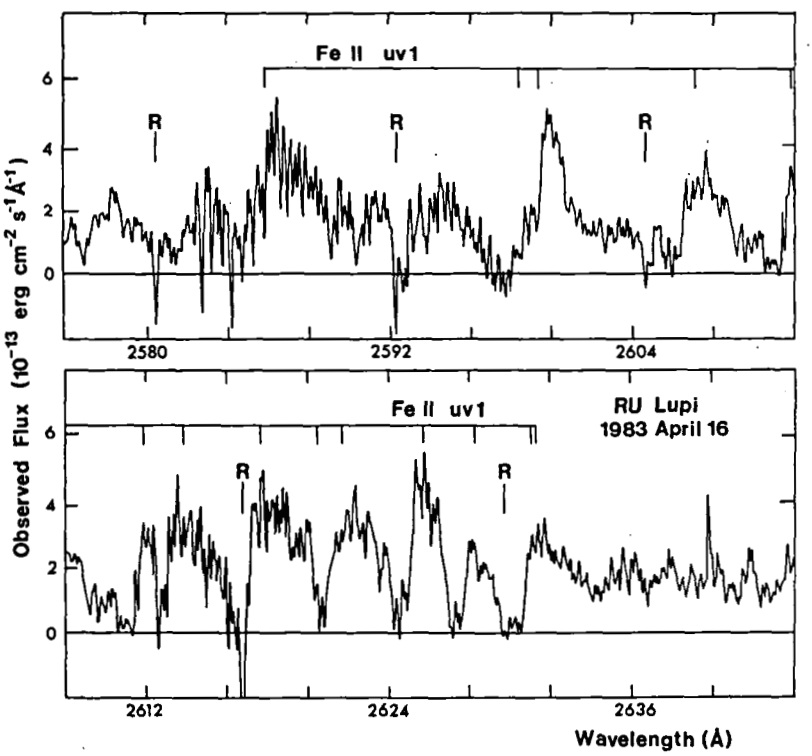

Fig. 3. High dispersion spectrum of the region containing the Fe II UV1 multiplet. The positions of the members of the UV1 multiplet are shown and clearly the lines show classical P Cygni profiles. The spectrum has been smoothed with a 3 point running mean. R denotes reseaux marks.

RESULTS PERTAINING TO THE ATMOSPHERIC PROPERTIES OF RU LUPI

The results derived from our preliminary analysis of these data are:

1. The Fe II UV1 and Mg II resonance lines show strong classical P Cygni line profiles formed in the stellar wind of RU Lupi. While such profiles are generally seen in the Mg II lines of T Tauri stars, strong P Cygni profiles in Fe II have not been seen before. These Fe II profiles are more extreme than the asymmetries seen in the lines of evolved cool giants and supergiants. We intend to model these profiles using co-moving frame radiative transfer techniques, which incorporate velocity fields, a chromospheric rise and PRD effects.

2. The observed line widths imply an increase in line broadening with temperature (i.e. the FWHM are ~125 km s^{-1} for Si II λ1808; ~155 km s^{-1} for Si III λ1892, and ~200 km s^{-1} for Si IV λ1394 and C IV λ1548). While some opacity broadening may be present in the resonance lines, this cannot be the case for the optically-thin Si III line. Kinematic effects, such as flows and turbulence, appear to be the dominant broadening mechanisms.

3. Assuming solar abundances, the Si III λ1892/C III λ1909 ratio of 3.3 indicates that the TR pressure at $\sim 6 \times 10^4$ K is $\sim 2 \times 10^{15}$ cm^{-3} K, equivalent to a local electron density of $\sim 3 \times 10^{10}$ cm^{-3}. The calibration of this line ratio used is that of Jordan (1983, private communication), which includes improved atomic data for Si III as compared to that of Doschek et al. (1978).

4. The emission measure distribution of chromospheric and TR plasma can be derived from the data in Table 1. We intend to calculate models of the temperature and density structure of RU Lupi using emission measure analysis (see, for instance, Brown, Ferraz and Jordan 1984). Since both the upper limit to the N V emission measure ($T_e \sim 2 \times 10^5$ K) is low and the Einstein X-ray upper limit (Gahm 1981) implies an even lower coronal ($T_e \sim 10^6$ K) emission measure, it seems that very little coronal plasma is present in the atmosphere of RU Lupi (Brown and Jordan 1983; Imhoff and Giampapa 1982).

Since emission from the stellar wind of RU Lupi dominates photospheric radiation in the UV and optical spectral regions, the combination of emission measure analysis, co-moving frame PRD calculations and previous optical studies should allow the consistent modeling of the atmosphere of RU Lupi.

REFERENCES

Brown, A., Ferraz, M. C. de M. and Jordan, C. 1984, M.N.R.A.S., in press.

Brown, A. and Jordan, C. 1983, IAU Colloq. No. 71, Activity in Red Dwarf Stars, Catania, August 1982, D. Reidel, p. 61.

Cohen, M. and Kuhi, L. V. 1979, Astrophys. J. Suppl., 41, 743.

Doschek, G. A. et al. 1978, Astrophys. J. (Letters), 226, L35.

Gahm, G. 1981, Astrophys. J. (Letters), 242, L163.

Imhoff, C. L. and Giampapa, M. S. 1982, in Proc. Symp. "Advances in Ultraviolet Astronomy: Four Years of IUE Research," NASA-CP 2238, p. 456.

Lago, M.T.V.T. 1982, M.N.R.A.S., 198, 445.

Penston, M. V. and Lago, M.T.V.T. 1982, in Proc. Symp. Third European IUE Conference, Madrid, p. 95.

Savage, B. D. and Mathis, J. S. 1979, Ann. Rev. Astr. Ap., 17, 73.

Mg II EMISSION OF POP. II LONG-PERIOD CEPHEIDS

M. Parthasarathy
Indian Institute of Astrophysics, Bangalore

and
Sidney B. Parsons
Astronomy Programs, Computer Sciences Corporation

ABSTRACT

The Population II Cepheid pulsational variables AL Vir (P = 10.3 days) and W Vir (P = 17.3 days) were observed with IUE at two phases each. Only low-dispersion mid-UV exposures were feasible, but were sufficient to show a great range in Mg II emission behavior. The relationship to phase variation of emission in classical (Pop. I) Cepheids of long period is unclear.

RESULTS

W Vir showed Mg II 2800 emission well in excess of the local continuum at both times (JD 2445561.65 and 2445755.18). The FES magnitudes at these two times were 10.0 and a faint 10.7. This means that the second observation was taken near minimum light. The actual phase values are in doubt, pending investigation of recent ground-based data, since the period and form of light curve are known to vary. If we adopt the elements 2436576.687 + 17.2736 E from the Second Supplement to the Third Edition of the General Catalogue of Variable Stars, the provisional phases are 0.16 and 0.36, respectively.

AL Vir showed only photospheric absorption in Mg II at both times (JD 2445561.75 and 2445755.11). FES magnitudes were 9.5 and 10.1, and provisional phases from 2437823.45 + 10.30256 E are 0.10 and 0.87. The spectrum resembles early F-type luminous stars with their pronounced Fe II absorption features.

DISCUSSION

Schmidt and Parsons (1982, 1984) found that among classical Cepheids with periods near 10 days, Mg II emission strength builds rapidly at the time of maximum outward acceleration of the photosphere, around phase 0.7--

0.8. This emission subsequently fades toward much smaller but still detectable levels at minimum light. In this framework, the observations of both Pop. II Cepheids are surprising.

If similar mechanisms of shock heating and radiational cooling operate in both population types with similar efficiencies, then AL Vir should have had detectable emission, and the enormous emission in W Vir is unexpected. There is a trend among Pop. I Cepheids for greater overall emission strength at longer periods; the current sample of two stars would give a much steeper slope to such a trend. There are too many variables, however, including differences in light curve shape (i.e. pulsation dynamics), to be able to conclude at present whether the abundance differences between Pop. I and Pop. II have a direct affect on the nature of Cepheid chromospheres.

REFERENCES

Schmidt, E.G., and Parsons, S.B. 1982, Ap.J. Suppl., 48, 185.

Schmidt, E.G., and Parsons, S.B. 1984, Ap.J., 279, ___. (April 1)

BLUE COMPANIONS OF CEPHEIDS

Erika Böhm-Vitense and Charles Proffitt
University of Washington, Seattle

ABSTRACT

Nineteen Cepheids, known or suspected to have blue companions, have been observed. For 11 of them, blue companions were indeed seen, though many of them were fainter in the UV than suspected. For four Population I Cepheids the suspected companions were not seen. For none of the Population II Cepheids could a companion be detected.

For the observed companions we have determined T_{eff}, luminosities and masses from their position in the HR diagram.

INTRODUCTION

The masses of Cepheids have been a long debated subject (see Cox 1980 for a review). While originally pulsational masses were about 30-40% lower than evolutionary masses, larger distances and smaller T_{eff} for the observed Cepheids have reduced this discrepancy, at least for Cepheids with periods <12 days. For Cepheids showing beat phenomena in their amplitudes, indicating the excitation of two modes, the masses derived from the ratio of the periods are still a factor of two to three smaller than the masses derived from other methods.

As Hofmeister (1967) and Becker, Iben and Tuggle (1981) pointed out, there appears to be a surplus of Cepheids with long periods in comparison with the birth rates of massive stars. This problem would be eased if a large fraction of long period Cepheids have actually smaller masses than presently thought. For Cepheids with periods longer than 10^d, Burki (1983) finds Wesselink masses lower by about 15 to 20% than those found from evolutionary tracks.

Because of these discrepancies between different mass determinations it would be of great help to have dynamical mass determinations for a few Cepheids with different pulsational periods.

Suitable binaries should be identified. As Cepheids have visual magnitudes much brighter than their main sequence counterparts, any companion with a mass less than that of the Cepheid is expected to be much fainter but much bluer than the Cepheid unless it has a much smaller mass than the Cepheid, in which case it will be very hard to detect.

For a large number of Cepheids, Madore (1977) observed their paths in the two-color diagram during their pulsational cycle. For several of them open loops in the two-color diagram were found, which he attributed to the presence of a blue companion.

We have observed many of the suspected binaries in addition to Cepheids whose radial velocities indicated an orbital velocity superimposed on the pulsational velocity curves (Lloyd Evans 1982, Jacobsen 1974). Companions for T Mon and η Aql were observed by Mariska, Doschek and Feldman (1980a and 1980b), who determined temperatures of about 10000 and 9500K for the companions.

THE OBSERVATIONS

Table 1 gives the list of stars which have been observed by us and by other IUE guest observers. The observed energy distributions were corrected for interstellar reddening with the E(B-V) given by Dean, Warren and Cousins (1978) and with the average galactic extinction curves as given by Seaton (1979). The distances are obtained from the period, color, luminosity relation for the Cepheids. We used the relation given by Sandage and Tammann (1969). Assuming that the companions are main sequence stars, we can determine the surface flux $F_\lambda\ (T_{eff})$ for any given wavelength λ, for instance, from Kurucz's 1979 tables. For main sequence stars we also know the radius $R\ (T_{eff})$. We can therefore use the equation

$$f_\lambda \cdot d^2 = F_\lambda\ (T_{eff}) \cdot R^2\ (T_{eff})$$

to determine T_{eff}. Here, f_λ is the observed flux at wavelength λ. We used the wavelengths 1950 A and 1550 A. For 1950 A the Cepheid itself sometimes contributes a small fraction to the observed flux. We therefore obtain an upper limit to the T_{eff} from this λ.

In order to check whether our assumption that the companions are main sequence stars is correct, we compare the observed, reddening corrected, energy distributions with model energy distributions as given by Kurucz (1979). For most of the companions we find good agreement (see Figure 1), except for the RW Cam, SV Per and RY Nor companions, for which we find rather large discrepancies, as discussed by Böhm-Vitense and S. Borutzki (1983). It is interesting to note that these are all Cepheids with periods longer than 10 days.

For the main sequence companions we can use their T_{eff} to determine their masses. The results are shown in Figure 2, where we have plotted the relation between evolutionary and pulsational masses and the lengths of the periods, and also the masses for the companions of the Cepheids studied here.

For the stars with nearly equal masses, the companion is relatively bright and hot in comparison with the Cepheid. We therefore have a very good chance to observe the companion with high resolution and determine the radial velocities. Studies for SU Cyg and S Mus are underway by N. Evans, by us, and by Eichendorf. It appears that KN Cen would also be a good candidate and optical studies should be undertaken to determine the orbital periods and orbital velocities for this Cepheid. Once the orbital velocities of the Cepheids are known in principle, one velocity ratio will

then determine the mass ratio of the two stars.

Studies of the radial velocities of the W Sgr, V636 Sco, and U Aql companions are also underway. It is hoped that in the near future we will finally be able to determine dynamical masses for the Cepheids.

REFERENCES

Becker, S.A., Iben, I. and Tuggle, K.S. 1977, Ap.J. 218, 633.
Böhm-Vitense, E., Borutzki, S. and Harris, H. 1983, Proceedings of IAU Colloquium 105, Geneva.
Burki, G. 1983, preprint.
Cox, A.N. 1980, Ann. Rev. Astron. Astrophys. 18, 15.
Dean, C.A., Warren, W.H. and Cousins, A.W.J. 1978, MNRAS 183, 569.
Eichendorf, W. 1982, private communication.
Evans, N. 1982, private communication.
Hofmeister, E. 1967, Z.f. Astrophys. 65, 194.
Jacobsen, T.S. 1974, Ap.J. 191, 691.
Kurucz, K. 1979, Ap.J. Suppl. 40, 1.
Lloyd Evans, T. 1982, MNRAS 199, 925.
Madore, B.F. 1977, MNRAS 178, 505.
Mariska, J.T., Doschek, G.A. and Feldman, U. 1980a, Ap.J. Letters 238, L87.
Mariska, J.T., Doschek, G.A. and Feldman, U. 1980b, Ap.J. 242, 1083.
Sandage, A.R. and Tammann, G. 1969, Ap.J. 157, 683.
Seaton, M.J. 1979, MNRAS 187, 73.

Table 1
Properties of Cepheids with Main Sequence Companions

Star	$\langle m_V \rangle$	$\langle B \rangle - \langle V \rangle$	E(B-V)	P[d]	M_V	d[pc]	T_{eff} [1] comp.	M/M_o [1] comp.
SU Cyg	6.9	0.64	0.12	3.85	-3.14	830	12000±100	4.8±.2
V636 Sco	6.6	0.92	0.22	6.80	-3.54	780	9400±100	2.9±.2
U Aql	6.5	1.04	0.36	7.02	-3.66	620	9300±100	2.8±.2
η Aql	3.9	0.80	0.14	7.18	-3.73	270	9500±100	2.5±.2
W Sgr	4.7	0.75	0.13	7.60	-3.91	430	9400±100	2.9±.2
S Mus	6.1	0.82	0.27	9.66	-4.43	870	17300±400	7.3±.2
T Mon	6.1	1.20	0.18	27.02	-4.79	1150	10000±200	3.8±.2
KN Cen	9.8	1.57	0.9 ?	34.01	-6.02	3870	26000±2000	13 ±1 (?)

1. The uncertainty limits given ignore the uncertainty in the reddening corrections.

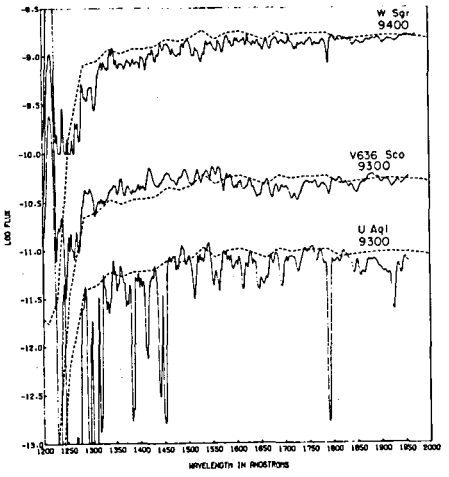

Figure 1. The observed reddening corrected energy distributions for the companions of W Sgr, V636 Sco and U Aql are compared with model energy distributions for log g = 4 and the temperatures given, as interpolated from the model energy distribution given by Kurucz 1979.

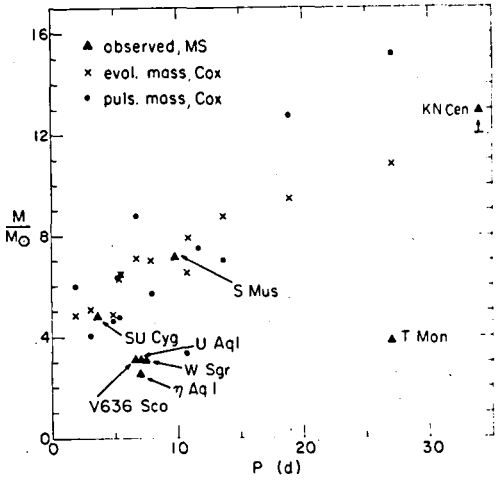

Figure 2. Evolutionary and pulsational masses of Cepheids are shown as a function of their pulsational periods for the stars studied by Cox 1980. Also shown are the masses for the main sequence companions of the Cepheids studied here.

ULTRAVIOLET OBSERVATIONS OF POPULATION II CEPHEIDS

Erika Böhm-Vitense, Charles Proffitt and George Wallerstein
University of Washington, Seattle

ABSTRACT

The two Population II Cepheids, ST Pup and W Vir, have nearly the same length of period and B-V colors, yet spectral types are very different, indicating large differences in metal abundances. We have determined metal abundances, T_{eff} and the color excess from the observed discontinuities at 1700 A, at 2600 A, the ultraviolet to visual colors, and the 2400 A absorption band. The observations for ST Pup were made shortly after maximum light. For ST Pup we found E(B-V) = 0.2, T_{eff} = 6600 + 100K at 0.5 days after maximum. A metal abundance of [A/H] = -1.7 $\pm$ 0.2 was determined. For W Vir a metal abundance of [A/H] $\sim$-0.9 is suggested.

INTRODUCTION

The two Population II Cepheids, ST Pup and W Vir, have nearly the same periods: 18.44 days for ST Pup and 17.8 days for W Vir. Their B-V colors differ only slightly, but ST Pup has much weaker metallic lines. It is therefore suspected that ST Pup is much more metal deficient than W Vir. For W Vir, Abt (1954) used nearly solar metal abundances. Barker et al. (1971) determined [A/H] = -1.2 from spectrum analysis. Böhm-Vitense (1974) found agreement of the UBV color variations with phase assuming [A/H] = -1. We are not aware of any analysis of ST Pup.

As has been shown previously (Böhm-Vitense 1980), the discontinuity in the energy distribution at 1700 A observed for late A and F stars provides an excellent opportunity to determine [A/H], if T_{eff} is known, for instance, from ultraviolet to visual flux ratios after correction for interstellar extinction. Another temperature and metal abundance sensitive apparent discontinuity is observed at 2600 A. We have used these two discontinuities and the overall energy distribution to determine the atmospheric parameters of these two Population II Cepheids, together with a determination of the color excess. We will report here on the results.

THE OBSERVATIONS

We tried to observe both stars one-half to one day after maximum light, such that we might expect to have nearly optimum flux in the ultraviolet, yet have the atmosphere be close to equilibrium; i.e., that the outmoving shocks would not be of serious influence. At these phases the comparison with equlibrium model stellar atmospheres should be correct. For ST Pup V. Smith (1982) kindly made a new phase determination about one-half year before the observations. For W Vir we did not foresee any phase shifts, but it appeared that maximum light was delayed by two days. With one day separation between the two observations, we measured the same visual magnitude on both days, always close to maximum light. The observations of

W Vir met with the additional difficulty that the Earth gets in the way a few hours into the US1 shift. Therefore, uninterrupted long exposures are not possible on this side of the Atlantic. W Vir also appears to have a higher metal abundance than ST Pup and therefore has less flux in the UV, which makes the observations in the short wavelength range more difficult. Our observations are therefore best for ST Pup. We have two short wavelength low resolution exposures for ST Pup 1/2 day and 1-1/2 days after maximum light. We also have one long wavelength exposure one-half day after maximum light. For W Vir we have one short wavelength exposure and three long wavelength exposures at phases near maximum light. The second SWP exposure for ST Pup and the SWP exposure for W Vir were too weak to measure the 1700 A discontinuity with confidence.

SPECTRUM ANALYSIS

We used the flux ratios of the following wavelength pairs 3112:1892; V:1892; V:2712; 1892:1635 (1700 A discontinuity), 2712:2562 ("discontinuity" at 2600 A); and the broad absorption band at 2400 A. The flux ratios from the two wavelength pairs including the visual are less reliable than the other pairs because we only have FES measurements for the visual magnitudes which are uncertain by ± 0.2 magnitudes.

All the flux ratios depend on T_{eff}, log g, [A/H] and E(B-V). Log g is approximately known from M_V and $M/M_o \sim 0.5$. For the determination of the unknowns we have three independent flux ratios and the 2400 A absorption band.

For an assumed value of E(B-V) we get from each flux ratio and for the 2400 absorption band a relation between T_{eff} and [A/H] that will give the observed value. For the correct value of E(B-V) all these curves should intersect at one point. For an incorrect reddening correction or possibly an incorrect value for log g the measured flux rations are inconsistent and the different T_{eff} [A/H] curves derived from the different kinds of measurement do not intersect at one point. In Figure 1 we show the relations obtained for ST Pup for assumed values of E(B-V) = 0.15, 0.20 and 0.22. We used Seaton's average galactic extinction curve for the extinction correction. Model atmosphere energy distributions for log g =2 were used for the theoretical relations. This log g is somewhat larger than expected from M_V and $M/M_o \sim 0.5$, but seems to give better agreement than smaller values. Since we observed ST Pup shortly after maximum light, the higher pressure may not be surprising. The best agreement for the different relations is found for E(B-V) = 0.22, but for E(B-V) = 0.20 only the somewhat uncertain flux ratio of the visual to the 2712 A flux is in disagreement. From Figure 1 we conclude that the color excess is E(B-V) = 0.20 ± 0.02 and that [A/H] is -1.7 ± 0.15 for ST Pup. At the phase of this observation T_{eff} was $6600 + 100$°K. In his last study of the surrounding stars, Demers (1982) determined E(B-V) = 0.20 for ST Pup.

In Figure 2 we show the corresponding diagrams for our first set of observations of W Vir. For this star our results are somewhat disappointing because our short wavelength spectrum is underexposed and we cannot use the discontinuity at 1700 A. The absorption band at 2400 A is very weak and may be weakened by emission. For the expected gravity of log g = 1.3 we find one intersection only for E(B-V) $\simeq$ 0.20; see Figure 2. This is unreasonable in comparison with other determinations, which all give E(B-V) $\lesssim$ 0.10. For this E(B-V) we need log g =3.0 to get a 2400 A absorption band nearly as weak as observed. It appears that the 2400 A band is weakened by some unknown reason and that log g = 2 and E(B-V) = 0.10 are probably the best values. For these we find T_{eff} = 5900 $\pm$ 200 and [A/H] = -0.9 + 0.2, which is in agreement with earlier results (Barker et al. 1971, Böhm-Vitense 1974) for phase 0.9. We have to admit, however, that for lower log g values temperatures up to 300° higher and metal abundances higher by a factor of 2 may be obtained. We need longer exposure, short wavelength spectra in order to get more accurate results.

REFERENCES

Abt, H.A. 1954, Ap.J. Suppl. 1, 63.
Böhm-Vitense, E. 1980, Ap.J. 243, 213.
Barker, T. et al. 1971, Ap.J. 165, 67.
Böhm-Vitense, E. 1974, Ap.J. 188, 571.
Demers, S. 1982, private communication.
Smith, V. 1982, private communication.

FIGURE CAPTIONS

Figure 1: T_{eff} (log Z/Z_o) relations are shown as obtained from the flux ratios at different wavelengths measured for ST Pup for a phase 0.5 days after maximum light. The wavelength pairs used for the flux ratios are noted on the curves. Also used was the equivalent width of the absorption band at 2400 A. Figures, a, b, c were obtained assuming log g = 2 and different values of E(B-V), Figures d, e f were obtained assuming log g = 1.3. The best one point intersection is obtained for log g = 2 and E(B-V) = 0.22.

Figure 2: Similar to Figure 1, but for the flux ratios measured for W Vir, probably shortly before maximum light. The 2400 A absorption band is too weak. Perhaps an overlying emission, due to the outward moving shock, weakens this absorption band.

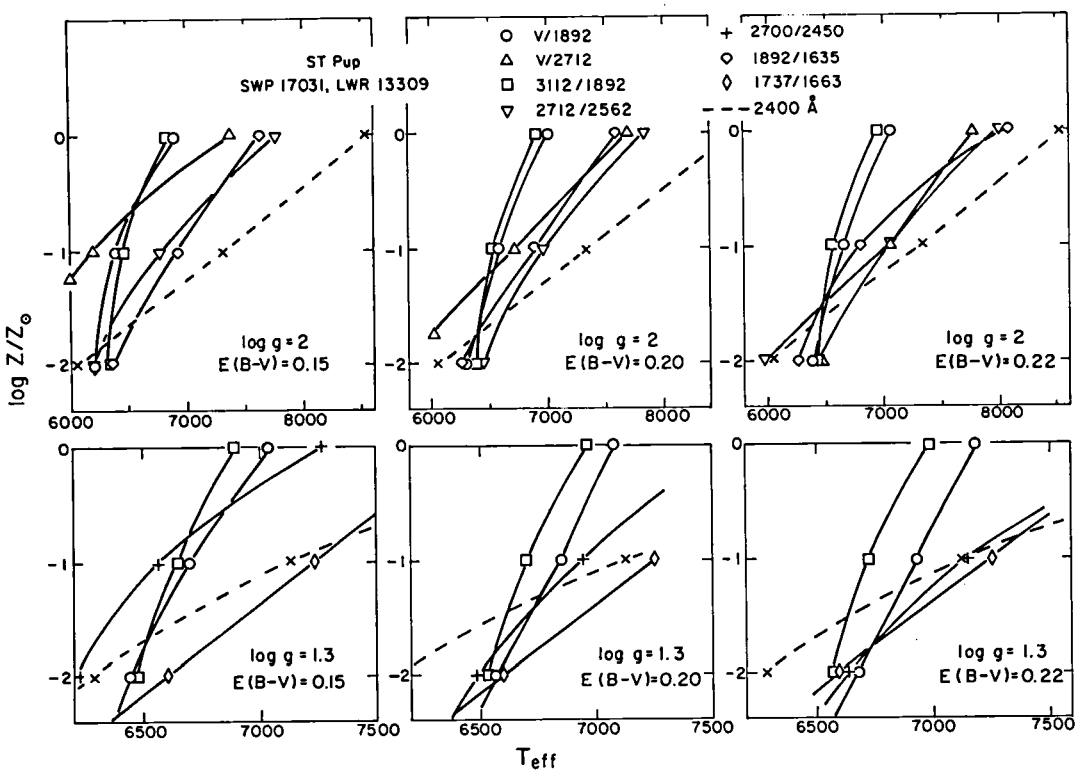
ST Pup
SWP 17031, LWR 13309
V/1892
V/2712
3112/1892
2712/2562
2700/2450
1892/1635
1737/1663
2400 Å
log g = 2
E(B-V) = 0.15
log g = 2
E(B-V) = 0.20
log g = 2
E(B-V) = 0.22
log g = 1.3
E(B-V) = 0.15
log g = 1.3
E(B-V) = 0.20
log g = 1.3
E(B-V) = 0.22
log Z/Z⊙
Teff

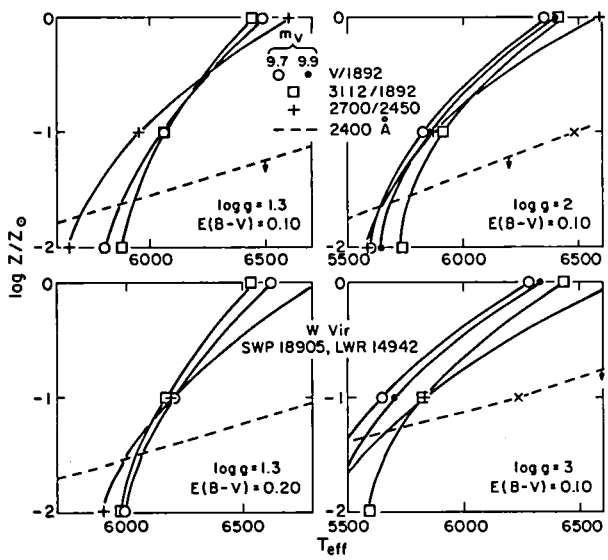
mv
9.7 9.9
V/1892
3112/1892
2700/2450
2400 Å
log g = 1.3
E(B-V) = 0.10
log g = 2
E(B-V) = 0.10
W Vir
SWP 18905, LWR 14942
log g = 1.3
E(B-V) = 0.20
log g = 3
E(B-V) = 0.10
log Z/Z⊙
Teff

ULTRAVIOLET ANALYSIS OF THE PECULIAR F SUPERGIANT HD 112374

Erika Böhm-Vitense and Charles Proffitt
University of Washington, Seattle

ABSTRACT

We have studied the ultraviolet energy distribution of the metal-poor supergiant HD 112347. We need a temperature T_{eff} = 5500+ 100K, log g = -0.3±0.3 and a metal deficiency of log $Z/Z_\odot$ = -0.7 in order to find agreement between theoretical and observed ultraviolet energy distributions with a reddening of E(B-V) $\leq$ 0.1, consistent with its galactic latitude of +36°.

INTRODUCTION

The star HD 112374 = HR 4912 is an F3Ia supergiant (Hoffleit and Jascheck 1982) at a galactic latitude of +36°. Arellano Ferro (1981) found it to be variable with an amplitude of ΔM_B = 0.32 and a period of either 43.96, 53.33 or 67.8 days. The scatter is smallest for P = 43.96 days. These authors call the star a Cepheid-like supergiant. Luck, Lambert and Bond, 1983, recently analyzed the star and found it to be metal-poor. They obtained [A/H] = -1.2 in the average, but the light elements are less depleted than Fe. From the excitation and ionization, the authors found T_{eff} = 6000 to 5700K and log g = 0.4 to 0.8. E(B-V) was then found to be 0.25, which is surprising because of the large galactic latitude. The authors suspected circumstellar absorption.

This star appears to be rather similar to W Vir, the prototype Pop. II Cepheid, whose period is, however, only 17.8 days. Circumstellar extinction for such a star would therefore be very interesting, suggesting mass loss for Population II Cepheids. The average metal deficiencies of the two stars appear to be very similar. Barker et al. (1971) find [A/H] = -1, but less for s process elements in W Vir.

We therefore wanted to observe this star as a "Standard" star to test our methods of UV analysis of the Population II Cepheids. Since we observed the Cepheids at $m_V \sim 9.8$, we expected it to be easy to observe this star with m_V = 6.6. Our IUE observations revealed, however, immediately that the UV intensities for this star are relatively much lower than for W Vir around maximum light. The temperature must be lower or Z higher or the UV extinction much larger than for W Vir at maximum or log g much lower. In the following we will describe our observations and analysis.

THE OBSERVATIONS

On June 15, 1983 we took a short wavelength low resolution spectrum with 40 min exposure time which showed nothing. We then took two LWR low resolution exposures with 6 and 25 min exposure time; the latter was overexposed for $\lambda >$ 2600 A. At 2400 A the flux was still too small and noisy

to measure the 2400 A absorption feature with confidence. Figure 1 shows the spectrum for the LWR region.

THE ANALYSIS

Since the short wavelength spectrum could not be observed nor could the 2400 A absorption feature, our analysis could make use only of the 2600 A discontinuity and of the continuum energy distributions. We used the flux ratios of the wavelengths 2662 A and 2537 A to describe the discontinuity at 2600 A. This is the best known quantity. We also used the B-V colors and the V: (2662 A) colors. For B-V we used the value given by Luck et al. (1983) and a visual magnitude of $6^m.6$, presumably the average visual magnitude, since we do not know the exact values at the time of our observations. Apparently, the B-V colors do not vary much. Our visual magnitude could be wrong by 0.20, which means our visual flux might be wrong by $\Delta \log f_v = \pm 0.08$.

Our calibration plot for the visual to 2662 A flux ratio is shown in Figure 2. Also indicated is the observed flux ratio for different assumed values of E(B-V). From the B-V color we obtain for each assumed E(B-V) a $(B-V)_o$ and a relation between T_{eff} and [A/H] which will give the $(B-V)_o$, which is slightly dependent on the luminosity. These relations are shown in Figure 3. The observed discontinuity at 2600 A requires another relation between T_{eff} and $\log Z/Z_\odot$. See Figure 3. For each E(B-V) we find one intersection with this curve. For each value of E(B-V) we therefore obtain a pair T_{eff}, [A/H] as a possible solution. We can interpolate the V/2662 A flux ratio as a function of log g for these pairs of T_{eff} and [A/H] as shown in Figure 2. We now have to fit the measured points on one of these curves depending on E(B-V). The intersections give very low values for $\log g \approx -0.3$, which is, however, not inconsistent with the very long period and luminosity of this variable, though it is smaller than the value found by Luck et al. For E(B-V) = 0.25 we would find a rather large T_{eff} and small $\log Z/Z_\odot$ which would be inconsistent with the instability strip. Making use of the fact that we expect $E(B-V) \lesssim 0.1$ from the galactic latitude of the star, we find $\log Z/Z_\odot = -0.7$ with $T_{eff} = 5600K$. It seems we observed the star at a lower temperature and gravity than Luck et al., though this value of T_{eff} is at the lower error limit given by them. The metal deficiency found here corresponds to the deficiency found by Luck et al. for the light elements. Since it follows mainly from the discontinuity at 2600 A, it measures the abundance of the elements responsible for this discontinuity, which is probably mainly MgI, though strong Fe lines are superimposed in the region $2550 < \lambda < 2650$ A.

REFERENCES

Arellano Ferro, A. 1981, PASP 93, 351.
Barker, T., et al. 1971, Ap.J. 165, 67.
Hoffleit, D. and Jaschek, C. 1982, Catalogue of Bright Stars, 4th ed., New Haven, Yale University Observatory
Luck, R.E., Lambert, D.L. and Bond, H.E. 1983, PASP 95, 413.

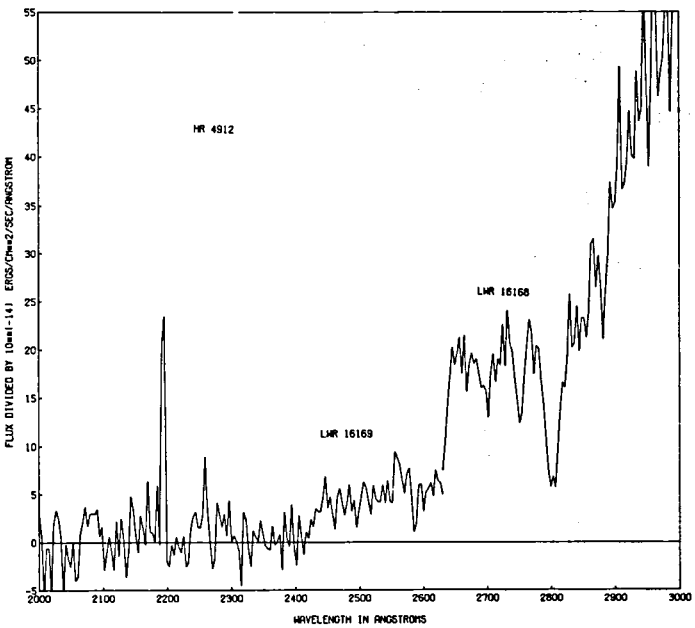

Figure 1. The long wavelength range low resolution spectrum of HD 112374.

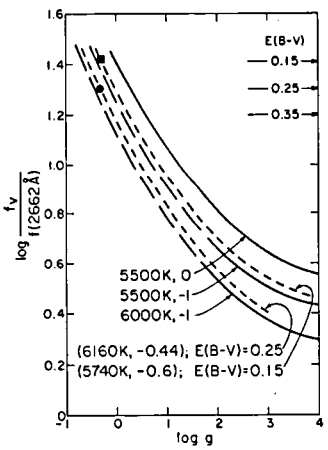

Figure 2. Model atmosphere (Kurucz 1979) flux ratios visual to 2662 A as a function of log g for different effective temperatures and [A/H], solid lines. The dashed lines are interpolated curves for pairs of T_{eff} and [A/H] suggested by our observations; see text.

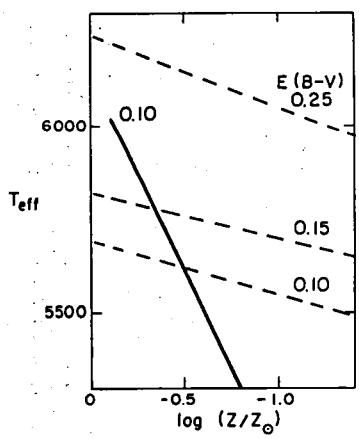

Figure 3. The relations T_{eff} [A/H] obtained for different values of E(B-V). Also shown is the relation T_{eff} [A/H] required by the measured discontinuity at 2600 A (thick line).

BINARY STARS

Accretion in the zeta Aurigae and 32 Cygni Shock Cones

by

I. A. Ahmad,[1] R. D. Chapman,[2], R. Stencel,[3] and Y. Kondo[2]

[1]Imad-ad-Dean, Inc., 4323 Rosedale Avenue, Bethesda, MD 20814
under contract to
the National Aeronautics and Space Administration

[2]NASA, Goddard Space Flight Center,
Laboratory for Astronomy & Solar Physics, Greenbelt, MD 20771

[3]NASA Headquarters, Code EZ-7, Washington, DC 20546

Abstract

Zeta Aurigae and 32 Cygni are binary stars consisting of a cool supergiant primary and a hot dwarf secondary. We have observed variations in the Mg II 2800 A and C IV 1550 A doublets of these stars near the time of secondary minimum. Longward-shifted absorption is seen in the Mg II lines of both stars which may be due to material accreting onto the B star behind the shock front. We have observed a reverse P-Cygni profile in the C IV lines at some phases of zeta Aur. This phenomenon seems transient and recurrent, and may suggest streaming. An abrupt strengthening and broadening of the absorption--especially at higher positive radial velocities--manifested in the CIV lines coincides with the onset and termination of the Mg II accretion absorption. We speculate that this is the effect of the abrupt increase in optical depth as the line of sight aligns with the shock front.

Parameters for the interaction dynamics in the case of zeta Aur confirms the general conclusions of Ahmad, Chapman and Kondo (1983) although there may be small secular differences from the preceding cycle. In the case of 32 Cygni the observed aberration angle is similar to that of zeta Aur, but the system seems more difficult to model in detail. For zeta Aur the angle of aberration of the accreting material from the radial direction is about 38° and the half width of the shock cone is about 11°. For 32 Cygni the aberration angle is about 44°.

INTRODUCTION

Zeta Aurigae is the prototype for eclipsing binaries in which an early type secondary moves through the extended atmosphere of a late type supergiant. The B star has been successfully used as a probe of the atmosphere and

inner wind region of the red giant. Recently, Chapman (1981) and Ahmad, Chapman and Kondo (1983) have shown that variations in the Mg II and C IV line profiles are related to the presence of a column of material accreting onto the B star inside a shock cone trailing the B star in its orbit. We have systematically monitored two zeta Aurigae systems--zeta Aur and 32 Cyg--with the IUE instrument during that part of their phases in and around which we expect the effects of the shock cone to be apparant. In this paper we report the results as manifested in the Mg II 2800 and C IV 1550 profiles.

OBSERVATIONS

Zeta Aur and 32 Cygni were observed approximately monthly from February, 1983 through December, 1983. No observations were scheduled for November, and Zeta Aur was not observed in May or June due to the solar constraint. In the reduced spectra shown, absolute flux is plotted against wavelength in the reference frame of the interstellar medium, calibrated by the use of interstellar absorption lines.

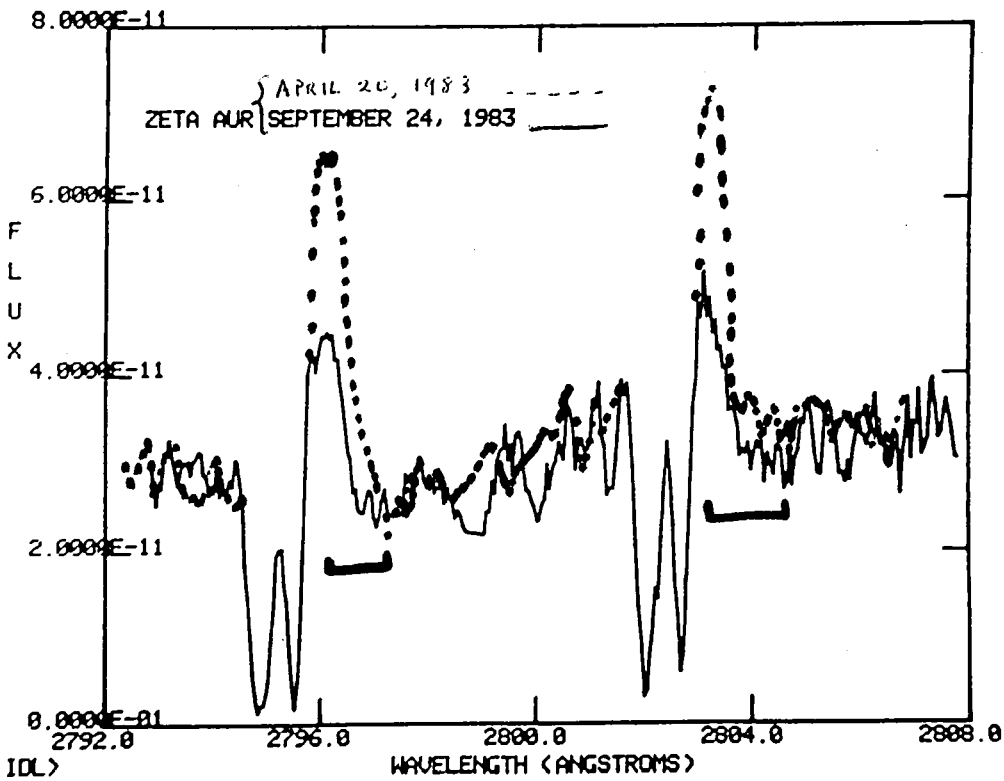

Figure 1. Mg II Lines in zeta Aur

ANALYSIS OF THE Mg II LINES

Secondary minimum occurred in April for Zeta Aur and in May for 32 Cygni.

Only days before secondary minimum, Zeta Aurigae had the same appearance as it usually does away from primary minimum (Fig. 1, dotted line). By July a pronounced absorption component had appeared at the long wavelength side of the P-Cygni emission. This increased in strength in August and again in September (Fig. 1, solid line). In October it had become very weak and by December was gone. We believe this absorption, longward shifted by about 100 km sec^{-1}, is due to absorption by the accretion column which Chapman (1981) observed in C IV. The fact that this absorption can be seen throughout the period from July to October suggests it is of a very large scale.

According to the model of Ahmad, Kondo and Chapman (1983), the absorption is due to accretion in a shock cone due to the motion of the B star through the K star wind. The accretion column inside the shock wave is basicly a turbulent wake behind the B star. The shortward shifted absorption line in the Mg II profile is broad and shallow, as one would expect for a line formed in a turbulent medium. The line widths suggest a turbulence velocity of order 80 km s^{-1}. The accretion phenomenon should be visible in the IUE spectrum as long as the line of sight to the B star passes inside the shock cone. The fact that the absorption is most pronounced five months after secondary minimum implies that the shock cone is aberatted behind the radial between the two stars by about 38^{o}. This is consistent with Ahmad *et al.*'s estimated aberration angle of about 35^{o}. Using their method of analysis, we conclude that the K star wind has a velocity of about 60 km s^{-1} and that the shock cone has a Mach angle (half width) of about 11^{o}. Both of these values confirm the estimates of Ahmad *et al.* obtained for the preceding cycle. There may be some secular differences in the data from the earlier cycle, however. Although the equivalent width of the accretion absorp-tion appears similar, it may have been wider and more shallow in 1980 than in 1983.

32 Cygni shows a similar phenomenon, with the maximum accretion absorption occuring four months after secondary minimum. The case of 32 Cygni is somewhat more difficult to analyze, however, because of the larger inclination of the system's orbital plan to the line of sight. Nonetheless, it is reasonable to infer an aberration angle of 44^{o} (plus or minus 8^{o}) from the date of the peak absorption, given the orbital characteristics of the system.

ANALYSIS OF THE C IV LINES

Figure 2 shows the C IV 1550 A doublet of zeta Aur throughout the period observed (with an offset in flux for all but the December observations). A remarkable reverse P Cygni profile is seen in the July and December observations, and may be marginally present in the others. We are as yet unable to account for behavoir of the emission component and speculate it may evidence for streaming.

The absorption component of the lines is strongest and broadest in the

period July through October (coinciding with the period in which we are looking into the shock cone). It is particularly strong at the beginning (July) and end (October) of this period, with the most dramatic enhancement occuring on the long wavelength side of the line (highest positive radial velocities). We speculate that there may be more C IV along the line of sight as we look into the shock cone, especially at the shock front. The C IV lines of 32 Cygni show no signs of a reverse P-Cygni profile.

Conclusions

The Mg II profiles observed in zeta Aurigae provide evidence for the accretion column model of Ahmad, Chapman, and Kondo (1983). Variations in the C IV lines may provide insights into the temperature structure along the accretion column.

REFERENCES

Ahmad, I. A., Chapman, R.D., and Kondo, Y. 1983, Astr. and Ap., **126**, L5.

Chapman, R.D. 1981, Ap. J. **248**, 1043.

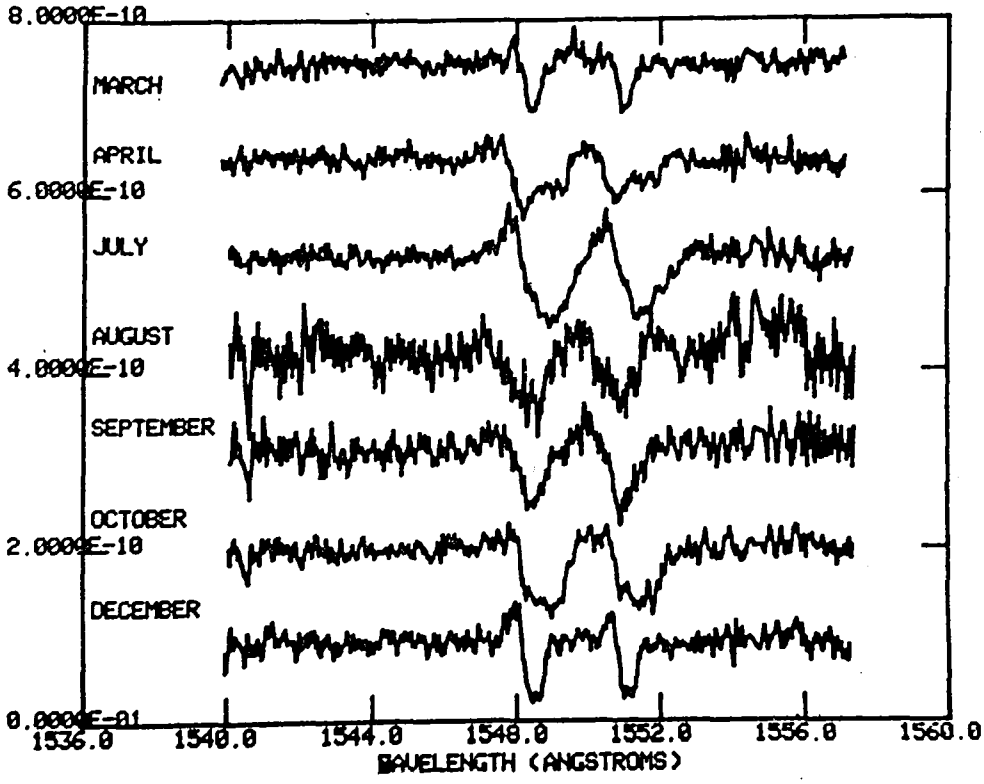

Figure 2. Stacked CIV Lines of zeta Aur

ECLIPSE OBSERVATIONS OF EPSILON AURIGAE

Thomas B. Ake
Astronomy Operations, Computer Sciences Corporation

Theodore Simon
Institute for Astronomy, University of Hawaii

ABSTRACT

We summarize the major characteristics in the UV of the 1982-84 eclipse of ϵ Aur, from first through third contact. From 1500 to 3200 A, the spectrum is dominated by periodic changes in continuum levels, apparently due to Cepheid-like pulsation of the primary, superimposed upon the decrease in light due to the eclipse itself. There is disagreement between various observers about the wavelength dependence of the UV eclipse due to a brightening that occurred prior to first contact. We find no large increase in the 2200 A dip, so that if the cool disk found by Backman et al (1983a,b) is comprised of cool dust grains, they must be larger than typical interstellar grains. Comparison with other A-F supergiants are inconclusive as to whether a hot companion is seen, although excess UV flux is present shortward of 1400 A. The only strong emission lines in the UV are O I 1304 and Mg II 2800. O I is present outside of eclipse and shows variations of a factor of two during totality. The absence of strong eclipse effects on it leaves some doubt as to whether it arises from the F-type primary, the secondary, or intrasystem gas. The Mg II emission, which was unveiled as the F star continuum decreased on ingress, has developed a broad, blue-shifted component of -300 ks^{-1}, which we speculate may be a signature of accretion by the secondary of gas ejected by the primary.

CONTINUUM VARIATIONS

The shape of the UV light curve, particularly its wavelength dependence, depends upon the geometry and opacity of the occulting body. In figure 1, we plot our broadband (100-200 A) photometric points in regions centered between 2850 and 1260 A, as well as visual magnitudes obtained from the FES at the time of observation. As characteristic of the Cepheids, pulsational variations are enhanced in the UV continua down to 1500 A (Schmidt and Parsons 1982). The IUE data indicate maxima occurred near JD 2445050, 5200 and 5375, but are difficult to determine because of inadequate phase sampling and complications arising from the eclipse itself. After mid-eclipse the variations became smaller except for a strong peak near the predicted time of third contact ($\sim$JD 2445710).

Based on preliminary analyses of ingress observations, there is some disagreement about the wavelength dependence of the eclipse. Ake and Simon (1983) suggest the eclipse is wavelength dependent, being 0.5 mag. deeper at 3000 A and 1 mag. deeper at 1500 A. Chapman, Kondo and Stencel (1983) find the eclipse to be much deeper in the far UV and strongly wavelength dependent, which they attribute to dust in the vicinity of the secondary. Parthasarathy and Lambert (1983), however, report the eclipse is only slightly deeper in the

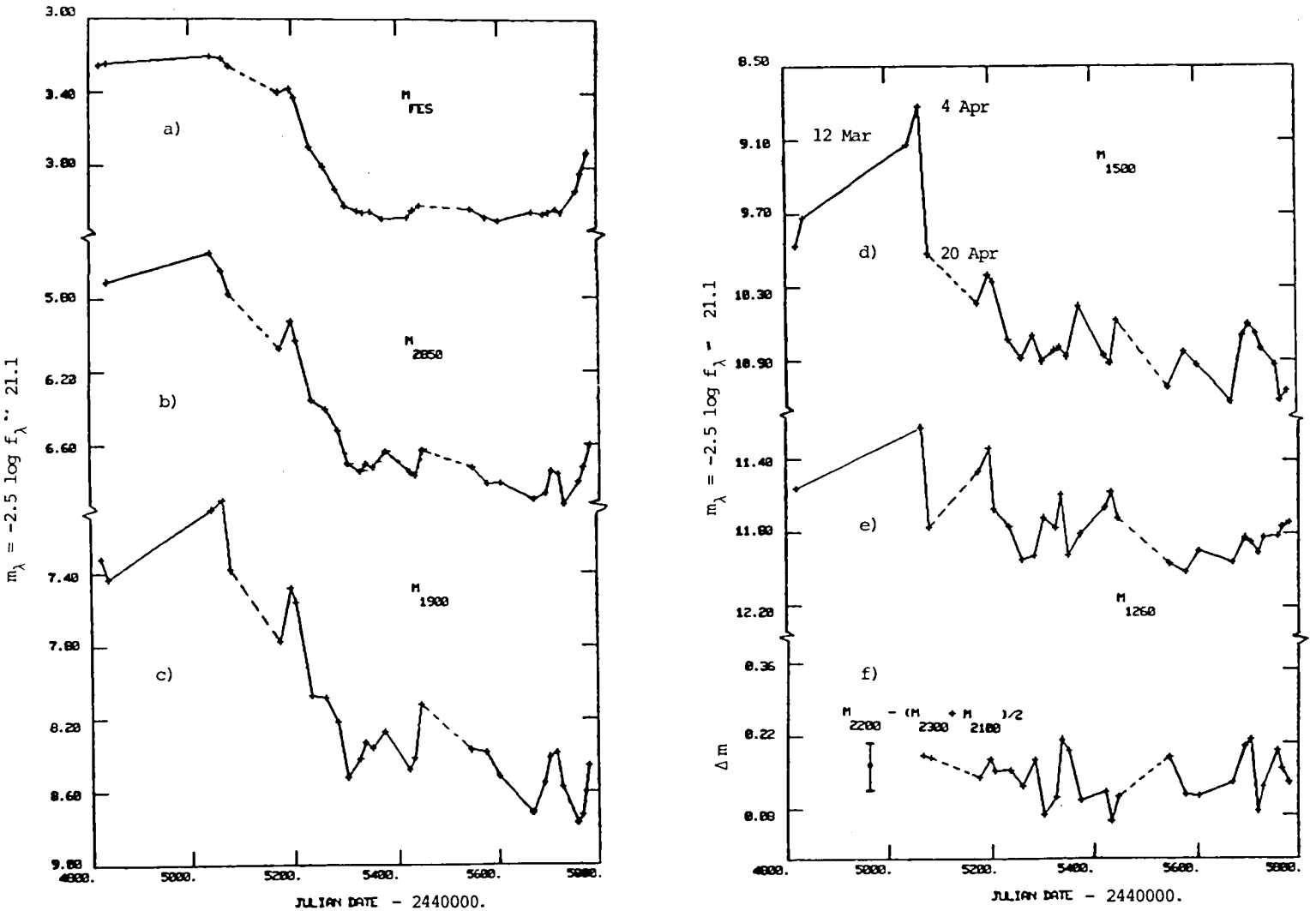

Figure 1. (a-e). Light curves of ζ Aur at different wavelength continua. Scales are magnitudes where $m_\lambda = 3.64 \times 10^{-9}$ ergs/cm^2/sec/A. (f). 2200 A absorption measurement determined as magnitude depth from adjacent continua; vertical bar is estimated measurement error. Dotted lines indicate dates when ε Aur was unobservable due to its proximity to the Sun.

UV, is nearly wavelength independent down to 1600 A, and at 1250 A, there is no eclipse at all!

These seemingly discrepant observations are the result of a brightening in the UV prior to first contact (fig. 1d). Ake and Simon chose a March 1982 observation by Chapman to be an out-of-eclipse reference; the Chapman, Kondo and Stencel pre-eclipse point was taken near the peak in early April; and Parthasarathy and Lambert chose a 25 April level just after the precipitous drop off from that peak. Ake and Simon (1982) attributed this peak to a maximum in the Cepheid-like pulsation as seen in the visual region, but Parthasarathy and Lambert speculate that a hot secondary may have become visible through tunnels in the disk at this time.

Without adequate pre-eclipse data, we conclude that there is a modest change in the slope of the UV continuum to 1400 A during the eclipse, and shortward of this the eclipse is indeed much shallower. There is certainly no large increase in the 2200 A absorption dip (fig. 1f), so if dust grains are responsible for the primary eclipse, they must be larger than typical interstellar grains.

LINE VARIATIONS

The only strong emission features seen are O I 1304 and Mg II 2800. Too few observations are available outside of eclipse to determine if the factor of two variation of O I during totality is intrinsic to the eclipse. Relative to Mg II, it is an order of magnitude stronger compared to typical cool-star chromospheric spectra (Simon, Linsky and Stencel 1982), but comparable to shock induced emission in long-period Cepheids (Schmidt and Parsons 1982).

The Mg II line cores have a P-Cygni like structure that was revealed as the surrounding continuum level decreased during ingress. One could associate the emission either with the chromospheric structure of a secondary star, which is partially obliterated by interstellar absorption, or with intrasystem gas. If a secondary's chromosphere, the full width at the base of the emission yields $M_V = +0.8$ according to the Weiler and Oegerle (1979) relation. Since $M_V = -8.5$ for the primary, the secondary would not be detectable.

The Mg II emission core has remained constant during all of the eclipse, but after mid-totality in July 1983 a broad, blueshifted absorption with a terminal velocity of $-300\ ks^{-1}$ arose. In the optical region, smaller velocity blue-shifted features have occurred at this time in previous eclipses and have been interpreted as arising from rotation of a disk around the secondary. The higher velocity absorption may arise from a gas stream between the two stars and is possibly the signature of accretion by the secondary of gas ejected by the primary.

EVIDENCE FOR A HOT SOURCE

Hack and Sevelli (1979) reported finding a trace of a B5 V continuum in an SWP low dispersion spectrum obtained with IUE, but the line spectrum is unconvincing and the true absolute flux was indeterminant since the exposure was taken through the small aperture. Parthasarathy and Lambert note that a B0 main sequence star buried within a disk and seen through a few small tunnels may explain the shallow eclipse below 1400 A. The data may also be explained by a model where the primary is assymetric such that its poles, which are uneclipsed, are warmer than the occulted part of the surface.

Figure 2 compares ϵ Aur (dereddened for E(B-V)=0.35) with the A9 Ia star HR 4110 (dereddened for E(B-V)=0.37) and the B5 standard ρ Aur. Note that while ϵ Aur has a far UV excess, its line spectrum below 1400 A does not match that for a B5 star or for HR 4110.

REFERENCES

Ake, T.B and Simon, T. 1982, Bull. Am. Astr. Soc., 14, 979
_____ 1983, I.A.U. Circular, No. 3763
Backman, D., Becklin, E.E., Cruishank, D., Simon, T., Tokunga, A. and Joyce, R. 1983a, I.A.U. Circular, No. 3763
_____ 1983b, Ap. J. submitted
Chapman, R., Kondo, Y. and Stencel, R.E. 1983, Ap.J.(Letters), 269, L17
Hack, M. and Sevelli, P.L. 1979, Astron. Astrophys., 75, 316
Parthasarathy, M. and Lambert, D.L. 1983, Pub. Astr. Soc. Pac., 95, 1012
Schmidt, E.G. and Parsons, S.B. 1982, Ap. J. Suppl., 48, 185
Simon, T., Linsky, J.L. and Stencel, R.E. 1982, Ap. J., 257, 225
Weiler, E. and Oegerle, W. 1979, Ap. J. Suppl., 39, 537

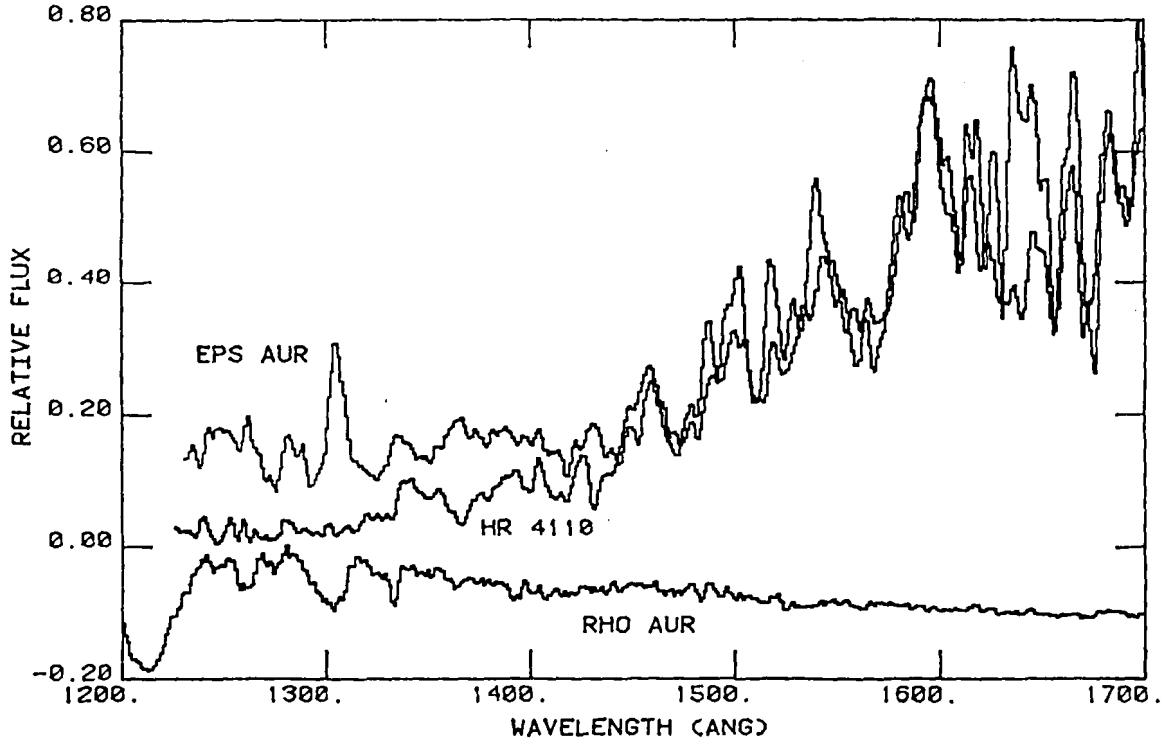

Figure 2. Far UV line spectrum of ϵ Aur (A8 Ia) compared to HR 4110 (A9 Ia) and ρ Aur (B5 V). ϵ Aur and HR 4110 were dereddened and normalized to the fluxes in the 1500-1700 A region.

UV Observations of Epsilon Aurigae During Ingress and Totality

Bruce M. Altner
Applied Research Corporation

Robert D. Chapman and Yoji Kondo
Laboratory for Astronomy and Solar Physics
NASA, Goddard Space Flight Center

and

Robert E. Stencel
NASA Headquarters/ EZ-7

Analysis of SWP and LWR spectra of Epsilon Aurigae taken during the pre-eclipse, ingress and total phases of the present eclipse has provided further constraints on models of this enigmatic system. High dispersion images show no significant change in the strength of the Mg II emission lines during the course of the eclipse. Both high and low dispersion spectra indicate that the eclipse starts earlier, ends later and is deeper in the UV compared to visual wavelengths. In addition, we confirm our earlier observation that the eclipse depth is wavelength dependent shortward of 2400 A. Abrupt changes in the light curve appear at all wavelengths, suggestive of discontinuities in the opacity of a ring of material surrounding the secondary object.

INTRODUCTION

At various times in the past the secondary in the Epsilon Aurigae binary system has been described as a swarm of meteorites (Ludendorff, 1924), a giant infrared star (Kuiper, et al., 1937), a small infrared star plus an ionized gas stream (Struve, 1956), a hot B star surrounded by an ionized gas shell (Hack, 1961), a bar of optically thick material (Huang, 1965), a proto-planetary system (Kopal, 1971), a black hole plus a semi-transparent disk (Cameron, 1971) and a black hole within a thin, opaque disk with a central opening (Wilson, 1971). This rather lengthy list serves to underscore Wilson's comment that Epsilon Aurigae is the only binary system that can be described "with complete justification, as mysterious". In this paper we present SWP and LWR spectra taken in both the high and low dispersion modes from pre-eclipse right through to the beginning of egress and compare these data to visual observations.

OBSERVATIONS

The primary star (A8 - F2 Ia), an irregular period cepheid variable with an ampltude of 0.2 magnitudes, is visible during all phases of the eclipse. The additional cepheid variability complicates the eclipse light curve and makes the choice of a pre-eclipse fiducial spectrum a decision of some importance. With this in mind, and given the sparse sampling of the IUE data, we see that it is difficult to determine the actual dates of first and second contact in the UV eclipse, which are not necessarily the same as for the optical eclipse. A fairly reliable indicator of the time displacement between the UV and visible light curves may be obtained by matching the ingress slopes and the mid-eclipse brightening feature, as shown in Figure 1. The units of "eclipse phase" used in this and later figures are such that first contact corresponds to phase 0.00 and last contact to phase 1.00, based on contact dates predicted by Gyldenkerne (1970). In these units second contact is phase 0.20 and third contact is 0.79. The shift of 0.15 used to align the light curves in Figure 1 corresponds to approximately 100 days. It will be interesting to watch the system as the UV eclipse ends to see if a similar delay exists for the egress phase. At the time of this writing egress appears just to have begun in the UV whereas it is already well along according to the latest UBV photometry (Hopkins and Stencel, 1984). Figure 1 also illustrates that the UV eclipse is deeper than the 0.8 magnitude drop noted in the longer wavelength observations.

The most interesting high dispersion feature is the Mg II resonance doublet, seen in emission. A narrow (30 - 50 km/s) blueward absorption feature present in all the spectra is interpreted as being of interstellar origin. The emission lines became more pronounced as the eclipse progressed but this was due to the decreasing light level of the surrounding continuum. Figure 1 also shows just how little the flux in the Mg II K line changed relative to the continuum in the same echelle order. Thus, whatever source is responsible for the emission lines is probably not associated with the primary star.

Many of the models cited above are based on the belief that the eclipse is "gray", i.e., that eclipse depth is independent of wavelength. The IUE data we have obtained shows that this property holds in the UV all the way to 2400 A. However, in the wavelength range $1500 < \lambda < 2400$ A the eclipse appears to be non-gray, being deeper at shorter wavelengths. Chapman, Kondo and Stencel (1983) noted this in the earliest stages of the eclipse and interpreted it as an indication of a cloud of small grains surrounding the secondary. Such a cloud, extending above, below, in front of and behind the material responsible for the wavelength independent eclipse would explain the deeper and longer eclipse in the UV data. In Figure 2 we have plotted curves of eclipse depth versus wavelength for several typical phase points during ingress and totality to illustrate this wavelength dependence. The pre-eclipse SWP and LWR spectra we have chosen as our reference point

were taken on April 4, 1982 (phase, - 0.17) by T. Ake and T. Simon. The almost vanishing eclipse depth shortward of 1500 A has been discussed elsewhere (Parthasarathy and Lambert, 1983) and does indeed suggest the existence of an uneclipsed hot source associated with the extended occulting material. Hack (1961) first proposed this hot source to be a main sequence B star and Plavec (1981) speculated that it might be associated with heating as material from the supergiant wind falls onto the accretion disk of the secondary. It is noteworthy that the system has shown no secondary minimum in the past and no spectroscopic evidence for a hot star, other than the UV excess shortward of 1500 A first observed by Hack and Selvelli (1979).

In Figure 3 we have plotted eclipse depth versus phase for several wavelength bands (data are averaged in 100 A bins). The sharp jumps in light level at certain phases are too large to be attributed solely to the cepheid variability of the primary. We call attention to the downward slope of the light curve during totality which is also evident in the light curves of the 1929 and 1956 eclipses and which Wilson (1971) interpreted as a small tilt in the major axis of his proposed ring as it transits the primary. Certainly the discontinuities we note in the light curve are consistent with some kind of ring structure, i.e., gaps in a disk. That the discontinuities are deeper at the shorter wavelengths suggests that the gaps might be associated with the small particle component of the eclipsing object.

The question that arises from our observations to this point is clear: how does this obscuring material compare to matter responsible for interstellar extinction? To facilitate this comparison we have renormalized Seaton's (1979) mean extinction curve to E(1800-2900). Figure 4 shows this renormalized interstellar curve superimposed on the data for Epsilon Aurigae at several representative phases. Because we have been unable to remove the effects of the hot component from the eclipse curve, we display data longward of 1500 A only. The most noteworthy feature in Figure 4 is the large variability in the region $2000 \leqslant \lambda \leqslant 2400$ A. Unfortunately for this kind of analysis, the most interesting part of the interstellar curve, the broad hump centered at 2200 A, falls on the least sensitive part of the LWR camera. Nevertheless, some of this variability may be intrinsic to the Epsilon Aurigae system. If so, it argues for a mixed population of grain sizes and types in the secondary cloud. Comparisons with model extinction curves for other kinds of small particle grains are planned.

REFERENCES

Cameron, A.G.W. 1971, Nature, 229, 178.

Chapman, R.D., Kondo, Y. and Stencel, R.E. 1983, Ap. J. (Letters), 269, L17-19.

Gyldenkerne, K. 1970, Vistas in Astronomy, (Oxford: Pergamon Press), 12, 199.

Hack, M. 1961, Mem. Soc. Astr. Italiana, 32, No. 4.

Hack, M. and Selvelli, P.L. 1979, Astr. Ap., 75, 316.

Hopkins, J.L. and Stencel, R.E., eds. 1984, Epsilon Aurigae Campaign Newsletter, No. 10.
Kopal, Z. 1971, Ap. and Space Science, 10, 332.
Kuiper, G.P., Struve, O. and Stromgren, B. 1937, Ap. J., 86, 570.
Ludendorff, H. 1924, Sitz. ber. Preuss. Akad. Wiss. (Math.-Naturwiss. Kl.), 9, 49.
Parthasarathy, M. and Lambert, D.L. 1983, Pub. A.S.P., 95, 1012.
Plavec, M.J. 1981, in "The Universe at Ultraviolet Wavelengths: The First Two Years of IUE", ed. R.D. Chapman, NASA CP-2171.
Seaton, M.J. 1979, M.N.R.A.S., 187, 73.
Struve, O. 1956, Pub. A.S.P., 68, 27.
Wilson, R.E. 1971, Ap. J., 170, 529.

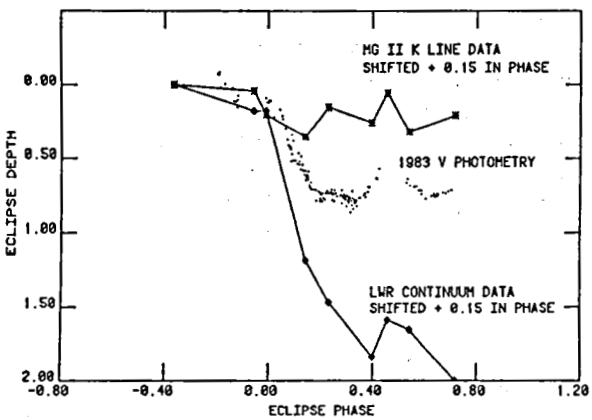

Figure 1.

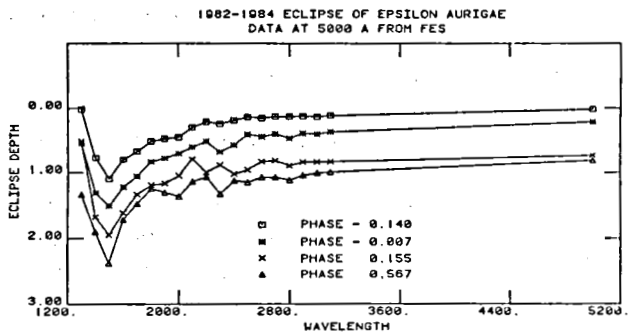

Figure 2.

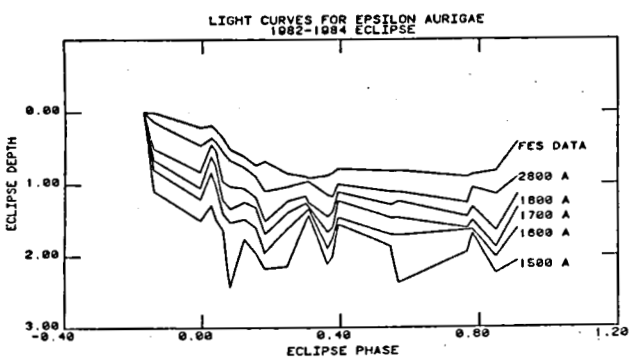

Figure 3.

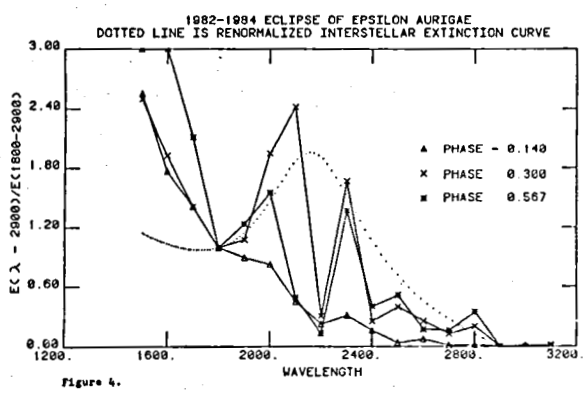

Figure 4.

EGRESS SPECTRA OF THE NEW ECLIPSING SUPERGIANT 22 VULPECULAE

Thomas B. Ake, III and Sidney B. Parsons
Astronomy Operations, Computer Sciences Corporation

Yoji Kondo
Laboratory for Astronomy and Solar Physics
Goddard Space Flight Center

ABSTRACT

The G-type primary in the single-lined spectroscopic binary 22 Vul (HD 192713, G3p Ib-II, period 249 days) was found with IUE in April 1983 to eclipse its recently identified B9 main sequence companion. The system thus joins the few known Zeta-Aurigae systems in which a hot dwarf can be used to probe the extended atmosphere of a cool supergiant. Outside of eclipse, a wind from the system with terminal velocity of 300 ks^{-1} is conspicuous in the Mg II lines. Enhanced Fe II absorption seen well away from geometrical eclipse implies an extensive envelope around the G star. Some of the 22 Vul spectra closely resemble those of other interacting binaries, suggesting common properties of relatively dense, warm plasmas in these systems.

INTRODUCTION

The Zeta-Aurigae systems exhibit the phenomenon of atmospheric eclipses caused by the passage of a hot dwarf behind the extended atmosphere of an evolved, cool supergiant. Four such systems are known: Zeta Aur, 31 Cyg, 32 Cyg and VV Cep. These binaries provide an excellent opportunity to study the outer atmospheres of and winds from the late-type supergiants by using the light from the hot secondary as a probe during eclipse. Ultraviolet spectra are particularly important as the temperatures and densities of the plasmas involved are such that the spectral signatures are most effectively seen in that spectral region.

In April 1983, a fifth member of this class of binaries was discovered, 22 Vul (HD 192713; Parsons and Ake 1983a,b). This system is unique because the spectral type of the evolved component, G3 Ib-II, makes it the earliest type of such systems; the spectral type of the secondary, B9, is the latest of the secondaries; and its binary period, 249 days, is the shortest in these systems, implying the separation of the components is also the smallest.

OBSERVATIONS

22 Vul was originally placed on our IUE program to determine mass ratios of giant and supergiant stars with hot companions. In these systems, the flux contribution from the two components is nearly the same in IUE's long wavelength region and so velocity differences from the composite spectra are easy to measure. Optically 22 Vul was known to be a single-lined spectroscopic binary and exhibited weak Ca II h and k lines. Parsons (1981b) estimated from TD-1 fluxes that the secondary is nearly 3 magnitudes fainter

visually than the primary and is of spectral class B7-B9.

The first IUE observations of this star exhibited a strong, high-velocity component in Mg II (fig. 1), while the SWP spectrum was that for a normal B9 star (fig. 2). Interpreted as a wind, the terminal velocity of the absorption is about 300 ks^{-1}. Since our mass ratio observations were timed to occur at quadratures of maxmimum velocity separation, we did not expect to see structures indicative of streaming or eclipses.

An observation was obtained later at phase 0.07 after the G star passed in front of the B star and the character of the composite spectrum changed appreciably. Numerous low excitation-level absorption lines presumably from the extended atmosphere of the supergiant became apparent. The B star itself took on the appearance of a supergiant due to the extra absorption features. Such characteristics are reminiscent of HR 4511 in which Parsons (1981a) found the B-type secondary to resemble a supergiant rather than the giant type implied by the magnitude difference from the continuous flux distribution.

Parsons (1983) derived new orbital elements for the primary of 22 Vul with McDonald Reticon radial velocity data and predicted mid-totality of a possible eclipse of the secondary in April 1983. IUE observations at that time confirmed the eclipsing nature of the system as the spectrum of the hot star disappeared leaving only an emission-line spectrum visible (fig. 2). Eight days later (phase 0.03) the SWP flux level returned to about half its previous height but the continuum and line spectrum looked little like a normal star.

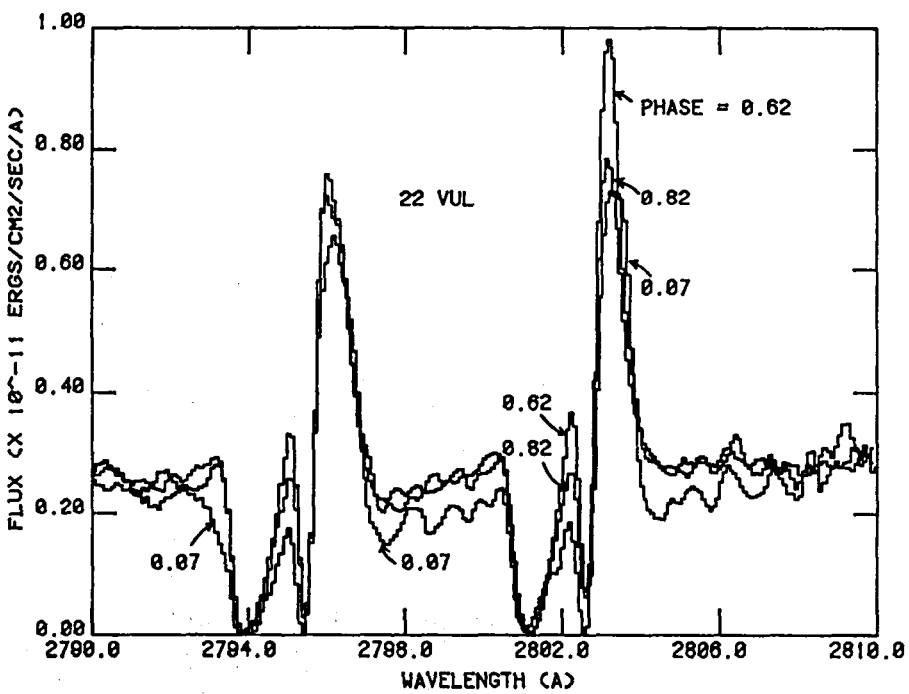

Figure 1. Three observations of 22 Vul showing the region of the Mg II resonance lines. The peak of the Mg II k-line is saturated in all spectra. The orbital phases are counted from mid-totality of the eclipse of the B star as predicted by the orbital determination of the G3 Ib-II primary. Considerable shortward-shifted absorption is seen with the characteristic of an accelerated wind.

DISCUSSION

Fitting together the observations from the April and December 1983 eclipses, we estimate that totality lasts about 17 days. Partial obscuration of the secondary lasts for at least 10 days after totality and implies that there is an large envelope around the G supergiant extending at least 2 stellar radii. From the radial velocity differences between the components measured with IUE and the orbital determinations of the primary's velocity from the ground, the mass ratio is about 0.7. Assuming an inclination of 90° and a normal size for the B9 secondary, we find $M_{G*} = 4.3\ M_\odot$ and $M_{B*} = 3.0\ M_\odot$. Optical photometric data, which should show eclipse effects in the blue and near ultraviolet regions, would yield more definitive values of the system parameters.

Line identifications in progress of the high dispersion data indicate that the majority of the absorption features superimposed on the B9 spectrum during egress is due to Fe II from the outer atmospheric layers of the G3 Ib-II star. The lines show multiple components at various phases with velocity separations on the order of 100 ks^{-1}.

The emission line spectrum during totality is rather different from the chromospheric emission of single stars. For instance, the lines in general are found to have fluxes comparable to the G2 Ib-II star Beta Dra, but 22 Vul is two magnitudes fainter visually. The ratios of different ions are quite different, with Si IV, C II and especially Al II lines having greater observed flux in 22 Vul. Furthermore, a high dispersion observation of the December 1983 eclipse shows substantial structure in the emission components, particularly a red-biased component indicating a flow of material away from the observer and towards the secondary. As in other Zeta-Aur systems, the zero-volt Fe II lines are in fluorescence during totality.

The importance of 22 Vul then is not just the extension of the Zeta-Aur phenomenon to study atmospheres of earlier-type supergiant stars. There is a close correspondence between the SWP spectra at different phases and those of other interacting binaries such as SX Cas (Plavec et al 1982) and HD 207739 (Parsons et al 1983). The totality SWP emission spectrum is quite similar to that of SX Cas in eclipse, while the partial egress absorption spectrum (phase 0.03) resembles SX Cas out of eclipse and HD 207739.

This suggests a common property between these systems of the existence of a relatively dense, warm plasma surrounding one component and/or the entire system. Preliminary indications are that in 22 Vul the plasma is roughly but not tightly concentrated around the G star. As the separation of the components, as indicated by the binary period, is intermediate between those of the interacting binaries and other Zeta Aur systems, 22 Vul provides a transition case between what has so far been considered to be two separate classes of objects.

References

Parsons, S.B. 1981a, Astrophys. J., 245, 201.
_____ 1981b, Astrophys. J., 247, 560.
_____ 1983, Astrophys. J. Suppl., 53, No. 3.
_____ and Ake, T.B. 1983a, Inf. Bull. Var. Stars, No. 2334.
_____ and Ake, T.B. 1983b, Bull. Am. Astr. Soc., 15, No. 3.
_____, Holm, A.V. and Kondo, Y. 1983, Astrophys. J. (Letters), 264, L19.
Plavec M J, Weiland J L and Koch R H 1982, Astrophys. J., 256, 206.

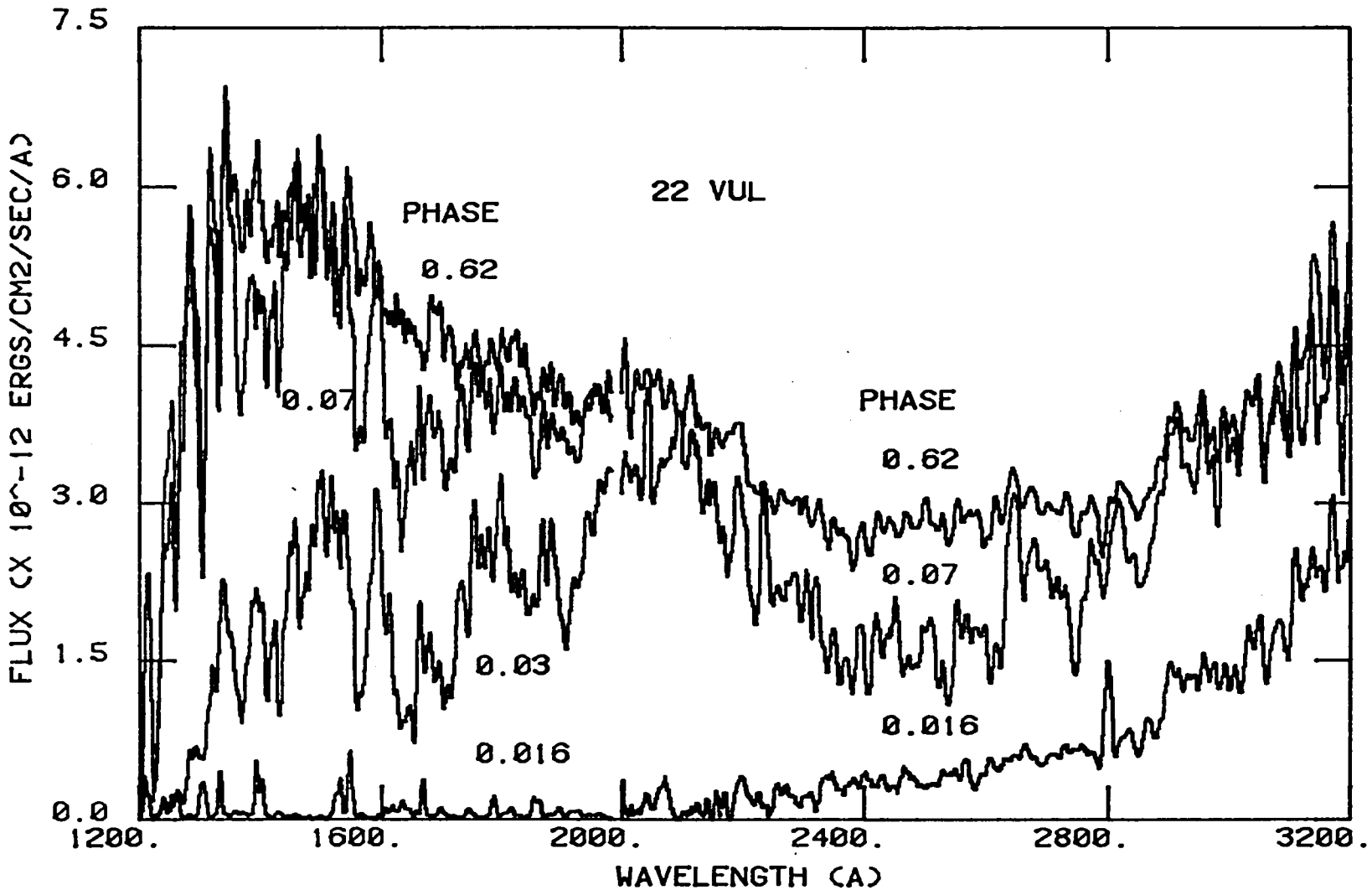

Figure 2. IUE flux spectra of 22 Vul at different orbital phases. Far from eclipse, the SWP spectrum is that of a B9 star. Observations at 0 = 0.016 indicate total eclipse of the hot component and prominent emission lines of C II 1335, Si IV 1400, Si II 1526/33, C IV 1549, Al II 1671 and Mg II 2800 are present. The SWP spectrum at phase 0.03 is similar to the interacting binary SX Cas when out of eclipse. At phase 0.07, when the hot star line of sight is probably about one cool star's radius away from the limb of the cool component, there is still considerable absorption at some wavelengths.

THE STELLAR WIND IN THE BO V-TYPE ECLIPSING BINARY Y CYGNI

N. D. Morrison

Ritter Astrophysical Research Center
The University of Toledo

and

C. D. Garmany

Joint Institute for Laboratory Astrophysics
University of Colorado

ABSTRACT

The double-lined eclipsing binary system Y Cygni (HD 198846) has well-determined orbital elements, absolute dimensions, and rate of apsidal motion. In several high-dispersion SWP images taken near (but not in) eclipse and in one at quadrature, we studied the profiles of the resonance lines of Si IV, C IV, and N V. C IV is very broad, and the absorption minima are shortward shifted by 160 km s^{-1} with respect to Si IV. N V is weak but is shortward shifted by a similar amount and has a broad shortward wing. In general, the spectrum is similar to that of the single BO V-type star τ Scorpii. In the spectrum obtained at quadrature, the C IV profile is shifted in accordance with the orbital motion of the hotter, less massive star. Therefore, it is likely that the wind-borne C IV absorption originates in this star.

By fitting the C IV and N V lines with synthetic profiles computed from the program written by Olson (1982 and references therein), we obtained a terminal velocity of 1500 km s^{-1}. Application of the technique of Garmany et al. (1981) yields $\dot{M} = 10^{-8.4} M_{\odot}$ yr^{-1}.

INTRODUCTION

Y Cygni is a double-lined eclipsing binary that is noteworthy in being one of the best-determined cases of apsidal motion. It consists of a pair of BO V-type stars. Giuricin et al. (1980) give the most recent tabulation of the absolute dimensions of the components. They find that the radii of the hotter and the cooler star are 0.182 and 0.237, respectively, times the mean separation. Therefore, the system is well detached, and we expect the components to be structurally similar to single stars. The rotation velocity of each, 145 km s^{-1} (Levato 1975), is significantly greater than the synchronous rotational velocity, 100 km s^{-1}. On the basis of an early IUE observation, Heap (1981) informed us that the system has a stellar wind.

OBSERVATIONS AND RESULTS

We obtained a high-dispersion image (SWP 19650) of the system with IUE just before primary eclipse, when the spectrum was single-lined. The two stars contribute roughly equally to the combined light: from the equatorial temperatures and the luminosity ratio given by Giuricin et al. (1980) and from fluxes given by Kurucz (1979), we estimate that the hotter star is about 20% brighter at 1500 Å.

The principal evidence for a wind is that the short-wavelength wing of the C IV resonance doublet ($\lambda\lambda$1548,1550) is broad, and that its absorption minima are shifted by about 160 km s^{-1} toward shorter wavelengths relative to the photosphere. The N V doublet ($\lambda\lambda$1238,1242) is also present, although weakly, at a similar radial velocity. The motion of the photosphere is represented by the radial velocities of the Si IV resonance lines, which are symmetrical and usually originate in the photosphere in stars of this spectral type.

Heap's original image, SWP 6388, was obtained at quadrature, when the hotter star was approaching with a heliocentric radial velocity of -310 km s^{-1}. In this image, the absorption minima of C IV appear at a radial velocity of -470 km s^{-1}, again shortward shifted by 160 km s^{-1}. N V shows the same behavior. Thus, the orbital motion of the stellar wind follows that of the hotter star, and we conclude that the wind is associated with this star.

We have compared the spectrum that we obtained at conjunction with archival IUE spectra of single BO-type stars. The C IV profile in Y Cyg is similar to that in τ Scorpii (BO V), except that the Doppler shift of the minima in the latter star is only -100 km s^{-1} relative to the photosphere. Since the Si IV lines have a noticeably broad shortward wing in τ Sco but not in Y Cyg, however, the two stars are certainly not identical. On the other hand, the BO.3 IV-type star δ Scorpii shows only minimal wind broadening of the C IV doublet, and its N V lines are narrow. That such differences exist among single stars of the same spectral type makes it understandable that the components of Y Cyg have winds of different strengths.

A plausible hypothesis might be that the wind of the hotter component of Y Cyg is spectroscopically similar to that of τ Sco, while the cooler component has a wind like that of δ Sco. Then, the composite, single-lined spectrum shows the C IV line cores at their true depths, because they are approximately equal in depth in the two stars, while the C IV wing and the N V lines are weaker in the composite spectrum than they are in the hotter star alone, because their light is diluted with light from the companion, which has a weak wind. In order to test this hypothesis, it would be necessary to obtain an exposure at mid-eclipse.

ANALYSIS AND CONCLUSIONS

We computed synthetic C IV and N V profiles at the Colorado Regional Data Analysis Facility with the program COMPAR (Olson 1982 and references therein), and we fitted them to the observed profiles in both Y Cyg and τ Sco. Table 1 lists the parameters that gave a good fit to each star; T is the line-center radial optical depth for the shortward component of the doublet (Olson 1982) and v_∞ is the terminal velocity of the wind.

TABLE 1

Profile Fitting Parameters from COMPAR

Star (Image)	v_∞ (km s^{-1})	T(C IV)	T(N V)
Y Cyg (SWP 19650)	1500	0.65	0.15
τ Sco (SWP 13713)	1500	0.60	0.20

With these values, we used the procedure given by Garmany et al. (1981) to estimate the mass-loss rate, $\dot{M}$. The fact that the procedure was designed for hotter (O-type) stars means that the assumed ionization balance may not be correct in our case. The procedure assumes that nearly all the carbon in the wind is quadruply ionized and that the only important ions of C and N are the third and the fourth. To check the reliability of our results, Table 2 compares values of $\dot{M}$ derived by this technique with values derived by more sophisticated analyses of τ Sco and μ Columbae.

TABLE 2

Comparison with Independently Derived Mass-Loss Rates

Star	Type	Author	log $\dot{M}$ ($M_\odot$ yr^{-1}) (other study)	log $\dot{M}$ ($M_\odot$ yr^{-1}) (this technique)
Y Cyg	(BO V)x2	---	---	-8.4
τ Sco	BO V	Hamann (1981)	-8.9 $\pm$ 0.5	-8.3
μ Col	O9 V	Olson and Castor (1981)	-8.2	-8.1

The agreement is reasonably good. We conclude that, even for effective temperatures near 30000 K, the technique of Garmany et al. (1981) gives a

reasonable estimate of $\dot{M}$.

Since our spectrum of the hotter component of Y Cyg is diluted with light from the companion, which has a weaker wind, the mass-loss rate given in Table 2 is a lower limit to the mass-loss rate of the hotter component. Its accuracy could be improved if a spectrum at mid-secondary eclipse could be obtained. Then, only about 20% of the combined light would come from the cooler star.

Since the mass and radius of the hotter component are well determined from the orbit, this star could be important in the study of the dependence of terminal velocity and mass-loss rate on the stellar parameters, provided that the properties of the wind are not strongly influenced by the companion. That the wind does behave approximately as the wind of a single star is suggested, firstly, by the fact that, in a series of exposures taken as the system approached primary eclipse, the C IV profile does not vary noticeably with orbital phase. Secondly, if the wind is like that of τ Sco, then, according to Hamann's (1981) model, it reaches terminal velocity 2.5 stellar radii from the center of the star. In Y Cyg, this distance equals 0.46 times the average separation of the stars, a. Since the companion's photosphere lies at a distance of 0.76 a, the wind reaches it only after attaining terminal velocity. Thus, provided that the wind of the cooler star is truly very weak, so that wind-wind interactions are unimportant, the hotter star's wind probably acts like that of a single star.

We gratefully acknowledge the capable assistance of the staffs of the IUE Observatory, the Regional Data Analysis Facilities at Goddard and at the University of Colorado, and the National Space Science Data Center. We also thank H. J. G. L. M. Lamers for helpful discussions.

REFERENCES

Garmany, C. D., Olson, G. L., Conti, P. S., and Van Steenberg, M. 1981, Ap. J., 250, 660.
Giuricin, G., Mardirossian, F., and Mezzetti, M. 1980, Astr. Ap. Suppl., 39, 255.
Hamann, W. -R. 1981, Astr. Ap., 100, 169.
Heap, S. R. 1981, private communication.
Kurucz, R. L. 1979, Ap. J. Suppl., 40, 1.
Levato, H. 1975, Astr. Ap. Suppl., 19, 91.
Olson, G. L. 1982, Ap. J., 255, 267.
Olson, G. L. and Castor, J. I. 1981, Ap. J., 244, 179.

OBSERVATIONS OF CATACLYSMIC VARIABLE STAR WINDS

France A. Córdova, Los Alamos National Laboratory
and
Keith O. Mason, Mullard Space Science Laboratory

ABSTRACT

High velocity winds are common among cataclysmic variables stars (CVs) with luminous accretion disks. Here we summarize what has been learned about these winds from IUE spectrophotometry.

INTRODUCTION

The observation that under some conditions CVs can exhibit high-velocity winds marks one of IUE's most interesting discoveries. These close binary systems can potentially offer much information about the driving mechanisms of winds in general because (a) the orbital elements of many of these binaries and their geometry is well understood, allowing the spectral line profiles to be studied as a function of inclination and stellar mass; and (b) changes in the luminosity of these stars are dramatic and, in some cases, fairly predictable, so that the effect on the winds of changes in the radiation field can be studied.

The earliest announcement of evidence for winds from compact binaries was made at the first IUE symposium in 1980 (refs. 6,7). Two novalike stars, CD-42°14462 and TT Ari, were observed to show C IV λ1549 in emission with associated shortward-shifted absorption, giving the appearance of a P Cygni profile. P Cygni-like profiles for the C IV and N V lines of three old novae, RR Pic, HR Del, and V603 Aql were subsequently reported[13]. Dwarf novae in outburst also evidence mass loss on the basis of shortward-shifted absorption lines of N V λ1240, O IV λ1340, C III λ1176, Si III/O I/Si II λ1300, in addition to P Cygni-type profiles of Si IV λ1400 and C IV (refs. 1,8,11,15).

THE OBSERVATIONS

1. When are winds observed in CVs? The present authors noted[1] that there is a correlation between winds and luminosity. An example is shown in Fig. 1, which follows the progress of the dwarf nova AB Dra through an outburst. During its quiescent luminosity state the system shows only broad emission lines; at the point in the outburst when a very hot far-UV continuum component manifests itself, the lines develop shortward-shifted absorption components symptomatic of mass loss. The high luminosity of dwarf novae during outbursts is thought to be due to an increase in the rate of mass accretion through the disk ($\dot{m}_{acc} \sim 10^{-8}\ M_\odot\ yr^{-1}$). This idea is supported by fits to the continuum distribution with steady-state, optically thick disk models or hot stellar atmospheres (refs. 5,6,7,8,11,13,14,15).

2. High velocities in the wind. The terminal velocities in the wind implied by the absorption line profiles is $(3 - 5) \times 10^3$ km s^{-1}, about the escape velocity from the surface of a white dwarf.

3. From where does the wind originate? The high velocities suggest an origin near the central, accreting degenerate dwarf. This is further supported by observations of CVs at various inclination angles. For example, AB Dra (Fig. 1) is

probably viewed from above the accretion disk (i.e. at a relatively low inclination, $i \leq 60^{\circ}$), since no orbital variation has yet been observed for this star. RW Tri, in contrast (see Fig. 2), is viewed at a very high inclination ($i \sim 85^{\circ}$), i.e. along the plane of the disk, and has very different line profiles. No absorption component is seen in RW Tri's spectrum, but the peaks of all the spectral lines[3] are markedly red-shifted with respect to the line centers, suggesting an accelerating wind which is not seen in projection against a continuum source. Fig. 2 shows that during the eclipse of the continuum in RW Tri the C IV line emission changes very little. This indicates that the wind is extensive.

4. Orbit-related variations in the line profiles. There are few observations of CVs around their binary orbits. RW Tri shows no line profile variability outside of eclipse[3], but HR Del and TT Ari do show evidence for such variations[4,7]. This variability has not been sufficiently studied to interpret it properly. The eclipsing novalike star UX UMa shows line profile behavior remarkably similar to that of RW Tri, except that at a phase that is normally associated with the mass transfer "bright spot" on the edge of the disk, the asymmetric, red-shifted emission line profile is cut by a deep absorption near the rest wavelength[9].

5. The ionizing spectrum. Many plausible arguments suggest that photoionization provides the underlying structure of the wind,[1,10,12] but the nature of the ionizing spectrum is not known. The fact that a few high luminosity systems do not show velocity-shifted UV lines could be because the gas is in a different ionization state in these stars, perhaps because the photoionizing spectrum is different. The ubiquitous hard X-rays in CVs[2] can produce the observed ion fractions[10], but there is probably not enough energy in the X-ray component to provide all of the observed line emission[3]. The energy to drive the wind could easily be supplied by far UV or EUV radiation from the inner disk.

6. The mass loss rate. Some estimates of the mass loss rate, $\dot{m}$, come from comparisons with the theoretical line profiles developed for OB stars. It is usually impossible, however, to fit the absorption and emission components simultaneously in CV spectra. An alternate method relies on deriving an ionization parameter for the wind using X-ray nebular models. Both methods give $\dot{m} \sim 10^{-11}$ to 10^{-10} $M_{\odot}$ yr^{-1} (refs. 1,5,8,10,11,13,15). The uncertainty in $\dot{m}$ is high because of uncertainties in the ion fractions and the size of the emitting region. The ratio of $\dot{m}$ to the mass accretion rate is probably between 10^{-3} and 10^{-2}.

7. Driving mechanism for the wind. In OB supergiants the driving mechanism is believed to be radiation pressure in the lines. This mechanism may also be responsible for accelerating CV winds to the high velocities observed, as evidenced by: (a) the observation of winds only in high luminosity systems; (b) the fact that the terminal velocities of CV winds are of the magnitude of the escape velocity from the white dwarf surface; and (c) the fact that the momentum rate of the radiation, i.e. $L_{tot}/c = 10^{24}$ g cm s^{-2}, is of the same order as the momentum rate of the wind.[1]

8. Comparison with other mass-losing stars. Among stars losing mass, CVs exhibit winds with the highest terminal velocities, e.g. 5000 km s^{-1} as compared to 2000 to 4000 km s^{-1} for OB stars and 100 km s^{-1} for red supergiant stars. The probable mass loss rates from CVs, i.e. 10^{-11} to 10^{-10} $M_{\odot}$ yr^{-1}, fall between the mass loss rates for dwarf stars like the Sun (10^{-14} $M_{\odot}$ yr^{-1}) and those for O V stars (10^{-8} to 10^{-7} $M_{\odot}$ yr^{-1}). The luminosities of CVs is ≤ 20 $L_{\odot}$, several orders of magnitude less than the luminosities of OB stars. The ratio of the observed X-ray flux to the total luminosity is much higher for CVs (i.e. 10^{-2} to 10^{-4}) than it is for any other wind-emitting system (e.g. for OB stars this ratio is 10^{-5}). The ratio of the luminosity in the wind to the total luminosity is also much higher for

CVs (10^{-2}) than it is for the other systems (e.g. 10^{-4} to 10^{-3} in OB stars; 10^{-4} in red supergiants; $10^{6.7}$ in the Sun). The momentum flux of the wind in CVs is similar to that of red supergiants, but a few orders of magnitude less than the flux of the most luminous OB stars.

EPILOGUE

Observations of winds in CVs are at the limit of what IUE can do. CVs are so faint ($m_v > 10$) that high spectral resolution observations, which could be used to decipher structure in the line profiles and distinguish bands of weak lines, cannot be performed. Fast timing analysis (e.g. to search for correlations between the UV profiles and optical or X-ray flickering that occurs on timescales of minutes) is not possible because of the relatively long readout time required for the IUE cameras.

There are, however, at least two areas where progress on CV winds using IUE can be anticipated. The first is more comprehensive phase-resolved observations of wind-emitting CVs sampling a variety of inclination angles; these could be done in conjunction with simultaneous X-ray and optical observations to further refine our ideas about the location and geometry of the wind. The second area is more detailed studies of correlated changes in the radiation field with changes in the line profiles: dwarf novae represent the best candidates for this investigation because of their frequent changes in luminosity. The nature of the underlying photoionizing spectrum could be elucidated in this way.

This research is supported by the U.S. Dept. of Energy and the U.K. Science and Engineering Research Council.

REFERENCES

1. Córdova, F.A., and Mason, K.O. 1982, Ap.J., 260, 716.
2. _____ 1983, in Accretion Driven Stellar X-ray Sources, eds. Lewin, W.H.G., and Van den Heuvel, E.P.J. (Cambridge University Press: Cambridge), p. 147.
3. _____ 1984, Ap.J., submitted.
4. Friedjung, M., Andrillat, Y., and Puget, P. 1982, Astron. Astrophys., 114, 351.
5. Greenstein, J.L., and Oke, J.B. 1982, Ap.J., 258, 209.
6. Guinan, E.F., and Sion, E.M. 1980, NASA Conf. Publ. 2171, p. 471.
7. _____ 1980, NASA Conf. Publ. 2171, p. 477.
8. Hassall, B.J.M., Pringle, J.E., Schwarzenberg-Czerny, A., Wade, R.A., and Whelan, J.A.J. 1983, M.N.R.A.S., 203, 865.
9. Holm, A.V., Panek, R. J., and Schiffer III, F.H. 1982, Ap.J., 252, L35.
10. Kallman, T.R. 1983, Ap.J., 272, 238.
11. Klare, G., Krautter, J., Wolf, B, Stahl, O., Vogt, N., Wargau, W., and Rahe, J. 1982, Astron. Astrophys., 113, 76.
12. King, A.R., Frank, J., Jameson, R.F., and Sherrington, M.R. 1983, M.N.R.A.S., 203, 677.
13. Krautter, J., Klare, G., Wolf, B., Duerbeck, H.W., Rahe, J., Vogt, N., and Wargau, W. 1981, Astron. Ap., 102, 337.
14. Mayo, S.K., Wickramasinghe, D.T., and Whelan, J.A.J. 1980, M.N.R.A.S., 193, 793.
15. Szkody, P. 1982, Ap.J., 261, 200.

Fig. 1 Three of these IUE spectra of the dwarf nova AB Dra were taken during the course of a single outburst in 1982. The faintest spectra were taken during quiescence (bottom plot), and far down on the decline of an earlier outburst in 1979, and show only emission lines. As the spectrum brightens and steepens, the lines develop shortward-shifted absorption profiles. C IV also has enhanced emission, giving it the appearance of a P Cygni profile. The disk in AB Dra is probably viewed at a low inclination.

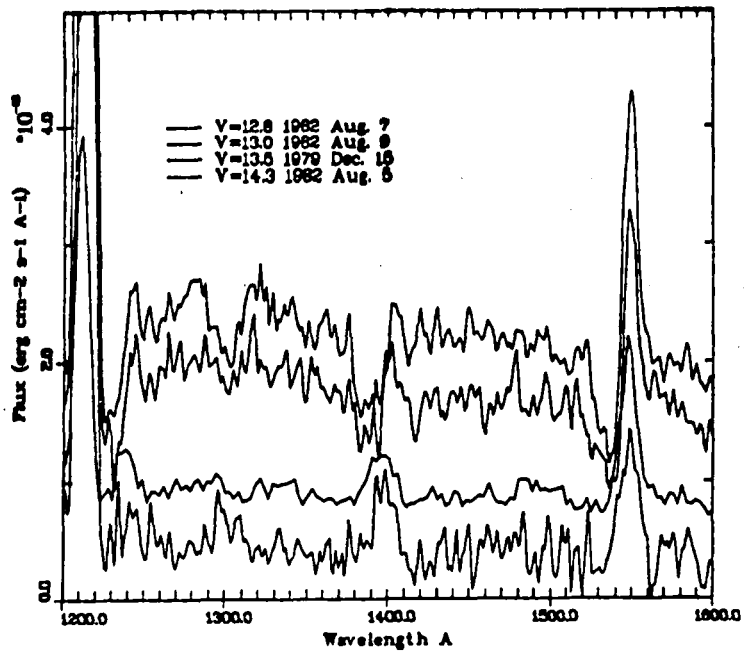

AB Dra
Montage of Spectra in various Outburst States

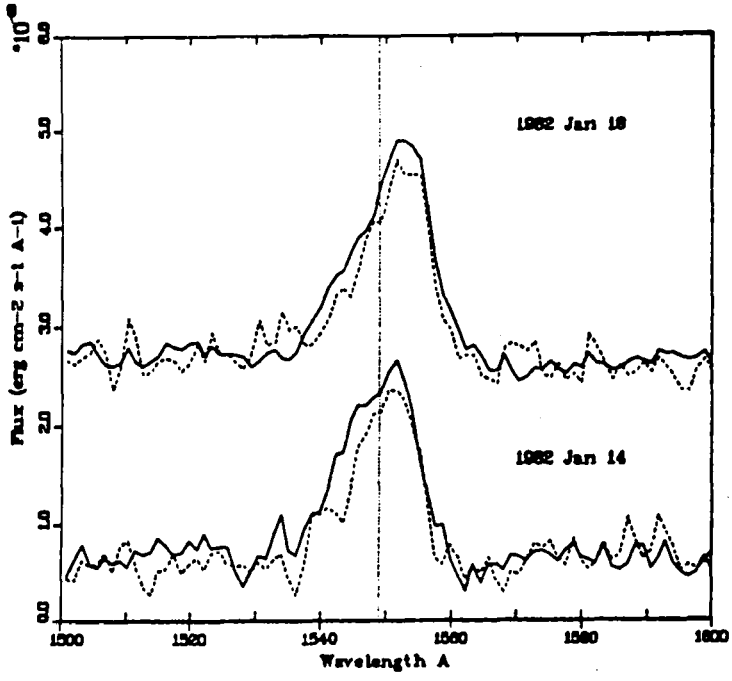

RW Tri CIV Line
broken line : in eclipse
solid line : out of eclipse

Fig. 2 The eclipsing, novalike variable RW Tri is viewed at a high inclination, i.e., along the plane of the accretion disk, and shows emission lines with no absorption below the continuum. The peaks of the lines appear to be shifted longwards of the line centers, suggesting an expanding wind. Each plot represents the average of several spectra taken on the day indicated. The top plot has been offset by 20 units for clarity. An additional offset has been added to the eclipse continuum in both plots in order to compare the relative line fluxes. The fact that there is little difference in the emission in and out of eclipse indicates that the wind is extensive.

Table 1: Comparison of Wind Parameters

Object	$\frac{\text{Log } \dot{m}}{(M_\odot\ yr^{-1})}$	$\frac{v_\infty}{(x\ 10^3 km\ s^{-1})}$	$\frac{\text{Log } L_{bol}}{(L_\odot)}$	$\text{Log}\left(\frac{L_x}{L_{bol}}\right)$	$\text{Log}(L_{wind}/L_{bol})$	$\frac{\text{Log}(mv_\infty)}{(gm\ cm\ s^{-2})}$	$\frac{\text{Log}(L_{bol}/c)}{(g\ cm\ s^{-2})}$
Sun	-14	0.5	0	-5	-6.7	19.5	23
OB	-6,-5 (Of) -8,-7 (O)	2-4	4.5-6.5	-5	-4,-3	26-29	27-29
WR	-4.6	2	5.4	-7	-1.2	29.5	28.5
Red SG	-8	0.1	2	---	-4	24.8	25
Red G	-6	0.02	4.7	---	-6.3	26.1	27.8
CVs	-11,-10	3-5	0-1.3	-2,-4	-2	24-25	24

ULTRAVIOLET SPECTROSCOPY OF THE INTERACTING BINARY U SAGITTAE

George E. McCluskey, Jr.
Division of Astronomy
Department of Mathematics, Lehigh University

and

Yoji Kondo
Laboratory for Astronomy and Solar Physics
Goddard Space Flight Center

ABSTRACT

The interacting Algol-type binary U Sagittae (B8 V + G2 III-IV) has been observed with the International Ultraviolet Explorer (IUE). Eleven high resolution spectra in the far-ultraviolet and nine high resolution spectra in the mid-ultraviolet were obtained during one orbital cycle in June 1983. The resonance lines of Si IV and C IV are present in absorption of moderate strength at all observed phases. The resonance lines of N V are probably present at several phases. The presence of Si IV and C IV indicates the existence of regions considerably hotter than a normal B8 V photosphere and which are visible at all of the observed phases. The existence and behavior of these features suggests that a hot "pseudo-photosphere" is created around the B8 star by matter flowing from the G-type companion.

1. INTRODUCTION

The eclipsing binary U Sagittae = HD 181182 (B8 V + G2 III-IV) is a typical Algol-type system with a period of 3.38 days. Struve (1949) and McNamara (1951a) have made extensive spectroscopic studies while McNamara and Feltz (1976) have derived the photometric elements.

Struve (1949) noted that from the beginning of the primary eclipse at phase 0.92 until phase 0.97, many lines narrowed and deepened such that the equivalent widths remained approximately constant. However, from phase 0.97 until totality at phase 0.99 the lines increase in width and weaken. He explained this in part as due to decreasing rotational broadening as the B-star is eclipsed. He estimated the rotational velocity of the B-star to be 100 kms^{-1} while the synchronous velocity would be 63 kms^{-1}. Levato (1976) gives 76 kms^{-1} for the observed rotational velocity of the B-star.

Struve (1949) analyzed the complex behavior of the Balmer lines and postulated the existence of extensive gas streams around the B-star originating from the G-star.

McNamara (1951a) also found the Balmer lines to be affected by gas streams and noted rapid velocity variations at several phases. Emission lines were discovered just before totality by McNamara (1951b). They were evidently not present during the investigations of Struve (1949).

These studies all indicate that U Sge is an active Algol system. For this reason the system was observed with IUE as part of our general program of investigation of interacting binaries.

2. OBSERVATIONS

In 1980, four high resolution LWR and four high resolution SWP exposures of U Sge were obtained. The presence of Si IV and C IV absorption lines and of non-orbital velocities indicated that a more extensive investigation was warranted. In 1983, a total of twenty high resolution spectra of U Sge were obtained during one orbital cycle. In all, observations near phases 0.05, 0.26, 0.35, 0.49, 0.61, 0.65, 0.76 and 0.78 were obtained.

3. DISCUSSION

The most striking features in the spectra of U Sge are the Si IV and C IV resonance doublets which are present in absorption at all of the observed phases. At phases 0.049, 0.063, 0.613, 0.641, 0.759 and 0.782 one or both of the N V resonance doublet lines are tentatively identified with weak absorption features. In addition, lines of Al II, Al III, C II, Fe II, Fe III, Mg II, Mn II, Ni II, Si II, Si III, and Zn II are present. No significant emission was detected in any of the spectra.

During the partial phases of primary eclipse Struve (1949) observed a deepening and narrowing of some spectral lines as discussed above. This same effect is clearly seen in many lines at phase 0.063 and even more strongly at phase 0.049. Numerous lines of Fe II with widths of 0.3 - 0.6A and residual intensities of 0.6 - 0.7 which are essentially undetectable outside of eclipse are easily seen at phase 0.049. Outside of eclipse the residual intensities of the Si IV, C IV and Al III doublets are approximately 0.48, 0.54, and 0.42, respectively, while at phase 0.049 the corresponding values are 0.20, 0.19 and 0.16. The residual intensities are relatively constant outside of eclipse, although the lines appear to strengthen slightly near phase 0.77.

No significant change in the equivalent widths occurs at any phase with the exception that at phase 0.257, observed in 1980, the Si IV, C IV and Al III lines were distinctly weaker.

With regard to radial velocities, all of the lines follow the motion of the B-star closely with the exception of the putative N V lines. At phases 0.641 and 0.759 the N V lines have more positive velocities than the B-star by 50-150 kms^{-1}. All other lines tend to have a slightly more negative velocity at all phases than the B-star. For example, not using phase 0.257 which is peculiar, the average deviation over all phases of the line velocity from the orbital velocity of the B-star is -24 kms^{-1} for Si II, -21 kms^{-1} for Si IV, -22 kms^{-1} for Al III and -28 kms^{-1} for C IV. The phase dependence of this behavior is minimal with somewhat smaller deviations occurring near phases 0.35 and 0.50 and larger deviations elsewhere.

At phase 0.257 the velocities of the Si IV and C IV, lines deviate by -50 to -100 kms^{-1}. Unfortunately, no observations near this phase could be obtained in 1983 so that it is not known if this peculiar behavior is persistent.

The Fine Error Sensor (FES) measurements show that the system was about $0^m.10$ brighter near phases 0.35 and 0.65 than at phase 0.75. A secondary minimum of depth $0^m.05$ with respect to phase 0.75 was detected at phase 0.50.

Ultraviolet light curves were generated at various wavelengths by measuring continuum intensities in line free regions. All intensities were normalized to phases 0.759 (SWP) or 0.764 (LWR). No significant wavelength dependences were found. The partial primary eclipse intensities are as expected from ground-based solutions. Outside of this eclipse we find average intensities of 1.00, 0.95, 0.96 and 1.00 near phases 0.35, 0.50, 0.65 and 0.75, respectively. It appears that the system exhibited an extended "secondary minimum" from phases 0.49 - 0.66 in 1983. The 1980 observations are consistently fainter than the 1983 data by 2-5%. This may be due to some systematic change in the IUE system for which we have not yet corrected.

The existence of Si IV, C IV and N V lines in the ultraviolet spectra of various Algol binaries is well known (Kondo et al. 1979, 1981; McCluskey 1982; Polidan and Peters 1982; Plavec 1983). Similar superionization is seen in numerous Be stars. The energy source for this ionization in Algol systems is generally attributed to matter from the subgiant accreting onto the early-type star.

The spectra of U Sge show that the heated region is closely associated with the B8 V primary and probably is visible at all phases. The velocities and widths (FWHM $\sim$ 1.5Å outside of eclipse) of the Si IV and C IV lines make it seem unlikely that they are formed in an extensive disk since these values are close to those of ions of Si II, Al II, Fe II and Si III which presumably arise in, or very close to, the photosphere of the B8 star.

It would appear that a relatively hot (20,000-100,000K) region lies around the B-star, at least in the equatorial regions, not far above the photosphere. This region is essentially transparent except in the resonance lines where it is semitransparent. Whether we call this a "pseudo-photosphere" or transition region is really a matter of definition at this time. High spatial and time resolution spectroscopy during the primary eclipse will be required to construct a detailed model.

The narrowing and deepening of lines during the partial phases of the primary eclipse may be due in part to a decreasing rotational broadening as the B-star is eclipsed. However, this is probably not the main effect as only about 1/5 of the B-star is covered at phase 0.049. Struve (1949) noted that this effect had been observed in several Algol binaries in which it appears that the broadening of lines occurs near the limb of the hot star while near the center of the disk the lines are sharp. This might be due to the distribution and observing geometry of the accreting matter.

4. CONCLUSION

The interacting binary U Sge is in a state of active mass flow. No high velocity (> 50 kms^{-1}) components are observable for any lines with the possible exception of N V and no detectable emission occurred outside of totality. The ultraviolet absorption spectrum arises primarily in a "pseudo-photosphere" close to the surface of the B-star. The line forming region may be expanding at 20-30 kms^{-1} and surrounds the entire B-star. The physics of this line forming region would seem to be similar to that occurring in numerous Be stars (e.g., Slettebak and Carpenter 1983) which show very similar lines due to superionization of Si IV and C IV.

We thank the US IUE project team for their competent assistance in obtaining the data. One of the authors (G.E.M.) was partially supported in this research by NASA Grant NSG 5386.

REFERENCES

Kondo, Y., McCluskey, G.E., and Stencel, R.E., 1979, Ap. J., 233, 906.

Kondo, Y., McCluskey, G.E., and Harvel, C.A., 1981, Ap. J., 247, 202.

Levato, H., 1976, Ap. J., 203, 680.

McNamara, D.H., 1951a, Ap. J., 114, 513.

McNamara, D.H., 1951b, P.A.S.P., 63, 68.

McNamara, D.H. and Feltz, K.A., Jr., 1976, P.A.S.P., 88, 688.

McCluskey, G.E., 1982, in Advances in Ultraviolet Astronomy, ed. Y. Kondo, J.L. Mead, and R.D. Chapman (NASA Conf. Pub. 2238), p. 102.

Plavec, M.J., 1983, Ap. J., 275, 251.

Polidan, R.S. and Peters, G.J., 1982, in Advances in Ultraviolet Astronomy, ed. Y. Kondo, J.L. Mead, and R.D. Chapman (NASA Conf. Pub. 2238), p. 534.

Slettebak, A. and Carpenter, K.G., 1983, Ap. J. Suppl. 53, 869.

ULTRAVIOLET OBSERVATIONS OF CIRCUMSTELLAR MATTER IN ALGOL TYPE BINARY SYSTEMS

Geraldine J. Peters
Department of Astronomy
University of Southern California

Ronald S. Polidan
Lunar and Planetary Laboratory
University of Arizona

ABSTRACT

Properties of four components to the circumstellar matter in Algol type interacting binary systems which have been investigated with the aid of timed high resolution IUE observations are discussed. Included are the high temperature accretion region (HTAR), gas stream, restricted domains of material outflow, and the general wind. In particular, we comment on the geometrical distribution in the system, physical conditions, flow patterns, and stability. CX Dra serves as our illustrative example and a model for the circumstellar matter in this system is presented.

INTRODUCTION

Since the far ultraviolet spectral region contains numerous resonance lines from abundant ions and absorption lines from these ions can be detected even if the column density of matter is relatively low, spacecraft observations of Algol type binaries have produced a wealth of information on the nature and behavior of the circumstellar matter (CM) in these systems. Accordingly, we have employed timed high resolution IUE observations of selected systems in order to investigate the geometrical distribution, flow patterns, physical conditions, and stability of this material. Some components to the CM include the high temperature accretion region (HTAR), gas stream, apparent narrow domains of mass outflow, the general wind, and disk. In this paper, we present selected results from our analyses of absorption lines formed in all but the latter of the above mentioned components to the CM. Systems considered in the study are CX Dra (B2.5Ve + F:), AU Mon (B5V + F-G:), U CrB (B6V + F8III-IV), TX UMa (B8V + F8III), and RS Vul (B5V + G0:). CX Dra, a Be binary which appears to be a counterpart to classical Algol systems, will serve as our illustrative example in this short presentation.

THE HIGH TEMPERATURE ACCRETION REGION (HTAR)

The HTAR was discovered from the (variable) presence of strong absorption lines of N V, C IV, and Si IV in the spectra of Algol primaries whose photospheres are much too cool to form such ions. The properties of this region, which has been found in all of the above mentioned systems, is discussed in detail in Peters and Polidan (1984). The observed radial velocity behavior

and phase dependence in the strengths of the lines formed in the HTAR provide compelling evidence that this region is associated with the primary and the source of the heating is the shock from the impact of the gas stream onto the photosphere. The latter is supported by the fact that the HTAR is observed only about primaries whose radii are larger than ϖ_{min} (Lubow and Shu 1975). To illustrate the observed behavior of features formed in the HTAR, consider selected profiles of N V, C IV, and Si IV seen in CX Dra (Figure 1). We see variations with phase as well as with time. A pair of observations secured at the same phase (≈0.6) but four cycles apart demonstrate that the HTAR can fade on a time scale of days-months. Observations of CX Dra as well as other systems (Peters and Polidan 1984) show the strong phase dependence of the HTAR. Generally speaking, the lines formed in the HTAR tend to be strongest between phases 0.4 to 0.9 (on the hemisphere of the star receiving the gas stream impact. The sometimes observed large line depths (Figure 1) imply that the HTAR has substantial thickness perpendicular to the orbital plane($\gtrsim R_p$). Using an ionization equilibrium code, we have found that the HTAR lines are formed in a collisionally dominated region of $T_e \sim 100{,}000$K and $N_e \sim 10^9$ cm^{-3}. We find evidence of extreme carbon depletion (note the observed weakness of the C IV lines compared with the N V line), $C \sim 10^{-3} C_\odot$, which suggests that the gas in the HTAR is composed of matter that has been processed by the CNO cycle in the core of the transformed secondary. Since the HTAR lines often are broader than photospheric features, it appears that the HTAR is not in co-rotation with the accreting component. Mass motion and turbulence are probably responsible for

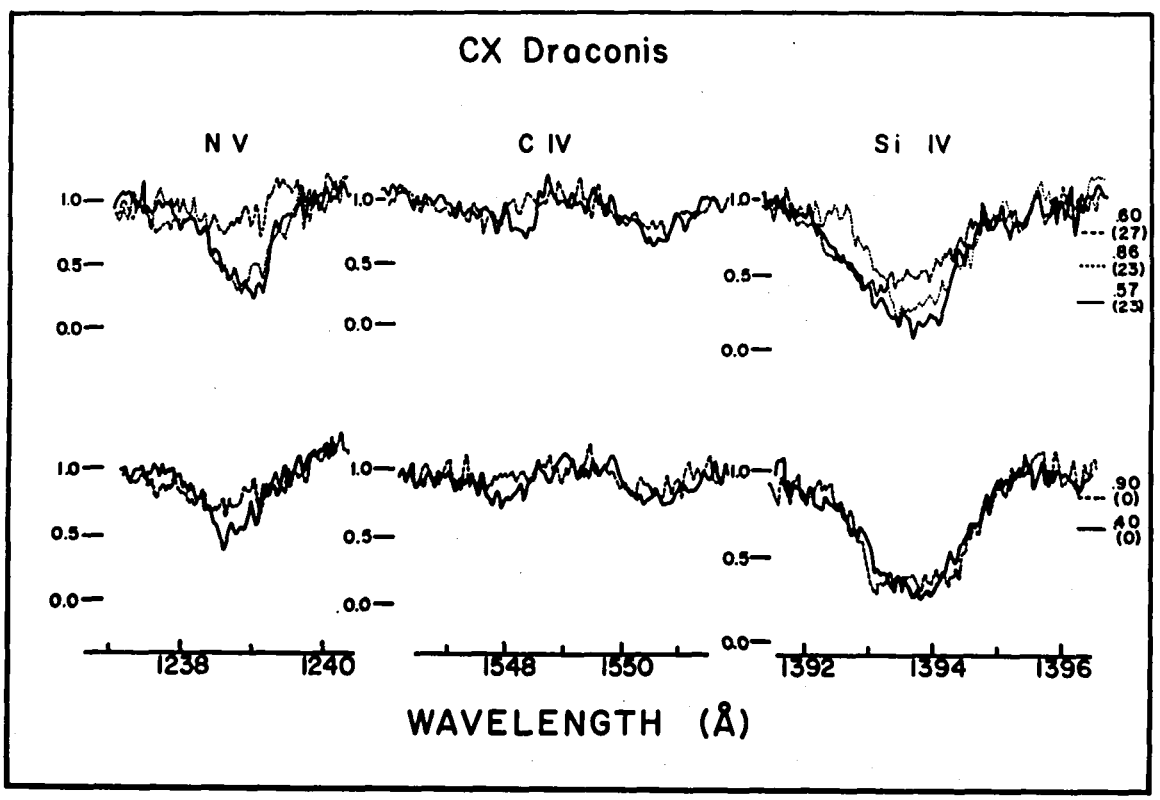

Fig. 1 - Observed profiles of selected features formed in the HTAR in CX Dra versus phase (noted on right; cycle numbers in parentheses).

the line broadening. The role of turbulence, which could be the source of the collisional ionization, is discussed in Peters and Polidan (1984).

THE GAS STREAM

Gas streams are usually detected from the presence of red-shifted absorption components to the resonance lines of abundant species. Both intermediately (i.e. Mg II, Si II) and more highly ionized species (i.e. Si IV, Al III) are observed. In general, one observes these features between phases 0.8 - 0.9, but in certain systems (i.e. AU Mon), such absorption is unexpectedly weak. Examples of typical gas stream features are shown in Figure 2. One might get the impression that reliable mass transfer rates can be deduced from the observed "extra" redward absorption but problems abound. To mention two, we are uncertain about the projection of the gas stream along our line of sight but, more important is the fact that the gas stream most likely does not cover the entire stellar surface. Measured column densities tend to yield unreasonably low mass transfer rates. Shallow, broad gas stream lines such as one observes in TX UMa (Peters and Polidan 1984) are probably saturated features formed in a geometrically small domain and the observed depths of these lines can be used to estimate the fractional coverage of the photosphere. There is some evidence of variability in gas stream features over a time scale of hours, which suggests possible clumpiness to the streams, but this must be confirmed with future observations. The more highly ionized gas stream lines could be formed in regions of collisional ionization and their presence/strength could be correlated with the instantaneous rate of mass transfer.

RESTRICTED DOMAINS OF MATERIAL OUTFLOW

In several systems, we have seen curious evidence for mass loss over a restricted interval in phase. Violet-shifted absorption components are ob-

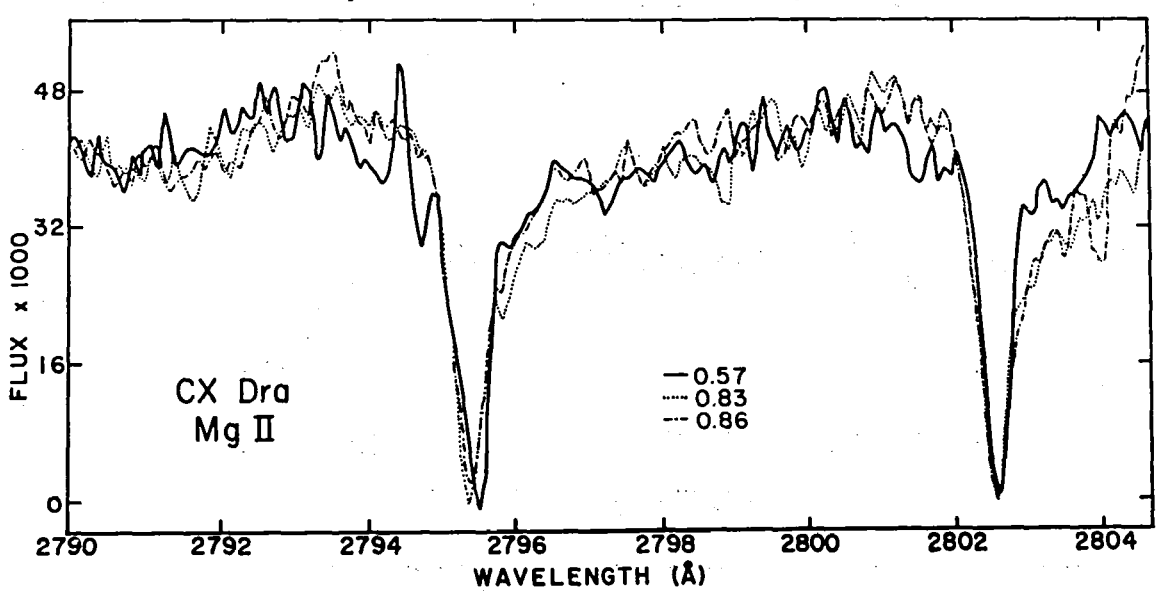

Fig. 2 - Gas stream components to the complex Mg II features in CX Dra are clearly seen near phase 0.85. Note the broad photospheric feature.

served to persist for only $0^p.1$ in phase or less and this mass loss is usually seen between phase 0.0 and 0.5. We recently observed high velocity (-700 km s^{-1}) components to Si III, IV of column density 10^{14} cm^{-2} in CX Dra at phase 0.24 but uncertainty in the path length precludes a reliable estimate of $\dot{M}$.

GENERAL WINDS

Winds are observed in Algol primaries and usually the mass flow is what we would expect from the star's spectral type. But the winds are highly variable with time and there is also some evidence for a phase dependence as illustrated in Figure 1 for CX Dra. From the Si IV profiles we see that the wind appears to be enhanced near the conjunction points but suppressed near phase 0.85. We also see a similar behavior in AU Mon.

CONCLUSIONS

IUE observations of the CM in CX Dra have suggested the model presented in Figure 3. We show the HTAR (with a radial extent of a few R_p) observed primarily between phases 0.4 and 0.9, the gas stream (seen from phase 0.8-0.9), and the domain of high velocity outflow. Through future observations it should be possible to ascertain whether the presence/strength of the HTAR is associated with an enhanced mass transfer rate and if the gas stream is clumpy. The nature of and cause for the directional outflow, seen near phase 0.24 in CX Dra, should be investigated further. This project has been supported in part by NASA NSG 5422.

REFERENCES

Lubow, S. H., and Shu, F. H. 1975, Ap.J., 198, 383.
Peters, G. J., and Polidan, R. S. 1984, Ap.J., 283 (in press).

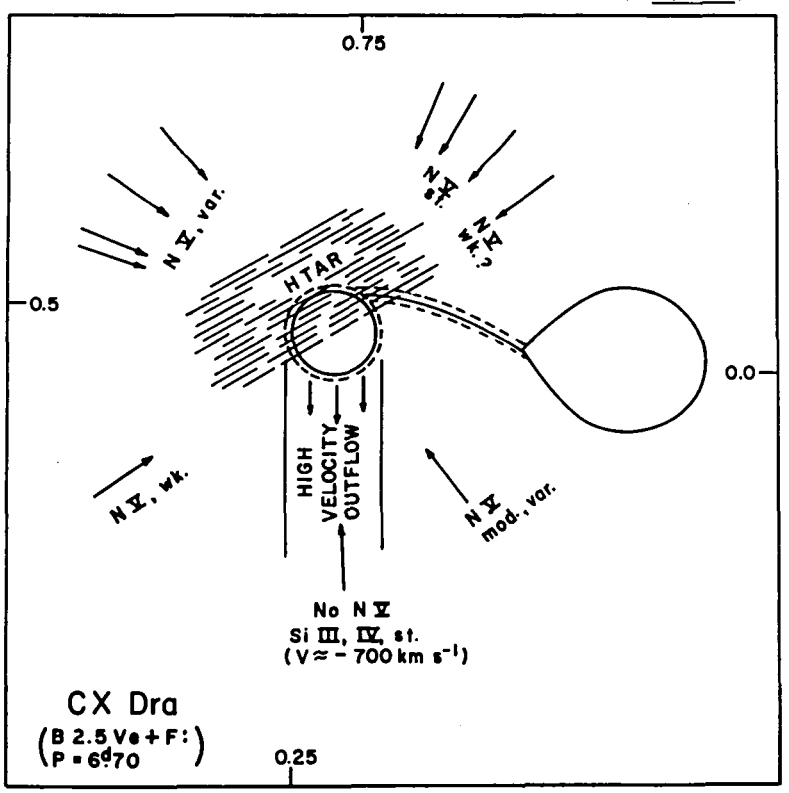

Fig. 3 - Model for the CM in CX Dra. Arrows indicate the lines of sight for our IUE observations. The gas stream (size ≃ ε) and the extent of the dense disk (Lubow and Shu 1975) are shown with the dashed lines.

THE ESSENCE OF BINARY STAR COALESCENCE - A COORDINATED GROUND-BASED PHOTOMETRIC AND IUE ULTRAVIOLET STUDY OF FK COMAE

J. D. Dorren, Institute of Physics and Astronomy
National Central University, Republic of China
and
E. F. Guinan, Department of Astronomy
Villanova University, Villanova, PA

INTRODUCTION

FK Comae (= HD 117555) is a rapidly rotating ~G5 giant (Walter et al. 1984 find: V sin i ≃ 200 kms^{-1}) which has very strong and variable chromospheric and transition region line emissions, similar in number and strength to those observed for the most active RS CVn stars (see Bopp 1982; Bopp and Stencel 1981 and references therein). It is also a variable star which has low amplitude, quasi-sinusoidal light variations with a period of ~2.40 days (Chugainov 1966; 1976). As in the case of RS CVn variables, these light variations have been modelled with dark star spots (e.g. Holtzman and Nations 1984; Dorren, Guinan and McCook 1984). In addition, energetic flare-like events (lasting from a few hours to days) have been observed spectroscopically (Walter and Basri 1982; McCarthy 1982) and photometrically (Morris and Milone 1983; Holtzman and Nations 1984; and Dorren, Guinan and McCook 1983, 1984).

The rapid rotation observed for FK Comae is most unusual for an evolved single star, since it would imply a main-sequence rotational velocity ($V \sin i > 1000$ kms^{-1}) that would exceed its breakup speed. However, detailed radial velocity observations fail to reveal that FK Comae is a close binary system (McCarthy and Ramsey 1983), which could account for its rapid rotation through tidal synchronization. Since radial velocity observations have failed so far to reveal any evidence that FK Comae is a close binary, Bopp and Stencel (1981) have suggested that the star was once a binary system that now has coalesced into a single, rapidly rotating star. The evolutionary models of Webbink (1976) suggest that W Ursae Majoris binaries coalesce after going through the contact stage of their evolution. Furthermore, Ramsey, Nations, and Barden (1981) have suggested that the very broad H-alpha feature observed in FK Comae originates in the excretion disk expected in Webbink's scheme.

On the other hand, Walter and Basri (1982) propose that FK Comae is a terminally evolving Algol-type (high mass ratio: $q \simeq 1/20$) binary system in which the giant star is still accompanied by a Roche-filling companion of very low mass. In this model the line emissions as well as the light variations are produced by the effects of gas streaming from the low mass object on the visible star. In the most recent version of this model, Walter et al. (1984) propose that FK Comae evolved from a binary with an initial total mass of 5-6 $M_\odot$ which now consists of stars with masses of 4 $M_\odot$ and 0.2 $M_\odot$ and with radii of 6 $R_\odot$ and 2.8 $R_\odot$, respectively. The constraint on the system masses is obtained from the requirement that the core of secondary not be degenerate (since then it would be visible at UV wavelengths - contrary to what is observed).

DISCUSSION OF THE OBSERVATIONS

Multi-bandpass photoelectric observations of FK Comae have been carried out at Villanova University Observatory since March 1982. Additional photometry was obtained at KPNO during May-June 1983. The photometry obtained during 1982 indicated that systematic changes in the shape and amplitude of the light curve as well as the photometric period occur over a few months (see Dorren, Guinan, and McCook 1984). As shown in Fig. 1, the red (λ6600) light curve of the star obtained during the June-August 1983 is characterized by a small light amplitude of $\sim$0.06 mag (and $\sim$0.08 mag at λ4500), while the light curve obtained about six months later during the Winter of 1984, has a larger light amplitude of $\sim$0.12 mag in red (and $\sim$ 0.20 mag at λ4530). The photometric phases were computed with the light elements of Rucinski (1981):

$$T_{MIN} = \text{HJD } 2442192.345 + 2^{d}.400 \cdot E \qquad (1).$$

The cyclic nature of the light curve changes is illustrated in Fig. 2, in which the light amplitudes at blue wavelengths are plotted against time. As shown in the figure, the light amplitude appears to vary cyclically between $\sim 0^{m}.08$ and $\sim 0^{m}.22$ with a characteristic time-scale of 1.0 - 1.3 yrs. Preliminary modelling of the light curves over this interval indicates that variations in the light amplitude arise chiefly from latitudinal changes of the spot forming regions on the star's surface. In accord with the results of our analysis of the 1982 light curves, the present light curves were modelled with two spots about 800 K cooler than the surrounding photosphere and which cover about 10-15% of the star's visible hemisphere.

Ultraviolet observations of FK Comae were obtained with the IUE on 27 and 28 July 1983 (at photometric phases $\sim$0.04P and $\sim$0.48P, respectively) also on 14 and 15 March 1984 (at photometric phases $\sim$0.37P and $\sim$0.78P respectively). Spectra were secured on these dates with both the shortwave (SWP :$\lambda\lambda$1150-2000) and longwave (LWR + LWP :$\lambda\lambda$2000-3200) cameras. In addition, careful measurements of the optical brightness of the variable were made with the Fine Error Sensor (FES) on board the satellite. The FES measures of FK Comae were made differentially relative to the comparison (HD 117567) and check (HD 117876) star used in the ground-based photometric program and the transformed differential FES magnitudes are plotted (as triangles) in Fig.1 . The phases over which the IUE spectra were secured are also shown in the figure. Although the IUE observations obtained on 27 and 28 July were scheduled near the expected times of minimum ($\sim$0.0P) and maximum ($\sim$0.5P) of the light variation, it appears that during July 1983 the minimum and maximum brightness occurred near $\sim$0.80P and $\sim$0.30P, respectively. Because of the apparent shift in phase of minimum, and maximum light (and also because of the low light amplitude during July 1983), the IUE spectra were obtained at times when the star had nearly the same optical brightness ($\bar{V}$ (FES) = + $8^{m}.22$ on 27 July 1983; $\bar{V}$ (FES) = + $8^{m}.23$ on 28 July 1983). This was contrary to what had been planned when scheduling the observing dates two months earlier. Although the optical brightness of the star was nearly the same on 27 July and 28 July, the IUE spectra obtained on these days were significantly different. As shown in Fig. 3, the emission line fluxes on 28 July are on the average about 1.4 - 1.6 x greater than observed on the previous day. The Mg II h + k line emission also changed by about the same amount between the two days. However, during March 1984, IUE spectra were secured near the extrema of the large amplitude light curve. On March 14 (at 0.37P; V (FES) = + $8^{m}.18$) the

UV line fluxes were about the same as observed on 27 July 1983 while on 15 March (at 0.78P; V (FES) = + $8^{m}.28$), the UV emission line fluxes were about the same as observed on 28 July 1983. A preliminary examination of the spectra available in the IUE archives (including the spectra published by Bopp and Stencel 1981), reveals no definite correlation between the overall UV emission line strength with photometric phase, brightness or light amplitude. If there is a phase correlation, it is masked by what appears to be frequent flare-like enhancements in the UV emission line strengths. These random variations in the UV emission lines are probably related to the enhancements observed at visible wavelengths in the H-alpha line and in the continuum (e.g. see Dorren, Guinan and McCook 1984).

CONCLUSIONS

Although the photometry and UV observations do not rule out the existence of a low mass companion for FK Com, they do diminish or eliminate, however, the need for such a companion to explain the light variations and the origin of the intense emission features. We conclude that the light variations, the strong chromospheric and transition region line emissions, and the apparently frequent and random flare-like events that occur in the UV and visible regions are manifestations of extreme surface activity. These phenomena most likely arise from energetic magnetic fields generated by a powerful dynamo, which is driven by the star's rapid rotation and maintained by its deep convection zone. The level of surface activity observed for FK Comae is consistent with that expected from the period-activity relations found for the chromospherically active RS CVn variables (Bopp and Stencel 1981).

Considering the apparent frequent occurrence of flare-like events and its rapid rotation and low surface gravity, we speculate that there may be significant non-uniform mass outflows from the star. The asymmetries reported in the emission line profiles by Walter and Basri (1982), Ramsey, Nations and Barden (1983), and Walter et al. (1984) could be due to large mass outflows occurring, perhaps preferentially, from active sites on the star's surface. The inferred large mass loss combined with magnetic breaking could cause the star to lose its angular energy at a very rapid rate. If this is so, then it could spin down at a rapid rate and then be spectroscopically indistinguishable from a normal field grant. From this we conclude that this stage of binary-star evolution may be very short, making these kinds of objects extremely rare.

ACKNOWLEDGEMENTS

We wish to thank the IUE staff at GSFC for their help in obtaining and reducing the UV observations. We also wish to thank the following students at Villanova University for obtaining photometric observations: E. Dombrowski, R. Donahue, S. Draus and S. Wacker. We gratefully acknowledge the support of this research from NASA through grant NAG 5-382 to Villanova University. The manuscript was prepared for publication by C. F. McMenamin.

REFERENCES

Bopp, B. W. 1982, in the Second Cambridge Workshop on Cool Stars, Stellar Systems, and the Sun, M. S. Giampapa and L. Golub, eds.; SAO Special Report 392, p. 207.

Bopp, B. W. and Stencel, R. E. 1981. Ap. J. 247, L. 131.

Chugainov, P. F. 1966 Inf. Bull. Var. Stars, No. 172.

Chugainov, P. F. 1976, Izv. Krymskoj Astrof. Obs. 54, 89.

Dorren, J. D., Guinan, E. F. and McCook, G. P. 1983. Inf. Bull. Var. Stars, No. 2276.

Dorren, J. D., Guinan, E. F. and McCook, G. P. 1984. Publ. Astron. Soc. of Pacific (in press).

Holtzman, J. A. and Nations. H. L. 1984, Preprint.

McCarthy, J. K. 1982. B. S. Senior Thesis, Penna. State University.

McCarthy, J. and Ramsey, L. W. 1982. Bull. A.A.S. 14, 780.

Morris, S. L. and Milone, E. F. 1983, Publ. Astron Soc. of Pacific 95, 376.

Ramsey, L. W., Nations, H. L. and Barden, S. C. 1981, Ap. J. 251, L 101.

Rucinski, S. M. 1981, Astron. Astrophys. 104, 260.

Walter F. M. and Basri, G. 1982, Ap. J. 260, 735.

Walter, F. M., Neff, J. E., Bopp, B. W. and Stencel, R. E. 1984, in Third Cambridge Workshop on Cool Stars, Stellar Systems, and the Sun, S. L. Baliunas and L. Hartman eds., Springer-Verlag (in press).

Webbink, R. 1976, Ap. J. 209, 829.

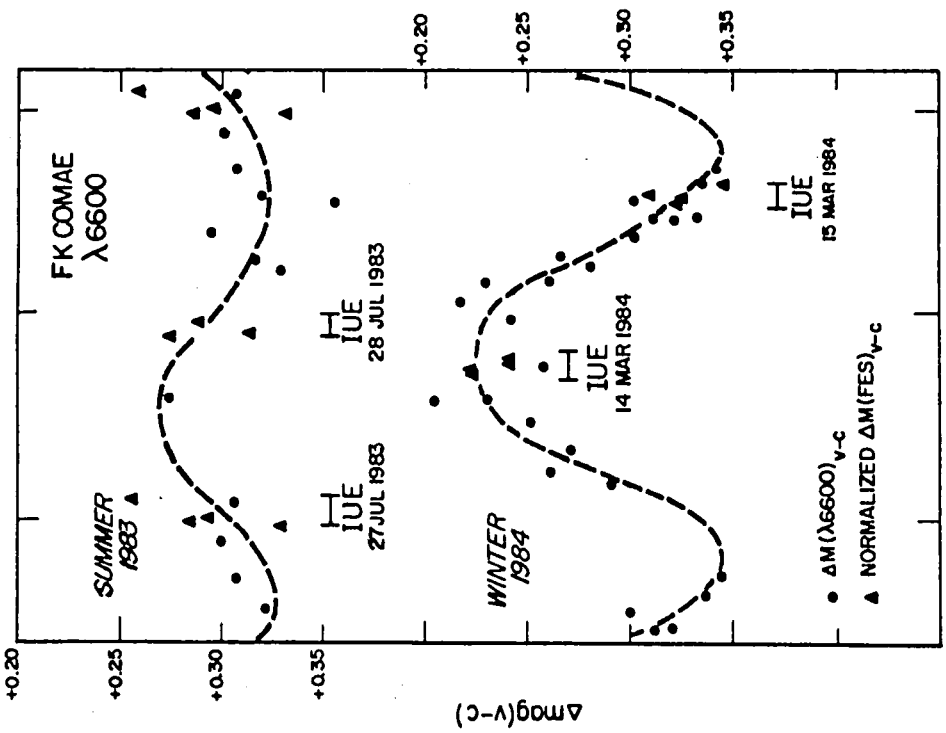

Fig.1. The light curves of FK Comae obtained during June-Aug. 1983 (upper panel) and during Dec.1983-Mar.1984 (lower panel). The phases over which IUE observations were obtained are indicated in the figure along with the differential magnitudes obtained with the FES. The light curves have been modeled with dark spots on the rotating star.

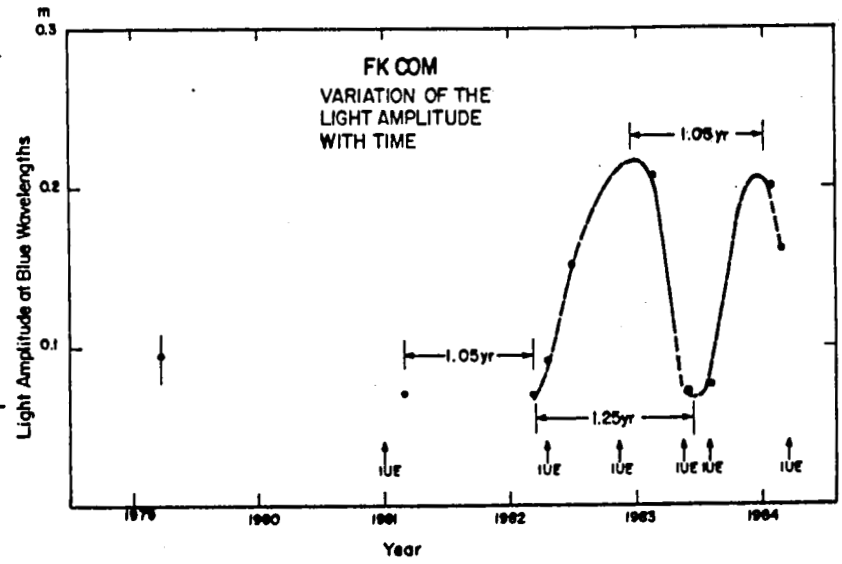

Fig. 2. The variation of the (blue) light amplitude of FK Comae with time. The variation appears to be cyclic having a characteristic time-scale of about 1-1.3 years. Analysis of the light curves with the star-spot model indicates that the amplitude variations arise chiefly from systematic variations of the latitudes and longitudes of the spot groups on the star's surface.

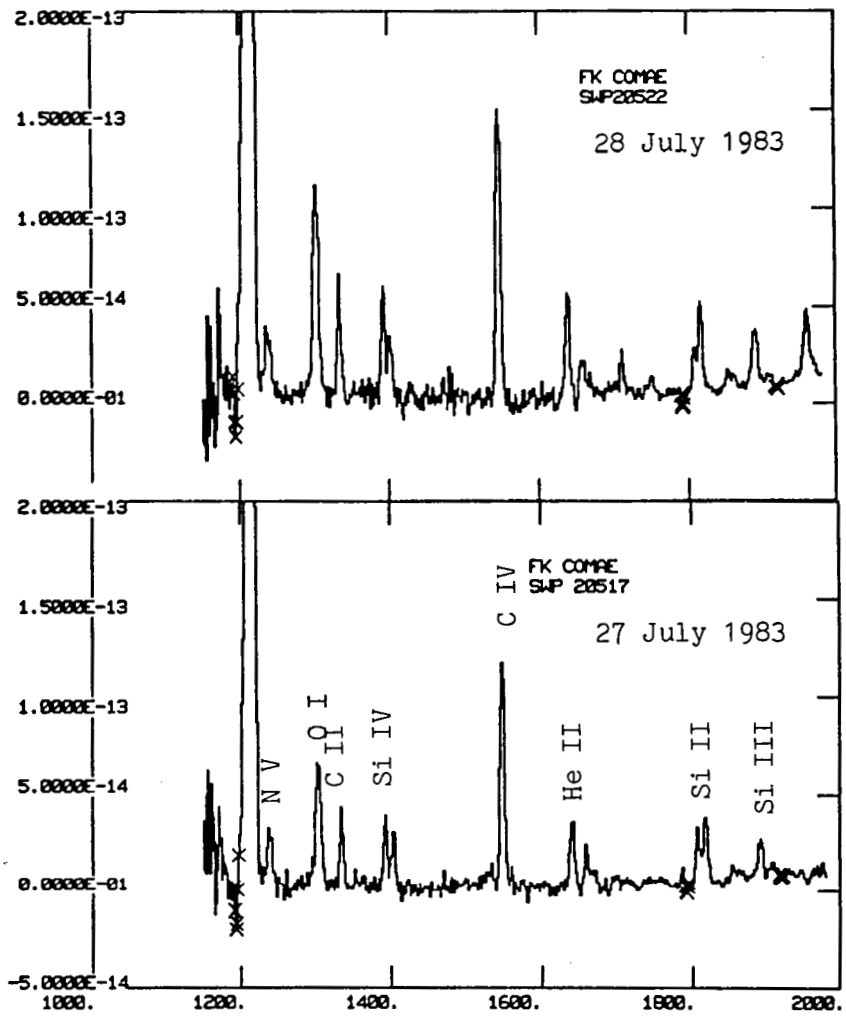

Fig. 3. The observed monochromatic fluxes (in units of ergs cm^{-1} s^{-1} A^{-1})of FK Comae. The lower panel shows the FUV spectrum obtained with the SWP camera on 27 July 1983,near photometric phase 0.04P. The upper panel shows the FUV spectrum of FK Comae obtained on 28 July 1983 ,near phase 0.47P. The strongest emission lines are identified in the figure.Although the optical brightness of the star was essentially the same on these two days, the FUV emission line fluxes varied by 1.4-1.6x between the two dates.

STRANGE F + Be BINARY STAR SYSTEMS

Sidney B. Parsons
Astronomy Programs, Computer Sciences Corporation

Bernard W. Bopp
Department of Physics and Astronomy, University of Toledo

and
Yoji Kondo
Laboratory for Astronomy and Solar Physics, Goddard Space Flight Center

ABSTRACT

IUE spectra of 5 stars with F or F + B optical spectra and strong Be-star-like H alpha emission have been obtained on several dates. No two exposures of the strange optical variable HD 37453 are quite alike, Mg II emission is strong, and the SWP region has some resemblance to known interacting binaries such as SX Cas. HD 43246 shows significant Si IV absorption against an otherwise normal late B spectrum. HD 166612 shows early B main-sequence spectral features except for evidence of a strong stellar wind. HD 207739, discovered in 1982 to show UV characteristics of a strongly interacting system, showed general brightening in the September observations, opposite to the visual flux which decreased slightly. The far-UV spectrum of HD 207739 was seen to evolve but to remain in between the two extremes seen in 1982, which differed greatly both in character and in absolute flux.

INTRODUCTION

Several star systems with F-type or composite F + B ground-based spectra are known to exhibit strong H-alpha emission. The H-alpha line profiles are being monitored in a program using KPNO facilities by Bopp, and profiles typical of Be stars are seen in most cases. One of these, HD 207739, was found by Parsons, Holm, and Kondo (1983) to have very strange UV characteristics, and an IUE program was undertaken to investigate these systems in the UV region and look for possible relationships.

SPECTROSCOPIC OBSERVATIONS

Five stars were oserved during 4 US1 and 2 US2 IUE shifts in September 1983. One set of high-dispersion spectra was obtained for HD 50820 (B3 pe

+ F n); these spectra look qualitatively like other early B main-sequence stars and have not been analyzed further to date. Samples of low-dispersion SWP spectra for other systems are illustrated in Figure 1.

HD 166612 (F e + B:) exhibits an SWP spectrum which is nearly normal in comparison to stars in the spectral type domain B0.5 V - B2 III. However, the Si IV and C IV features are deeper than normal, and there is an apparently double strong feature measured at 1235 and 1238 A (N V ?). These are most likely due to a strong stellar wind, but among "normal" stars such winds are found only in supergiants. The observed spectrum does not match those of supergiant stars.

HD 43246 (gF2e + B?) also exhibits consistently strong Si IV absorption, while otherwise the SWP spectrum resembles a normal main-sequence star of class around B8. Two high-dispersion LWR spectra show variation in the strong double-lobed Mg II emission profile. Bopp's H-alpha observations show slow changes of profile with time. HD 43246 is a known spectroscopic binary with period of 23.2 days. From K-line measurements by R.M. Petrie the hotter component has been estimated to have roughly twice the mass of the F star.

HD 37453 (F5 II + Be) was observed entirely at low-dispersion, but this is sufficient to show complex variation: no two spectra are quite alike, the flux varies on the order of 20%, but often different parts of the UV spectrum behave oppositely in terms of increasing or decreasing flux. There is always strong Mg II emission, and slight evidence for variation in its profile. The SWP region has a complex pattern of (primarily at least) absorption features similar to the out-of-eclipse spectra of SX Cas (Plavec, Weiland, and Koch 1982) and to HD 207739 (below). Recent optical observations by Bopp show dramatic variability: at one epoch the H-alpha profile had symmetrical double emission, very broad absorption wings, and little evidence of metallic absorption, whereas at epochs before and after, separated by many months, there was primarily an F-type spectrum with superimposed strong asymmetric, centrally reversed emission.

HD 207739 (F8 II + Be:) continues to be a puzzle. The September UV spectra show a general brightening and a corresponding evolution in spectral features intermediate between the two previous observations. The initial, very complex 17 February 1982 spectrum ("low") also resembles SX Cas out of eclipse, while the second epoch spectrum (5 October 1982, "high") qualitatively resembles early B-type giants with mild stellar winds (Parsons 1983). Five high-dispersion SWP exposures, including one at the "high" epoch, have now been taken to aid the interpretation of features seen. The only pronounced emission feature besides the Mg II 2800 doublet is very broad C II 1335 emission with black central absorption. Various ions from N V to Si II and Fe II show P Cygni profiles, with the absorption component normally dominant. Al II 1671 is a notable exception, having a prominent emission lobe on the redward side of the profile. H-alpha region observations continue to show a rotationally-broadened F-type spectrum with superimposed strong asymmetric, centrally reversed emission.

Originally we speculated that HD 207739 would have a binary period as short as 1 month, based on an F II star nearly filling its Roche surface. Recently R.F. Griffin has communicated to us numerous radial velocity observations between July 1983 and January 1984 and a preliminary orbital fit with period 140.8 days and eccentricity near zero. Other values obtained or collected by us, including two observations by W.I. Beavers, fit this well. The range in the cool component's velocity is from -83 to +55 km/s, a sin i = 190 solar radii, and the system's mass function is a large 4.8 solar masses. The hot object is then most likely the more massive; if the F star is really a bright giant with mass around 6, then the hot object has mass of order 12 solar masses. A lower mass ratio and hence greater mass for the F star would imply greater luminosity and account more easily for its domination of visible light.

OTHER OBSERVATIONS AND DISCUSSION

Recent KPNO photometry of HD 43246 by J.L. Africano shows about 0.1 mag variability in V, with a double sine curve suggesting ellipsoidal shape. HD 37453 shows photometric variability as well, but radial velocities are lacking, and no period is yet known. R.H. Bloomer has done extensive UBV photometry of HD 207739 between July and December 1983. The V magnitude shows roughly a double sine curve with respect to Griffin's period, with a range of about 0.2 mag, but with much fluctuation during the decline in light when the F-type component is going from being broadside to us towards being in front of the hot object. These are the phases during which the September IUE data were taken, showing increasing UV flux (and hence probably no eclipse of the hot component). The phases of the first two IUE epochs can now be found: the "low" state was with the system broadside, just before the phases of the September spectra, while the "high" state was when the hot component is closest to us.

A possible but not unique or definitive explanation for the HD 207739 observations is that gas streams or a disk partially obscure the hot object (probably early B type) at some times and that there is a hot region or "spot" with variable flux in between the two stars which comes into view after the broadside phase. The erratic behavior of HD 37453 and the mutual similarities with SX Cas indicate that it too is probably a closely interacting system.

REFERENCES

Parsons, S.B. 1983, Bull. A.A.S., 15, 619.

Parsons, S.B., Holm, A.V., and Kondo, Y. 1983, Ap.J., 264, L19.

Plavec, M.J., Weiland, J.L., and Koch, R.H. 1982, Ap.J., 256, 206.

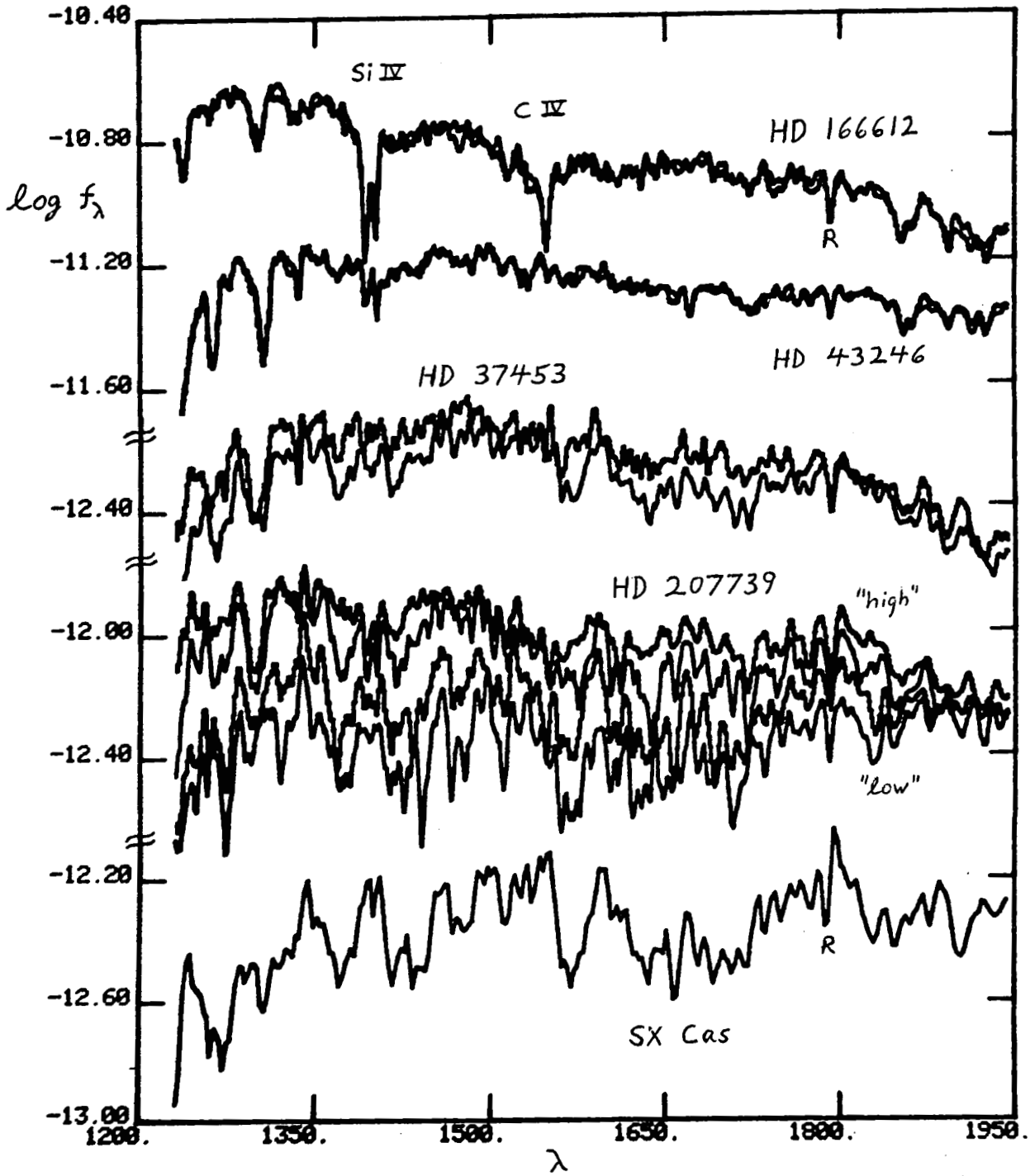

Figure 1. -- Far UV low-dispersion IUE spectra of unusual binary systems: from top to bottom, HD 166612 (16 and 23 Sep 1983), HD 43246 (21 and 23 Sep 83), HD 37453 (12 and 21 Sep 83), HD 207739 (5 Oct 82, 23 and 6 Sep 83, and 17 Feb 82), and SX Cas out of eclipse (SWP 2249).

MULTI-YEAR & POSSIBLY PERIODIC VARIATIONS IN THE UV SPECTRUM OF 56 PEGASI

Robert E. Stencel (NASA-HQ & JILA)
James E. Neff (A.P.A.S., Univ. Colorado), and,
Robert D. McClure (Dominion Astrophys. Obs.)

Abstract

Radical variations in the Mg II emission profile of the late type supergiant 56 Peg have been observed to occur during the course of five years of IUE operations. Pronounced and possibly periodic changes in asymmetry, emission relative velocity and photospheric radial velocity are reported. Implications for the study of cool star chromospheres and interacting binaries are discussed.

Introduction

Timescales in nature do not always conform to human attention spans, but thanks to the remarkable continuity of the IUE Observatory, we can report the discovery of significant ultraviolet spectral variability in the K supergiant star 56 Peg, with a 4 to 5 year characteristic timescale. One conceivable interpretation of the data is that 56 Peg is a binary in a dynamic stage of evolution. Alternately, an infrequent, flare-like event on a single star may have been observed.

As one of the few bright K type supergiants (Keenan classified 56 Peg as K0 IIp and noted its strong Ba II line), attention was drawn to it by G. Basri in connection with its unusual Ca II K line emission profile (cf. Linsky et al. 1979). The K line more nearly resembles a solar plage than that of a mass losing red giant. Although systematic observations of the K line have not been pursued to date, observations by the first author and others suggest no significant K line profile changes over several years.

IUE Observations

The initial LWR spectra obtained in June 1979, as part of a Mg II survey of cool supergiants, showed a doubly reversed, red asymmetric emission profile typical of mass losing objects. The initial far UV spectrum revealed an unexpectedly hot continuum, which was estimated by Schindler et al. (1982) to correspond to a 32,000K white dwarf. The SWP also showed a variety of strong, high temperature emission lines similar to those seen in some RS CVn stars. The soft x-ray flux detected with HEAO-2 IPC was

ascribed by Schindler et al. to wind accretion on to the surface of the white dwarf.

After a year of attempting to compute a synthetic spectrum for the discrepant Ca II and Mg II profile asymmetries, we returned for a second LWR exposure in late July 1980, and discovered a radical increase in total flux, plus a profile asymmetry opposite the initial observation. Since then, a series of LWR observations showed the total flux has slowly declined and the asymmetry gradually returned to the mass loss sense by early 1984 (Figure 1). A second SWP showed no measurable changes in either line or continuum flux. During the same several years, McClure at DAO began to study Ba II star radial velocity changes using precision photoelectric techniques (cf. Fletcher et al. 1982) and has monitored 56 Peg at our request.

Figure 2 displays the correlations among: (a) the Mg II profile asymmetry (defined by the ratio of k2 peak fluxes); (b) the relative shift between the centroid of the Mg II emission envelope (fit by gaussians) and the k3 central reversal (presumed to be fixed and interstellar); and, (c) the optical, photospheric radial velocity data. The data can be viewed as either reflecting binary motion, or a strong enhancement (flare?) in the Mg II forming region, on a 4 to 5 year timescale. During the Julian Day interval 4400-5100 (modulo 2,440,000), the Mg II emission and the radial velocity both show a redshift trend, suggesting the Mg II is associated with the cool star and not the white dwarf. After JD 5100, the Mg II variation slows and the radial velocities become stochastic. One interpretation of this is that the side of the K star facing the white dwarf is heated, while the opposite side is a relatively normal turbulent cool photosphere and mass losing chromosphere. How the chromospheric Mg II is affected, yet the Ca II is not, remains to be understood.

Further UV and radial velocity observations are planned, and polarimetry is encouraged. Details of this research will be published elsewhere.

References

Fletcher, J.M., Harris, H.C. and McClure, R.D. 1982 PASP 94, 1017.

Linsky, J.L., Worden, S.P., McClintock, W. and Robertson, R. 1979 Ap.J. Suppl. 41, 47.

Schindler, M., Stencel, R.E., Linsky, J.L., Basri, G.S. and Helfand, D. 1982 Ap.J. 263, 269.

Zirin, H. 1982 Ap.J. 260, 655.

Figure 1

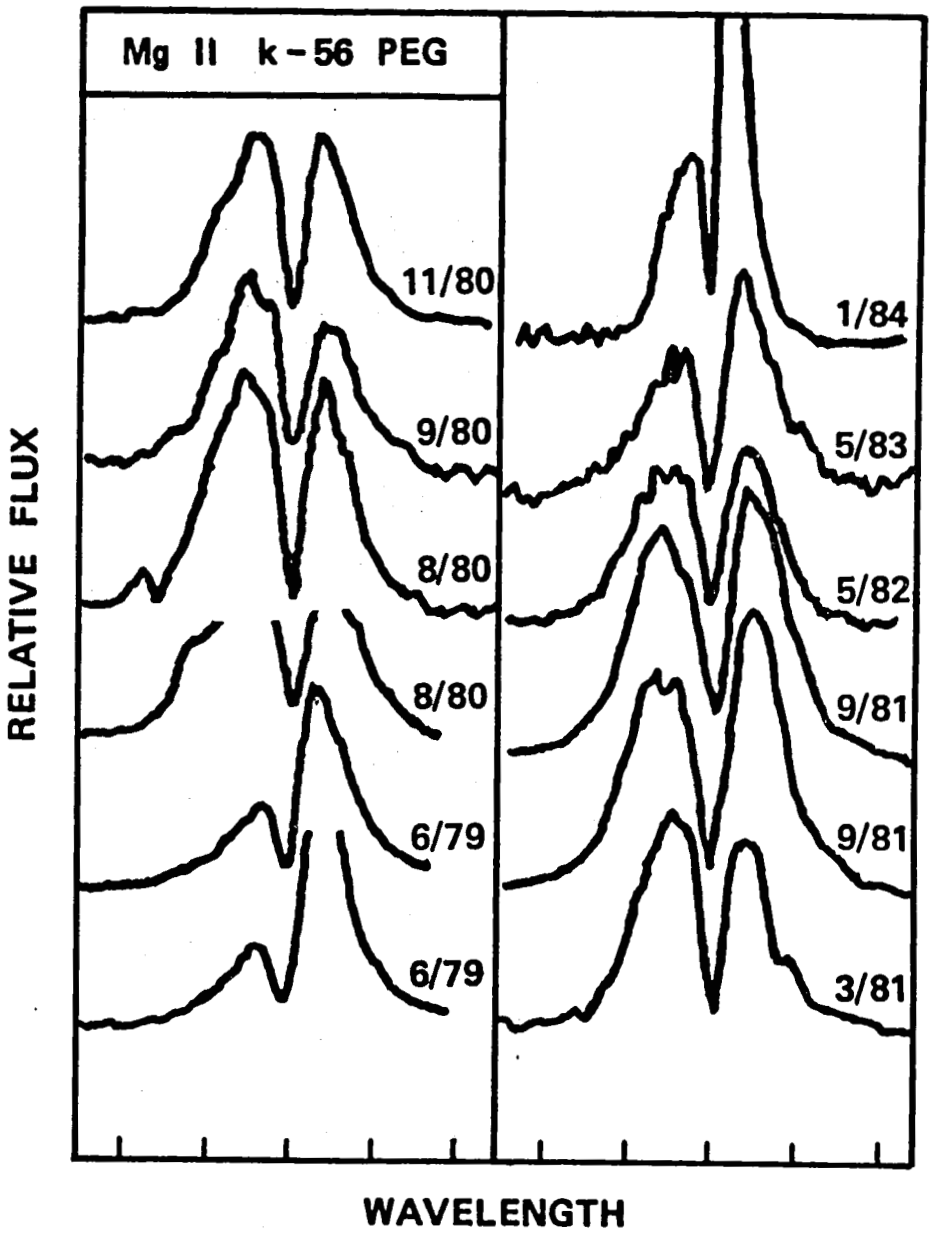
Mg II k-56 PEG
11/80
9/80
8/80
8/80
6/79
6/79
1/84
5/83
5/82
9/81
9/81
3/81
RELATIVE FLUX
WAVELENGTH

Figure 2

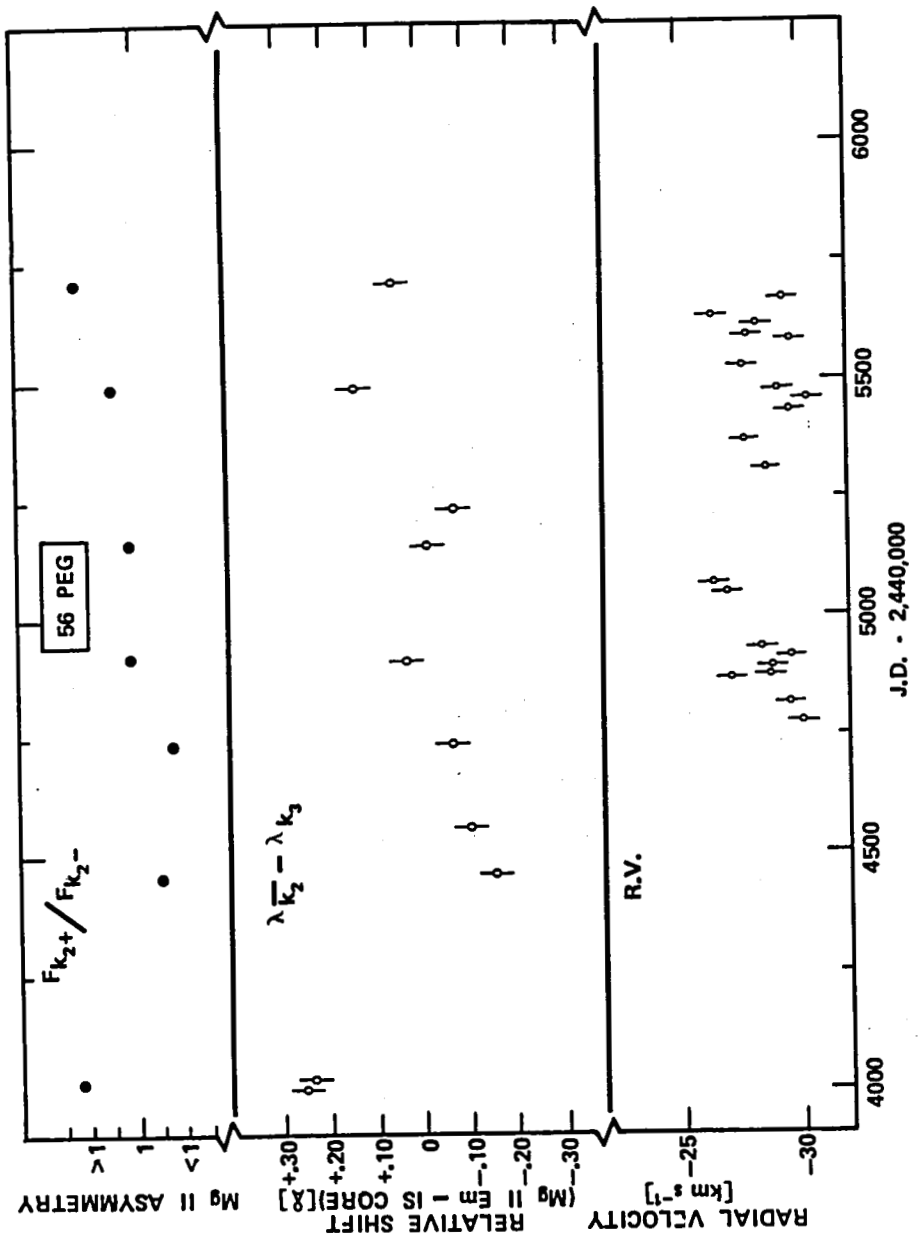
56 PEG
F_{k_2+}/F_{k_2-}
$\lambda_{k_2} - \lambda_{k_3}$
R.V.
Mg II ASYMMETRY
RELATIVE SHIFT (Mg II Em − IS CORE)[Å]
RADIAL VELOCITY [km s⁻¹]
J.D. - 2,440,000
>1
1
<1
+.30
+.20
+.10
0
−.10
−.20
−.30
−25
−30
4000
4500
5000
5500
6000

THREE SHORT-PERIOD BINARIES SEEN AT HIGH-DISPERSION: UX ARI, IOTA TRI AND HR5110

Irene R. Little-Marenin
Joint Institute for Laboratory Astrophysics
University of Colorado and National Bureau of Standards
Boulder, Colorado 80309

Thomas R. Ayres
Laboratory for Atmospheric and Space Physics
University of Colorado, Boulder, Co 80309

Theodore Simon
Institute for Astronomy, University of Hawaii, Honolulu, HI

The three short-period binary systems UX Ari (P=6.43791 days), iota Tri (P=14.732 days) and HR5110 (P=2.61328 days) represent three different evolutionary stages: a)an evolved subgiant primary with a secondary still on the mainsequence (UX Ari), b)two evolved G giants that appear to be crossing the Hertzsprung gap for the first time together (iota Tri), and c)an evolved subgiant that fills its Roche lobe and has lost mass to the secondary to the point where the original secondary is now about 3.5 times as massive (Conti 1967) as its evolved K0IV companion (HR5110). The first two systems are classical RS CVn binaries whereas HR5110 has the characteristics of an Algol system. All three systems are assumed to be in synchronous rotation. Hence the larger, usually cooler star rotates faster. All three systems show strong UV emission lines indicative of plasmas ranging in temperature from 5000K to 200,000K. X-ray emission has been detected from UX Ari and HR5110 indicating hot coronae. The chromospheric, transition region and coronal activity appears to be related primarily to the rotational velocity of the stars (but also to other parameters such as the depth of the convection zone) (Ayres and Linsky 1980). Hence to establish unambigiously which component is the site of the UV emission, we analyzed high-dispersion short-wavelength as well as long-wavelength IUE spectra of all three systems.

UX ARI

The K0IV primary and the G5V secondary have a mass ratio of 1.12 and we view the system at an inclination of about 60° (estimated from the assumed mass of .93 $M_\odot$ for the G5V star and the orbital data of Carlos and Popper (1971)). Two high-dispersion short-wavelength spectra (SWP15211, SWP15240) and two high-dispersion long-wavelength spectra (LWR11729, LWR11755) were taken at two consecutive quadratures (phase about 0.25 and 0.75). Measuring the velocity difference between the stronger emission lines (CI, SiII, HeII, CIV, CII, MgII and MgI) at opposite quadratures gives a value of 115+/-10 km/sec (in good agreement with the velocity of 120 km/sec predicted from the Carlos and Popper (1971) orbit). This

emission follows the cooler star as was found previously for the MgII emission (Simon and Linsky 1980; Simon, Linsky and Schiffer 1980). Hence the chromospheric and transition region emission is located around the cooler, more rapidly rotating primary and is a true stellar phenomenon. The FWHM of the chromospheric lines (SiII, CI) are slightly narrower (about 70 km/sec) than the transition region (TR) lines (about 100 km/sec). The line fluxes are slightly lower than those for HR1099 (Ayres and Linsky 1982) as expected due to the fact that the K0IV star of UX Ari rotates more slowly. The MgII profiles show that a significant fraction (10%-20%) of the emission can be attributed to the secondary as found by Simon and Linsky (1980). A careful analysis of the lines in the SWP-Hi spectra revealed no convincing evidence for emission due to the secondary.

IOTA TRI

Iota Tri is the brighter (A) component of a visual binary with a magnitude difference of 1.6. Both components (A and B) are double-line spectroscopic binaries (Harper 1921) with mass ratios close to unity. Iota Tri has been classified as a G0III+G5III system (Harlan 1969) or a G5III+G5III (Evans 1977) with the spectrum of the secondary being about 20% fainter than the primary (Harper 1921). The rise of the continuum seen in an IUE low-dispersion shortwavelength spectrum (SWP11034) agrees better with the G0III classification. Using the classification of Buscombe (1980) of F6V for the visual B component gives an absolute magnitude of +1.9 for iota Tri (more in line with a III-IV classification). We view the system at an inclination of about 55^{o} +/-10^{o} (assuming a mass between 1.5 and 3.0 $M_{\odot}$ for the G0III(IV) component). Iota Tri has unusually strong CaII emission and Young and Koniges (1977) indicated that this emission is single and follows the orbit of the fainter G5III star. To establish if chromospheric and transition region activity is also observed in the UV and if this activity follows the cooler component, we analyzed five LWR-Hi spectra at different phases (LWR9691, phase 0.07; LWR9721, phase 0.40; LWR11573, phase 0.07; LWR13664 and 13665, phase 0.30) and one SWP-Hi (SWP17412) spectrum near quadrature (phase 0.29). The Mg II emission is strong with a deep central absorption feature. Measuring the velocity of the centroid of emission relative to the central (interstellar) absorption feature at four different phases shows that the velocity of the centroid follows the orbit of the cooler star with roughly the correct velocity amplitude (assuming the deeper dip in the photometric lightcurve of Hall, Louth and Lovell (1980) does indeed occur when the hotter star is behind (phase =0.0)). There is no evidence that the brighter, hotter star contributes significantly to the MgII emission. Analysis of the high-dispersion SWP17412 spectrum (phase=0.29) showed emission from lines of CIV, HeII, SiII, CI, OI and CII with weak emission from CIII, SiIII and SiIV. We determined an absolute velocity shift of the stronger lines relative to the sun of about +60+/-20km/sec. The orbit of Harper (1921) predicts a velocity of +40km/sec for this phase for the fainter star (marginally within the error of the measurement). Hence it appears that both the chromospheric and transition region emission is located around the cooler, fainter (G5III) star. The spectrum of iota Tri has a relatively strong lithium line

(Alschuler 1975) and the lines are rotationally broadened (vsini is 18km/sec (Huang 1952) or 36 km/sec (Hoffleit and Jaschek 1982)) implying a relatively young star crossing the Hertzsprung gap for the first time. (But from the data it is unclear to which of the spectra the Li line and vsini belong.) The fact that the cooler star is also the fainter one implies (from evolutionary tracks) that we are seeing the unique situation of catching two stars of the same system crossing the Hertzsprung gap together for the first time. Hence the mass ratio must be very close to unity indeed. The fact that only one of the stars shows chromospheric activity can be understood in terms of the rotation-activity connection since the cooler, larger primary has to rotate roughly twice as fast as the secondary. (But it is surprising that no contribution from the secondary is observable). Iota Tri appears to be an analog of the Capella system (F9III+G6III), but with a shorter period. Hence in Capella the primary could spin down (not being tidally locked to the secondary) so that chromospheric activity is seen almost exclusively from the secondary (Ayres and Linsky 1980), whereas in iota Tri the chromospheric activity is seen around the more rapidly rotating primary which is tidally locked to its secondary.

HR5110

This system consists of an F2IV primary and an evolved K0IV secondary with a mass ratio of 0.28 (Conti 1967). (Based on the IJHKLM colors of HR5110, the system does not appear to consist of an F2IV star and a G0V star as suggested by Shore and Adleman (1984)). The secondary appears to fill its Roche lobe. Hence HR5110 needs to be considered as a mass-exchange Algol system which is unusual since we view it nearly pole-on ($i=13^{o}$). Little is known about the secondaries of Algol systems since their hotter components dominate the spectrum and during primary eclipse the UV emission spectrum appears to be due primarily to an accretion disk (Plavec 1983). Only in HR5110 does the UV emission spectrum appear to be the typical spectrum of a rapidly rotating K star as found in RS CVn binaries allowing us to study the secondary of an Algol system. But to establish that the UV emission spectrum does indeed come from the secondary and not from an accretion disk, we measured precisely the velocity shifts of the emission lines relative to the photospheric absorption lines in a high-dispersion (SWP13669) spectrum of HR5110 taken at phase 0.27 when the maximum velocity shift of about +45km/sec relative to the primary is observed. The photospheric absorption lines (which arise from the F star) were aligned with those of Procyon (F5IV/V) and the average velocity difference of the two sets of emission lines was then determined to be +40+/-10 km/sec. Hence this analysis shows unambigiously that even in this Algol system the active chromosphere and transition region is a true stellar phenomenon around the cooler star and not due to an accretion disk around the F star. Emission at the velocity of the F star was not observed and chromospheric emission of the K star longward of about 1700A (such as SiII) is also not observed. Since the radii of the two components are comparable (giving similiar rotation rates), we interpret the lack of an active chromosphere as being related to another parameter such as the different depth of the convection zones in the two

components. The flux in the emission lines is in between those of UX Ari and HR1099 (Ayres and Linsky 1982)

We wish to thank the staff of the IUE Observatory for their help in acquiring the stellar spectra, and the staff (especially T. Armitage) of the RDAF in Boulder, operated under grant NAS5-26409, for their help in reducing these data. This work is in part supported through grants NAGS-199 to the University of Colorado and grant NAGS-146 to the University of Hawaii. IL-M wishes to thank JILA for the support given during her year as a visiting fellow.

REFERENCES

Alschuler, W.R. 1975, Ap.J., 195, 649
Ayres, T.R., and Linsky, J.L. 1980, Ap.J., 241, 279
Ayres, T.R., and Linsky, J.L. 1982, Ap.J., 254, 168
Ayres, T.R., Schiffer, H.F.III, and Linsky, J.L. 1983, Ap.J., 272, 223
Buscombe, W., 1980, MK Spectral Classifications: Fourth General Catalogue (Northwestern University)
Carlos, R.C., and Popper, D.M. 1971, Pub.A.S.P., 83, 804
Conti, P.S. 1967, Ap.J., 149, 629
Evans, T.L. 1977, M.N.Astr.Soc.So.Af., 6, 41
Hall, D.S., Louth, H., and Lovell, L.P. 1980, Inf.Bull.Var.Star, #1764
Harlan, E.A. 1969, A.J., 74, 916
Harper, W.E. 1921, P.Dom.Ap.O., 2, 129
Hoffleit, D., and Jaschek, C. 1982, The Bright Star Catalogue (Yale Univerity Observatory)
Huang, S. 1953, Ap.J., 118, 285
Plavec, M.J. 1983, Ap.J., 275, 251
Simon, T., and Linsky, J,L. 1980, Ap.J., 239, 911
Simon, T., Linsky, J.L., and Schiffer, F.H.III 1980, Ap.J., 241, 759
Shore, S.N., and Adleman, S.J. 1984, Ap.J.Supp., 54, 846
Young, A., amd Koniges, A., 1977, Ap.J., 211, 836

PHYSICAL MODELS FOR THE UV CONTINUA OF SYMBIOTIC STARS

Scott J. Kenyon
Harvard-Smithsonian Center for Astrophysics

ABSTRACT

Low resolution IUE spectra represent a unique opportunity to examine the hot component in a symbiotic binary. Reddening-free color indices have been developed which serve to identify the nature of the hot components in these interesting systems. The hot components are divided into two categories: accreting main sequence stars and hot stellar sources. Symbiotic stars are therefore not a homogeneous group of variables, and at least two formation mechanisms are needed to produce the observed sample.

INTRODUCTION

Symbiotic stars were discovered by Cannon and Merrill as M-type variables with intense H I, He I and He II emission lines. IR photometry has confirmed that a late-type star is present in nearly all symbiotics, and usually this is an M-type giant (Allen 1982). The observations of bright emission lines and a veiling blue continuum in these systems are naturally explained by a binary model in which the high-temperature features are associated with a hot companion to the giant. Recent IUE observations of symbiotic systems support this idea, as the UV spectra are dominated by intense emission lines (He II, C IV, N V) superposed on a hot continuum source (e.g., Slovak and Lambert 1982).

The advent of IUE has for the first time permitted the direct observation of an extended underlying continuum attributable to the hot component in a symbiotic system. Several attempts have been made to fit these continua to stellar atmospheres with mixed success: certain systems (e.g., AG Peg: Gallagher, et al. 1979; Keyes and Plavec 1980) appear to conform closely to this model, whereas others (e.g., CI Cyg: Stencel, et al. 1982) defy such simple explanations. This paper reports on a new method to analyze the continua of symbiotic stars, and summarizes results derived in previous papers.

CALCULATIONS

A symbiotic star is considered to be a binary consisting of (i) a late-type giant star, (ii) a hot component, being either an accretion disk surrounding a low mass main sequence or white dwarf star, or a hot, compact star similar to a planetary nebula central star, and (iii) a surrounding gaseous nebula. The continuous spectrum from the nebula and hot component has been calculated using a method described by Kenyon and Webbink (1984), and may be

characterized by continuum magnitudes, m = -2.5 log (F) - 21.1, at 1300, 1700, 2200 and 2600 A. These points were chosen to span the continuum range covered by IUE, and to exploit the 2200 A interstellar absorption feature. The four magnitudes have been combined to define two reddening-free color indices, C_1 and C_2, given by:

$$C_1 = (m_{1300} - m_{1700}) - 0.46(m_{2200} - m_{2600})$$

$$C_2 = 0.55(m_{1700} - m_{2600}) - 0.45(m_{1300} - m_{1700})$$

For a given symbiotic model, C_1 and C_2 are unique functions of either (i) the accretion rate or (ii) the effective temperature of the hot component. Once a solution for the accretion rate or the effective temperature is obtained from (C_1,C_2), the reddening may be determined from the individual colors, $(m_{1300} - m_{1700})$, $(m_{1700} - m_{2600})$ and $(m_{2200} - m_{2600})$.

Figure 1 shows C_2 as a function of C_1 for a complete set of theoretical models, and it is obvious that each class of model occupies its own region in the color-color plot. Superimposed on this Figure are the observed (C_1,C_2) indices for selected symbiotic stars (additional systems are discussed in Kenyon and Webbink [1984]). Most systems lie near only one of the model sequences, and have unique solutions within the framework of the models. More than one plausible solution exists for a few systems, but the derived reddening and the predicted optical nebular spectrum usually serve to eliminate multiple solutions. Based on Figure 1 and these other considerations, Y CrA, CI Cyg, YY Her and AX Per are identified as main sequence stars accreting at rates of roughly 10^{-5} $M_\odot$ yr^{-1}. The remaining systems are hot stellar sources, with effective temperatures ranging from 30,000 K to 150,000 K.

DISCUSSION

A large number of symbiotics have been observed with IUE, and very few of the S-type objects fail to conform to the three-component model described above (Kenyon and Webbink 1984; the (C_1,C_2) indices are unreliable diagnostics for D-type symbiotics). Six systems are unambiguously identified as accreting main sequence stars (Y CrA, CI Cyg, YY Her, AR Pav, AX Per and CL Sco). The late-type giants of these systems should fill their tidal lobes; this requirement is satisfied for CI Cyg and AR Pav, but additional IR data is needed to determine if the other systems have lobe-filling giants. The remaining symbiotic stars appear to contain hot stellar sources with effective temperatures ranging from 10,000 K to >100,000 K and radii < 1 $R_\odot$ (Z And, EG And, UV Aur, TX CVn, BF Cyg, AG Dra, V443 Her, RW Hya, SY Mus, AG Peg and LMC S63). It is not necessary for the late-type giants in these systems to fill their tidal

lobes, although some (e.g., RW Hya) may do so.

The existence of two distinct types of hot components in symbiotic stars requires two radically different formation mechanisms. Assuming a symbiotic star initially contains two normal main sequence stars, each formation process can be sketched qualitatively. The primary star, being more massive, is the first to evolve off the main sequence and ascend the giant branch. For binary periods, P, less than 1000-2000 days, this star fills its Roche lobe on the giant branch or asymptotic giant branch, and forms a symbiotic star if the accretion rate is sufficiently high (as shown above). Such rates are realized in the detailed evolutionary calculations discussed by Webbink (1979). The hot stellar sources present in other symbiotics resemble the central stars of planetary nebulae, and must therefore have ascended the giant and asymptotic giant branches (without filling their tidal lobes) and ejected planetary nebulae. This requires P > 3-4,000 days, and the ejection of the planetary nebula must carry away a sufficient amount of mass and angular momentum to shorten the period to a value comparable to that observed in most symbiotic stars (P = 200-1000 days). Whether this can happen in a long period binary is, as yet, an unsolved problem.

REFERENCES

Allen, D.A. 1982. in IAU Colloquium No. 70, The Nature of Symbiotic Stars, ed. M. Friedjung and R. Viotti (Dordrecht: Reidel), p. 27.

Gallagher, J.S., Holm, A.V., Anderson, C.M. and Webbink, R.F. 1979. Ap. J., 229, 994.

Kenyon, S.J. and Webbink, R.F. 1984. Ap. J., 279, No. 1.

Keyes, C.D. and Plavec, M.J. 1980. in IAU Symposium No. 88, Close Binary Stars: Observations and Interpretation, ed. M.J. Plavec, D.M. Popper and R.K. Ulrich (Dordrecht: Reidel), p. 365.

Slovak, M.H. and Lambert, D.L. 1982. in IAU Colloquium No. 70, The Nature of Symbiotic Stars, ed. M. Friedjung and R. Viotti (Dordrecht: Reidel), p. 103.

Stencel, R.E., Michalitsianos, A.M., Kafatos, M. and Boyarchuk, A.A. 1982. Ap.J. (Letters), 253, L77.

Webbink, R.F. 1979. in IAU Colloquium No. 46, Changing Trends in Variable Star Research, ed. F.M. Bateson, J. Smak and I.H. Urch (Hamilton, NZ: U. of Waikato Press), p. 102.

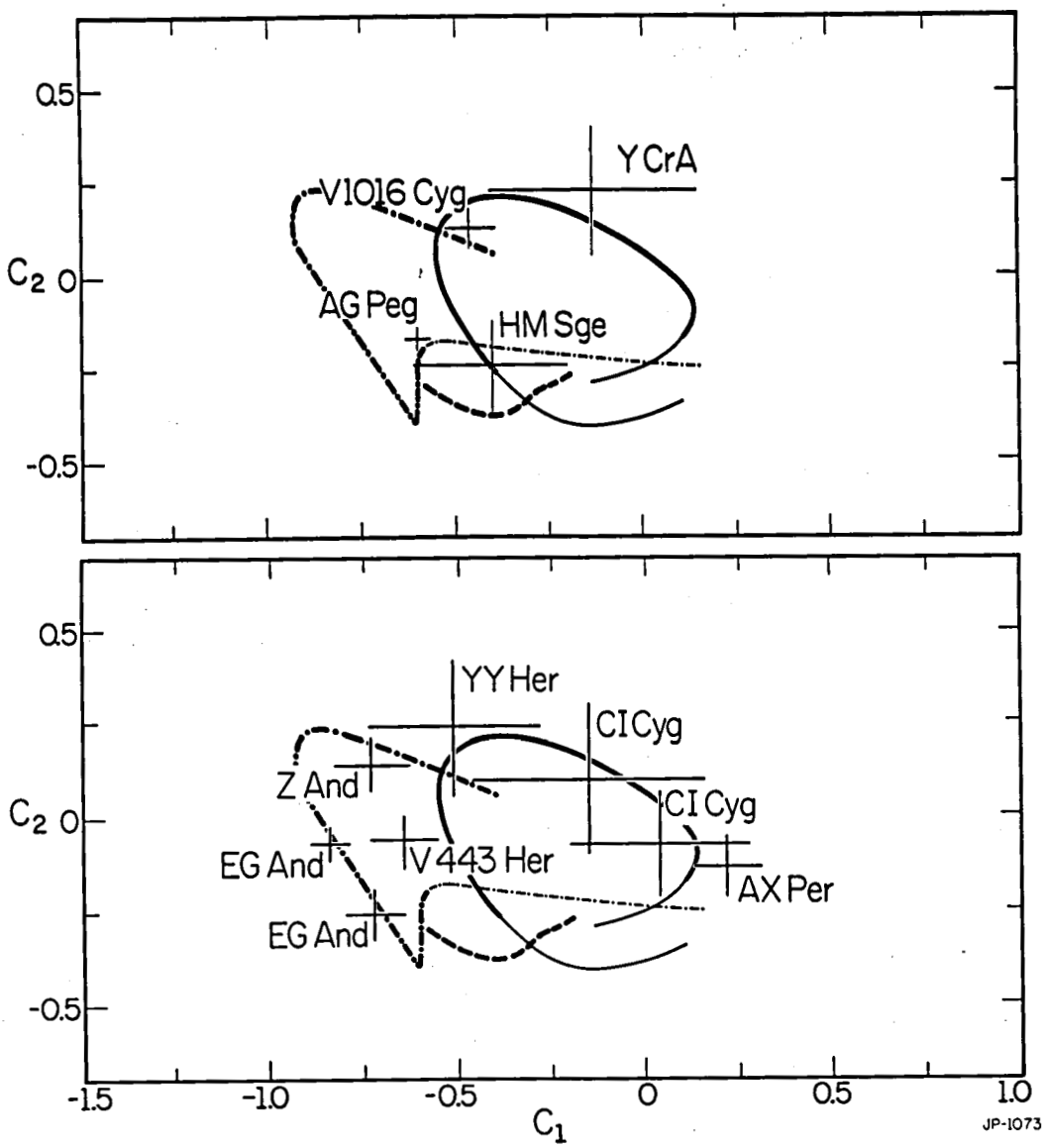

FIGURE 1 - Reddening-free color-color plot for model symbiotic stars. The solid curve correspnds to the locus of accreting main sequence stars, with mass accretion rate increasing clockwise around the curve. The dashed curve is the locus of accreting white dwarf stars, with the accretion rate increasing from right to left. Finally, the dot-dashed curve corresponds to the locus of hot stellar sources, with effective temperature increasing from right to left. Additional information regarding this plot can be found in Kenyon and Webbink (1984).

THE ECLIPSING BINARY U SAGITTAE:

EVIDENCE FOR CNO PROCESSING AND MASS EXCHANGE IN THE PAST

Jan J. Dobias and Mirek J. Plavec
Department of Astronomy, University of California, Los Angeles

ABSTRACT

We have determined the system parameters of U Sagittae. The components are of spectral types B7.5 V and G4 IV-III, and the system is at a distance of approximately 290 pc. We confirm the conclusion by Tomkin that the masses are about 5.5 and 1.9 solar masses, respectively. The system is a typical semidetached system of the Algol type, but it is almost completely dormant, with only the barest traces of circumstellar material. This enabled us to study the photospheric lines of the hotter star in good detail. The profiles of the absorption lines on high-dispersion IUE spectra can be matched if we assume solar abundances except for carbon and nitrogen. The abundance of carbon is only 9% of its solar abundance, and N is overabundant by about a factor of 4.5. We conclude that the system underwent large mass transfer.

FLUX DISTRIBUTION AND OTHER CHARACTERISTICS

U Sagittae is a practically dormant Algol-type semidetached binary. This can be seen from various pieces of evidence. The period of the system, 3.38 days, is more stable than that of many other well-observed Algols. The radial velocity curve of the primary component is rather uncomplicated. Shell lines are either weak or absent. Emission lines of the Balmer series were observed only once (McNamara 1951). Also the ultraviolet spectrum is almost purely stellar: in our IUE observations of a total eclipse of the hotter component in U Sagittae, we saw only the barest traces of the emission lines of N V, Si IV, C IV , and other emission lines typical for interacting binaries.

On top of all this, U Sagittae is relatively very bright, about 6.5 mag visually, and the reddening is small: we found E(B-V) = 0.06 mag. Thus the system is easily observable at high dispersion, except, unfortunately, for the deep total eclipse. The lack of a substantial circumstellar envelope makes it easier to study the stellar photospheres in greater detail, and the later-type G4 III-IV component does not affect the spectrum in the IUE spectral range.

Under these circumstances, we have been able to determine the spectral parameters of the components with a high degree of accuracy. We combined our IUE spectra with optical scans obtained with the Lick Observatory ITS scanner, thus covering the wavelength interval 120 -720 nm with almost no gap. The flux distribution of the primary component is perfectly well matched by an (interpolated) Kurucz normal model atmosphere with an effective temperature of 12,250 K and log g = 3.85. The primary is a B7.5 V star. The spectral type

of the secondary component has been determined from our Lick scans to be G4 IV-III. The system is at a distance of about 290 pc. After years of uncertainty, the masses of the components are now fairly well known thanks to the work of Tomkin (1979), supported by our own results. The mass ratio is quite close to 3, and the masses are 5.5 and 1.9 solar masses, respectively. The secondary component fills its critical Roche lobe, and U Sagittae is therefore a classical semidetached system of the Algol type. Since it is nearly dormant, it is possible to believe that the mass-transfer episode is practically over. Can we use this system to support the general idea that Algols are products of a large-scale mass transfer? We believe that the answer is very strongly in the affirmative.

SPECTRUM SYNTHESIS SHOWS EFFECTS OF CNO PROCESSING

The method of spectrum synthesis has been applied to the line profiles derived from IUE high-dispersion spectra. Line broadening parameters have been derived from absorption lines of Fe II and other metals. The profile fitting led us to postulate a microturbulence velocity parameter of 8 km/s, and an effective macroturbulence velocity of 80 km/s. The latter parameter actually represents rotation; the value of v sin i must lie between 80 km/s and 100 km/s, and is somewhat higher than the synchronized rotational velocity, which would be 65 km/s. With these parameters, a very good agreement with observed profiles is obtained when the solar abundances of these elements are assumed.

However, the profile of C II at 1335 Å indicates a substantially reduced abundance of carbon, down to about 9% of the solar value (see Figure 2). At the same time, the N I lines at 1493/1495 Å are better fitted if an overabundance of nitrogen is postulated by about a factor of 4.5. Optical studies of the cool component by Parthasarathy et al. (1983) are in qualitative agreement with our results.

We conclude that U Sagittae, although dormant now, was subject to large-scale mass transfer in the past. The mass-losing star (the present G4 subgiant) has been stripped so thoroughly that material at least partially processed by the CNO cycle was exposed, and eventually partly transferred to the surface of the B8 V gainer. All this strongly corroborates the theory of the evolution of the Algol-type semidetached binaries through a large-scale mass transfer.

One exciting question remains: Why is U Sagittae dormant and U Cephei so much more active, when both systems are rather similar to each other? Is it only a transient situation? Or are they at different evolutionary stages?

REFERENCES

McNamara, D.H. 1951, Astrophys. J. 114, 513 and Pub. Astr. Soc. Pacif. 63, 38.

Parthasarathy, M., Lambert, D.L., and Tomkin, J. 1983, Mon. Not. 20, 1063.

Tomkin, J. 1979, Astrophys. J. 244, 546.

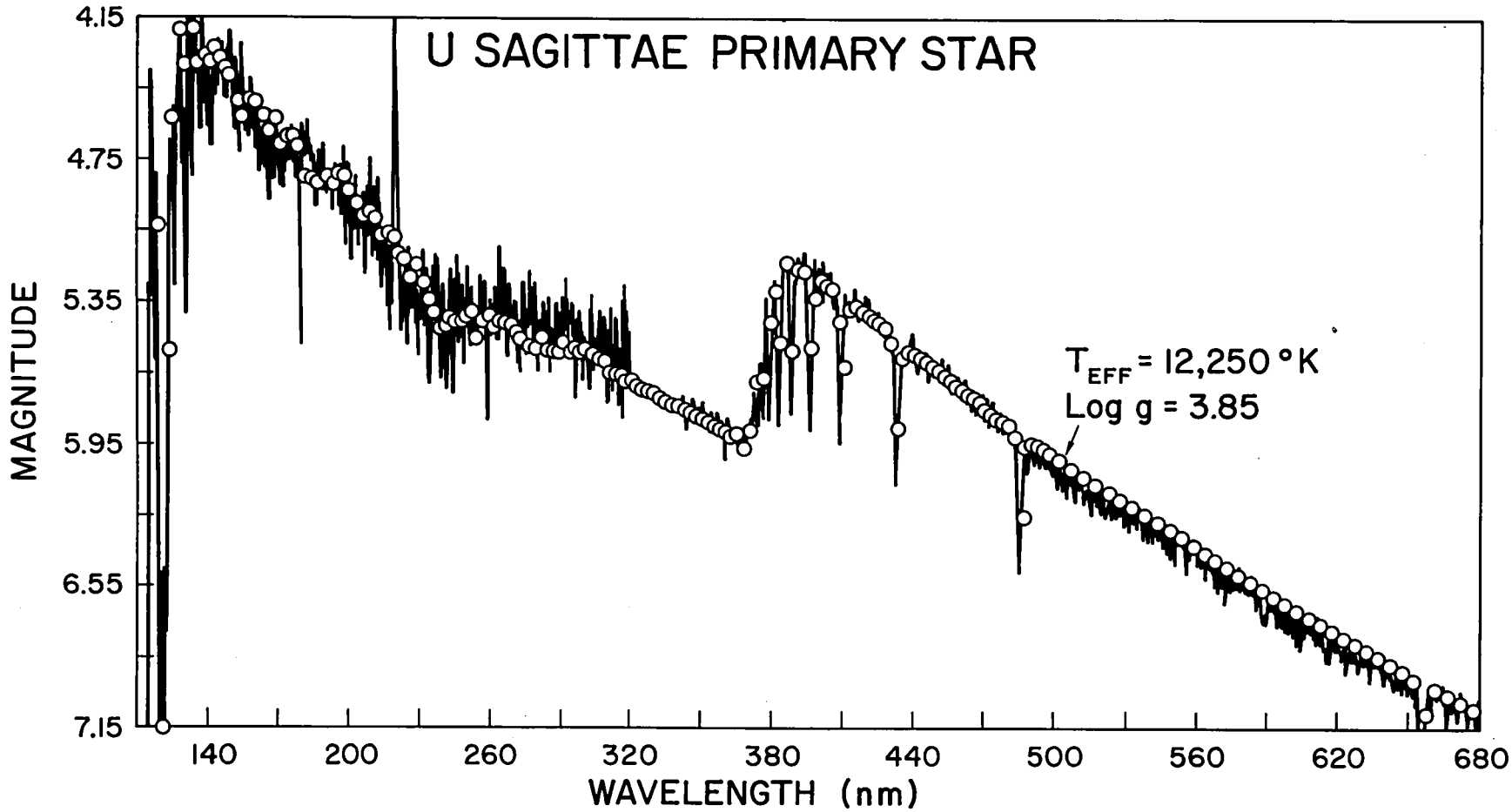
U SAGITTAE PRIMARY STAR
T_{EFF} = 12,250 °K
Log g = 3.85
MAGNITUDE
4.15
4.75
5.35
5.95
6.55
7.15
140
200
260
320
380
440
500
560
620
680
WAVELENGTH (nm)

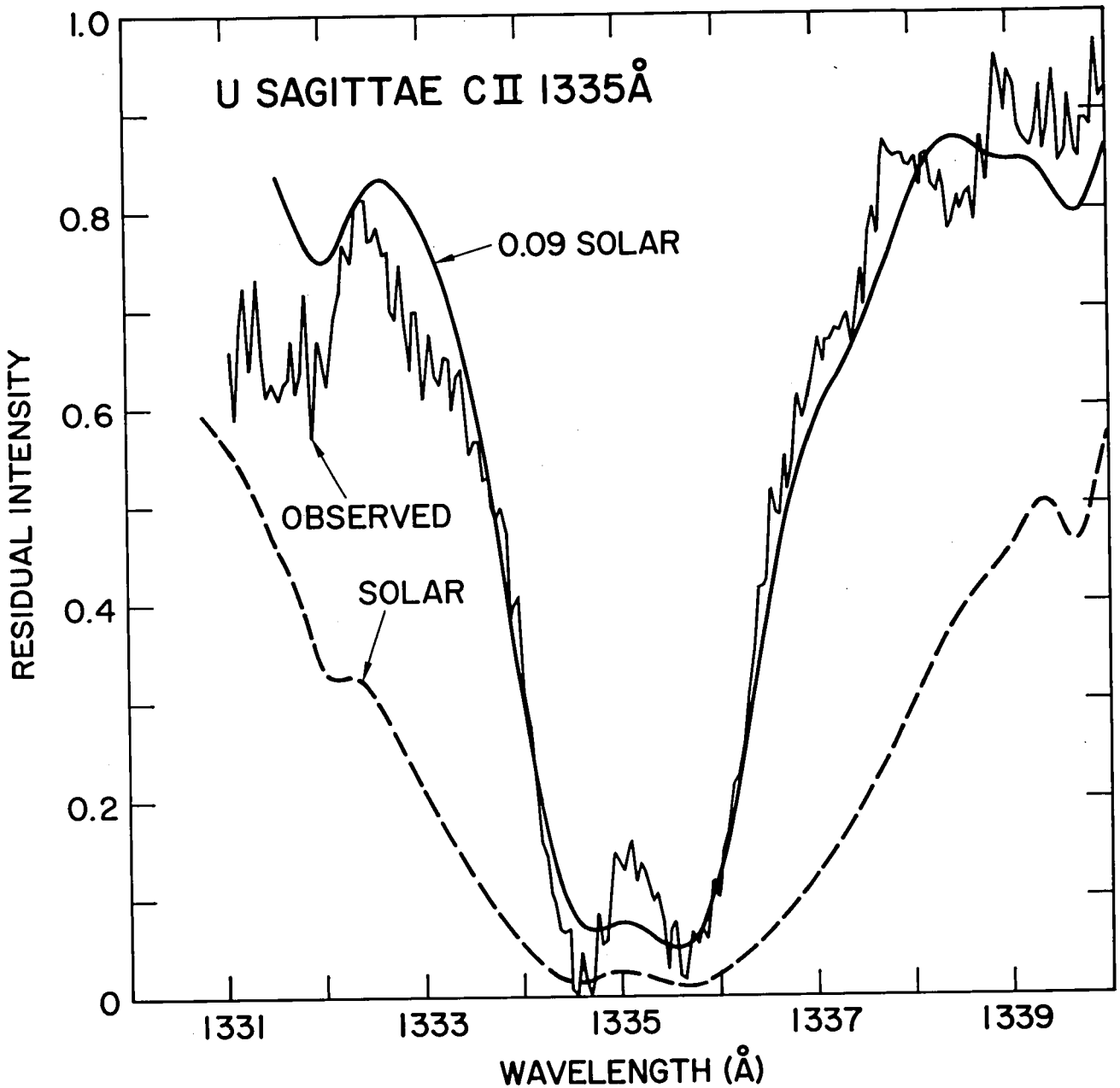
U SAGITTAE C II 1335Å
0.09 SOLAR
OBSERVED
SOLAR
RESIDUAL INTENSITY
1.0
0.8
0.6
0.4
0.2
0
1331
1333
1335
1337
1339
WAVELENGTH (Å)

IUE AND OPTICAL OBSERVATIONS OF LMC X-RAY BINARIES.

Luciana Bianchi
Osservatorio Astronomico di Torino, Italy
Manfred Pakull
Technische Universitat Berlin, W.Germany

ABSTRACT

The first IUE observations of two LMC X-Ray binary candidates, LMC X-1 (star 32) and 1E0501.8 (Sk-7036) are presented. Both sources were observed with IUE at two phases of the optical light curve, to search for possible effects of the X-Ray flux on the primary's wind.

From consideration of the 220.0nm interstellar extinction dip and of the overall continuum distribution, we derive the foreground reddening to be E(B-V)= 0.05 and the additional reddening in the LMC to be E(B-V)=0.11 for Sk-7036 and E(B-V)=0.32 for LMC X-1.

The spectra of Sk-7036 show a significant variation of the continuum , the flux at 1300Å beeing stronger at phase 0.2 by 40% compared to the flux observed at a minimum of the light curve. The latter can be represented by a model atmosphere with Teff=25000K, log g =3.0, in agreement with the spectral type derived from the optical colors.

The UV continuum of star 32 (LMC X-1) can be modeled with Teff=35000K, log g = 3.5,which is appropriate for an O7-9 giant.

INTRODUCTION

Ultraviolet spectroscopy of X-Ray binaries is a very important complement to the optical and X-Ray data, as it gives information about the UV continuum distribution and stellar wind (mass loss) of the hot primary and, hence, on the rate and mechanism of mass accretion onto the compact secondary. Moreover, the influence of the X-Rays on the primary's wind ionization conditions and the presen= ce of a possible hot accretion disk can be studied with UV phase dependent observations.

Following an extensive optical identification work we are therefore observing with IUE optical candidates of X-Ray sources. We present here the first observations of two sources in the LMC.

LMC X-1

Optical

The Einstein 3arcsec error circle for LMC X-1 (LHG78) still includes the bright B3-5 supergiant R148 and star32 (Cowley et al.,1978, Pakull,1980). Optical spectroscopy of R148 revealed no apparent peculiarities whereas star 32 exhibits weak variable HeII4686 and NIII λ 4640-60 emission (Pakull,1980) typical for optical counterparts of high luminosity X-Ray binaries. From the ratio HeI λ4540 to HeI λ 4471 Pakull(1983) classified star 32 as O7-9. Optical spectra of the star and of the surrounding HII region N159 at different positions indicate that star 32 is located within N159, and there is evidence for interaction of a strong X-Ray source with the low density HII region: e.g.,an increase of temperature of $\gtrsim$5000K in the neighbohood of the star (from the OIII lines ratio, Pakull,1983) and some possible HeII nebular emission (Hutchings et al.1983), not observed at other posi=

tions around the star, as expected from a normal HII region.

Hutchings et al.(1983) reported RV variations with a period of approximately 4 days, making star 32 a black hole candidate.

IUE observations.

We observed star 32 with IUE over the total range (1150-3200Å) on Apr.10,1982. With the SWP camera we obtained an exposure also two days before.

Star 32 is one of the most reddened objects in the LMC, beeing embedded in the N149 HII region, and due to the presence of the nearby much brighter supergiant R148, the reddening is difficult to estimate from optical photometry. Indeed, existing determinations are quite discrepant: Pakull (1983) derives E(B-V)=0.6 from the Balmer decrement in the vicinity of the star in N159, while Hutchings et al.(1983) estimate E(B-V)=0.20, however allowing also E(B-V)=0.34.

From the UV continuum distribution a good reddening estimate can be derived. Using the standard Galactic extinction curve by Savage and Mathis (1979) for the foreground extinction and the LMC extinction curve by Nandy et al.(1981) we derive the best correction to our spectrum to be E(B-V)=0.05 in the Galaxy plus E(B-V) between 0.30 and 0.32 in the LMC. The dereddened spectrum of Apr.10 is shown in Fig.1. The observed distribution is well represented by a model atmosphere with Teff=35000K, logg=3.5,consistent with the spectral type O8III. The corresponding model from Kurucz(1979) is also shown in Fig.1. The scaling factor to superimpose the model to the observed dereddened flux gives a magnitude for the star of $V=V_o+A_v$ =14.5 in agreement with the optical photometry.

A detailed discussion of the line spectrum is given in Bianchi and Pakull (1984) here we just point out that some of the emission could be of stellar origin (Of?). The strong FeIII and FeII blends indicate that the star is a giant.

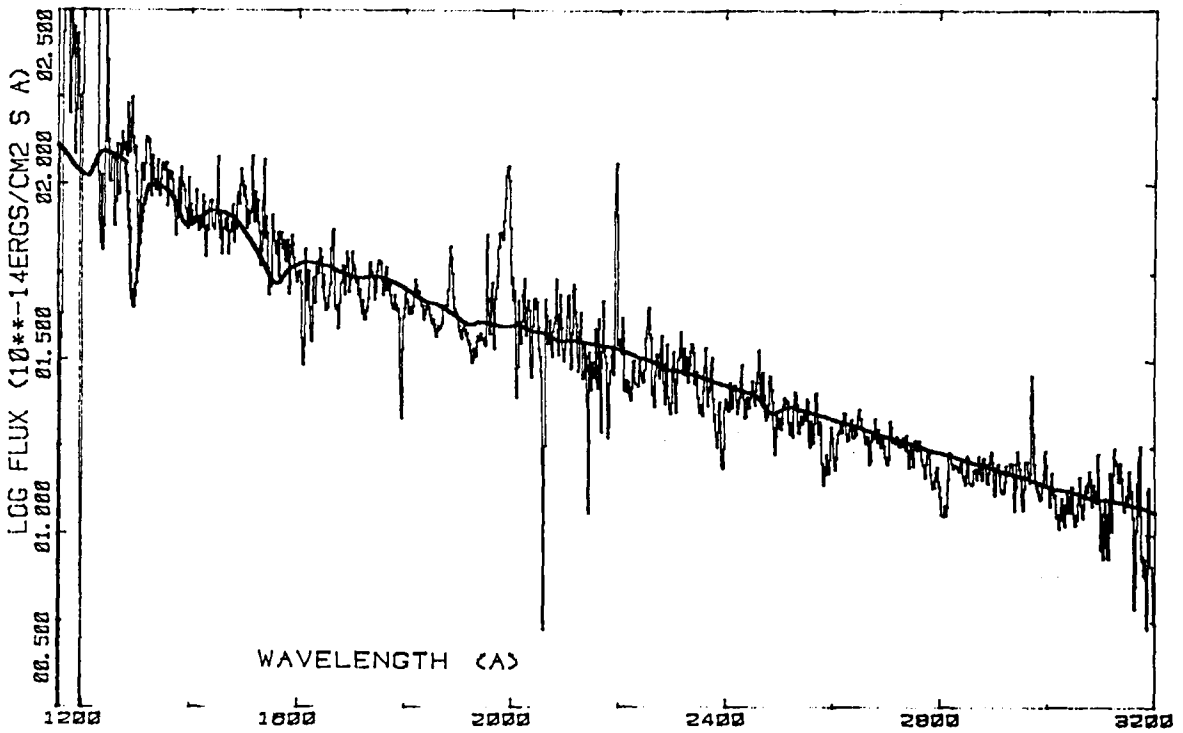

Fig.1 The UV spectrum of LMC X-1 (star 32) is shown, dereddened for E(B-V)= 0.05(galactic)+0.3(LMC).Superimposed is a model with Teff=35000,logg=3.5.

The IUE images also show an extended emission from the surrounding nebula, which we extracted separately from the stellar spectrum. The observed nebular spectrum looks hotter than a nebular continuum (H and He recombination and two-photons continuum) computed for $Ne=100cm^{-2}$, Te=12000K (values derived from the optical line ratios), indicating maybe some scattering of the stellar light. (see Bianchi and Pakull, 1984).

Sk-70 36 (1E0501.8-7036 ?)

Optical data

The B1-2I star Sk-7036 was proposed by Pakull (1982) as one possible candi= date for the hard X-Ray source 1E0501.8-7036. While the other early type star included in the IPC error circle (HV2289) showed long term (~ months) variations by about 0.3 mag (Be star?), Sk-7036 exhibits an "ellipsoidal" light curve with period P=6.94d and amplitude $\Delta V=0.2$ mag, indicating a Roche-lobe filling primary seen at orbital inclination, which makes it an excellent candidate for a massive X-Ray binary.The photometric double wave curve is shown in Fig.2. The U-B beha= viour is very puzzling, the amplitude in the U band beeing larger that in B and V colors. This might suggest the presence of a thick accretion disk.

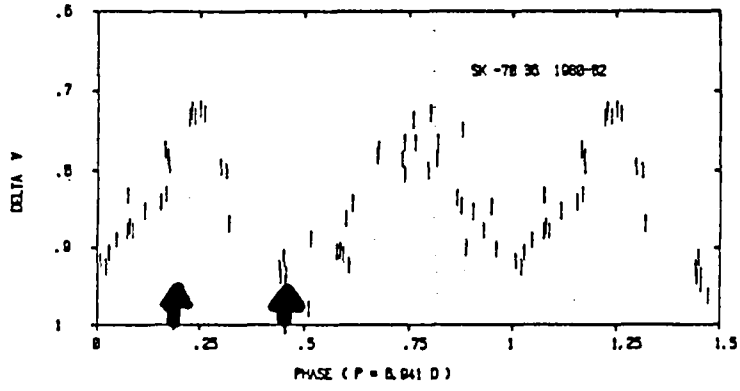

Fig.2. Light curve for Sk-7036. Phases of our two IUE observations are indicated (arrows).

IUE data

We observed Sk-7036 with IUE (SWP+LWR) near one minimum and one maximum of the optical light curve. Details of the observations are given in Bianchi and Pakull (1984). The two full range spectra are plotted toghether in Fig.3, to show the strong difference of the continuum distributions. The UV spectrum at a maximum is stronger by 20% to 40% than the other one, the difference beeing larger at shorter wavelengths. This fact is consistent with the optical U-B behaviour mentionned earlier, and may support the hypothesis of an accretion disk. A detailed discussion of this possibility will be given elsewhere, as well as the description of the line spectrum. We just mention here the strong variations of NV(1): strong emission in one spectrum, pure absorption in the other one (see Fig.3) which might be an effect of X-Ray heating , and of MgII λ2800, which is present in emission in antiphase with NV (perhaps related to the accretion disk).

Assuming that the fainter spectrum corresponds to the hemisphere of the star not heated by the X-Rays, we use this one to derive stellar parameters. From the optical colors, very little reddening is inferred for Sk-7036,E(B-V)=

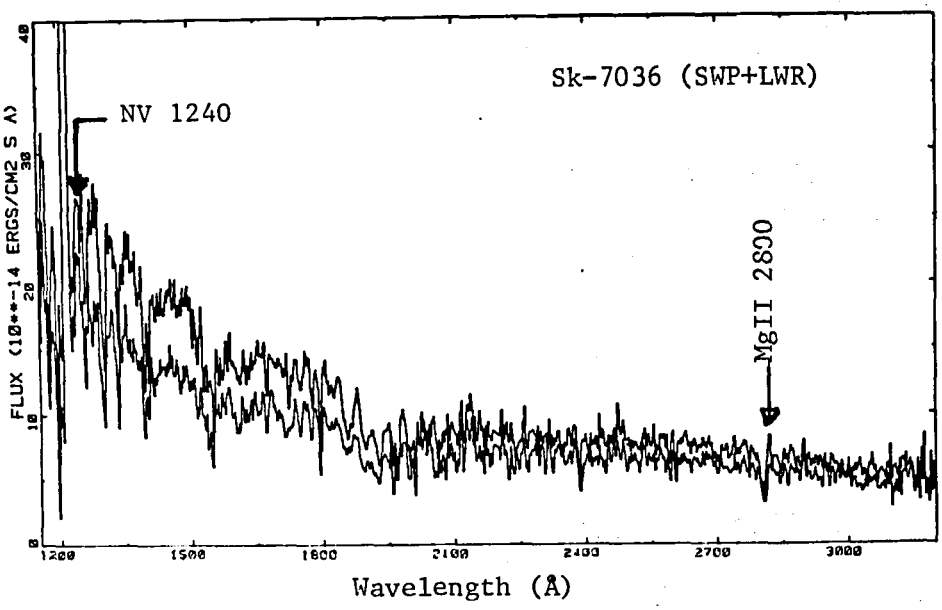

Fig.3. The IUE spectra of Sk -7036 (Apr.8 and 10,1984). The lines showing the strongest variations (NV and MgII) are indicated.

=0.165. The UV spectra confirm this value. In Fig.4 the Apr.10 spectrum is shown,corrected for foreground galactic extinction with E(B-V)=0.05 and for the LMC extinction with E(B-V)=0.11. In Fig .4 the best model atmosphere fit is also plotted, a Kurucz (1979) model with T_{eff}=25000K and log g=3.0, which confirms the spectral type B1-2I. Extrapolation of the model fit gives V= V_o+A_v=13.77, in agreement with the observed V mag. at minimum.

REFERENCES.
Bianchi,L.,and Pakull,M.,1984, in preparation
Cowley,A.,Crampton,D.,and Hutchings,J.,1978,A.J.,83,1619
Hutchings,J., Crampton,D.,and Cowley,A.,1983, Ap.J.,275,443
Nandy,K.,Morgan,D.,Willis,A.,Wilson,R.,and Gondhalekar,P.,1981,M.N.R.A.S,196,955
Pakull,M.,1980, IAU Circ. N.3318
Pakull,M.,1983, IAU Symp. N.108,p.173

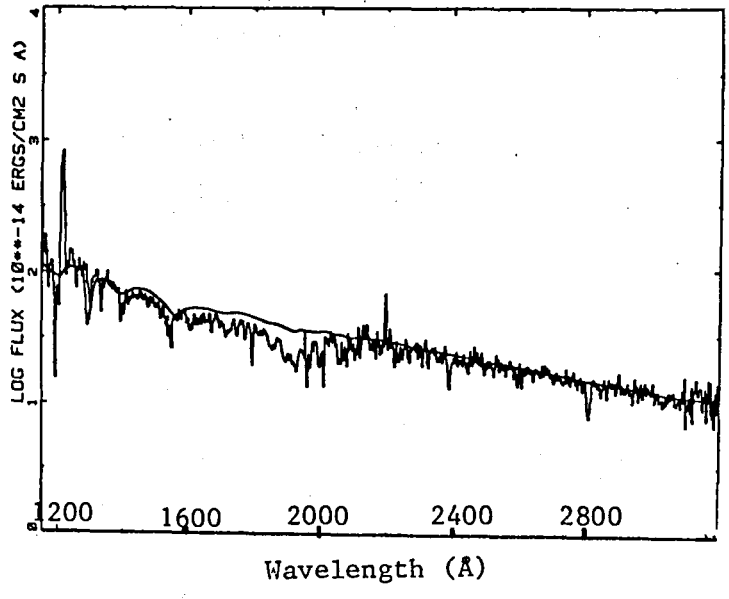

Fig.4. SWP+LWR spectrum of Sk-7036 (Apr.10,1984),deredde= ned for E(B-V)=0.05(galactic) +E(B-V)=0.11(LMC). The fit is a Kurucz model with T_{eff}= 25000K, log g=3.0.

CIRCUMSTELLAR MATERIAL IN ALGOLS AND SERPENTIDS

Mirek J. Plavec, Jan J. Dobias, Paul B. Etzel, and Janet L. Weiland
Department of Astronomy, University of California, Los Angeles

ABSTRACT

The observations of the emission lines of C IV, N V, Si IV, etc. in interacting binaries of the Algol and W Serpentis types are reviewed. So far, seven "Serpentids" are known, and seven bona fide Algol-type semidetached systems have been found to display the same kind of emnission lines, only on a weaker scale. Interesting differences are observed in both the absolute and relative strengths of the emission lines. In some systems, the C IV resonance doublet is the strongest, while in others, the N V doublet is definitely stronger. The main cause of this dichotomy is suspected to be the varying degree of CNO processing of the observed material. But the variable ratio of the strength of the C II line to that of the C IV line suggests temperature differences between the emitting regions of the individual systems, too.

SURVEY OF INTERACTING BINARIES WITH "HOT" EMISSION LINES

One of the first discoveries made with the IUE in the field of close binary stars was the detection of the emission lines of C II, CIV, N V, Si II, Si IV, Fe III, and Al III in the SWP spectra of W Serpentis, V367 Cygni, SX Cassiopeiae, RX Cassiopeiae, and W Crucis in August 1978 (Plavec and Koch 1978). Before that, only one similar emission-line spectrum was known, namely that of β Lyrae, discovered with Copernicus. At first sight, these six systems have little in common, except that they are strongly interacting binaries and are surrounded by so much circumstellar matter that it is hard to establish the character of the components. The presence of the circumstellar matter was known before, from observations of optical emission lines and of shell absorption lines. Although we are still far from fully understanding the nature of these six "W Serpentis-type systems", evidence has been gradually mounting that they are semidetached interacting binaries in a stage of rather rapid mass transfer. If so, then they represent extreme cases of the general class of the Algol-type semidetached binaries.

Now some more "classical" Algols also display a fairly high degree of activity, which is manifested by period changes and the presence of optical emission lines as well as shell absorption lines. It can be conjectured that these active Algols may represent transition cases between quiescent Algols and the W Serpentis stars. A program has therefore been started in which we systematically survey the brighter Algols. The progress has been rather slow since the anticipated "hot" emission lines are rather weak compared to the continuous flux of the hotter component, and observations must therefore be made during the total eclipse of that component.

So far, we have detected far ultraviolet emission lines in the spectra of the following Algols:

star	period (days)	components	comments on UV emission lines
RW Tauri	2.77	B8 V + K0 III-IV	Contaminated. C IV seen, N V dbtfl
U Cephei	2.49	B9 V + G8 III-IV	C IV dominates: F(C IV)/F(N V) = 3.9
U Sagittae	3.38	B8 V + G4 IV-III	C IV dominates, N V weak; lines weak
RY Persei	6.86	B6 III+ F8 III	N V dominates: F(N V)/F(C IV) ≈ 5
TT Hydrae	6.95	B9 V + K0 III	C IV dominates, N V hardly seen
UX Monocer.	5.90	A7 ?? + G2 IV	C IV dominates, N V uncertain
V356 Sagit.	8.90	B3 V + A1.5 II	N V dominates: F(N V)/F(C IV) = 6.1

On the negative side, no emission lines were detected in:

W Delphini	4.81	B9 V + G5 IV	no emission seen in deep eclipse
S Velorum	5.93	A5 V + K5 III	observed only outside eclipse
RZ Eridani	39.28	F2 V + K1 III	observed only outside eclipse
BM Cassiop.	197.3	A5 I? + ?	observed only outside eclipse

W Delphini is known to be mildly active, with Hβ observed in emission by Struve (1946). The three following stars have not been observed in eclipse, but their hotter components are sufficiently cool so that their fluxes shortward of 1600 Å should not obliterate the emission lines, if present. Yet perhaps the exposure times were not long enough. S Velorum should certainly be tested once more, since it does show optical emission lines. So does, in fact, BM Cas, while RZ Eri seem to be dormant.

From the above statistics it transpires that whenever we can observe an Algol system in total eclipse, chances are very good that the "hot" emission lines will be detected, but we cannot be 100% sure. If the system is not totally eclipsing, then the prospect is not good, since the emission lines are on the whole quite weak compared to the continuous flux of the primary component. Only in the genuine Serpentids β Lyr, SX Cas, W Ser, V367 Cyg, and W Cru are the emissions strong enough to show even in full light -- although the SWP fluxes for all of them are considerably higher than the optical spectral types of the hotter components would predict. RX Cas is an interesting anomaly: there is no stellar component visible in the SWP spectrum and both stars appear to be no earlier than spectral type G.

It is interesting to speculate how many more "mild Serpentids" or "active Algols" would be detected if some Be stars were eclipsing. Actually one of them, KX Andromedae (HD 218393), which used to be classified as an active shell star and was later discovered to be an interacting binary (Kriz and Harmanec 1975; Polidan 1976; Plavec 1979) has emission lines strong enough to show even without eclipses: this is, therefore, an example of a non-eclipsing Serpentid.

STATISTICS OF THE EMISSION LINES

Naturally it is very important to compare the absolute powers emitted in the "hot" emission lines. Unfortunately, reliable statistics emerges only slowly, because it prerequires a good knowledge of the distance to each system, which in turn requires a reliable knowledge of the nature of at least one component.

At the present time we can say with good confidence that the emission lines in SX Cas are absolutely about 100 times stronger than those in U Cep. Emission lines in U Sge are very weak, probably about 3 times weaker than those in U Cep, but uncertainties in distances may affect this ratio. TT Hydrae appears to have emissions of about the same strength as U Cep.

Somewhat more reliable is an intercomparison of the relative strengths of the emission lines within the same spectrum. Certainly most interesting is the ratio of strengths of the resonance doublet of C IV at 1550 Å to the doublet of N V at 1240 Å. We can anticipate that this ratio will be a good indicator of the degree by which the circumstellar material was exposed to CNO processing at the time when it was deep in the interior of the loser (the presently less massive star).

The uncertainty entering this statistics stems from uncertain amount of reddening and, in some systems, from difficulties of determining the position of the continuum. Nevertheless, we can say with good confidence that there exist surprising differences between the individual systems. In U Cep, U Sge, TT Hya, UX Mon, and V367 Cyg, the C IV line is definitely stronger. On the other hand, in RY Per and V356 Sgr, the N V line is strikingly stronger than the C IV line. In β Lyr, SX Cas, RX Cas, and W Ser, the N V line is also stronger than C IV, but the difference is not so pronounced. It appears that RY Per and V356 Sgr should be most advanced in the mass transfer episode, or, more precisely, that the loss of mass from the gainer went deeper into its interior. It has long be suspected that V356 Sgr is at the end of the mass transfer period (Wilson and Caldwell 1978); about RY Per we have less definite knowledge. Somewhat puzzling in this interpretation is U Sagittae. It is practically dormant and we can surmise that for it, too, the mass transfer episode ended. Then we expect that the surface layers of the gainer should be carbon-poor and nitrogen-rich, and this is exactly what we find from an analysis of the line profiles of these elements (see the article by Dobias and Plavec in this volume). But then it is puzzling why the emission line of C IV is still stronger than that of N V.

The "hot" emission lines are probably formed in a kind of stellar wind, induced by accretion. The necessary conversion of energy probably occurs in a relatively hot, strongly turbulent layer surrounding the gainer (i.e. the accreting star) (Plavec 1983; Peters and Polidan 1984). It is likely that the temperature of the turbulent layer and the temperature of the expanding medium in which the emission lines are formed will be different from object to object. Some information on the temperatures may be obtained from the ratio of the lines C II/C IV and Si II/Si III/Si IV.

A quick semiquantitative look at the ratios P(C II 1336Å)/P(C IV 1550 Å) does reveal differences between the systems. As a rule, the C II line is the weaker of the two. The ratio is about 3 in favor of C IV in U Cep, TT Hya, and V356 Sgr; it is about 2 in RX Cas and UX Mon; less than 2 in RY Per, V367 Cyg, and β Lyr. The two lines are nearly equal in strength in SX Cas and W Ser. In an interestingly contrasting case, in W Cru, the C II lines is more than twice as strong as the C IV line. The non-eclipsing Serpentid KX And does not seem to have any emission at C IV or N V, but C II is conspicuously in emission. There is very little doubt that these varying ratios depend on the temperature of the circumstellar region where the emission lines are formed. Unfortunately, this statistics, too, is not easy to interpret, since we must assume temperature stratification.

The location and extent of the line-emitting region is another problem of great interest. The eclipses help in studying this question, but low brightness and poor time resolution are serious obstacles. Qualitatively speaking, the eclipses reduce the strength of the emission lines, but the diminution is not large in the partially-eclipsing systems β Lyrae and W Ser, as well as in the totally eclipsing systems RX Cas and SX Cas. Relative large decrease in the intensity of the emission lines during totality has been observed in U Cephei (Plavec 1983) and it seems that in that system, the main seat of the emission is quite close to the gainer. In the other systems, the emitting region may be much more extended or possibly partly surrounds the whole system. All these problems require patient gathering and analysis of data before we can be more definitive.

REFERENCES

Kriz, S. and Harmanec, P. 1975, Bull. Astron. Inst. Czech. 26, 65.
Plavec, M.J. 1979, Bull. Amer. Astron. Soc. 11, 648.
Plavec, M.J. 1983, Astrophys. J. 275, 251.
Plavec, M.J. and Koch, R.H. 1978, Inf. Bull. Var. Stars No. 1482.
Polidan, R.S. 1976, in Be and Shell Stars, ed. A. Slettebak, Dordrecht: Reidel, 401.
Struve, O. 1946, Astrophys. J. 104, 253.
Wilson, R.E. and Caldwell, C.N. 1978, Astrophys. J. 221, 917.

MU SAGITTARII AND BETA LYRAE: COMBINED IUE/VOYAGER OBSERVATIONS

Mirek J. Plavec,
Department of Astronomy, University of California, Los Angeles

Ronald S. Polidan,
Lunar and Planetary Laboratory, University of Arizona, Tucson, Arizona

ABSTRACT

A hot companion to the B8 Ia supergiant μ Sagittarii was discovered by observations with three satellites: Copernicus, IUE, and Voyager. The companion is probably a B2 V star, but could be as hot as B0. Voyager observations in the region 900 - 1700 Å have been started also for β Lyrae, and show that the disk-shaped secondary is the dominating source in the EUV.

INTRODUCTION

The binary systems β Lyrae and μ Sagittarii are in many respects very dissimilar. β Lyrae is a well-known peculiar interacting binary with a period of 12.9 days; μ Sagittarii has a much longer period of 180 days, and is probably not interacting. However, spectrophotometrically these two binaries pose very similar problems. In both systems, the optically less luminous component becomes dominant in the far ultraviolet, thus offering us the possibility of determining its character. Moreover, in both systems, the optically dominant component is a luminous B8 star (B8 II in β Lyrae and B8 Ia in μ Sagittarii).

In β Lyrae, the source of this far ultraviolet excess is the disk-shaped secondary component, whose flux becomes higher than that of the primary star at about 1500 Å. Unfortunately, the excess is not sufficiently large and the spectrum is complicated by numerous emission lines. Eclipses help in separating the fluxes of the two components, but the eclipses are only partial.

In μ Sagittarii, the existence of another star was, before the advent of IUE, known only indirectly, from the fact that μ Sagittarii was found to be a single-spectrum spectroscopic binary already by Foster and Adams in 1904. The mass function obtained from the orbital solution is so large ($f(m) = 2.64$) that a fairly massive companion must be postulated. The plausible range of mass ratios appears to be between 0.5 and 0.7. Thus if we assume that the B8 Ia supergiant has, say, 20 solar masses, then the unknown companion must have about 12 solar masses. Such a star should show up in some spectral region. When we failed to detect it in the near infrared, we turned our attention to the far ultraviolet, and indeed found evidence for it with three satellites: Copernicus, IUE, and Voyager.

A small decline in optical brightness of μ Sagittarii at the time of conjunction was reported by Morgan and Elvey in 1938 and by Hall in 1941, and interpreted as a shallow eclipse. However, as Plavec pointed out in 1979, it must be the secondary eclipse, since the B8 supergiant is behind the unknown companion at that time. Plavec therefore predicted a primary eclipse for September 1978, March 1979, and September 1979.

Copernicus scans of μ Sgr on September 10-14, 1978 did indeed show much lower fluxes in five narrow spectral regions between 1065 - 1205 Å, compared to scans made in late May and early August of the same year. Encouraged by this evidence of eclipses, we started a program on the IUE in 1978 and continued over the years as much as proposal evaluations permitted. Another definite evidence of eclipses has been established. The low-dispersion spectra taken on 23 September 1979 and on 3 September 1980 show a much lower flux in the SWP camera than other spectra, specifically those from 16 August 1978, 13 July 1979, and late May 1980.

A very plausible spectrum of an early-type star results from subtraction of these two sets of spectra. As already reported (Plavec 1980) the source appears to be an early-type main-sequence star, probably of a spectral type between B0 - B2. It is not easy to determine its effective temperature more accurately from IUE observations only, because interstellar reddening is not small and not well known (it probably lies near E(B-V) = 0.30), and mainly because the flux distribution is well-established only over a short interval of wavelengths. The worst source of uncertainty is a quasi-periodic brightness variation of the supergiant, discovered by Guinan and Dorren. This variation seems to affect IUE spectra, too, but if it is really due to the supergiant, it should become negligible in the EUV.

Therefore, Copernicus and Voyager observations are extremely important. The first Voyager data by RSP are most exciting. They show a very large flux excess over that expected for a B8 Ia star all over the studied wavelength interval from 1700 Å down to 916 Å. The observed flux distribution of μ Sgr outside eclipse seems to be best matched by a star of an effective temperature of about 24,000 K. In this result, both the Voyager data and our revised IUE data agree, although the IUE data show a good fit over a broad interval of effective temperatures between 24,000 and 35,000 K.

Our Figure 1 shows the good overlap of the Voyager and IUE data at full light. In Figure 2, the IUE spectrum taken during an eclipse is matched by the Voyager scan of β Orionis (B8 Ia) shifted by 2.25 mag. It is seen that the Copernicus observations in eclipse fit in very well.

The first Voyager scan of β Lyrae shows that the secondary component has a much higher color temperature between 900 - 1400 Å than the B8 II primary. More Voyager observations are planned. The importance of these studies cannot be overestimated. In β Lyrae, we have the case of a very extensive, optically and geometrically thick disk. In μ Sagittarii, we have a unique case where the extended atmosphere of an early-type supergiant can be studied by means of a stellar probe, as it passes behind in an eclipse.

Ref.: Plavec, M.J. 1980, in The Universe at Ultraviolet Wavelengths, p. 399.

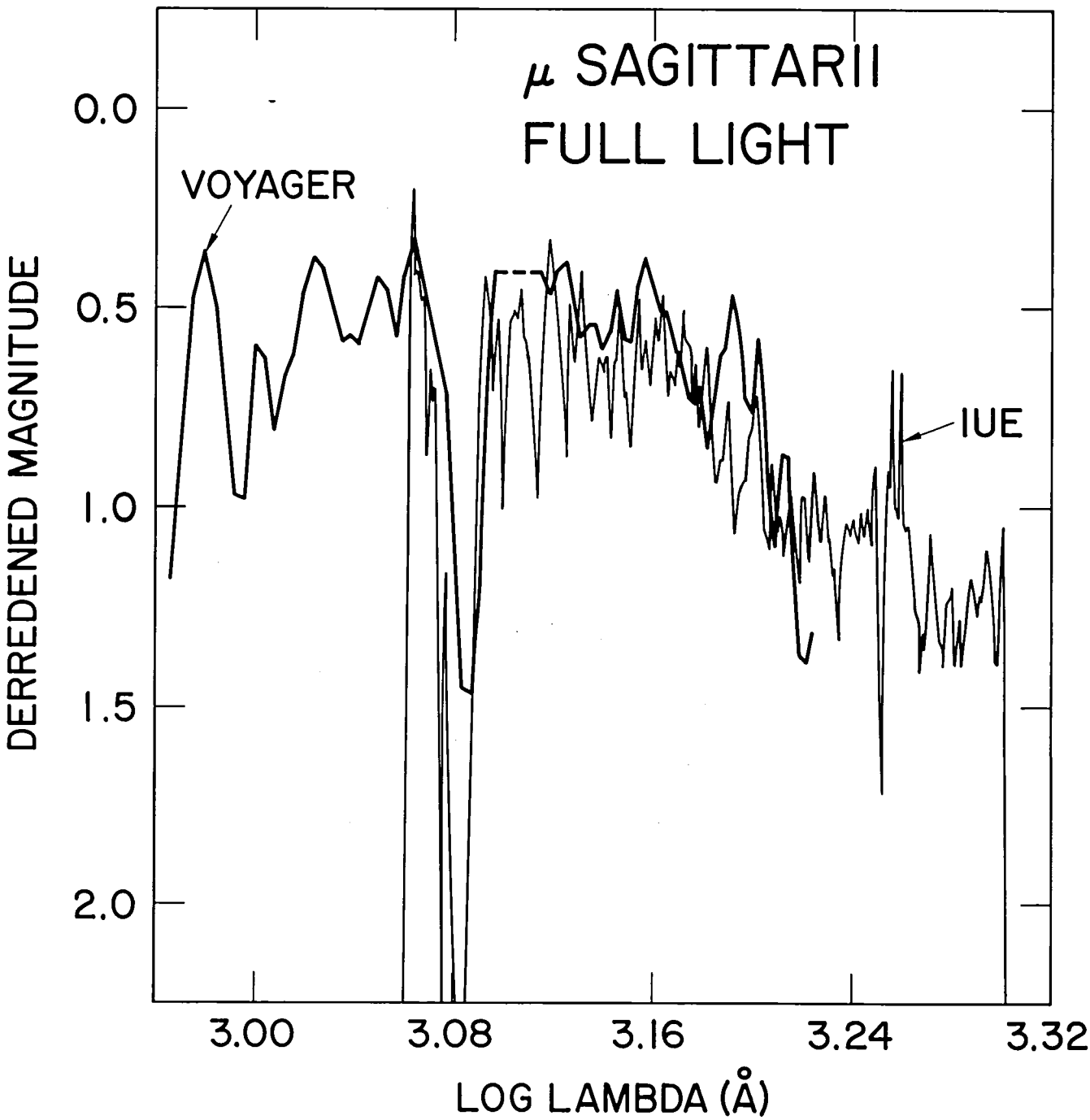
μ SAGITTARII
FULL LIGHT
VOYAGER
IUE
DERREDENED MAGNITUDE
0.0
0.5
1.0
1.5
2.0
3.00
3.08
3.16
3.24
3.32
LOG LAMBDA (Å)

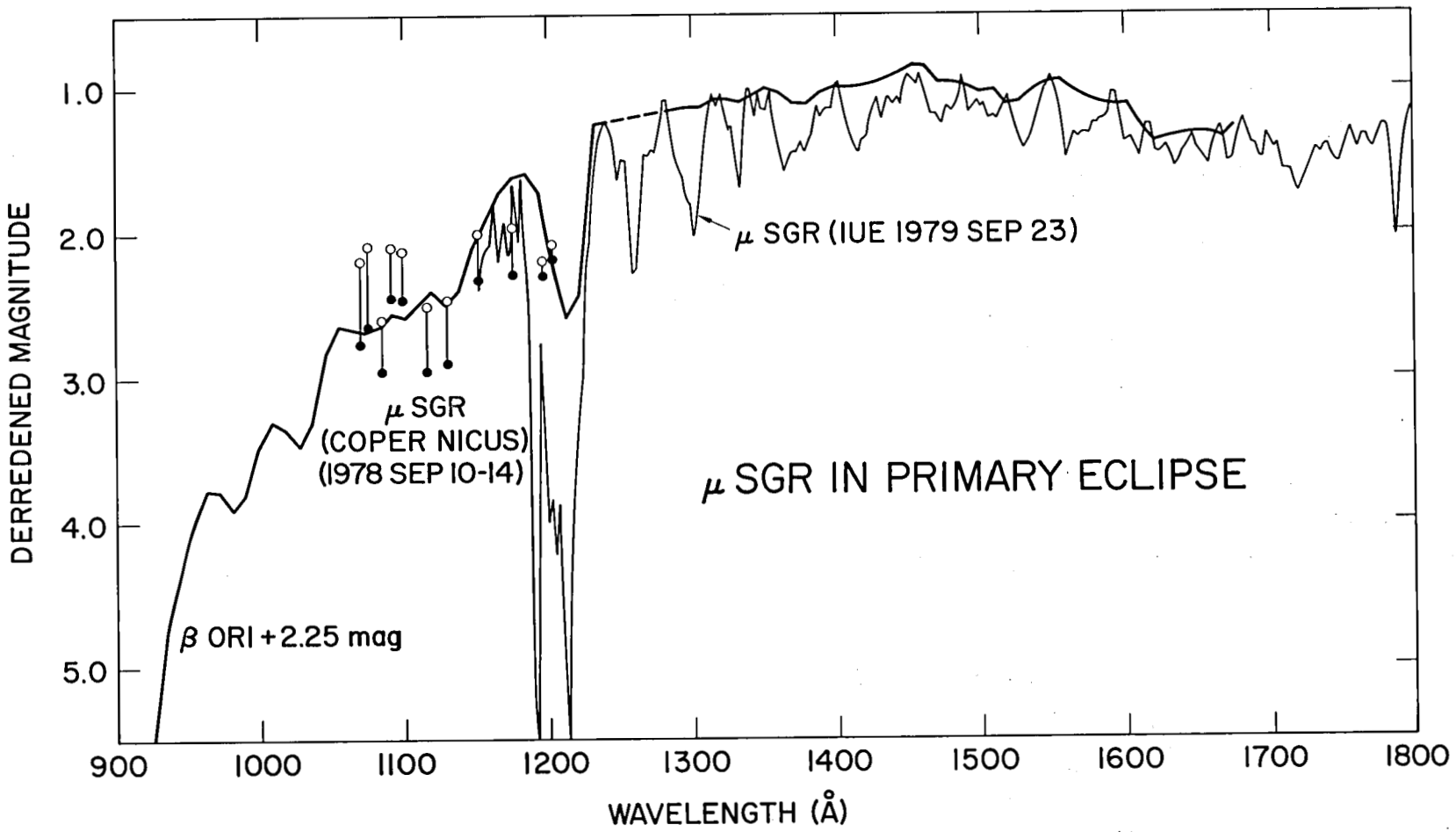
DERREDENED MAGNITUDE
1.0
2.0
3.0
4.0
5.0
900
1000
1100
1200
1300
1400
1500
1600
1700
1800
WAVELENGTH (Å)
μ SGR (IUE 1979 SEP 23)
μ SGR
(COPER NICUS)
(1978 SEP 10-14)
μ SGR IN PRIMARY ECLIPSE
β ORI + 2.25 mag

A SEARCH FOR THE SPECTROSCOPIC BINARY COMPANION OF POLARIS USING IUE SPECTRA

Nancy Remage Evans
Astronomy Program
Computer Sciences Corporation

Abstract

Polaris has a spectroscopic orbit from an extensive series of observations as well as more uncertain astrometric elements. Spectra exposed down to 3200 Å have previously been searched for light from a companion, presumably a hotter main sequence star, but none has been found. In this study IUE low dispersion spectra have been searched for any light from a companion by forming ratios with observations of stars with spectral types similar to Polaris. There is no sign of a companion as early as A7V. Mass limits are discussed.

I. Introduction.

Interest in Polaris (=HD 8890 = Alpha UMi) is due to a number of factors, both questions it raises and the potential for answering some of them.

As a classical Cepheid it has an unusually low amplitude. It is even more markedly peculiar in a unique characteristic recently discovered by Arellano Ferro (1983), the fact that the light amplitude is only half what it was 50 years ago. This fact together with the large period variation for a short period star makes it desirable to make as few assumptions as possible about its properties and evolutionary state.

The fact that it has both a spectroscopic orbit (Roemer 1965) and an astrometric orbit (Wyller, 1957) makes it possible to determine some information about the mass of the Cepheid, although the errors in the astrometric elements lead to large uncertainties.

II. Predictions of Ultraviolet Flux

Spectra exposed down to 3200 Å have previously been searched for light from the spectroscopic binary companion. However since a number of spectra have now been obtained with the International Ultraviolet Explorer (IUE) satellite, a search has been made in the region 1600 to 3200 Å for light from the companion.

Figure 1 summarizes the unreddened magnitudes expected from an F8Ib supergiant and various main sequence stars. $\langle M_V \rangle = -3.^m17$ is adopted for Polaris from the period luminosity relation of Caldwell (1983). The colors for supergiants are taken from Parsons (1981), for main sequence stars from Wessilius, et al. (1980). For main sequence stars, the luminosity calibration of Schmidt-Kaler (1982) was adopted. Very small bolometric corrections were also added.

Figure 1 shows that for an F8Ib supergiant (appropriate for Polaris, as confirmed by the results of Section III.) a main

sequence star A5V or earlier should dominate the short wavelength region of the IUE spectra (2000 to 1200 Å). An A7V or A8V star would double the amount of light seen at 1800 Å. Any main sequence star later than that would be essentially impossible to detect.

III. Ultraviolet Spectra.

Archival spectra of Polaris were ratioed with spectra of nonvariable supergiants of similar types and Delta Cep at two suitable phases to look for a flux increase at the short wavelength. Table 1 summarizes the image numbers, spectal types, intrisic colors, and phases which were used. For the variables Polaris and Delta Cep only pairs of long and short wavelength spectra which were obtained during the same shift were used. Color excesses and colors of supergiants were taken from Fernie (1982), color excesses for Cepheids from Dean, Warren, and Cousins (1978). Colors were read from the curve of Moffett and Barnes (1980) for Delta Cep (using the same period they used), and from the curve of Arellano Ferro (1983) for Polaris. The difficulty of obtaining uniformly well exposed spectra for these late type stars is very clear from Figure 1; the final ratios (dereddened) contain only suitably exposed portions of the spectra. Figure 2 shows the results in increasing order of spectral type. As expected, the proportion of flux from Polaris decreases with decreasing wavelength in comparison to Alpha Per (F5Ib) and increases in comparison to Beta Aqr (G0Ib) down to 1700 Å. Both Gamma Cyg (F8Ib) and Delta Cep (at phase 0.15) are good matches for Polaris (though of course a significant change in the reddening would affect the results). There is no indication of a doubling of the flux of Polaris as would be expected from an A7V companion. The signal to noise decreases markedly in two regions: from 1600 to 1700 Å in all spectra and from 2000 to 2400 Å in Gamma Cyg. The behavior of the ratios from 1700 to 1600 Å is more difficult to interpret, but presumably the very weak spectra, possible scattered light and possible incipient emission (which is present for Beta Aqr) combine to distort the simple temperature dependence evident in the rest of the ratios. In summary, the IUE spectra show no sign of a companion as early as A7V.

IV. Discussion

If we use Popper's compilation of masses (1980) a companion later than A7V must be less massive than 1.8 $M_\odot$. This upperlimit is significantly lower than the limit which can be deduced from ground-based spectra. It does not conflict with orbital information about the system. An evolutionary mass for Polaris (5.5 $M_\odot$), for instance, is consistant with this lower limit and any inclination larger than 40°.

Bibliography

Arellano Ferro, A. 1983 Ap. J., 274, 755.
Caldwell, J. A. R. 1983, The Observatory, 103, 244.
Dean, J. F., Warren, P. R., and Cousins, A. W. J. 1978, M. N. R. A. S., 183, 569.
Fernie, J. D. 1982, Ap. J., 257,193.
Moffett, T. J. and Barnes, T. G. 1980, Ap. J. Suppl., 44, 427.
Parsons, S. B. 1981, Ap. J., 247, 560.
Popper, D. M. 1980, Ann. Rev. Astr. Ap., 18,115.
Roemer, E. 1965, Ap. J., 141, 1415.
Schmidt-Kaler, T. 1982 in Landolt-Bornstein, ed. K. Schaifers and H. H. Voigt (New York: Springer Verlag) 2b, p. 18.
Wesselius, P. R., Duinen, R. J. van, Aalders, J. W. G., and Kester, D. 1980, Astr. Ap, 85, 221.
Wyller, A. A. 1957, A. J., 62, 389.

Table 1

Spectra

	Spectral Type	$(B-V)_0$	E(B-V)	SWP	LWR	Phase
Alpha Per	F5Ib	0.44	0.04	15316	7094	
Delta Cep		0.40	0.09	10475	9143	0.05
Delta Cep		0.49	0.09	10479	9151	0.13
Gamma Cyg	F8Ib	0.65	0.02	3667	3276	
Beta Aqr	G0Ib	0.81	0.03	7124	3290	

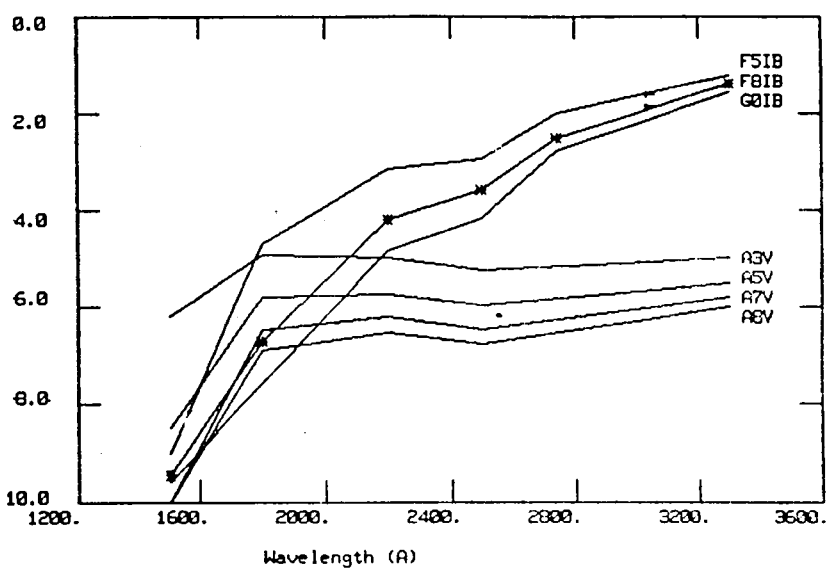

Figure 1. Magnitude differences for supergiants and main sequence stars all with respect to V=0.0 for Polaris.

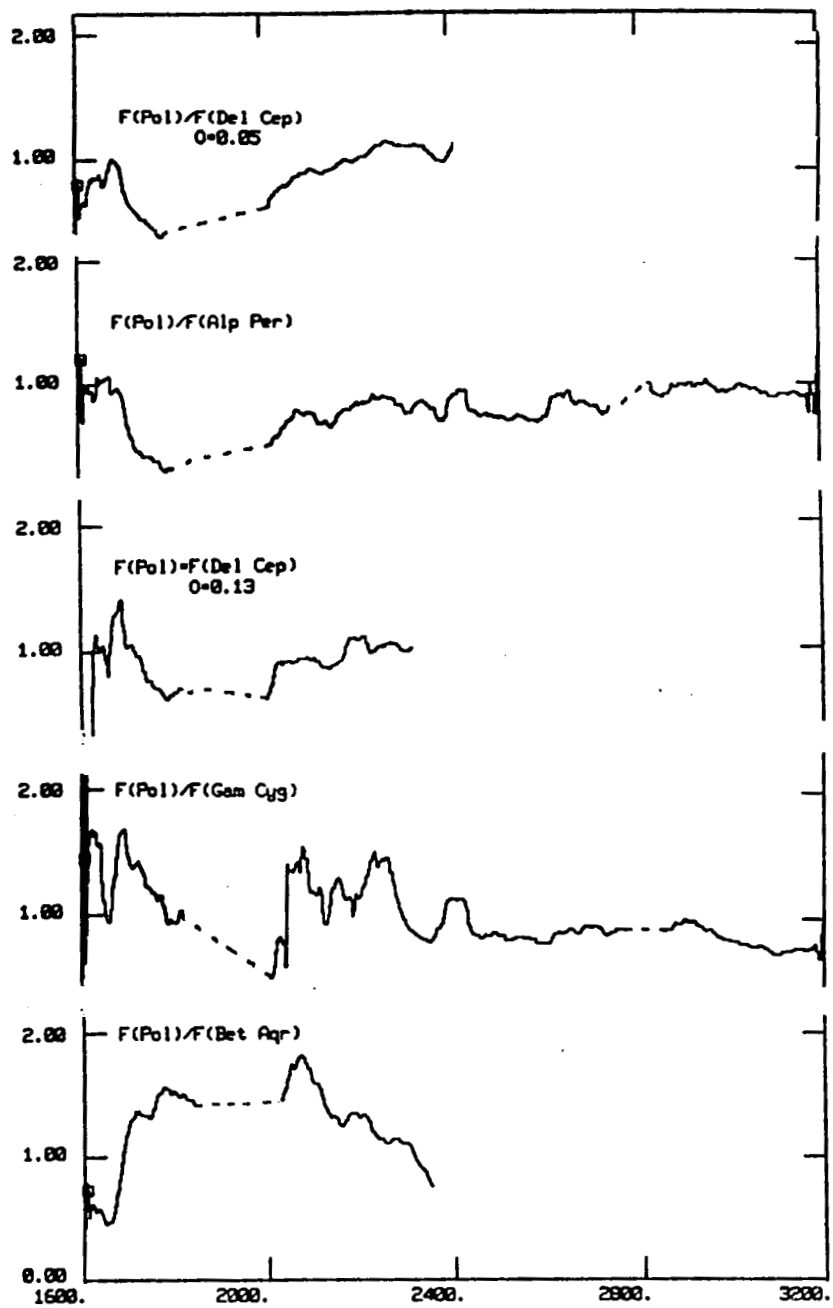

Figure 2. Flux ratios of Polaris to comparison stars in order of $(B-V)_o$. Ratios have been arbitrarily set approximately to 1.0 in the long wavelength region and shifted vertically. Regions where one spectrum is overexposed are represented by dotted lines.

TASKS FOR OBSERVATIONS OF CLOSE BINARY SYSTEMS IN THE EXTREME ULTRAVIOLET

Zdenek Kopal
Department of Astronomy
University of Manchester
Manchester, England

Jurgen Rahe
Remeis-Observatory Bamberg
Astronomical Institute
University Erlangen-Nurnberg
Bamberg, F.R.G.

Close binary systems, which by virtue of the inclination of their orbits to the celestial sphere happen to be eclipsing variables, have in the past century contributed greatly to our knowledge of the physics of their constituent stars; and much more can be expected to be learned from them in the future--not the least because of new observations which can be carried out from spacecraft operating well outside the terrestrial atmosphere, such as the present IUE and its successors of subsequent generations. The aim of the present brief communication should, therefore, be some more specific contributions which can in confidence be expected from them once the sensitivity of their detectors extend beyond the Lyman limit of the hydrogen atom which sets in at $\lambda 912$ Å.

As is well known, an analysis of the light changes of eclipsing variables within minima (at least, of certain types) can disclose--inter alia--the distribution of light over the apparent discs of the stars undergoing eclipse, which in simpliest cases (cf. e.g., Chandrasekhar and Münch, 1949) can be described by the coefficient u of (linear) limb-darkening, given by

$$u = \left\{1 + \frac{2}{3}\left(\frac{8}{a} - 1\right)\frac{K_\lambda}{\bar{K}}\right\}^{-1},$$

where $K_\lambda/\bar{K}$ stands for the ratio of the absorption to opacity coefficients in the respective atmospheric layers; and

$$a = \frac{b}{1 - e^{-b}}, \qquad b = \frac{hc}{\lambda k T_e}$$

represents a logarithmic derivative of the intensity-distribution in the blackbody continuum of effective temperature T_e; and where h = Planck constant, c = velocity of light, and k = Boltzmann constant. In atmospheres consisting predominantly of hydrogen, the coefficient u of limb darkening can, accordingly, be expected to jump up beyond the head of each spectral series (Lyman, Balmer, etc.) as a consequence of the electrons being liberated by ionization, and a difference between the values of u

deduced from observations at effective wavelengths above and beyond the limit of the respective series can then be utilized to indicate the electron density of the medium.

A quest for an empirical value of this difference above and below the Balmer limit at λ3647 Å was already attempted from ground-based facilities in the years past but without much success, because the vagaries of atmospheric extinction at these wavelengths did not permit attainment of sufficient precision of the underlying observations. Resorting to spacecraft operating above the atmosphere and utilizing detectors which remain sensitive down to the Lyman limit at 912 Å should enable us not only to bypass all deleterious effects of atmospheric extinction but also to measure a quantity much more significant from the observational point of view (because the difference in darkening on either side of the Lyman limit should be considerably larger than is the case with the Balmer limit).

A second--and closely related--aspect should also be mentioned in this connection. In recent years, much speculation has been indulged in about the presence of circumstellar hydrogen (and helium) in which components of close binary systems are imbedded--often, however, without sufficient consideration of the physical state of such a hypothetical gas or of the quantitative aspects of the effects which such a gas should produce in accessible parts of the spectra.

If, however, the density of such circumstellar gas (again predominantly hydrogen) were to exceed a certain limit, the apparent limb of the star undergoing eclipse, deduced from observations at wavelengths below the Lyman limit, need not have anything in common with the position of this limb observable at optical frequencies that are accessible from the ground. In other words, the fractional dimensions of the components of eclipsing systems deduced from an analysis of the light curves observed at λ912 Å need not refer to the optical limb (i.e., the photosphere) of the respective star, but rather to the dimensions of the Stromgren spheres (or lobes!) separating the HI and HII regions in the system--just as the eclipse of our Sun by the Moon, observed in the microwave domain of the radio-spectrum, does not commence at the time of first contact of the two discs but rather hours before--when the Moon commences to encroach on the solar corona! The first steps toward the development of a theory of Stromgren lobes in close binary systems have aready been taken by one of us (cf. Kopal, 1981) to which the reader may be referred for fuller details, but much work remains still to be done before this subject can be placed on a more solid basis.

The question can, of course, be asked: how many of the known eclipsing systems could be actually observable with our present (or proposed) space telescopes through the intervening interstellar haze at wavelengths below the Lyman limit? It is true that the transparency of interstellar space for λ912 Å diminishes rather rapidly with distance--especially in the plane of the Galaxy. Nevertheless, more than a dozen eclipsing systems of adequate apparent magnitude and suitable for the proposed analysis are

known to us at intermediate galactic latitudes where interstellar absorption is weak, and which should be observable with the present optics of the IUE if the sensitivity of its detectors at the Lyman limit were comparable with that attained at L_α.

A list of such binaries can easily be compiled; it is hoped that it may be kept in mind by future investigators in this enchanted field of double-star astronomy. Suitable stars are certainly not lacking in numbers; and the technical problem is essentially one of detectors. Once, however, this latter problem has been resolved, the opening up of the Lyman limit domain to photometers in space, directed to observe close binaries at intermediate galactic latitudes, will without doubt inaugurate a new and exciting chapter in stellar astrophysics.

References

Chandrasekhar, S. and Münch, G.: Harvard Circular No. 453, 1949.

Kopal, A.: NATO Advanced Study Institutes Series (D. Reidel Publ. Co., Dordrecht), Vol. 69, p. 535, 1981.

COOL STARS

THE SOLAR STELLAR CONNECTION IN THE FAR ULTRAVIOLET

J.O. Bennett, T.R. Ayres, and G.J. Rottman, Department of Astrophysical, Planetary, and Atmospheric Sciences, and Laboratory for Atmospheric and Space Physics, University of Colorado

1.0 Introduction

We compare the far-ultraviolet "activity" of solar type stars, as measured with the IUE, to that of the Sun, as measured by the Solar Irradiance Monitor of the Solar Mesosphere Explorer (Rottman et al., 1982, Geophys. Res. Letters, 9, 587). The goal of our study is to explore the relationships between the "ultraviolet activity" at different levels of the atmospheres of solar type stars, after the manner of Ayres, Marstad and Linsky (1981, Ap. J. 247, 545). In particular, we have produced diagrams that depict correlations of fluxes of ultraviolet emission lines formed at different temperatures in the stellar outer atmosphere. Secondary goals are to establish, quantitatively, the strength of the solar ultraviolet activity within the class of solar-type stars, and to examine the amplitudes of rotational modulations of the solar emission lines during the declining portion of the current sunspot cycle.

A unique aspect of our study is that the spectral resolution of the SME instrument (7.5 Å) compares very favorably with that of the low dispersion mode of the IUE (5 Å). Furthermore, the SME instrument measures the full-disk solar irradiance, analogous to the spatially unresolved spectra of stars obtained by the IUE. Accordingly, the solar and stellar data can be reduced in a nearly identical fashion, thereby minimizing systematic errors that otherwise might be a concern.

2.0 Observations

The lines chosen for the present study were C IV (λ1550), C II (λ1335), C I (λ1657) and O I (λ1305). C IV is formed in the transition zone at 10^5 K; C II is formed in the high chromosphere at about 3×10^4 K; and the multiplets of neutral oxygen and carbon are formed deep in the chromosphere at 6,000 K.

Data for main sequence solar type stars, ranging in spectral type from F8 through G5, were obtained from the IUE archives at the Colorado RDAF. In some cases, several spectra of a given star were available, and were treated individually in the subsequent analysis.

The solar data set consisted of weekly averages of SME irradiance spectra taken over an 11 month period in 1982. The absolute flux scale of the SME spectra is maintained by periodic flights of calibration rockets.

3.0 Data Reduction

Owing to the large amounts of stellar (and solar) data to be analyzed, and our concerns of operator biases in interactive fitting procedures, we developed an automatic numerical algorithm to find, and measure, the reference emission lines in each spectrum.

Since the important C IV and C I features are located on top of a significant photospheric continuum in solar-type stars, we required a systematic technique to determine the appropriate continuum shape for each spectrum. First, the spectrum is smoothed by a median filter, and one pass of a running mean. Next, a "clipped" spectrum is created by taking the minimum of the smoothed spectrum or the original spectrum point-by-point, thereby effectively eliminating sharp emission structure. Last, the clipped spectrum is smoothed further by an additional pass of a running mean to provide an approximate continuum

background. This approach is straightforward to implement in an automatic algorithm, and has the important advantage that the continuum fit is systematically applied to all spectra without an operator bias.

Once the continuum level was determined, and subtracted from the spectrum, the automatic procedure identified the reference lines and measured their fluxes by means of a least-squares Gaussian fitting procedure. The results of the measurement procedure were stored in a disk file for later processing. Measurement errors were determined for the line fluxes according to the RMS deviation of the observed profile from the fitted Gaussian and the semi-empirical relations given by Landman, Roussel-Dupre and Tanigawa (1982, Ap. J., 261, 732). In this regard, the solar and stellar data were treated somewhat differently, since the former is governed by photon statistics, while the latter is dominated by readout noise and particle radiation fogging.

4.0 Results

Figure 1 illustrates sample spectra of the Sun and two nearby solar type stars: χ^1 Orionis and α Centauri A. The stellar spectra shown are composites of up to ten individual IUE spectra. The solar spectrum is an average of the entire set of SME data for the 11 months of 1982. The three spectra are qualitatively similar, although it is clear that χ^1 Ori is an order of magnitude more "active" than the Sun or α Cen A.

Figure 2 depicts the weekly averaged fluxes of several important solar lines over the course of 1982. Note that a pronounced rotational modulation is seen in all of the lines during the latter half of the year, but almost no modulation is apparent during the first half. The onset of the prominent modulation coincided with the development of a major active region on one hemisphere of the Sun near the middle of 1982 which persisted for many rotations. The modulation of over 25% seen in the second half of the year in H I Lyα is consistent with that observed in other solar-type dwarfs by Hallam and Wolff (1981, Ap. J. [Letters], 248, L73.)

Finally, we present diagrams comparing the normalized fluxes (i.e. f_L/f_{bol}, where f_{bol} is the bolometric flux of the star) of different line pairs for the Sun and our sample of solar-type stars. Figure 3 illustrates C IV versus C II; Figure 4, C IV versus C I; and Figure 5, C I versus O I. For both the stellar data and the solar data, power laws were fitted to the observed normalized fluxes and plotted. The solar data covers a smaller range than the stellar data, but the slopes of the power laws appear to agree reasonably well within the uncertainties of the fits.

5.0 Discussion

The steepest power law slopes are for the correlation of the highest excitation line (C IV) against the lowest excitation line (C I). An analogous behavior was seen in the study by Ayres, Marstad and Linsky between the combined flux of N V + C IV + Si IV and the chromospheric species Mg II. This behavior was interpreted to indicate that the heating rates of the chromosphere and transition zone are strongly related, but are not identical functions of increasing activity. Furthermore, the C IV-C II flux correlation exhibits a unit power law slope in both the solar and stellar data, indicating a one-to-one correspondance between the fluxes formed at somewhat different temperatures in the transition zone, and suggesting a unity of the heating rates above about 3×10^4 K. However, the fact that the C I-O I correlations do not exhibit a one-to-one correspondance in either the stars or the Sun is somewhat of a mystery, but perhaps is related to the partial production of oxygen triplet emission by Lyβ pumping.

For the future, we hope to use these correlations and measurements of apparent Lyα emission from G-type dwarfs in the solar neighborhood to probe the abundance of neutral hydrogen in the local interstellar medium.

This study was supported by NASA through grant NAG5-199 to the University of Colorado. We thank the staff of the Colorado RDAF for their help in the analysis of the stellar spectra.

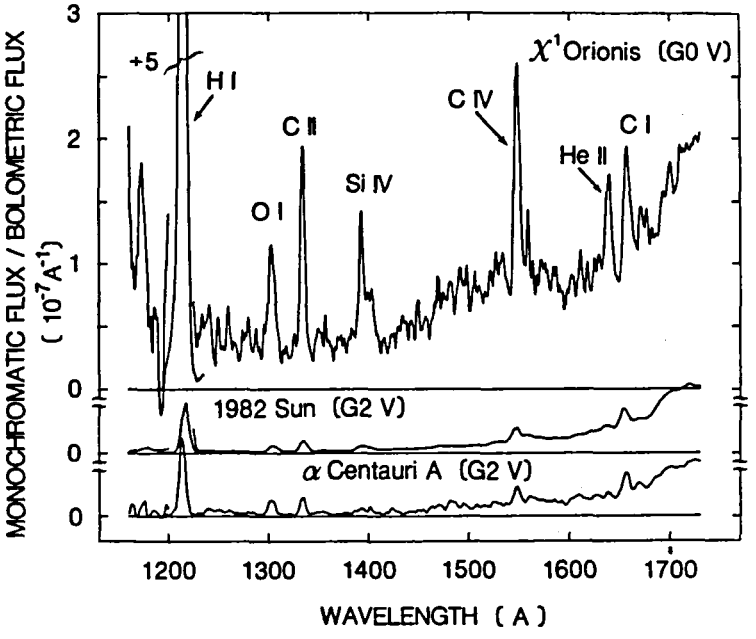

Figure 1.

Sample spectra taken by the IUE for two solar-type stars, and by the SME for the Sun.

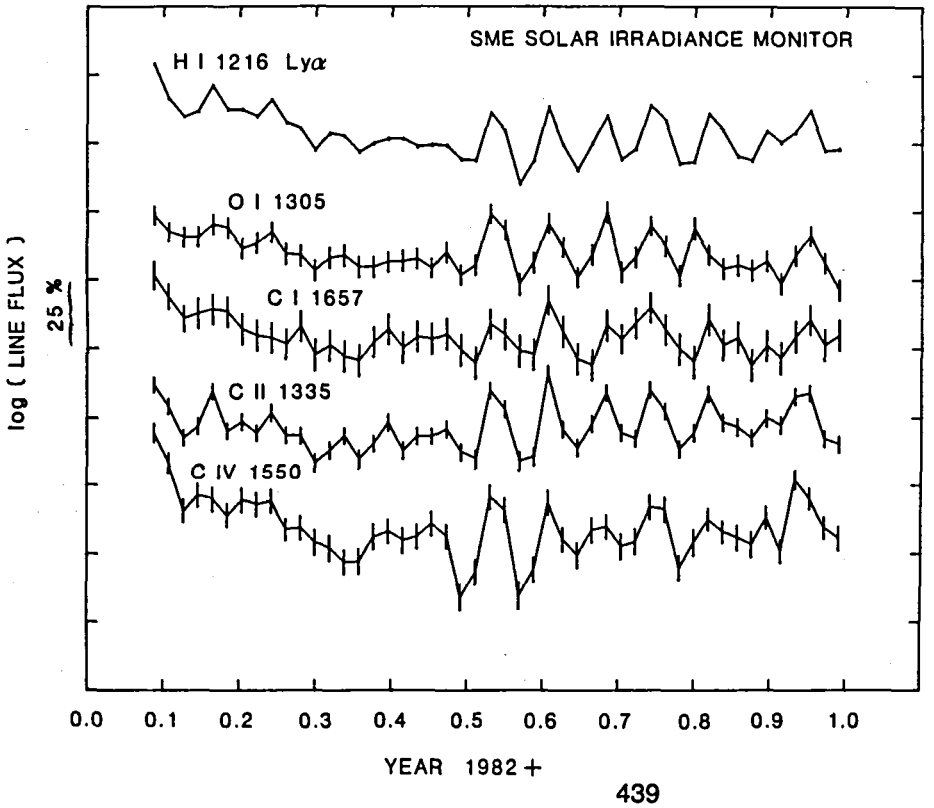

Figure 2.

Weekly averaged fluxes for several lines in the Sun during 1982.

Solar-type stars (IUE)

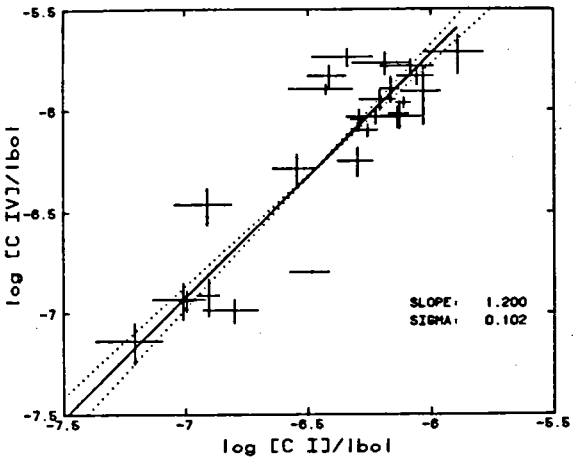

Sun (SME)

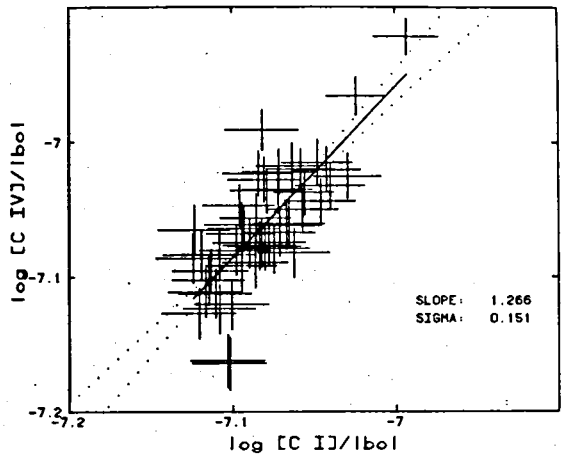

Figure 3.

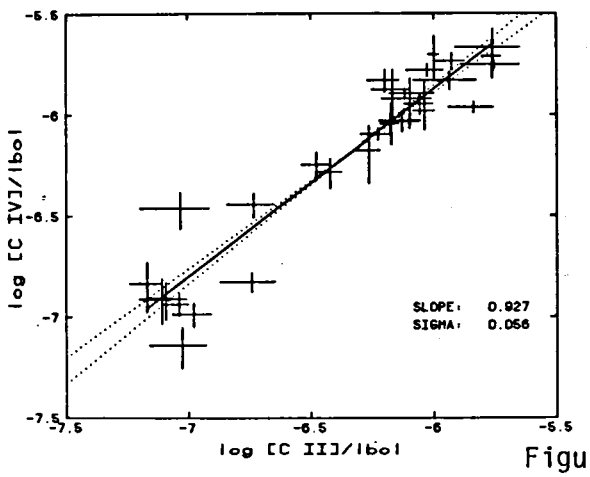

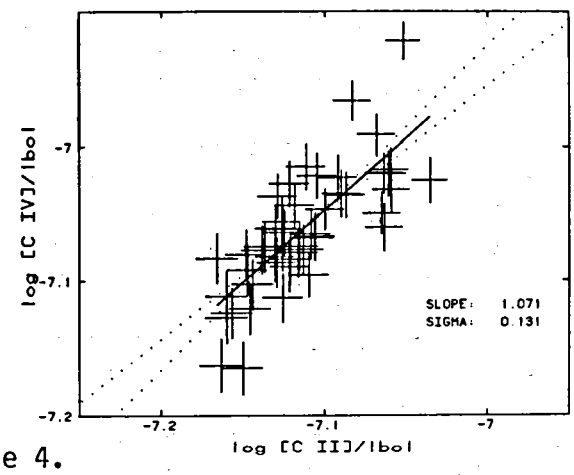

Figure 4.

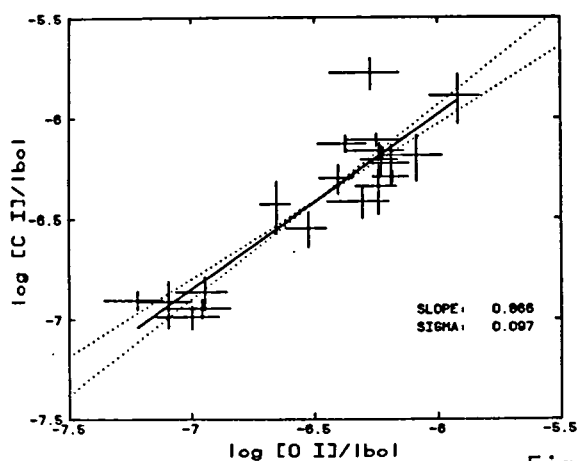

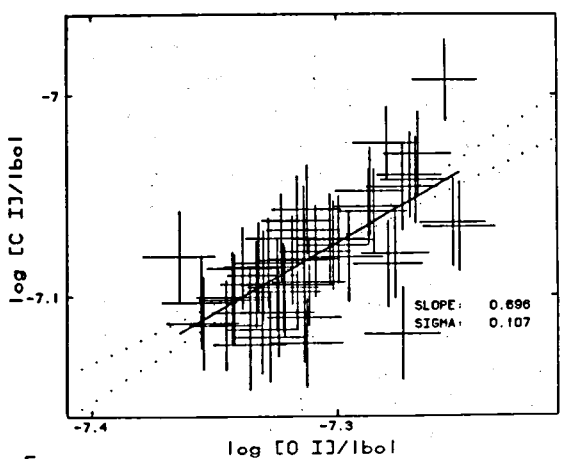

Figure 5.

CHROMOSPHERIC ACTIVITY IN M GIANTS

Thomas Y. Steiman-Cameron
Mt. Wilson and Las Campanas Observatories
of the
Carnegie Institution of Washington

Hollis R. Johnson, R. Kent Honeycutt
Astronomy Department, Indiana University

Low-resolution IUE spectra have been obtained with the LWR camera for fifteen cool giant stars ranging in spectral type from K4.8 thru M5.9. These spectra have been used to examine chromospheric activity in late type giants and to evaluate the extent to which nonradiative heating affects the upper levels of cool giant photospheres. The program stars are from the Ridgway et al. (1980) sample used in the study of effective temperatures of late-type field giants. These stars were chosen because they all have well determined wide band colors, TiO band strengths (from Wing photometry), angular diameters (determined from lunar occultations), apparent bolometric fluxes as seen from Earth, and effective temperatures. In this paper we present the preliminary analysis of these observations.

Fluxes in the resonance lines (h and k) of Mg II ($\lambda\lambda$2796,2803) and integrated fluxes in the wavelength region 2830 to 2950 A (hereafter referred to as F289) were measured using the facilities of the Regional Data Analysis Facility (RDAF) at Goddard Space Flight Center. Mg II emission is a major source of chromospheric cooling and Linsky and Ayres (1978) have argued that the total chromospheric radiative loss rate in spectral lines should be roughly proportional to the radiative loss rate in the Mg II lines. Therefore the flux in the resonance lines provides a direct measure of the level of chromospheric activity. Because the h and k lines are not separately resolved in the LWR spectra, our measured fluxes are the combined fluxes in both lines. Measured Mg II and F289 fluxes are tabulated in Table 1.

The accurate determination of Mg II fluxes requires that the IUE spectra have well exposed, but not overexposed, h and k lines. In two spectra (HD75156 and BS 7900) obtained on October 10, 1983 these lines were saturated providing only lower limits for the resonance line flux. However, only one pixel was saturated in each case, therefore the limits obtained are probably quite close to the correct value. One of these stars (HD75156) was subsequently observed a second time on January 1, 1984. This presented an opportunity to look for short term (3 month) variability in the spectrum. The Mg II flux found in January was ~ 20% lower than that found in October while the integrated continuum flux f289 remained constant to within the accuracy of the observations. The amount of variability found in the Mg II lines is consistent with rotation carrying an active region out of the visible disk. Ca II emission, also an indicator of chromospheric activity, has previously been found to vary at this level and this variation has been ascribed to rotational modulation.

TABLE 1.

BS/HD	Sp.†	V-K	T(eff)† K	F(bol)† E-8 cgs	ang. dia.† E-3 arcsec	F(MgII h&k) E-12 cgs	F289 E-12 cgs
224	K4.8	3.57	3560 +/-400	121.	4.75 +/-1.13	1.42	2.52
601	M3.3	4.57	4070 +/-380	64.3	2.65 +/-0.51	1.68	3.72
867	M5.9	6.65	3350 +/- 30	433.	10.2 +/-0.2	4.84	3.07
29051	M1.1	5.12	3680 +/- 90	55.1	3.01 +/-0.15	0.34	0.68
2938	M0.0	3.87	4090 +/-200	82.3	2.97 +/-0.29	4.20	10.0
75156	M3.3	4.60	2810 +/-110	35.6	4.13 +/-0.32	>1.30(a)	1.42(a)
						1.08(b)	1.40(b)
3950	M1.7	4.11	3710 +/-110	150.	4.88 +/-0.28	5.70	11.7
6861	M4.1	6.24	4950 +/-590	253.	3.55 +/-0.89	1.20	1.86
7023	M5.2	6.57	3170 +/- 30	274.	9.03 +/-0.17	1.18	1.68
176124	M4.3	5.39	4030 +/-610	71.5	2.85 +/-0.92	1.02	2.86
7900	M2.1	4.30	3540 +/-190	116.	4.72 +/-0.52	>5.00	6.92
8318	M3.4	4.74	3840 +/-390	72.4	3.16 +/-0.68	2.20	3.04
8698	M2.0	4.42	3750 +/-100	442.	8.21 +/-0.44	10.0	120.
8834	M1.5	4.00	3770 +/-300	199.	5.44 +/-0.89	7.20	16.9
9047	M4.6	5.49	3390 +/-110	174.	6.30 +/-0.40	3.12	3.73

† From Ridgway et al. (1980)
(a) October 10, 1983
(b) January 1, 1984

Figure 1 shows the log of the Mg II h and k fluxes, normalized to the apparent bolometric fluxes, plotted against the effective temperatures found by Ridgway et al. (1980). Though a certain amount of scatter exists, it is apparent that chromospheric activity, as measured by Mg II, diminishes rapidly at lower effective temperatures. This type of behavior has been previously noted (c.f. Basri and Linsky 1979; Linsky 1980; Catalano 1983), though the rate of decrease with effective temperature found here is more rapid than previously thought. This discrepancy stems from the more accurate determination of effective temperature for the stars observed in this study. Because the program stars have reasonably well determined angular diameters, the Mg II fluxes can be used to determine the intensity of Mg II radiation averaged over the disk of the star. With the definition $I(Mg) = F(Mg)/r^2$, where r is the angular diameter, Figure 2 shows the log of I(Mg) plotted against effective temperature. Again, the intensity drops rapidly at lower temperatures but the scatter is somewhat smaller than that found in Figure 1.

Two stars (HD75156 and BS 6861) show substantial deviations from the general trends found in Figures 1 and 2, and this will be discussed below. Although a smooth line can be drawn in Figure 2 which includes the error boxes of all but one of the remaining stars (HD29051) it is probable that much of the scatter is real. Physical variables which might be expected to play a role in chromospheric activity in cool giants include mass, age,

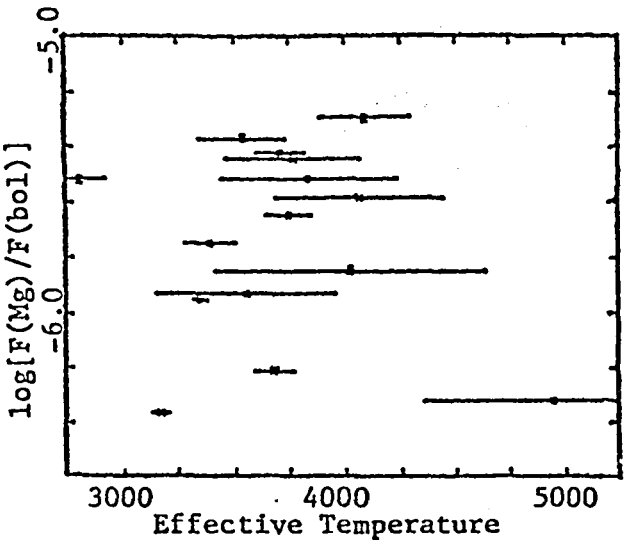

Figure 1. Log of the normalized MgII h and k flux as a function of stellar effective temperature.

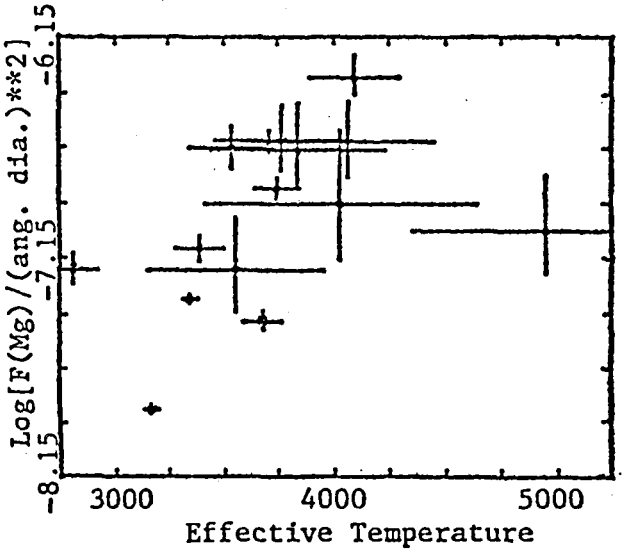

Figure 2. Log of the intensity (averaged over stellar disk) of Mg II h and k radiation as a function of effective temperature.

metallicity, rotation rate, magnetic field strength (probably not strictly independent of rotation rate), and the presence of companions (see Linsky 1980). Discussions of the dependence of chromospheric activity on rotation (among main sequence stars) and age can be found in Wilson (1963), Skumanich (1972), Vaughn and Preston (1980), Hartmann et al. (1984), and references therein. While it is impossible at present to determine the origins of scatter found in Figures 1 and 2, it is interesting to note that on a purely statistical basis we would expect the main sequence precursors of these stars to have been in the range of late A thru early G. This spans the transition of main sequence stars from rapid rotators (earlier than mid F) to slow rotators (later than mid F). It would not be unreasonable to expect that some of this rotational variation would be carried over into the red giant phase, though with considerably slower rotation rates. Chromospheric activity among main sequence stars is known to have a correlation with rotation rate (see references cited above) and order of magnitude variations in F(Mg)/F(bol) among main sequence stars of a given effective temperature have been attributed to this effect (Catalano 1983). It is possible, therefore, that rotationally induced scatter may exist in the chromospheric activity of red giants of a given effective temperature which arises from differences in their main sequence precursors.

Errors in the measured angular diameters, and hence effective temperatures, would introduce noise into the relations of Figures 1 and 2. Since these quantities are often not as accurate as one would like (as evidenced by the large quoted uncertainties for some stars in Table 1) we have replotted the normalized Mg II fluxes against a well observed quantity, the wide band color V-K. This is shown in Figure 3. While some scatter

persists, the relation is much tighter than in the earlier figures. The stars HD75156 and BS 6861, which deviated greatly from the rest of the stars in Figures 1 and 2, do not deviate from the trend in Figure 3. This agreement plus the fact that both stars lie far off the color temperature (from Wing photometry) - effective temperature relation found using the total sample of Table 1 suggests that the effective temperatures determined for these stars may be in error.

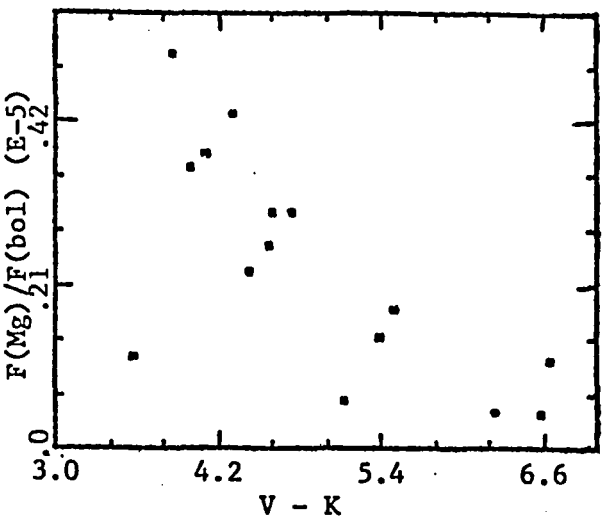

Figure 3. Normalized Mg II h and k fluxes as a function of the Johnson V-K color index.

The third star which deviated from the trends of Figures 1 and 2, HD 29051, also is discordant in Figure 3. All three figures suggest that this star has a chromosphere which is underactive for stars of similar characteristics. It is interesting to note that this star is noted for having a spectral type (as determined by TiO bandstrengths) which is abnormally early for its observed color (Ridgway et al. 1980). In the coming year we expect to acquire additional observations of both "normal" stars (stars whose spectral types are consistent with their wide band colors) and stars with abnormal spectral types for their colors. We hope to use this data to further our understanding of the interplay between the chromosphere and the outer layers of the photosphere where the spectral type determinant for M giants (TiO) is formed.

REFERENCES

Basri, G. S., and Linsky, J. L. 1979, Ap. J., 234, 1023.

Catalano, S. 1983, Mem. S. A. It.,54, No. 2, 553.

Hartmann, L., Sonderblom, D.R., Noyes, R.W., Burnham, N., and Vaughn, A.H. 1984, Ap. J., 276, 254.

Linsky, J.L., and Ayres, T.R. 1978, Ap. J., 220, 619.

Linsky, J.L. 1980, Ann. Rev. Astron. Astrophys., 18, 439.

Ridgway, S.T., Joyce, R.R., White, N.M., and Wing R.F. 1980, Ap. J., 235, 126.

Skumanich, A. 1972, Ap. J., 171, 565.

Vaughn, A.H., and Preston, G.W. 1980, Pub. A.S.P., 92, 235.

Wilson, O. 1963, Ap. J., 138, 832.

A PROGRESS REPORT ON THE ANALYSIS OF LONG EXPOSURE SWP HIGH RESOLUTION SPECTRA OF COOL STARS

J. L. Linsky,[1,2] T. R. Ayres,[3] A. Brown,[1] K. Carpenter,[1]
C. Jordan,[4] P. Judge,[4] B. Gustafsson,[5] K. Eriksson,[5]
M. Saxner,[5] O. Engvold,[6] E. Jensen,[6] O. K. Moe,[6] T. Simon[7]
[1]Joint Institute for Laboratory Astrophysics, University of Colorado and National Bureau of Standards, Boulder, CO 80309.
[2]Staff Member, Quantum Physics Division, National Bureau of Standards.
[3]Laboratory for Atmospheric and Space Physics, Univ. Colo., Boulder, CO 80309.
[4]Department of Theoretical Physics, Oxford University, UK.
[5]Astronomiska Observatoriet, Uppsala University, Sweden.
[6]Institute of Theoretical Astrophysics, University of Oslo, Norway.
[7]Institute for Astronomy, University of Hawaii, Honolulu, HI 96821.

I. INTRODUCTION

IUE is the first experiment with sufficient sensitivity to obtain high resolution spectra ($\lambda/\Delta\lambda \approx 10{,}000$) of many cool stars in the vitally important 1200-2000 Å spectral region. These data provide qualitatively new information with which to understand the properties of and structures in the outer atmospheres of these stars. Also, these cool star spectra will be extremely useful in planning for the Space Telescope High Resolution Spectrograph, which will be 10^4 times more sensitive than IUE but will be hampered by limited observing time and limited spectral bandwidth in each exposure.

During the last few years we have obtained very long exposure, high-dispersion SWP spectra of many stars located throughout the cool half of the HR diagram. These 12-21 hour exposures were obtained by combining NASA and Vilspa shifts so as to obtain the longest possible exposures at times of low background. Included are dwarf stars of spectral type G0 V-M2 V, G9.5 III-M5 II giants, G2 Ib-M2 Iab supergiants, a number of RS CVn-type systems, and Barium stars. Table 1 is a nearly complete summary of our data set, deleting only the very short exposures and observations of premain sequence stars. Given the importance of this data set and the many questions that it can answer with appropriate data reduction and extensive modeling efforts, we summarize briefly what has and is being done with these data.

II. SEPARATION OF CLOSE LINE BLENDS

High resolution spectra are essential in identifying which emission lines are the dominant contributors to the blends generally observed in the IUE low resolution spectra. Table 2 summarizes which lines contribute to the important grouping of emission lines at 1294-1306 Å, 1393-1407 Å, 1640-1641 Å, 1807-1826 Å, 1892-1914 Å. For additional information the reader is referred to Refs. (2) and (15) and to the references for each star listed in Table 1. We note the importance of S I features in the 1295-1306 Å, 1807-1826 Å, and 1892-1915 Å regions in the cool giants and especially the cool supergiants (2,9,11,14,15). Deep exposures of the 1393-1407 Å region in active stars,

Table 1

Summary of Well-Exposed, High-Dispersion SWP Spectra Obtained by the Authors

HD	Star	Spectral Type	m_v	Program	Exposure Time (min)	Remarks and References
39587	χ^1 Ori	G0V	4.4	CCDTA	420	(7)
				CSFTA	845,†870,†840†	(2)
128620	α Cen A	G2V	0.0	CSCJL	400	+ shorter exposures (2),(6),(7),(9),(11)
131154	ξ Boo A	G8V	4.5	CCDTA	952	(2),(7)
128621	α Cen B	K1V	1.3	CSCJL	340	+ shorter exposures (2),(6),(7)
22049	ε Eri	K2V	3.7	CCDTA	447†	(7),(11)
				CSFTA	530†	(2)
	AU Mic	M2Ve	8.6	DMEJL	1080	Flare star (3)
61421	α CMi	F5IV-V	0.4	UK252	90	(12)
				CSFTA	110,†60†	(2)
2151	β Hyi	G2IV	2.8	CSDJL	938	
4128	β Cet	G9.5III	2.0	LGDRS	795	(2),(11)
62509	β Gem	K0III	1.1	UK482	374	
				CCFJL	1010†	
124897	α Boo	K2III	0.1	CSCJL	420†	(9)
				LGFTA	1290†	Longest SWP-HI exp. (2)
29139	α Tau	K5III	0.9	UK252	400†	
6860	β And	M0III	2.0	LGFJL	930†	
159181	β Dra	G2Ib-II	2.9	CSDRS	1273	Longest continuous SWP-HI exp. (6),(11),(13),(14)
214952	β Gru	M3II	2.2	CSEJL	975†	
156015	α Her	M5II+G5III+A	3.1	LGFJL	790†	
48329	ε Gem	G8Ib	3.1	CCFJL	†	New exposure 5 Apr 1984
78647	λ Vel	K5Ib	2.3	CSEJL	976	
39801	α Ori	M2Iab	0.8	LGDRS	930	
118216	HR 5110	F2IV+K	5.0	OD49B	378	After flare of 6 Apr 1981
34029	α Aur	G6III+F9III	0.1	CEJLL	180†	+ many shorter exposures (4),(6)
				RSETA	148†	+ 5 shorter exposures (conjunction) (1),(2),(8),(11)
13480	ι Tri	G5III+G5III	5.5	RSETA	730	
222107	λ And	G8III-IV	3.9	CSCJL	450†	(6),(11)
				CSFTA	730†	(2)
22468	HR 1099	K0IV+G5V	6.0	CSCJL	435,375	Opposite quadratures (5)
				RSDJL	120†	During flare of 3 October 1981
				FSETA	420†	6 phases
21231	UX Ari	K0IV+G5V	6.6	FSDJL	400,450	Opposite quadratures
62044	σ Gem	K1III+?	4.2	RSETA	420,425	Near conjunction (10)
204075	ζ Cap	G4Ib+WD	3.7	CBEJL	987	Barium star
218356	56 Peg	K0Ib+WD	4.8	CSDRS	1040	Barium star (2),(16)

†Observations obtained, or to be obtained, with a procedure to ensure a precise radial velocity scale.

Table 2

Close Blends Resolved in IUE High-Dispersion Spectra

Wavelength (Å)	Ion	G Dwarf	G Supergiant	K Dwarf	Early K Giant	Later K Giant	K Supergiant	M Dwarf	M Giant	M Supergiant	RS CVn System
		χ^1 Ori (G0V)	β Dra (G2Ib-II)	ε Eri (K2V)	β Cet (G9.5III)	α Boo (K2III)	λ Vel (K5Ib)	AU Mic (M2Ve)	β Gru (M3II)	α Ori (M2Iab)	α Aur (F9III+)
1294.534	SiIII	--	--	--	VW	--	--	--	--	--	--
1295.653	SI	W	S	--	W	W	S	--	W	W	W
1296.174	SI	--	W	--	VW	W	S	--	S	W	VW
1296.726	SiIII	--	--	--	S	--	--	--	--	--	--
1302.169	OI	S	VS	S	S	S	VS	S	S	--	VS
1302.337	SI	--	S	--	W	?	--	--	--	VW	--
1302.863	SI	--	--	--	VW	W	S	--	W	--	VW
1303.111	SI	--	--	--	--	--	--	--	--	--	--
1304.858	OI	S	VS	S	VS	VS	VS	S	S	--	VS
1305.883	SI	--	--	--	--	--	--	--	--	--	--
1306.029	OI	S	VS	S	VS	VS	VS	S	S	--	VS
1393.755	SiIV	S	S	S	S	--	--	--	--	--	S
1401.156	OIV	--	W	--		--		--			W
1402.770	SiIV	--	S	W	S	--	--	--	--	--	S
1404.812	OIV	--	W	--		--		--			W
1407.386	OIV	--	--	--							--
1640.151	FeII	--	--	--	--	--	--	--	--	--	--
1640.474	HeII	S	S	S	S	--	--	S	--	--	S
1641.305	OI	--	W	--	--	S	S	--	S	S	W
1807.311	SI	--	--	--	--	W	S	--	S	VS	
1808.012	SiII	S	S	S	S	VS	S	S	W	W	S
1816.928	SiII	S	VS	S	VS	W	VS	S	S	S	S
1817.451	SiII	S	S	S	W	S	--	S	VW	--	S
1820.323	SI	--	--	--	--	W	S	--	S	VS	
1826.245	SI	--	--	--	--	W	S	--	S	VS	
1892.030	SiIII	S	VS	S	S	W	--	--	--	--	S
1900.286	SI	--	W	--	VW	S	S	--	S	S	
1908.734	CIII	S	S	--	W	VW	--	--	--	--	S
1914.698	SI	--	W	--	--	S	S	--	S	S	

VS = Very strong compared to other lines in the group.
S = Strong compared to other lines in the group.
W = Weak compared to other lines in the group.
VW = Very weak compared to other lines in the group.
-- = Not present in the deepest spectra so far obtained.

e.g. β Dra and α Aur, reveal the O IV lines, which are useful in density sensitive line ratios (1,14). The 1640 Å region is interesting as the He II feature dominates in active dwarfs, giants, and RS CVn systems, whereas the Fe II line is important in quiet dwarfs like α Cen A and B, and the intersystem O I line dominates in the cooler giants and supergiants (2,7,9,15). Coaddition of many deep exposures of Capella now reveal the O V 1218 Å intersystem line in the wing of Lα (1). The absence of bright emission lines at 1340, 1380, and 1545 Å in high dispersion spectra of α Boo implies that the strong features observed at low dispersion are fluorescent CO bands (9).

III. SEPARATION OF INDIVIDUAL STARS IN CLOSE BINARY SYSTEMS AND EVIDENCE FOR ACTIVE REGIONS

The 30 km s^{-1} resolution of IUE is sufficient to identify which star is the dominant emitter in RS CVn-type systems, where the radial velocity separation is typically 100 km s^{-1}. Extensive studies of Capella by Ayres and his collaborators, for example, have shown that the rapidly rotating F9 III star in this long period system is responsible for 90% of the C IV flux (4,8). In the shorter period systems like HR 1099, the K0 IV component has the brighter transition region lines, but in surface flux units the two stars are more nearly similar (5). IUE has also been able to Doppler image bright active regions as they rotate across the disks of RS CVn systems. Two examples of systems for which changes in the central wavelengths of emission lines are detected and likely due to the rotation of an individual active region are HR 1099 (5) and σ Gem (10). The absence of time variability to high precision in the emission line flux in Capella (1) likely indicates that the F9 III star in this system has a large number of active regions.

IV. LINE SHIFTS AND WIDTHS

One of the major new unexpected results from IUE is the discovery of the redshift of high temperature emission lines relative to low temperature chromospheric lines. This effect is now seen unambiguously in β Dra, Capella, λ And, and the active GK dwarfs taken as a group (2,11,14). Small aperture observations of Capella and spectra obtained with platinum lamp exposures for wavelength calibration confirm that the red shifts are valid on an absolute wavelength scale. While redshifts can be produced in optically thick lines by differential expansion, the observed redshifts of the C III, Si III, O III, and O V intersystem lines in Capella and β Dra imply that 10^5 K plasma is moving downward in these stars (1,14).

In G-M dwarf stars the widths of transition region emission lines appear to be independent of spectral type and activity, except that these lines in AU Mic (M2 Ve) may be slightly broader (3,7). There is a width-luminosity effect, however, seen in the G and K giants. For example, the intersystem lines of Si III and C III are broader in β Dra (G2 Ib-II) and α Aur Ab (F9 III) than in active dwarfs, implying the turbulence increases with luminosity (6,14). In addition, the permitted transition region lines (e.g. C IV and Si IV) are broader than the intersystem lines, implying that the permitted lines are optically thick (6). Opacity broadening may also explain the widths of chromospheric emission lines in α Boo (9).

V. MODELS OF STELLAR CHROMOSPHERES AND TRANSITION REGIONS

An important goal of this program is to derive models for the chromospheres and transition regions of cool stars and to use these models in assessing the energy balance and heating mechanisms. This is a difficult task requiring much effort. To date models have been constructed for α CMi (12) and β Dra (14) and models are now being constructed for the giants β Cet and β Gem and the dwarfs χ^1 Ori, α Cen A, ξ Boo A, α Cen B, and ε Eri. These models are based in part on an emission measure analysis of the low dispersion line fluxes, but the high dispersion spectra are needed to separate close blends and measure the line widths. For example, the important density-sensitive lines O IV 1401, 1405 Å and O III 1666 Å must be resolved. Line widths provide information on whether lines are optically thick or thin, which can be used to place constraints on transition region pressures. Also, line widths can be used to infer turbulent broadening and thus estimate the mechanical energy contained in waves passing through an atmospheric layer and available to heat higher layers. Such data have led to the conclusion that the outer atmospheres of α CMi and β Dra are not heated by purely acoustic waves, but they may be heated by MHD waves (12,14).

This work is supported by NASA grants NAG5-82 and NGL-06-003-057 to the University of Colorado.

REFERENCES

(1) Ayres, T. R. 1984, Ap. J., in press.
(2) Ayres, T. R., Engvold, O., Kjeldseth Moe, O., Simon, T., Jordan, C., Judge, P., Brown, A., and Linsky, J. L. 1984, this volume.
(3) Ayres, T. R., Eriksson, K., Linsky, J. L., and Stencel, R. E. 1983, Ap. J. (Letters), 270, L17.
(4) Ayres, T. R., and Linsky, J. L. 1980, Ap. J., 241, 279.
(5) Ayres, T. R., and Linsky, J. L. 1982, Ap. J., 254, 168.
(6) Ayres, T. R., Linsky, J. L., Basri, G. S., Landsman, W., Henry, R. C., Moos, H. W., and Stencel, R. E. 1982, Ap. J., 256, 550.
(7) Ayres, T. R., Linsky, J. L., Simon, T., Jordan, C., and Brown, A. 1983, Ap. J., 274, 784.
(8) Ayres, T. R., Schiffer, F. H. III, and Linsky, J. L. 1983, Ap. J., 272, 223.
(9) Ayres, T. R., Simon, T., and Linsky, J. L. 1982, Ap. J., 263, 791.
(10) Ayres, T. R., Simon, T., and Linsky, J. L. 1984, Ap. J., to appear.
(11) Ayres, T. R., Stencel, R. E., Linsky, J. L., Simon, T., Jordan, C., Brown, A., and Engvold, O. 1983, Ap. J., 274, 801.
(12) Brown, A., and Jordan, C. 1981, MNRAS, 196, 757.
(13) Brown, A., Jordan, C., Ayres, T. R., Linsky, J. L., and Stencel, R. E. 1982, Third European IUE Conference, p. 142.
(14) Brown, A., Jordan, C., Stencel, R. E., Linsky, J. L., and Ayres, T. R. 1984, Ap. J., in press.
(15) Engvold, O., Kjeldseth Moe, O., Jensen, E., Jordan, C., Stencel, R., and Linsky, J. L. 1984, in Proceedings of the Third Cambridge Workshop on Cool Stars, in press.
(16) Jordan, C., Brown, C., Ayres, T. R., Linsky, J. L., and Stencel, R. E. 1982, Third European IUE Conference, p. 161.

CHROMOSPHERIC EMISSION LINES IN HIGH-RESOLUTION LWR SPECTRA (2200 - 3000 Å) OF GAMMA CRU (M3 III) AND ALPHA ORI (M2 Iab)

Kenneth G. Carpenter
Joint Institute for Laboratory Astrophysics
University of Colorado and National Bureau of Standards

ABSTRACT

The identity and characteristics of the chromospheric emission features in the 2200-3000 Å region of high-resolution spectra of γ Cru and α Ori are summarized. The velocities, fluxes, and asymmetries of a set of Fe II lines which share common upper or lower energy levels are discussed and the information gained from flux measurements of the C II (UV 0.01) lines is presented. An analysis of the Fe II lines in the α Ori spectra indicates the general shape of the velocity versus radius relation in its wind. The C II (UV 0.01) data are combined with measures of the C II (UV 1) flux to estimate the electron density and temperature in the wind and the geometric extent of the C II emitting region in both stars.

THE SPECTRA AND THEIR CONTENTS

The α Ori data consist of four high-resolution, large aperture LWR spectra taken during April 1978 - November 1982 and thus cover nearly a full period in the semi-periodic photospheric radial velocity variation (Goldberg, 1984). The γ Cru data consist of two spectra -- a long exposure to record the Fe II and C II features properly, plus a short exposure which records the Mg II lines without saturating the detector. The spectra, listed in Table 1, were obtained from the IUE archives at the National Space Science Data Center (NSSDC) and analyzed at the Colorado IUE Regional Data Analysis Facility (RDAF).

Over 80% of the emission features in these spectra are due to lines of Fe II, which occur throughout the full range of the spectra. The strongest features not attributed to Fe II are due to the Mg II doublet near 2800 Å, the Aℓ II line near 2669 Å, and the C II lines near 2325 Å. Other elements represented in these spectra include definitely Si II, Cr II, Mg I, and the fluorescent Fe I (at 2823 and 2844 Å, pumped by the Mg II k-line) and Co II (at 2330 Å, pumped by Fe II and Si II at 2344 Å) lines and probably Ni II, Mn II, and Si I. A more detailed list of the identified emission features in the 2500-3230 Å region of the 120 minute γ Cru spectrum is given in Wing, Carpenter and Wahlgren (1983). In both stars, a substantial fraction of the total chromospheric radiative losses occurs through the numerous Fe II lines, which together produce a total loss rate approaching that of the primary cooling channel, the Mg II resonance lines. Thus the Fe II lines, which are usually ignored, should be included in chromospheric models of stars similar to these.

THE Fe II LINES OF MULTIPLETS UV 1-3, 32, 33, 35, 36, AND 60-64

The lines of these multiplets, which share a number of common upper or lower energy levels, represent the strongest Fe II transitions in this spectral

TABLE 1. High-Resolution IUE Spectra of α Ori and γ Cru

Star	Image #	Date Taken Year	Day	Exp. Time	Program ID
α Ori	LWR 1371	1978	113	120^{min}	LTRFW
α Ori	2100	1978	229	35	CEJLL
α Ori	9600	1980	364	30	CSCRW
α Ori	14673	1982	324	35	CCEJL
γ Cru	1356	1978	111	120	LTRFW
γ Cru	10651	1981	139	4	MGDDM

Note: LTRFW/CSCRW spectra were obtained by Wing and Carpenter.
CEJLL/CCEJL spectra were obtained by Linsky and Stencel.
MGDDM spectrum was obtained by D. Mullan.

region. In α Ori, many of these lines are self-reversed and all of them are quite broad (FWHM ~ 120 km/sec), while in γ Cru, the same lines show no reversals and are considerably narrower (~40 km/sec). Because of the great breadth of the lines in α Ori, blending is quite frequent and greatly complicates the interpretation of its Fe II spectra. Weymann (1962), after an examination of the Fe II lines near 3200 Å in α Ori, concluded that some Fe II lines are also "mutilated" by overlying absorption lines of other elements, thus further complicating the picture. Using the relatively clean γ Cru spectrum as a guide, I have identified and measured a subset of 42 Fe II lines, listed in Table 2, which are visible in all the spectra and which appear to be free of blending and mutilation in the α Ori spectra. The mean velocity of these lines is close to that of the photospheric Fe I absorption lines in α Ori, although the Fe II lines do not seem to follow strictly the six-year radial velocity variation of

TABLE 2. Selected Unblended, Unmutilated Fe II lines

λ_{lab}	UV Mult.	λ_{lab}	UV Mult.	λ_{lab}	UV Mult.
2338.005	3	2591.542	64	2755.733	62
2354.884	35	2593.722	64	2759.336	32
2362.014	35	2607.086	1	2761.813	63
2368.593	36	2625.664	1	2768.940	63
2370.494	35	2628.291	1	2772.719	63
2373.733	2	2692.826	62	2868.874	61
2375.192	36	2709.373	62	2880.750	61
2379.275	36	2714.414	63	2892.822	61
2391.475	35	2724.879	62	2907.853	60
2402.597	36	2727.538	63	2916.150	60
2505.217	33	2730.735	62	2917.465	61
2566.908	64	2732.441	32	2926.584	60
2577.920	64	2739.545	63	2945.262	60
2585.876	1	2749.324	62	2970.510	60

the latter. In the one deep γ Cru spectrum the lines appear to show a small redshift, relative to the photosphere, on the order of 5 km/sec. The existence of the self-reversals in some but not all of the Fe II lines in α Ori and the lack of any reversals in γ Cru indicate that these lines represent a wider range of optical thickness in the supergiant and that, at least in some lines, the α Ori wind is considerably thicker.

In α Ori the presence or absence of the self-reversals and the asymmetry of the Fe II lines that do show the reversals correlate well, within a given multiplet, with intrinsic line strength (e.g. gf-value). The strongest reversed lines in multiplets UV 60-64 show a violet asymmetry (i.e. have more flux to the violet of the self-reversal than to the red), while the weaker reversed lines show a red asymmetry. The remaining multiplets are represented in these spectra by too few unmutilated, unblended lines of sufficiently different intrinsic strength for any correlation to be proven or disproven in these cases. The variation of the Fe II profiles with intrinsic strength in α Ori is illustrated in Figure 1. This correlation suggests that the weaker lines form in a region relatively low in the chromosphere with a positive velocity gradient, while the intrinsically stronger lines are formed in a region in the upper reaches of the wind with a negative velocity gradient.

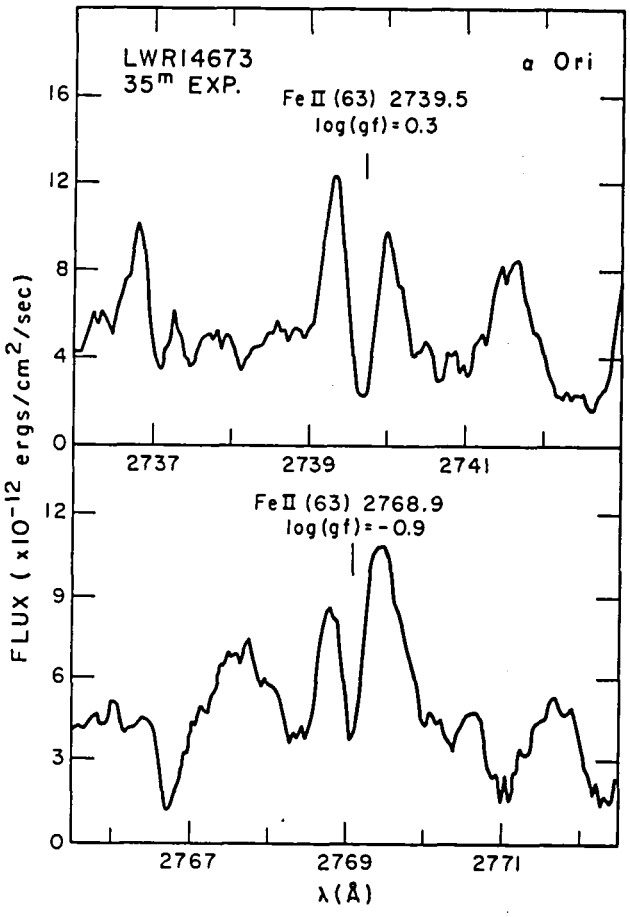

Fig. 1. Fe II profiles from multiplet UV 63 illustrating the correlation of line asymmetry with intrinsic line strength seen in high-resolution IUE spectra of α Ori.

THE C II LINES: THE DENSITY AND TEMPERATURE OF THE WIND

The relative fluxes of the C II (UV 0.01) intercombination lines near 2325 Å are sensitive to the electron density in the winds about cool luminous stars (Stencel et al., 1981), while the ratio of the total flux in the multiplet to that in the C II (UV 1) doublet near 1335 Å provides a measure of the electron temperature (Hayes and Nussbaumer, 1984; Brown and Carpenter, 1984). The total UV 0.01 flux plus the temperature and density estimates can be combined in an emission measure analysis to provide an estimate of the geometric extent of the emitting region. The flux ratios indicate $N_e \sim 3.2 \times 10^7 - 1.3 \times 10^8$ cm^{-3}, $T_e \sim 8300$ K in α Ori and $N_e \sim 1.6 \times 10^8$ cm^{-3}, $T_e \sim 8000$ K in γ Cru. These values, combined with the total UV 0.01 fluxes of 2.05×10^{-11} in α Ori and 1.04×10^{-11} ergs/cm^2/sec in γ Cru, indicate that the extent (measured from the base of the chromosphere) of the C II emitting region is in the range of 0.1-1.1 R_* in α Ori and ~1.1 R_* in γ Cru. The uncertainty in these results can be reduced when more accurate atomic data relevant to the relative transition strengths within multiplet UV 0.01 become available.

Further details on the analysis of the Fe II and C II features in the α Ori spectra will be given in Carpenter (1984).

This work was supported in part by NASA grant NAG5-82 to the University of Colorado.

REFERENCES

Brown, A. and Carpenter, K. G. 1984, Ap. J. (Letters), submitted.
Carpenter, K. G. 1984, Ap. J., submitted.
Goldberg, L. 1984, P.A.S.P., submitted.
Hayes, M. A. and Nussbaumer, H. 1984, Astr. Ap., in press.
Stencel, R. E., Linsky, J. L., Brown, A., Jordan, C., Carpenter, K. G., Wing, R. F., and Czyzak, S. 1981, M.N.R.A.S., 196, 47p.
Weymann, R. 1962, Ap. J., 136, 844.
Wing, R. F., Carpenter, K. G., and Wahlgren, G. W. 1983, Perkins Obs. Spec. Publ. No. 1.

ACTIVE LATE-TYPE STARS AND THE APPLICABILITY OF CORONAL LOOP MODELS

Mark S. Giampapa, National Solar Observatory and
L. Golub, G. Peres, S. Serio, G. S. Vaiana
Harvard-Smithsonian Center for Astrophysics

ABSTRACT

We combine far ultraviolet IUE observations with existing soft X-ray measurements obtained by Einstein (HEAO-B) satellite observatory for a sample of solar-type stars. We utilize the resulting data-set and a new coronal loop model numerical code developed at the Harvard-Smithsonian Center for Astrophysics to perform a preliminary investigation of the applicability of coronal loop models to solar-type stars. In particular, we find that reasonable agreement between the predictions of single-component, coronal loop model atmospheres and the observational data is achieved for a relatively well defined, plausible range of stellar atmospheric parameters for the sample of solar-type stars considered herein. We thus demonstrate that semi-empirical, coronal loop models can be applied to account for observed stellar transition region and coronal emission. This result is corroborative evidence for the presence of magnetic field structures analogous to solar coronal loops on the surfaces of solar-type stars. Moreover, we suggest that observed stellar transition region emission arises predominantly from the base of quiescent coronal loop configurations.

INTRODUCTION

The atmosphere of the Sun exhibits a variety of structural inhomogeneities that are defined by magnetic field configurations. We now recognize these atmospheric inhomogeneities as a fundamental property of the solar outer atmosphere. In particular, magnetic field configurations that define atmospheric thermal inhomogeneities are especially evident in the solar corona which is characterized by open and closed coronal loop structures (e.g., see Vaiana and Rosner 1978). Previous investigations have delineated the physical structure of open (Rosner and Vaiana 1977) and closed field regions in the solar corona, culminating in the development of scaling laws relating loop size, temperature and pressure for coronal loops in hydrostatic equilibrium (Rosner, Tucker and Vaiana 1978; hereafter RTV). The results of the solar investigations may be applicable to stars given that the occurrence of stellar surface features similar to solar plage and sunspots is now well established. The existence of stellar surface inhomogeneities, analogous to solar surface features, provides compelling circumstantial evidence for the presence of coronal magnetic field structures on stars that are similar to solar coronal loops.

Recently, coronal loop models have been utilized by several investigators to explain the observed soft X-ray emission from active stars (e.g. Golub et al. 1982; and references therein). These investigations reveal that, without additional constraints, coronal loop models deduced solely on the basis of stellar X-ray observations can only yield a locus of

possible atmospheres in the coronal pressure - filling factor (p-f) plane. Consequently, we have utilized observed far ultraviolet line fluxes of prominent transition region emission lines, as obtained with the International Ultraviolet Explorer (IUE) satellite, combined with measurements of coronal soft X-ray emission, acquired by Einstein Observatory, to construct semi-empirical, single-component loop model atmospheres that best fit the aforementioned observations for a sample mainly composed of solar type stars. In this way, we (1) test the applicability to solar-type stars of solar coronal loop models, (2) obtain estimates of stellar coronal properties such as coronal base pressure and the filling factor of coronal loops, and (3) ascertain the extent to which the addition of UV transition region observations to X-ray measurements can constrain the range of possible loop atmospheres. The observations, detailed model computations and results are given by Giampapa et al. (1984). We summarize the basic results and conclusions herein.

RESULTS

Following Golub et al. (1982a), we envisage a stellar atmosphere consisting of loops of magnetically confined plasma where each loop is subject to the constraint imposed by the RTV scaling law

$$T = 1.4 \times 10^3 (pL)^{1/3}, \quad (1)$$

or the generalization of this law given by Serio et al. (1981). We adopt the theoretical constraints outlined by Pallavicini et al. (1981) for the static stellar loop models we construct. The observational constraints that a model must satisfy include the value of the coronal temperature, assumed to characterize the maximum loop temperature which, in turn, occurs at the top of the loop (RTV 1978), and the observed ultraviolet line fluxes combined with the soft x-ray flux. The ultraviolet lines used include C IV 1550, N V 1240 and Si IV 1400 (we apply a correction to the observed Si IV-O IV 1400 blend to account for the contribution from O IV).

The results of the model computations are displayed in Table 1. We show relevant stellar parameters in the first three columns of Table 1. The remaining columns include the coronal temperature, T_{max}, coronal loop base pressure, p, and the filling factor f of identical loops characterized by length L necessary to best fit the observed UV and X-ray emission.

DISCUSSION

Consistent with the results of Golub et al. (1982), we find a locus of allowed values in the (p,f) - plane which would satisfy the observational constraints provided by measurements of only f_x and T_{corona}. Examination of Table 1, however, reveals that the addition of the transition region emission line fluxes severely constrains the range of permissible values in the (p, f) - plane that yield acceptable loop model atmosphere that satisfy both the far ultraviolet and X-ray data for the solar-type stars considered in this investigation. We note that the assumed primary emitter in the RS CVn system HD5303 is characterized by high pressure loop structures with loop lengths L > R and a filling factor f > 1. Both Swank et al. (1981) and

Walter et al. (1980) find similar results in their investigations of RS CVn systems within the context of loop model atmospheres. The inferred loop length $L > R$ can be attributed to the high coronal temperature ($T_{corona} = 2.5 \times 10^7$) combined with a consideration of the RTV scaling law (equn. 1). Thus the inferred filling factor is more representative of a volume, rather than surface, filling factor of emitting loops. Additional evidence for these kinds of loop structures is given by Simon, Linsky and Schiffer (1980) in the specific case of the RS CVn system UX Ari.

TABLE 1

STELLAR ATMOSPHERIC LOOP MODEL PARAMETERS

Object	g (cm s^{-2})	d (pc)	T_{max} R/R_o	p (K)	f (dynes cm^{-2})	L	(cm)
α Cen B (K1 V)	3.23(4)	1.34	0.87	2.4(6)	0.56	1.68	9.5(9)
i Per (G4 V)	2.91(4)	11.6	0.95	2.6(6)	0.65-0.85	1.25-1.69	7.5(9)-9.8(9)
μ Her (G5 IV)	5.06(3)	8.06	3.10	2.6(6)	0.35	0.27	1.8(10)
σ Dra (K0 V)	2.95(4)	5.68	0.85	2.3(6)	4.0-16.0	0.04-0.16	2.8(8)-1.1(9)
HR 3538 (G3 V)	2.88(4)	11.8	0.98	3.2(6)	5.0-10.0	0.085-0.17	1.1(9)-2.2(9)
ε Eri(K2 V)	3.08(4)	3.31	0.82	3.5(6)	5.0-20.0	0.54-0.22	7.5(8)-3.0(9)
HD 206860-1[a] (G0 V)	2.75(4)	17.5	1.05	4.4(6)	6.0-8.0	0.35-0.47	3.8(9)-5.0(9)
HD 206860-2[a] (G0 V)	2.75(4)	17.5	1.05	-	-	-	-
HD 5303 (G2 V+F)	2.75(4)	66	1.0	24(6)	25.0	3.64	2.2(11)

[a]Multiple ultraviolet observations available for this object.

In brief summary, inspection of Table 1 reveals that, in general, reasonable agreement between the predictions of coronal loop model atmospheres and the observational data is achieved for plausible stellar atmospheric parameters (i.e., T_{max}, p, f, L) for the sample of solar-type stars considered herein. Hence the results of this preliminary investigation demonstrate that semi-empirical coronal loop models can be applied to account for the observed transition region and coronal emission from solar-type stars. This conclusion represents corroborative evidence for the existence of magnetic field configurations analogous to solar coronal loops on the surfaces of solar-type stars.

The aforementioned results are particularly intriguing in view of the (1) occurrence of variability in stellar transition region and coronal emission, and (2) the lack of simultaneous UV and X-ray observations for this study. Consequently, we suggest that the amplitude of UV and X-ray variability in solar-type stars must rarely exceed factors of 2-3. This low-amplitude variability is a characteristic of static, quiescent ($L \leq s_p$) loop structures which have evolved from originally compact ($L < s_p$) high pressure, newly-emerged flux loops. Hence the implication of this suggestion is that the observed far UV stellar transition region line emission predominately arises from the footpoints of quiescent coronal loop structures. Furthermore, we have examined the applicability of high pressure, compact loops. We find that these kinds of loops can correctly predict the observed X-ray emission but they completely fail to account for the far UV emission due to the low filling factor ($f \ll 1$) of these loops (e.g., see Swank et al. 1981). This fact constitutes additional evidence for our claim that stellar UV emission is principally diagnostic of the transition regions at the base of quiescent loop structures.

Finally, we note that intrinsic stellar variability may account for

some of the discrepancies between the model predictions and the observations. In particular, we obtained models that satisfactorily predicted the observed X-ray emission and the initial UV observations for HD 206860 (designated HD 206860-1 in Table 1). However, no acceptable model could account for both the X-ray emission and the second set of UV observations acquired for this star (designated HD 206860-2 in Table 1). More specifically, all models that correctly predicted the X-ray emission consistently overpredicted the UV emission in all lines. Low pressure loops correctly predicted the UV emission of HD 206860-2 but they underpredicted the X-ray emission by at least an order of magnitude. Moreover, these low pressure models were characterized by physically unrealistic filling factors of $f>>1$. The transition region UV emission of the initial observation of HD 206860 (HD 206860-1) was enhanced relative to the later observation (HD 206860-2). Thus the single measurement of the X-ray emission from the star must be more compatible with the relatively enhanced transition region of HD 206860-1 than that of the later observation of this object. A similar result was obtained for models of the dMe flare star AD Leo. These models were based on recent (non-flaring) IUE observations and an earlier X-ray measurement that likely contained a flare contribution. We therefore suggest on the basis of these results that intrinsic stellar variability can contribute to the discrepancies between the observations and the model predictions for the stars considered in this investigation.

We gratefully acknowledge useful discussions with R. Rosner. We acknowledge support of NASA grants NAG 5-87 to SAO and a NASA grant via interagency agreement S-04160D to the National Solar Observatory. The National Solar Observatory is operated by AURA, Inc. under contract to the NSF.

REFERENCES

Giampapa, M. S. et al. 1984, Ap. J. in press.
Golub, L., Harnden, F. R., Jr., Pallavicini, R., Rosner, R., and Vaiana, G. S. 1982, Ap. J., 253, 242.
Pallavicini, R., Peres, G., Serio, S., Vaiana, G. S., Golub, L. and Rosner, R. 1981, Ap. J., 247, 692.
Rosner, R., and Vaiana, G. S. 1977, Ap. J., 216, 141.
Rosner, R., Tucker, W. H., and Vaiana, G. S. 1978, Ap. J., 220, 643.
Serio, S. Peres, G., Vaiana, G. S., Golub, L., and Rosner, R. 1981, Ap. J., 243, 288.
Simon, T., Linsky, J. L., and Scheffer, F. H. III 1980, Ap. J., 239, 911.
Swank, J. H., White, N. E., Holt S. S., and Becker, R. H. 1981, Ap. J., 246, 208.
Vaiana, G. S., and Rosner, R. 1978, Ann. Rev. Astr. Ap., 16, 393.
Walter, F. M., Cash, W., Charles, P. A., and Bowyer, C. S. 1980, Ap. J., 236, 212.

CO-ROTATING INTERACTION REGIONS IN STELLAR WINDS

D. J. Mullan
Bartol Research Foundation of The Franklin Institute
University of Delaware
Newark, DE 19716

ABSTRACT

A co-rotating interaction region (CIR) forms in a stellar wind when a fast stream from a rotating star overtakes a slow stream. CIR's have been studied in detail in the solar wind over the past decade. Here, we point out their usefulness in interpreting several spectroscopic features in stars of various types, including "hybrid" stars, OB stars, and cool supergiants.

INTRODUCTION

Stars emit wind with a velocity which is not in general spherically symmetric. Since all stars rotate, it is possible for faster wind to catch up with slower wind and form an interaction region which co-rotates with the star. CIR's have been the subject of extensive study for the past decade in the solar wind, mainly because they act as sources of energetic charged particles. When a CIR is fully developed, it consists of a forward shock, a stream-stream interface, and a reverse shock. The shock pair separates in time: at radial distance r, the separation of the shock pair is typically 0.1r in the solar wind.

A detector passing through a CIR in the solar wind records variations in density, temperature, and velocity as shown schematically in Figure 1. For present purposes, it is important to note that between the forward and reverse shocks, the velocity has a plateau. The velocity plateau remains well-defined as the CIR propagates out through the wind (Holzer, 1979). The density has a marked peak while the velocity is passing through its plateau.

The temperature profile in the CIR is complicated. Particle acceleration at the shocks suggests (Smith and Wolfe, 1977) that MHD turbulence is enhanced there. The detailed temperature structure in the CIR depends on how this turbulence is dissipated. Model calculations of non-turbulent CIR evolution (Hundhausen, 1973) suggest that strong cooling is expected to occur in the CIR as it evolves. The dashed lines in Fig. 1 are meant to indicate that this prediction may be modified in particular cases. In any case, the temperature jumps at the shocks to values which can be predicted.

For the case of stellar observations, the most readily detectable features of CIR's are the velocity plateau and the shock heating. We

propose that narrow absorption features observed in the spectra of various types of stars, with associated enhanced levels of ionization, are formed when light from the central star passes through the CIR on the line of sight.

Velocities in CIR's

The plateau velocity, v_a, is intermediate between the velocity of slow wind, v_0, and fast wind, v_f. In the solar wind, $v_f \lesssim 2v_0$. We will assume that the wind velocity can also vary by factors of about 2 in stellar winds. Then the velocity jumps across the forward and reverse shocks are $\Delta v = v_a - v_0 \approx 2v_0 - v_a$. In cases where v_0 is unknown, an upper limit on Δv can be derived: $\Delta v \lesssim v_a$.

Narrow absorption features are observed in OB stars at velocities which are typically 0.7 times terminal speed v_t (Lamers et al, 1981). With $v_t \simeq (1\text{-}3)\times 10^3$ km/sec, the velocity difference between "normal wind" and CIR's in such stars is of order 300-1000 km/sec. In "hybrid" stars, narrow absorption features are observed at velocities of 80-150 km/sec (Reimers, 1982). In such stars, v_0 is unknown: $\Delta v \lesssim$ 80-150 km/sec. In the cool supergiant Betelgeuse, absorption features are observed at 8 and 16 km/sec relative to the photosphere (Goldberg, 1983). Again, v_0 is not known, and so: $\Delta v \lesssim 8$, 16 km/sec. Narrow features are also known to be present in the spectra of other stars, such as T Tauri stars (cf. Mundt, 1984). Finite lifetimes of the narrow absorption features in all cases can be ascribed to propagation time-scales of the CIR's through the wind: in the outlying regions of the wind, the CIR velocity remains essentially unchanged, but the column density along the line of sight ($\propto r^{-3}$) eventually falls below detectability.

Temperatures in CIR's

At a shock where the velocity jump is Δv, the Rankine-Hugoniot relations predict the temperature jump. In the limit of a strong shock, with $\gamma \approx 5/3$, we find $\Delta T \approx (\mu/3R_g)\ (\Delta v)^2$, where μ is the mean molecular weight, and R_g is the gas constant.

In OB stars, this yields $\Delta T \approx (2\text{-}20) \times 10^6$ K, sufficient to make the CIR's acts as sources of X-rays. This is an alternative to the Lucy-White mechanism of X-ray emission from "blobs" in the winds. Particle acceleration at the shocks in the winds of OB stars can also provide non-thermal electrons. Moreover, enhanced temperatures in CIR's explain why the ionization level is higher in the narrow absorption components (Lamers et al, 1982).

In Betelgeuse, with $\Delta v \lesssim 8$ km/sec, the shocked gas remains neutral ($\mu \approx 1.3$), and hence $\Delta T \lesssim 3300$ K. With $\Delta v = 16$ km/sec, ionization occurs, and $\mu \approx 0.62$; hence $\Delta T \lesssim 6400$ K. Adding these to the boundary temperature of Betelgeuse, we predict CIR temperatures (at the shocks) of

6000-9000 K. This overlaps with the observed range of temperatures in the "chromosphere" of Betelgeuse, 7000-9000 K (Wischnewski and Windker, 1981). We suggest that the chromosphere of Betelgeuse begins in the wind.

In hybrids, we find $\Delta T \lesssim (1\text{-}3) \times 10^5$ K. This suffices to produce ions such as CIV, SiIV, and NV (which have been detected by IUE), but certainly insufficient to produce X-rays (consistent with the absence of Einstein detections). The widths of emission lines in CIR shocks are predicted to be about twice the plateau velocity, since emission from both near and far sides of the shocked shell will contribute to an emission component. Thus, widths of order 160-300 km/sec are expected for emission lines from the CIR shocked region. These are consistent with IUE data (Hartmann et al, 1982).

Interaction Distance

Suppose "slow" wind emerges from a star at speed v_0, and that the wind speed has a gradient G=dv/dw with respect to longitude, w, on the stellar surface (r=R*). Then with a stellar rotation velocity of v_r, the distance where fast gas catches up with slow gas is at least

$$r_i/R* \approx 1 + (v_0/v_r)(v_0/G) \qquad (1)$$

where we have assumed that the fast stream axis is separated in longitude by Δw from the slow wind, and we have allowed $\Delta w \to 0$. To obtain an upper limit on r_i, we allow Δw to becomes 2π. In this case, we find

$$r_i/R* \approx 1 + 2\pi\ (v_0/v_r) \qquad (2)$$

In the solar wind, (1) predicts $r_i/R* \approx 60$, while (2) predicts $r_i/R* \approx 1200$. Thus, the geometrical mean of these two limits is $r_i/R* \approx 270$, i.e. $r_i \approx 1.2$ A.U., in good agreement with observations of CIR formation distances in the solar wind (Hundhausen, 1973).

Other stars have (v_0/v_r) ratios which may be much smaller than the solar value (200). Hence, CIR's are predicted to form much closer to the surfaces of other stars. In OB stars, with $v_0 \approx (1\text{-}3) \times 10^3$ km/sec and $v_r \approx (1\text{-}3) \times 10^2$ km/sec, v_0/v_r is typically smaller than solar by an order of magnitude. In such stars, CIR's should form at a few tens of stellar radii. At such radii, CIR's have sufficient emission measure to account for much of the Einstein X-ray emission in, say, ζ Puppis.

In Betelgeuse, v_r is not known, but evolutionary calculations (Endal and Sofia, 1979) suggest that v_r may be a few km/sec. In that case, v_0/v_r may be almost 2 orders of magnitude smaller than the solar value. CIR's could then form quite close to the star, within 1-2 stellar radii. In view of the temperatures we have estimated above for CIR's in Betelgeuse wind, these results have a bearing on the claim for an "extended chromosphere" in Betelgeuse and similar cool giants (Stencel, 1982).

In hybrid stars, recent work (Brosius et al, 1983) based on archival

IUE MgII data (interpreted in terms of rotational modulation) suggests that v_r 20 km/sec in some hybrids. If these can be confirmed, they suggest that v_0/v_r in hybrids is intermediate between values in OB stars and those in Betelgeuse. Thus, in hybrids, CIR's are predicted to form at about 10 R_*. With mass loss rates of order 2×10^{-9} M_0/yr, CIR's at such distances contain sufficient emission measures to account for the observed intensities of NV emission in the hybrids.

References

Brosius, J.W., Mullan, D.J., and Stencel, R.E., 1983, submitted.
Endal, A. and Sofia, S. 1979, Ap.J. 232, 533.
Goldberg, L. 1983, preprint.
Hartmann, L., Dupree, A.K., and Raymond, J. 1982, Ap.J. 252, 214.
Holzer, T. 1979, in Solar System Plasma Physics (eds. E. Parker et al) (North Holland), p. 101.
Hundhausen, A. 1973, J. Geophys. Res. 78, 1528.
Lamers, H. et al, 1982, Ap.J. 158, 186.
Mundt, R. 1984, preprint.
Reimers, D. 1982, Astron. Astrophys. 107, 292.
Smith, E.J. and Wolfe, J.H. 1977 in Study of Travelling Interplanetary (Phenomena (eds. M. Shea et al) (Reidel), p. 227.
Stencel, R.E. 1982, SAO Spec. Report 392, P. 137.
Wischnewski, E. and Wendker, H.J. 1981, Astron. Astrophys. 96, 102

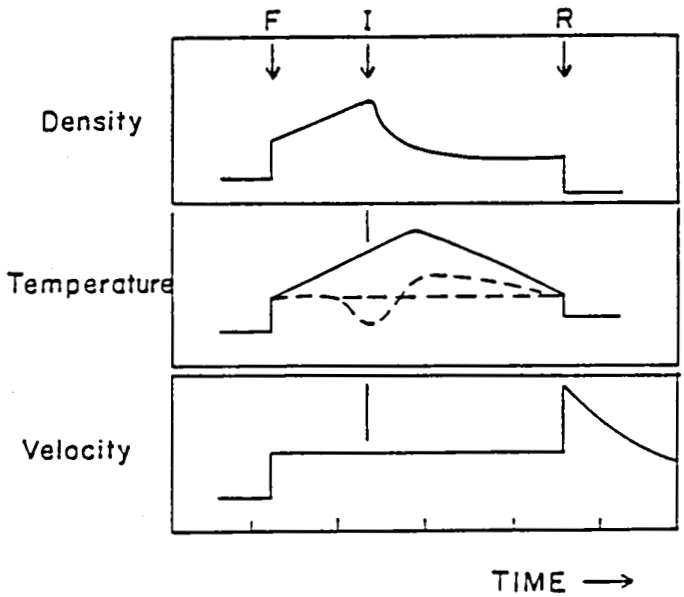

Fig. 1 Variations of solar wind parameters as CIR sweeps past a spacecraft (courtesy of E.J. Smith). The spacecraft, initially in slow wind, is overtaken by F, a forward shock. I is the interface between fast and slow wind, where density has a maximum. R is a reverse shock where the spacecraft emerges into the fast wind. Note the velocity plateau between F and R.

BETELGEUSE AT MAXIMUM LUMINOSITY

A. K. Dupree[1], G. Sonneborn[2], S. L. Baliunas[1], E. F. Guinan[3], L. Hartmann[1], and D. P. Hayes[4]

[1] Harvard-Smithsonian Center for Astrophysics, Cambridge, MA 02138
[2] Goddard Space Flight Center/CSC, Code 685, Greenbelt, MD 20771
[3] Department of Astronomy, Villanova University, Villanova, PA 19085
[4] Astronomy Department, Columbia University, New York, NY 10027

ABSTRACT

Betelgeuse (Alpha Ori; M2 Iab) was extremely bright at optical wavelengths and in the Mg II resonance lines during January and February 1984 when an intrinsic brightening occurred in the photosphere and chromosphere. Linear polarization in the B-band at this time was not anomalous when compared to earlier epochs. The core of the Hα line was redshifted by about 10 km/s with respect to the photospheric lines during January/February as compared to measurements made five months previously. There may be periodic variations in the chromospheric flux.

INTRODUCTION

Betelgeuse (Alpha Orionis), a semiregular red supergiant star is one of the brightest stars in the sky and as such is eminently suitable to intensive analysis by a variety of techniques. This star has commanded a great deal of attention because observations of high precision are possible and variability is present on different time scales. The star shows irregular light fluctuations on the order of 100 to 200 days (Stebbins 1931; Guinan 1984) superposed on an underlying long term variation of about half a magnitude in a period of slightly less than six years (see Figure 1, also). As Goldberg (1979) has noted, several components to the atmosphere can be defined: a photosphere that exhibits regular velocity variations and irregular brightenings; an extended chromosphere in which outward mass flow exists; and two stationary circumstellar shells. In this picture, downward flowing material must also coexist as suggested by Boesgaard's (1979) measurements of redshifted Fe II lines.

Both Sanford (1933) and Spitzer (1939) remarked on the similarity between Betelgeuse and a pulsating star, but the presence and effect of large photospheric convective elements as suggested by Schwarzschild (1975) has not been incorporated into a pulsation model. Guinan (1984) and Hayes (1984) have speculated that the 100 to 200 day variation in light and polarization may result from the ejection of hot material from the stellar photosphere - perhaps corresponding to a convective element.

The 1984-1985 observing season is particularly attractive for observations because it represents a time near maximum luminosity and minimum radial velocity. We have begun an intensive multifrequency observing program to coincide with the Seventh Round of IUE Observing Program, and the first results of the two months, January and February 1984 are discussed here with

particular comparison to earlier epochs. Director's discretionary time was kindly allotted by Y. Kondo to take advantage of the exceptional brightening of Betelgeuse in December 1983 and January-February 1984.

OBSERVATIONS (See Figure 1)

a.) The optical B-band photometry shows agreement in seasonal average with the Stebbins (1931) photoelectric ephemeris and a period of 5.781 years. A brightening of $\sim$ 0.3 magnitudes such as occurred in 1984 (and 1981) appears superposed on the long-term variation.

b.) Polarization does not follow the long-term brightness variation, however the 100 to 200 day polarization events generally correspond to optical brightenings. In 1984, however the polarization was a 0.3 percent level - not anomalously high in spite of the substantial optical brightening.

c.) The ultraviolet measures indicate that the Mg II flux corresponds to the optical brightening. The Mg II profiles in Figure 2 show that a true chromospheric enhancement occurred (and not simply a modification of the circumstellar envelope). The λ1300 feature (S I and O I) also showed a slight increase in flux. Fluxes for the Mg II and λ1300 feature are contained in Tables 1 and 2.

d.) The Hα profiles (Figure 3) obtained with a Cassegrain echelle spectrograph and reticon detector at the Oak Ridge Observatory of SAO, show variability in the wings as well as a 10 km s^{-1} redshift during a five month period. The velocity of the photosphere in this period (as determined from five lines of Fe I, Ti I, and Ca I) was approximately constant at + 17 km s^{-1}.

DISCUSSION

The brightening event of Betelgeuse in 1984 gives evidence for variability in photospheric and chromospheric structure. The observation of ordered variations in the polarization in conjunction with optical brightening suggests the appearance of a bright element (or few elements) on or close to the stellar surface.

The evidence from the Hα core for ordered downflow at the top of the extended chromosphere may be associated with the optical brightening in December 1983 or may simply be similar to the infall that Boesgaard (1979) inferred from Fe II emission. However, the Hα core indicates a motion relative to the photosphere as distinct from Boesgaard's conclusion that the Fe II emission displayed photospheric variations in conjunction with steady downflow. The extent of the association of Hα with the photospheric brightness and velocity variations is of crucial importance to assess the dynamics of the atmosphere.

The long-term variability of the Mg II flux (see Figure 4) is particularly intriguing for there is clear evidence of chromospheric variability. The Mg II fluxes do not appear to match the optical variations, but a shift of the optical ephemeris by six months improves the correlation. If confirmed, such a shift suggests that the chromospheric enhancement is displaced to follow,

and hence may result from, the maximum in photospheric luminosity. In Cepheids, it is known that the Ca II emission is displaced later with respect to the optical phase with increasing Cepheid period (Kraft 1957; Whitney 1958). And long period variables with periods of $\sim$ 4000 days show emission distinctly after maximum light (Whitney 1958). Attempts have been made to obtain the phase dependence of chromospheric lines in a few Cepheids, and while the emissions are variable, the pattern of variability with both phase and the stellar period has not been explored in depth (Schmidt and Weiler 1979; Schmidt and Parsons 1982, 1984).

We are just entering a year of concerted observations of Betelgeuse, and acquiring such phase and velocity information should give insight into at least two major current problems of stellar astrophysics, namely chromospheric structure and activity in a low gravity object, and the physics of stellar winds and mass loss.

We are grateful to N. Burnham and R. Hewett for timely reduction of the spectroscopic data. This research is supported in part by NASA Grant NAG5-87 to the Smithsonian Astrophysical Observatory.

REFERENCES

Boesgaard, A. M. 1979, Ap. J., 232, 485.
Goldberg, L. 1979, Q.J.R. Astr. Soc., 20, 361.
Guinan, E. F. 1984, in Cool Stars, Stellar Systems, and the Sun, (ed. S. L. Baliunas and L. Hartmann) Springer: New York, p. 336.
Hayes, D. 1980, Ap. J. Lett., 241, L165.
Hayes, D. 1981, Pub. A.S.P., 93, 752.
Hayes, D. 1984, in Cool Stars, Stellar Systems, and the Sun, (ed. S. L. Baliunas and L. Hartmann) Springer: New York, p. 342.
Kraft, R. P. 1957, Ap. J., 125, 336.
Krisciunas, K. 1982, I.A.U., I.B.V.S., No. 2104.
Sanford, R. F. 1933, Ap. J., 77, 110.
Schmidt, E. G., and Parsons, S. B. 1982, Ap. J. Suppl., 48, 185.
Schmidt, E. G., and Parsons, S. B. 1984, Ap. J., April 1.
Schmidt, E. G., and Weiler, E. S. 1979, A.J., 84, 231.
Schwarzschild, M. 1975, Ap. J., 195, 137.
Spitzer, L., Jr. 1939, Ap. J., 90, 494.
Stebbins, J. 1931, Pub. of the Washburn Obs. of Univ. of Wisconsin, 15, 177.
Whitney, C. 1958, 8th Leige International Colloq. on Astrophysics, Soc. Roy. Sci. Liege, Ser. 4, XX, 298.

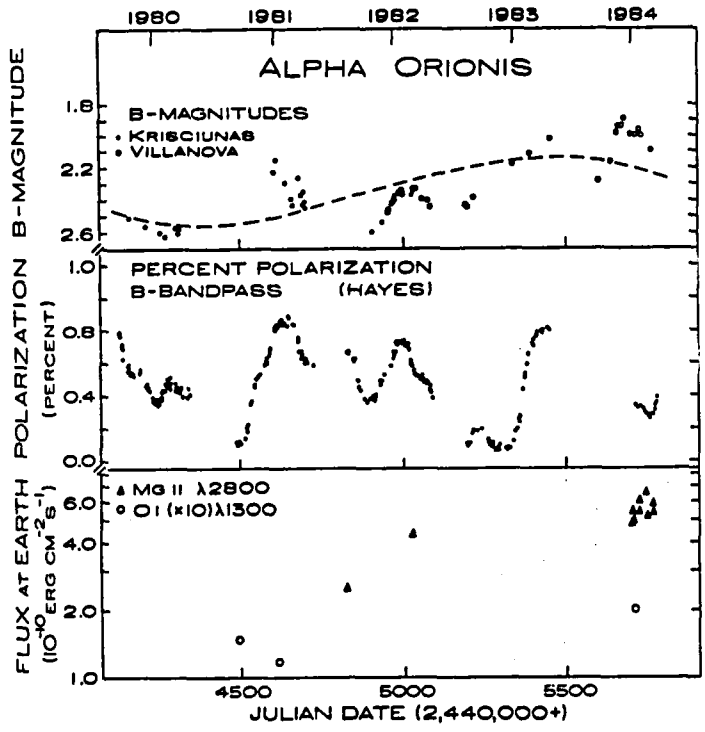

Figure 1. Measurements of Alpha Orionis from 1980 to 1984. The top panel contains the B-magnitudes from Krisciunas (1982)and from Guinan at Villanova. The broken curve represents Stebbins' (1931) ephemeris with a period of 5.781 years that is extrapolated from his photoelectric measurements from 1916 to 1931. The middle panel represents the percentage polarization in the B-bandpass as measured by Hayes (1980, 1981, 1984). The lower panel displays the Mg II and O I (and S I) fluxes obtained during 1980-1984 by us and from IUE Archival data. This figure is adapted and extended from one published by Guinan (1984).

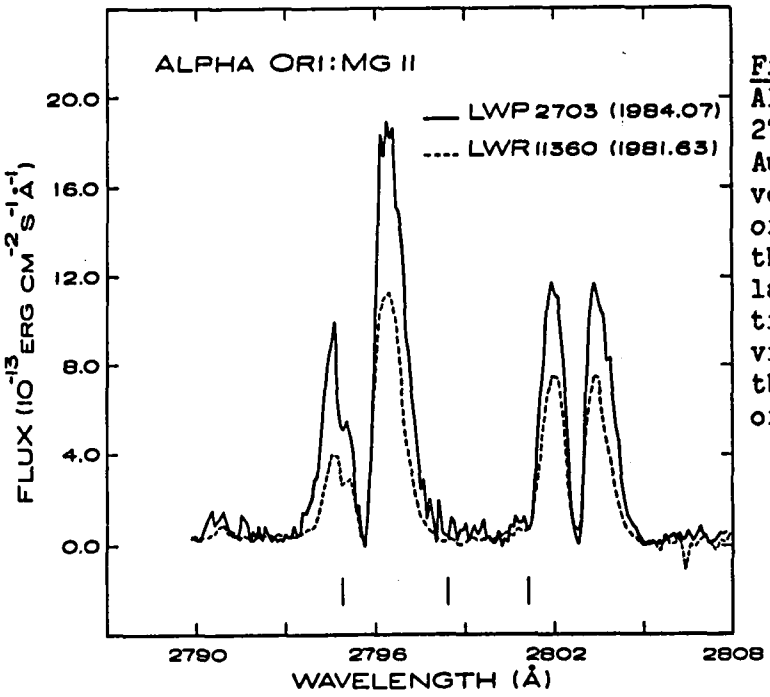

Figure 2. The Mg II profiles of Alpha Ori on 24 January 1984 (LWP 2703) and at a previous time, 19 August 1981 (LWR 11360). The vertical lines mark the position of resonant Mn I absorption lines that may arise in the circumstellar shell. The two Mn I transitions at longer wavelengths are visible in our deep exposures that saturate the emission peaks of the Mg II lines.

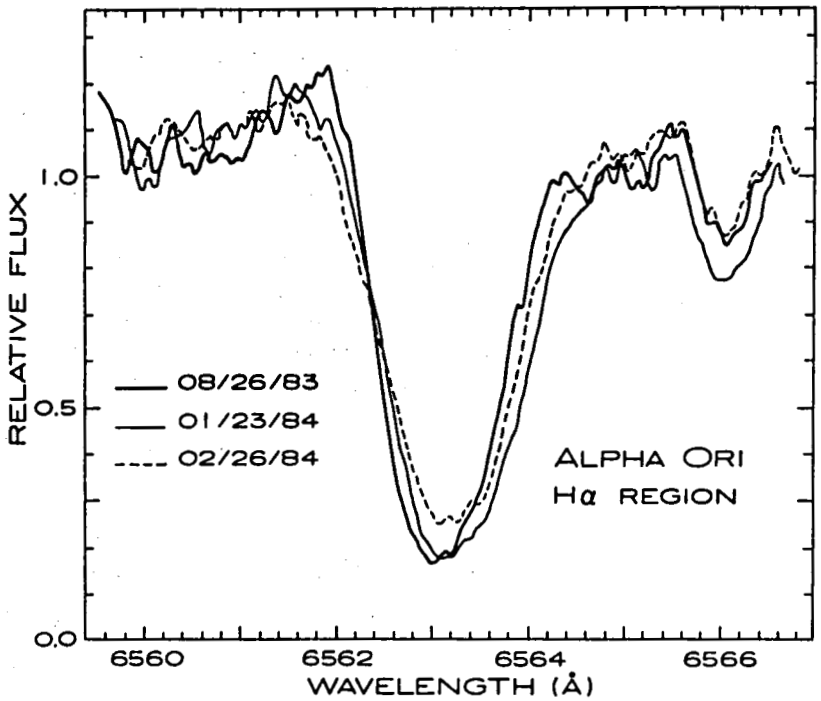

Figure 3. The Hα core region of Alpha Ori where the redward shift of the core is apparent as is the varying emission in the wings. For display, this figure was aligned on the photospheric V I line at λ6566.

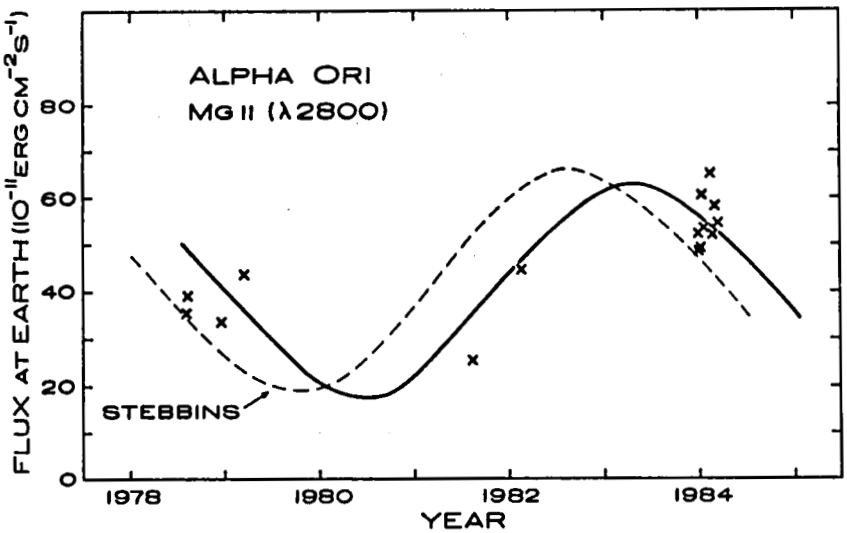

Figure 4. Mg II fluxes in Alpha Ori as measured from all suitable IUE spectra. The broken curve results from Stebbins' (1931) photoelectric ephemeris that predicts maximum light in late 1983 (see Figure 1); the solid line is the same curve of Stebbins that has been arbitrarily advanced by about 0.5 year to give better agreement with the Mg II flux variations.

TABLE 1

OBSERVED FLUXES AT λ1300 (SI, OI FEATURE)

Date	Image No.+	Flux (10^{-13} erg cm^{-2} s^{-1})
1978.63	SWP 2322	16.5
1978.96	SWP 3629	15.6
1979.22	SWP 4729	12.5
1979.68	SWP 6426	22.6
1980.68	SWP 10030	15.4
1981.00	SWP 10917	12.5
1984.02	SWP 21967	21.3
1984.16	SWP 22371	23.5

+ All images in low dispersion through the large aperture.

TABLE 2

OBSERVED Mg II FLUXES FROM ALPHA ORI

Date	Image No.+	Disp.	k-Line (λ2795) (units of 10^{-11} erg cm^{-2} s^{-1})	h-Line (λ2803)	Total
1978.63	LWR 2099	H	18.3	17.0	35.3
1978.63	LWR 2116	L			39.7
1978.96	LWR 3195	H	18.4	15.7	34.1
1979.22	LWR 4090	H	22.2	21.3	43.5
1981.63	LWR 11360	H	14.8	10.8	25.6
1982.15	LWR 12668 *	L			45.0
1984.02	LWP 2574a *	L			54.2
1984.02	LWP 2574b	L			49.6
1984.02	LWP 2573	H	27.9	21.8	49.7
1984.07	LWP 2702	L			60.4
1984.07	LWP 2703	H	30.6	22.9	53.5
1984.13	LWP 2791	L			65.3
1984.13	LWP 2792	H	29.6	22.6	52.2
1984.16	LWP 2860	L			58.6
1984.16	LWP 2861	H	31.6	23.0	54.5

+ All exposures in large aperture.
* Two exposures in large aperture.

PRECISE MEASUREMENTS OF RADIAL VELOCITIES OF EMISSION LINES IN THE FAR-ULTRAVIOLET SPECTRA OF LATE-TYPE STARS

T.R. Ayres, Laboratory for Atmospheric and Space Physics, University of Colorado
O. Engvold and O. Kjeldseth Moe, Institute for Theoretical Astrophysics, University of Oslo
T. Simon, Institute for Astronomy, University of Hawaii
C. Jordan and P. Judge, Department of Theoretical Physics, University of Oxford
A. Brown and J.L. Linsky[1], Joint Institute for Laboratory Astrophysics, National Bureau of Standards and University of Colorado

We have measured the radial velocities of emission lines in deep SWP echelle exposures of several late-type dwarf and giant stars, taken with special observing precautions to ensure the assignment of precise wavelength scales. Our goal was to search for absolute and differential Doppler shifts of emission lines formed at different temperatures in the stellar outer atmospheres analogous to the redshifts of C IV λ1548 (10^5 K) known to occur in the solar transition zone. In addition to new exposures of ε Eridani (K2 V: 530 minutes), χ^1 Orionis (G0 V: 845, 870, and 840 minutes), λ Andromedae (G8 III-IV: 730 minutes), α Aurigae Ab (F9 III: 5 pairs of short [22.5 minutes] and long [>80 minutes] exposures symmetrical about single-line phase 0), and α Canis Minoris A (F5 IV-V: 110 minutes, 3×60 minutes), we have reanalyzed existing images, taken without the precise radial velocity precautions, of five dwarf stars--χ^1 Ori, α Centauri A (G2 V), α Centauri B (K1 V), ξ Bootis A (G8 V), and ε Eri; four giant stars--λ And, β Ceti (G9.5 III), α Bootis (K2 III), and α Trianguli Australis (K3 II); and three supergiants--β Aquarii (G0 Ib), α Aquarii (G2 Ib), and 56 Pegasi (K0 Ib). A list of the spectra analyzed for this study is provided in Table 1.

The spectra were reduced at the Regional Data Analysis Facility in Boulder using standard procedures. For the stars for which multiple spectra were available, we interpolated the individual observations onto a common wavelength scale and coadded them to produce a composite spectrum of uniformly higher signal-to-noise. Wavelength registration was accomplished by a weighted mean velocity of the prominent, narrow low-excitation lines in each spectrum, except for α CMi A and α Aur Ab where we coadded the spectra on the assigned heliocentric wavelength scale, from which had been subtracted the stellar radial velocity. In all cases where multiple spectra were summed to form a composite spectrum, the rms deviation of the individual observations from the mean was calculated point-by-point. The rms record contains structure when one of the observations differs significantly from the others, owing to a cosmic ray hit for example, and provides a means to identify regions of the composite spectra that are so affected.

Selected examples of the reduced spectra, primarily the previously unpublished composite spectra, are provided in Figures 1 (late-G and K stars) and 2 (F and early-G stars).

We measured in the composite spectra, and in the single exposures, the apparent wavelengths of about 25 emission lines using a least-squares Gaussian fitting algorithm. Not all of the lines could be measured in every spectrum. We define a transition zone (TZ) velocity index based on the mean

velocity of the Si IV λλ1393.8,1402.8 and C IV λλ1548.2,1550.8 doublets, weighted by the statistical significance of each line flux, and a chromospheric velocity index based on a similarly weighted mean of narrow, low excitation lines from multiplets of Si II (dwarfs only), S I, O I, C I, and Cl I. We also constructed a third index based on the weighted mean velocity of the optically thin intersystem lines of Si III (λ1892) and C III (λ1909). The values obtained for these indices are provided in Table 1.

Among the supergiants, only 56 Peg exhibits a positive TZ-chromosphere index, and then only at the 2σ level. The early K-giant α Boo shows no evidence for high temperature lines, aside from a marginal detection of Si III], but the absolute chromospheric velocity index is within 1σ of the stellar photospheric velocity. The K bright giant α TrA exhibits weak C IV emission in the composite spectrum (2155 minutes of exposure), but the presence of significant continuum emission in the 1900 Å region raises the possibility that the high temperature lines are from a previously unrecognized main sequence F-type companion. The two active giant stars, α Aur Ab and λ And, exhibit substantial differential TZ indices (10 km s^{-1}, significant at the 4σ level). However, the middle-F subgiant Procyon has an absolute TZ index within about 1σ of the stellar radial velocity. Individually, the dwarfs are found to have, at best, only marginally positive differential TZ indices, but collectively exhibit a differential index of +4 km s^{-1} which is significant with respect to the standard error of the sample mean at the 3σ level. The collective redshift for the dwarfs is intriguing because it is approximately the value expected from scaling solar observations, obtained by the OSO-8 UV spectrometer, to full-disk (Sun as a star) averages. Nevertheless, at this level of precision, systematic errors in the wavelength scales of the SW echelle and uncertainties in laboratory wavelengths become quite important, and remain to be investigated in adequate detail.

TABLE 1 : SUMMARY OF VELOCITY MEASUREMENTS

Star	Sp. Type	SWP Image Nos.	V(lowX)	ΔV(Si III], C III])	ΔV(Si IV, C IV)
χ^1 Ori	G0 V	13643, 21462, 22223, 22244	(+0.1 ± 0.4)	+ 0.3 ± 0.5	+ 8.5 ± 1.7
α Cen A	G2 V	11017	-9.4 ± 2.4	---	+3.4 ± 2.5
ξ Boo A	G8 V	14792	+ 31.3 ± 1.8	+ 1.9 ± 5.0	+ 2.2 ± 3.4
α Cen B	K1 V	9036	- 21.1 ± 0.9	+ 3.5 ± 1.1	+ 3.7 ± 1.1
ε Eri	K2 V	13553, 21192	(+1.3 ± 1.3)	+ 4.2 ± 1.9	+ 2.4 ± 1.8
α CMi	F5 IV-V	20048, 21194, 21195, 21196	$[-6.0 \pm 0.3]_{abs}$	---	$[+ 1.7 \pm 1.4]_{abs}$
α Aur Ab	F9 III	18779, 781, 786, 788, 792,794 799, 801, 803, 805, 810, 812	$[- 0.3 \pm 0.8]_{abs}$	+ 8.6 ± 2.5	+12.4 ± 3.0
λ And	G8 III-IV	9057, 18480, 21186	(- 0.3 ± 0.7)	+ 2.0 ± 0.9	+ 11.8 ± 2.5
β Cet	G9.5 III	14786	- 19.6 ± 5.6	+ 13 ± 6	+ 13 ± 7
α Boo	K2 III	20044	$[- 1.2 \pm 1.2]_{abs}$	+ 4 ± 4	---
α TrA	K3 II	8569, 8986, 15494	(2.1 ± 0.8)	+ 1.2 ± 1.5	+ 2.4 ± 5
β Aqr	G0 Ib	10265	+ 35.3 ± 2.9	+ 0.7 ± 2.9	- 1 ± 11
α Aqr	G2 Ib	17060	+ 2.2 ± 2.7	+ 7.6 ± 2.7	- 15 ± 22
56 Peg	K0 Ib	15283	- 19.7 ± 1.9	+ 5.1 ± 3.5	+ 14 ± 7

Notes: V(lowX) is the measured weighted mean velocity of low excitation lines in single or composite spectra. Parantheses indicate that the low X lines were used to register the individual exposures to a common velocity scale. Brackets indicate single spectra or composite spectra registered to the stellar radial velocity frame by means of an 'absolute' velocity measurement. The final two columns provide the differential velocities of the Si III] + C III] or Si IV + C IV features relative to V(lowX), except for Procyon where the measurement is 'absolute'. The uncertainties in the V's are standard errors of the weighted means. The uncertainties in the ΔV's are quadratic sums of errors. In the single spectra, the V(lowX) have not been corrected for the Earth, satellite or stellar radial velocities, and therefore can depart significantly from zero.

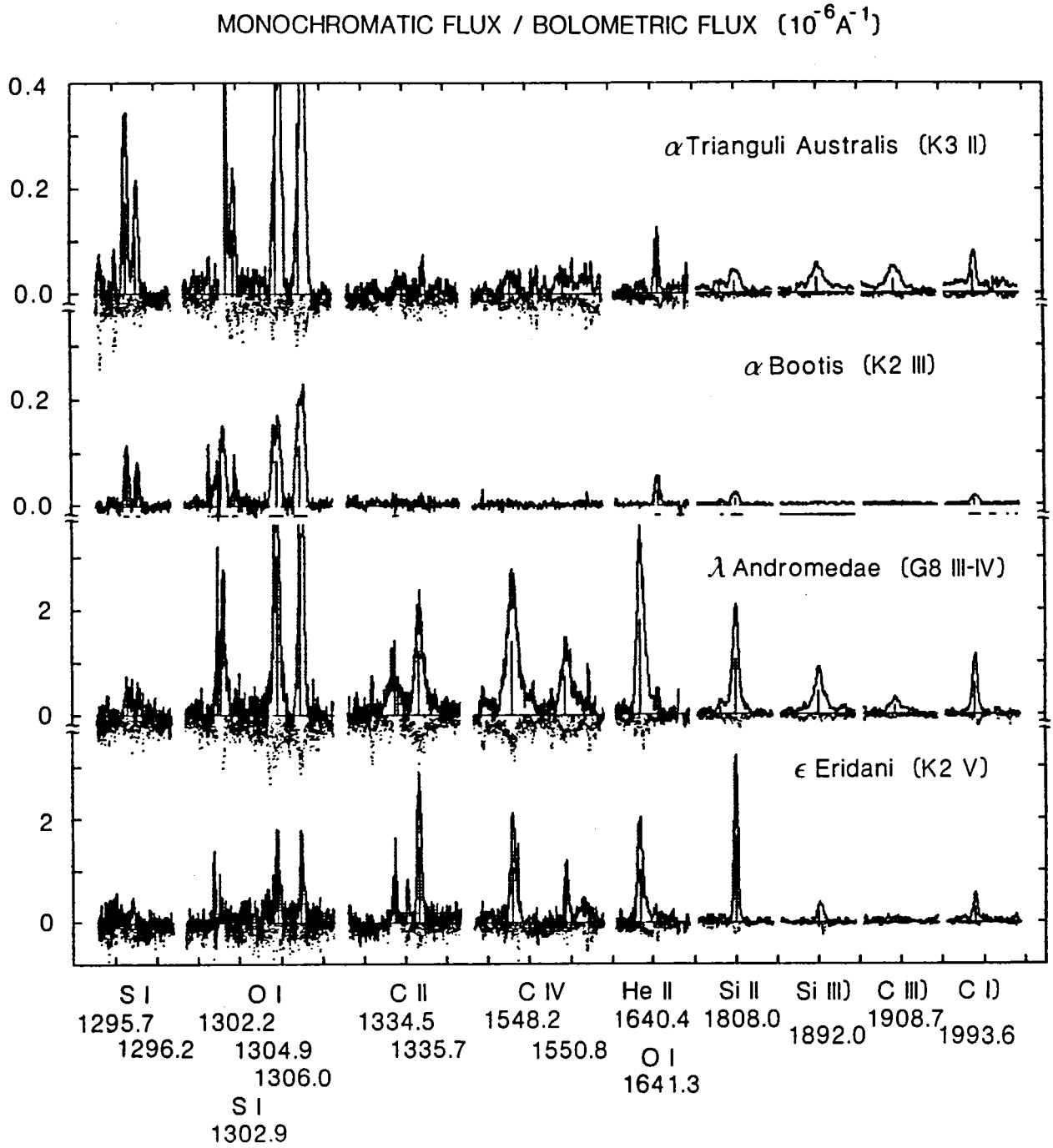

Figure 1: The ordinate is the monochromatic flux divided by the bolometric flux of the star, and is ananlogous to a surface flux. The abscissa is a segmented wavelength scale (the tick marks are 2 A apart). For the composite spectra, the negative of the rms vector is plotted for each spectral interval. For example, sharp dips in the -rms indicate the presence of cosmic ray "hits." The vertical strokes in each line represent the laboratory wavelengths in the rest frame of the low-excitation species. Note that O I 1302.2 and C II 1334.5 are affected by reseau marks in addition to interstellar absorption.

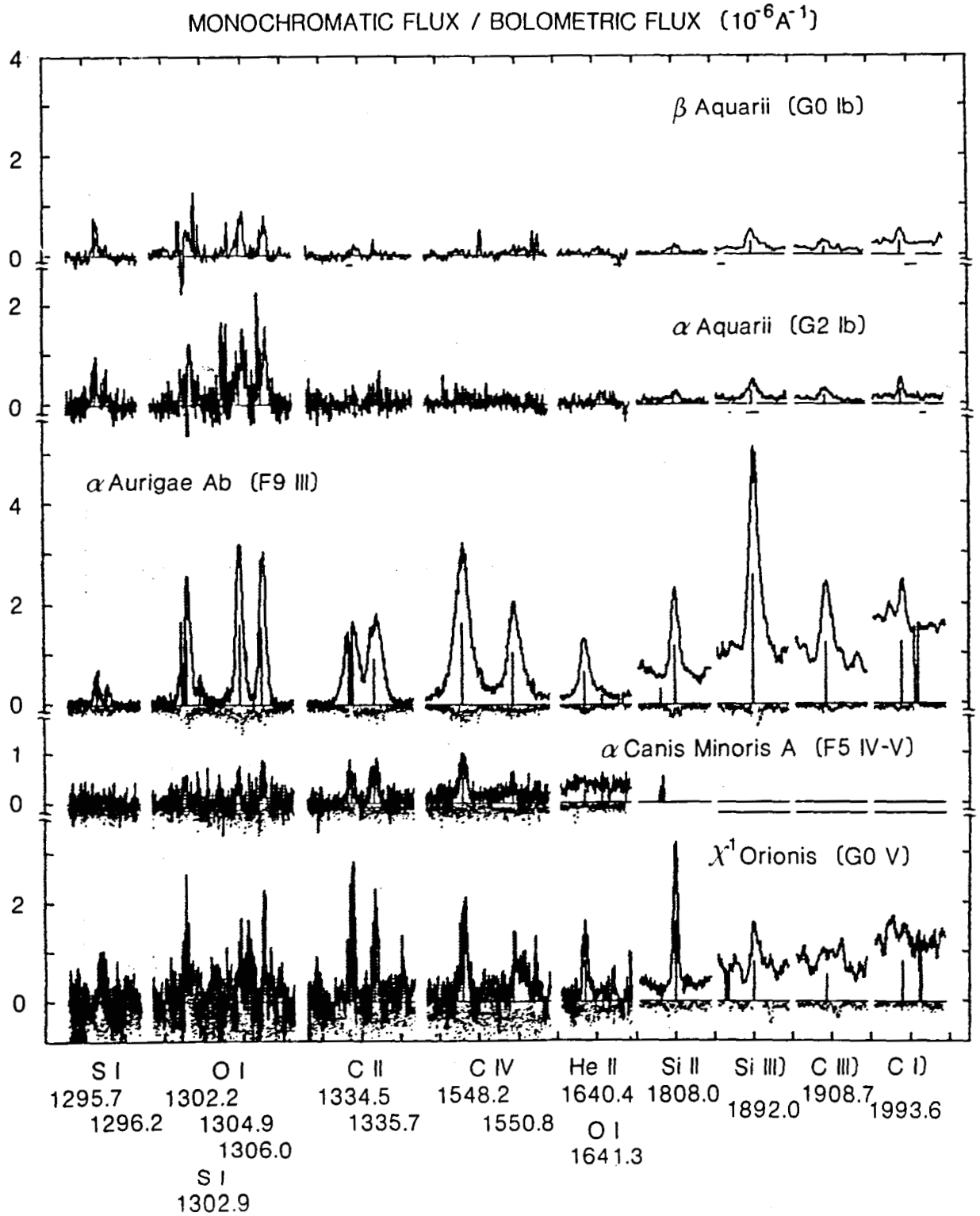

Figure 2: Same as Figure 1 for F and early-G stars. In the single spectra, and in the longwavelength portion of the Procyon composite spectrum, dips below the zero line in each panel indicate regions of the spectra which are overexposed or, in some cases, affected by reseau marks. The reference frames for the Procyon and Capella composite spectra are barycentric 'absolute.'

This work was supported by Guest Observer grants from NASA, SERC, and ESA.

ULTRAVIOLET, RADIO AND X-RAY OBSERVATIONS OF HYBRID STARS

Stephen A. Drake, Alexander Brown and Jeffrey L. Linsky*
Joint Institute for Laboratory Astrophysics, University of Colorado
and National Bureau of Standards, Boulder, Colorado 80309

ABSTRACT

In order to understand the nature of the circumstellar regions in the so-called hybrid (-chromosphere) stars, we have analyzed existing long wavelength IUE data of these stars, obtained new 6 cm radio observations with the VLA, and compiled all available X-ray observations. We conclude that the low-velocity absorption components seen in the Mg II h and k lines of hybrids are almost certainly interstellar and that only the high-velocity components are indicative of the stellar wind speeds. The mass loss rates of ionized material obtained from the radio data are $\lesssim 2\text{-}4 \times 10^{-9}$ $M_\odot$ yr^{-1} for the three hybrids observed to date. The emission measures of coronal material can be obtained from the X-ray data; of the four hybrids observed by Einstein, three were not detected, and one (θ Her) was possibly detected, implying that hybrid stars are not intrinsically strong X-ray sources.

INTRODUCTION

Hartmann, Dupree and Raymond (1980) introduced the term hybrid (-chromosphere) star to refer to those luminous, late-type stars that show spectroscopic evidence for both a cool ($T \sim 10^4$ K), high-velocity ($v \sim 100$ km s^{-1}) wind (as indicated by short-wavelength-shifted absorption in the Mg II h and k lines) and a solar-type transition region (as indicated by emission lines such as C IV formed at $T \sim 10^5$ K). This apparent dual nature of the outer atmospheres of the hybrid stars is very interesting because these stars lie in a region of the H-R diagram separating stars with solar-like hot coronae (as implied by X-ray emission) from those with cool, massive winds (as evidenced by shortward-shifted "circumstellar" absorption components) (Linsky and Haisch 1979; Ayres et al. 1981). Thus the hybrid stars could be in transition between these two types of atmospheric structure, perhaps due to evolution to the right in the H-R diagram. Reimers (1982) proposed possible new hybrid stars on the basis of the two (high and low velocity) absorption features in either the Mg II or the Ca II resonance lines, since all six hybrids known to that date had this characteristic.

Hartmann, Dupree and Raymond (1981, hereafter HDR) proposed as an additional property of the hybrid stars that the low-velocity absorption components seen in the Mg II lines in these stars are intrinsically circumstellar. These authors applied the Alfvén-wave driven stellar wind theory of Hartmann and McGregor (1980) to model the Mg II lines and the strengths and widths of

---

*Staff Member, Quantum Physics Division, National Bureau of Standards.

the Si III, C III and C IV lines. Their hybrid star model envelopes had the following properties: (1) A temperature structure which rises from $T_e \sim 10^4$ K just above the photosphere (region A) to a maximum of $\sim 8 \times 10^4$ K at 2-3 stellar radii r_* (region B) and then declines back down to $\lesssim 10^4$ K at 10 r_* (region C). (2) A velocity field increasing from $\lesssim 10$ km s^{-1} (region A) to ~ 100 km s^{-1} (region B) and then staying fairly constant. (3) A mass loss rate of 4-5 $\times$ 10^{-9} $M_\odot$ yr^{-1}.

We present here a re-analysis of the Mg II profiles of hybrid stars (obtained from spectra available in the IUE Archives of the Univ. of Colorado RDAF), present new radio observations of 3 hybrid stars (ι Aur, θ Her and γ Aql), and discuss the available Einstein X-ray data on these stars. We compare this observational material with the properties of the HDR model.

THE NATURE OF THE ABSORPTION COMPONENTS IN THE Mg II LINES

Because of inconsistencies between the various authors who have measured the radial velocities of the Mg II absorption components, we have remeasured the best spectra for all seven confirmed hybrid stars. We have used Fe I and Cr II absorption lines in the region 2765-2875 Å to determine the photospheric radial velocities. On the basis of their repeatability from spectrum to spectrum, we estimate that the measured relative radial velocities of the absorption features with respect to the photosphere should be accurate to ± 3 km s^{-1} (1σ). The major inferences that we have directly drawn from our study of the Mg II lines in these stars can be summarized as follows: (i) In each star the low-velocity absorption component is always narrower than the high-velocity component, and is generally unresolved at the 30 km s^{-1} resolution of the LWR camera. (ii) The low-velocity component for each exposure of a given star is always at the same radial velocity relative to the stellar photosphere. The values obtained from measurements of different exposures for the same star have a standard deviation of 2-4 km s^{-1}, which is equal to our expected measurement error for a feature that is at constant radial velocity. (iii) The high-velocity component is clearly variable in velocity in α TrA and probably also in ι Aur and this component is variable in shape in many of the stars, confirming that it is circumstellar in origin.

Since the low-velocity absorptions in all seven hybrids are narrow and constant in heliocentric radial velocity, we have investigated the hypothesis that they are due to interstellar absorption. The interstellar medium within ~30-50 pc of the Sun (the Local Interstellar Medium, LISM), can be modeled to a fair degree of approximation as a discrete entity with a coherent velocity vector (V_I, α_0, δ_0) with respect to the Sun. Crutcher (1982) and Frisch (1981) have reviewed the evidence supporting this simple model and determined values for this vector. Freeman et al. (1980) have modeled the resonant scattering of the solar He I λ584 Å emission by material flowing through the solar system to obtain a local value for this vector which is in good agreement with the value obtained from observations of the interstellar absorption seen toward nearby hot stars (Kondo et al. 1978) and cool stars (McClintock et al. 1978; Böhm-Vitense 1981).

Comparing the predicted radial velocities obtained from these different estimates of the LISM vector we find a spread in the values, for a given direction, of up to 18 km s^{-1}, with typical standard deviations about the mean of ~6 km s^{-1}. If the flow of the LISM were truly coherent, then this uncertainty would presumably be a consequence of measurement errors. Since we do not expect the radial velocities to be this imprecise, a more likely reason for the uncertainty in the LISM radial velocities is that the LISM flow is not as simple kinematically as our model assumes. Thus, if we use the "global" LISM assumption, we should not expect to predict the exact radial velocity in a given direction to better than ±5-10 km s^{-1}. In Fig. 1, we plot the measured radial velocities of the low-velocity components (V_{low}) in the hybrid stars against the predicted LISM radial velocities (V_I) in the stellar reference frames using averaged values of the global LISM vector. The graph shows a good correlation between the predicted LISM absorption radial velocity and that observed for the low-velocity component. Most of the scatter is probably due to the inherent inaccuracies in representing the LISM by a single kinematic entity. Indeed, when we use LISM velocities determined from hot stars nearly in the same direction as two of the hybrids (θ Her and γ Aql), in both cases the "better" values of V_I move closer to the observed values of v_{low}. We therefore conclude that the low-velocity absorption in hybrid stars can be entirely explained by local interstellar absorption.

RADIO AND X-RAY OBSERVATIONS OF HYBRID STARS

We have observed θ Her, γ Aql and ι Aur at 6 cm with the VLA. We did not detect any of these stars, with 3σ flux upper limits of ~0.2 mJy. Using the Wright and Barlow (1975) theory for the thermal radio emission from a constant

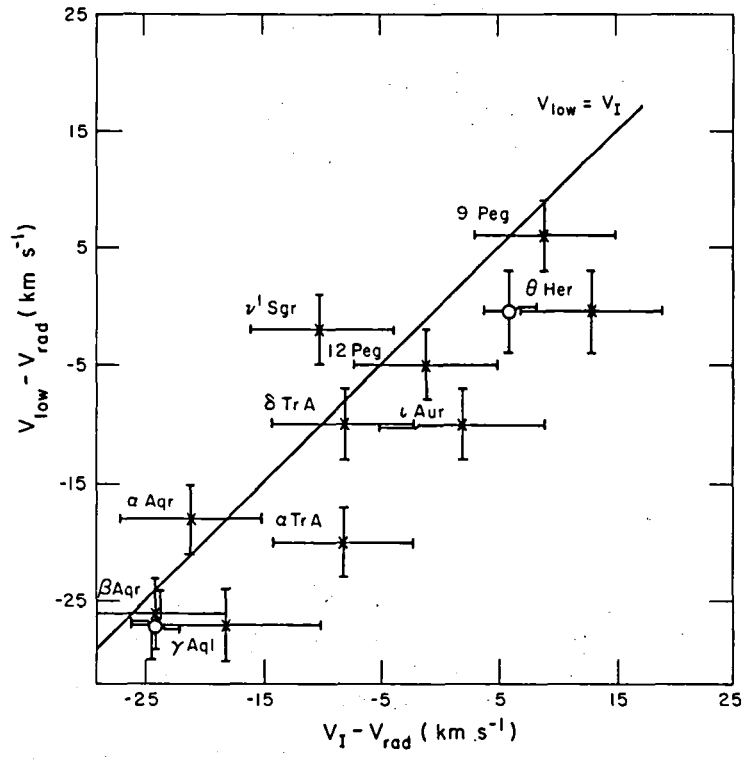

Fig. 1. Comparison of the measured radial velocities of the low velocity components of the hybrid star Mg II lines (V_{low}) with the predicted local interstellar medium (LISM) radial velocities (V_I), both corrected for the radial velocity of the stellar photosphere (V_{rad}). The $V_{low} = V_I$ line is indicated. For two stars, θ Her and γ Aql, the circles indicate that V_I was determined from the interstellar velocity toward a nearby hot star rather than from the mean global LISM vector, thereby improving the agreement with the $V_{low} = V_I$ line.

velocity, ionized wind, the wind velocities and distances for these stars taken from Drake et al. (1984), and the 6 cm upper limits, we obtain upper limits to the ionized mass loss rates of 2×10^{-9} $M_\odot$ yr^{-1} (γ Aql and ι Aur) and 4×10^{-9} $M_\odot$ yr^{-1} (θ Her).

We have also compiled published Einstein X-ray fluxes for these stars. For three hybrids (α Aqr, β Aqr, and γ Aql) no flux was observed with upper limits of 6×10^{-14}, 2×10^{-13}, and 2×10^{-13} ergs cm^{-2} s^{-1}, respectively (Haisch and Simon 1982). Given the great distance of α and β Aqr ($\gtrsim$300 pc), their non-detections are not surprising. For θ Her, there is an unpublished 2.5σ X-ray detection of 2×10^{-13} ergs cm^{-2} s^{-1} corresponding to log L_x = 29.75 (Caillault and Helfand 1982). Unfortunately, no X-ray data are presently available for the two nearest hybrid stars α TrA and ι Aur.

CONCLUSIONS

HDR adopted a model for hybrids that could form both the low- and high-velocity Mg II absorptions in the expanding circumstellar envelope. Their model predicted no X-ray emission (since $T_{max} \ll 10^6$ K). We conclude from our analysis that interstellar absorption is sufficient to account for the observed low-velocity features, so that only the high-velocity absorptions are formed in the winds themselves. Thus, we believe that what makes the kinematics of hybrid star winds interesting are the observed high wind velocities (70-140 km s^{-1}) compared to other G-K I-III stars (typically 10-40 km s^{-1}) and not, as previously believed, the supposed "twin circumstellar" absorptions. To verify the possibility of 10^6-10^7 K plasma existing in the circumstellar regions of these stars, further X-ray data are clearly needed. The present data are not yet conclusive. Finally, the mass loss rates for hybrids, as determined from radio continuum observations, are so small as to imply that mass loss will have no effect on the evolution of the stars during this phase, since typical evolutionary times through this region of the HR diagram are $<10^7$ years and the derived mass loss rates are $\lesssim10^{-9.3}$ $M_\odot$ yr^{-1}.

REFERENCES

Ayres, T. R. et al. 1981, Ap. J., 250, 293.
Böhm-Vitense, E. 1981, Ap. J., 244, 504.
Caillault, J.-P. and Helfand, D. J. 1982, private communication.
Crutcher, R. M. 1982, Ap. J., 254, 82.
Drake, S. A., Brown, A. and Linsky, J. L. 1984, Ap. J., in press.
Freeman, J. et al. 1980, Astr. Ap., 83, 58.
Frisch, P. C. 1981, Nature, 293, 377.
Haisch, B. M. and Simon, T. 1982, Ap. J., 263, 252.
Hartmann, L. et al. 1980, Ap. J. (Letters), 263, L143.
_____. 1981, Ap. J., 246, 193 [HDR].
Hartmann, L. and McGregor, K. B. 1980, Ap. J., 242, 260.
Kondo, Y. et al. 1978, Ap. J. (Letters), 220, L97.
Linsky, J. L. and Haisch, B. M. 1979, Ap. J. (Letters), 229, L27.
McClintock, W. et al. 1978, Ap. J., 225, 465.
Reimers, D. 1982, Astr. Ap., 207, 292.
Wright, A. E. and Barlow, M. J. 1975, Mon. Not. R.A.S., 170, 41.

ROTATIONAL MODULATION OF CHROMOSPHERIC EMISSION IN COOL GIANTS AND "HYBRID" STARS

J. W. Brosius and D. J. Mullan
Bartol Research Foundation of the Franklin Institute
and
R. E. Stencel
NASA Headquarters

ABSTRACT

We have used IUE archival data to study temporal variations of the MgII h and k emission lines in 8 late-type giants. We present evidence that the variations are periodic in nature. We argue that the periodicities can be interpreted in terms of rotation. We find that the four fastest rotators in our sample are "hybrid" stars.

INTRODUCTION

We searched the IUE archives for G and K giants and supergiants with 4 or more images well-exposed in the MgII h and k lines. After eliminating known doubles (Ba stars), we settled upon the following 8 stars: α Aqr (G2 Ib), β Aqr (G0 Ib), α Tra (K4 II-III), ι Aur (K3 II), θ Her (K1 IIa), γ Aql (K3 II), α Cas (K0 IIIa), ζ Cyg (G8 II). (The spectral types are taken from Morgan and Keenan, 1973.) Of these, the first 5 had been previously classified as hybrids, stars exhibiting evidence of both cool massive winds and warm material (N V and C IV emission lines), but no X-rays (Reimers, 1982).

71 images for the 8 stars were reduced at the IUE RDAF at Goddard Space Flight Center. We obtained the fluxes for each of the h and k lines by integrating above a continuum level designated by the minima surrounding each of the emission lines (FNET in the IUE software). We also obtained S/L values where the shortward emission component rose significantly above the noise (for α Cas and ζ Cyg). We estimate that the noise in FNET (due to temperature drifts, reproducibility uncertainty, and pixel saturation) is $\leq$ 4%.

RESULTS

The variability of chromospheric emission in cool giants has already been demonstrated (Mullan and Stencel, 1982), but the question of periodicity is addressed here for the first time. We wish to fit our data to a curve of the form

$$C_i = K + A\sin(\omega t_i + \phi)$$

where A is the amplitude, ω is the angular frequency, ϕ is a phase factor, t_i is the time in days since the first exposure in the series (t_1=0), and K is the d.c. (mean) term. In the case of α Aqr, where we have 16 good,

independent exposures, we find that the first 6 images fit (to < 1%) an angular frequency of $\omega = 0.0288$ (period of 218 days) and the 9th-15th images fit $\omega = 0.0313$ (period of 201 days). The 7th, 8th, and 16th points fit neither of these two curves. See Figure 1. Because these periods are much longer than expected pulsation periods for stars in our sample, we ascribe the periodicity to rotational modulation. This requires that the chromospheric emission from a star is dominated by emission from a small number (ideally, one) of active regions, where the active regions live for one or more rotational periods (Vaughan et.al., 1981). We interpret the results for α Aqr to mean that the chromospheric emission is dominated by one active region through and including the first 6 images, and a different active region (located at a different stellar latitude) for the 9th-15th images. This yields an estimate on the life expectancy of active regions on α Aqr to be ~ 1.5 years. (We similarly obtain life expectancies of ~ 1-2 years for the other stars in our sample.) We note that similar angular frequencies (0.0293 and 0.0301, respectively) fit the h-line data for α Aqr (to < 2%), although here we have only 5 and 5 points fitting the same time intervals. For the other stars in our sample, we have extracted periods of 390 days (β Aqr), 100 days (ι Aur), 430 days (γ Aql), 116 days (α TrA), 146 days (α Cas), 323 days (ζ Cyg), 56 days (θ Her). The corresponding rotational velocities are 9.2, 32, 7.4, 22, 4.9, 5.6, 42, and 20 km/sec for α Aqr. Note that the four fastest rotators are "hybrids".

Since the periods we have determined were obtained by using relatively sparse data, we sought to confirm our results by the use of other methods. We employed the periodogram method of Scargle (1983) and Black and Scargle (1983) for unevenly sampled data. Note that uneven sampling drastically reduces effects of aliasing. See Figure 2, where we plot the periodogram for α Aqr for frequencies up to the Nyquist frequency $\omega_N = 0.392$. The 4 main peaks in Fig. 2 were investigated with the period analysis technique described above, and the best fit (most points fitting the given curve to < 1%) was found to be the 2 values quoted above. The peak at $\omega \sim 0.03$ corresponds to a confidence level of >99.9%. Scargle's method, applied to the other stars in our sample, again yields several peaks similar in strength to the main peaks, but in all cases the period which fits the data best corresponds to the value of ω as obtained by the algorithm described above. Thus, the periodogram supports our conclusions, although it indicates that other, shorter, periods may also be present.

As a test of the rotational interpretation of our periodicities, we first compare our value of rotational velocity V for α Cas with the range of values of V obtained by Gray (1982) for stars of spectral type K0 III. Gray obtains values in the range 3.1-4.3 km/sec (assuming $\sin(i)=\pi/4$), in good agreement with our value of 4.9 km/sec. Second, we compared the widths of FeI absorption lines (e.g., in the range 2906-2916 Å) in the spectra of two stars which we have determined to be rotating with very different periods, although their spectral types are almost identical: γ Aql (7.4 km/sec) and θ Her (42 km/sec). We confirm that the features in the spectrum of the slower rotator are significantly narrower than they are in the spectrum of the more rapid rotator. Third, for the 4 bright giants θ Her, γ Aql, ι Aur,

and α TrA, we correlated the C IV and N V fluxes (Hartmann et.al., 1981; Reimers, 1982) with our derived values of ω and found a clear-cut ordering of the surface fluxes: the larger our estimate of ω, the larger the surface flux of both C IV and N V (see Figure 3). It is already established (Basri et.al., 1983) that the surface flux of the warm lines in the spectra of cool dwarfs and subgiants is positively correlated with the angular velocity of rotation; we think it is not unlikely that a similar "rotation-activity connection" is present in the bright giants.

For these reasons, we believe that we have obtained estimates of rotational velocities in the stars of our sample. The confidence level we assign to the extracted periods is highest in the stars with most data points (α Aqr, β Aqr), and poorest in the cases of ζ Cyg and α Cas (4 and 5 points, respectively). Of the other stars (γ Aql, α TrA, ι Aur, θ Her), the periodogram analysis suggests that our most reliable determination of period is for ι Aur, while θ Her's period is considerably less certain.

This work has been supported in part by NASA Grant NAG5-378.

REFERENCES

Basri, G., Laurent, R., Walter, F., 1983, IAU Symp. 102 (ed. J. Stenflo), p.199.
Black, D., Scargle, J., 1982, Ap. J. 263, 854.
Gray, D. F., 1982, Ap. J. 262, 682.
Hartmann, L., Dupree, A. K., Raymond, J. C., 1981, Ap. J. 246, 193.
Morgan, W. W., Keenan, P. C., 1973, Ann. Rev. Astron. Ap. 11, 29.
Mullan, D. J., Stencel, R. E., 1982, Ap. J. 253, 716.
Reimers, D., 1982, Astron. Ap. 107, 292.
Scargle, J., 1982, Ap. J. 263, 835.
Vaughan, A. H. et.al., 1981, Ap. J. 250, 276.

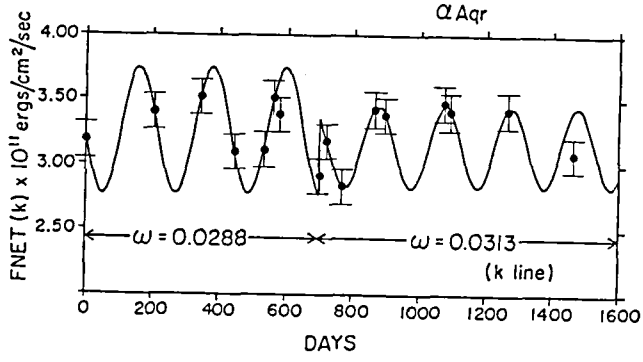

Figure 1. Fit of 13 FNET(k) data points for α Aqr to two sinusoids, with slightly different angular frequencies before and after t=700 days. K, A, and φ also alter abruptly at t=700 days. Error bars correspond to a maximum possible error of 4%.

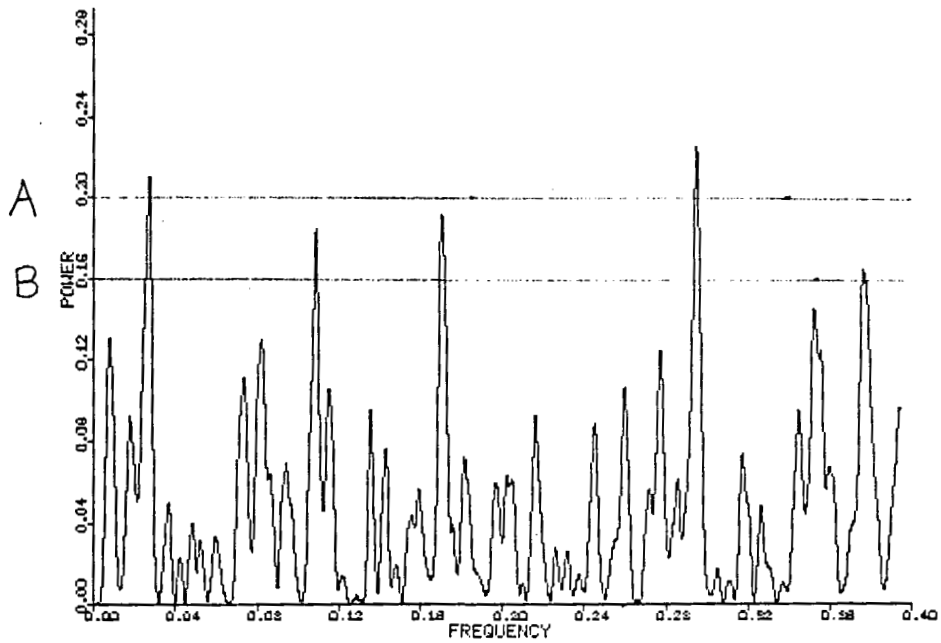

Figure 2. Periodogram power vs. angular frequency for α Aqr. Indicated are the 99.994% (A) and 99.94% (B) confidence levels.

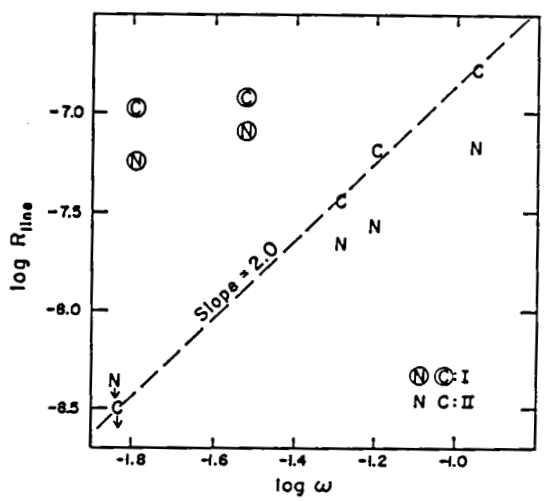

Figure 3. Surface fluxes of CIV and NV emission in 4 bright giants (uncircled symbols) and 2 supergiants (circled symbols) as a function of our estimated ω values. R_{line} is the ratio of surface flux to σT^4_{eff}.

HELIUM-WEAK STARS

ULTRAVIOLET AND OPTICAL SPECTROSCOPY AND POLARIMETRY OF THE HELIUM WEAK STAR HD 21699: EVIDENCE FOR A MAGNETICALLY CONTROLLED STELLAR WIND

Douglas N. Brown[1], Steven N. Shore[2], C.T. Bolton[3], Stephen J. Hulbert[2], and George Sonneborn[4]

1. Department of Astronomy, University of Washington
2. Warner and Swasey Observatory, Case Western Reserve University
3. David Dunlap Observatory, University of Toronto
4. Resident Astronomer, IUE Observatory and Computer Sciences Corporation

ABSTRACT

We have obtained high dispersion SWP spectra with IUE, and contemporaneous optical Zeeman polarimetry and spectroscopy, of the helium weak star HD 21699 = HR 1063. All IUE observations were made during Sept. 1983 and Feb. 1984. The C IV 1548,1550 doublet varies on a timescale consistent with the photometric and magnetic period, while no other strong lines in the UV display obvious variations in profile or strength. Only the helium weak star HD 5737 = α Scl shows a similarly strong C IV line among the helium weaks. We discuss this set of observations in the context of a magnetic star which is losing mass, having constrained that outflow to corotate with the stellar surface. If the magnetic period is correct, the greatest mass outflow seems to be from above the polar regions. The comparison between optical and UV spectrum phenomenology is also briefly discussed.

INTRODUCTION

The helium weak star HD 21699 = HR 1063 is a member of the α Persei cluster, and was discussed as such by Molnar et al.(1978). The MK type for the star is B8, but the UBV colors indicate a B4 or B5 effective temperature and extreme helium deficiency (leading to a too late MK type). Mallama and Molnar (1974) determined an effective temperature of 15050 K (log g = 4.0) with a helium depletion of a factor of 3. The star would have to be cooler than 13000 K in order to render it helium normal, as is typically the result for the helium weak stars.

Winzer (1974) published UBV photometry for the star. He found a single wave variation (roughly sinusoidal) with all colors in phase and a U amplitude larger than B or V, and a period of 2.47 days. Mallama and Molnar (1974) revised this period to $2^{d}.4928$ using additional UBV photometry. Spectrum variations were first mentioned by Bruckner (1973, M.Sc. thesis,Toronto),who also provided a line identification list.

Our interest in this star arose from its membership in the cluster and as part of our general survey of the 1540 - 1560 region among the helium peculiar main sequence stars. HD 21699 is a slow rotator, and the velocity and published period are nearly identical to HD 34452, the most extreme Si star. Otherwise, it appeared undistinguished. Somewhat to our surprise, the behavior of HD 21699 has proven exciting in its own way. We here merely

present a summary of our results. A complete paper is in preparation.

ULTRAVIOLET VARIATIONS

We have obtained eight high dispersion SWP spectra (SWP 21081,21096, 21110, 21118,21123,21127,21133) during 1983 Sept. and SWP 22197 in 1984 Feb. All are 7 min. exposures. Since all of the September 1983 data was obtained in a one week period, we shall concentrate on this set. The Feb.1984 spectrum is consistent with the average Sept. spectra. The gallery of CIV results is shown in fig.1. The region is dominated by numerous strong FeIII lines, but there is clearly a strong, variable and broad line at each of the C IV lines. In fact, these are the only lines in the region which are varying with any amplitude. Figure 2 shows the differenced spectra, relative to SWP 21081. Note the asymmetry of the CIV line and that the FeIII 1558,1559 lines disappear on differencing. Fig.3 shows the SiIV 1400 region for the most extreme SWP spectra. Again note that the CIV is variable with a far greater amplitude than even SiIV. The FeIII is not variable. For comparison we refer the reader to the theoretical spectra in the accompanying CIV survey paper for T_{eff} = 17000 K and 90 km s^{-1}. The most nearly equal spectra (SWP 21081,21110) are $2^d.25$ apart and we feel the evidence is good for periodic, rather than stochastic, variation of C IV.

Having examined especially the 1800 - 1900 region (FeII and FeIII,Al III dominant) and the SiIV 1400 region, we again emphasise that only C IV appears to be distinctly variable. The terminal velocity is about 600 km s^{-1}.

MAGNETIC MEASUREMENTS

The magnetic measurements were performed at the Mt. Palomar 1.5 m telescope using the Univ. of Michigan filter polarimeter (Brown *et al.* 1977) modified for Hβ Zeeman polarimetry. The technique is identical to that of Landstreet (1980). Observations of well known magnetic CP stars confirm the comparability of measurements made with the UM and UWO polarimeters. The data re shown in fig.4. Clearly, HD 21699 is a magnetic star and it appears that the field reverses sign. It was not previously known to be magnetic. The best fitting magnetic period does not differ substantially from Mallama and Molnar's period (and the timescale for comparison of the Zeeman and IUE data being sufficiently short can be taken as about $2^d.5$). The measured values range from -1.3 to +1.0 kilogauss. A sinusoidal variation gives the crude oblique rotator parameters i = 60 ± 20^o(inclination),β ≈70^o(obliquity). This high value is not unusual among the CP2 stars, and the measured field is of the same magnitude as observed for the helium weak stars by Borra *et al.* (1983).

OPTICAL SPECTROSCOPY

As part of a continuing program, over the past decade 8 and 12 A mm^{-1} IIaO and IIIaJ spectra have been obtained at DDO with the cassegrain spectrograph on the 1.88 m. Preliminary analysis of this material confirms that the Si II optical lines vary by about a factor of two, and also vary in v_{rad}, but the best fitting periods for Si II are $1^d.01$ and $1^d.99$. The magnetic, UV and photometric period doesn't give significent results in the power spectrum analysis. The hydrogen lines display a long term variation (the two data

sets are 1970-1980 and 1983-1984) of about 7.5 km s^{-1}, but the details are still uncertain.

DISCUSSION

At present, we can only provide a crude interpretation of these data. If the magnetic and photometric periods are correct, the C IV variations can be explained by a wind emerging from above the magnetic poles of HD 21699. As the rotation of the star transports this "plume" across the line of sight the absorption profile and terminal velocity change. The cylindrical structure of the plume would explain both the single wave variation and the lack of emission, as well as qualitatively fitting the line profile. We cannot now specify the required mass loss rate, but the profile we are observing at C IV should be entirely from the wind. The constancy of the Fe III lines, we believe, argues forcefully for the intrinsic variability of the C IV lines as opposed to merely blending. It is interesting to note that of the dozen stars in our sample of helium weaks, only the two "sn" stars (Abt's classification showing diffuse and sharp lines) display strong C IV. We hope to observe other members of this class for comparison.

DNB wishes to thank Research Corporation for support of his polarimetry. We also thank Drs. W.P. Bidelman and J.D. Landstreet for discussions.

REFERENCES

Borra,E.F., Landstreet,J.D. and Thompson,I. 1983,Ap.J.Suppl.,53,151.
Brown,D.N.,Rich,A.,Williams,W.L. and Vauclair,G. 1977,Ap.J.,218,227.
Landstreet,J.D. 1980,A.J.,85,611.
Mallama,A.D. and Molnar,M.R. 1974,BAAS,6,307.
Molnar,M.R.,Stephens,T.C. and Mallama,A.D. 1978,Ap.J.,223,185.
Winzer,J.E. 1974,A.J.,79,45.

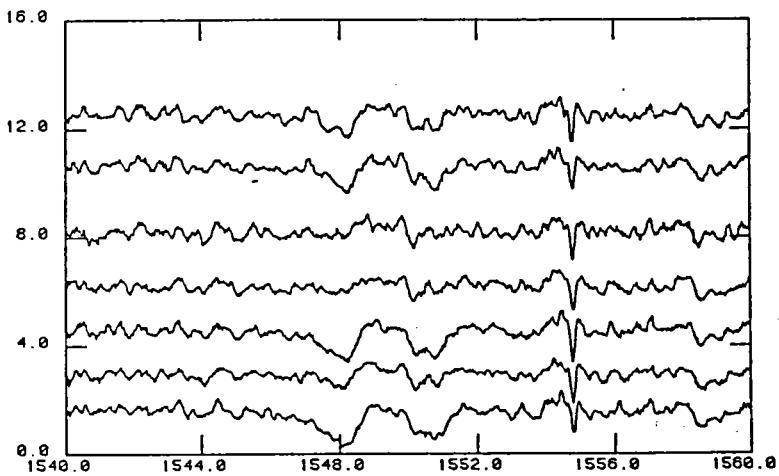

Fig.1.Gallery of CIV Profiles. Bottom to top: SWP 21081, 21096, 21110 21118, 21123, 21127, 21133. A three point filter has been applied.

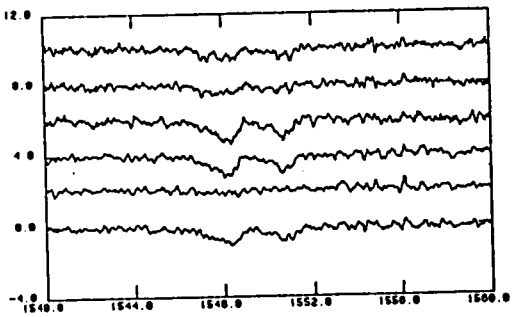

Fig. 2. Differenced profiles for C IV region. Taken relative to SWP 21081. Three point filtering. The order is the same as figure 1.

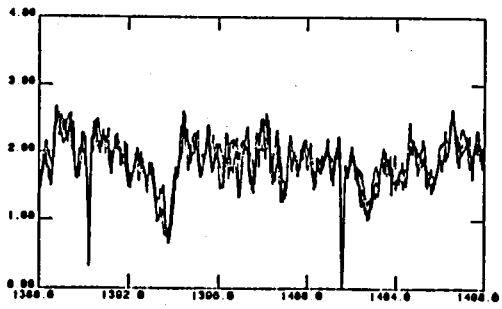

Fig. 3. Three extreme phases of HD 21699, plotted at Si IV 1400. SWP 21081, 21096, 21110 with a three point filter applied.

Figure 4 (below). Magnetic curve for HD 21699, based on Zeeman polarimetry. ϕ_0 = 0.0512. Ephemeris is: JD (SWP21081 ϕ = 0^p) = 2445595.778 + $2^d.4819$ E (magnetic best fit period).

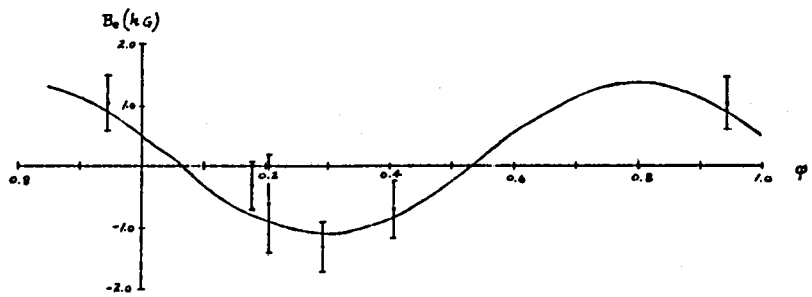

MAGNETOSPHERES AND WINDS IN THE HELIUM WEAK STARS: OBSERVATIONS OF C IV IN UPPER MAIN SEQUENCE CP STARS

Douglas N. Brown[1], Steven N. Shore[2], Paul K. Barker[3], George Sonneborn[4]

1. Dept. of Astronomy, University of Washington, Seattle, WA 98195
2. Warner and Swasey Obs.,Case Western Reserve Univversity, Cleveland, OH
3. Dept. of Astronomy, Univ. of Western Ontario, London, ON Canada
4. IUE Resident Astronomer, Computer Sciences Corp., GSFC

ABSTRACT

We present a sample of eleven helium weak and Si stars, observed at high dispersion. These are HD 5737, 21699, 28843, 34452, 125823, 131120, 142301, 142990, 144334, 175362 and 215441. The stars span the range B2.5 to B6 and include both magnetic and nonmagnetic as well as rapid and slow rotators. In the two stars designated "sn" by Abt, the C IV profile is strong (HD 5737 and 21699) while all of the other stars can be explained by numerous blended lines of Fe III and similar ions. Most of the stars have been observed several times, and only HD 21699 appears to show large amplitude spectral variations.

INTRODUCTION

This paper represents a continuation of our study of magnetospheres and winds in the helium rich stars (Shore and Adelman 1981, Barker et al. 1982a, 1982b), and continues down the main sequence from that survey. The fact that even the coolest of the helium rich stars display spectral variations at CIV 1548,1550 which are suggestive of nonisotropic distributions of low density gas about these (magnetic) stars, leads to the question: at what effective temperature do the winds in the CP stars turn on? The problem is naturally parallel to that posed by normal main sequence stars, and can be viewed as ancillary to any such study. Since many of the helium weak stars have strong (or detectable) magnetic fields, and appear to obey the oblique rotator model well, we have chosen a sample of well studied He weak and Si stars to see whether there is in fact some place on the main sequence at which the presence of a chemical anomaly and/or magnetic field plays any role in the mass loss by the star.

OBSERVATIONS AND RESULTS

Most of the stars in our sample have been observed by Borra, Landstreet and Thompson (1983, BLT) using Zeeman polarimetry. In the case of HD 21699, additional observations have been obtained in 1983. The stars are listed below and illustrated in figures 1. All observations have been obtained at high dispersion with the SWP camera of IUE. HD 21699, 28843, 142301, 142990, 144334 and 175362 have been observed during 1983. All other spectra

are archival. The data have been reduced at the RDAF at Goddard Space Flight Center using standard programs. A discussion, in the companion papers, of the low dispersion SWP data and of the time-dependent variations of HD 21699, supplement this discussion. All quoted magnetic measurements are from BLT except for HD 21699.

HD 5737 (Vsini = 10 km s^{-1}, B5): CIV 1548,1550 very strong (residual inten. of about 15%. Sharp FeIII 1558,1559 well resolved, as is blend at 1550. Two archival spectra at about the same phase, no variations detected.

HD 21699 (Vsini= 40 km s^{-1}, B5): CIV variable (!), going from about as strong as HD 5737 to invisibility. Total of seven spectra, taken in one week, suggest periodic variations of the CIV component of the line. The Fe lines do not vary, nor do the SiIV 1400 lines. The star has a detected field of about 1 kG (see paper, this session).

HD 28843 (No Vsini published, B5): CIV extremely weak, if present. Only Fe III lines appear to dominate the 1540 to 1560 A region. Four spectra, at three different phases, do not show variations. The 1548, 1550 lines are about the median strength for the helium weak stars. Possible that the rotational velocity is 60 - 100 km s^{-1} on the basis of the Fe lines. Upper limit for B_{eff} is 250 G. North (1984, preprint) gives a period of 1.37 days.

HD 34452 (Vsini=60 km s^{-1}, B6): Only archival spectra available. FeIII 1550 and 1559 strong; no evidence for CIV. Spectral variations probably due to Fe variations. The star has a weak, variable magnetic field (430 G) and a period of about 2.5 days. The Si is extremely strong in this star (see accompanying paper).

HD 125823 (17 km s^{-1}, B3): This star has been extensively discussed by Fahey (1981 and references therein). We have used archival images taken subsequent to his study for comparison. No CIV is present, and the numerous sharp absorption lines in the region compare quite well with model calculations. The B_{eff} is 500 G, and reverses symmetrically with a period of about 8.8 days. This star serves as a "standard" for comparison with the models.

HD 131120 (90 km s^{-1}, B2.5): The profile is dominated by FeIII absorption. The 1548, 1550 blend is about as strong as FeIII 1558, 1559. Only one spectrum was obtained, but the profile is "normal" for the helium weak stars. No period is known, and only an upper limit of 170 G is given by BLT. The star is quite similar to HD 142990 at CIV; no CIV indicated.

HD 142301 (50 km s^{-1}, B3.5): Two spectra available at essentially the same phase. No CIV detected and the FeIII 1558,1559 agrees with the Vsini. The 1550 line is boxlike, with the 1550,1551 iron lines visible and about the same strength as 1548. The profile is a good match for the intermediate strength in HD 21699, and for HD 175362. The r.m.s. field is 2.1 kG and a period is given by North of 1.46 days.

HD 142990 (150 km s^{-1}(:), B3): This star is the most rapid rotator in our sample, being comparable with the helium rich stars. The 1548,1550 lines are probably entirely FeIII. The spectrum compares well with the model calculations. All suggested periods for this star are less than one day. The r.m.s. field is 1.4 kG. Only one SWP spectrum obtained.

HD 144334 (45 km s^{-1}, B4): Two phases have been observed (one archival). CIV is very weak if present at all. The available spectrum fits the

mean profile of HD 175362 quite well. BLT give an r.m.s. field of 780 G with a period of 3.61 days; North finds a period of 1.49 d.

HD 175362 (28 km s^{-1}, B2.5): We have, including archival spectra, six SWP spectra at five phases. No marked variations are observed, although the period is well covered. No CIV appears present beneath the 1548, 1550 Fe lines. Some weak variability of the metallic lines may be happening. The line strengths are consistent with those of HD 125823 with some slight rotational broadening. The measured field is 3.9 kG variable with He on a 3.67 d period.

HD 215441 ($<$ 5 km s^{-1}, B4): Two archival spectra are available for this star at different phases. Numerous sharp absorption lines make specification of the continuum level a problem, but there appears to be no CIV in either spectrum. The lines are stronger (FeIII) than in HD 125823. The measured field is the strongest of any of the He peculiar stars, 10 kG, and the period the longest, 9.49 d, of any of the stars in our sample.

DISCUSSION AND MODELS

We have computed a series of rotationally broadened spectra, using the OSU version of ATLAS 6, for T_{eff} from 17000 to 25000 (log g = 4.0) and a virial parameter of 0.5 (an equatorial velocity of about 200 km s^{-1}). The models have a von Zeipel gravity darkening and normal He/H ratio (we have also computed models with X = 0.53, Y = 0.47 but these do not differ by more than 5% on any of the lines). No CIV is visible until about 25000 K, and then the residual intensity for a normal model is 50 percent. We here show (figs.2) the model for 17000 K, with i = 0° and 30°. The match with most of the He weak stars is, in our judgement, good. Only the "sn" stars in our sample, HD 5737 and 21699, appear to show enhanced absorption due to CIV. In fact, the profiles in these stars are as strong as we see in any of the helium rich stars. All other stars can be described by broadened and blended Fe III and other metallic ion lines blanketing the 1540-1560 spectral region. A more complete discussion is in preparation.

In conclusion, although at present only a tentative statement can be made, we find that only the "sn" stars among the helium weak class show any evidence for stellar winds.

REFERENCES

Barker,P.K.,Brown,D.N.,Bolton,C.T. and Landstreet,J.D. 1982a, Adv. in UV Astronomy (NASA CP-2238)p. 589.

Barker,P.K.,Brown,D.N.,Landstreet,J.D. and Shore,S.N. 1982b, BAAS, 14,651.

Borra,E.F., Landstreet,J.D. and Thompson,I. 1983, Ap.J.Suppl.,53, 151.

Shore,S.N. and Adelman,S.J. 1981, 23rd Liege Symp., p. 429.

Fahey, R.P. 1981, in The Universe at UV Wavelengths (NASA CP-2171),p. 177.

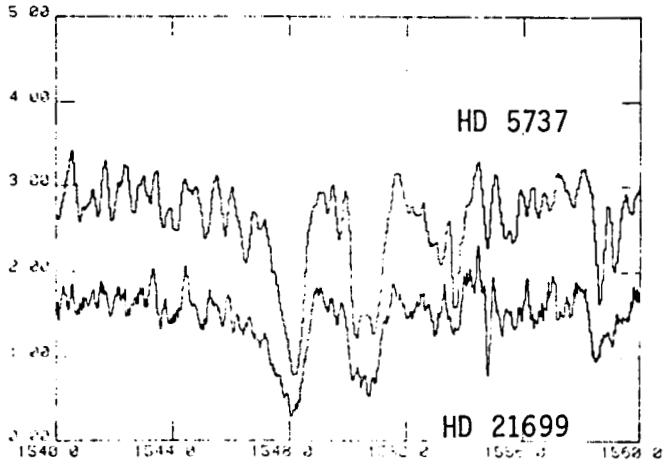
HD 5737
HD 21699

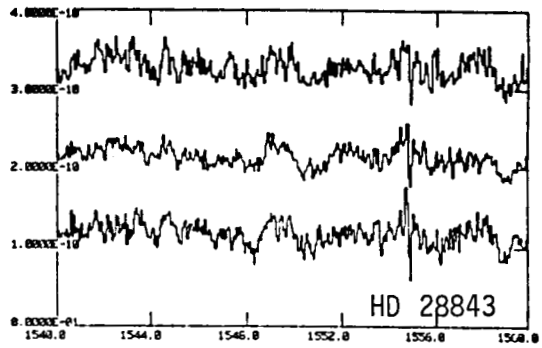
HD 28843

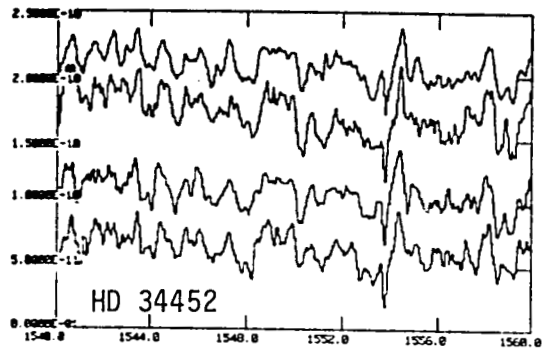
HD 34452

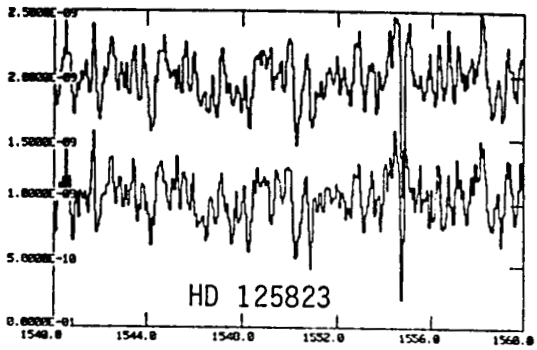
HD 125823

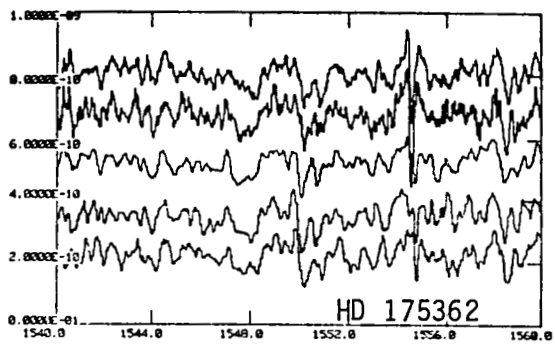
HD 175362

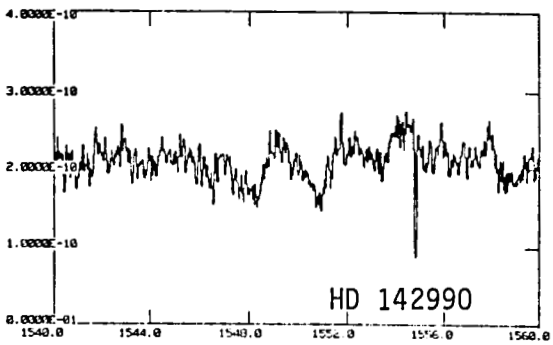
HD 142990

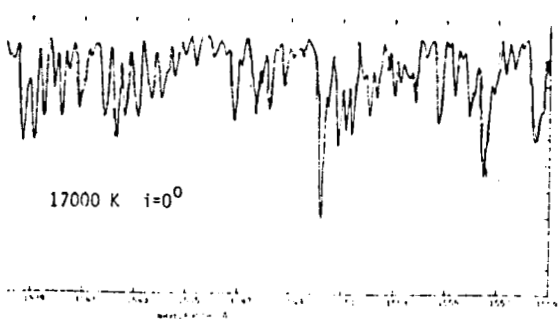
17000 K i=0°

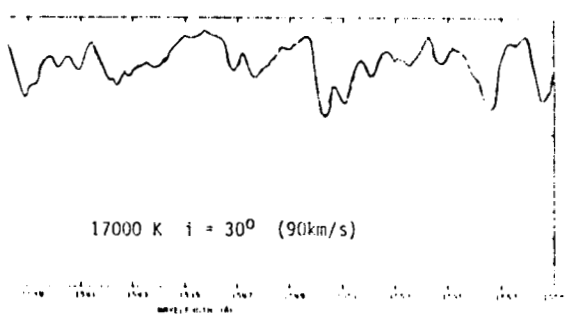
17000 K i = 30° (90km/s)

IUE SPECTROPHOTOMETRY OF HELIUM WEAK AND SILICON STARS

Steven N. Shore
Warner and Swasey Observatory
Case Western Reserve University

and

Douglas N. Brown
Department of Astronomy
University of Washington

ABSTRACT

We have surveyed a sample of helium weak stars using the low dispersion SWP and LWR cameras of IUE during 1983. The aim is to study systematics of the broad continuum feature at 1400 A as a function of effective temperature, spectral anomaly and age. For the Orion association, we have five stars (HD 35456, 36313, 36526, 36668, 37140); for Sco-Cen we have two (HD 142301 and 144334) and for Alpha Per we have one (HD 21699). We cover the range from B2 to B6. Only HD 34452, the most extreme silicon star in the sample, has a very strong 1400 feature.

INTRODUCTION

Recent surveys by Maitzen (1976, 1980) and Joncas and Borra (1981) (see Adelman 1981 for further discussion) have shown that the broad continuum feature at 5200 A is an effective tool for discovering both magnetic and CP2 stars photometrically. Artru et al. (1981) have argued that the broad feature observed in Ap and Bp stars with TD-1 at 1400 A , which they attribute to an autoionizing transition of Si II, is perhaps even better as a fingerprint of chemical peculiarity (see Jamar et al. 1978). In order to test the idea that this is associated with a Si enhancement, and to see if there is some way of quantitatively observing the development of this anomaly with time, we have observed a sample of helium weak and Si stars with the SWP and LWR cameras of IUE. The satellite was employed as a spectrophotometer for this work, and the observations parallel those of the high dispersion study (Brown et al., this conference) and Panek and Sonneborn (1984, preprint)(for 56 Ari).

SAMPLE STARS

Our sample consists of the following stars (see table I for details): HD 21699, 34452, 35456, 36313, 36526, 36668, 131120, 142301, 144334, 175362, and 215441. Accidentally (the FES locked onto the common proper motion companion of HD 34452), we also obtained an observation of the Hg-Mn star AR Aur = HD 34364. Multiple observations were obtained of HD 21699,

34452 and 175362. One additional star, the He rich star HD 184927, was also observed.

RESULTS

With the exception of HD 131120, all of the sample stars are shown in figs. 1. As is immediately obvious from the continuua, only HD 34452 is markedly different from any of the stars in the sample. Both the continuum $\lambda \lesssim 1400$ A and the depth of the 1400 feature are consistent with the results of Panek and Sonneborn concerning the influence of silicon on the spectral appearance of CP2 stars. HD 215441, which is also known as a strong silicon star, is also possessed of a peculiar continuum, having the next strongest 1400 feature . Most of the other stars in the sample appear quite similar, with the 1400 feature being about 15 $\pm$ 4 A equivalent width. Two of the Orion stars, HD 36313 and 37140, have essentially the same continuum distribution below 1500 A, but differ at longer wavelength. It should be noted that the Orion stars do not appear to have a systematically weaker 1400 feature than any of the other stars in the sample, even dispite their youth, so that if the silicon anomaly is really connected directly with the strength of this feature, the Si abundance enhancement is "normal" in these stars.

There is no obvious relation between 1400 and magnetic field strength. HD 21699 and 131120 are about equal (as is 175362) but range over three kilogauss in field strength. HD 34452 is only weakly magnetic (about 400 G) while HD 215441 is the most strongly magnetic CP star in the sky. Only in the helium rich star HD 184927 is there no obvious absorption at 1400, consistent with the suggestion that the helium rich stars are not Si rich (Shore 1978, thesis; Shore and Adelman 1981, 23rd Liege Symp., p.426).

There does not appear, at present, any obvious correlation between the 1400 feature and anything peculiar about the star other than the Si enhancement -- not magnetic field, T_{eff}, V sin i or helium anomaly. It does appear that to produce the feature, "a little dab'll do ya" but that not a great deal else can be learned quantitatively about the star from the presence of this feature.

We wish to thank Dr. W.P. Bidelman for helpful discussions and Dr. George Sonneborn for his continuing collaboration on the age question and the Si anomaly.

REFERENCES

Artru,M.C.,Jamar,C.,Petrini,D. and Praderie,F. 1981,Astron.Ap.,96,380.
Adelman,S.J. 1981, 23rd Liege Symp., p.13.
Jamar,C.,Macau-Hercot,D. and Praderie,F. 1978, Astron.Ap., 63, 155.
Joncas,G. and Borra,E.F. 1981,Astron.Ap., 94, 134.
Maitzen,H.M. 1976, Astron.Ap., 51, 255.
———————. 1980, Astron.Ap., 84, L9.

Table I

Sample Stars

Star(HD)	B-V	U-B	V sini (km/s)	B_{eff}(r.m.s.)	W(1400)(Å)	$\overline{\Delta a}$ (1)
21699	-0.10	-0.57	40	730 G	16.3± 1.2	-----
34452	-0.19	-0.55	60	430	35.3± 1.7	-----
35456	-0.05	-0.49	--	615	12.7	0.028
36313	-0.07	-0.40	--	915	12.7	0.020
36526	-0.11	-0.60	--	2130	11.9	0.006
36668	-0.12	-0.46	--	900	19.7	0.023
37140	+0.09	-0.41	≤25	450	12.7	0.002
131120	-0.16	-0.72	90	110:	18.6	-----
142301	-0.06	-0.58	50	2100	16.6	-----
144334	-0.08	-0.55	45	780	16.5±1.0	-----
175362	-0.14	-0.71	28	3920	15.7±0.6	-----
215441	+0.03	-0.51	≤5	16900	20.2	-----

Note:(1) Data from Joncas and Borra (1981). Magnetic fields for the Ori stars are from Borra (1981,Ap.J.(Letters), 249, L39).

Figure 1. Low dispersion SWP continuua of helium peculiar stars.

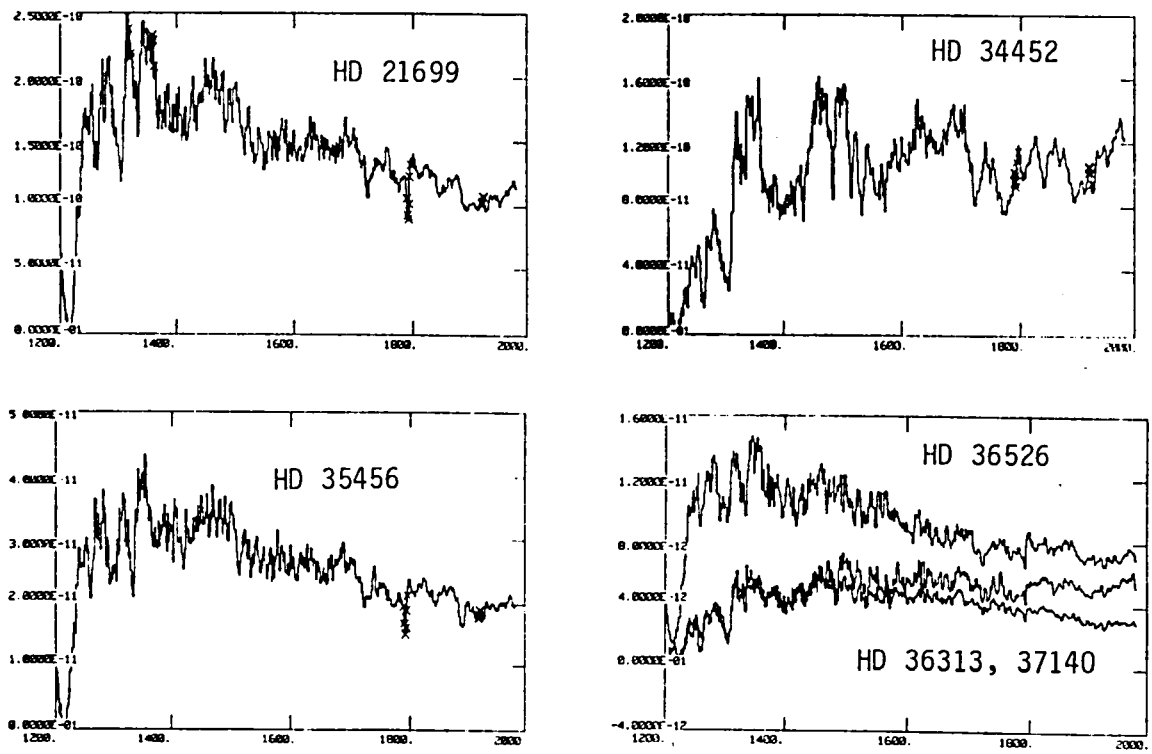

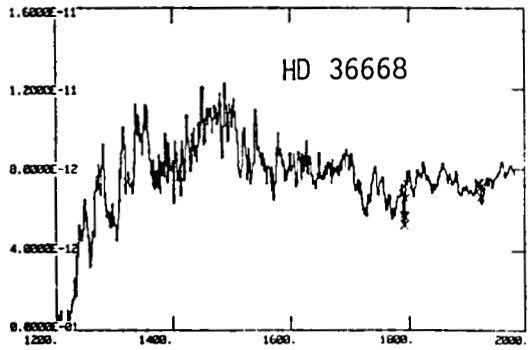
HD 36668

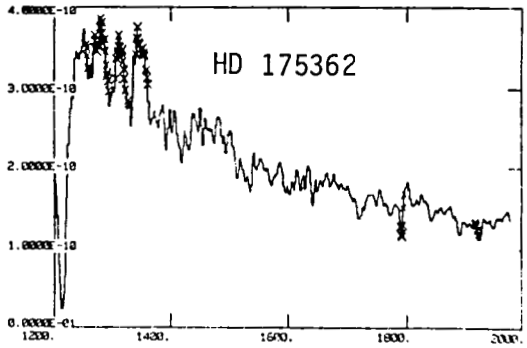
HD 175362

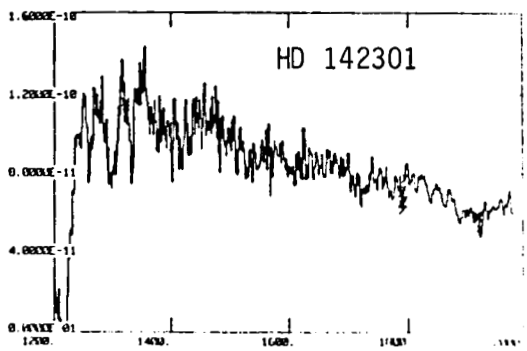
HD 142301

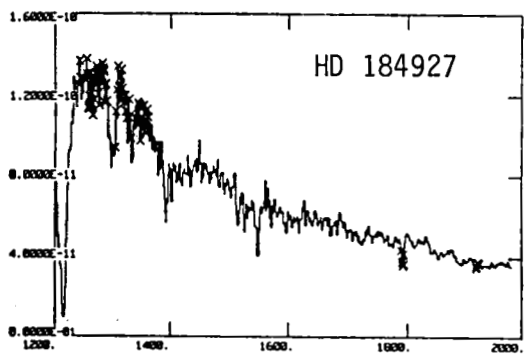
HD 184927

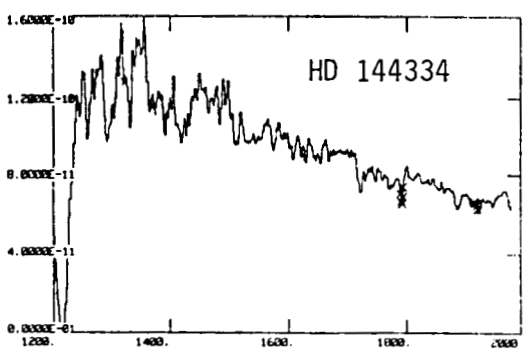
HD 144334

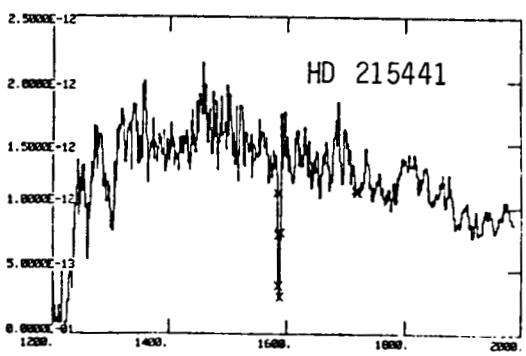
HD 215441

SOLAR SYSTEM

THE SPATIAL DEPENDENCE OF THE JOVIAN AURORAL EMISSIONS

T. E. Skinner, H. W. Moos, and G. E. Ballester

Physics Department, The Johns Hopkins University
Baltimore, Maryland 21218

Auroral emissions from the northern hemisphere of Jupiter have previously been monitored using the IUE observatory during a one year period beginning in 1981 January (Durrance, Feldman, and Moos 1982; Skinner, et al. 1984). The intensity of the north pole emissions shows a marked variation with central meridian longitude λCML (System III [1965] coordinates), rising to a maximum near λCML = 185° and then falling again toward zero. Changes in auroral zone orientation with respect to the instrument field of view as the planet rotates could account for much of the observed variation. However, the spatial resolution in the large aperture of the short-wavelength spectrograph (∿5") is not sufficient to resolve the actual auroral zone, so that the amount of the auroral oval contained within the aperture as a function of λCML cannot be explicitly determined from the observations.

In order to distinguish between the effects of the emission geometry and changes in auroral intensity, Skinner et al. (1984) modeled the observations on the basis of the geometry and the intensity of the emissions using two auroral zones taken from the O_4 plus current sheet model of Connerney, Acuna, and Ness (1981). The observed variation in flux with λCML was shown to be inconsistent with a uniform brightness as a function of longitude in either the torus or the magnetotail auroral zones. The data was best fitted by confining the emissions to the region of the torus auroral zone defined by $120° \lesssim \lambda III \lesssim 240°$. A spatially nonuniform emission from the magnetotail auroral zone could also be used to fit the data, but the longitudinal variations were more complex. In addition, the model implied variations by a factor of 4 in the brightness of the enhanced region over the course of the observations, with variations by a factor of 1.5 over a time as short as one rotation of the planet.

Preliminary results of 3 observations of the south pole aurora show a definite variation in the emission flux with λCML. The observations were performed on 1983 July 6, 1984 March 21, and 1984 March 23. The maximum flux of the observations varies by an overall factor of 2, with a factor of ∿1.5° variation within a 2 day period, again similar to the temporal variations seen in the intensity of the aurorae at the north pole.

Since the auroral zones in the southern hemisphere are more nearly centered about the planet's rotational axis (see, for example, Connerney, Acuna, and Ness 1981), the model fluxes produced by a uniform emission from either the torus or magnetotail auroral zones at the south pole show very little variation with λCML. Thus, the case for some kind of longitudinally asymmetric emission is even more dramatic than at the north pole. It appears that the emissions are enhanced within the longitude sector $60° \gtrsim \lambda III \gtrsim 245°$ of the torus auroral zone. By adjusting both the longitudinal extent of the enhanced region and the model emission rate for the different observations, we are able to obtain a very good fit to the data. At this time, we still can not rule out a similar asymmetric emission from the magnetotail auroral zone. However, there is now evidence for a longitudinal asymmetry in both the north and south pole auroral emissions. In order to compare the morphology of the north and south pole aurorae, continued monitoring of the south pole aurora is needed to increase the data base and allow a more accurate determination of the characteristic temporal variations in the brightness of the south pole aurorae.

The assistance of the IUE Observatory staff in the acquisition and reduction of the satellite data is gratefully acknowledged. This work was supported by NASA grant NSG 5393.

References

Connerney, J.E.P., Acuna, M.H., and Ness, N.F. 1981, J. Geophys. Res., 86, 8370.

Durrance, S.T., Feldman, P.D., and Moos, H.W. 1982, Geophys. Res. Letters, 9, 652.

Skinner, T.E., Durrance, S.T., Feldman, P.D., and Moos, H.W. 1984, Ap. J., 278, 411.

THE JOVIAN STRATOSPHERE IN THE ULTRAVIOLET

Richard Wagener and John Caldwell

Department of Earth and Space Science
Stony Brook, New York 11794

Abstract

The center-of-disk reflectivity of Jupiter in the wavelength range from 1500 to 3000 Å has been computed from 31 low dispersion IUE spectra taken during solar maximum in 1979/80. The spectra were normalized to a reflectivity scale with the improved solar spectrum of July, 1980 by Mount et al. (JGR **86**, 9193, 1981 and JGR 88, 5403, 1983). Consideration of wavelength shifts between different IUE spectra and within the solar spectrum improved the apparent noise, especially longward of 2000 Å. Six out of seven ammonia bands between 1900 and 2200 Å have been detected. A vertically inhomogeneous radiative transfer program is used to compute model reflectivities for various stratospheric compositions. In addition to ammonia, the abundance of acetylene is also well determined because these molecules show narrow absorption bands in the ultraviolet. The abundances of the other molecules in our models (C_3H_4, C_2H_4, C_4H_2, C_2H_6, C_3H_6) are very uncertain and therefore are quoted only as upper limits. The best model fit is consistent with infrared observations by Voyager IRIS (Kunde et al., Ap.J. 263, 443, 1982).

This work has been supported by NASA grant NAG 5275 in Stony Brook.

LONG TERM VARIABILITY OF THE IO TORUS

H.W. Moos, T.E. Skinner, P.D. Feldman, and S.T. Durrance
Physics Department, The Johns Hopkins University

and

J.L. Bertaux
Service d'Aéronomie du CNRS, Verrierès-le-Buisson, France

and

M.C. Festou
Institut d'Astrophysique de Paris, Paris, France

The ultraviolet emissions from the Io plasma torus have been monitored by IUE since the Voyager 1 encounter in early 1979. Recently, it has been shown that the prominent feature near 1729 Å is definitely due to S^{++}, eliminating the problem with Lyα contamination of SIII 1199 (Moos et al, 1983). Thus, it is now possible to estimate the long term variation of the S^{+}, S^{++}, and (to a lesser extent) S^{+++} concentrations in the high electron temperature "core" plasma of the torus. The effects of the viewing geometry and the rocking of the torus about the centrifugal axis were modeled using the plasma density and electron temperature profiles derived by Smythe and Shemansky (1983) from Voyager data, the assumption that an ion mixing ratio was the same throughout the torus, and local charge neutrality. This procedure was checked by using a crude spatial scan consisting of three five-hour observations obtained back to back at elongations of 5.0, 6.0, and 7.0 R_J. The S^{+}, and S^{++} (and a smaller number of S^{+++}) concentrations are presented for thirteen observations from 1979 March 1 to 1984 March 21. Significant variations in the plasma density have clearly occurred. A more detailed description will be submitted for publication at a later date. The assistance of the IUE Observatory staff in the acquisition and reduction of this data is gratefully acknowledged. This research was supported by NASA grant NSG 5393.

References

Moos, H.W., Durrance, S.T., Skinner, T.E., Feldman, P.D., Bertaux, J.L., and Festou, M.C., 1983, Ap. J., 275, L19.

Smyth, W.H., and Shemansky, D.E., 1983, Ap. J., 271, 865.

ULTRAVIOLET OBSERVATIONS OF URANUS AND NEPTUNE BELOW 3000 Å

John Caldwell, Richard Wagener and Tobias Owen

Department of Earth and Space Science
State University of New York
Stony Brook, New York 11794, USA

Michel Combes and Therese Encrenaz

Observatoire de Paris
Meudon 92190, France

Abstract

From 2000 to 3000 Å, both Uranus and Neptune have albedos that are about two times higher than Jupiter or Saturn's, implying that the outer giants have stratospheres that are relatively free of aerosol absorption. Uncertainties in the absolute calibration procedure allow discrepancies of order 15% between conservative models and the observations. A small amount of aerosol absorption is therefore possible. Below 2000 Å the derived albedo is highly dependent on the solar spectrum source used in the data reduction. The most recent result for Uranus is consistent with a secular change in C_2H_2 mixing ratio from $\sim 3 \cdot 10^{-8}$ in 1980 to $\leq 10^{-9}$ in 1983. These values are ~2 orders of magnitude less than the mixing ratios of this gas on Saturn, and comparable to the amount on Jupiter.

The work has been supported in part by NASA grant NSG 5250 at Stony Brook.

IMPLICATIONS OF THE PRESENCE OF S_2 IN COMETARY ICE

P. D. Feldman
Physics Department, The Johns Hopkins University

and

M. F. A'Hearn
Astronomy Program, University of Maryland

The discovery, by IUE, of the sulphur dimer, S_2, in the near nucleus region of comet IRAS-Araki-Alcock (1983d) during the very close approach of the comet to Earth in May 1983 provides us with a new diagnostic tool for studying cometary structure and evolution. The IUE data indicate that the photochemical lifetime of S_2 is very short (of the order of 500 seconds) and that the S_2 is most likely a parent molecule coming directly from the nucleus rather than being produced in the gas phase from other parent molecules (A'Hearn et al. 1983). Thus, observations of S_2 can be used to monitor short term fluctuations in cometary activity, and in fact the IUE observations, spaced over a period of ~ 32 hours, showed a marked decrease in S_2 surface brightness (a factor of 20) over this period. The other ultraviolet emissions also decreased during this time but only by about a factor of 4. The ultraviolet data, coupled with the FES counts data obtained in the course of the tracking procedure debeloped by T. B. Ake, lead to a lower limit of ~ 28 hours for the rotation period of the comet (Feldman et al. 1984). This result is based on the assumption of a single localized region of volatile ices containing S_2 on the surface of the cometary nucleus.

The presence of S_2 in the cometary ice also implies that significant irradiation of the cometary material must have occurred in its early evolutionary history. However, since the irradiation would have affected only the outer ~ 1 meter of the cometary ice and since this much material is lost in a single perihelion passage of the comet (period ~ 10^3 yr), it is unlikely that irradiation which has occurred since the formation of the comets is significant. More likely is the possibility of strong irradiation of "cometesimals" during the pre-solar nebula phase in the interstellar medium. A fuller discussion of this problem is given by A'Hearn and Feldman (1984).

The success of the IUE in observing comet IRAS-Araki-Alcock is due to the tireless efforts of the IUE Observatory staff for which we are extremely thankful. This work was supported by NASA grants NSG-5393 to the Johns Hopkins University and NAG 5-279 to the University of Maryland

REFERENCES

A'Hearn, M. F., and Feldman, P. D., 1984, in Proceedings of NATO Advanced Workshop "Ices in the Solar System", in press.

A'Hearn, M. F., Feldman, P. D. and Schleicher, D. G. 1983, Ap. J. (Letters), 274, L99.

Feldman, P. D., A'Hearn, M. F. and Millis, R. L. 1984, Ap. J., 282, in press.

SPECTRAL CLASSIFICATION

IUE LOW-DISPERSION REFERENCE ATLAS

A. Heck[1,2], D. Egret[2], M. Jaschek[2], C. Jaschek[2]

[1] - IUE Observatory, Astronomy Division, ESA, Madrid, Spain
[2] - Observatoire Astronomique, Strasbourg, France

ABSTRACT

This atlas, published by ESA and essentially devoted to normal stars, presents 229 graphic spectra together with the corresponding fluxes and an ultraviolet spectral type. The preparation of this publication has indeed confirmed that MK classifications cannot simply be transferred to the ultraviolet range. A set of transparencies are illustrating the reference sequences constructed from the ultraviolet data. A magnetic-tape copy of all the spectra pertaining to this atlas is available from the Stellar Data Center in Strasbourg.

INTRODUCTION

The programme of ultraviolet spectral classification was initiated in 1978 with the specific goal of building up a set a representative IUE low-disersion spectra from which a classification scheme could be constructed in the UV. This undertaking was strongly supported by the participants to the VILSPA workshop on "UV Stellar Classification" held in October 1981 who stressed in their final resolution its basic importance not only for stellar and extragalactic astronomy, but also for the preparation of spectroscopic programmes on future space missions.

From a previous study in the ultraviolet range based on data from the S2/68 experiment on board the ESRO/ESA's TD1 satellite (see i.a. Cucchiaro et al., 1978 and the references quoted therein), it was found that about 90% of the spectra fit a two-dimensional frame whose parameters are correlated with the temperature and luminosity, and which parallels that of the MK classification in the visible range (Jaschek & Jaschek, 1982). The remaining 10% of the stars did not fit in such a scheme, in the sense that they were abnormal in one wevalength region and normal in the other.

Similar conclusions have been reached with the present work, namely that one cannot simply transfer MK spectral classifications to the ultraviolet, the order in the MK system being not identical to that which can be established in the ultraviolet spectral range.

THE MATERIAL

Compared with the previous work on TD1 data, the present programme represents a significant improvement bacause the spectra cover a larger wavelength range at a higher resolution. Moreover IUE has observed a much broader range of stellar types than TD1 and has also reached significantly fainter magnitudes.

Table 1 : Designations used for the UV spectral classifications

Designation	Name	Rough MK equivalent
d	dwarf	V
g-	subgiant	IV
g	giant	III
g+	bright giant	II
s-	supergiant	Ib
s+	bright supergiant	Ia

Table 2 : Stars appearing in the atlas

Identifier	IUE Sp.T.	MK Sp.T.	Identifier	IUE Sp.T.	MK Sp.T.
HD 698	B3 pec	B5 III e	HD 36673	s FO	FO Ib
2905	s+B1	B1 Ia	36824	d B2.5	B2.5 V
3360	d+B1.5	B2 IV	36879	O7 p	O7.5 III
4142	d B4	B5 V SB	37042	d BO.5	BO.5 V
4727	d+B4	B5 V SB	37061	d+BO.5	BO.5 V
5448	d A4	A5 V	37129	d+B2.5	B2.5 Vs
6619	d A5	A1 V, Am	37367	d+B2.5	B2 IV-V
8890	s F8	F7:Ib-II SB,V	37744	d B1.5	B1.5 V
9132	d A1	A1 V	37776	d B2	B2 V
10250	d B9	B9 V	37903	d B1.5	B1.5 V
10307	d G1.5	G1.5 V	38206	d AO	AO Vs
11031	d A2	A3 V	38666	d O9	O9 V
11636	d A5	A5 V SB, A5m	40136	d F2	F2 V
12301	s-B8	B8 Ib	40893	g O9.5	BO IV:
12311	g FO	FO V	40932	d A4	Am SB, VB
15570	s O4	O4 If	41117	s+B2	B2 Ia
15629	d O5	O5 V ((f))	42690	d B2	B2 V
17138	d A3	A3 V	46056	d O8	O8 V
20346	g:A2	A2 IV	46149	d+O8	O8.5 V
20630	d G5	G5 V var	46150	d O5	O5 V ((f))
20902	s F5	F5 Ib	46202	d+O9	O9 V
21071	d B7	B7 V	46223	d O4	O4 V ((f))
21291	s B9	B9 Ia	46769	d B6	B8 Ib
21389	s AO	AO Ia SB:	47054	d B8	B8 V
22049	d K	K2 V	47129	g+O7	O7.5 III (f)
22928	g B5	B5 III SB	47240	s+B1	B1 Ib
23302	g B6	B6 III	47432	s+O9	O9.5 I
23324	d B8	B8 V	47755	d B3	B9
23408	g B6	B7 III	48250	d A2	A3 V
23432	d B8	B8 V	48329	s G8	G8 Ib var
23480	d B6	B6 IV (e)	48434	BO.5:	BO III
23630	g B7	B7 III (e)	50138	B9 pec	B6 III
23753	g B8	B8 Vn	51283	g B2	B2 III
23850	g B8	B8 III	51309	g+B3	B3 II
25340	d B5	B5 V	52266	g O9	O9.5 V
27176	d FO	FO V	52721	d B2:	B2 Vne
27290	d F1	F4 III	52918	d+B1	B1.5 III
27396	d B4	B4 IV	52942	d B1.5	B3n
27962	d A2	A2 IV	53138	s+B3	B3 Iab
28319	g A7	A7 III	53367	g BO	BO III
29335	d B6	B7 V	53974	g BO.5	BO.5 III
29365	d B8	B8 V	54306	d B1	B2 V
29646	d A1	A2 V	54439	d:B1.5	B2 IIIn
30614	s+O9	O9.5 Ia	55857	d BO.5	BO.5 V
31295	d A2 p	AO V lambda Boo	57061	g+O9.5	O9 II
31726	d B2	B1 V	57682	d O9.5	O9 V
32630	d B3	B3 V	58142	d+A1	A1 V
34078	d+O9.5	O9.5 V	58350	s+B5	B5 Ia
34759	d B4	B3 V	58946	d F2	F2-3 Vas
34816	d BO.5	BO.5 IV	59612	s A5	A5 Ib
36512	d BO	BO V	60753	d B3	B3 V
36629	d B2	B2.5 IV	61429	d B7	B8 IV

Identifier	IUE Sp.T.	MK Sp.T.	Identifier	IUE Sp.T.	MK Sp.T.
HD 61831	d B2.5	B2.5 V	HD 152247	g+09	09 II
63922	d+B0	B0 III	152248	s 07	07 Ib: (f) p
64760	s-B0.5	B0.5 Ib	152249	s-09	09 Ib
64802	d B2.5	B2.5 IV	152667	s+B0.5	B0.5 Ia
65456	d A5	A2 V var	156208	g A1	A2 V
74180	s F2	F3 Ia	159561	g A5	A5 III
74273	d B1.5	B1.5 V	159876	F2 p	Delta Del
75821	g B0	B0 III	161817	d:A3 p	A2 VI
76644	d A7	A7 IV	162374	d B6	B6 V
76756	d:A5	A5m	162978	g+07	07.5 II ((f))
77370	d F4	F3 V	163181	s B1	B1 Ia pe
77581	s+B0.5	B0.5 Ia	164353	s-B5	B5 Ib
78362	g F3	F3 III-IVm, vs	164402	s-B0	B0 Ib
79439	d A5	A5 V	164794	d 03	04:V ((f))
79447	d+B3	B3 III	165024	g+B1	B2 Ib
80081	d A2	A1 V	165052	d 07	06.5 V
83183	g+B6	B5 II	166205	d A2	A1 Vn
83754	d B5	B5 V	166937	s+B8	B8 Ia
85504	d+A0	A0 Vs	167264	s+B0	B0 Ia
86360	d+B9	B9 IV	167756	s-B0.5	B0.5 Ia
86440	s-B5	B5 Ib	167838	s+B5	B5 Ia
87696	d A7	A7 V	168076	d 04	04 f
87737	s A0	A0 Ib	168905	d B2.5	B2.5 Vn
87901	d B7	B7 V	170153	d F6	F8 Vb, vw
89025	g F2	F0 III	173502	g B1	B1 II
90589	d F3	F2 IV	173667	d F6	F6 V
90772	s A5	A6 Ia	177724	d A0	A0 Vn
90994	d B6	B6 V	183143	s+B7	B7 Ia
91316	s-B1	B1 Ib SB	183914	d B8	B8 Ve
92741	g+B1	B1 II	188209	s-09.5	09.5 Iab
93028	d+09.5	09 V	189849	g A5	A4 III
93130	g 05	06 III (f)	190603	s B2	B1.5 Ia
93204	d:03	05 V	190993	d B2.5	B3 V
93205	d 03	03 V	192281	d 04	05 V ((f)) p
93250	d 03	03 V ((f))	192685	d B2.5	B3 V
93403	g 05	05 III (f)	193682	g:04	05
95418	d A1	A1 V	197345	s A2	A2 Ia
99028	g F3	F3 III SB	197392	g B8	B8 II-III
100600	d B2.5	B4 V	198478	s+B3	B3 Ia
102870	d F9	F9 V	199478	s+B8	B8 Ia
103287	d A0	A0 V SB	200120	d B0.5	B1 Ve
104035	s A2	A3 Ib	200310	d B1	B1 Ve
107832	d+B8	B8-B9 V	201908	d B8	B8 Vn
108767	d B9	B9 Vn	202444	d:F3	F1 IV
109387	d+B7	B6 IIIp	206165	s-B2	B2 Ib
111775	d+A0	A0 IV	206901	d F4	F4 IV SB
116842	d A5	A5 V SB	207260	s+A pec	A2 Ia var
120315	d B3	B3 V SB	207330	g B2.5	B2.5 III
122879	s+B0	B0 Ia	209481	g 09	08.5 III
123008	s+09	ON9 Ia	210221	s A3	A3 Ib
125162	d A2 p	A0 p lambda Boo	210424	d B7	B7 III
128167	d F3	F3 Vvw	210839	s 05	06 If
137422	g+A2	A3 II-III	212571	d B1	B1 III-IVe
144470	d B1	B1 V	214680	d 09	09 V
147394	d B5	B5 IV	215835	d 05	05.5
147547	g F0	A9 III	216701	d A5	A7 III
148379	s+B2	B1.5 Ia	216956	d A3	A3 V
148605	d B2	B2 V	219188	g B0.5	B0.5 II-IIIn
148743	s A7	A7 Ib	HDE 242908	d 04 p	05
149212	g B9	A0 III	303308	d 03	03 V
149881	g:B0.5	B0.5 III	BD +60°497	d 07	07 V
150898	g+B0:	B0.5 Ia	+60°2522	s 07	06.5 IIIef
152233	g 05	06 III (f) p			

TD1 data have, however, the advantage of resulting from a survey and thus represent a magnitude-limited unbiased sample of bright stars whereas IUE is pointed only to preselected targets from accepted proposals, thereby providing

a highly biased sample, mainly towards earlier spectral types.

Most of the spectra we used have been retrieved from the low-dispersion IUE data base with preference given to trailed spectra. The existing gaps in the data were bridged as far as possible via observations performed during the very limited number of shifts allocated to this programme. The absolute flux calibration applied has been that of Bohlin & Holm (1980). The short- and long-wavelength spectra have been combined into a single file and the instrumental peaks around λ2200 have been truncated. The geo-coronal Ly α lines have not been removed, since some contain a stellar component.

THE ULTRAVIOLET SPECTRAL TYPE

We tried to produce natural sequences of standard stars in which the features transit smoothly from one standard to the next, staying however as far as possible within the general MK frame. This has been done essentially by a morphological approach described in the atlas introduction (see also Jaschek & Jaschek, 1984) and confirmed by an independent statistical process (Egret et al., 1984). To avoid confusion with the MK system, a set of designations gathered in Table 1 have been introduced. To illustrate the differences which may appear between MK and UV spectral sequences, we are listing in Table 2 the stars catalogued in the atlas with both classifications.

THE ATLAS

The body of the atlas consists of the presentation of flux tables (left-hand pages) and the corresponding composite graphs (right-hand pages) for 229 stars, most of them exhibiting a normal behavior in the ultraviolet range. A few peculiar stars have, however, been included to illustrate typical abnormalities. Adjacent to the graphs are the identifications of the IUE images used, as well as basic astronomical data retrieved from the SIMBAD data base at the Strasbourg Stellar Data Center. A set of 34 transparencies are also provided for the most representative standard stars, to allow direct comparison with the spectra and easy illustration of the spectral sequences.

BIBLIOGRAPHY

Bohlin, R., Holm, A.V. 1980, NASA IUE Newsl. 10, 37

Cucchiaro, A., Jaschek, M., Jaschek, C. 1978, An atlas of ultraviolet stellar spectra, Liège & Strasbourg

Egret, D., Heck, A., Nobelis, Ph., Turlot, J.C. 1984, this meeting

Jaschek, M., Jaschek, C. 1982, in Ultraviolet Stellar Classification, ESA SP-182, p. 9

Jaschek, M., Jaschek, C. 1984, in MK Spectral Classification: Criteria and Applications, in press

Note: The atlas can be ordered (ref. ESA SP-1052) from the Scientific and Technical Publications Branch, ESTEC, Postbus 299, NL-2200 AG Noordwijk, The Netherlands. A magnetic-tape copy of all the spectra pertaining to the atlas is available (ref. 3083) from the Centre de Données Stellaires, Observatoire Astronomique, 11 rue de l'Université, F-67000 Strasbourg, France.

AN IUE HIGH-RESOLUTION ATLAS OF O-TYPE SPECTRA

Nolan R. Walborn
Space Telescope Science Institute

Robert J. Panek
Raytheon Company and Wellesley College

Joy N. Heckathorn
Computer Sciences Corporation

The IUE archives provide an unprecedented sample of uniform, high-quality ultraviolet stellar spectra. In particular, they contain high-resolution, SWP data for nearly 200 different O stars. We have undertaken a survey of the 1200-1900Å region in about 120 of them having homogeneous optical spectral classifications, to investigate systematically the behavior of the ultraviolet features, including the prominent stellar wind profiles, and the degree to which they correlate with the optical types. The standard extracted spectrograms have been rebinned to a constant wavelength resolution of 0.25Å and uniformly normalized (not dereddened) at the GSFC RDAF. They are then plotted at 10Å/cm, with reseau, photometric quality, and echelle order junction flags available. This resolving power of 6000 at 1500Å can be compared with that of 4000 used for similar studies in the blue-violet spectral region; it permits clear discrimination between stellar and interstellar features.

The results show a high degree of correlation between the ultraviolet features, both photospheric and stellar-wind, and the optical spectral types/luminosity classes for the majority of normal stars. For instance, the stellar wind effect in the Si IV resonance doublet displays a pronounced luminosity dependence which has not been completely described before. Other useful UV classification criteria have also been found. Hence, the normal spectra provide a well-defined, two-dimensional empirical reference frame relative to which peculiar objects can be recognized and described. For example, a group of luminosity class V stars with weak winds for their types has been isolated; there is evidence that they may be nearer to the zero-age-main-sequence than the typical class V objects. Also, a number of ON and OC spectra display marked anomalies in the ultraviolet CNO features. We are preparing a large-format spectral atlas, to be published by NASA, illustrating the full 1200-1900Å range in about 100 of these objects. The tracings will extend across two facing pages with four or five objects per montage, showing spectral-type and luminosity sequences as well as peculiar spectra. This atlas could be the forerunner of a series concerned with various types of stars, which will be an important development of the information content in the IUE archives, as well as a resource for future ultraviolet spectroscopic programs.

STATISTICAL CLASSIFICATION OF IUE LOW-DISPERSION STELLAR SPECTRA : PROGRESS REPORT

D. Egret[1], A. Heck[2], Ph. Nobelis[3] and J.-C. Turlot[3]
[1]Centre de Données Stellaires, Observatoire de Strasbourg, France
[2]Observatoire Astronomique, Strasbourg, France
[3]Centre d'Etudes Statistiques, Strasbourg, France

ABSTRACT

Statistical data analysis methods have been applied to a set of stellar low-dispersion IUE spectra. From distances between flux vectors in an adequate multivariate space, these algorithms build statistical classification schemes in the UV which can be confronted to classical morphological approaches. A progress report of the study is given.

INTRODUCTION

The ultraviolet classification programme, based on spectra collected by the IUE satellite has already been presented by Heck et al. (1982), and the "IUE Low-Dispersion Reference Atlas" is described by Heck et al. (1984) at this meeting. Independent of the essentially morphological approach used for the Atlas, we have carried out a statistical analysis of the same spectra by applying mathematical algorithms to distances between flux vectors in an adequate multivariate space. Our aim is to derive an automatic classification procedure in the UV, only through statistical methods, and to compare it with the morphological frame (ultraviolet and MK spectral classification). This work is still in progress, but we shall give in the following some of our preliminary results.

THE DATA

Details on the preparation of the material can be found in the atlas introduction, and especially on the ultraviolet spectral type (refer also to Jaschek and Jaschek, 1984). The sample at hand consists of 373 low-dispersion IUE spectra (1150 to 3200 Å) de-archived from the IUE data base for the purpose of the UV classification programme. Images of poor quality (affected by saturation, microphonic noise or other defects) have been discarded.

The available data for each star consist of a table of 410 values of the absolute flux, by 5 Å steps. To compare flux values for stars with different apparent magnitudes, a normalization of the flux scale of each spectrum is necessary. We have divided, for this reason, each spectrum by the averaged value over the complete interval, which is equivalent to normalizing the integrated value of the ultraviolet flux over the whole spectral range.

THE METHOD

The statistical methods suitable for an objective classification of the stars on the basis of their UV fluxes have already been discussed in a previous paper by Egret and Heck (1983). In this specific application, we used a statistical software package developed by Lebart and Morineau (1982): SPAD (Système Portable pour l'Analyse des Données).

The first step was a principal-component analysis establishing the number of significant dimensions of the problem and the second step a cluster analysis aggregating the stars into groups around moving centers ("nuées dynamiques"). In a third step we tried to interpret the resulting clustering especially by analysing the MK and ultraviolet classifications of the stars within each group.

THE VARIABLES

Our choice of variables was influenced by the facts that we want to be able to interpret the results astrophysically and to establish later classification criteria (this is a future step of our work). Therefore we believed it appropriate to define our variables as follows:

-a) variables linked to the "continuum": we chose the median values of the flux by intervals of 65 Å (31 variables);

-b) variables representative of the variations relatively to this continuum: we used the maximum deviations from the median flux in the same intervals, in "emission" (31 variables) and in "absorption" (31 variables).

We were thus dealing with 93 variables for each object. The corresponding matrix (373 x 93) could be treated without any difficulty by the standard programmes at hand.

THE RESULTS

The first factor of the principal-component analysis is strongly correlated to the temperature, whereas the luminosity effect and a significant contribution of the reddening are carried by the second factor. The cumulative contribution of the first three factors to the variance is 87%.

The cluster analysis aggregated 20 classes of stars on the basis of their mutual distance in the multivariate space defined by the first twenty factors of the principal-component analysis. The distribution of the classes in the plane of the first two factors is given in Figure 1. Each class has been named according to the ultraviolet classification of the stars closest to the barycenter of the class.

The distribution of the ultraviolet classification within each class is quite homogeneous, but one class still covers several decimal subclasses: for instance the group named B8 contains B7, B8 and B9-type stars. The same is true for luminosity classes. We have to consider a larger number of classes

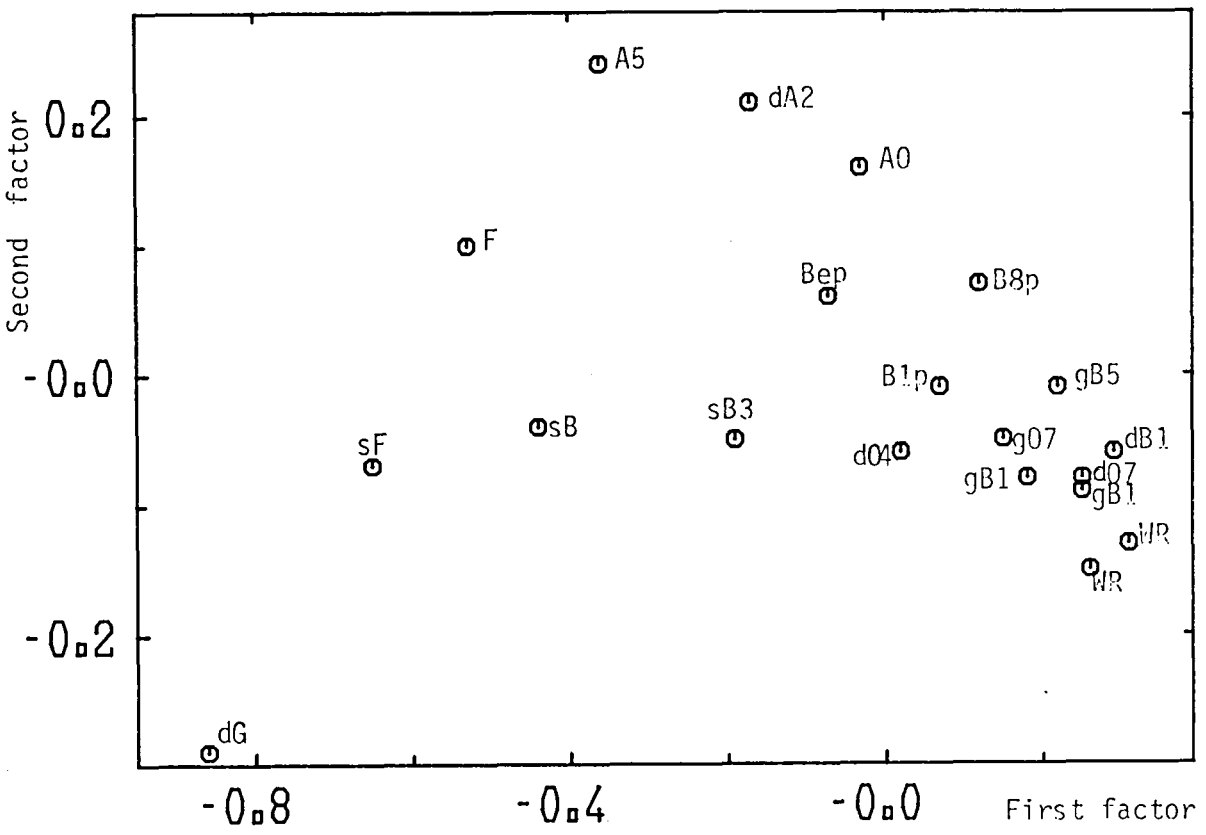

Figure 1 : Distribution of the classes in the plane of the first two factors.

if we want to reproduce a classification scheme consistent with the MK (or ultraviolet) subdivisions. It appears however that the number of objects (373 stars, including a number of peculiar stars) is too small to obtain directly a more satisfactory result. We intend to refine the methodology in a near future (especially by introducing a weight for the most discriminant variables, linked for instance to characteristic features) in order to build an automatic procedure applicable to new sets of spectra.

CONCLUSION

We showed it is feasible to use purely statistical methods in order to classify low-dispersion IUE spectra into classes consistent with the ultraviolet spectral types introduced by Jaschek and Jaschek (1984). Nevertheless, due to the relatively small number of objects presently available, the classification scheme is still less precise that the UV or MK systems. We hope to improve this precision by introducing new refinements in the methodology and by increasing the sample.

REFERENCES

Egret, D., Heck, A. : 1983, in *Statistical Methods in Astronomy*, ESA Sp-201, p. 59
Heck, A. et al. : 1982, in *Third European IUE Conference*, ESA SP-176, p. 327
Heck, A., Egret, D., Jaschek, M., Jaschek, C. : 1984, *this meeting*
Jaschek, M., Jaschek, C. : 1984, in *MK Spectral Classification: Criteria and Applications*, in press
Lebart, L., Morineau, A. : 1982, *Système Portable pour l'Analyse des Données*, C.E.S.I.A., Paris

IUE OBSERVATIONS OF FAINT STANDARD STARS FOR CALIBRATION OF THE SPACE TELESCOPE

A. W. Harris*, C. Gry, P. Benvenuti+, A. Cassatella, R. Gilmozzi, B.J.M. Hassall, A. Talavera and W. Wamsteker.

E.S.A. Satellite Tracking Station, Apartado 54065, Madrid, Spain

ABSTRACT

Many scientific programmes envisaged for the ST will require spectrophotometric observations with precise determination of absolute flux as a function of wavelength. However, the occurate calibration of the ST instruments throughout the extremely broad (UV-IR) operational wavelength range presents a major challenge to the ST project. The aim of our programme, which is being carried out in collaboration with the ST calibration team, is to provide accurate, absolute IUE spectrophotometric data for a number of faint standard stars with magnitudes near the limit of IUE's observing capability. The scope of the programme and the precautions taken to maximise the accuracy of the IUE data are discussed.

INTRODUCTION

The full exploitation of the Space Telescope's unprecedented sensitivity will depend critically on the provision of a large set of stars with accurately determined absolute fluxes for use as a calibration sequence. The number of such stars and their spatial distribution should be such that some calibration sources are available to the ST at all times. All 5 of the ST's scientific instruments will be used in the UV down to $\lambda \simeq 1100$ Å; a wavelength range for which absolute flux data for suitable targets are seriously lacking. IUE, however, offers a unique opportunity to provide calibration data for the ST project in the wavelength range 1150-3200 A. IUE's extensive on-going calibration monitoring programme guarantees the accuracy of absolute flux measurements and enables corrections to be made for any temporal variations in sensitivity. Although the IUE calibration standards themselves are too bright for the ST, it is possible to provide absolute fluxes, tied to the IUE calibration system, for stars with brightness down to the practical limit of IUE's sensitivity ($m_v \simeq 16$).

* On secondment from The Rutherford Appleton Laboratory, Chilton, Didcot, U.K.

+ Present address: European Coordinating Facility for the Space Telescope, ESO, Garching, nr. Munich, West Germany.

PROCEDURE

Observations made from VILSPA are coordinated with those made by the ST calibration team from GSFC and scheduled contemporaneously with IUE calibration shifts wherever possible. This enables the accuracy of the IUE data to be closely monitored and facilitates corrections for any variation in IUE sensitivity. Criteria used for target selection are 1. suitability of spectrum: it should be smooth and featureless, 2. brightness: a wide range of magnitudes is required to enable checks on ST instrument linearity to be made, and 3. position: the distribution of calibration stars should be such that some are observable by the ST at any time and all ground-based observatories can observe a good selection of them. The VILSPA programme is devoted to observations of relatively faint stars ($13 < m_v < 16$) and 4 white dwarfs have been selected for the initial phase: HZ4, LB 227, LDS 235B, HZ 21. Ideally we aim to observe each star 3 times on at least two separate occasions at low dispersion, in both short-and-long-wave spectrographs. In practice, however, it may not be possible to achieve this degree of coverage for all target stars due to observing time constraints.

This observational plan will enable any variable stars to be identified and eliminated from the sequence and will allow spectra to be averaged, thereby enhancing the signal/noise ratio. By comparing the IUE data with ground-based optical data of the same stars we should be able to provide accurate absolute fluxes through the difficult IUE-optical overlap region. The final data will be presented as tables of absolute flux values for 5 Å intervals, corrected for any variability of the IUE instruments.

ACCURACY OF THE DATA

The accuracy of the IUE absolute calibration is $\lesssim$ 10% but substantial improvements on this are possible by comparing data with that of IUE standards taken at about the same time. The noise in IUE data includes a non-random component ("fixed pattern noise") which gives rise to somewhat lower signal/noise ratios after co-adding spectra than would be expected if the noise were entirely random. In Table 1 values of the signal level divided by the RMS noise are given for 3 single spectra, and an average spectrum derived from these, for each of the SWP and LWP cameras. The values were derived by dividing each spectrum by a smooth curve fitted to the continuum and then calculating the RMS deviation from unity over wavelength intervals of 200 Å. It is seen that the accuracy of the final data will depend somewhat on wavelength but by averaging 6 spectra a signal/noise ratio of > 30 would be achievable over most of the IUE spectral range.

LB 227

λ [Å]	SWP 21837	SWP 21855	SWP 21872	Mean	Average Spectrum
1400	19.2	27.0	23.3	23.2	33.3
1600	23.8	18.5	17.5	19.9	30.3
1800	27.8	34.5	25.0	29.1	38.5

HZ 4

λ [Å]	LWP 2458	LWP 2476	LWP 2489	Mean	Average Spectrum
2200	9.2	6.1	7.9	7.7	10.1
2400	13.0	12.8	12.8	12.9	18.9
2600	19.6	19.2	22.2	20.3	27.8
2800	16.7	20.4	27.8	21.6	33.3
3000	16.7	14.1	17.2	16.0	25.0

TABLE 1: Signal-to-noise ratios in 3 SWP and 3 LWP low dispersion spectra of LB 227 and HZ 4 respectively. The spectra were binned at 5 Å intervals and the S/N ratios derived over 200 Å ranges. The final column gives the S/N values derived after co-adding the 3 individual spectra in each case.

HARDWARE/EXPERIMENTS

CALIBRATIONS OF WAVELENGTHS IN SWP ECHELLE SPECTRA

M.D. De La Pena and T.R. Ayres, Department of Astrophysical, Planetary and Atmospheric Sciences and Laboratory for Atmospheric and Space Physics, University of Colorado

1.0 Introduction

In order to obtain high quality radial velocity measurements of emission lines in the far ultraviolet with IUE, it is crucial to minimize sources of random and systematic errors in the echelle wavelength scales. In addition to the systematic shift owing to the Earth and satellite motions, which is easily rectified, the major sources of velocity shifts which can affect echelle spectra are: offsets of the image from the aperture center; inaccurate laboratory wavelengths; failure of the assigned dispersion relations to faithfully model the dispersion properties of the particular image; and read beam deflections caused by accumulations of charge on saturated portions of the vidicon target. Inaccuracies of the maneuver of the stellar image into the center of the aperture can be minimized by careful observing techniques. However, the fidelity of the dispersion relations, and the related question of nonlinearities induced by read beam deflections, are a cause for concern. For example, the deflections could, in principle, induce effective nonlinearities in the derived wavelength scales which would be "hidden" by the systematic nature of the effect because only a single exposure time is used for the standard calibration spectra.

In addition to the foregoing problems, the two-minute integration time of the standard wavelength calibration images is long enough to guarantee that the strongest Pt II emission lines at the long wavelength end of the spectrum will be exceedingly overexposed. Unfortunately, the remaining Pt II emission features not only are intrinsically quite faint, with the result that their laboratory wavelengths might be less reliable than those of the stronger Pt II lines, but also the unsaturated features are rather sparsely distributed. Hence, the dispersion relations in the spectral region longward of 1800 angstroms are dependent upon Pt II features that are less than optimum.

Here we address these questions by analyzing wavelength calibration spectra secured from our own observing programs and from the IUE Archives.

2.0 Observations

Our investigation began with the analysis of six 120 second (standard) wavelength calibration spectra obtained in mid-December of 1982 in connection with a fifth year observing program. These results were presented at the "IUE - Observing at the Limit" meeting in August of 1983. Subsequently, we have supplemented the original investigation with an examination of seventeen calibration spectra spanning approximately one year (1982) taken from the Archives (PHCAL program). Further, a series of seven non-standard (18 second) wavelength images also have been secured from a sixth year observing program.

These short exposure wavecals are far less saturated longward of 1800 angstroms than the standard wavecals, and therefore provide many more features with which to undertake the registration of the wavelength scales in that region. (An additional advantage of a shorter wavecal exposure is that it need not be followed by an XPREP.)

3.0 Data Analysis

The spectra were reduced using standard software at the IUE Regional Data Analysis Facility in Boulder. The platinum lines were measured using an interactive procedure incorporating a least squares Gaussian fitting algorithm. The measurements were stored in a disk file for subsequent processing.

The two sets of line position data for the 120 second and 18 second wavecals were then analyzed by two different statistical methods. For both methods, line displacements were expressed in terms of the equivalent velocity shift (i.e. [observed wavelength minus laboratory wavelength] divided by observed wavelength times the speed of light). For Method "One", a mean velocity of each image was calculated by averaging the velocity shifts of the individual lines (108 lines [120 seconds] or 64 lines [18 seconds]). Residual velocities (line velocity minus mean image velocity) were then determined for each line. Finally, a mean residual velocity was calculated for each line by averaging over the set of wavecals. Method "Two" is similiar to Method One except lines within the same order were first averaged to provide a mean order velocity. The goal of Method One is to investigate systematic behavior of the individual line velocities from image to image; Method Two accomplishes the same goal, but for the individual orders.

4.0 Conclusions

* The standard deviation of the PHCAL wavecals (+/- 1.1 km/sec using 1982 data only) is less than was found for the 6 wavecals (+/- 3.1 km/sec) obtained on consecutive days in December of 1982 in our previous study. The latter were taken under less than optimum conditions. We conclude that it is essential to obtain nearly contemporaneous wavecals to register velocity scales of stellar high dispersion observations.

* The standard deviation of the mean residuals of the orders averaged over 1982 is 2.2 km/sec, which can be interpreted as the internal consistency of the IUE SW wavelength scales. However, the order residuals are very stable. The stability suggests that the IUE wavelength scales might be improved. In particular, if one can determine the origin of the systematic behavior of the line and order residuals, for example systematic errors in the laboratory wavelengths of the calibration lines, then the dispersion relations could be modified to account for these deviations.

This work was supported by NASA grant NAG5-199.

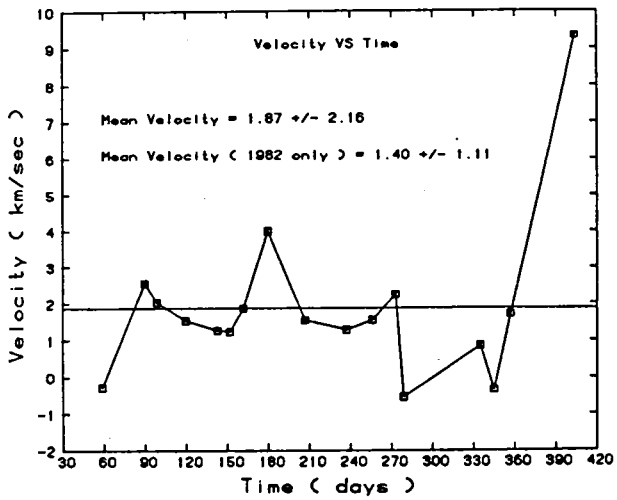

FIGURE 1A - MEAN VELOCITY OF IMAGES FOR 1982 AND EARLY 1983. TIME IS DAYS AFTER 1982.0.

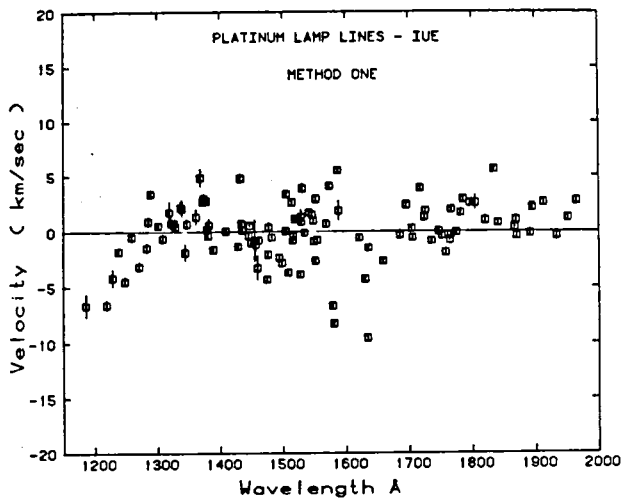

FIGURE 1B - METHOD ONE: MEAN RESIDUAL VELOCITIES (SEE TEXT) OF INDIVIDUAL LINES FOR 120 SECOND WAVECALS.

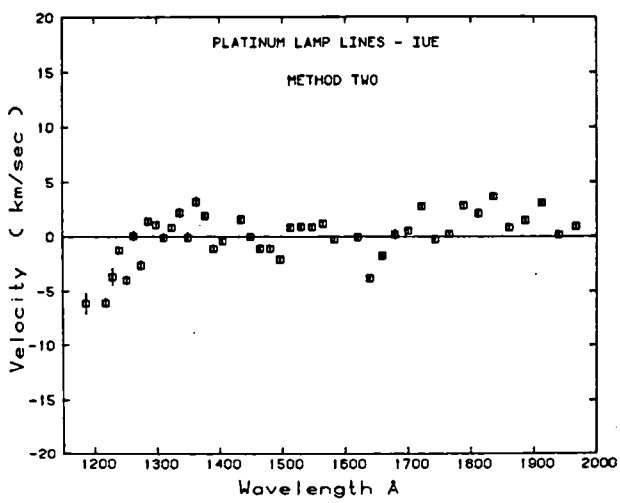

FIGURE 1C - METHOD TWO: MEAN RESIDUAL VELOCITIES (SEE TEXT) OF INDIVIDUAL ORDERS FOR 120 SECOND WAVECALS.

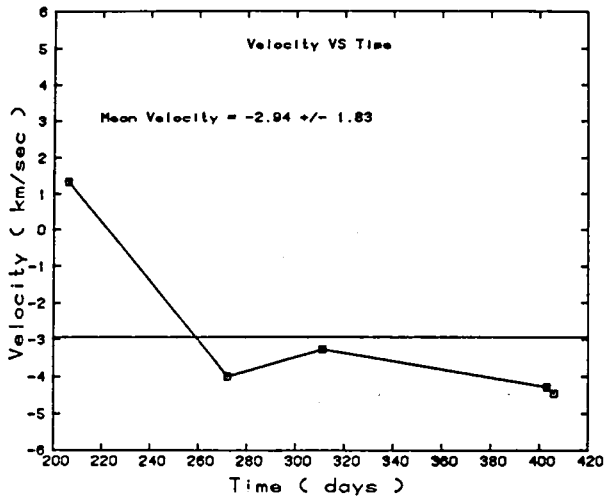

FIGURE 2A - SAME AS FIGURE 1A FOR 13 SECOND WAVECALS.

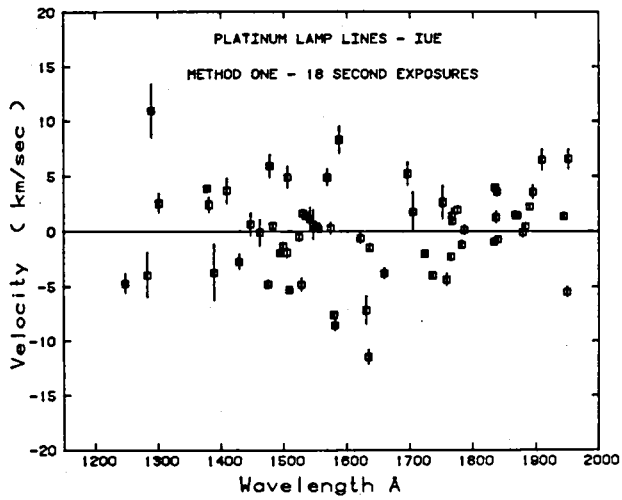

FIGURE 2B - SAME AS FIGURE 1B FOR 13 SECOND WAVECALS.

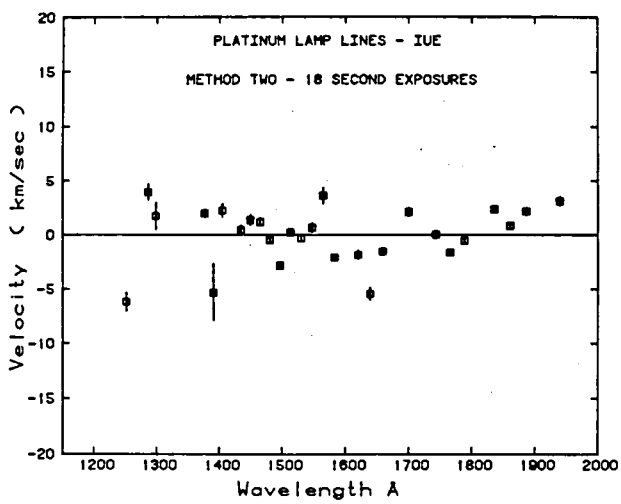

FIGURE 2C - SAME AS FIGURE 1C FOR 13 SECOND WAVECALS.

IMPROVED CONTINUUM DEFINITION IN HIGH-BACKGROUND IUE IMAGES

Richard L. Hackney and Karen R. H. Hackney
Department of Physics and Astronomy
Western Kentucky University

Yoji Kondo
Laboratory for Astronomy and Solar Physics
Goddard Space Flight Center

ABSTRACT

A technique is described for automatically filtering low-dispersion IUE images of untrailed point sources during extraction from the guest observer tape, for the purpose of reducing the effects of radiation events and "bright pixels" and obtaining improved definition of the continuum in long duration or high-background exposures. The method is based upon fitting a gaussian point-spread-function (PSF) to crosscuts of the sample orders in ESSR or LBLS files, which can be processed on a relatively small computer. Several adjacent crosscuts are binned during the fit to permit discriminating against errant samples lying directly along the dispersion line (and narrow spectral lines). The procedure results in a significant reduction of discrepancies in the fitted power-law indices for repeated exposures of faint BL Lac objects, compared with the results of previously attempted automatic filtering techniques.

INTRODUCTION

The impact of effects other than photon statistics in the determination of continuum levels in IUE images is evident in the comparison of repeated exposures of some feature-less-spectrum BL Lac objects, such as Mk 180 and Mk 501, which are believed to exhibit little intrinsic variation. With exposures of several hours accumulating background levels between 1/6 and 1/2 the gross signal exposure level, radiation effects (and non-linear effects exacerbated by the relatively high background levels) make substantial contributions to the extracted net spectra of such faint targets.

Using standard extraction procedures in the ESSR or LBLS files, the spectral indices (negative of slopes in log-log plots) of power-law fits to multiple images of Mk 180 and Mk 501 are found to range up to 17 times the average one-sigma errors indicated for the fits from the sampling statistics in the bins. Discrepancies are noticeable even between quasi-simultaneous pairs of SWP and LWR images. Figure 1 illustrates the disagreement between power-law fits to SWP only, to LWR only, and to both taken together for two pairs of Mk 501 whole-shift exposures in which the LWR and SWP components were obtained within a day of each other. After extraction and calibration to absolute fluxes (1980 May version), the data were binned and least-squares fitted with a power law, with bins individually weighted according to the inverse square of the standard deviation indicated for the bin mean from the standard deviation of the samples in the bin. No reddening correction was considered to be necessary, assuming $E(B-V) = 0.0 \pm 0.03$ for the line of sight to Mk 501 based on the work of Burstein and Heiles (1978). Moreover, a trial dereddening assuming the upper uncertainty limit, $E(B-V) = 0.03$, did not materially reduce the discrepancy among the fitted power-law indices. We infer that factors intrinsic to the observing and reduction systems cause the discrepant behavior, which if seen in only one image pair might easily be interpreted as a significant indication of source behavior, since the magnitude of the effect is several times the statistical error indicated

internally from the sampling. The images were extracted from line-by-line files using a standard summation procedure, with median filtering for background smoothing. Correction for the erroneous intensity transfer function (ITF) used for the SWP camera was made using the algorithm of Cassatella et al. (1980) with quadratic decomposition of the samples (Holm and Schiffer 1980).

PROCEDURE

Various attempts have been made to reduce effects of radiation events and noise in IUE spectra using filtering procedures that could be applied during or following the extraction from the GO tape. Practical limitations of a small-core computer prevent us from working with the large, unresampled files, and the detectability of sharp features such as "bright pixels" is reduced by the resampling performed in generating the ESSR or LBLS files with which we must work. Initially, we tried filtering the extracted image by rejecting spectral points that deviated from the local median by more than a specifiable number of local standard deviations. We next studied application of a similar procedure within each of the gross-signal "orders" during the assembly. The effects of some "bright pixels" and radiation events were reduced using this procedure, but the discrepancies in the fitted spectal indices were not significantly affected.

Our most successful automated filtering procedure is a variation of extraction procedures (e.g., Koorneef and de Boer 1979; Panek 1983) involving least-squares fitting of a gaussian PSF to sample crosscuts perpendicular to the dispersion line. Our PSF fitting was implemented in the ESSR or LBLS files using a procedure adapted from Bevington (1969), with free parameters including background base level, integrated signal in the profile (which is directly extracted), location of the center of light, and dispersion of the PSF. Within this fitting procedure, we added an optionally selectable filter which rejects samples that deviate by more than a specifiable amount (typically, 2 standard deviations) from the fitted profile and iterates the fit. Since no strong discrete features are expected in the spectra of BL Lac objects and since we seek to isolate the continuum, we pool several contiguous crosscuts to permit detection and rejection of deviant points that may occur within the gross-signal (central) orders, as illustrated in Figure 2, as well as elsewhere (see Figure 3). Only about 6 samples in each crosscut lie within the PSF, and the number of such points used to determine each fit is increased by this pooling of data from several adjacent crosscuts, for which the PSF dispersion, light center, background, and incident continuum flux should be essentially the same. The final extraction is made in a second, similar pass for the image, except that the dispersion of the PSF is forced to the (wavelength-dependent) values indicated by a linear regression of the sample dispersion estimates obtained in the initial pass with dispersion as a free parameter. Image-to-image focus variations are thus accommodated by determining the dispersion function of the PSF for each individual image.

The improvement in continuum definition that resulted with the gaussian fitting and filtering procedure revealed apparently significant image-to-image variations in the indicated LWR fluxes in the low-sensitivity region $\lambda < 2300$ A. Apparently the non-linearity of the camera response severely affects data in this region, where low flux and low sensitivity result in low net exposure compared to the high background. The behavior seems to preclude reliable independent determinations of the reddening from IUE images of faint targets with significant background levels; and, indeed, inconsistent results are frequently obtained in reddening extractions using different LWR/SWP image pairs. The erratic behavior of the LWR points with $\lambda < 2300$ A led us to omit them from our fits, resulting in further reduction of the disagreement among indices of power laws fit to different images. Omission of these points from extractions made before the gaussian fitting and filtering procedure did not significantly affect the discrepancy. For the images

previously illustrated in Figure 1, Figure 4 shows the improved inter-image agreement in power-law indices that resulted when the images were extracted using the gaussian fitting and filtering procedure and LWR points with $\lambda < 2300$ A were omitted from the power-law fits. The scatter in fitted indices, previously 17 times the average indicated standard deviation of the fit based on internal sampling statistics, was reduced to 6 times the average standard deviation. Similar results were obtained for 5 additional unpaired SWP images of Mk 501 and for a Mk 180 image pair.

CONCLUSIONS

Comparisons of the results of extractions using various procedures and filters are made in Figures 5 and 6, separately treating two different Mk 501 image pairs. In each case, filtering during or after a standard sample-summation extraction had little effect on the discrepant indices of fits to SWP only, LWR only, and the pair together. Omission of LWR points with $\lambda < 2300$ A also had little effect. Gaussian fitting without filtering gave ambiguous results. Gaussian extraction with filtering improved the agreement between fits to SWP and to both, but gave ambiguous results for the LWR fits. Finally, the further omission of LWR points with $\lambda < 2300$ A reduced the discrepancies to the minimum observed among the investigated treatments. This ultimate treatment gives relatively good agreement between the results obtained from the two different image pairs (compare final sets of points in Figures 5 and 6).

However, remaining in the data are differences in fitted indices that may be significantly larger than expected on the basis of the internal sampling statistics (assuming uncorrelated samples). Also evident in the data of Figures 1 and 4 is the artifact shape that appears in some SWP spectra, previously reported by Hackney, Hackney, and Kondo (1982). Goodness-of-fit measures for the power laws are poor (chi-square/d.o.f. ~ 3 to 7), even with the best extraction treatment (as judged by reduction of the discrepancy in indices). Relative to the internal sampling errors indicated for the bin means, the bins show significant deviations from the linear fits, with similar deviations or spectral shapes occurring systematically in different targets of various classes. These effects may be due to "fixed-pattern noise" or to residual non-linearities in the ITFs (Holm 1982), which would strongly affect the spectra of all faint sources for which the necessarily long exposures result in significant background exposures. Such effects should be evaluated quantitatively — after needed improvement of the ITF has been accomplished — in order to permit estimation of the ultimate systematic limits on the definition of source continua in IUE images of faint targets.

REFERENCES

Bevington, P. R. 1969, Data Reduction and Error Analysis for the Physical Sciences, (New York: McGraw-Hill), 235.

Burstein, D., and Heiles, C. 1978, Ap. J., 225, 40.

Cassatella, A., Holm, A., Ponz, D., and Schiffer, F. H. 1980, IUE NASA Newsletter, 8, 1.

Hackney, R. L., Hackney, K. R., and Kondo, Y. 1982, Advances in Ultraviolet Astronomy: Four Years of IUE Research, NASA CP-2238, 335.

Holm, A. V. 1982, Advances in Ultraviolet Astronomy: Four Years of IUE Research, NASA CP-2238, 339.

Holm, A. V., and Schiffer, F. H. 1980, IUE NASA Newsletter, 8, 45.

Koorneef, J., and de Boer, K. 1979, IUE NASA Newsletter, 5.

Panek, R. J. 1983, IUE NASA Newsletter, 21, 43.

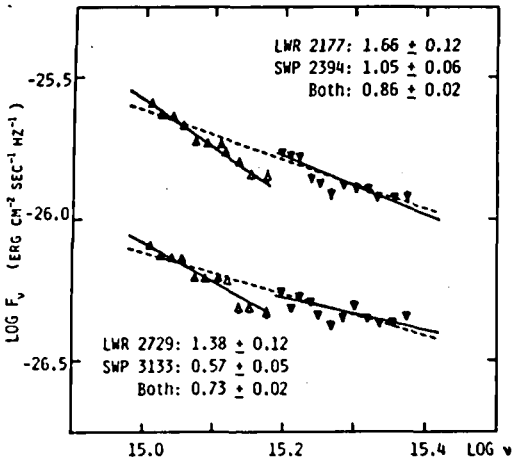

FIG. 1 -- Power-law fits for LWR bins (▲, omitting Δ), SWP bins (▼), and both sets for two MK 501 image pairs extracted by summing in ESSR files, after filtering in the orders. The lower pair is offset vertically by -0.5 unit. Indices are given with 1-sigma formal errors.

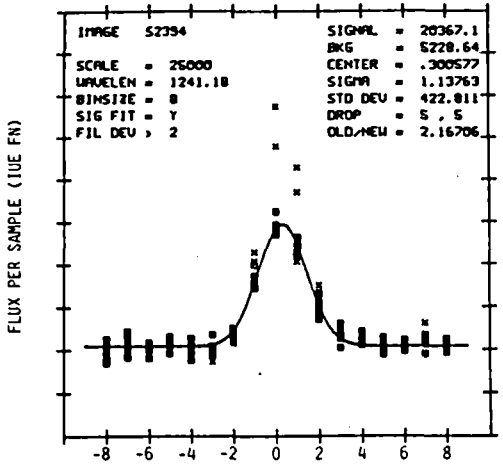

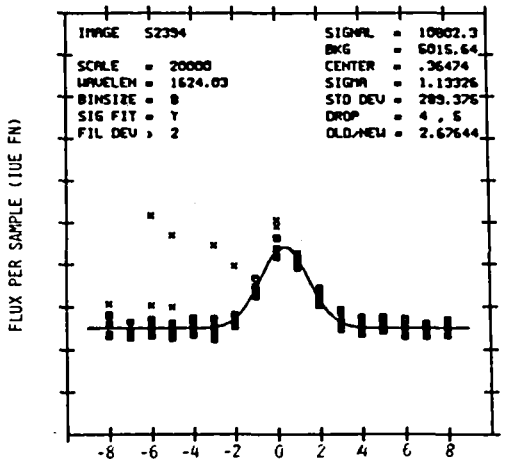

FIGS. 2 & 3 -- Flux (FN) per sample versus order number (with central order as order 0) in the ESSR file for MK 501 image SWP 2394, binning 8 adjacent crosscuts of the orders. Filtered points (x) deviate from the fitted gaussian PSF profile by more than twice the standard deviation of the remaining points. Figure 2 shows filtered points in a narrow feature occurring in orders normally summed for the gross signal. In Figure 3, non-central orders are mainly affected by the filtered points, which can be identified in plots of the orders as fixed-pattern-noise features.

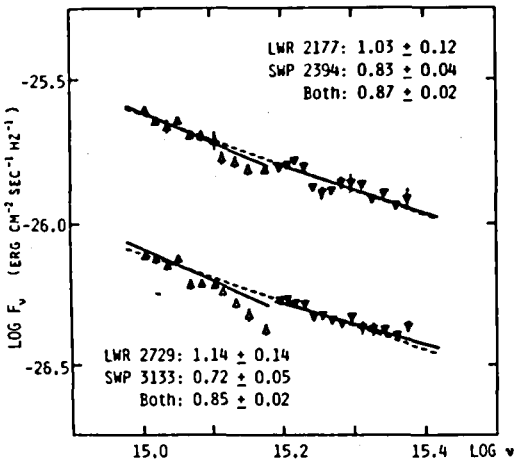

FIG. 4 -- Power-law fits for LWR bins (▲, omitting Δ), SWP bins (▼), and both sets for two MK 501 image pairs extracted by gaussian PSF fitting and filtering. The lower pair is offset vertically by -0.5 unit. Indices are given with 1-sigma formal errors.

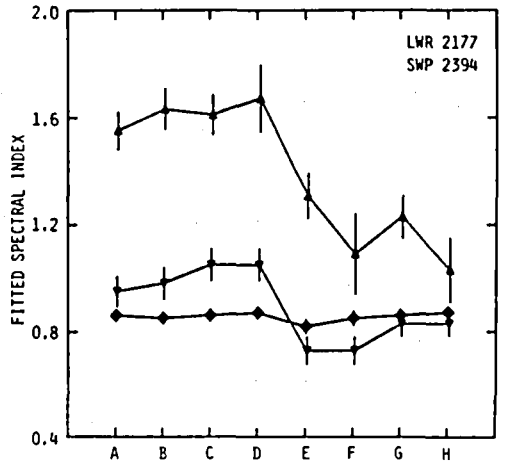

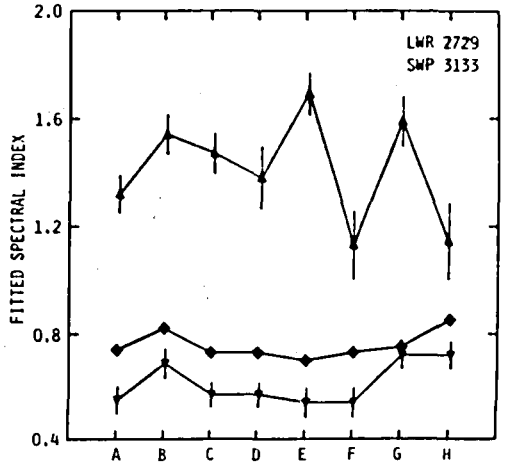

FIGS. 5 & 6 -- Indices of power-law fits to LWR only (▲), to SWP only (▼), and to both together (◆) for pairs of images LWR 2177 / SWP 2394 (Fig. 5) and LWR 2729 / SWP 3133 (Fig. 6) for various extraction methods: (A) summation and median-filtered background; (B) summation followed by filter; (C) summation of filtered orders; (D) same as C, except omitting LWR < 2300 Å; (E) gaussian fitting without filtering; (F) same as E, omitting LWR < 2300 Å; (G) gaussian fitting with (2-sigma) filtering; and (H) same as G, omitting LWR < 2300 Å. Points are connected to aid the eye.

A New Generation of Spectrometer Designs for Ultraviolet Astronomy, M. Hettrick and S. Bowyer, U.C. Berkeley, Space Sciences Laboratory, Berkeley, CA 94720. Many crucial topics in current astrophysics require high spectral resolution, $\lambda/\Delta\lambda \sim 10^3$ - several x 10^4, in the 100-1200 Å band. Recent advances in the design of grazing incidence reflection grating spectrometers capable of achieving such performance are presented. These designs are shown to constitute a new geometric class of spectrometer, in which a plane grating (or combination of plane gratings) directly intercepts, diffracts and focuses at grazing incidence the light collected by a preceding mirror. Such compact and efficient designs are made possible by discarding historical constraints on groove patterns of reflection gratings. The common feature to the resulting gratings is a smooth spatial variation in the groove spacings. Two complementary solutions are derived:

(1) Grooves which diffract within the plane of incidence, and which are spaced quadratically with the distance from focus; and
(2) Grooves which diffract conically, and which fan-out linearly with the distance from a ruling focus located behind the mirror focus.

Several variants of these solutions are analyzed through both analytic calculations and raytraces, which describes the imaging properties. Both solutions possess the unique property that the grating aberrations do not increase as the graze angle of reflection becomes small. However, due to the significantly diminished dispersive power of the conical fan solution, it is shown that the in-plane grating mount is required if resolutions in excess of approximately 1000 are needed.

A stigmatic variant of the in-plane class of solutions, one having grooves concentric about a common line, is raytraced and delivers in the extreme UV a $\lambda/\Delta\lambda \sim 10^4$ over a few percent in wavelength. In combination with a conical fan low resolution cross-disperser, it is revealed that a two-element echelle spectrometer operates at several x 10^4 over a factor of two in wavelength simultaneously. Due to its highly symmetric pattern of concentric grooves, the echelle grating can be ruled mechanically, and the resulting efficiency of this spectrometer is maximized. Such an instrument can address questions in ultraviolet astrophysics requiring high resolution.

THE MULTI-ANODE MICROCHANNEL ARRAY DETECTOR SYSTEM:

CURRENT STATUS AND FUTURE PROSPECTS

J. Gethyn Timothy
Center for Space Science and Astrophysics
Stanford University, Stanford CA 94305

ABSTRACT

The Multi-Anode Microchannel Arrays (MAMAs) are a family of photoelectric pulse-counting array detectors that are being developed specifically for use in space. MAMA detectors with formats as large as 256 x 1024 pixels are currently under evaluation in the laboratory, and a (24 x 1024)-pixel extreme-ultraviolet (EUV) MAMA detector was recently flown succesfully on a sounding rocket. A (256 x 1024)-pixel ultraviolet MAMA detector system is now being prepared for flight on the Balloon-Borne Ultraviolet Stellar Spectrograph (BUSS). The performance characteristics of this detector system are briefly described in this paper and the implications for the design of the detectors for the FUSE (now Columbus) mission are discussed.

INTRODUCTION

Two different types of MAMA detector systems have been developed; namely the discrete-anode arrays and the coincidence-anode arrays and descriptions of both systems have been presented in the literature (see, for example, Timothy and Bybee, 1983; Timothy, 1983).

The components of a coincidence-anode MAMA detector system consist of first, a tube assembly (sealed or open) containing an array of metallic anodes and a single curved-channel MCP with the appropriate photocathode material deposited directly on, or located in proximity-focus with, the front face (see Fig. 1), and, second, the associated amplifiers, discriminators, Random-Access Memory (RAM), and low- and high-voltage power supplies. In the coincidence-anode arrays, the simultaneous detection of charge pulses on two or more electrodes makes it possible to uniquely identify a very large number of pixels using only a limited number of amplifier and discriminator circuits. The coincidence-anode detector systems currently in operation are the (1 x 1024)-pixel array (64 amplifiers), the (16 x 1024)-pixel array (80 amplifiers), the (24 x 1024)-pixel array (88 amplifiers), and the (256 x 1024)-pixel array (96 amplifiers). The (256 x 1024)-pixel ultraviolet MAMA detector system, which is the prototype imaging system for space astrophysics missions, is briefly described in this paper.

THE (256 X 1024)-PIXEL MAMA DETECTOR SYSTEM

The (256 x 1024)-pixel coincidence-anode array with 25 x 25 microns^2 pixels is shown in Fig. 2. The curved-channel MCP used with this array has 12-micron-diameter channels on 15-micron centers and an active area of about 9 x 27 mm^2 (see Fig. 3). The electrodes in the array are 12.5 microns wide on 25-micron centers and the locations of charge pulses which illuminate two or

three electrodes in each axis (to allow for the spreading of the charge cloud from the MCP) are decoded by the logic circuits.

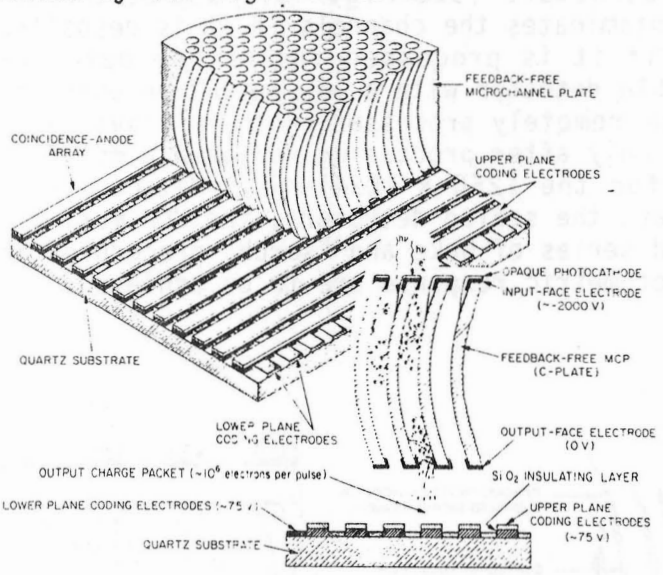

Figure 1. Schematic of coincidence-anode MAMA detector.

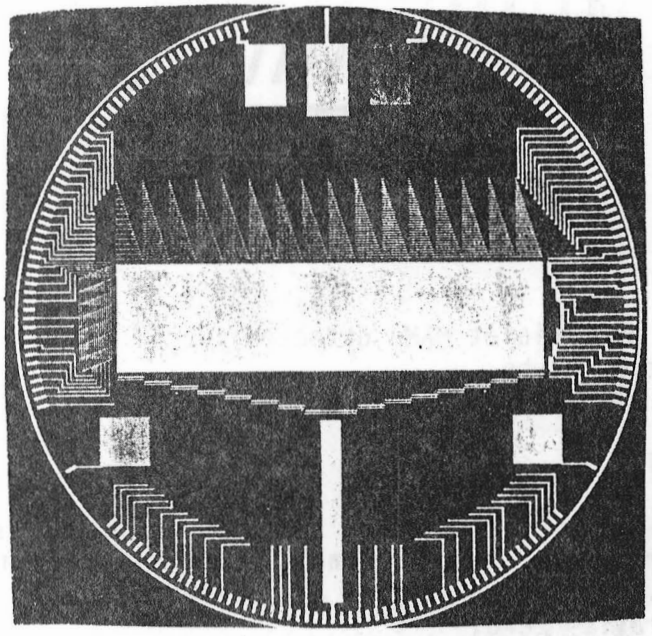

Figure 2. (256 x 1024)-pixel array.

Figure 3. Curved-channel MCP with rectangular active area.

It is now clear that two different tube structures must be used at ultraviolet wavelengths, as shown in Fig. 4. At EUV and soft x-ray wavelengths an open-structure tube is used with an opaque photocathode deposited directly on the front face of the MCP (see Fig. 4a). Funneling the channels to increase the open area increases the detection efficiency at EUV wavelengths because of the increase in the quantum efficiency when the photocathode is illuminated at high angles of incidence. On the basis of data recorded to date, CsI which is stored under high vacuum at all times, appears to be the best photocathode material

now available for the EUV spectral region. At vacuum ultraviolet wavelengths a sealed tube structure (see Fig. 4b) must be employed. The activated Cs_2Te photocathode contaminates the channels if it is deposited directly on the face of the MCP or if it is processed inside the detector tube. The result is a noisy and unstable detector with a low detective quantum efficiency. The photocathode must be remotely processed on the ultraviolet transmitting window and the tube sealed only after processing has been completed. This tube structure is being used for the (256 x 1024)-pixel detector for the BUSS. For both the open-structure and the sealed detectors, the MCP must be conditioned by a carefully controlled series of bake and "scrub" procedures if a low dark count rate and a stable photometric response are to be achieved.

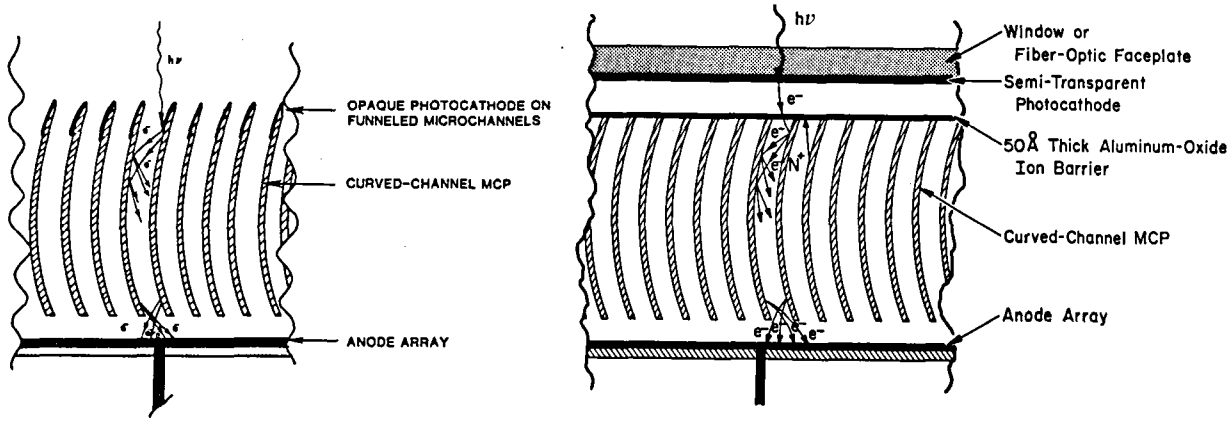

(a) (b)

Figure 4. Schematics of ultraviolet MAMA detector tubes.
a. Open-structure EUV tube.
b. Sealed vacuum ultraviolet tube.

SUMMARY OF PERFORMANCE CHARACTERISTICS

The preliminary performance characteristics of the BUSS detector system are now being determined. The first ultraviolet image recorded with this detector system is shown in Fig. 5. Key parameters are as follows:

Number of defects in anode array: Zero.
Quantum efficiency: 16.8% at 1850 A, 18.0% at 2537 A, 9.8% at 2930 A.
Modal gain: 4×10^5 electrons $pulse^{-1}$.
Spatial resolution: 1-2 pixels FWHM (>20% contrast at 16 line pairs mm^{-1}).

At present this modal gain is too low for the first generation amplifiers (threshold 1×10^5 electrons $pulse^{-1}$), causing a low detective quantum efficiency. A new tube is now being built using an MCP with longer channels to produce a higher gain for use with the BUSS flight electronics. The existing tube, however, performs with a high detective quantum efficiency with the second generation amplifiers (threshold 5×10^4 electrons $pulse^{-1}$).

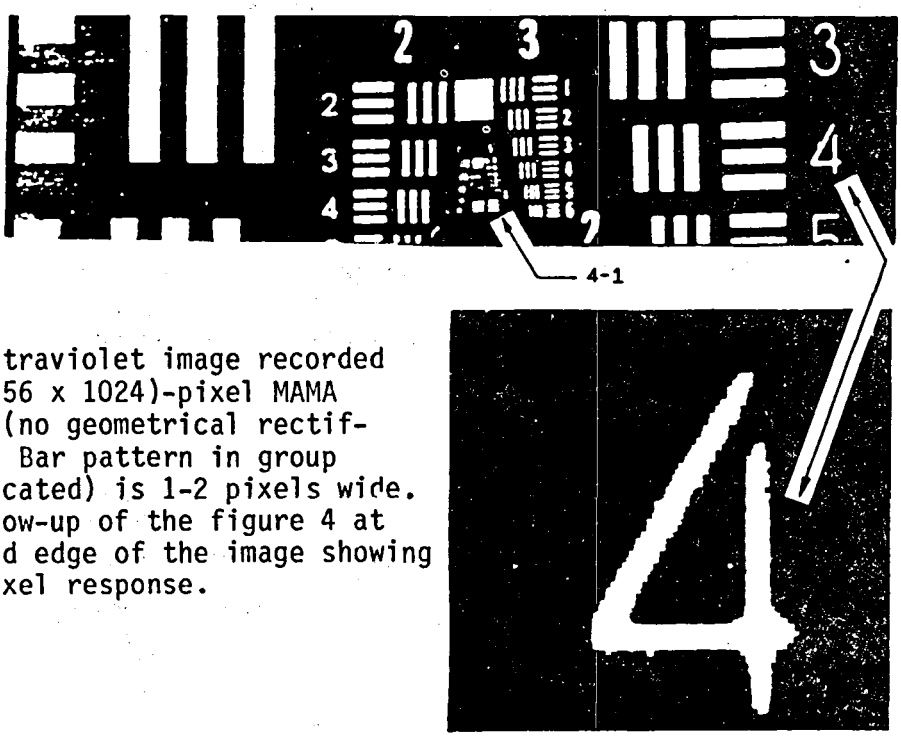

Figure 5. Upper: Ultraviolet image recorded with a (256 x 1024)-pixel MAMA detector (no geometrical rectification). Bar pattern in group 4-1 (indicated) is 1-2 pixels wide. Lower: Blow-up of the figure 4 at right hand edge of the image showing single pixel response.

FUTURE DEVELOPMENTS

It is now clear that, for a stable photometric response over the lifetimes required for space astrophysics missions, MCPs must be carefully conditioned prior to operation. The resulting modal gains, in the range from 10^5 to 10^6 electrons pulse^{-1}, set clear requirements on the design of the MCP readout system and on the sensitivity of the amplifier circuits. Accordingly, the two-fold and four-fold coincidence-detection systems used in the one- and two-dimensional MAMA arrays respectively, seem at this time to offer the optimum compromise between the number of encoded pixels and the photometric performance for high-resolution spectroscopic missions such as FUSE (now Columbus). The performance characteristics of the (256 x 1024)-pixel detector system will now be optimized and the construction of the (1024 x 1024)-pixel MAMA detector system will be initiated. The 40-mm-diameter curved-channel MCP with an active area of 27 x 27 mm^2 for this detector system is already in hand.

I am happy to acknowledge the support received from Jim Abraham at Litton Electron Tube Division with the fabrication of the sealed MAMA detector tubes and from Dick Bybee at Ball Aerospace Systems Division with the design and test of the detector system electronics. This development program is supported at Stanford University by NASA grants NAGW-551 and NAG5-622.

REFERENCES

Timothy, J. G., and R. L. Bybee, Proceedings AIAA 21st Aerospace Sciences Meeting, Reno, Nevada, January 1983.

Timothy, J. G., Publications Astron. Soc. Pacific.,95, 810, 1983.

STELLAR ULTRAVIOLET FLUX DISTRIBUTIONS IN THE 912-1200 A WAVELENGTH RANGE

George R. Carruthers, Harry M. Heckathorn, and Chet B. Opal
E. O. Hulburt Center for Space Research, Naval Research Laboratory

ABSTRACT

We have conducted a series of three sounding rocket experiments aimed at measurement of stellar ultraviolet flux distributions in the wavelength range below 1200 A, the effective limit of previous calibrations such as those of OAO-2, TD-1, and IUE. Previous sounding rocket and Voyager UVS measurements in this wavelength range were discordant with each other and with model atmosphere predictions. We describe the calibration and data reduction procedures used for our investigations, as well as preliminary results.

INTRODUCTION

The wavelength range 912-1200 A in the spectra of hot stars is not presently as well known as at longer UV wavelengths, particularly the absolute brightnesses and flux distributions of stars in this range. Although many stars have been observed by the Copernicus satellite for studies of stellar atmosphere and interstellar medium absorption lines, there have been no extensive, well-calibrated measurements of flux distributions comparable to those obtained by OAO-2 and TD-1 at longer wavelengths. Rocket experiments conducted by the Johns Hopkins University (Brune, Mount,and Feldman 1979) and the Naval Research Laboratory (Carruthers, Heckathorn, and Opal 1981), and observations with the Voyager UV spectrometers (Holberg et al., 1982) have yielded results in wide disagreement with each other and with model atmosphere predictions, such as those of Kurucz, (1979). Hence, we subsequently carried out a series of three sounding rocket investigations with particular emphasis on obtaining accurate measurements of stellar flux distributions in the 900-1200 A range.

INSTRUMENTATION AND CALIBRATIONS

Our instrument was an objective grating spectrograph (Fig. 1), based on an electrographic "Schmidt" camera operated with an annular aperture in place of the conventional refractive Schmidt corrector. The instrument field of view was 11° in diameter, and the spectral resolution was about 3 A. For the first flight, in which stars in Cygnus were observed, the optics were coated with Al + LiF for best reflectance down to 1000 A. For the two later flights, the optics were coated with osmium to extend the wavelength range to below 900 A and to provide a flatter and more stable response in the 900-1200 A range. The second flight observed stars in central Orion, whereas in the third flight the region of 15 Mon and northern Orion were observed.

For each flight, laboratory calibrations were performed in the 900-1200 A range to establish the relative spectral response of the instrument.

Calibrations were also made using the NBS SURF-II synchrotron light source facility to establish the absolute sensitivity of the instrument, and to extend the relative sensitivity curve toward longer wavelengths (providing overlap with OAO-2 and other previous measurements).

The film-recorded flight and calibration spectra were digitized on either the NRL Grant or Goddard PDS microdensitometer for computerized data reduction and analysis. Corrections were made for emulsion and/or microdensitometer induced nonlinearities and, for the first flight, for distortion caused by nonuniformity of the focusing magnetic field. (A self-shielded permanent magnet assembly of the reluctor-ring type was used in the two later flights and provided improved geometric fidelity.) The overall instrument calibration was derived by joining the calibrations based on the reduced synchrotron spectra and on the laboratory (molecular hydrogen light source) measurements in the range of overlap, 1100-1200 A. Problems encountered including the lack of a wavelength reference in the synchrotron spectra, and uncertainties in the calibration of the laboratory calibration reference detector (a windowless Channeltron).

RESULTS

The highest quality data came from the second flight, in which the instrument had the flattest spectral response. This flight also observed the largest number of stars, with more than 40 objects yielding measureable spectra. Figure 2 shows OAO-2 measurements (Code and Meade 1979) and the Voyager UVS measurements (Holberg, private communication, 1982) of the star σ Orionis (spectral type O9.5 V). Figure 3 shows our present best estimate of our instrument sensitivity vs. wavelength for the second flight, with instrumental intensity (density area of the spectrum, integrated transverse to the dispersion) vs. wavelength of a spectrum of σ Orionis. Convolution of the sensitivity vs. wavelength curve with the instrumental intensity spectrum yields the corrected spectral intensity curve, shown in the lower part of Figure 3.

In comparison to our previous observation of σ Ori, we find that the flux distribution still shows a downturn below 1050 A but not as marked as before. There is also an indication of an excess in the 1050-1150 A range. We are presently continuing efforts to refine our instrumental sensitivity vs. wavelength curve; once this is finalized it can be immediately applied to all of the stars observed in this flight. The data from the other two flights are being analyzed in an analogous fashion. It is anticipated that, once a reliable calibration of stellar fluxes in the 912-1200 A wavelength range has been obtained, that the stars we have observed can serve as reference standards for future observations with the Hopkins Ultraviolet Telescope (HUT) and the Far Ultraviolet Spectrographic Explorer (FUSE, recently renamed Columbus).

REFERENCES

Brune, W. A., Mount, G. H., and Feldman, P. D. 1979, Ap. J., 227, 884.

Carruthers, G. R., Heckathorn, H. M., and Opal, C. B. 1981, Ap. J., 243, 855.

Code, A. D. and Meade, M. R. 1979, Ap. J. Suppl., 39, 195.

Holberg, J. B., Forrester, W. T., Shemansky, D. E., and Barry, D. C. 1982, Ap. J., 257, 656.

Kurucz, R. L. 1979, Ap. J., 40, 1.

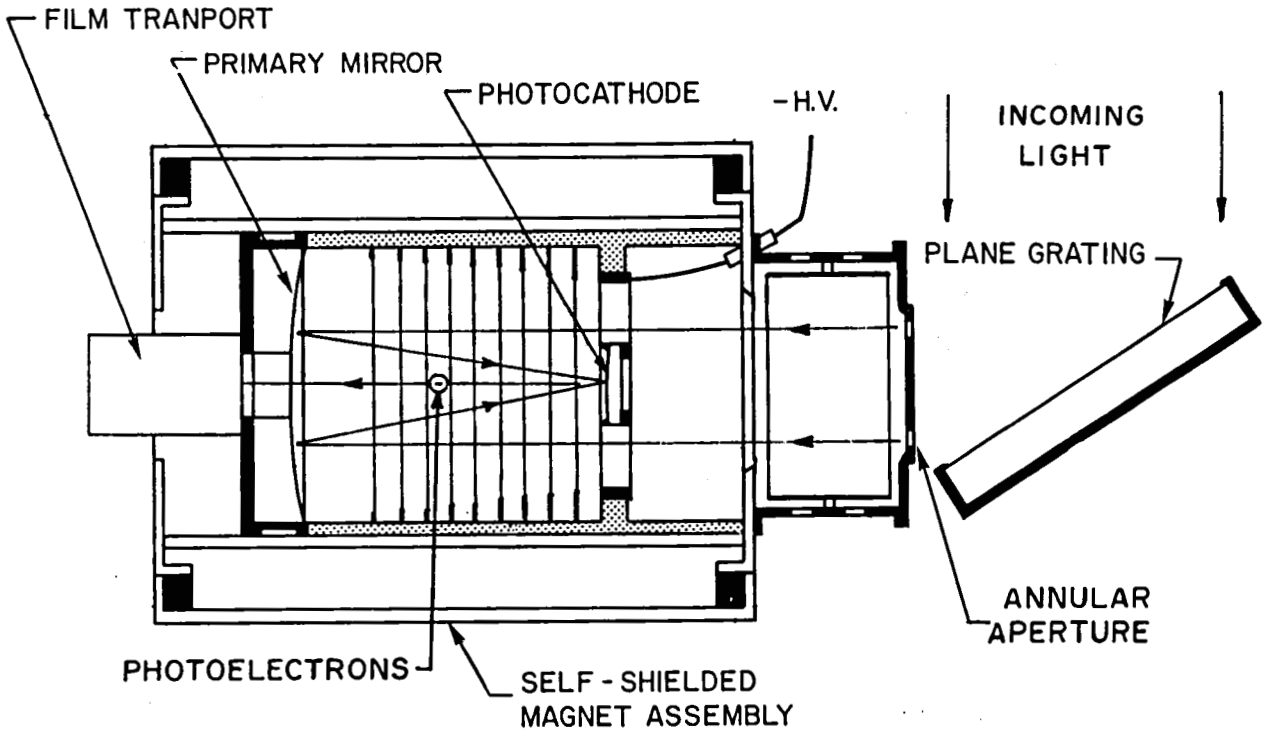

Figure 1. Diagram of the rocket objective spectrograph used for stellar observations in the 900-1600 A wavelength range.

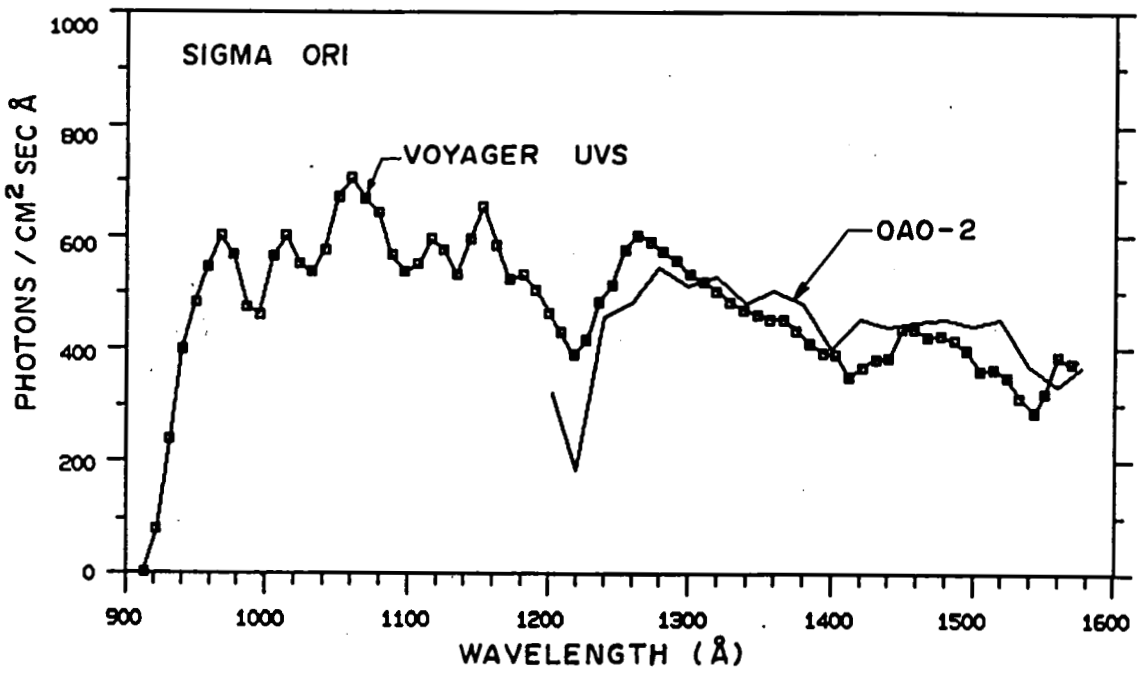

Figure 2. Comparison of far ultraviolet flux distributions for the star σ Orionis (spectral type O9.5 V) observed by OAO-2 and Voyager.

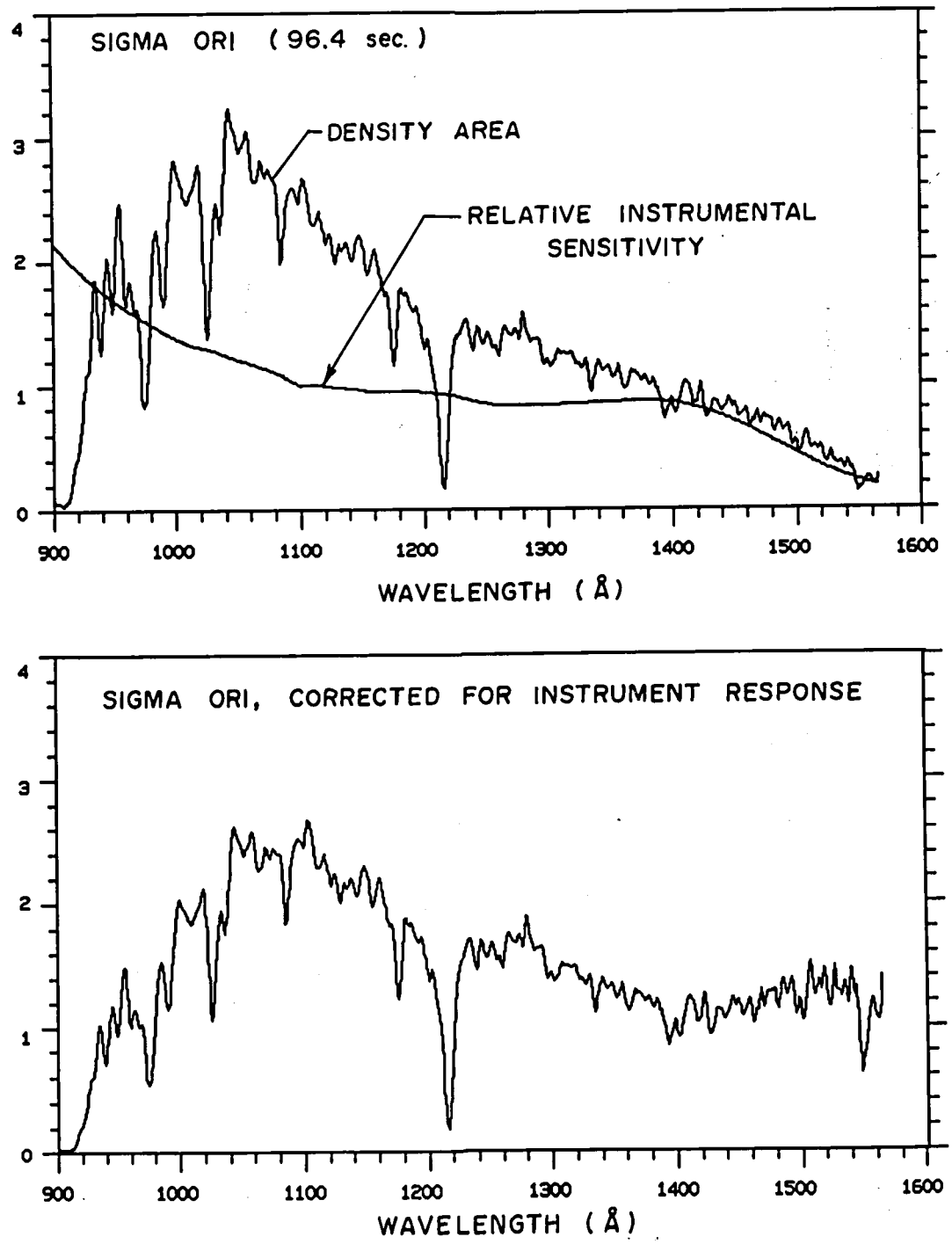

Figure 3. (TOP) Instrumental spectral intensity distribution (density area) of a rocket spectrum of the star σ Orionis, and preliminary curve of relative instrumental sensitivity vs. wavelength. (BOTTOM) Spectral distribution (relative photon flux) for σ Ori, corrected for instrumental response.

INDEX TO AUTHORS

INDEX TO AUTHORS

BIBLIOGRAPHIC DATA SHEET

1. Report No.	2. Government Accession No.	3. Recipient's Catalog No.
NASA CP-2349		

4. Title and Subtitle	5. Report Date
FUTURE OF ULTRAVIOLET ASTRONOMY BASED ON SIX YEARS OF IUE RESEARCH	December 1984
	6. Performing Organization Code

7. Author(s)	8. Performing Organization Report No.
Jaylee M. Mead, Robert D. Chapman, and Yoji Kondo, Editors	85B0016

9. Performing Organization Name and Address	10. Work Unit No.
Laboratory for Astronomy & Solar Physics NASA-Goddard Space Flight Center Greenbelt, MD 20771	11. Contract or Grant No.
	13. Type of Report and Period Covered
12. Sponsoring Agency Name and Address	
National Aeronautics and Space Administration Washington, D.C. 20546	Conference Publication
	14. Sponsoring Agency Code

15. Supplementary Notes

16. Abstract

This volume contains the invited and contributed papers presented at a symposium held at the Goddard Space Flight Center April 3-5, 1984, to mark the beginning of the seventh year of guest observations with the International Ultraviolet Explorer (IUE) satellite. The program emphasized physical insights into the various astronomical objects which have been studied using the observatory. Topics covered at the symposium included galaxies, cool stars, hot stars, close binaries, variable stars, the interstellar medium, the solar system, and IUE follow-on missions.

17. Key Words (Selected by Author(s))	18. Distribution Statement
International Ultraviolet Explorer (IUE), ultraviolet astronomy, solar system, stars, binary stars, nebulae, interstellar medium, galaxies	Unclassified-Unlimited Subject Category 89

19. Security Classif. (of this report)	20. Security Classif. (of this page)	21. No. of Pages	22. Price*
Unclassified	Unclassified	544	A20

*For sale by the National Technical Information Service, Springfield, Virginia 22161
☆U.S. GOVERNMENT PRINTING OFFICE: 1984-537-086/ 36

National Aeronautics and
Space Administration

Washington, D.C.
20546

Official Business
Penalty for Private Use, $300

SPECIAL FOURTH CLASS MAIL
BOOK

Postage and Fees Paid
National Aeronautics and
Space Administration
NASA-451

NASA

POSTMASTER: If Undeliverable (Section 158
Postal Manual) Do Not Return